

**UNIVERSIDADE FEDERAL DE MINAS GERAIS
INSTITUTO DE CIÊNCIAS BIOLÓGICAS
PROGRAMA DE PÓS-GRADUAÇÃO EM MICROBIOLOGIA
TESE DE DOUTORADO**

**Desvendando características biológicas e moleculares dos
vírus gigantes: predição e análise de motivos promotores em
marseillevírus, faustovírus e kaumoebavírus e caracterização
do efeito citopático do tupanvírus em *Acanthamoeba
castellanii*.**

GRAZIELE PEREIRA OLIVEIRA

Belo Horizonte, 27 de Agosto de 2018

GRAZIELE PEREIRA OLIVEIRA

**Desvendando características biológicas e moleculares dos
vírus gigantes: predição e análise de motivos promotores em
marseillevírus, faustovírus e kaumoebavírus e caracterização
do efeito citopático do tupanvírus em *Acanthamoeba
castellanii*.**

Tese de Doutorado apresentada ao Programa
de Pós-Graduação em Microbiologia do
Instituto de Ciências Biológicas da
Universidade Federal de Minas Gerais

Orientador: **Prof. Jônatas Santos Abrahão**
Coorientador: Prof. Flávio Guimarães da
Fonseca

Belo Horizonte, 27 de Agosto de 2018

043

Oliveira, Grazielle Pereira.

Desvendando características biológicas e moleculares dos vírus gigantes: predição e análise de motivos promotores em Marseillevirus, Faustovirus e Kaumoebavirus e caracterização do efeito citopático do Tupanvirus em *Acanthamoeba castellanii* [manuscrito] / Grazielle Pereira Oliveira. – 2018. 331 f. : il. ; 29,5 cm..

Orientador: Prof. Jônatas Santos Abrahão. Coorientador: Prof. Flávio Guimarães da Fonseca.

Tese (doutorado) – Universidade Federal de Minas Gerais, Instituto de Ciências Biológicas. Programa de Pós-Graduação em Microbiologia.

1. Microbiologia. 2. Marseillevírus. 3. Faustovírus. 4. Kaumoebavírus. 5. Tupanvírus. I. Abrahão, Jônatas Santos. II. Fonseca, Flávio Guimarães da. III. Universidade Federal de Minas Gerais. Instituto de Ciências Biológicas. IV. Título.

CDU: 579



UNIVERSIDADE FEDERAL DE MINAS GERAIS

INSTITUTO DE CIÊNCIAS BIOLÓGICAS
PROGRAMA DE PÓS-GRADUAÇÃO EM MICROBIOLOGIA

ATA DA DEFESA DE TESE DE GRAZIELE PEREIRA OLIVEIRA

Nº REGISTRO: 2015705010

Suplente interno: Prof^a. Dr^a. Betânia Paiva Drumond

Suplente externo: Dr^a. Ana Paula Moreira Franco Luiz

Às 14:00 horas do dia 27 de agosto de 2018, reuniu-se, no Instituto de Ciências Biológicas da UFMG, a Comissão Examinadora composta pelos

Drs. Francisco Pereira Lobo- Titular (UFMG), Graciela Kunrath Lima- Titular (UFMG), Pedro Augusto Alves- Titular (Centro de Pesquisas René Rachou/Fundação Oswaldo Cruz), Danilo Bretas de Oliveira - Titular (Faculdade de Medicina (FAMED) da UFVJM) e o Prof. Jônatas Santos Abrahão - Orientador, para julgar o trabalho final "Desvendando características biológicas e moleculares dos vírus gigantes: predição e análise de motivos promotores em marseillevirus, faustovirus e kaumoebavirus e caracterização do efeito citopático do tupanvirus em *Acanthamoeba castellanii*.", da aluna **Graziele Pereira Oliveira**, requisito final para a obtenção do Grau de **DOCTOR EM CIÊNCIAS BIOLÓGICAS: MICROBIOLOGIA**. Abrindo a sessão, o Presidente da Comissão, Prof. Flávio Guimarães da Fonseca - Coordenador do Programa, após dar a conhecer aos presentes o teor das Normas Regulamentares do Trabalho Final, passou a palavra à candidata, para a apresentação de seu trabalho. Seguiu-se a arguição pelos Examinadores, com a respectiva defesa da candidata. Logo após, a Comissão se reuniu, sem a presença da candidata e do público, para julgamento e expedição de resultado final. A candidata foi considerada **APROVADA**. O resultado final foi comunicado publicamente à candidata pelo Presidente da Comissão. Nada mais havendo a tratar, o Presidente encerrou a reunião e lavrou a presente ata, que será assinada por todos os membros participantes da Comissão Examinadora. Belo Horizonte, 27 de agosto de 2018.

Dr. Francisco Pereira Lobo

Francisco P. Lobo

Dr^a Graciela Kunrath Lima

Graciela Kunrath Lima

Dr. Pedro Augusto Alves

Pedro Augusto Alves

Dr. Danilo Bretas de Oliveira

Danilo Bretas de Oliveira

Prof. Jônatas Santos Abrahão (Orientador)

Jônatas S. Abrahão

Prof. Flávio Guimarães da Fonseca
Coordenador

AGRADECIMENTOS

Eis que é chegada a hora de finalizar mais um dos capítulos que compõe o livro da minha vida: meu Doutorado. E aqui estou com meu fiel amiguinho do lado (Cadu), completamente perdida em pensamentos e recordações para tentar escrever em poucas palavras os agradecimentos que poderiam compor um livro.

Primeiramente, agradeço a Deus por me guiar e me fazer acreditar que tudo é possível quando se tem fé.

A minha mãe, por me amar e cuidar de mim em todos os momentos da minha vida: “Essa tese é dedicada a você”. E ao meu amado pai, por construir uma família forte e unida que é o pilar da minha vida.

Ao meu melhor amigo e grande amor Josaphat por toda paciência, compreensão, amor e cuidado diário: “Eu amo você”.

Aos meus irmãos e irmãs, obrigada pelo apoio e amizade: “Madrinha, sem o seu apoio nada na minha vida teria sido possível”; “Micááá, minha irmã e amiga Cristiane você me mostrou pela sua história de vida que o amor e o respeito pelo outro podem vencer tudo”; Meu irmão Magela, você é minha fonte de inspiração, caráter e amor”; “Meus irmãos Laerte e Paulo amo e admiro muito vocês”; “Meu irmão Humberto, mesmo longe sei que está torcendo por mim”: “Eu amo todos vocês e serei eternamente grata a tudo que fizeram por mim”... Agradeço também por terem escolhido ótimos cunhados e cunhadas, em especial a Márcia (uma amiga que admiro muito) e os mais lindos e inteligentes sobrinhos que existem: em especial ao meu afilhado Iury (Meu príncipe) e a Lavínia por me fazer ter vontade de largar tudo e fugir levando ela.

Ao meu amiguinho fiel nas madrugadas de estudo: Cadu.

A minha mais que amiga (minha irmã escolhida) Graciele por sempre me dar a mão quando eu precisei. As minhas amigas Bruna, Denise Anete e Denise Araújo (Eu tenho as melhores amigas do mundo): “Amo vocês”.

Ao meu orientador pela excelência com que exerce sua profissão e pelo brilhantismo que nos inspira: “Jônatas, obrigada pela oportunidade, pela paciência, pela dedicação diária, pelos ensinamentos, pelas ótimas idéias, por todo crescimento científico e por não me deixar esquecer que eu posso muito mais do que eu sou capaz de imaginar”.

A professora Erna pela oportunidade e por ter aberto as portas do laboratório de vírus para mim: “Obrigada por ter me mostrado diariamente, ao longo desses quase 10 anos, o que é ser uma verdadeira líder”.

Aos demais professores do laboratório de vírus Dr. Cláudio, Dr. Paulo, Dra. Giliane e Dra. Betânia pelas disciplinas enriquecedoras ofertadas e por todo conhecimento e dedicação. Ao prof. Flávio e ao seu aluno Thiago pela ajuda e ensinamentos no estudo de vírus recombinante.

Aos meus amigos presentes e egressos do Laboratório de Vírus, pela amizade e discussões produtivas. Em especial a Deinha, pela amizade e carinho sinceros. À Poli, pela companhia desde a graduação. Ao Maurício, pelas valiosas discussões e por me mostrar que independente do que aconteça em nossas vidas há sempre um caminho que nos permite seguir em frente. À Paulinha, por estar sempre disposta a ajudar, e pelo quanto me ajudou nessa fase da defesa. A todos os integrantes do Gepvig por me mostrar o quanto é bom trabalhar em grupo, em especial a Isa por colaborar com esse estudo e me permitir compartilhar um pouco da minha experiência, a Lud, Thalita e Ana Cláudia por serem mais que amigas de grupo sempre me ouvindo quando precisei: “Torço pelo sucesso de vocês, pois são merecedores”.

Aos funcionários do departamento de microbiologia e a gerência de resíduos pelo trabalho exercido, aos membros da banca pela disponibilidade e contribuições, e às agências de fomento pelo apoio financeiro.

Tenho consciência que palavras são pouco para demonstrar minha gratidão, mas ofereço estar sempre presente para retribuir com atitudes, palavras e quando preciso for: silêncio.

Obrigada!

RESUMO**Tese de Doutorado**

Programa de Pós-Graduação em Microbiologia-Universidade Federal de Minas Gerais

DESVENDANDO CARACTERÍSTICAS BIOLÓGICAS E MOLECULARES DOS VÍRUS GIGANTES: PREDIÇÃO E ANÁLISE DE MOTIVOS PROMOTORES EM MARSEILLEVIRUS, FAUSTOVIRUS E KAUMOEBAVIRUS E CARACTERIZAÇÃO DO EFEITO CITOPÁTICO DO TUPANVIRUS EM ACANTHAMOEBA CASTELLANII.**GRAZIELE PEREIRA OLIVEIRA**

ORIENTADOR: Prof. Jônatas Santos Abrahão

COORIENTADOR: Prof. Flávio Guimarães da Fonseca

Belo Horizonte, Agosto de 2018

A descoberta dos vírus gigantes levou à quebra de paradigmas no campo da virologia devido ao tamanho das partículas desses vírus e pela sua complexidade genômica e estrutural. Na última década, a busca por novos vírus gigantes foi intensificada levando a descoberta dos marseillevírus, faustovírus, kaumoebavírus e tupanvírus. Visto a necessidade de elucidar características biológicas e moleculares desses vírus que ainda permanecem sem resposta, esse trabalho teve como objetivo fazer a predição e análise de motivos promotores em vírus da família *Marseilleviridae*, em faustovírus e kaumoebavírus e a caracterização do efeito citopático do tupanvírus em *Acanthamoeba castellanii*. A predição e análise de motivos promotores levou a primeira caracterização de um octâmero (AAATATTT) que pode atuar como promotor em vírus da família *Marseilleviridae*. A distribuição e localização do motivo em relação ao códon de iniciação seguiu um padrão semelhante ao demonstrado para outros promotores descritos entre os membros que compõem o NCLDV. Além disso, a relevância biológica do octâmero predito foi demonstrada e a presença de repetições desse motivo nas regiões intergênicas do genoma de marseillevírus foi associada à elevada capacidade dos marseillevírus de adquirir genes por transferência gênica lateral contribuindo para explicar o seu mosaicismo e plasticidade genômica. Já a busca de motivos promotores em faustovírus e kaumoebavírus revelou que esses vírus compartilham em abundância as mesmas sequências promotoras (TATTT e TATATA) previamente descritas em vírus da família *Asfarviridae*. Foi demonstrado que os motivos preditos estão presentes em mais de 65% das regiões a montante dos genes compartilhados entre faustovírus, kaumoebavírus e asfarvírus reforçando a relação filogenética entre estes vírus. Além da regulação dos processos transcricionais, um importante desafio para os vírus na natureza é a busca por células hospedeiras. Nesse contexto nós realizamos uma caracterização detalhada do efeito citopático desenvolvido por tupanvírus em cultura de *Acanthamoeba castellanii* o que levou a descrição de um novo tipo de interação vírus-hospedeiro. Foi demonstrado que a infecção por tupanvírus é capaz de induzir a expressão de um gene que codifica uma proteína ligadora de manose viral e celular sugerindo a importância dessa proteína no ciclo de multiplicação do tupanvírus. Curiosamente, a adição de manose livre durante a multiplicação de tupanvírus levou não só a supressão do aumento do nível de transcritos dos genes da proteína ligadora de manose viral e celular como a inibição da formação do cacho de uma maneira concentração dependente, sugerindo que a formação de cachos correlaciona com a expressão dos genes que codifica a proteína ligadora de manose tanto viral quanto celular. Finalmente, nós demonstramos que os cachos formados durante a multiplicação de tupanvírus são capazes de interagir com células não infectadas contribuindo para a disseminação viral.

Palavras Chave: Marseillevírus, faustovírus, Kaumoebavírus, promotor, tupanvírus

ABSTRACT**Doctoral Thesis**

Programa de Pós-Graduação em Microbiologia-Universidade Federal de Minas Gerais

UNCOVERING BIOLOGICAL AND MOLECULAR CHARACTERISTICS OF GIANT VIRUSES: PREDICTION AND ANALYSIS OF PROMOTERS IN MARSEILLEVIRUS, FAUSTOVIRUS AND KAUMOEBAVIRUS AND CHARACTERIZATION OF THE CITOPATHIC EFFECT OF TUPANVIRUS IN *ACANTHAMOEBA CASTELLANII*.**GRAZIELE PEREIRA OLIVEIRA**

ADVISOR: Dr. Jônatas Santos Abrahão

CO-ADVISOR: Dr. Flávio Guimarães da Fonseca

Belo Horizonte, August 2018

The discovery of giant viruses led to the breakdown of paradigms in virology field due virus particle size and genomic and structural complexity. In the last decade, the search for new giant viruses intensified leading to the discovery of marseillevirus, faustovirus, kaumoebavirus and tupanvirus. In order to elucidate the biological and molecular informations of these viruses that remain unclear, this work aimed to predict and analyze the promoter motifs in *Marseilleviridae* family viruses, in faustovirus and kaumoebavirus, further to characterize the cytopathic effect of tupanvirus in *Acanthamoeba castellanii*. The analysis of promoter motifs led to the first characterization of an octamer (AAATATTT) that can act as a promoter in the *Marseilleviridae* family. The distribution and localization of the motif relative to the start codon followed a pattern similar to that demonstrated for other promoters described among NCLDV members. In addition, the biological relevance of the predicted octamer was demonstrated and the motifs repetitions in intergenic regions of the marseillevirus genome was associated with the high ability of the marseillevirus to acquire genes by lateral gene transfer contributing to explain their mosaicism and genomic plasticity. The search for promoter motifs in faustovirus and kaumoebavirus revealed that these viruses share in abundance the same promoter sequences (TATTT and TATATA), as previously described in viruses of the *Asfarviridae* family. It has been demonstrated that the predicted motifs are present in more than 65% of the genes shared among faustovirus, kaumoebavirus and asfarvirus, reinforcing the phylogenetic relationship between these viruses. In addition to the regulation of transcriptional processes, an important challenge for viruses in nature is the search for host cells. In this context, we performed a detailed characterization of the cytopathic effect of tupanvirus in the culture of *Acanthamoeba castellanii*, which led to the description of a new type of virus-host interaction involving the tupanvirus. Tupanvirus infection has been shown to be capable of inducing the expression of genes encoding a viral and cellular mannose binding protein (MBP), suggesting the importance of the MBP in tupanvirus multiplication cycle. Interestingly the presence of mannose led not only to suppression of the increase in transcripts level of the viral and cellular MBP genes, but also led to the inhibition of amoebal-bunches formation at a concentration dependent, suggesting that the bunches formation correlates with the expression of the viral and cellular MBP genes. Finally, we demonstrate that the amoebal-bunches formed during multiplication of tupanviruses are able to interact with uninfected cells contributing to viral spread.

Key words: Marseillevirus, faustovirus, Kaumoebavirus, promoter, tupanvirus

Oliveira, GP.

SUMÁRIO

1. INTRODUÇÃO	09
2. JUSTIFICATIVA	15
3. OBJETIVOS	16
3.1 Objetivo Geral	16
3.2 Objetivos Específicos	16
4. METODOLOGIA, RESULTADOS E DISCUSSÃO PARCIAL	18
4.1. ARTIGO 1_REVISÃO: Promoter Motifs in NCLDVs: An Evolutionary Perspective.....	18
4.2. ARTIGO 2: The Investigation of Promoter Sequences of Marseilleviruses Highlights a Remarkable Potential for Gene Acquisition and Genome Expansion	39
4.3. ARTIGO 3: Putative Promoter Motif Analyses Reinforce the Evolutionary Relationships Among Faustoviruses, Kaumoebavirus, and Asfarvirus	50
4.4. ARTIGO 4: Tupanvirus-infected amoebas are induced to aggregate with uninfected cells promoting viral dissemination.....	59
5. DISCUSSÃO	88
6. CONCLUSÕES.....	94
7. REFERÊNCIAS BIBLIOGRÁFICAS	96
8. EVENTOS CIENTÍFICOS E PRODUÇÕES.....	103
8.1 Participações em eventos científicos	103
8.2 Organização de evento científico	103
8.3 Artigos científicos publicados	104
8.4 Capítulos de livros publicados.....	107
8.5 Artigos em processo de revisão	108
9. ANEXOS_OUTROS ARTIGOS PUBLICADOS DURANTE O DOUTORADO.....	108

1. INTRODUÇÃO

Os vírus são parasitas intracelulares obrigatórios conhecidos principalmente com base em suas características ultramicroscópicas, bem como pelo seu genoma pequeno que codifica poucas proteínas (Lwoff, 1957). No entanto, a comunidade científica tem sido cada vez mais surpreendida com a descoberta de novos vírus que quebram esses paradigmas, sendo que a maioria deles está incluída no grupo denominado Vírus Grandes Núcleo-citoplasmáticos de DNA (NCLDV) (Yutin *et al.*, 2009). Esse grupo atualmente é composto pelas famílias *Poxviridae*, *Asfarviridae*, *Phycodnaviridae*, *Iridoviridae*, *Ascoviridae*, *Mimiviridae* e *Marseilleviridae*. Além disso, vírus recentemente descobertos, ainda não incluídos em famílias pelo Comitê Internacional de Taxonomia de Vírus (ICTV), também pertencem a esse grupo, como pandoravírus, pithovírus, mollivírus, cedratvírus, pacmanvírus, faustovírus, kaumobavírus e orpheovírus (Philippe *et al.*, 2013; Legendre *et al.*, 2014; ; Legendre *et al.*, 2015; Reteno *et al.*, 2015; Andreani *et al.*, 2016; Bajrai *et al.*, 2016; Andreani *et al.*, 2017; Andreani *et al.*, 2018). A prospecção e caracterização de vírus pertencentes ou relacionados a essas famílias e espécies tende a crescer uma vez que desde a descoberta dos mimivírus (o primeiro representante entre os vírus gigantes que foi caracterizado), inúmeros têm sido os isolamentos e caracterizações de vírus de complexidade genômica e estrutural semelhantes aos mimivírus (La Scola *et al.*, 2003; Claverie *et al.*, 2006; Yutin *et al.*, 2009; La Scola *et al.*, 2010; Philippe *et al.*, 2013; Legendre *et al.*, 2014; Andrade *et al.*, 2018; Abrahão *et al.*, 2018).

Os NCLDVs são caracterizados por extensos genomas de dupla fita de DNA, que variam entre aproximadamente 100 kb em vírus da família *Iridoviridae* a 2.5 Mb nos pandoravírus (Williams *et al.*, 2005; Philippe *et al.*, 2013). Vírus gigantes pertencentes a esse grupo apresentam um conteúdo genético peculiar nunca antes descrito entre os vírus, entre eles destacam-se genes relacionados não só ao processo transcricional, mas também traducional, tais como aminoacil-tRNA-sintetases (aaRS), RNA transportadores (tRNA) e fatores de tradução (Abergel *et al.*, 2007; Jeudy *et al.*, 2012; Abrahão *et al.*, 2017; Schulz *et al.*, 2017; Abrahão *et al.*, 2018). Com os estudos de prospecção de vírus gigantes, impulsionados pela descoberta dos mimivírus, novos vírus gigantes vêm sendo descobertos e caracterizados, dentre eles destaque os vírus alvos de estudo desse trabalho: marseillevírus, faustovírus, kaumobavírus e tupanvírus (Boyer *et al.*, 2009; Reteno *et al.*, 2015; Bajrai *et al.*, 2016; Abrahão *et al.*, 2018).

Marseillevirus marseillevirus (MsV) foi isolado em cultura de *Acanthamoeba polyphaga*, a partir de amostra de água coletada em uma torre de resfriamento de ar condicionado na cidade de Paris, na França (Boyer *et al.*, 2009). A descoberta desse vírus levou a criação de uma nova família viral, denominada *Marseilleviridae*, que constitui a mais recente família pertencente ao grupo NCLDV oficialmente aceita pelo ICTV (Colson *et al.*, 2013). Nos anos seguintes, outros vírus pertencentes a essa família foram isolados em diversos países e com base em características filogenéticas distintas reveladas por análises de genes conservados, tais como DNA polimerase B, helicase, genes da família das ATPase e fatores de transcrição da proteína principal do capsídeo, os marseillevírus foram classificados nas linhagens A, B, C, D e E. (Thomas *et al.*, 2011; Largier *et al.*, 2012; Aherfi *et al.*, 2013; Aherfi *et al.*, 2014a; Doutre *et al.*, 2014; Dornas *et al.*, 2016; Takemura, 2016; dos Santos *et al.*, 2016). O MsV é o protótipo do gênero *Marseillevirus* e um dos representantes da linhagem A (Boyer *et al.*, 2009). O lausannevírus constitui o único representante da linhagem B caracterizado até o momento, e foi isolado em cultura de *A. castellanii*, a partir de uma amostra de água de rio coletada na cidade de Paris, na França (Thomas *et al.*, 2011). Como representante da linhagem C destaca-se o tunisvírus, isolado a partir de uma amostra de água coletada em uma fonte decorativa na cidade de Tunis, na Tunísia (Aherfi *et al.*, 2014a). Mais recentemente, foi isolado pela primeira vez no Brasil, a partir de uma amostra de água proveniente da lagoa da Pampulha em Belo Horizonte, um representante dessa família, denominado brazilian marseillevirus (BrMsV), que levou a proposta da formação da linhagem D (Dornas *et al.*, 2016). Além disso, foi proposta a criação de uma quinta linhagem (E) para incluir uma amostra isolada a partir de água coletada do interior de mexilhões dourados oriundos do sul do Brasil denominado golden marseillevírus (dos Santos *et al.*, 2016). Além de inúmeros isolamentos provenientes de amostras ambientais, vírus pertencentes à família *Marseilleviridae* já foram isolados a partir de amostras clínicas, tal como o senegalvírus, isolado de amostra de fezes de humano e o giant blood marseillevirus isolado a partir de sangue humano (Largier *et al.*, 2012; Popgeorgiev *et al.*, 2013).

O MsV apresenta capsídeo de simetria icosaédrica, medindo cerca de 250 nm de diâmetro e circundado por fibrilas de aproximadamente 12nm. O genoma é composto por uma molécula de DNA circular dupla fita com aproximadamente 370.000 pares de bases, que codificam 428 proteínas preditas (Boyer *et al.*, 2009).

O genoma do MsV apresenta um grande número de genes ortólogos, bem como um número significativo de genes parálogos (Boyer *et al.*, 2009). Outra importante característica do genoma dos marseillevírus é a presença de inúmeros genes provenientes de transferência

gênica lateral (TGL) o que conferem a esse genoma um alto nível de mosaicismo (Boyer *et al.*, 2009). Com base em análises filogenéticas, foi demonstrado que 11% dos genes preditos em MsV demonstram alta similaridade com outros vírus, 11% com bactérias ou fagos e 19% com eucariotos (Aherfi *et al.*, 2014b). O elevado número de genes provavelmente provenientes de TGL no genoma de MsV pode estar relacionado ao estilo de vida simpátrico dos seres que parasitam amebas, entre eles bactérias, fungos, algas e vírus. Deste modo, foi hipotetizado que durante o processo de replicação do DNA dos marseillevírus podem ocorrer processos de transferências gênicas entre os organismos que coabitam o interior das amebas bem como a partir do próprio hospedeiro (Boyer *et al.*, 2009; Aherfi *et al.*, 2014b). Estudos demonstram que eventos de TGL contribuem para a diversidade dos genomas de vírus de amebas sendo assim considerado importante no processo evolutivo desses vírus e de outros organismos (Anderson *et al.*, 2009; Clarke *et al.*, 2013; Fillé *et al.*, 2008; Fillé *et al.*, 2010).

Além dos marseillevírus, foi demonstrado que faustovírus e kaumoebavírus possuem um genoma composto por inúmeros genes supostamente provenientes de eventos de TGL. Os faustovírus foram isolados em cultura de *Veramoameba vermiformes* a partir de amostras de água de esgoto coletadas nas cidades de Marseille na França e na cidade de Dakar no Senegal, respectivamente. Estes vírus são formados por capsídeo de simetria icosaédrica que mede aproximadamente 200 nm de diâmetro e genoma de dupla fita de DNA circular de aproximadamente 466.000 pares de bases (pb), com conteúdo de G/C de aproximadamente 35%, dos quais foram preditos cerca de 451 genes. Uma grande parte dos genes de faustovírus apresenta similaridade com genes de procariotos, eucariotos, bacteriófagos e principalmente outros membros pertencentes ao grupo NCLDV com destaque para os vírus da família *Asfarviridae* (Reteno *et al.*, 2015). Além dos faustovírus, outro vírus gigante foi demonstrado apresentar relação filogenética aos asfarvírus: o kaumoebavírus.

O kaumoebavírus foi isolado em *V. vermiformes* a partir de amostras de esgoto provenientes da cidade de Jeddah, na Arábia Saudita. Apenas um isolado de kaumoebavírus foi descoberto e caracterizado até o momento. Seu capsídeo apresenta simetria icosaédrica com aproximadamente 250 nm de diâmetro e o genoma é composto por uma molécula de dupla fita circular de DNA que contém 350,731 pb, com conteúdo GC de 43,7% e 465 genes preditos (Bajrai *et al.*, 2016). Estudos comparativos do genoma de kaumoebavírus, faustovírus e asfarvírus demonstraram que esses vírus são filogeneticamente relacionados sugerindo uma ancestralidade comum.

O controle da expressão gênica constitui um importante fator no contexto da interação vírus hospedeiro. Vários estudos foram desenvolvidos a fim de caracterizar o perfil de

expressão gênica e sequências promotoras nos NCLDV. Na família *Poxviridae* é observado um perfil de expressão temporal bem caracterizado com a presença de três sequências promotoras distintas ricas em A/T sendo elas AAAANTGAAAA, TAAA e TAAAT (Davison *et al.*, 1989; Yang *et al.*, 2011). Similar aos poxvírus, os vírus da família *Asfarviridae* apresentam um padrão de expressão gênica temporal associada à presença principalmente das seguintes sequências promotoras: TATTT e TATATA (Garcia-Escudero *et al.*, 2000). A presença de sequências ricas em A/T está presente também entre os phycodnavírus, tal como a sequência AAAAATANTT presente na região promotora do gene *kcv*, e as sequências ATGACAA e TATAAAT relacionados à expressão de genes precoces nesses vírus (Kang *et al.*, 2004; Kawasaki *et al.*, 2004). Na família *Iridoviridae* sequências promotoras tem sido descritas para poucos genes, no entanto a sequência AAAAT foi bem caracterizada como promotor de genes tardios, além disso, uma sequência composta de 19 pares de bases AAAATTGATTATTTGTTTT foi descrita como uma região responsável pela expressão do gene que codifica a DNA polimerase (Jakob *et al.*, 2001; Nalcacioglu *et al.*, 2007). São escassos os estudos envolvendo processos transcricionais entre os membros da família *Ascoviridae*, mas as sequências TAATTAAA e ATTTGATCTT foram associadas à regulação de genes em alguns vírus dessa família (Salem *et al.*, 2008). Assim como em outros membros do NCLDV, os genes dos mimivírus podem ser divididos em precoces, intermediários e tardios (Legendre *et al.*, 2010). A análise das regiões intergênicas do genoma do protótipo do gênero *Mimivirus*, o *Acanthamoeba polyphaga mimivirus* (APMV), revelou uma sequência conservada de oito nucleotídeos (AAAATTGA) associada com aproximadamente 45% dos seus genes (Suhre *et al.*, 2005). Além disso, a mesma sequência foi identificada em regiões intergênicas do genoma de cafeteria roenbergensis virus e do tupanvírus, ambos pertencentes à família *Mimiviridae* (Fischer *et al.*, 2010; Abrahão *et al.*, 2018). Apesar da identificação de sequências promotoras em diversas famílias pertencentes ao grupo NCLDV, estudos de promotores em outros vírus pertencentes a esse grupo ainda é um campo aberto dentre eles destaque os marseillevírus, faustovírus e kaumoebavírus.

Além do controle da expressão gênica, a disseminação viral constitui um ponto crítico na interação vírus hospedeiro. Dentre os vírus gigantes recém-descobertos que apresentam alta complexidade referente a genoma e estrutura destaca-se o tupanvírus. Tupanvírus pertence à família *Mimiviridae* e duas espécies foram isoladas pelo nosso grupo de pesquisa sendo uma delas proveniente de amostras de lagoas salinas coletadas no Pantanal (tupanvírus soda lake) e uma segunda amostra isolada a partir de solo de oceano (tupanvirus deep ocean) em Campos dos Goytacases, Rio de Janeiro (Abrahão *et al.*, 2018). Sendo assim, a ocorrência

de tupanvírus foi demonstrada em ambientes extremos como as lagoas salinas que representam um dos ambientes aquáticos mais extremos do planeta devido sua alta salinidade e pH. Tupanvírus foi assim nomeado em tributo às tribos indígenas Guarani que apresentam o Deus do trovão Tupã como principal figura mitológica. Ambas as amostras de tupanvírus apresentam uma partícula viral composta por um capsídeo de estrutura bastante similar ao dos mimivírus, com um tamanho aproximado de 450 nm, um vértice modificado em star-gate e fibrilas recobrando a parte externa. Além disso, uma membrana lipídica foi observada na parte interna do capsídeo e, assim como em outros vírus gigantes, está associada ao início do ciclo de multiplicação dos tupanvírus (Abrahão *et al.*, 2018). Tupanvírus apresenta uma cauda ligada a base do capsídeo de aproximadamente 550 nm de extensão e 450 nm de diâmetro. Sendo assim, cauda e capsídeo apresentam juntos aproximadamente 1,2 µm de comprimento e devido a plasticidade observada no tamanho da cauda, foram observadas partículas de até 2,3 µm. Tupanvírus soda lake e tupanvirus deep ocean apresentam um genoma de dupla fita de DNA linear de aproximadamente 1,4 e 1,5 Mb, respectivamente (Abrahão *et al.*, 2018). Um total de 1276 ORFs foram preditas em tupanvirus soda lake e 1425 ORFs foram preditas em tupanvirus deep ocean das quais 375 e 378 são ORFans (Abrahão *et al.*, 2018). Além do seu amplo genoma, tupanvírus apresenta o maior aparato traducional descrito até o momento dentre os vírus, composto por 20 ORFs que codificam aaRS e 67 e 70 tRNAs, associados a 46 e 47 códon, em tupanvírus soda lake e tupanvírus deep ocean respectivamente. Composto esse aparato traducional foram identificados no genoma de tupanvírus fatores de iniciação (IF2 alfa, IF2 beta, IF2 gama, IF4e, IF5a, SUI1,IF4a), um fator de alongação/iniciação (GTP-binding elongation/initiation), um fator de alongação (Ef-aef-2) e um fator de terminação (ERF1), além de fatores relacionados à maturação e estabilização de tRNAs, maturação de RNAm, *splicing* e modificação de proteínas ribossomais também foram relatados. Interessantemente foi demonstrado que o genoma de tupanvírus apresenta duas repetições de sequências similares a partes de regiões intrônicas de 18S, que são expressas durante o seu ciclo de multiplicação (Abrahão *et al.*, 2018).

Diferentemente dos outros vírus gigantes que infectam amebas até o momento descritos, os tupanvírus demonstram um amplo espectro de hospedeiros. Enquanto os outros vírus gigantes são capazes de multiplicar em apenas um gênero de amebas, o tupanvírus foi capaz de multiplicar em diferentes espécies do gênero *Acanthamoeba* tais como *A. castellanii*, *A. sp E4*, *A. polyphaga* e *A. griffini*, em *Dyctiostelium discoideum*, *Vermamoeba vermiformis*, e *Willaertia magna*. Além disso, foi demonstrado que tupanvírus é capaz de desencadear um

ciclo abortivo em *A. michelline* e *A. royreba* e citotoxicidade sem multiplicação viral em *Tetrahymena hyperangularis* (Abrahão *et al.*, 2018).

O ciclo de multiplicação do tupanvírus foi observado em *A. castellanii* e *V. vermiformes* e inicia-se com a adesão das partículas virais seguido de internalização por fagocitose. Em seguida, o genoma é liberado através da abertura do star-gate com a fusão da membrana interna do capsídeo com a membrana do fagossomo. Curiosamente, foi demonstrada uma invaginação da membrana do fagossomo para o interior da cauda, causando a liberação do conteúdo da mesma no citoplasma das amebas. Após a fase de eclipse, fábricas virais são formadas no citoplasma e a morfogênese começa a ser observada (7-12 h.p.i). A análise da morfogênese viral revelou que a cauda é ligada ao capsídeo somente após a formação e fechamento do mesmo. Em tempos tardios, (16-24 h.p.i), o citoplasma da ameba é preenchido com partículas virais maduras, seguido da lise celular e liberação dos vírus (Abrahão *et al.*, 2018).

Além das características estruturais e moleculares diferenciais demonstradas por tupanvírus, no contexto de sua descoberta foi observado que esses vírus eram capazes de gerar um efeito citopático peculiar caracterizado pela formação de agregados de amebas denominados cachos (Arantes, 2018). Essas características despertaram nosso interesse em investigar mais detalhadamente o efeito citopático desencadeado pela infecção por tupanvírus, bem como os fatores envolvidos na sua formação e sua relevância biológica, no contexto da interação vírus-hospedeiro.

2. JUSTIFICATIVA

A regulação dos processos transcricionais e a disseminação viral constituem importantes pontos a serem investigados no que confere as interações entre os vírus e seus hospedeiros. Desde a descoberta dos mimivírus, estudos têm sido desenvolvidos a fim de descobrir novos vírus gigantes, o que levou ao isolamento dos marseillevírus, faustovírus, kaumoebavírus e tupanvírus, que apresentam características genômicas e estruturais peculiares. Esses vírus pertencem ao grupo NCLDV e pouco ainda é conhecido sobre suas características biológicas e seu perfil de regulação gênica. Durante muitos anos, estudos têm sido feitos com intuito de melhor entender a regulação dos processos transcricionais. Nesse caminho, sequências promotoras vêm sendo descritas para membros que compõem o grupo NCLDV e a compilação de estudos revisando pela primeira vez essas sequências faz-se importante. Além disso, a busca por motivos promotores em vírus gigantes recém-isolados pode levar a valiosas descobertas e discussões. Os marseillevírus apresentam um repertório genômico composto por inúmeros genes originados a partir do hospedeiro e seus simbioses em eventos de transferência gênica lateral (TGL), o que torna o genoma desses vírus um verdadeiro mosaico. Embora os marseillevírus apresentem genoma com características peculiares, despertando interesse no seu estudo, pouco é conhecido acerca do seu padrão de expressão gênica bem como sobre os fatores que a regulam. Além de marseillevírus, faustovírus e kaumoebavírus também apresentam genes provenientes de TGL e são filogeneticamente relacionados a asfarvírus. Esse trabalho foi direcionado não só para a revisão de sequências promotoras em vírus gigantes, mas principalmente para a busca e caracterização de sequências promotoras nos vírus da família *Marseilleviridae*, nos faustovírus e kaumoebavírus levando a aquisição de novas informações acerca da biologia desses vírus. Além disso, a hipótese de que as sequências promotoras previamente caracterizadas em asfarvírus poderiam atuar como promotores em faustovírus e kaumoebavírus devido sua proximidade filogenética justifica uma das abordagens desse estudo. Além da regulação dos processos transcricionais o encontro de células hospedeiras é um desafio para os vírus. O isolamento e caracterização do tupanvírus despertaram a curiosidade acerca de suas características biológicas visto se tratar de um vírus com características moleculares e estruturais nunca antes observadas. No contexto do isolamento do tupanvírus, a observação de um efeito citopático peculiar caracterizado pela formação de agregados de amebas despertou nossa curiosidade acerca dos fatores envolvidos na formação desse efeito, e das possíveis implicações no valor adaptativo conferido ao tupanvírus.

3. OBJETIVOS

3.1 OBJETIVO GERAL

Fazer a predição e análise de sequências promotoras em vírus da família *Marseilleviridae*, em faustovírus e em kaumoebavírus e caracterizar o efeito citopático do tupanvírus em cultura de *Acanthamoeba castellanii*.

3.2 OBJETIVOS ESPECÍFICOS

- Revisar estudos de sequências promotoras em vírus pertencentes ao grupo NCLDV;
- Fazer a predição de sequências promotoras em vírus pertencentes às 4 linhagens da família *Marseilleviridae*;
- Avaliar o perfil de distribuição e a posição mais frequente dos motivos promotores preditos em relação aos códons de iniciação de cada gene, nas 4 linhagens da família *Marseilleviridae*;
- Avaliar o papel biológico das sequências promotoras preditas e a influência de eventuais mutações na expressão gênica;
- Avaliar a origem das regiões intergênicas do genoma de marseillevirus marseillevirus;
- Discutir e traçar hipóteses acerca do perfil de disposição das sequências promotoras no genoma dos vírus da família *Marseilleviridae*;
- Fazer a predição de sequências promotoras em faustovírus e kaumoebavírus com base nas sequências de asfarvírus previamente descritas;
- Avaliar o perfil de distribuição e a posição mais frequente em relação aos códons de iniciação dos motivos promotores preditos nos genomas de faustovírus, kaumoebavírus e asfarvírus;

- Avaliar a presença dos motivos preditos nos “core genes” de faustovírus, kaumoebavírus e asfarvírus;
- Caracterizar o efeito citopático de tupanvírus em cultura de *Acanthamoeba castellanii* utilizando MOI alta (10) e MOI baixa (0.01);
- Analisar a transcrição do gene que codifica a proteína ligadora de manose de *Acanthamoeba castellanii* e de tupanvírus na presença e ausência de manose durante o ciclo de multiplicação do tupanvírus;
- Analisar a transcrição do gene que codifica a proteína ligadora de manose em *Acanthamoeba castellanii* durante o ciclo de multiplicação do acanthamoeba polyphaga mimivirus;
- Avaliar o efeito do uso de manose na formação dos cachos durante a multiplicação do tupanvírus;
- Avaliar as possíveis implicações no valor adaptativo conferido pela formação dos cachos durante o ciclo de multiplicação do tupanvírus;

4. METODOLOGIA, RESULTADOS E DISCUSSÕES PARCIAIS SERÃO APRESENTADOS A SEGUIR NA FORMA DE ARTIGOS PUBLICADOS PRECEDIDOS DE UM BREVE RESUMO.

4.1. ARTIGO 1_REVISÃO: Promoter Motifs in NCLDV: An Evolutionary Perspective

Esta revisão foi publicada no periódico Viruses.

O grupo NCLDV é composto pelas famílias virais *Poxviridae*, *Iridoviridae*, *Phycodnaviridae*, *Ascoviridae*, *Asfarviridae*, *Mimiviridae* e *Marseilleviridae* além de outros vírus recém-descobertos tais como faustovírus, pandoravírus, phitovírus, cedratvírus, mollivírus e kauamoebavírus, ainda não inseridos em famílias. Com base no possível monofiletismo desse grupo foi proposta a criação de uma ordem viral para agrupar os vírus pertencentes ao grupo NCLDV que seria denominada “Megavirales”. Os vírus incluídos nesse grupo multiplicam completamente ou parcialmente no citoplasma da célula hospedeira e alguns deles sintetizam sua própria RNA polimerase, além de inúmeras outras proteínas relacionadas ao processo transcricional tais como helicases e fatores de transcrição, o que confere a esses organismos uma menor dependência da maquinaria transcricional do hospedeiro. A presença dessas e de outras proteínas que juntas compõem um robusto aparato transcricional constitui um dos fatores que tornam os vírus do grupo NCLDV, em especial os vírus gigantes, alvo de interessantes estudos e profundas discussões acerca da origem e evolução. A regulação dos processos transcripcionais é um campo vasto que vem sendo estudado há décadas principalmente em eucariotos e procariotos. Nesse contexto, são bem caracterizadas as sequências promotoras no genoma desses organismos. Além disso, sequências promotoras vêm sendo estudadas em inúmeros vírus, incluindo aqueles pertencentes aos NCLDVs. Nesse trabalho foi feita uma compilação de dados que resume os principais aspectos da regulação dos processos transcripcionais em procariotos e eucariotos com foco nas sequências promotoras seguido de uma revisão dos estudos que abordam as regiões promotoras até o momento descritas para os vírus pertencentes ao grupo NCLDV.



Review

Promoter Motifs in NCLDVs: An Evolutionary Perspective

Graziele Pereira Oliveira ^{1,†}, Ana Cláudia dos Santos Pereira Andrade ^{1,†},
Rodrigo Araújo Lima Rodrigues ¹, Thalita Souza Arantes ¹, Paulo Victor Miranda Boratto ¹,
Ludmila Karen dos Santos Silva ¹, Fábio Pio Dornas ¹, Giliane de Souza Trindade ¹,
Betânia Paiva Drumond ¹, Bernard La Scola ², Erna Geessien Kroon ¹
and Jônatas Santos Abrahão ^{1,*}

¹ Laboratório de Vírus, Departamento de Microbiologia, Instituto de Ciências Biológicas, Universidade Federal de Minas Gerais, Belo Horizonte 31270-901, Minas Gerais, Brazil; graziufmg@yahoo.com.br (G.P.O.); ana.andrade2008@hotmail.com (A.C.d.S.P.A.); rodriguesral07@gmail.com (R.A.L.R.); tsarantes@gmail.com (T.S.A.); pvboratto@gmail.com (P.V.M.B.); ludmilakaren@gmail.com (L.K.d.S.S.); fabiopiod154@gmail.com (F.P.D.); gitrindade@yahoo.com.br (G.d.S.T.); betaniadrumond@gmail.com (B.P.D.); ernagkroon@gmail.com (E.G.K.)

² Unité de Recherche sur les Maladies Infectieuses et Tropicales Emergentes (URMITE) UM63 CNRS 7278 IRD 198 INSERM U1095, Aix-Marseille Université, 27 Boulevard Jean Moulin, Faculté de Médecine, 13385 Marseille Cedex 05, France; bernard.la-scola@univ-amu.fr

* Correspondence: jonatas.abrahao@gmail.com; Tel.: +55-031-3409-3002

† These authors contributed equally to this work.

Academic Editor: Eric Freed

Received: 14 November 2016; Accepted: 5 January 2017; Published: 20 January 2017

Abstract: For many years, gene expression in the three cellular domains has been studied in an attempt to discover sequences associated with the regulation of the transcription process. Some specific transcriptional features were described in viruses, although few studies have been devoted to understanding the evolutionary aspects related to the spread of promoter motifs through related viral families. The discovery of giant viruses and the proposition of the new viral order Megavirales that comprise a monophyletic group, named nucleo-cytoplasmic large DNA viruses (NCLDV), raised new questions in the field. Some putative promoter sequences have already been described for some NCLDV members, bringing new insights into the evolutionary history of these complex microorganisms. In this review, we summarize the main aspects of the transcription regulation process in the three domains of life, followed by a systematic description of what is currently known about promoter regions in several NCLDVs. We also discuss how the analysis of the promoter sequences could bring new ideas about the giant viruses' evolution. Finally, considering a possible common ancestor for the NCLDV group, we discussed possible promoters' evolutionary scenarios and propose the term "MEGA-box" to designate an ancestor promoter motif ("TATATAAAATTGA") that could be evolved gradually by nucleotides' gain and loss and point mutations.

Keywords: megavirales; NCLDV; giant viruses; promoter; transcription; evolution; MEGA-box

1. Introduction

For decades, viruses have been strictly considered intracellular parasites, filterable in membranes of 0.22 nm, composed by genomes of DNA or RNA encoding only a few proteins, being entirely dependent on the metabolic machinery of the host cell [1]. However, viruses show a large diversity of genome size and organization, capsid architecture, mechanisms of replication, and interactions with host cells. The extreme diversity of viruses suggests that they must have had multiple evolutionary origins, thus being polyphyletic [2]. In 2001, a supposedly monophyletic

group named nucleocytoplasmic large DNA viruses (NCLDV) was proposed, composed of families *Poxviridae*, *Asfarviridae*, *Iridoviridae* and *Phycodnaviridae* [3]. This group gained notoriety two years later with the discovery of *Acanthamoeba polyphaga mimivirus* [4] and it is currently composed of the families mentioned above, as well as *Ascoviridae*, and the more recently incorporated *Mimiviridae* and *Marseilleviridae* [5]. Moreover, other recently discovered giant viruses such as pandoraviruses, faustoviruses and pithoviruses were classified as members of the NCLDV group [6–9]. This group has single features such as large genomes and a diverse gene repertoire, which encode some proteins never identified previously in viruses. Therefore, the creation of a new viral order named ‘Megavirales’, encompassing all families of the NCLDV group was proposed [5].

This proposed order comprises viruses with large double-stranded DNA (dsDNA) genomes, encoding hundreds of proteins and capable of infecting a wide-range of eukaryotic organisms. These viruses replicate completely or partly, in the cytoplasm of eukaryotic cells and some of them are able to synthesize RNA polymerases (RNA pol), helicases and transcription factors involved in the transcription initiation and elongation steps with lower dependence of the host’s transcriptional machinery [3]. The presence of a robust transcriptional apparatus in some Megavirales members, along with a quasi-autonomous glycosylation and translational machinery, especially in mimiviruses, boosted the discussion about the origin and evolution of giant viruses and their genome. Recent evolutionary reconstructions mapped about 25–50 genes encoding essential genes for the probable most recent common ancestor [10]. Concerning the origin of such giant genomes, different hypotheses have been proposed. Some authors suggest a “genome degradation hypothesis”, wherein the giant viruses are derived from a cellular ancestor through genome simplification linked to the adaptation to some host lineage [11,12]. Other authors argue in favor of a “genome expansion hypothesis”, wherein the giant viruses evolved from a smaller viral ancestor and the universal genes have been independently acquired from their eukaryotic hosts by progressive gene accretion and duplication. According to this theory, the genes of giant viruses have several origins and the origin of giant viruses is probably from a simpler ancestor [13,14].

On the other hand, the accordion-like model of evolution proposes that there is no trend of genome expansion or general tendency of genome contraction. Instead, viruses evolving by constant gene gain and loss originated from an ancestor giant virus [10]. All these theories are often contradictory and have stimulated discussion about the establishment of a fourth domain of life where the giant viruses of the proposed order Megavirales were suggested to share a common ancestral origin based on analyses of their sequences and gene repertoires and compose a new domain aside Bacteria, Archaea and Eukarya [14–16].

During the last years, a huge effort has been made to better understand the virus–host interaction on many levels. One of the most interesting research fields is how the viruses can explore host transcriptional machinery to express their genes. Nevertheless, it is important also to look into the transcription process of the cellular organisms. The upstream regions of eukaryotes and prokaryotes genes have been studied in different organisms in an attempt to discover sequences associated with the regulation of the transcription process. The same has been done for viruses, especially considering the proposed Megavirales order, where some putative promoter sequences have already been described. In this review, we summarize the main aspects of the transcription regulation process in the three domains of life, followed by a systematic description of current knowledge of the promoter regions of all members within Megavirales order. Finally, we discuss how the analysis of the promoter sequences found in giant viruses provides new insights into the evolutionary history of these complex and intriguing agents.

2. Gene Expression in Cells

In all cells, thousands of genes encoded in the DNA are transcribed into RNA and for the efficient occurrence of this process, multiple events must be triggered. In eukaryotes, the genome is coupled to histones and other proteins, forming the chromatin compact complex. Since wrapping

DNA around histones blocks the access to the genetic information, decondensation of DNA is required, to allow physical access to the the gene locus and the transcription initiation machinery formation [17–19]. The transcription initiation machinery is formed over a region of the genome, the promoter. The promoter is typically located 40 bp upstream and downstream of the transcription start of a gene, called transcription start sites (TSS). Several transcription factors mediate the transcription machinery assembly on the promoter region. There are thousands of transcription factors involved in the transcription process, such as TFIIA, TFIIB, TFIID, TFIIE, TFIIIF and TFIIH that recognize and bind the promoter region, called the core promoter, and recruit RNA polymerase (RNA pol) [20]. Eukaryotes have five types of RNA pol (I to V). RNA pol I transcribes ribosomal RNA, whereas the type II is the best characterized one and responsible for transcribing genes encoding proteins, and several noncoding RNA classes [18,21,22]. RNA pol III transcribes genes encoding short, untranslated RNAs, such as tRNAs, 5S ribosomal RNA (rRNA) and the spliceosomal U6 small nuclear RNA (snRNA) [23]. RNA pol IV and V transcribe siRNA in plants [24].

One classical element of the core promoter is the TATA-box, which is a consensus sequence (TATAAAT) located at –25 to –30 bp upstream of the TSS. Although the TATA-box sequence is a well-known promoter core motif, it is present only in a minority of mammalian promoters. This sequence is commonly associated with tissue-specific gene transcription and high conservation within species [25,26]. Other eukariotic promoter elements are Initiator (Inr); Downstream Promoter Element (DPE), Core Element Downstream (CED), TFIIB-Recognition Element (TRE), and Motif Ten Element (MTE) [20,27,28]. Together, these components act synergistically to increase transcription efficiency by providing recognition sites for transcription factors, and indicate the direction of transcription and also the DNA strand to be transcribed [20]. The transcription starts with the binding of the TFIID to the TATA-box region, the Inr sequence and/or other core promoter elements [27]. TFIID is a multiprotein complex comprising the TATA-box binding protein (TBP) and more than 10 different TBP associated factors (TAFs) [22]. After binding TBP to the TATA-box motif, the RNA pol II is recruited, and the transcription is triggered (Figure 1A).

Nevertheless, the transcription in eukaryotes is a much more complex process than previously thought and various strategies are used to increase the diversity of transcripts produced. Among mammals, previous analysis has shown that a large proportion of protein-coding genes (58%) use alternative promoters during transcription [25]. These alternative promoters may have different combinations of core promoter elements to increase the variability of transcripts [20,29,30].

There are many differences between the transcription process of eukaryotic and bacteria cells. The bacterial transcription is much simpler compared to the eukaryotic process since the transcription occurs using a single type of RNA pol and there are no transcription factors [31]. This enzyme is capable of synthesizing RNA from a DNA template, but it is unable to locate the promoter and transcription initiation site. Thus, a key factor to transcription is the free subunit named σ (sigma), which is responsible for recognizing the promoter region (Figure 1B) [32,33]. Although the majority of nucleotides within bacteria promoters vary in sequence, several short motifs are conserved. These include the hexamer (TATAAT), located 10 base pairs (bp) upstream of the TSS and is recognized by domain 2 of RNA pol σ subunit. Another motif is the the hexamer (TTGACA), located 35 base pairs (bp) upstream of the TSS and recognized by domain 4 of the RNA pol σ subunit [31,34,35]. In Archaea, there is a mix of eukarya and bacteria translational apparatus. Just as in eukaryotes, the archaea RNA pol is not able to recognize promoter sequences by itself and at least two transcription factors analogous to TBP and TFIIB are required [36–38]. The archeal TBP also recognizes specifically an AT-rich sequence, homologous to the TATA-box region of eukaryotes [39,40]. Although archaea transcription machinery is similar to that of eukaryotes, the characterization of transcription regulators of some archaeas showed that most of the transcriptional regulation in archaea is done by “bacterial-like” regulators, as two homologues of bacterial leucine-responsive regulatory protein (Lrp)—Lrs14 and Sa-Lrp and metal-dependent repressor 1 (MDR1) homologous to bacterial metal-dependent regulators (Figure 1C) [41–43].

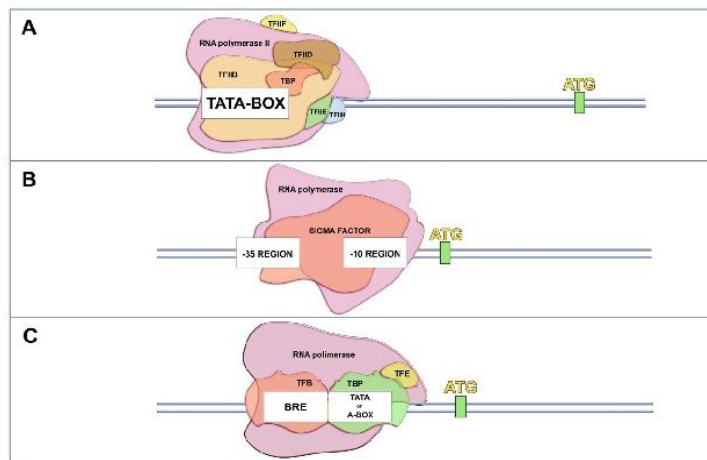


Figure 1. Main features in the transcription initiation machinery presented in the canonical Domains of Life. (A) In Eukarya, several components, called general transcription factors (represented as TFIIB, TFIID, TFIIE, TFIIH and TBP), are responsible for assembling over a region called the promoter, where they recruit an RNA polymerase to initiate the transcription process. A classical promoter presented in this group is the TATA-BOX region, located at the positions -25 and -30 from the initial transcription site; (B) In Bacteria, the sigma factor recognizes and recruits the RNA polymerase over the promoter regions. These regions are well conserved over the positions -35 and -10 upstream of the initial transcription site; (C) Archaea present a mixture of the transcription apparatus of the two other Domains. While the machinery itself is similar to that found in eukaryotes (the general transcription factors, a homologous TATA-BOX region and the RNA polymerase), the archaeal transcription regulators, activators and repressors are homologous to the bacterial ones.

Hypotheses regarding the evolutionary history of translational machinery among the living organisms have been raised during the last years, but the theme is still under debate [44]. Even considering the most recent proposals, the translational process of viruses remains out of the discussion, basically because these organisms are traditionally excluded from the canonical tree of life. However, this scenario has been changing since the discovery of giant viruses [16]. Therefore, it becomes interesting to examine if NCLDV members share similar transcription initiation strategies that could bring insights about how this correlates to giant viruses' evolution.

Gene Expression in NCLDVs

In contrast to cellular genomes, which are formed by dsDNA, viral genomes show a large diversity genome composition, structures, replication and transcription strategies with great implications in virus biology, as virus–host interactions [45]. The majority of the RNA viruses employ virus-coded specific enzymes (RNA-dependent RNA polymerases) to synthesize and modify their mRNA. DNA viruses showing small and intermediate size genomes such as the parvoviruses, papillomaviruses, and adenoviruses, depend on host-cell enzymes for transcription, including the RNA pol [45]. However, viruses with a large genome such as the giant viruses, mostly encode their transcriptional apparatus, which make them relatively independent from their host transcription machinery [15,46].

The transcription of a typical large DNA virus occurs in a temporal pattern in the host cytoplasm (Figure 2). At the start of infection, a subset of immediate early viral proteins is required for DNA replication and host cell manipulation [47,48]. The early mRNAs also encode enzymes and factors needed for transcription of the intermediate genes. Concomitantly with the expression of intermediate genes, the expression of the early genes is often repressed. Finally, late genes are transcribed, directing the synthesis of structural proteins, non-structural proteins and enzymes present in the mature particle

required for viral assembly [45,48]. The efficient transcription of late mRNA usually depends on intermediate gene products, as well as cellular transcription factors that may differ from those used by the early promoters. The products of the late genes include the immediate early transcription factors, which are packaged along with RNA pol and other enzymes within the virus progeny [47–50].

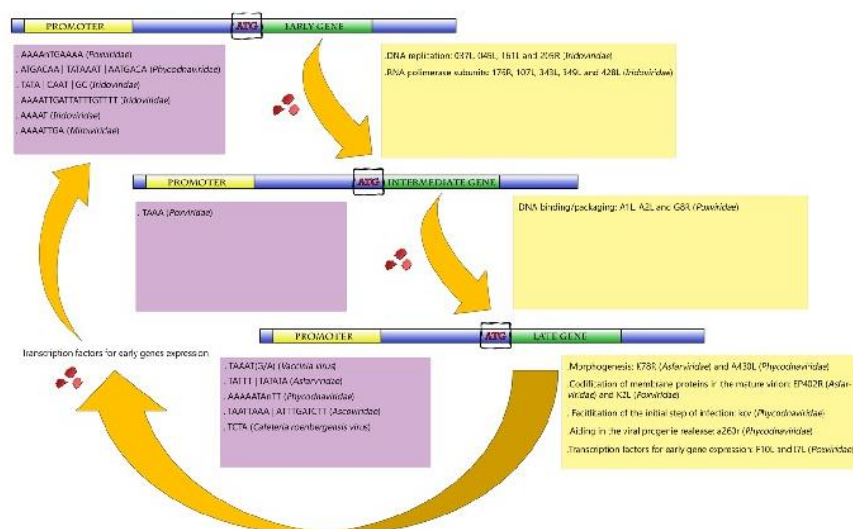


Figure 2. Representative scheme of the temporal gene expression in NCLDVs. During initial times of infection, the expression of genes related to the metabolism of nucleic acids is primarily activated (early and intermediate genes). After DNA replication, the activation of late genes is initiated. Those genes are involved in the production of viral structural proteins, in transcription factors used for early gene expression and also in proteins that facilitate the initial step of infection of the viral progeny in the next round of multiplication. Purple boxes represent the promoters described for giant viruses according to each gene category (early, intermediate and late genes). Yellow boxes exemplify the biological functions involved in each category, with some genes represented inside the parentheses.

This ability to regulate temporally the transcription of genes is characterized as an evolutionary advantage. This strategy is possible due to the presence of promoter codes that dictate when, where, and at what level the classes of early, intermediate, and late genes are transcribed [45,48]. These promoter sequences are different between the three genes classes, but there is a pattern of conservation within the same group. This indicates that during the evolution the gene promoters were selected to ensure the temporal gene expression, and therefore ensure the gene expression in the host cell during its replication [45,47,48,50].

In the following sections, we look closer at how the gene transcription is carried out in each family of the proposed Megavirales order, focusing on the current knowledge about the promoter sequence of these viruses.

3. Poxviridae Family

Among NCLDVs, the *Poxviridae* family is one of the most studied. These viruses have enveloped ovoid particles of around 200 nm in diameter and 300 nm in length and present a linear dsDNA genome of approximately 200 kbp coding nearly 200 open reading frames (ORFs). Poxviruses can infect a wide range of hosts, such as insects, birds, and mammals [48,51]. Extensive study of the poxvirus genome and replication cycle allowed a detailed identification of its promoters, as well as important transcription factors. Poxviruses possess their own DNA-dependent RNA polymerase (RNA pol) that is very similar to the eukaryotic protein, regarding size and subunit complexity. In the case of *Vaccinia virus* (VACV), a poxvirus prototype, the enzyme subunits are encoded by eight viral VACV genes

which, in most cases, are homologous to cellular RNAPol [52,53]. Gene transcription in poxviruses follows a typical temporal profile regulated by well-conserved promoters of early, intermediate and late genes (Figure 2) [47,48].

The transcription of early genes is characterized by an A/T-rich motif upstream of transcriptional start site with a critical core region located from -13 to -25 to that region. Figure 3 illustrates the promoter motifs described in megavirales members. The representative consensus sequence of the early promoter region is 'AAAANTGAAAA'. Mutagenesis in this promoter region of VACV causes a drastic negative effect on VACV gene transcription [54]. The intermediate genes are transcribed after DNA replication, before the transcription of the late genes. The intermediate core promoter is similar to the early promoter due to the A/T-rich content, but its specific sequence is given by the tetranucleotide 'TAAA'. Furthermore, the intermediate promoter sequence has a bipartite structure presenting a core and an initiator region with similar sequences (TAAA) [55–57]. Three (*A1L*, *A2L*, and *G8R*) of the 53 genes that compose the set of intermediate genes encode transcription factors that are directly related to the late stage of the replication cycle, important to DNA binding/packaging processes and to core-associated proteins [58].

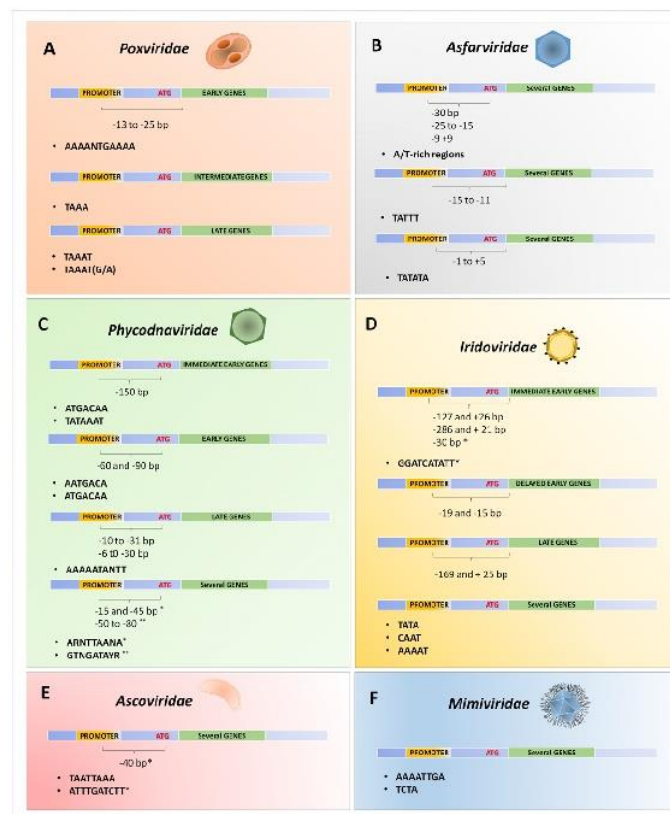


Figure 3. Schematic representation of the promoter's sequences described for different NCLDVs. Compilation of the described promoters for some viral families belonging to the proposed order Megavirales: *Poxviridae* (A); *Asfarviridae* (B); *Phycodnaviridae* (C); *Iridoviridae* (D); *Ascoviridae* (E) and *Mimiviridae* (F). Each promoter was related to the expression of immediate early, early, delayed early, intermediate and late genes, or related to the expression of genes independent of temporal expression (several genes). The distances between the transcription start site or translate start site (ATG) until the promoters are also indicated by brackets.

The transcription of late genes persists until the end of the replication cycle. Around 38 late genes have already been identified, with their main functions related to the codification of membrane proteins in the virion, morphogenesis steps, and also to the production of immediate early transcription factors [57,59]. Most of them are clustered in the central region of the poxviruses genome and also have A/T-rich sequence promoters. These regions consist of a core sequence of about 20 bp with some 'T' residues, separated by a region of about 5–7 bp of a conserved 'TAAAT' motif, which regulates the transcription initiation. Usually, G or A follows the late promoter sequence, performing a 'TAAAT (G/A)' transcription initiation sequence. This sequence is conserved among VACV late promoters, overlapping the site of transcription initiation that is absent in 5' untranslated regions (5'-UTR) [48,54]. Mutations within this conserved element were demonstrated to cause complete inactivation of the promoter, and almost 25% of the 'AAA' sequences are used as transcription initiation sites in VACV. Along with other factors, the viral RNA pol directs the synthesis of late mRNAs, finishing the transcription process [54,60–62].

The presence of complete transcriptional machinery in poxviruses allows a lower dependency of these viruses on their hosts. It permits that the mRNA transcription totally occurs in the host's cytoplasm, right after the virus entry. Additionally, the presence of well conserved promoter regulatory sequences in different poxviruses suggests a conserved evolutionary pattern among them. It is likely that such a complete transcriptional set was already present in their ancestor and was maintained over time. Alternatively, the presence of a robust transcriptional apparatus in all members of the *Poxviridae* family might be a result of evolutive convergence. Although less parcimonious, the different poxviruses might have had different evolutionary histories regarding the transcription process, including both protein-related elements and promoter sequence regions, but in the course of evolution, they became more similar to each other. It is not yet possible to determine which hypothesis is the correct, or even if other possibilities correspond to the real history of these complex viruses, and this discussion shall continue for a while.

4. *Asfarviridae*

African swine fever virus (ASFV), a large (~200 nm), icosahedral, and enveloped virus is currently the single member of the *Asfarviridae* family, infecting members of the *Suidae* family (pigs, hogs and boars) [63]. The genome is composed of a linear dsDNA molecule of approximately 170 kbp with terminal inverted repeats. It encodes approximately 150 ORFs separated by short intergenic regions [64,65]. ASFV encodes its own RNA pol and all ASFV genes are transcribed by its enzyme [66,67].

Similar to poxviruses, the ASFV gene transcription follows a temporal profile, where immediate early and early genes are expressed before the DNA replication that is followed by the expression of intermediate, late and immediate early genes. Transcription initiation and termination occurs at very precise positions in the genome, encoding a several genes involved in the transcription and modification of viral mRNAs. The transcriptional machinery of ASFV provides an accurate temporal control of gene expression regulated by cis-DNA elements, enhancers, and promoters together with a structural complexity of transcription factors [68]. Analysis of the base composition of the intergenic regions shows that they are rich in A/T sequences, similar to that observed in poxviruses [69–71]. A/T-rich regions located at approximately –30 bp upstream of the ATG translation start site are essential for the expression of the K9L gene, which encodes a protein with similarity to mammalian transcription elongation factor IIS [72]. Furthermore, upstream sequences presented in two intermediate genes exhibit highly conserved sequences at positions –25 to –15, and –9 to +9 to the translational start codon [70]. Experiments involving genetic deletions, linker scan substitutions and point mutations in the promoter sequence of the *p72* gene (major capsid protein) revealed that the replacement of the A/T-rich region by G/C residues strongly reduced the transcription rate, demonstrating the importance of this sequence for efficient late viral transcription [71].

Two other major essential regions for promoter activity are described: one region is located at position -15 to -11 upstream of the transcription start site (TATTT); and the second region at positions -1 to $+5$ (TATATA) [71]. Mutants presenting the 'TATATA' motif replaced by a G/C-rich sequence had the promoter activity completely abolished, suggesting that ASFV transcription is dependent on such sequence at (or near) the region of transcriptional initiation, similar to what is found in other large viruses [71]. The replacement of the equivalent 'TATATA' sequence on the late genes *K78R*, *EP402R* and *A137R* by the 'GCGC' motif was also demonstrated to be deleterious, suggesting that the A/T-rich sequence could be a motif for late promoter function as well [68,71]. Interestingly, the bipartite structure seen in the late promoter of ASFV is similar to the late and intermediate promoters in poxviruses that contain a core and an initiator region [54,55,62,71]. The similarities found in the transcriptional strategies reinforce the genetic data, indicating a close relationship between poxviruses and asfavirus, pointing to a common ancestor for both viral families.

5. Phycodnaviridae

The phycodnaviruses are large and icosahedral viruses (~ 100 – 220 nm), with dsDNA genomes ranging from 180 to 560 kbp [73]. Since they infect a diverse group of eukaryotic algae, they are one of the most important groups of organisms regulating the oxygen cycle in the Earth [74,75]. The family *Phycodnaviridae* consists of six genera, named according to the hosts that they infect: *Chlorovirus*, *Coccolithovirus*, *Prasinovirus*, *Prymnesiovirus*, *Phaeovirus*, and *Raphidovirus* [76]. As demonstrated by other giant viruses, the phycodnaviruses exhibit a temporal transcription profile. Early genes are transcribed within 5 to 60 min post-infection (p.i.), and transcripts of late genes begin to appear around 60–90 min p.i. However, some early genes can also be detected in later stages of infection [77,78].

The presence of A/T-rich promoters was also observed in phycodnaviruses. Analysis of the *kcv* gene, encoding a potassium ion channel protein in chlorella viruses, revealed a highly conserved 10-nt sequence (AAAAATANTT) in the promoter region of this gene, present in 16 out of 17 chlorellaviruses [77]. This sequence is located at 10–31 nucleotides upstream of the ATG translation start codon in all of the analyzed viruses, and it was associated with late gene transcription, since, apparently, *kcv* transcripts are produced during the late steps of infection. Furthermore, the region that precedes seven genes expressed at later times during the *Paramecium bursaria chlorella virus 1* (PBCV-1) replication cycle (*a85r*, *a237r*, *a248r*, *a260r*, *a292l*, *a430l*, and *a530r*) contain the same sequence or at least a subset of this sequence located at 6–30 nucleotides upstream of the ATG start codon [77]. The study of immediate early genes expressed in chlorovirus infections also revealed A/T-rich sequences as putative promoter regions. Two sequences determined by 'ATGACAA' and 'TATAAAT' (such as the eukaryotic "TATA-box") were located in a 150 bp region from the translation start codon in the upstream regions of almost all immediate early genes (20 of 23 studied) [78]. These elements, especially 'ATGACAA', were absent in all genes so far examined, expressed after 40 min p.i., including *A122R* (Vp260) [79], *A181-182R* (chitinase), *A292L* (chitosanase) [80], *A430L* (major capsid protein) [81], *vAL-1* [82].

Bioinformatics analysis revealed highly conserved nucleotide sequences in putative promoter regions involving three different chlorella viruses: PBCV-1, virus MT325 [83], and *Paramecium bursaria chlorella virus* NY-2A [84]. Three putative AT-rich sequence promoters, comprising seven to nine nucleotides (ARNTTAANA, AATGACA and GTNGATAYR), located at 150-nt upstream of the translation start codon of many ORFs were observed [85]. The 'ARNTTAANA' sequence is found between nucleotides -15 and -45 relative to the ATG translation start codon. This sequence occurs in the promoter region of 25% of PBCV-1 genes, 22% of NY-2A genes and 12% of MT325 genes. Regarding the entire genome, this sequence is present within the 200-nt promoter region during 44% of the time in PBCV-1, 49% of the time in NY-2A, and 37% of the time in MT325. The hotspot for the presence of the 'AATGACA' sequence is located between nucleotides -60 and -90 from the translational start codon. This sequence occurs in the promoter region of 16% of the PBCV-1 genes, 18% of NY-2A genes and 8% of MT325 genes. Regarding the entire genome, this sequence is present within the 200-nt promoter region in 54% of the PBCV-1 genes, 53% of the NY-2A genes, and 25% of the MT325 genes [85].

The 'AATGACA' sequence in PBCV-1 is associated with early genes during the replication cycle [85]. This sequence is very similar to a motif previously identified in some chlorella viruses (ATGACAA), which is also correlated with early transcripts [78]. Finally, the 'GTNGATAYR' sequence is mainly located at nucleotide positions –50 to –80 from the ATG initiation codon, occurring in the promoter region of 13% of PBCV-1 genes, 14% NY-2A genes, and in 11% of MT325 genes. Regarding the entire genome, this sequence is found specifically within the 200-nt promoter region in 28% of the PBCV-1 genes, 22% of the NY-2A genes, and 21% of the MT325 genes [85].

Unlike other members of the NCLDVs, phycodnaviruses do not encode their own RNA pol and need to appropriate the host's RNA pol to properly make their transcripts [86]. However, uniquely for the *Phycodnaviridae* family, *Emiliana huxleyi virus 86* (EhV-86), a coccolithovirus that infects the marine calcifying microalga *Emiliana huxleyi*, contains a total of six RNA pol subunits, which suggests that this virus partially encodes its own transcription machinery [87]. Although these viruses present some important elements for the mRNA synthesis, it is not possible to state that they have their own transcriptional complete apparatus, at least for the majority of them. Therefore, concerning the transcriptional process, the phycodnaviruses seem to present a different evolutionary history.

6. Iridoviridae

The *Iridoviridae* family is composed by five genera: *Ranavirus*, *Megalocytivirus* and *Lymphocystivirus* that infect vertebrates; *Iridovirus* and *Chloriridovirus* that infect invertebrates [88]. Iridoviruses have a linear dsDNA genome varying from 105 to 212 kbp, coding between 92 and 211 putative proteins. They present a non-enveloped icosahedral particle of 300 nm in size [89–92]. These large viruses also display a pattern of temporal gene expression regulation, wherein the genes are divided into three classes: immediate-early (IE or α), delayed-early (DE or β), and late (L or γ) genes [93–95]. Iridoviruses are typical nucleo-cytoplasmic viruses. They begin the replication cycle in the nucleus, followed by the second phase of genome replication in the cytoplasm [90].

Gene transcription and promoter sequences studies have been performed for only a few genes in members of the *Iridoviridae* family. The study of promoter sequences in iridovirus is focused mainly in the *Ranavirus* genus (using type species *Frog virus 3* (FV3)) and *Iridovirus* genus (using type species *Invertebrate iridescent virus 6* (IIV-6)), the type species of the *Iridovirus* genus. Notwithstanding, both the gene expression and promoter sequences studies have been performed for only a few genes in the *Iridoviridae* family. The most complex studies were performed with immediate-early *ICR-169* and *ICR-489* genes of FV3 [96,97]. Those studies revealed the importance of a 78 bp sequence before the transcription start site of an IE gene of the FV3 promoter. It was shown that an FV3 protein acts in trans to induce the transcription of the major FV3 IE gene, *ICR-169*, and is dependent on the 78 bp sequence located at the 5' position from the start site of the transcription of this gene [98]. Two years later, the same group demonstrated that a 23 bp sequence was possibly a critical *cis*-regulatory element for the occurrence of FV3 *trans*-activation, since a significant reduction of transcription occurred after its deletion, located at the 5' region, showing the sequence 'ATATCTCACAGGGGAATTGAAAC' [96]. Despite the importance of the approximately 23-nt sequence upstream of the transcription start site in the IE *ICR-169* gene of FV3, this sequence had no similarity with the promoter region of the intermediate gene *ICR489*. This lack of similarity indicated that the contemporary regulation of these two promoters is not controlled by sequences upstream of the start point of transcription [97]. It is worthy to note that in the *ICR489* gene, in an upstream region, 'TATA', 'CAAT', and 'GC' motifs were identified, which are similar to those of typical eukaryotic promoters [97].

Another study analyzed three genes—two early (*ICP-18* and *ICP-46*) and a late one [major capsid protein (MCP)] of *Bohle iridovirus* (another *Ranavirus* member)—looking for conserved regions to be considered as regulatory elements [99]. The authors demonstrated that all gene promoters included sequences located 127 to 281 bases upstream of the transcription initiation site (127 pb or ICB-18, 281 pb for ICP46, and 169 pb for MCP), but also sequences located from 21 to 26 bases downstream of this site (26 bases for *ICP-18*, 21 bases for ICP 46 and 25 bases for MCP) [99].

Moreover, a detailed study conducted in the following years identified an essential 'AAAAT' motif in a DE gene of IIV-6 (*Iridovirus*) [100]. The authors described a sequence of 19 bp (AAAATTGATTATTTGTTTT), located between −19 and −2 relative to the mRNA transcription start site, which is the putative region responsible for promoter activity of the DNAPol gene. Deletions and point mutations in the DNAPol promoter of IIV-6 showed that each of the 5-nt of 'AAAAT' motif located between −19 and −15 were equally essential for promoter activity. Mutations at the downstream side had a lower effect, but the role of individual nucleotides positioned at −14 to −5 was not analyzed in this study [100].

It is noteworthy that the same critical 'AAAAT' motif was found in the 100-nt upstream of the putative translational start codons of several other putative DE IIV-6 genes [91]. In *Invertebrate iridescent virus 3* (IIV-3), many homologues of these genes also presented the 'AAAAT' motif in proximity to their start codon. A great similarity was also found between the region upstream of the DNAPol ORF and the corresponding region in 12 iridovirus genomes [101]. Eight of these genomes showed a similar 'AAAAT' motif in the DNAPol upstream region and three sequenced ranavirus genomes also shared the related 'TAAAT' motif in their DNA pol promoter region, which may indicate a conserved regulation of DE promoter activity in iridoviruses [101].

A study that targeted a IE gene (012L) of IIV-6 showed that the transcription start site is located 30-nt upstream of the ATG translational start codon. Analyzing mutants (produced by deletion), it was established that the intergenic region located between −21 and −10 (GGATCATATT) upstream of the transcription start site comprised the promoter sequence promoter 012L gene. This type of sequence was not observed in upstream regions of other IE genes of IIV-6, such as 468R, 006L and 010R. The 'TATA' and 'CAAT' sequences were also identified in the intergenic region of this gene, as well as sequences similar to the 'AAAAT' motif described to the DNA pol gene, but this sequence had no promoter activity for the 012L, differently than demonstrated for the DNA pol gene. The 037L and 012L genes of IIV-6, both early genes, do not share conserved key promoter motifs. However, DNA pol is considered a DE gene and 012L an IE gene [100,102].

Despite the presence of homologs of RNA pol subunits in the iridoviruses genome, host RNA pol II is required for the synthesis of *Ranavirus* IE transcripts, and it is likely that the same is true from *Iridovirus* IE genes, contrasting to pox- and asfавiruses [103–106]. It has been proposed that the RNA pol subunits found in members of the *Iridoviridae* family are probably involved in the cytoplasmic phase of transcription in later stages of infection [91,107]. Such a paradox may reflect the long co-evolution period that these viruses had been through. It is possible that the ancestor of iridoviruses presented a complete transcription apparatus, but some elements were lost due to the adaptation to a more parasitic lifestyle. Other possibilities are the occurrence of events of horizontal gene transfer (HGT) between the viruses and their hosts. However, the lack of information about such events involving members of the *Iridoviridae* family prevents further insights into this alternative for the evolution of the transcription apparatus of these viruses.

7. Ascoviridae

The *Ascoviridae* family has two genera that include *Ascovirus*, with three species including *Spodoptera frugiperda ascovirus 1a* (SfAV-1a), the prototype of the genus, *Trichoplusia ni ascovirus 2a* (TnAV-2a), and *Heliothis virescens ascovirus 3a* (HvAV-3a), and the *Toursvirus* genus, with only one representative, *Diadromus pulchellus ascovirus 4a* (DpAV-4a) [108,109]. Ascoviruses are enveloped viruses, 300–400 nm long by 100–150 nm in diameter, with a circular dsDNA genome with sizes ranging from 116 to 185 kb, infecting arthropods, mainly lepidopterans [110–112].

The studies regarding the ascoviruses are still in their infancy. Information about the replication and more specifically, the transcription process, are extremely scarce. The current knowledge about transcription in ascoviruses come from the analyses of the *Ascovirus* genus [110,113]. A study performed using a possible variant of HvAV-3, the *Spodoptera exigua ascovirus 5a* (SeAV-5a) showed that the 5'-UTR region of the SeAV-5a MCP gene is composed of 25-nt [114]. The upstream region

of this gene does not present a typical eukaryotic class II promoter motif sequence ‘TATAAAT’ (TATA box). However, the putative 5’ transcription control region of the SeAV-5a MCP gene shares similarities with other ascoviruses and iridoviruses, containing a conserved TATA-box like motif (TAATTAAA) and an ‘ATTTGATCTT’ motif within 40-nt upstream of the translation initiation codon ATG [114]. The ‘TAATTAAA’ and ‘ATTTGATCTT’ motifs are located downstream and upstream of the transcription initiation site, respectively. Furthermore, the ORF p27 presents a similar 5’ downstream transcription promoter region, suggesting that such a region might be a truly regulatory sequence within ascoviruses [114].

Sequences from the promoter regions of the MCP genes from ascoviruses and IIV-6 (late genes), showed that ascoviruses and iridoviruses are closely related in this aspect, suggesting that the transcription regulation could be maintained during the viral evolution process in closely related viruses [115,116]. Furthermore, phylogenetic studies showed that ascoviruses probably evolved from the iridoviruses [116–118]. It is possible that the same pattern of temporary gene expression exhibited in iridoviruses (and the other members of proposed Megavirales order) was conserved in the ascoviruses lineage, and that such a mechanism might have been present in their common ancestor.

8. Mimiviridae and Other Amoebal Giant Viruses

The discovery of mimiviruses in 2003 and the establishment of the *Mimiviridae* family astonished the scientific community, making the term ‘giant virus’ more appropriated than ever. These viruses have particles visible in light microscopy, with sizes of ~700 nm in diameter. Viral particles have characteristics never described before in the virosphere, such as long proteic fibrils (~125 nm in length) immersed in a peptidoglycan matrix, and a star-shaped face, named stargate, responsible for the releasing of the genome inside the cytoplasm of their host (*Acanthamoeba* genus) [4,119–121]. The genome is a linear dsDNA molecule of about 1.2 Mbp, coding more than 1000 proteins, including a large set of transcriptional elements [15,122].

Similar to other NCLDV members, mimiviruses genes can be divided into early, intermediate and late categories according to three major temporal classes of transcription determined by mRNA deep sequencing [49]. The analysis of the intergenic regions of *Acanthamoeba polyphaga mimivirus*, the prototype species of *Mimivirus* genus, showed a conserved ‘AAAATTGA’ motif in nearly 50% of genes [50]. The intergenic regions of the genome of mimiviruses have an average size of 157-nt. In silico analyses showed that the conserved ‘AAAATTGA’ motifs are present within the 150-nt upstream regions of the translation start codon in 45% of all predicted mimivirus genes [50]. This motif is mainly associated to early (or the late-early) genes during the viral infectious cycle, and it is absent from the upstream regions of mimivirus late genes, such as DNA replication and particle morphogenesis and assembly. It is noteworthy that similar sequences were described regulating the early genes in other giant viruses, such as iridoviruses and phycodnaviruses, as described in the topics above. Besides the early promoter sequence, another A/T-rich motif (two 10-nt informative segments separated by a highly degenerated 4-nt sequence) was identified as a putative late promoter within mimiviruses, which is present in 24.2% of the considered late class genes. To the best of our knowledge, an intermediate promoter sequence has not already been described in mimiviruses [49,50].

In a distant relative, the *Cafeteria roenbergensis virus* [CroV (*Cafeteria* genus)], *Mimiviridae* family; the same early promoter motif was identified in the upstream region of 35% of genes [123]. However, considering the late promoter motif, this virus exhibits a different putative regulatory sequence compared to other mimiviruses, wherein the ‘TCTA’ tetramer flanked by A/T-rich regions on either side was found in the 5’ upstream of 124 late genes [123]. Moreover, CroV present eight RNA pol II subunits, six transcription factors, several helicases, among others, indicating the presence of nearly complete transcriptional machinery. This feature seems to be a mark to all members of the *Mimiviridae* family, which suggests that such a robust transcriptional apparatus was already present in the last common ancestor.

After the discovery of mimiviruses, other giant viruses infecting amoebae were described, such as marseilleviruses, which is currently classified in the family *Marseilleviridae* [124]. Other viruses have also been isolated but still not properly classified, namely faustoviruses [125], pandoraviruses [8,126], phitoviruses [127,128] and mollivirus [129]. Although these viruses are not yet officially recognized by the ICTV, they are genuine members of the NCLDVs [6,7,9]. In all of these giant viruses, a set of transcriptional elements has already been identified, including many RNA pol subunits, indicating a nearly autonomous process in these viruses. However, analysis of promoters and studies aiming to understand how gene expression is regulated in those newly discovered viruses remain to be performed.

9. MEGA-Box: A Putative Promoter Region in the Common Ancestor of Megavirales

The proposed Megavirales order comprises viral families that exhibit some unique features that allow their clustering into a monophyletic group [5]. In addition to some core genes that are shared among these viruses, they present other similarities, such as a temporal transcription profile. As described above, all viruses present elements to the transcriptional apparatus, most of them reaching up to the independence from their host in this step of the viral life cycle. Also, the presence of an A/T-rich promoter sequence has been described in many representatives of each family, even in those in which the genome presents a high G/C content. More interesting is the fact that some promoter sequences found in one family are very similar to others found in their relatives (Figure 3). This fact suggests that a possible common ancestor of the Megavirales order likely had an A/T-rich promoter sequence. More interesting is the fact that some promoter sequences found in one family are very similar to others found in their giant relatives. This fact suggests that such a common ancestor of Megavirales likely had an A/T-rich promoter sequence.

The origin of the members of the Megavirales order is still under debate, but the evolutionary history of some of its members is already being told, at least concerning genome evolution. The first members to be analyzed were the poxviruses. It has been demonstrated by phylogenetic analysis based on the presence/absence of genes that genomes from this family have been subject to frequent events of gene duplication, deletion, and HGT from their hosts. Many of these genes can interfere with host immune signaling, such as homologues of cytokines receptors which could confer some advantages in the interaction with the hosts [130–132]. By analyzing the poxviruses' closest relative, ASFV, it seems that it has been through the same pattern of evolution, at least considering the multigene and p22 gene families [133,134].

The “accordion-like” pattern of evolution was also identified in different members of the *Iridoviridae* family. It is particularly interesting the fact that iridoviruses infecting the same host-range exhibited a similar pattern of gene gain and loss, but this was slightly different when the viruses infected different hosts (fish vs. insect-infecting viruses), suggesting that such a pattern was driven by host–virus co-evolution [135]. Finally, the same evolutionary model for members of the families *Phycodnaviridae* and *Mimiviridae* has recently been described. The genomic comparisons of closely related viruses belonging to the *Mimiviridae* and *Phycodnaviridae* families show that genomes accumulating genomic mutations occur on successive cycles of genome expansion and reduction. In addition, there is no general tendency of genome expansion or contraction. Each family exhibits a specific pattern for gene acquisition, which might be a reflex of interaction with distinct hosts [10]. Since these viruses seem to exhibit a similar pattern of genome evolution, it is possible that a similar scenario has also happened with their promoter sequences. In the same way, it is reasonable to consider that NCLDVs' common ancestor evolved by the same “accordion-like” pattern, and thus it presented a promoter region that underwent an analogous mechanism.

Considering a common origin for the NCLDVs, a possible scenario is that the Megavirales' common ancestor presented a ‘TATATAAAATTGA’ promoter motif, which we named here as the “MEGA-box” (an allusion to the conserved TATA-box promoter found in cellular organisms). Over time, with the Megavirales' order radiation, the MEGA-box has been gradually evolved by nucleotides'

gain and loss, analogously to that reported for the entire genome, which evolved through gene gain and loss. The MEGA-box was slightly modified in the poxviruses lineage, at least concerning the early promoter motif. Considering the intermediate and the late promoter motifs of poxviruses, if they truly came from the MEGA-box, this could have happened through a series of nucleotide loss. However, it is also possible that the emergence of other promoters, rather than the early one, have emerged after the establishment of the poxvirus' lineage, thus not originating from the ancestral promoter sequence. The same might be true for mimiviruses, phycodnaviruses and iridoviruses. Considering asfavirus and ascoviruses, their promoter sequences might have originated from the MEGA-box through successive gain and loss of nucleotides. However, another scenario is also possible, wherein their promoter motifs emerged from the poxviruses and iridoviruses lineages respectively (closest evolutionary groups). This scenario is in agreement with the proposition that the Megavirales' ancestor was already a giant virus with a large genome [10]. In this aspect, the giant ancestor also had a large promoter sequence that evolved through constant nucleotide gain and loss, a pattern analogous to the accordion-like model of genome evolution. However, other scenarios are also possible, although less probable, considering the evolutionary data currently available for these viruses. One is that the ancestor had a very short promoter sequence, like a poxvirus intermediate promoter (TAAA), that underwent massive nucleotide gain over time, leading to very large promoter sequences in the majority of the giant viruses. Another one is just the opposite; wherein the ancestor had a very large promoter region that had been losing nucleotides during evolution. A third pathway, equally unlikely, would be the acquisition of promoter sequences by horizontal/lateral transfer. Similar to different genes, the MEGA-box promoter evolutionary pattern during the radiation of NCLDV members could be related to the co-evolution with different hosts over time.

Whether the NCLDVs came from a simple entity [14,136], or from an already complex organism [10,16,137], is still under debate. Despite this, increasing evidence that they originated from a common ancestor is emerging, and it suggests that such an ancestor evolved through an "accordion-like" pattern. By analyzing the promoter regions currently known for different giant viruses, we provide another piece of evidence to support this statement. Further, we propose how a conserved A/T-rich promoter sequence was present in the possible common ancestor, which might have evolved by continuous gain and loss of nucleotides, in addition to some point mutations in the MEGA-box original sequence. Other scenarios could also be discussed for the evolution of the promoter sequences of the NCLDVs, including selective sweep or convergence. However, these alternatives run off the diffused hypothesis of a common origin for the putative Megavirales order.

10. What Comes Next?

Most of the giant viruses have a powerful genetic arsenal, encoding several proteins necessary for the transcription system which provides a relative independence of their hosts for this process. In addition, the transcription of this high gene content is temporally regulated by promoter regions that exhibit some similarities, indicating a common origin of these regulatory elements. Although many studies have already been done in relation to almost all viral families of the Megavirales order, most of them remain without biological confirmation; i.e., the promoter motifs in many giant viruses were predicted, but not experimentally validated. Therefore, the performance of biological studies to confirm the existence and the effect of all promoter motifs described so far in giant viruses is imperative. This analysis will truly establish the common temporal regulation pattern predicted in these viruses, and will also corroborate (or even refute) the hypothesis of an A/T-rich promoter in the Megavirales common ancestor. Moreover, the deep analysis of the genome of the recently described giant viruses (Marseilleviruses, Pandoraviruses, Pithoviruses, Faustoviruses and Mollivirus), and also the discovery of new complex viruses, will strongly contribute to complete the puzzle of the origin and evolution of Megavirales.

On the other hand, the biotechnology field will also be boosted by the advance in the studies of promoters and gene expression in giant viruses. Among the NCLDVs, the poxviruses are by far the best

characterized group regarding the genome expression, especially the VACV. These viruses have been used as expression vectors for the synthesis of proteins and as vaccine candidates to prevent infectious diseases and treat cancer, mainly due to their high gene expression levels [69,138]. This attribute is clearly shared with other giant viruses that were recently described, and the real comprehension of their gene regulation and expression will bring uncountable possibilities for biotechnology purposes. Finally, the impact of the giant viruses on the basic comprehension of the origin and evolution of life is undeniable, as well as for their ecological, medical and technological importance. The discovery of even more complex viruses associated with the advance of many techniques used for genomic studies will certainly answer those remaining questions around the NCLDVs, and will surely bring new exciting challenges for the whole scientific community.

Acknowledgments: We would like to thank our colleagues from GEPVIG (Grupo de Estudo e Prospecção de Vírus Gigantes) and Laboratório de Vírus of Universidade Federal de Minas Gerais. In addition, CNPq (Conselho Nacional de Desenvolvimento Científico e Tecnológico), CAPES (Coordenação de Aperfeiçoamento de Pessoal de Nível Superior) and FAPEMIG (Fundação de Amparo à Pesquisa do estado de Minas Gerais). G.S.T., E.G.K. and J.S.A. are CNPq researchers. B.L.S., J.S.A. and E.G.K. are members of a CAPES-COFECUB project.

Author Contributions: G.P.O.; A.C.S.P.A.; R.A.L.R.; T.S.A.; P.V.M.B.; L.K.S.S. and F.P.D. wrote the paper. B.P.D., G.S.T., B.L.S., E.G.K. and J.S.A. approved and reviewed the final version.

Conflicts of Interest: The authors declare no conflict of interest.

References

1. Lwoff, A. The concept of virus. *J. Gen. Microbiol.* **1957**, *17*, 239–253. [[CrossRef](#)] [[PubMed](#)]
2. Durzyńska, J.; Goździcka-Józefiak, A. Viruses and cells intertwined since the dawn of evolution. *Virol. J.* **2015**, *16*, 169. [[CrossRef](#)] [[PubMed](#)]
3. Iyer, L.M.; Aravind, L.; Koonin, E.V. Common origin of four diverse families of large eukaryotic DNA viruses. *J. Virol.* **2001**, *75*, 11720. [[CrossRef](#)] [[PubMed](#)]
4. La Scola, B.; Audic, S.; Robert, C.; Jungang, L.; de Lamballerie, X.; Drancourt, M.; Birtles, R.; Claverie, J.M.; Raoult, D. A giant virus in amoebae. *Science* **2003**, *299*. [[CrossRef](#)] [[PubMed](#)]
5. Colson, P.; de Lamballerie, X.; Fournous, G.; Raoult, D. Reclassification of giant viruses composing a fourth domain of life in the new order Megavirales. *Intervirology* **2012**, *55*, 321–332. [[CrossRef](#)] [[PubMed](#)]
6. Sharma, V.; Colson, P.; Chabrol, O.; Pontarotti, P.; Raoult, D. *Pithovirus sibericum*, a new bona fide member of the “Fourth TRUC” club. *Front. Microbiol.* **2015**, *4*, 722. [[CrossRef](#)] [[PubMed](#)]
7. Sharma, V.; Colson, P.; Chabrol, O.; Scheid, P.; Pontarotti, P.; Raoult, D. Welcome to pandoraviruses at the “Fourth TRUC” club. *Front. Microbiol.* **2015**, *18*, 423.
8. Scheid, P. A strange endocytobiont revealed as largest virus. *Curr. Opin. Microbiol.* **2016**, *31*, 58–62. [[CrossRef](#)] [[PubMed](#)]
9. Benamar, S.; Reteno, D.G.; Bandaly, V.; Labas, N.; Raoult, D.; la Scola, B. Faustoviruses: Comparative genomics of new Megavirales family members. *Front. Microbiol.* **2016**, *5*, 3. [[CrossRef](#)] [[PubMed](#)]
10. Filée, J. Genomic comparison of closely related Giant Viruses supports an accordion-like model of evolution. *Front. Microbiol.* **2015**, *16*, 593. [[CrossRef](#)] [[PubMed](#)]
11. Suzan-Monti, M.; la Scola, B.; Raoult, D. Genomic and evolutionary aspects of Mimivirus. *Virus Res.* **2006**, *117*, 145–155. [[CrossRef](#)] [[PubMed](#)]
12. Claverie, J.M. Viruses take center stage in cellular evolution. *Genome Biol.* **2006**, *7*, 110. [[CrossRef](#)] [[PubMed](#)]
13. Moreira, D.; López-García, P. Comment on “The 1.2-megabase genome sequence of Mimivirus”. *Science* **2005**, *20*, 1114. [[CrossRef](#)] [[PubMed](#)]
14. Yutin, N.; Wolf, Y.I.; Koonin, E.V. Origin of giant viruses from smaller DNA viruses not from a fourth domain of cellular life. *Virology* **2014**, *38–52*, 466–467. [[CrossRef](#)] [[PubMed](#)]
15. Raoult, D.; Audic, S.; Robert, C.; Abergel, C.; Renesto, P.; Ogata, H.; la Scola, B.; Suzan, M.; Claverie, J.M. The 1.2-megabase genome sequence of Mimivirus. *Science* **2004**, *306*, 1344–1350. [[CrossRef](#)] [[PubMed](#)]
16. Boyer, M.; Madoui, M.A.; Gimenez, G.; La Scola, B.; Raoult, D. Phylogenetic and phyletic studies of informational genes in genomes highlight existence of a 4 domain of life including giant viruses. *PLoS ONE* **2010**, *2*, e15530. [[CrossRef](#)] [[PubMed](#)]

17. Schones, D.E.; Cui, K.; Cuddapah, S.; Roh, T.-Y.; Barski, A.; Wang, Z.; Wei, G.; Zhao, K. Dynamic regulation of nucleosome positioning in the human genome. *Cell* **2008**, *132*, 887–898. [[CrossRef](#)] [[PubMed](#)]
18. Fuda, N.J.; Ardehali, M.B.; Lis, J.T. Defining mechanisms that regulate RNA polymerase II transcription in vivo. *Nature* **2009**, *10*, 186–192. [[CrossRef](#)] [[PubMed](#)]
19. Lacadie, S.A.; Ibrahim, M.M.; Gokhale, S.A.; Ohler, U. Divergent transcription and epigenetic directionality of human promoters. *FEBS J.* **2016**, *283*, 4214–4222. [[CrossRef](#)] [[PubMed](#)]
20. Haberle, V.; Lenhard, B. Promoter architectures and developmental gene regulation. *Semin. Cell Dev. Biol.* **2016**, *57*, 11–23. [[CrossRef](#)] [[PubMed](#)]
21. Weiss, S.; Gladstone, L. A mammalian system for the incorporation of cytidine triphosphate into ribonucleic acid. *J. Am. Chem. Soc.* **1959**, *81*, 4118–4119. [[CrossRef](#)]
22. Thomas, M.C.; Chiang, C.M. The general transcription machinery and general cofactors. *Crit. Rev. Biochem. Mol. Biol.* **2006**, *41*, 105–178. [[CrossRef](#)] [[PubMed](#)]
23. Sabin, L.R.; Delás, M.J.; Hannon, G.J. Dogma derailed: The many influences of RNA on the genome. *Mol. Cell* **2013**, *49*, 783–794. [[CrossRef](#)] [[PubMed](#)]
24. Vannini, A.; Ringel, R.; Kusser, A.G.; Berninghausen, O.; Kassavetis, G.A.; Cramer, P. Molecular basis of RNA polymerase III transcription repression by Maf1. *Cell* **2010**, *143*, 59–70. [[CrossRef](#)] [[PubMed](#)]
25. Carninci, P.; Sandelin, A.; Lenhard, B.; Katayama, S.; Shimokawa, K.; Ponjavic, J.; Semple, C.A.; Taylor, M.S.; Engström, P.G.; Frith, M.C. Genome-wide analysis of mammalian promoter architecture and evolution. *Nat. Genet.* **2006**, *38*, 626–635. [[CrossRef](#)] [[PubMed](#)]
26. Cooper, S.J.; Trinklein, N.D.; Anton, E.D.; Nguyen, L.; Myers, R.M. Comprehensive analysis of transcriptional promoter structure and function in 1% of the human genome. *Genome Res.* **2006**, *16*, 1–10. [[CrossRef](#)] [[PubMed](#)]
27. Smale, S.T.; Kadonaga, J.T. The RNA polymerase II core promoter. *Annu. Rev. Biochem.* **2003**, *72*, 449–479. [[CrossRef](#)] [[PubMed](#)]
28. Maston, G.A.; Evans, S.K.; Green, M.R. Transcriptional regulatory elements in the human genome. *Annu. Rev. Genom. Hum. Genet.* **2006**, *7*, 29–59. [[CrossRef](#)] [[PubMed](#)]
29. Hansen, S.K.; Tjian, R. TAFs and TFIIA mediate differential utilization of the tandem Adh promoters. *Cell* **1995**, *82*, 565–575. [[CrossRef](#)]
30. Ren, B.; Maniatis, T. Regulation of Drosophila Adh promoter switching by an initiator-targeted repression mechanism. *EMBO J.* **1998**, *17*, 1076–1086. [[CrossRef](#)] [[PubMed](#)]
31. Browning, D.F.; Busby, S.J. Local and global regulation of transcription initiation in bacteria. *Nat. Rev. Microbiol.* **2016**, *14*, 638–650. [[CrossRef](#)] [[PubMed](#)]
32. Burgess, R.R.; Travers, A.A.; Dunn, J.J.; Bautz, E.K. Factor stimulating transcription by RNA polymerase. *Nature* **1969**, *221*, 43–46. [[CrossRef](#)] [[PubMed](#)]
33. Lee, D.J.; Minchin, S.D.; Busby, S.J. Activating transcription in bacteria. *Annu. Rev. Microbiol.* **2012**, *66*, 125–152. [[CrossRef](#)] [[PubMed](#)]
34. Murakami, K.S.; Masuda, S.; Campbell, E.A.; Muzzin, O.; Darst, S.A. Structural basis of transcription initiation: An RNA polymerase holoenzyme–DNA complex. *Science* **2002**, *296*, 1285–1290. [[CrossRef](#)] [[PubMed](#)]
35. Browning, D.F.; Busby, S.J. The regulation of bacterial transcription initiation. *Nat. Rev. Microbiol.* **2004**, *2*, 57–65. [[CrossRef](#)] [[PubMed](#)]
36. Hausner, W.; Wettach, J.; Hethke, C.; Thomm, M. Two transcription factors related with the eucaryal transcription factors TATA binding protein and transcription factor IIB direct promoter recognition by an archaeal RNA polymerase. *J. Biol. Chem.* **1996**, *271*, 30144–30148. [[CrossRef](#)] [[PubMed](#)]
37. Bell, S.D.; Jaxel, C.; Nadal, M.; Kosa, P.F.; Jackson, S.P. Temperature template topology, and factor requirements of archaeal transcription. *Proc. Natl. Acad. Sci. USA* **1998**, *95*, 15218–15222. [[CrossRef](#)] [[PubMed](#)]
38. Darcy, T.J.; Hausner, W.; Awery, D.E.; Edwards, A.M.; Thomm, M.; Reeve, J.N. Methanobacterium thermoautotrophicum RNA polymerase and transcription in vitro. *J. Bacteriol.* **1999**, *181*, 4424–4429. [[PubMed](#)]
39. Reiter, W.D.; Hudspohl, U.; Zillig, W. Mutational analysis of an archae bacterial promoter—Essential role of a TATA Box for transcription efficiency and start-site selection in vitro. *Proc. Natl. Acad. Sci. USA* **1990**, *87*, 9509–9513. [[CrossRef](#)] [[PubMed](#)]

40. Palmer, J.R.; Daniels, C.J. In vivo definition of an archaeal promoter. *J. Bact.* **1995**, *177*, 1844–1849. [[CrossRef](#)] [[PubMed](#)]
41. Kyrpides, N.C.; Ouzounis, C.A. Transcription in Archaea. *Proc. Natl. Acad. Sci. USA* **1999**, *96*, 8545–8550. [[CrossRef](#)] [[PubMed](#)]
42. Aravind, L.; Koonin, E.V. DNA-binding proteins and evolution of transcription regulation in the Archaea. *Nucleic Acids Res.* **1999**, *27*, 4658–4670. [[CrossRef](#)] [[PubMed](#)]
43. Bell, S.D.; Jackson, S.P. Mechanism and regulation of transcription in Archaea. *Curr. Opin. Microbiol.* **2001**, *4*, 208–213. [[CrossRef](#)]
44. Werner, F.; Grohmann, D. Evolution of multisubunit RNA polymerases in the three domains of life. *Nat. Rev. Microbiol.* **2011**, *9*, 85–98. [[CrossRef](#)] [[PubMed](#)]
45. Whelan, S. Viral Replication Strategies. In *Fields Virology*, 6th ed.; Knipe, D.M., Howley, P.M., Eds.; Lippincott, Williams and Wilkins: Philadelphia, PA, USA, 2014; Volume 2, p. 2160.
46. Abergel, C.; Rudinger-Thirion, J.; Giege, R.; Claverie, J.M. Virus-encoded aminoacyl-tRNA synthetases: Structural and functional characterization of mimivirus TyrRS and MetRS. *J. Virol.* **2007**, *81*, 12406–12417. [[CrossRef](#)] [[PubMed](#)]
47. Broyles, S.S.; Knutson, B.A. Poxvirus transcription. *Future Virol.* **2010**, *5*, 639–650. [[CrossRef](#)]
48. Moss, B. Poxviridae. In *Fields Virology*, 6th ed.; Knipe, D.M., Howley, P.M., Eds.; Lippincott, Williams and Wilkins: Philadelphia, PA, USA, 2014; Volume 2, p. 2129.
49. Legendre, M.; Audic, S.; Poirot, O.; Hingamp, P.; Seltzer, V.; Byrne, D.; Lartigue, A.; Lescot, M.; Bernadac, A.; Poulain, J.; et al. mRNA deep sequencing reveals 75 new genes and a complex transcriptional landscape in Mimivirus. *Genome Res.* **2010**, *20*, 664–674. [[CrossRef](#)] [[PubMed](#)]
50. Suhre, K.; Audic, S.; Claverie, J.M. Mimivirus gene promoters exhibit an unprecedented conservation among all eukaryotes. *Proc. Natl. Acad. Sci. USA* **2005**, *102*, 14689–14693. [[CrossRef](#)] [[PubMed](#)]
51. Damon, I.K. Poxviruses. In *Fields Virology*, 6th ed.; Knipe, D.M., Howley, P.M., Eds.; Lippincott, Williams and Wilkins: Philadelphia, PA, USA, 2014; Volume 2, p. 2160.
52. Baroudy, B.M.; Moss, B. Purification and characterization of a DNA dependent RNA polymerase from vaccinia virions. *J. Biol. Chem.* **1980**, *255*, 4372–4380. [[PubMed](#)]
53. Knutson, B.A.; Broyles, S.S. Expansion of poxvirus RNA polymerase subunits sharing homology with corresponding subunits of RNA polymerase II. *Virus Genes* **2008**, *36*, 307–311. [[CrossRef](#)] [[PubMed](#)]
54. Davison, A.J.; Moss, B. The structure of vaccinia virus early promoters. *J. Mol. Biol.* **1989**, *210*, 749–769. [[CrossRef](#)]
55. Baldick, C.J.; Keck, J.G.; Moss, B. Mutational analysis of the core, spacer and initiator regions of vaccinia virus intermediate class promoters. *J. Virol.* **1992**, *66*, 4710–4719. [[PubMed](#)]
56. Knutson, B.A.; Liu, X.; Oh, J. Vaccinia virus intermediate and late promoter elements are targeted by the TATA-binding protein. *J. Virol.* **2006**, *80*, 6784–6793. [[CrossRef](#)] [[PubMed](#)]
57. Yang, Z.; Bruno, D.P.; Martens, C.A.; Porcella, S.F.; Moss, B. Genome-wide analysis of the 5' and 3' ends of vaccinia virus early mRNAs delineates regulatory sequences of annotated and anomalous transcripts. *J. Virol.* **2011**, *85*, 5897–5909. [[CrossRef](#)] [[PubMed](#)]
58. Keck, J.G.; Baldick, C.J.; Moss, B. Role of DNA replication in vaccinia virus gene expression: A naked template is required for transcription of three late transactivator genes. *Cell* **1990**, *61*, 801–809. [[CrossRef](#)]
59. Yang, Z.; Reynolds, S.E.; Martens, C.A.; Bruno, D.P.; Porcella, S.F.; Moss, B. Expression profiling of the intermediate and late stages of poxvirus replication. *J. Virol.* **2011**, *85*, 9899–9908. [[CrossRef](#)] [[PubMed](#)]
60. Yang, Z.; Martens, C.A.; Bruno, D.P.; Porcella, S.F.; Moss, B. Pervasive initiation and 3'-end formation of poxvirus postreplicative RNAs. *J. Biol. Chem.* **2012**, *287*, 31050–31060. [[CrossRef](#)] [[PubMed](#)]
61. Broyles, S.S.; Liu, X.; Zhu, M.; Kremer, M. Transcription factor YY1 is a vaccinia virus late promoter activator. *J. Biol. Chem.* **1999**, *274*, 35662–35667. [[CrossRef](#)] [[PubMed](#)]
62. Hänggi, M.; Bannwarth, W.; Stunnenberg, H.G. Conserved TAAAT motif in vaccinia virus late promoters: Overlapping TATA box and site of transcription initiation. *EMBO J.* **1986**, *5*, 1071–1076. [[PubMed](#)]
63. International Committee on Taxonomy of Viruses. Available online: http://www.ictvonline.org/taxonomyHistory.asp?taxnode_id=20151927&taxa_name=Asfarviridae (accessed on 22 September 2016).
64. Sogo, J.M.; Almendral, J.M.; Talavera, A.; Vinuela, E. Terminal and internal inverted repetitions in African swine fever virus DNA. *Virology* **1984**, *133*, 271–275. [[CrossRef](#)]

65. Tulman, E.R.; Delhon, G.A.; Ku, B.K.; Rock, D.L. African swine fever virus. *Curr. Top. Microbiol. Immunol.* **2009**, *328*, 43–87. [PubMed]
66. Kuznar, J.; Salas, M.L.; Vinuela, E. DNA-dependent RNA polymerase in African swine fever virus. *Virology* **1980**, *101*, 169–175. [CrossRef]
67. Salas, J.; Salas, M.L.; Vinuela, E. Effect of inhibitors of the host cell RNA polymerase II on African swine fever virus multiplication. *Virology* **1988**, *164*, 280–283. [CrossRef]
68. Rodríguez, J.M.; Salas, M.L. African swine fever virus transcription. *Virus Res.* **2013**, *173*, 15–28. [CrossRef] [PubMed]
69. Moss, B. Genetically engineered poxviruses for recombinant gene expression, vaccination, and safety. *Proc. Natl. Acad. Sci. USA* **1996**, *15*, 11341–11348. [CrossRef]
70. Rodríguez, J.M.; Salas, M.L.; Vinuela, E. Intermediate class of mRNAs in African swine fever virus. *J. Virol.* **1996**, *70*, 8584–8589. [PubMed]
71. Garcia-Escudero, R.; Vinuela, E. Structure of African swine fever virus late promoters: Requirement of a TATA sequence at the initiation region. *J. Virol.* **2000**, *74*, 8176–8182. [CrossRef] [PubMed]
72. Yates, P.R.; Dixon, L.K.; Turner, P.C. Promoter analysis of an African swine fever virus gene encoding a putative elongation factor. *Biochem. Soc. Trans.* **1995**, *23*, 1395. [CrossRef]
73. Van Etten, J.L.; Graves, M.V.; Müller, D.G.; Boland, W.; Delaroque, N. Phycodnaviridae—Large DNA algal viruses. *Arch. Virol.* **2002**, *147*, 1479–1516. [CrossRef] [PubMed]
74. Van Etten, J.L.; Meints, R.H. Giant viruses infecting algae. *Annu. Rev. Microbiol.* **1999**, *53*, 447–494. [CrossRef] [PubMed]
75. Wilson, W.H.; van Etten, J.L.; Allen, M.J. The *Phycodnaviridae*: The story of how tiny giants rule the world. *Curr. Top. Microbiol. Immunol.* **2009**, *328*, 1–42. [PubMed]
76. International Committee on Taxonomy of Viruses. Available online: http://www.ictvonline.org/taxonomyHistory.asp?taxnode_id=20153552&taxa_name=Phycodnaviridae (accessed on 22 September 2016).
77. Kang, M.; Graves, M.; Mehmel, M.; Moroni, A.; Gazzarrini, S.; Thiel, G.; Gurnon, J.R.; van Etten, J.L. Genetic diversity in chlorella viruses flanking *kcv*, a gene that encodes a potassium ion channel protein. *Virology* **2004**, *326*, 150–159. [CrossRef] [PubMed]
78. Kawasaki, T.; Tanaka, M.; Fujie, M.; Usami, S.; Yamada, T. Immediate early genes expressed in chlorovirus infections. *Virology* **2004**, *318*, 214–223. [CrossRef] [PubMed]
79. Chuchird, N.; Nishida, K.; Kawasaki, T.; Fujie, M.; Usami, S.; Yamada, T. A variable region on the chlorovirus CVK2 genome contains five copies of the gene for Vp260, a viral-surface glycoprotein. *Virology* **2002**, *10*, 289–298. [CrossRef] [PubMed]
80. Yamada, T.; Hiramatsu, S.; Songsri, P.; Fujie, M. Alternative expression of a chitosanase gene produces two different proteins in cells infected with Chlorella virus CVK2. *Virology* **1997**, *14*, 361–368. [CrossRef] [PubMed]
81. Graves, M.V.; Meints, R.H. Characterization of the major capsid protein and cloning of its gene from algal virus PBCV-1. *Virology* **1992**, *188*, 198–207. [CrossRef]
82. Sugimoto, I.; Hiramatsu, S.; Murakami, D.; Fujie, M.; Usami, S.; Yamada, T. Algal-lytic activities encoded by Chlorella virus CVK2. *Virology* **2000**, *10*, 119–126. [CrossRef] [PubMed]
83. Fitzgerald, L.A.; Graves, M.V.; Li, X.; Feldblyum, T.; Hartigan, J.; van Etten, J.L. Sequence and annotation of the 314-kb MT325 and the 321-kb FR483 viruses that infect Chlorella Pbi. *Virology* **2007**, *20*, 459–471. [CrossRef] [PubMed]
84. Fitzgerald, L.A.; Graves, M.V.; Li, X.; Feldblyum, T.; Nierman, W.C.; van Etten, J.L. Sequence and annotation of the 369-kb NY-2A and the 345-kb AR158 viruses that infect Chlorella NC64A. *Virology* **2007**, *20*, 472–484. [CrossRef] [PubMed]
85. Fitzgerald, L.A.; Boucher, P.T.; Yanai-Balser, G.M.; Suhre, K.; Graves, M.V.; van Etten, J.L. Putative gene promoter sequences in the chlorella viruses. *Virology* **2008**, *25*, 388–393. [CrossRef] [PubMed]
86. Van Etten, J.L. Unusual life style of giant chlorella viruses. *Ann. Rev. Genet.* **2003**, *37*, 153–195. [CrossRef] [PubMed]
87. Wilson, W.H.; Schroeder, D.C.; Allen, M.J.; Holden, M.T.; Parkhill, J.; Barrell, B.G.; Churcher, C.; Hamlin, N.; Mungall, K.; Norbertczak, H.; et al. Complete genome sequence and lytic phase transcription profile of a Coccolithovirus. *Science* **2005**, *12*, 1090–1092. [CrossRef] [PubMed]

88. International Committee on Taxonomy of Viruses. Available online: http://www.ictvonline.org/taxonomyHistory.asp?taxnode_id=20153003&taxa_name=Iridoviridae (accessed on 22 September 2016).
89. Darai, G.; Delius, H.; Clarke, J.; Apfel, H.; Schnitzler, P.; Flugel, R.M. Molecular cloning and physical mapping of the genome of fish lymphocystis disease virus. *Virology* **1985**, *146*, 292–301. [[CrossRef](#)]
90. Williams, T.; Barbosa-Solomieu, V.; Chinchar, V.G. A decade of advances in Iridovirus research. *Adv. Virus Res.* **2005**, *65*, 174–248.
91. Jakob, N.J.; Muller, K.; Bahr, U.; Darai, G. Analysis of the first complete DNA sequence of an invertebrate iridovirus: Coding strategy of the genome of Chilo iridescent virus. *Virology* **2001**, *286*, 182–196. [[CrossRef](#)] [[PubMed](#)]
92. Chinchar, V.G.; Yu, K.H.; Jancovich, J.K. The molecular biology of frog virus 3 and other iridoviruses infecting cold-blooded vertebrates. *Viruses* **2011**, *3*, 1959–1985. [[CrossRef](#)] [[PubMed](#)]
93. Barry, S.; Devauchelle, G. Protein synthesis in cells infected by Chilo iridescent virus: Evidence for temporal control of three classes of induced polypeptides. *Virology* **1987**, *138*, 253–261.
94. D’Costa, S.M.; Yao, H.; Bilimoria, S.L. Transcription and temporal cascade in Chilo iridescent virus infected cells. *Arch. Virol.* **2001**, *146*, 2165–2178. [[CrossRef](#)] [[PubMed](#)]
95. D’Costa, S.M.; Yao, H.J.; Bilimoria, S.L. Transcriptional mapping in Chilo iridescent virus infections. *Arch. Virol.* **2004**, *149*, 723–742. [[CrossRef](#)] [[PubMed](#)]
96. Willis, D.B. DNA sequences required for trans activation of an immediate-early frog virus 3 gene. *Virology* **1987**, *161*, 1–7. [[CrossRef](#)]
97. Beckman, W.; Tham, T.N.; Aubertin, A.M.; Willis, D.B. Structure and regulation of the immediate-early frog virus 3 gene that encodes ICR489. *J. Virol.* **1988**, *62*, 1271–1277. [[PubMed](#)]
98. Willis, D.B.; Granoff, A. Transactivation of an immediate-early frog virus 3 promoter by a virion protein. *J. Virol.* **1985**, *56*, 495–501. [[PubMed](#)]
99. Pallister, J.; Goldie, S.; Coupar, B.; Hyatt, A. Promoter activity in the 59 flanking regions of the Bohle iridovirus ICP 18, ICP 46 and major capsid protein genes. *Arch. Virol.* **2005**, *150*, 1911–1919. [[CrossRef](#)] [[PubMed](#)]
100. Nalcacioglu, R.; Ince, I.A.; Vlak, J.M.; Demirbag, Z.; van Oers, M.M. The Chilo iridescent virus DNA polymerase promoter contains an essential AAAAT motif. *J. Gen. Virol.* **2007**, *88*, 2488–2494. [[CrossRef](#)] [[PubMed](#)]
101. Nalcacioglu, R.; Demirbag, Z.; Vlak, J.M.; van Oers, M.M. Promoter analysis of the Chilo iridescent virus DNA polymerase and major capsid protein genes. *Virology* **2003**, *317*, 321–329. [[CrossRef](#)] [[PubMed](#)]
102. Dizman, Y.A.; Demirbag, Z.; Ince, I.A.; Nalcacioglu, R. Transcriptomic analysis of Chilo iridescent virus immediate-early promoter. *Virus Res.* **2012**, *167*, 353–357. [[CrossRef](#)] [[PubMed](#)]
103. Goorha, R. Frog virus 3 requires RNA polymerase II for its replication. *J. Virol.* **1981**, *37*, 496–499. [[PubMed](#)]
104. Goorha, R.; Willis, D.B.; Granoff, A. Macromolecular synthesis in cells infected by frog virus 3. VI. Frog virus 3 replication is dependent on the cell nucleus. *J. Virol.* **1977**, *21*, 802–805. [[PubMed](#)]
105. Goorha, R.; Murti, G.; Granoff, A.; Tirey, R. Macromolecular synthesis in cells infected by frog virus 3. VIII. The nucleus is a site of frog virus 3 DNA and RNA synthesis. *Virology* **1978**, *84*, 32–50. [[CrossRef](#)]
106. Baroudy, B.M.; Moss, B. Sequence homologies of diverse length tandem repetitions near ends of vaccinia virus genome suggest unequal crossing over. *Nucleic Acids Res.* **1982**, *25*, 5673–5679. [[CrossRef](#)]
107. Tidona, C.A.; Darai, G. Molecular anatomy of lymphocystis disease virus. *Arch. Virol. Suppl.* **1997**, *13*, 49–56. [[PubMed](#)]
108. Federici, B.A.; Bigot, Y.; Granados, R.R.; Hamm, J.J.; Miller, L.K.; Newton, I.; Stasiak, K.; Vlak, J.M. Family Ascoviridae. In *Virus Taxonomy: 8th Report of the International Committee on Taxonomy of Viruses*; Fauquet, C.M., Mayo, M.A., Maniloff, J., Desselberger, U., Ball, L.A., Eds.; Elsevier Academic Press: San Diego, CA, USA, 2005; pp. 261–265.
109. International Committee on Taxonomy of Viruses. Available online: http://www.ictvonline.org/taxonomyHistory.asp?taxnode_id=20151919&taxa_name=Ascoviridae (accessed on 22 September 2016).
110. Cheng, X.W.; Wang, L.; Carner, G.R.; Arif, B.M. Characterization of three ascovirus isolates from cotton insects. *J. Invertebr. Pathol.* **2005**, *89*, 193–202. [[CrossRef](#)] [[PubMed](#)]
111. Asgari, S.; Davis, J.; Wood, D.; Wilson, P.; McGrath, A. Sequence and organization of the *Heliothis virescens* ascovirus genome. *J. Gen. Virol.* **2007**, *88*, 1120–1132. [[CrossRef](#)] [[PubMed](#)]

112. Bigot, Y.; Rabouille, A.; Sizaret, P.Y.; Hamelin, M.H.; Periquet, G. Particle and genomic characterization of a new member of the Ascoviridae, *Diadromus pulchellus ascovirus*. *J. Gen. Virol.* **1997**, *78*, 1139–1147. [[CrossRef](#)] [[PubMed](#)]
113. Cheng, X.W.; Carner, G.R.; Arif, B.M. A new ascovirus from *Spodoptera exigua* and its relatedness to the isolate from *Spodoptera frugiperda*. *J. Gen. Virol.* **2000**, *81*, 3083–3092. [[CrossRef](#)] [[PubMed](#)]
114. Salem, T.Z.; Turney, C.M.; Wang, L.; Xue, J.; Wan, X.-F.; Cheng, X.-W. Transcriptional analysis of a major capsid protein gene from *Spodoptera exigua ascovirus 5a*. *Arch. Virol.* **2008**, *153*, 149–162. [[CrossRef](#)] [[PubMed](#)]
115. Zhao, K.; Cui, L.W. Molecular characterization of the major virion protein gene from the *Trichoplusia ni ascovirus*. *Virus Genes* **2003**, *27*, 93–102. [[CrossRef](#)] [[PubMed](#)]
116. Stasiak, K.; Renault, S.; Demattei, M.V.; Bigot, Y.; Federici, B.A. Evidence for the evolution of ascoviruses from iridoviruses. *J. Gen. Virol.* **2003**, *84*, 2999–3009. [[CrossRef](#)] [[PubMed](#)]
117. Chinchar, V.G.; Hyatt, A.; Miyazaki, T.; Williams, T. Family *Iridoviridae*: Poor viral relations no longer. *Curr. Top. Microbiol. Immunol.* **2009**, *328*, 123–170. [[PubMed](#)]
118. Piégu, B.; Asgari, S.; Bideshi, D.; Federici, B.A.; Bigot, Y. Evolutionary relationships of iridoviruses and divergence of ascoviruses from invertebrate iridoviruses in the superfamily Megavirales. *Mol. Phylogenet. Evol.* **2015**, *84*, 44–52. [[CrossRef](#)] [[PubMed](#)]
119. Zauberman, N.; Mutsafi, Y.; Halevy, D.B.; Shimoni, E.; Klein, E.; Xiao, C.; Sun, S.; Minsky, A. Distinct DNA exit and packaging portals in the virus *Acanthamoeba polyphaga mimivirus*. *PLoS Biol.* **2008**, *13*, 114. [[CrossRef](#)] [[PubMed](#)]
120. Xiao, C.; Kuznetsov, Y.G.; Sun, S.; Hafenstein, S.L.; Kostyuchenko, V.A.; Chipman, P.R.; Suzan-Monti, M.; Raoult, D.; McPherson, A.; Rossmann, M.G. Structural studies of the giant mimivirus. *PLoS Biol.* **2009**, *28*, e92. [[CrossRef](#)] [[PubMed](#)]
121. Rodrigues, R.A.; dos Santos Silva, L.K.; Dornas, F.P.; de Oliveira, D.B.; Magalhães, T.F.; Santos, D.A.; Costa, A.O.; de Macêdo Farias, L.; Magalhães, P.P.; Bonjardim, C.A.; et al. Mimivirus fibrils are important for viral attachment to the microbial world by a diverse glycoside interaction repertoire. *J. Virol.* **2015**, *89*, 11812–11819. [[CrossRef](#)] [[PubMed](#)]
122. Legendre, M.; Santini, S.; Rico, A.; Abergel, C.; Claverie, J.M. Breaking the 1000-gene barrier for Mimivirus using ultra-deep genome and transcriptome sequencing. *Virol. J.* **2011**, *4*, 8–99. [[CrossRef](#)] [[PubMed](#)]
123. Fischer, M.G.; Allen, M.J.; Wilson, W.H.; Suttle, C.A. Giant virus with a remarkable complement of genes infects marine zooplankton. *Proc. Natl. Acad. Sci. USA* **2010**, *9*, 19508–19513. [[CrossRef](#)] [[PubMed](#)]
124. Colson, P.; de Lamballerie, X.; Yutin, N.; Asgari, S.; Bigot, Y.; Bideshi, D.K.; Cheng, X.W.; Federici, B.A.; van Etten, J.L.; Koonin, E.V.; et al. “Megavirales”, a proposed new order for eukaryotic nucleocytoplasmic large DNA viruses. *Arch. Virol.* **2013**, *158*, 2517–2521. [[CrossRef](#)] [[PubMed](#)]
125. Reteno, D.G.; Benamar, S.; Khalil, J.B.; Andreani, J.; Armstrong, N.; Klose, T.; Rossmann, M.; Colson, P.; Raoult, D.; La Scola, B. Faustovirus, an asfarvirus-related new lineage of giant viruses infecting amoebae. *J. Virol.* **2015**, *89*, 6585–6594. [[CrossRef](#)] [[PubMed](#)]
126. Philippe, N.; Legendre, M.; Doutre, G.; Couté, Y.; Poirot, O.; Lescot, M.; Arslan, D.; Seltzer, V.; Bertaux, L.; Bruley, C.; et al. Pandoraviruses: Amoeba viruses with genomes up to 2.5 Mb reaching that of parasitic eukaryotes. *Science* **2013**, *341*, 281–286. [[CrossRef](#)] [[PubMed](#)]
127. Legendre, M.; Bartoli, J.; Shmakova, L.; Jeudy, S.; Labadie, K.; Adrait, A.; Lescot, M.; Poirot, O.; Bertaux, L.; Bruley, C.; et al. Thirty-thousand-year-old distant relative of giant icosahedral DNA viruses with a pandoravirus morphology. *Proc. Natl. Acad. Sci. USA* **2014**, *111*, 4274–4279. [[CrossRef](#)] [[PubMed](#)]
128. Levasseur, A.; Andreani, J.; Delerce, J.; Bou Khalil, J.; Robert, C.; La Scola, B.; Raoult, D. Comparison of a modern and fossil pithovirus reveals its genetic conservation and evolution. *Genome Biol. Evol.* **2016**, *25*, 2333–2339. [[CrossRef](#)] [[PubMed](#)]
129. Legendre, M.; Lartigue, A.; Bertaux, L.; Jeudy, S.; Bartoli, J.; Lescot, M.; Alempic, J.M.; Ramus, C.; Bruley, C.; Labadie, K.; et al. In-depth study of *Mollivirus sibericum*, a new 30,000-y-old giant virus infecting *Acanthamoeba*. *Proc. Natl. Acad. Sci. USA* **2015**, *112*, 5327–5335. [[CrossRef](#)] [[PubMed](#)]
130. McLysaght, A.; Baldi, P.F.; Gaut, B.S. Extensive gene gain associated with adaptive evolution of poxviruses. *Proc. Natl. Acad. Sci. USA* **2003**, *23*, 15655–15660. [[CrossRef](#)] [[PubMed](#)]
131. Hughes, A.L.; Friedman, R. Poxvirus genome evolution by gene gain and loss. *Mol. Phylogenet. Evol.* **2005**, *35*, 186–195. [[CrossRef](#)] [[PubMed](#)]

132. Elde, N.C.; Child, S.J.; Eickbush, M.T.; Kitzman, J.O.; Rogers, K.S.; Shendure, J.; Geballe, A.P.; Malik, H.S. Poxviruses deploy genomic accordions to adapt rapidly against host antiviral defenses. *Cell* **2012**, *17*, 831–841. [[CrossRef](#)] [[PubMed](#)]
133. Dixon, L.K.; Chapman, D.A.; Netherton, C.L.; Upton, C. African swine fever virus replication and genomics. *Virus Res.* **2013**, *173*, 3–14. [[CrossRef](#)] [[PubMed](#)]
134. Portugal, R.; Coelho, J.; Höper, D.; Little, N.S.; Smithson, C.; Upton, C.; Martins, C.; Leitão, A.; Keil, G.M. Related strains of African swine fever virus with different virulence: Genome comparison and analysis. *J. Gen. Virol.* **2015**, *96*, 408–419. [[CrossRef](#)] [[PubMed](#)]
135. Huang, Y.; Huang, X.; Liu, H.; Gong, J.; Ouyang, Z.; Cui, H.; Cao, J.; Zhao, Y.; Wang, X.; Jiang, Y.; et al. Complete sequence determination of a novel reptile iridovirus isolated from soft-shelled turtle and evolutionary analysis of Iridoviridae. *BMC Genomics* **2009**, *14*, 224. [[CrossRef](#)] [[PubMed](#)]
136. Koonin, E.V.; Krupovic, M.; Yutin, N. Evolution of double-stranded DNA viruses of eukaryotes: From bacteriophages to transposons to giant viruses. *Ann. N. Y. Acad. Sci.* **2015**, *1341*, 10–24. [[CrossRef](#)] [[PubMed](#)]
137. Nasir, A.; Kim, K.M.; Caetano-Anolles, G. Giant viruses coexisted with the cellular ancestors and represent a distinct supergroup along with superkingdoms Archaea, Bacteria and Eukarya. *BMC Evol. Biol.* **2012**, *24*. [[CrossRef](#)] [[PubMed](#)]
138. Moss, B. Reflections on the early development of poxvirus vectors 2013. *Vaccine* **2013**, *6*, 4220–4222. [[CrossRef](#)] [[PubMed](#)]



© 2017 by the authors; licensee MDPI, Basel, Switzerland. This article is an open access article distributed under the terms and conditions of the Creative Commons Attribution (CC BY) license (<http://creativecommons.org/licenses/by/4.0/>).

4.2. ARTIGO 2: The Investigation of Promoter Sequences of Marseilleviruses Highlights a Remarkable Potential for Gene Acquisition and Genome Expansion

Este artigo foi publicado no periódico Journal of Virology.

Durante vários anos as regiões intergênicas dos genomas de eucariotos e procariotos vêm sendo estudadas com o intuito de melhor entender as sequências envolvidas na regulação dos processos transcricionais. Nesse contexto, estudos têm sido feitos a fim de desvendar a regulação dos processos transcricionais nos vírus e conseqüentemente sequências promotoras vêm sendo descritas nos vírus que compõem o grupo NCLDV. Apesar da existência de estudos envolvendo sequências promotoras nesse grupo, muitos estudos ainda necessitam ser desenvolvidos para a identificação e caracterização biológica de promotores nos vírus recém-descobertos e recentemente inseridos no grupo. Nesse contexto destacam-se os vírus da família *Marseilleviridae* que permaneciam até o desenvolvimento desse trabalho em total desconhecimento acerca de seus possíveis promotores. No estudo aqui apresentado, foi identificada pela primeira vez uma sequência composta por oito nucleotídeos (AAATATTT) que está associada a 55% dos genes preditos de marseillevírus, conservada em todas as linhagens da família *Marseilleviridae*. A importância biológica dessa sequência foi demonstrada nesse estudo por ensaios *in vitro*, realizados em parceria com a Aix Marseille University. Através de análises dos genes transferidos por TGL nos hospedeiros doadores associado à busca por similaridade em relação a sequências intergênicas de marseillevírus nós sugerimos que a sequência promotora predita no genoma de marseillevírus aparentemente tem origem independente do organismo doador dos genes. Outro dado aqui demonstrado se refere à presença de múltiplas repetições de motivos não associados a genes em todas as linhagens de marseillevírus. Com base no grande número de genes presentes no genoma dos marseillevírus possivelmente adquiridos por TGL nós propusemos que esses promotores não associados a genes poderiam funcionar como regiões propícias a incorporação e expressão de novos genes contribuindo para a plasticidade do genoma dos marseillevírus.



The Investigation of Promoter Sequences of Marseilleviruses Highlights a Remarkable Abundance of the AAATATTT Motif in Intergenic Regions

Graziele Pereira Oliveira,^a Maurício Teixeira Lima,^a Thalita Souza Arantes,^a Felipe Lopes Assis,^a Rodrigo Araújo Lima Rodrigues,^a Flávio Guimarães da Fonseca,^a Cláudio Antônio Bonjardim,^a Erna Geessien Kroon,^a Philippe Colson,^b Bernard La Scola,^b Jônatas Santos Abrahão^a

Laboratório de Vírus, Departamento de Microbiologia, Instituto de Ciências Biológicas, Universidade Federal de Minas Gerais, Belo Horizonte, Minas Gerais, Brazil^a; URMITE, Aix Marseille Université, UM63, CNRS 7278, IRD 198, INSERM 1095, IHU-Méditerranée Infection, AP-HM, Marseille, France^b

ABSTRACT Viruses display a wide range of genomic profiles and, consequently, a variety of gene expression strategies. Specific sequences associated with transcriptional processes have been described in viruses, and putative promoter motifs have been elucidated for some nucleocytoplasmic large DNA viruses (NCLDV). Among NCLDV, the *Marseilleviridae* is a well-recognized family because of its genomic mosaicism. The marseilleviruses have an ability to incorporate foreign genes, especially from sympatric organisms inhabiting *Acanthamoeba*, its main known host. Here, we identified for the first time an eight-nucleotide A/T-rich promoter sequence (AAATATTT) associated with 55% of marseillevirus genes that is conserved in all marseilleviruses lineages, a higher level of conservation than that of any giant virus described to date. We instigated our prediction about the promoter motif by biological assays and by evaluating how single mutations in this octamer can impact gene expression. The investigation of sequences that regulate the expression of genes relative to lateral transfer revealed that the promoter motifs do not appear to be incorporated by marseilleviruses from donor organisms. Indeed, analyses of the intergenic regions that regulate lateral gene transfer-related genes have revealed an independent origin of the marseillevirus intergenic regions that does not match gene-donor organisms. About 50% of AAATATTT motifs spread throughout intergenic regions of the marseilleviruses are present as multiple copies. We believe that such multiple motifs are associated with increased expression of a given gene or are related to incorporation of foreign genes into the mosaic genome of marseilleviruses.

IMPORTANCE The marseilleviruses draw attention because of the peculiar features of their genomes; however, little is known about their gene expression patterns or the factors that regulate those expression patterns. The limited published research on the expression patterns of the marseilleviruses and their unique genomes has led us to study the promoter motif sequences in the intergenic regions of the marseilleviruses. This work is the first to analyze promoter sequences in the genomes of the marseilleviruses. We also suggest a strong capacity to acquire foreign genes and to express those genes mediated by multiple copies of the promoter motifs available in intergenic regions. These findings contribute to an understanding of genomic expansion and plasticity observed in these giant viruses.

KEYWORDS lateral gene transfer, *Marseilleviridae*, gene expression, promoter

Received 29 June 2017 Accepted 4 August 2017

Accepted manuscript posted online 9 August 2017

Citation Oliveira GP, Lima MT, Arantes TS, Assis FL, Rodrigues RAL, da Fonseca FG, Bonjardim CA, Kroon EG, Colson P, Scola BL, Abrahão JS. 2017. The investigation of promoter sequences of marseilleviruses highlights a remarkable abundance of the AAATATTT motif in intergenic regions. *J Virol* 91:e01088-17. <https://doi.org/10.1128/JVI.01088-17>.

Editor Rozanne M. Sandri-Goldin, University of California, Irvine

Copyright © 2017 American Society for Microbiology. All Rights Reserved.

Address correspondence to Jônatas Santos Abrahão, jonatas.abrahao@gmail.com.

Since the discovery of the *Acanthamoeba polyphaga mimivirus* (APMV) in 2003 (1), new giant viruses, including *Marseillevirus marseillevirus* (MsV), have been isolated from clinical and environmental samples (2–12). According to phylogenies that are based on a set of core genes, the family *Marseilleviridae* encompasses four distinct lineages: lineage A, composed of the prototype MsV; lineage B, composed of *Lausannevirus*; lineage C, composed of *Tunisvirus*; and lineage D, composed of *Brazilian marseillevirus* (BR-MsV) (2, 4, 7, 8, 13, 14). MsV has an extensive genome, with circular, double-stranded DNA. It is approximately 370 kbp, it has a GC content of 45%, and it encodes 428 proteins, of which 187 were encoded by genes that originated from a putative lateral gene transfer (LGT) (2).

Some studies have described putative A/T-rich promoter sequences for nucleocytoplasmic large DNA viruses (NCLDV) from different families (15–21). In 2005, the mimivirus promoter sequence was identified. It showed a level of conservation unreported among eukaryotes, being present for about 45% of open reading frames (ORFs) in the mimivirus (22).

In this paper, we describe the identification of an octamer promoter motif, AAATATTT, present in 55% of marseillevirus genes. We used biological assays to confirm the prediction of a promoter sequence in the genome of a giant virus. We also performed an analysis of the distribution of motifs in the intergenic regions (IRs) that are associated with lateral gene transfer in marseilleviruses. Results showed that marseillevirus IRs are of an independent origin that is unrelated to respective donor organisms. Furthermore, multiple copies of available AAATATTT promoter motifs in IRs that are not associated with a downstream gene may help explain why the marseilleviruses have the ability to acquire foreign genes that contribute to its fitness and genome expansion.

RESULTS AND DISCUSSION

The AAATATTT motif is associated with more than half of the MsV genes. The conserved AAATATTT motif (Fig. 1E) was found to be associated with 55.1% of MsV genes, which revealed an unprecedented conservation of the regulatory motif between viruses and eukaryotes. Similar conservation profiles were observed in all other marseilleviruses lineages: 49.5% in *Lausannevirus*, 41.9% in *Tunisvirus*, and 38.7% in BR-MsV (some overlapping genes in marseilleviruses seem to be regulated by a single motif). The AAATATTT motif occurred in 55.6% of MsV IRs, 49.4% of *Lausannevirus* IRs, 42.9% of *Tunisvirus* IRs, and 39.7% of BR-MsV IRs. These data reveal a strongly conserved motif in IRs across all lineages of the *Marseilleviridae* family. Such a high prevalence of motifs is not random; we found 350 to 700% more motifs in IRs than in coding regions (Fig. 1A to D). A total of 450 motifs were detected in MsV IRs, 397 in *Lausannevirus* IRs, 418 in *Tunisvirus* IRs, and 341 in BR-MsV IRs. In comparison, only 56, 87, 73, and 59 were found in coding regions of MsV, *Lausannevirus*, *Tunisvirus*, and BR-MsV, respectively (Fig. 1A to D). The presence of the motif upstream of marseillevirus genes was highly significant ($P = 1.61 \times 10^{-42}$ by Fisher exact test). These data are represented by the circles in Fig. 1A to D. Furthermore, the search for the AAATATTT motif in the *Acanthamoeba castellanii* genome showed that the motif is poorly represented; only about 35 AAATATTT motifs were found in the available genome. The presence of an A/T-rich promoter sequence has been described in the genomes of NCLDV, even in those presenting a high GC content, such as those in the following: phycodnaviruses (~40% GC content) (23), iridoviruses (~48% GC content) (24), and marseilleviruses (~45% GC content) (2). As previously mentioned, bioinformatics studies on the mimivirus identified a nucleotide sequence (AAAATTGA) that occurs in about 45% of mimivirus open reading frames (22). In addition, the *Cafeteria roenbergensis* virus, another representative of the *Mimiviridae* family which is distantly related to mimiviruses, showed this promoter motif in the upstream region of 35% of its genes (25). Therefore, the AAATATTT promoter motif in marseilleviruses is the most representative and widespread motif considering members from different lineages of marseilleviruses.

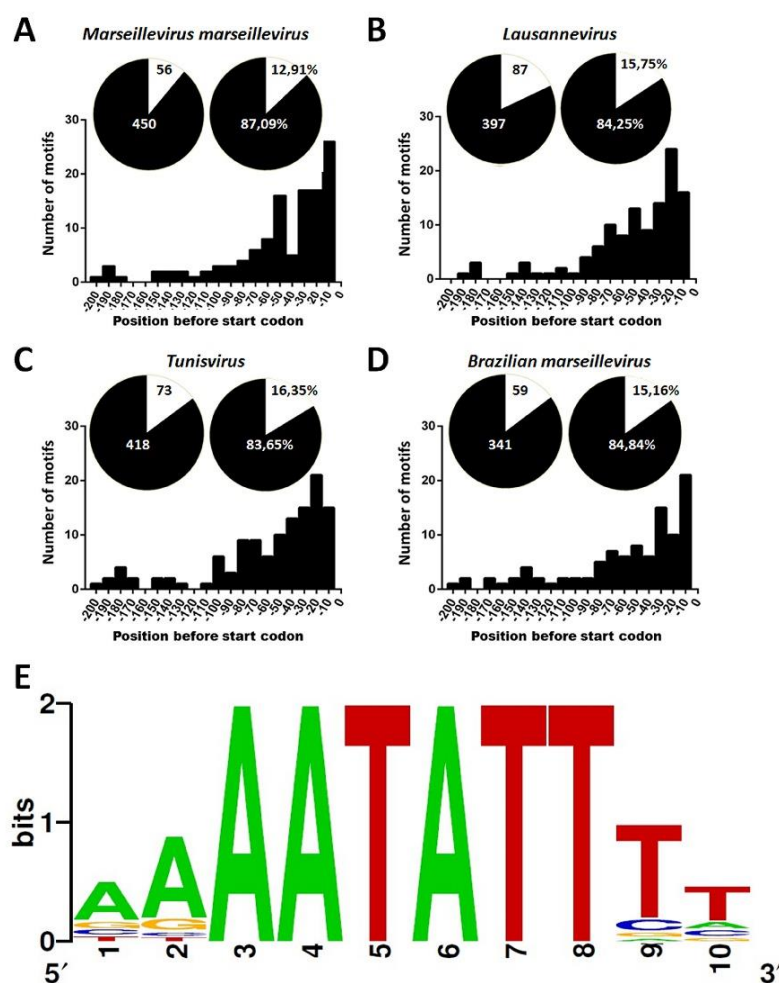


FIG 1 AAATATT motif in intergenic regions of marseillevirus lineages. (A to D) The distribution of the AAATATT motif in intergenic and coding regions is represented by a circle graphic with black and white colors, respectively. The bar graphs represent the distribution -200 bp upstream of the ATG start codon in all marseillevirus lineages. (E) The promoter motif sequence logo that was generated using the Berkeley Logo platform.

The AAATATT motifs are located mainly at -1 to -100 bp upstream of ATG.

The AAATATT motifs are mainly distributed in positions that are -1 to -100 bp upstream of translation start codons (ATG) for all lineages of marseillevirus (Fig. 1A to D). This predominant localization is consistent with the promoter patterns demonstrated for most organisms, including NCLDV members (21). In eukaryotes, one classic

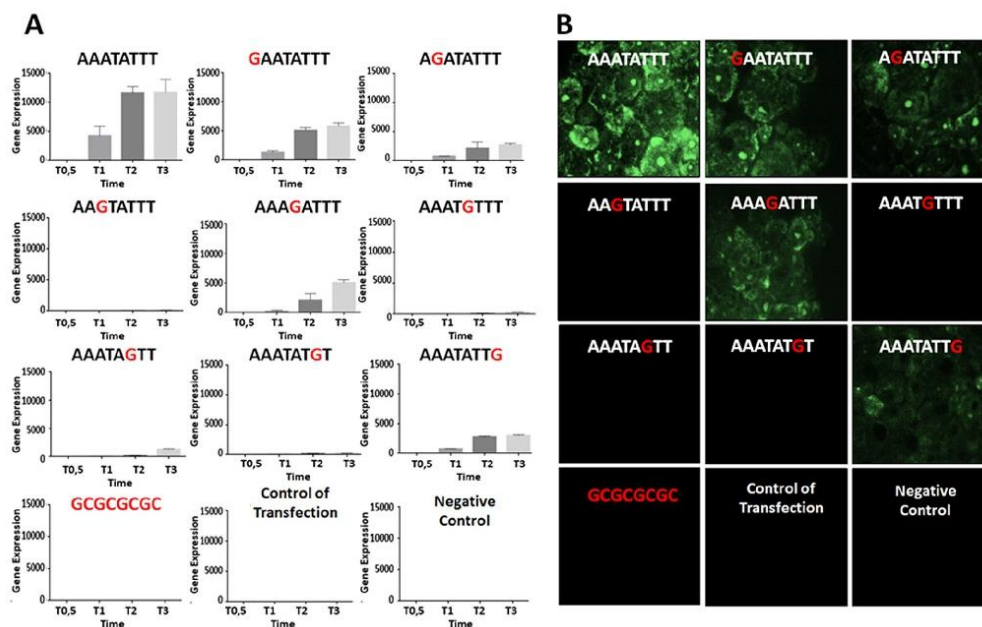


FIG 2 Biological assays confirm that the AAATATTT motif is a promoter sequence of MsV. (A) Enhanced green fluorescent protein (eGFP) expression was measured by quantitative PCR (qPCR). *Acanthamoeba castellanii* cells were infected with MsV and transfected with plasmids that contained the GFP gene under the control of the AAATATTT motif and other similarly mutated motifs (position -10 bp from ATG). Cells were collected at different times postinfection (0.5 h, 1 h, 2 h, and 3 h), and expression of eGFP transcripts was measured by qPCR. The data were calculated using the $2^{-\Delta\Delta CT}$ method and were represented as the standard deviations from two independent biological assays. (B) eGFP expression was detected by fluorescence microscopy. *Acanthamoeba castellanii* cells were infected with MsV (multiplicity of infection of 10) and then transfected with the indicated construct plasmids. eGFP expression was visualized at 3 h postinfection.

element of the core promoter is the TATA box, which is represented by the consensus sequence TATAAAT that is located at 25 to 30 bp upstream from the transcription start sites (26). Bacterial genomes present short conserved motifs such as the hexamers TATAAT and TTGACA, which are located at 10 and 35 bp upstream of the transcription start site, respectively (27). Base composition analyses of the IRs of the poxviruses, asfarviruses, phycodnaviruses, iridoviruses, and mimiviruses show that NCLDV members present A/T-rich motifs associated with transcription that is located, in general, within a 150-bp region upstream from the start codon (16, 17, 22, 28, 29). These results reinforce our findings for marseilleviruses.

Biological validation confirmed the importance of the AAATATTT motif for MsV gene expression. *Acanthamoeba castellanii* cells infected with MsV and transfected with plasmids containing the wild-type promoter motif (AAATATTT) showed high expression of enhanced green fluorescent protein (eGFP) transcripts at 1 h, 2 h, and 3 h postinfection (Fig. 2A). However, considerable reductions in eGFP transcript levels were detected for all mutant versions of this motif (including GAATATTT, AGATATTT, AAGTATTT, AAAGATTT, AAATGTTT, AAATAGTT, AAATATGT, and AAATATTG), even though the expression levels were not completely abolished when some motifs (GAATATTT, AGATATTT, AAAGATTT, and AAATATTG) were used in the assays. eGFP transcripts were not detected at 0.5 h postinfection in all cases, which may be due to the time needed for viral RNA polymerases to encounter the plasmids and trigger gene expression or the absence of complete RNA polymerase subunits in the virion (3). Furthermore, cells infected with MsV and then transfected with the plasmid containing

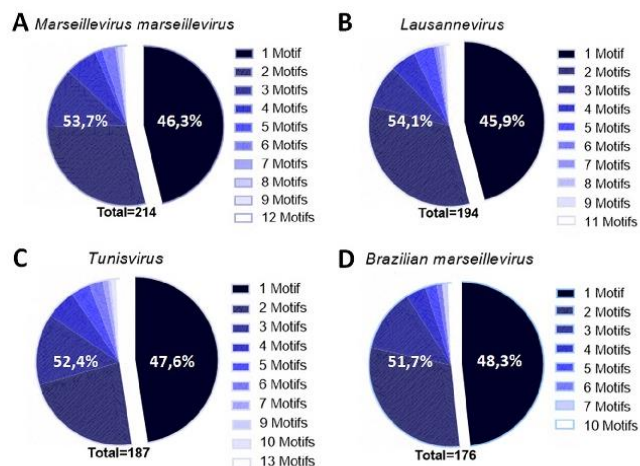


FIG 3 Most marseillevirus intergenic regions present more than one promoter motif. Shown is a graphic representation of the number of repetitions of the motifs in different lineages of marseilleviruses.

the GC-rich sequence showed no transcript expression, which is consistent with the lack of expression observed for the controls. eGFP expression, which was analyzed by fluorescence microscopy, corroborated the importance of the AAATATTT motif (Fig. 2B). Higher eGFP expression was observed in cells transfected with plasmids containing the sequence AAATATTT, while a negative effect on gene expression was observed for GAATATTT, AGATATTT, AAAGATTT, and AAATATTG sequences. For the remaining sequences, expression was completely abolished, similar to what was demonstrated for eGFP transcripts. Because substitution of these eight nucleotides can result in a decline or loss of promoter activity, these results confirmed that the AAATATTT motif can act as a promoter sequence during the MsV replication cycle.

Marseillevirus intergenic regions display multiple repetitions of the AAATATTT motif. More than 50% of the IRs of the marseilleviruses contain more than one copy of the AAATATTT motifs (Fig. 3). We found 450, 397, 418, and 341 motif repeats in a total of 214, 194, 187, and 176 IRs in MsV, *Lausannevirus*, *Tunisvirus* and BR-MsV, respectively. All marseilleviruses lineages presented more than one promoter motif sequence in approximately 50% of their IRs that contained the motif. Interestingly, some IRs harbored large numbers of up to 13 such repeats (Fig. 3). In MsV, more than one motif copy was observed in 53.7% of the IRs (between 2 and 12 repeats) (Fig. 3A). In *Lausannevirus*, more than one repeat was observed in 54.1% of the IRs (between two and 11 repeats) (Fig. 3B). In *Tunisvirus* and BR-MsV, more than one motif was found in 52.4% (with up to 13 repeats) and 51.7% of the IRs, respectively (Fig. 3C and D). These noteworthy findings motivated us to investigate the implications of repetitions in the MsV genome.

The marseillevirus intergenic regions seem to have a different origin than those of respective genes acquired by LGT. As previously mentioned, some research suggests that lateral gene transfer events are common among the marseilleviruses (2, 30). In our research, we observed that approximately 60% of genes that have been involved in LGT are regulated by IRs that present the AAATATTT motif (Fig. 4B). We decided to verify if the AAATATTT motif could have been acquired from donor organisms at the same time as the gene during LGT (that is, the transfer of the promoter plus gene). To investigate this, we analyzed the upstream promoter regions of all LGT donor organisms. Interestingly, the AAATATTT motif was present in only 14 of the 179 (7.8%) upstream regions in the LGT-associated donor genes that we

evaluated ($P = 4.17 \times 10^{-25}$ by Fisher exact test) (data not shown). In addition, the search for sequences with similar IRs (cutoffs were an E value of <0.001 and coverage of $>40\%$) revealed that only 4 of 317 (1.3%) IRs were similar to any organisms in the NCBI GenBank database ($P = 1.85 \times 10^{-47}$ by Fisher exact test) (Fig. 4A). These results suggest that neither the motif nor the IRs originated from LGT-related donors.

Multiple repetitions of the promoter motif in marseillevirus intergenic regions could help to explain their ability to acquire foreign genes. Although our results showed that the AAATATTT motif is associated with expression of genes in the marseilleviruses, we also observed the presence of a large percentage of motifs in the IRs that do not appear to be associated with any gene. A total of 52.6% of the motifs found in MsV IR are not associated with genes. This high availability of free motifs was observed in all marseillevirus lineages: 50.4% in *Lausannevirus*, 54.5% in *Tunisvirus*, and 47.7% in BR-MsV (Fig. 4C). In addition, the analysis of the motif distribution within the marseillevirus genome revealed that the motifs are distributed preferentially in the IR and that these motifs are homogeneously distributed in the IR of marseillevirus genomes (Fig. 4D). Interestingly, 62% (148) of the genes that present the AAATATTT motif are core genes and/or genes acquired by LGT (Fig. 4B). Taken together, these data led us to propose a hypothesis supporting that the initial fixation of foreign genes in the marseilleviruses depends not only on stochastic processes, such as genetic drifts and point mutations, but also on an increase in the likelihood of a prompt expression of a given just-acquired gene. This dynamic can speed the fixation of favorable genes and the exclusion of less competitive modified viral genomes (Fig. 5). The homogeneity of the distribution of motifs in genomes reinforces our hypothesis, since LGT can occur in many IRs within the genome. It was hypothesized that the high prevalence of free motifs in IRs reflects the number of potentially available motifs for the regulation of new genes acquired by LGT, revealing the great evolutionary potential of the marseilleviruses. This hypothesis may help to explain the genome plasticity of the marseilleviruses. However, more studies need to be done in order to confirm this hypothesis. To date, there are no differences of GC% content and codon usage among marseillevirus genes, which suggests an adaptation of a given LGT-acquired gene after the incorporation (data not shown). Moreover, a large number and wide distribution of free promoter motifs may confer a selective adaptive advantage in the sympatric lifestyle of an amoeba.

Conclusions. Here, we describe for the first time a conserved eight-nucleotide A/T-rich sequence (AAATATTT) associated with most of the genes of the marseilleviruses and its lineages. The motif AAATATTT is associated with 55% of genes in the marseilleviruses, which is a remarkable level of conservation among giant viruses and eukaryotes. Furthermore, variations in the motif sequence caused a negative effect on gene transcription. LGT events contributed to the diversity of the amoebal virus genomes and are considered to be important for evolutionary processes (2, 31, 32). The homogeneously distributed motifs within the IRs of the marseilleviruses, in addition to the possibility that the IRs were not transferred by LGT, strongly suggest that free motifs can act as major players in the prompt expression of recently acquired genes. In this scenario, within its amoeba host, marseilleviruses are able to find new genes from diverse sources and promptly incorporate those genes. The absence of fragments in MsV IRs that are similar to other organisms suggests that the free AAATATTT motifs did not originate from MsV LGT genes. Instead, the remarkable amount of AAATATTT motifs seems to be an original and ancient characteristic of the *Marseilleviridae* family, contributing to its genomic mosaicism and plasticity.

MATERIALS AND METHODS

Bioinformatic analyses. To investigate the promoter motif that regulates the marseilleviruses, the genomic sequences of a representative relative of each lineage of the *Marseilleviridae* family were analyzed: *Marseillevirus marseillevirus* strain T19 (representative of lineage A), *Lausannevirus* (representative of lineage B), *Tunisvirus* Fontaine 2 strain U484 (representative of lineage C), and *Brazilian marseillevirus* strain BH2014 (representative of lineage D). These genome sequences are available in

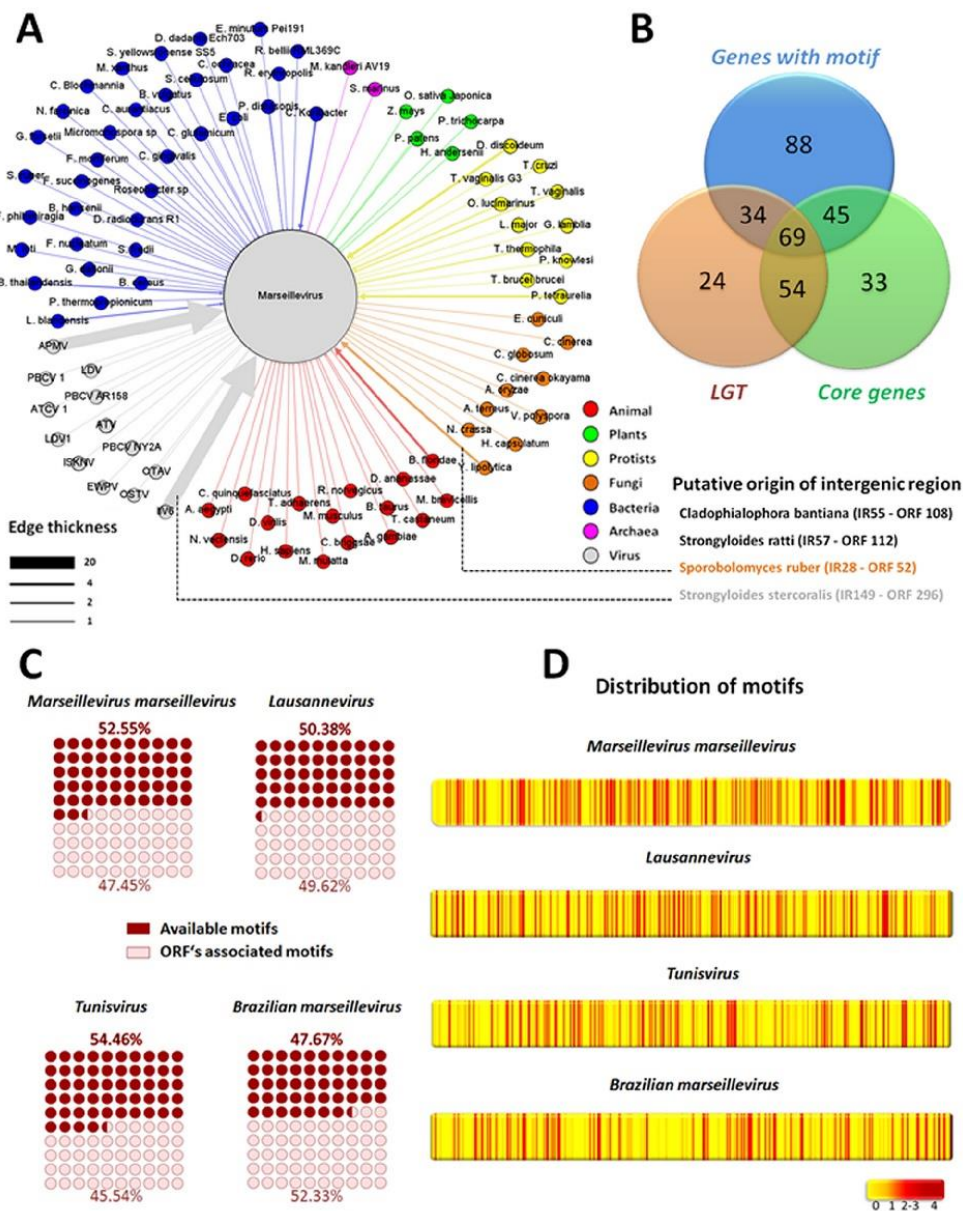


FIG 4 Intergenic regions upstream of genes acquired by lateral gene transfer were not acquired from LGT donor organisms. (A) The network of LGTs in MsV. Gene donor organisms are represented as colored circles connected to MsV. The thickness of the edges is proportional to the number of open reading frames transferred from an organism to MsV. The putative origins of intergenic regions found in MsV are depicted. (B) Venn diagram demonstrating the relationship among core genes, LGT genes, and genes regulated by the AAATATTT motif. (C) Representation of the number of motifs that control genes or available motifs that are present but do not control any genes. (D) Heat map showing that the AAATATTT promoter motif is homogeneously distributed in the genomes of marseillevirus lineages. APMV, Acanthamoeba polyphaga mimivirus; ATCV1, Acanthamoeba turfacea virus 1; ATV, Ambystoma tigrinum virus; EWPV, Erwinia phage; ISKNV, infectious spleen and kidney necrosis virus; IIV6, invertebrate iridescent virus 6; LDV, lymphocystis disease virus; OTAV, Ostreococcus tauri virus; OSTV, Ostreococcus virus; PBCV, Paramecium bursaria chlorella virus.

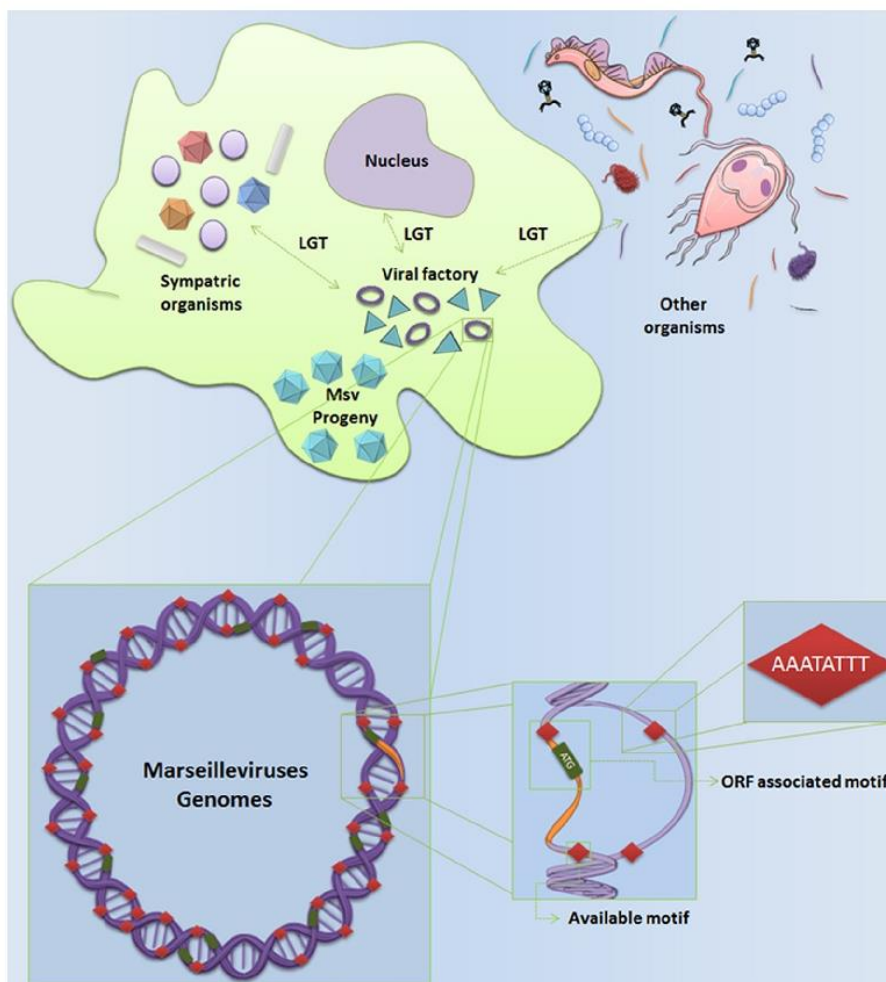


FIG 5 AAATATT motif may contribute to explanation of the plasticity of the marseilleviruses genome. Available genes from amoeba hosts or sympatric organisms would be incorporated into the genome of the marseilleviruses and expressed because of the large number of available promoter motifs in the intergenic regions.

GenBank under accession numbers [NC_013756.1](#), [NC_015326.1](#), [KF483846.1](#), and [NC_029692.1](#), respectively.

The IRs of these marseilleviruses species were obtained using the data set that is available under the accession numbers associated with each sequence and by using Artemis software for analysis (33). After extraction of the IRs, we identified the following number of genomic IRs: 402 from the MsV genome (196 were located in the positive strand and 206 were located in the negative strand), 412 from the *Lausannevirus* genome (198 were in the positive strand and 214 were in the negative strand), 450 from the *Tunisvirus* genome (225 were in the positive strand and 225 were in the negative strand), and 460 from the BR-MsV genome (221 were in the positive strand and 239 were in the negative strand). The IRs that contained ≥ 8 bp were not considered, because these IRs were too short to host the motif. The number of IRs that we considered here were 385, 394, 437, and 443 in MsV, *Lausannevirus*, *Tunisvirus*, and BR-MsV, respectively.

The search for motif occurrences was performed using the Find Individual Motif Occurrences (FIMO) software and by a manual search to validate the software results (34). The promoter sequence logo (Fig. 1E) was generated using a Berkeley Logo platform (<http://weblogo.berkeley.edu>). The search for promoter motifs was performed both in marseillevirus IRs and coding regions. The distance between the promoter and the ATG initiation codon was calculated for all genes that contained the motifs of interest. This was undertaken for all viral lineages being investigated in this study.

The LGT analysis was performed on the basis of results described by Boyer et al. (2). Similar searches of the IRs were performed using the Nucleotide Basic Local Alignment Search Tool platform, and regions

with more than 40 bp were considered in this analysis. Furthermore, the presence of the AAATATT motif in the *Acanthamoeba castellanii* genome was evaluated using a whole-genome shotgun (WGS) project, and sequences were deposited at DDBJ/EMBL/GenBank (accession number AHJ00000000; WGS, AHJ01000001-AHJ01003192; WGS_SCAFLD, KB007791-KB008174). The graphs were completed using GraphPad Prism version 7.00 for Windows (GraphPad Software).

Biological assays: gene expression analyses. *Acanthamoeba castellanii* cells (ATCC 30010) were grown in peptone yeast glucose medium that was supplemented with 25 mg/ml of amphotericin B (Fungizone; Cristalia, São Paulo, Brazil), 500 µg/ml of penicillin, and 50 mg/ml gentamicin (Schering-Plough, Brazil) at 32°C. *Marseillevirus marseillevirus* was replicated in *Acanthamoeba castellanii* cells at a multiplicity of infection of 0.01. After the appearance of a cytopathic effect, the cells and supernatant were collected, purified by ultracentrifugation with a 25% sucrose cushion at $36,000 \times g$ for 2 h, and then quantified using the 50% tissue culture infectious dose (TCID₅₀) method (35). To understand the biological relevance of the AAATATT motif in the gene expression pattern of the marseilleviruses, plasmids were drawn that contained the AAATATT sequence and progressive variations of that sequence (GAATATTT, AGATATTT, AAGTATTT, AAAGATTT, AAATGTTT, AAATAGTT, AAATATGT, and AAATATTG). The sequences were located at position -10 relative to the initiation of the eGFP reporter gene. In addition, a GC-rich sequence (GCGCGCGC), a noninfected/transfected amoeba, and a noninfected/nontransfected amoeba were used as controls. One microgram of each plasmid was used to transfect *Acanthamoeba castellanii* cells infected with MsV (multiplicity of infection of 10). The transfections were carried out in duplicate using a Lipofectamine reagent according to the manufacturer's instructions.

For the gene expression analysis, total RNA was purified from cells at 0.5 h (T0.5), 1 h (T1), 2 h (T2), and 3 h (T3) postinfection using a TRIzol reagent (Invitrogen) that was treated with DNase (Invitrogen) and reverse transcribed using Moloney murine leukemia virus reverse transcriptase (200 U/liter; Thermo Fisher Scientific) according to the manufacturer's instructions. The resulting cDNAs were used as a template in a StepOne thermocycler (Applied Biosystems) quantitative PCR assay to target the eGFP gene. Thermal cycling conditions were the following: one cycle at 95°C for 10 min, 40 cycles at 95°C for 10 s and 60°C for 40 s, a melting curve analysis at 95°C for 15 s and 58°C for 15 s, a temperature increase of 1°C per 2 s until a temperature of 95°C was reached, and a final cycle at 95°C for 15 s. The results were analyzed by StepOne software and were analyzed with the $2^{-\Delta\Delta CT}$ method. The amoebas were observed using a Zeiss (LSM 510 META) microscope at 3 hpi.

ACKNOWLEDGMENTS

We are grateful to our colleagues from Laboratório de Vírus of Universidade Federal de Minas Gerais. In addition, we thank CNPq (Conselho Nacional de Desenvolvimento Científico e Tecnológico), CAPES (Coordenação de Aperfeiçoamento de Pessoal de Nível Superior), and FAPEMIG (Fundação de Amparo à Pesquisa do estado de Minas Gerais).

E.G.K., C.A.B., F.G.F., and J.S.A. are CNPq researchers. B.L.S., J.S.A., and E.G.K. are members of a CAPES-COFECUB project.

We have no conflicts of interest to declare.

REFERENCES

- La Scola B, Audic S, Robert C, Jungang L, de Lamballerie X, Drancourt M, Birtles R, Claverie J-M, Raoult D. 2003. A giant virus in amoebae. *Science* 299:2033. <https://doi.org/10.1126/science.1081867>.
- Boyer M, Yutin N, Pagnier I, Barrassi L, Fournous G, Espinosa L, Robert C, Azza S, Sun S, Rossmann MG, Suzan-Monti M, La Scola B, Koonin EV, Raoult D. 2009. Giant Marseillevirus highlights the role of amoebae as a melting pot in emergence of chimeric microorganisms. *Proc Natl Acad Sci U S A* 106:21848–21853. <https://doi.org/10.1073/pnas.0911354106>.
- Fabre E, Jeudy S, Legendre M, Trauchessec M, Claverie J, Abergel C. 2017. Noumeavirus replication relies on a transient remote control of the host nucleus. *Nat Commun* 8:15087. <https://doi.org/10.1038/ncomms15087>.
- Aherfi S, Pagnier I, Fournous G, Raoult D, La Scola B, Colson P. 2013. Complete genome sequence of Cannes 8 virus, a new member of the proposed family "marseilleviridae." *Virus Genes* 47:550–555.
- Poggeorgiev N, Boyer M, Fancello L, Monteil S, Robert C, Rivet R, Nappes C, Azza S, Chiaroni J, Raoult D, Desnues C. 2013. Marseillevirus-like virus recovered from blood donated by asymptomatic humans. *J Infect Dis* 208:1042–1050. <https://doi.org/10.1093/infdis/jit292>.
- Poggeorgiev N, Michel G, Lepidi H, Raoult D, Desnues C. 2013. Marseillevirus adenitis in an 11-month-old child. *J Clin Microbiol* 51:4102–4105. <https://doi.org/10.1128/JCM.01918-13>.
- Dornas FP, Assis FL, Aherfi S, Arantes T, Abrahão JS, Colson P, La Scola B. 2016. A Brazilian marseillevirus is the founding member of a lineage in family Marseilleviridae. *Viruses* 8:76–85. <https://doi.org/10.3390/v8030076>.
- Aherfi S, Boughalmi M, Pagnier I, Fournous G, La Scola B, Raoult D, Colson P. 2014. Complete genome sequence of Tunisivirus, a new member of the proposed family Marseilleviridae. *Arch Virol* 159:2349–2358. <https://doi.org/10.1007/s00705-014-2023-5>.
- Doutre G, Philippe N, Abergel C, Claverie JM. 2014. Genome analysis of the first Marseilleviridae representative from Australia indicates that most of its genes contribute to virus fitness. *J Virol* 88:14340–14349. <https://doi.org/10.1128/JVI.02414-14>.
- Aherfi S, Colson P, Raoult D. 2016. Marseillevirus in the pharynx of a patient with neurologic disorders. *Emerg Infect Dis* 22:2008–2010. <https://doi.org/10.3201/eid2211.160189>.
- Aherfi S, Colson P, Audoly G, Nappes C, Xerri L, Valensi A, Million M, Lepidi H, Costello R, Raoult D. 2016. Marseillevirus in lymphoma: a giant in the lymph node. *Lancet Infect Dis* 10:225–234.
- Takemura M. 2016. Morphological and taxonomic properties of Tokyo-virus, the first Marseilleviridae member isolated from Japan. *Microbes Environ* 31:442–448. <https://doi.org/10.1264/jsm.e2.ME16107>.
- Thomas V, Bertelli C, Collyn F, Casson N, Telenti A, Goesmann A, Croxatto A, Greub G. 2011. Lausannevirus, a giant amoebal virus encoding histone doublets. *Environ Microbiol* 13:1454–1466. <https://doi.org/10.1111/j.1462-2920.2011.02446.x>.
- Boughalmi M, Pagnier I, Aherfi S, Colson P, Raoult D, La Scola B. 2013. First isolation of a marseillevirus in the diptera *Syrphidae eristalis tenax*. *Intervirology* 56:386–394. <https://doi.org/10.1159/000354560>.
- García-Escudero R, Viñuela E. 2000. Structure of African swine fever virus late promoters: requirement of a TATA sequence at the initiation region. *J Virol* 74:8176–8182. <https://doi.org/10.1128/JVI.74.17.8176-8182.2000>.

16. Nalçacıoğlu R, Ince IA, Vlak JM, Demirbâ Z, van Oers MM. 2007. The Chilo iridescent virus DNA polymerase promoter contains an essential AAAAT motif. *J Gen Virol* 88:2488–2494. <https://doi.org/10.1099/vir.0.82947-0>.
17. Fitzgerald LA, Boucher PT, Yanai-Balser GM, Suhre K, Graves MV, Van Etten JL. 2008. Putative gene promoter sequences in the chlorella viruses. *Virology* 380:388–393. <https://doi.org/10.1016/j.virol.2008.07.025>.
18. Salem TZ, Tumey CM, Wang L, Xue J, Wan XF, Cheng XW. 2008. Transcriptional analysis of a major capsid protein gene from *Spodoptera exigua ascovirus* 5a. *Arch Virol* 153:149–162. <https://doi.org/10.1007/s00705-007-1081-3>.
19. Legendre M, Audic S, Poirot O, Hingamp P, Seltzer V, Byrne D, Lartigue A, Lescot M, Bernadac A, Poulain J, Abergel C, Claverie JM. 2010. mRNA deep sequencing reveals 75 new genes and a complex transcriptional landscape in mimivirus. *Genome Res* 20:664–674. <https://doi.org/10.1101/gr.102582.109>.
20. Yang Z, Reynolds SE, Martens CA, Bruno DP, Porcella SF, Moss B. 2011. Expression profiling of the intermediate and late stages of poxvirus replication. *J Virol* 85:9899–9908. <https://doi.org/10.1128/JVI.05446-11>.
21. Oliveira G, Andrade A, Rodrigues R, Arantes T, Boratto P, Silva L, Dornas F, Trindade G, Drummond B, La Scola B, Kroon E, Abrahão J. 2017. Promoter motifs in NCLDVs: an evolutionary perspective. *Viruses* 9:16–32. <https://doi.org/10.3390/v9010016>.
22. Suhre K, Audic S, Claverie J-M. 2005. Mimivirus gene promoters exhibit an unprecedented conservation among all eukaryotes. *Proc Natl Acad Sci U S A* 102:14689–14693. <https://doi.org/10.1073/pnas.0506465102>.
23. Van Etten JL, Graves MV, Müller DG, Boland W, Delaroque N. 2002. *Phycodnaviridae*-large DNA algal viruses. *Arch Virol* 147:1479–1516. <https://doi.org/10.1007/s00705-002-0822-6>.
24. Jakob NJ, Müller K, Bahr U, Darai G. 2001. Analysis of the first complete DNA sequence of an invertebrate iridovirus: coding strategy of the genome of Chilo iridescent virus. *Virology* 286:182–196. <https://doi.org/10.1006/viro.2001.0963>.
25. Fischer MG, Allen MJ, Wilson WH, Suttle CA. 2010. Giant virus with a remarkable complement of genes infects marine zooplankton. *Proc Natl Acad Sci U S A* 107:19508–19513. <https://doi.org/10.1073/pnas.1007615107>.
26. Haberer V, Lenhard B. 2016. Promoter architectures and developmental gene regulation. *Semin Cell Dev Biol* 57:11–23. <https://doi.org/10.1016/j.semcdb.2016.01.014>.
27. Browning DF, Busby SJ. 2004. The regulation of bacterial transcription initiation. *Nat Rev Microbiol* 2:57–65. <https://doi.org/10.1038/nrmicro787>.
28. Davison AJ, Moss B. 1989. Structure of vaccinia virus early promoters. *J Mol Biol* 210:749–769. [https://doi.org/10.1016/0022-2836\(89\)90107-1](https://doi.org/10.1016/0022-2836(89)90107-1).
29. Yates PR, Dixon LK, Turner PC. 1995. Promoter analysis of an *African swine fever virus* gene encoding a putative elongation factor. *Biochem Soc Trans* 23:1395. <https://doi.org/10.1042/bst0231395>.
30. Raoult D, Boyer M. 2010. Amoebae as genitors and reservoirs of giant viruses. *Intervirology* 53:321–329. <https://doi.org/10.1159/000312917>.
31. Andersson JO. 2009. Gene transfer and diversification of microbial eukaryotes. *Annu Rev Microbiol* 63:177–193. <https://doi.org/10.1146/annurev.micro.091208.073203>.
32. Clarke M, Lohan AJ, Liu B, Lagkouvardos I, Roy S, Zafar N, Bertelli C, Schilde C, Kianianmomeni A, Bürglin TR, Frech C, Turcotte B, Kopec KO, Synnott JM, Choo C, Paponov I, Finkler A, Heng Tan CS, Hutchins AP, Weinmeier T, Rattei T, Chu JSC, Gimenez G, Irimia M, Rigden DJ, Fitzpatrick DA, Lorenzo-Morales J, Bateman A, Chiu C-H, Tang P, Hegemann P, Fromm H, Raoult D, Greub G, Miranda-Saavedra D, Chen N, Nash P, Ginger ML, Horn M, Schaap P, Caler L, Loftus BJ. 2013. Genome of *Acanthamoeba castellanii* highlights extensive lateral gene transfer and early evolution of tyrosine kinase signaling. *Genome Biol* 14:R11. <https://doi.org/10.1186/gb-2013-14-2-r11>.
33. Rutherford K, Parkhill J, Crook J, Horsnell T, Rice P, Rajandream MA, Barrell B. 2000. Artemis: sequence visualization and annotation. *Genomics* 16:944–945.
34. Bailey TL, Elkan C. 1994. Fitting a mixture model by expectation maximization to discover motifs in bipolymers. *Proc Second Int Conf Intell Syst Mol Biol* 28–36.
35. Reed LJ, Muench H. 1938. A simple method of estimating fifty per cent endpoints. *Am J Hyg* 27:493–497.

4.3. ARTIGO 3: Putative Promoter Motif Analyses Reinforce the Evolutionary Relationships Among Faustoviruses, Kaumoebavirus, and Asfarvirus.

Este artigo foi publicado no periódico *Frontiers in Microbiology*.

Faustovírus e kaumoebavírus são vírus gigantes relacionados aos vírus da família *Asfarviridae* e pertencentes ao grupo NCLDV. Estudos anteriores demonstraram o papel de motivos ricos em A/T como promotores em asfarvírus. As relações filogenéticas entre esses vírus nos levaram a investigar se as regiões promotoras previamente identificadas no genoma dos vírus da família *Asfarviridae* poderiam ser compartilhadas por faustovírus e kaumoebavírus. Neste estudo, foi confirmada a presença de motivos ricos em A/T nas regiões intergênicas do genoma de asfarvírus e, além disso, foi demonstrado que os motivos TATTT e TATATA também estão presentes em abundância no genoma de faustovírus e kaumoebavírus. Os motivos TATTT e TATATA estão presentes principalmente nas regiões intergênicas do genoma de faustovírus e kaumoebavírus se comparado a sua presença na região codificadora e estão amplamente distribuídos entre 0 e 100 pares de bases a montante do início da tradução. Observamos que os motivos aqui estudados apresentam repetições nas regiões intergênicas do genoma de faustovírus, kaumoebavírus e asfarvírus, o que é similar ao descrito anteriormente para marseillevírus. Os motivos promotores foram identificados na maioria dos genes compartilhados entre faustovírus, kaumoebavírus e asfarvírus sugerindo que os motivos já poderiam estar presentes no ancestral desses vírus antes da irradiação deste grupo. Assim, tomados em conjunto, os resultados demonstrados nesse estudo, fornecem uma análise das possíveis sequências que atuam como promotores em kaumoebavírus e faustovírus, o que reforçou a relação filogenética entre kaumoebavírus, faustovírus e asfarvírus.



Putative Promoter Motif Analyses Reinforce the Evolutionary Relationships Among Faustoviruses, Kaumoebavirus, and Asfarvirus

Grazielle P. Oliveira[†], Isabella L. M. de Aquino[†], Ana P. M. F. Luiz and Jônatas S. Abrahão*

Laboratório de Vírus, Departamento de Microbiologia, Instituto de Ciências Biológicas, Universidade Federal de Minas Gerais, Belo Horizonte, Brazil

OPEN ACCESS

Edited by:

John R. Battista,
Louisiana State University,
United States

Reviewed by:

Hetron Mweemba Munang'andu,
Norwegian University of Life Sciences,
Norway

Chen Peng,
National Institute of Allergy
and Infectious Diseases (NIAID),
United States

*Correspondence:

Jônatas S. Abrahão
jpnatas.abraha@gmail.com

[†]These authors have contributed
equally to this work.

Specialty section:

This article was submitted to
Evolutionary and Genomic
Microbiology,
a section of the journal
Frontiers in Microbiology

Received: 23 January 2018

Accepted: 02 May 2018

Published: 23 May 2018

Citation:

Oliveira GP, de Aquino ILM,
Luiz APMF and Abrahão JS (2018)
Putative Promoter Motif Analyses
Reinforce the Evolutionary
Relationships Among Faustoviruses,
Kaumoebavirus, and Asfarvirus.
Front. Microbiol. 9:1041.
doi: 10.3389/fmicb.2018.01041

Putative promoter motifs have been described in viruses belonging to the nucleocytoplasmic large DNA viruses (NCLDV) group; however, few studies have been conducted to search for promoter sequences in newly discovered amoebal giant viruses. Faustovirus and kaumoebavirus are two *Asfarviridae*-related giant viruses belonging to the NCLDV group. The phylogenetic relationships among these viruses led us to investigate if the promoter regions previously identified in the asfarvirus genome could be shared by its amoebal virus relatives. Previous studies demonstrated the role of A/T-rich motifs as promoters of asfarvirus. In this study, we reinforce the importance of A/T rich motifs in asfarvirus and show that the TATTT and TATATA motifs are also shared in abundance by faustovirus and kaumoebavirus. Here, we demonstrate that TATTT and TATATA are mostly present in faustovirus and kaumoebavirus genomic intergenic regions (IRs) and that they are widely distributed at 0 to –100 bp upstream to the start codons. We observed that putative promoter motifs are present as one to dozens of repetitions in IRs of faustovirus, kaumoebavirus, and asfarvirus, which is similar to that described previously for marseilleviruses. Furthermore, the motifs were found in most of the upstream regions of the core genes of faustovirus, kaumoebavirus, and asfarvirus, which suggests that the motifs could already be present in the ancestor of these viruses before the irradiation of this group. Our work provides an in-depth analysis of the putative promoter motifs present in asfarvirus, kaumoebavirus, and faustovirus, which reinforces the relationship among these viruses.

Keywords: faustovirus, kaumoebavirus, asfarvirus, promoter, core-genes

INTRODUCTION

The nucleocytoplasmic large DNA viruses (NCLDV) group has been expanding in number and diversity since the discovery of the *Acanthamoeba polyphaga mimivirus* (APMV) in 2003 (La Scola et al., 2003; Boyer et al., 2009; Pagnier et al., 2013; Philippe et al., 2013; Legendre et al., 2014, 2015). Faustovirus and kaumoebavirus are two Asfarvirus-related giant viruses that belong to the NCLDV group (Reteno et al., 2015; Bajrai et al., 2016). Faustoviruses strains were first isolated in France and Senegal on *Vermamoeba vermiformis* (Reteno et al., 2015). In addition, the

detection of a faustovirus-like virus has already been described in hematophagous arthropods and in their animal hosts and in human samples (Temmam et al., 2015). Faustovirus has a double-stranded DNA with a circular shape genome (except for the Faustovirus Liban strain for which a linear genome was suggested) with approximately 466 kbp encoding 451 predicted proteins. These viruses form 200 nm particles (icosahedral symmetry) with a unique structure and two protein shells (Reteno et al., 2015; Benamar et al., 2016; Klose et al., 2016; Louazani et al., 2017). Its unique architecture combined with a large number of introns and exons found in gene coding the major capsid protein were associated with the virus's ability to adapt to new environments or hosts (Klose et al., 2016). About two-thirds of the faustovirus genes are ORFans (ORFs with no detectable homolog). Furthermore, paralogous genes represent 19% of the faustovirus gene complement (Boyer et al., 2010; Rinke et al., 2013; Reteno et al., 2015). Similar to marseilleviruses and other giant viruses that infect amoebas, the faustoviruses exhibit a high level of genomic mosaicism, which were identified as proteins hits with other giant viruses, bacteria, eukaryotes, archaea and phages, and that best matches with proteins identified from African swine fever virus (ASFV) (Boyer et al., 2009; Reteno et al., 2015). A phylogenetic analysis revealed a relationship between faustoviruses and asfarvirus, which suggests a shared origin (Reteno et al., 2015; Benamar et al., 2016).

Currently, ASFV is a single member of the *Asfarviridae* family and *Asfivirus* genus. ASFV is a large (~200 nm), icosahedral, and enveloped virus that infects members of the Suidae family (Tulman et al., 2009). Its genome is composed of a linear dsDNA molecule of approximately 170 kbp that encodes approximately 150 ORFs (Yáñez et al., 1995). ASFV encodes its own RNA pol and ASFV genes are transcribed by its enzyme (Kuznar et al., 1980; Salas et al., 1988). The asfarvirus intergenic genomic regions are rich in A/T sequences and the characterization of the promoter motifs for the late asfarvirus gene B646L coding the major capsid protein showed the importance in gene expression of A/T rich regions containing TATTT and TATATA motifs, wherein the sequence located at -2 to +2 appears to be a more critical region for B646L promoter activity (Yáñez et al., 1995; García-Escudero and Viñuela, 2000; Rodríguez and Salas, 2013). Furthermore, biological experiments involving genetic deletions, linker scan substitutions and point mutations in these genomic regions revealed that the replacement of the A/T-rich region by G/C residues strongly reduced the transcription rate and demonstrated the importance of this sequence for viral transcription (Rodríguez et al., 1996; García-Escudero and Viñuela, 2000; Rodríguez and Salas, 2013).

Contributing to the expansion of the NCLDV group, a new giant virus was isolated in sewage water from Saudi Arabia and named Kaumobavirus (Bajrai et al., 2016). The kaumobavirus have a morphology (~250 nm icosahedral capsids) and genome (350,731 bp double-stranded DNA genome coding 465 genes) similar to faustoviruses. Furthermore, this giant virus was isolated on the same amoeba as faustovirus (*Vermamoeba vermiformis*) and the best matches to its proteins are to faustoviruses and asfarviruses. Accordingly, phylogenetic analysis showed

that kaumobavirus is a distant relative of faustoviruses and asfarviruses (Bajrai et al., 2016).

Promoter motifs have been described in viruses that belong to the NCLDV group such as in poxviruses, iridoviruses, phycodnaviruses, ascovirus, and asfarvirus (García-Escudero and Viñuela, 2000; Suhre et al., 2005; Nalçacioğlu et al., 2007; Fitzgerald et al., 2008; Salem et al., 2008; Legendre et al., 2010; Yang et al., 2011; Oliveira et al., 2017a). However, little is known about the promoter sequences in giant viruses since the putative promoter motif has been described only for the mimivirus and marseillevirus families (Suhre et al., 2005; Oliveira et al., 2017b). Here, we reinforce the importance of A/T rich motifs (TATTT and TATATA) in asfarvirus and for the first time identified those motifs as supposed sequences that can function as putative promoters in faustovirus and kaumobavirus. Furthermore, in conjunction with core gene analyses, we suggest that TATTT and TATATA motifs could be present in the ancestor of faustovirus, kaumobavirus, and asfarvirus.

MATERIALS AND METHODS

Motif Analyses

The genomic sequences of faustoviruses, kaumobavirus, and asfarvirus were analyzed: seven faustovirus strains (faustovirus strain E12-the prototype member, faustovirus D5a, faustovirus D5b, faustovirus D6, faustovirus E23, faustovirus E24, and faustovirus ST1); kaumobavirus (kaumobavirus isolate Sc) and asfarvirus (ASFV strain BA71V). The genome sequences used here are available in GenBank under accession numbers KJ614390.1; KU702950.1; KU702949.1; KU702951.1; KU702952.1; KU702948.1; LT839607.1; NC_034249.1; and NC_001659.2. The intergenic regions (IRs) of these viruses were obtained using Artemis software (Rutherford et al., 2000). A total of 489 genomic IR were obtained from the faustovirus E12 genome (274 in the positive strand and 215 in the negative strand), 487 from the faustovirus D5a genome (272 in the positive strand and 215 in the negative strand), 484 from the faustovirus D5b genome (208 in the positive strand and 276 in the negative strand), 486 from the faustovirus D6 genome (271 in the positive strand and 215 in the negative strand), 492 from the faustovirus E23 genome (277 in the positive strand and 215 in the negative strand), 492 from the faustovirus E24 genome (275 in the positive strand and 217 in the negative strand), 470 from the faustovirus ST1 genome (272 in the positive strand and 198 in the negative strand), 423 from the kaumobavirus genome (260 in the positive strand and 163 in the negative strand), and 141 from the asfarvirus genome (70 in the positive strand and 71 in the negative strand). The accession numbers and the IR data are shown in **Table 1**. The total number of IR that we considered in the analysis were 485 for faustovirus E12, 484 for faustovirus D5a, 478 for faustovirus D5b, 480 for faustovirus D6, 487 for faustovirus E23, 488 for faustovirus E24, 467 for faustovirus ST1, 417 for kaumobavirus, and 135 for asfarvirus (the IR that contained less than 8 bp were not considered). The search for motifs was performed in IR and in coding sequences (CSs) by manual analysis for all of the viral species mentioned above. The

TABLE 1 | Accession numbers and intergenic regions data of the faustoviruses, kaumoebavirus, and asfarvirus strains.

	Strains	Accession number	Number of intergenic regions	
			Positive strand	Negative strand
Faustoviruses	E12	KJ614390.1	274	215
	D5a	KU702950.1	272	215
	D5b	KU702949.1	208	276
	D6	KU702951.1	271	215
	E23	KU702952.1	277	215
	E24	KU702948.1	275	217
	ST1	LT839607.1	272	198
Kaumoebavirus	Sc	NC_034249.1	260	163
Asfarvirus	BA71V	NC_001659.2	70	71

distance between the motifs and the start codon was calculated for faustovirus E12, kaumoebavirus, and asfarvirus. The graphs were generated using GraphPad Prism version 7.00 (GraphPad Software).

Phylogenetic Analyses

Complete DNA polymerase B protein sequences were aligned using the MUSCLE program (Edgar, 2004). Evolutionary analyses were conducted in MEGA7 (Kumar et al., 2016). The phylogenetic analyses were inferred by using the maximum likelihood method based on the JTT matrix-based model (Jones et al., 1992). The percentage of trees in which the associated taxa clustered together is shown next to the branches. The bootstrap values above 800 are shown. The analysis involved 41 DNA polymerase B amino acid sequences. The accession numbers are shown in the phylogenetic tree.

Core-Genes Analysis

The Proteinortho tool (Lechner et al., 2011) was used to define the strict core of orthologs shared among the Faustovirus E12 strain, the Kaumoebavirus isolate Sc and ASFV strain BA71V. The core of orthologs shared among the Faustovirus E12 strain and the Kaumoebavirus isolate Sc and among were defined, among the Kaumoebavirus isolate Sc and the ASFV strain BA71V and among the Faustovirus E12 strain and the ASFV strain BA71V. The thresholds for the *e*-value, identity and coverage of amino acid sequences were 10^{-5} , 25 and 50%, respectively. The distribution of the motif sequences was evaluated in upstream regions of the core genes by manual analyses.

RESULTS

A/T Rich Promoters Motifs of the Asfarvirus in Genomic Intergenic Regions of the Faustovirus and Kaumoebavirus

The search for repeated motifs in the IR of faustovirus and kaumoebavirus revealed the presence of regions containing A/T

rich motifs, which play a promoter role in asfarvirus. To evaluate the distribution of motifs in the IR of faustovirus, kaumoebavirus, and asfarvirus, we searched and counted the number of IR that present any of the motifs. We observed that the motifs occurred in 418 of the 485 (86.19%) genomic IR of the faustovirus. In kaumoebavirus and asfarvirus, the motifs were found in 278 of 417 (66.67%) genomic IR and 112 of 135 (82.96%) genomic IR, respectively (Figure 1A). Moreover, the motifs were found alone (TATTT or TATATA) or in pairs (TATTT/TATATA) in the same IR of faustovirus, kaumoebavirus, and asfarvirus. A total of 41.03% (199/485) of the IR of the faustovirus presented only the TATTT motif, 2.27% (11/485) of the faustovirus IR presented only the TATATA and 42.89% (208/485) of the faustovirus IR presented both motifs (Figures 1B,C). In kaumoebavirus, 43.41% (181/417) of the IR presented only TATTT, 3.12% (13/417) of the IR only presented TATATA and 20.14% (84/417) presented both motifs (Figures 1B,C). In asfarvirus, 34.07% (46/135) of the IR presented only TATTT, 6.67% (9/135) of the IR only presented TATATA and 42.22% (57/135) presented both motifs (Figures 1B,C).

Distribution of the TATTT and TATATA Motifs and Its Localization Upstream of the ATG

A search and quantification of the motifs TATTT and TATATA was conducted in the genomic IR and in CSs of the strains of faustoviruses, kaumoebavirus, and asfarvirus. A total of 2608 (68.24% of the total motifs) TATTT motif copies were found in the IR of the faustovirus E12 strain, 1132 (69.45%) TATTT motif copies were found in the IR of the kaumoebavirus and 865 (65.18%) TATTT motif copies were found in the IR of the asfarvirus. Significantly less copies were found of this motif in the CS: 1214 (31.76%) TATTT motif copies were found in the CS of the faustovirus, 498 (30.55%) TATTT motif copies were found in the CS of the Kaumoebavirus and 462 (34.82%) TATTT motif copies were found in the CS of the asfarvirus (Figure 2A). Although it is present in a smaller quantity if compared to the TATTT motif, a higher prevalence in the IR was also demonstrated for the TATATA motif, which was found 590 (66.44%) TATATA motif copies in the IR of the faustovirus E12 strain and only 298 (33.56%) in the CS, 150 (71.09%) TATATA motif copies in the IR of the kaumoebavirus and only 61 (28.91%) in the CS. For asfarvirus were found 157 (73.36%) TATATA motif copies in the IR and only 57 (26.64%) times in the CS (Figure 2A). We expanded this analysis to other faustovirus isolates, and we observed similar results (Figure 2B). In the faustovirus D5a strain, 69.73% of the total TATTT motifs were found in their IR; in the faustovirus D5b, D6, E23, E24 and ST1 strains, this motif was found in 68.56, 68.55, 69.31, 69.39, and 68.92% of the IR, respectively. TATATA was found in 68.50, 71.78, 71.96, 67.49, 67.27, and 69.03% of the TATATA motifs in the IR of the faustovirus strains D5a, D5b, D6, E23, E24, and ST1, respectively. The localization relative to the start codon was identified for both motifs in faustovirus, kaumoebavirus, and asfarvirus. The TATTT and TATATA motifs are located mainly up to -100 base pairs (bp)

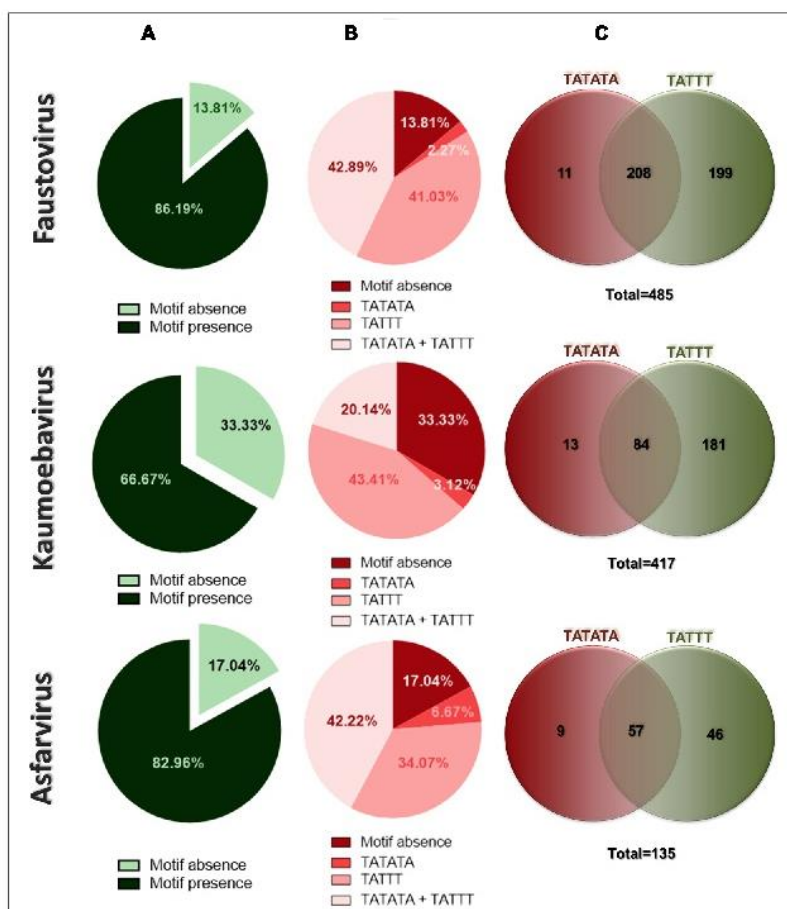


FIGURE 1 | Percentage of intergenic regions (IRs) containing the TATTT and TATATA motifs: faustovirus, kaumobavirus, and asfarvirus. **(A)** The total distribution of TATTT and TATATA motifs in the IRs. **(B)** The differential distribution of only the TATTT or TATATA motifs of both motifs in the same IR. **(C)** A Venn diagram representing the absolute number of IRs containing only TATTT or TATATA motifs and of those with both motifs.

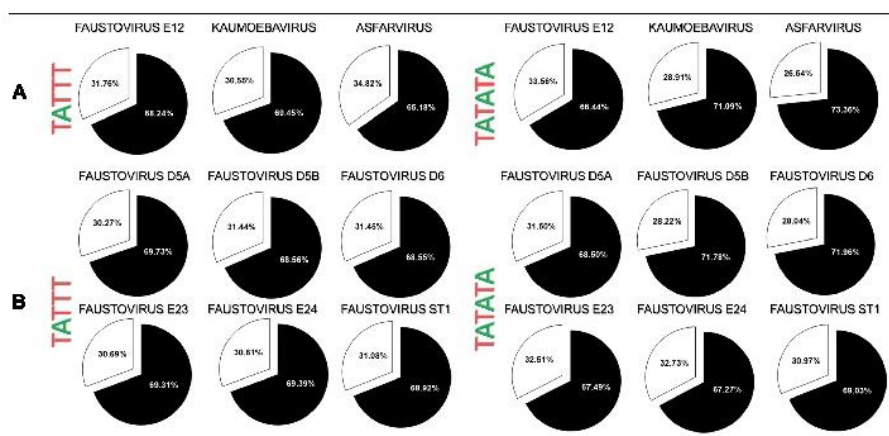
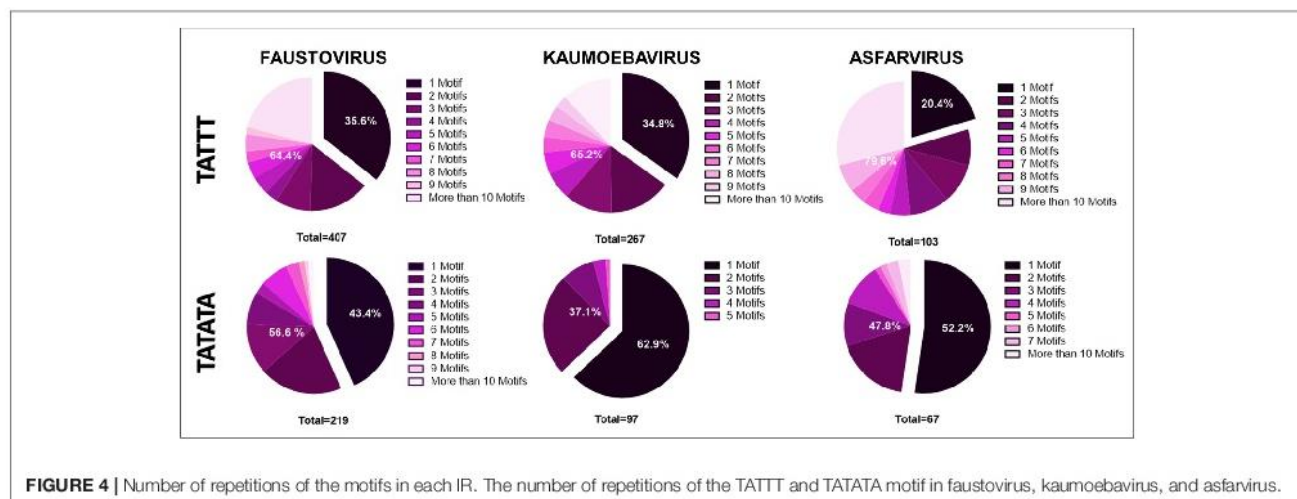
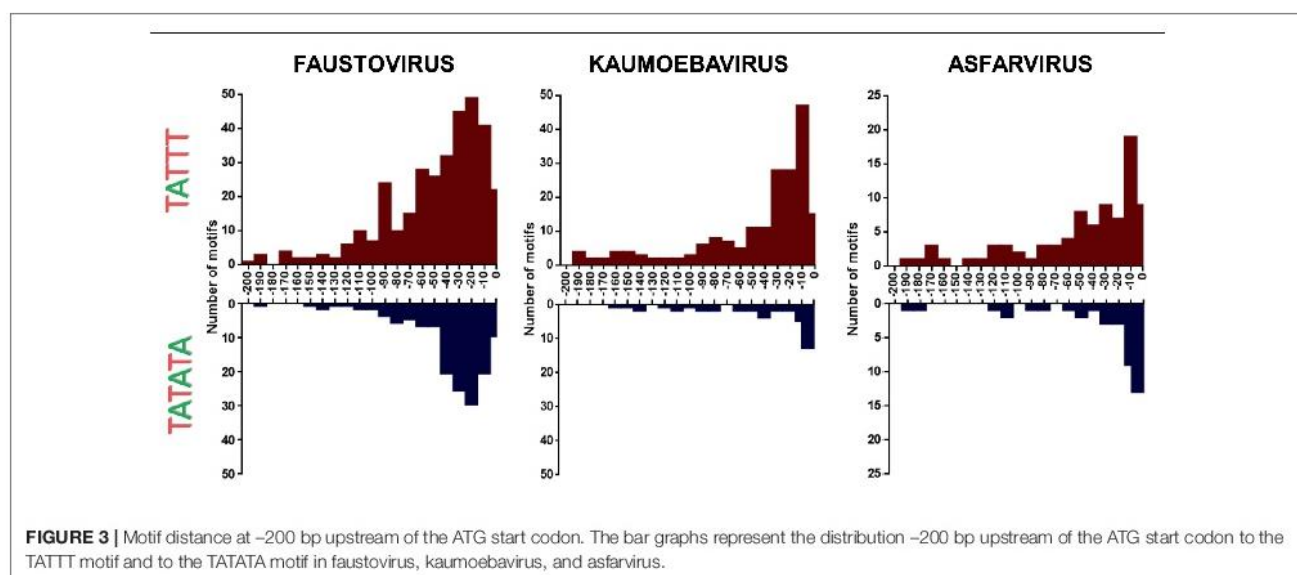


FIGURE 2 | Occurrence of the TATTT/TATATA motifs in genomic IRs or coding sequences (CSs) of faustovirus, kaumobavirus, and asfarvirus genomes. **(A)** The prevalence of the TATTT/TATATA motifs in faustovirus E12, kaumobavirus, and asfarvirus genomes and in other faustovirus strains **(B)**. The distribution of the TATTT/TATATA motifs in genomic IRs and in CSs is represented by a circle with black and white colors, respectively.



upstream of ATG (Figure 3). More specifically, the TATTT motifs are located mainly at 0 to -100 bp upstream from the ATG and the TATATA motifs are located mainly at 0 to -50 bp of faustovirus genes, while in kaumobavirus and asfarvirus the TATTT and TATATA motifs are located mainly at 0 to -50 bp and 0 to -20 bp from the start codon, respectively (Figure 3).

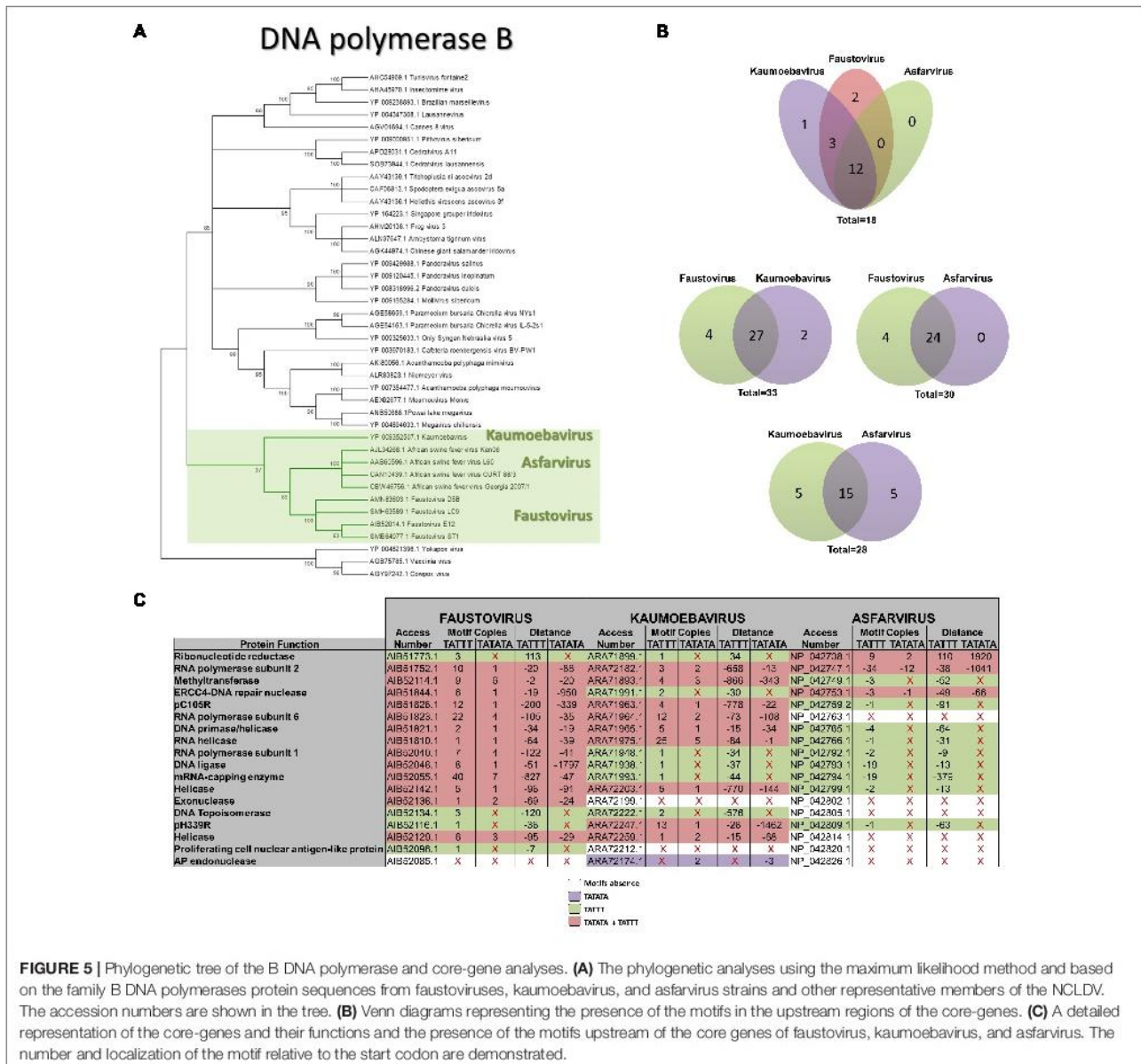
Repetitions of the TATTT and TATATA Motif in Genomic Intergenic Regions

The quantification of the motifs present in each genomic IR showed that 35.6% (145/407) of the faustovirus IR have only one copy of the TATTT motif and 64.4% (262/407) present more than one copy of the same motif (Figure 4). In kaumobavirus, only one copy of the TATTT motif was found in 34.8% (93/267) of the IR and more than one TATTT motif copy was observed in 65.2% (174/267) of the IR (Figure 4). A similar profile was observed in asfarvirus since 20.4% (21/103) of its

IR presents only one copy of the TATTT motif and 79.6% (82/103) show more than one copy of the motif (Figure 4). Regarding the TATATA motif, the occurrence of one motif copy in 43.4% (95/219), 62.9% (61/97), and 52.2% (35/67) of the genomic IR of the faustovirus, kaumobavirus, and asfarvirus was demonstrated, respectively (Figure 4). More than one copy of the TATATA motif was observed in 56.6% (124/219) of the faustovirus genomic IR, in 37.1% (36/97) of the kaumobavirus genomic IR and in 47.8% (32/67) of the asfarvirus genomic IR (Figure 4).

Distribution of the TATTT and TATATA Motifs at Core Genes' Upstream Regions of Faustoviruses, Kaumobavirus, and Asfarvirus

The phylogenetic relationship among faustovirus, kaumobavirus, and asfarvirus was reinforced in this study by the phylogenetic



reconstruction based on family B DNA polymerase (Figure 5A). We performed a comparative analysis of the faustovirus, kaumobavirus, and asfarvirus complete gene set with the aim of determining the core genes among this group of viruses. Our data reveals 18 genes that are shared by these three viruses, 28 core-genes that are shared between kaumobavirus and asfarvirus, 30 core-genes that are shared between faustovirus and asfarvirus and 33 core-genes that are shared between faustovirus and kaumobavirus. The search by the TATTT and TATATA motif sequences in the upstream regions of these genes revealed that most of the core genes (12/18) of the faustovirus, kaumobavirus, and asfarvirus had at least one of the motifs in their upstream region (Figures 5B,C). We also observed that among the 33 core-genes shared by faustovirus

and kaumobavirus, 27 present the putative promoter motifs. Considering faustovirus and asfarvirus, we observed that among their 30 core-genes, 24 shared the motifs, and among the 28 core-genes shared by kaumobavirus and asfarvirus, 15 present the putative promoter motifs (Figure 5B). This represents the presence of at least one of the motifs in 94.4, 88.9, and 66.7% at the IR upstream to the core genes of faustoviruses, kaumobaviruses and asfarviruses, respectively. Furthermore, it represents a higher perception of motif presence in core genes than that observed for the rest of the genome of faustovirus (86.2%) and kaumobavirus (66.7%); however, for asfarviruses, the perception of core genes presenting at least one of the promoter motifs is smaller than the rest of the genome (82.9%).

DISCUSSION

Genomic studies have revealed that faustovirus, kaumobavirus, and asfarvirus are phylogenetically related (Reteno et al., 2015; Bajrai et al., 2016). In this study, the search for repeated motifs in the IR of faustovirus and kaumobavirus revealed the wide distribution of the TATTT and TATATA motifs that play a promoter role in asfarvirus (Rodríguez et al., 1996; García-Escudero and Viñuela, 2000; Rodríguez and Salas, 2013). Given the phylogenetic proximity demonstrated between faustovirus, kaumobavirus, and asfarvirus and associated with the wide distribution of the same motifs in the IR of these viruses, we suggest that the regions containing the motifs TATTT and TATATA can also play an important role in the gene expression of faustovirus and kaumobavirus. It has already been demonstrated that ASFV encodes its own RNA pol and ASFV genes are transcribed by its enzyme (Kuznar et al., 1980; Salas et al., 1988). The RNA pol sequences were also predicted in the genome of faustovirus and kaumobavirus. Although studies have not been conducted to demonstrate the actual activity of RNA polymerase in the expression of their genes, we believe that this is the case, which reinforces the presence of a similar promoter sequence in these viruses since their RNA polymerase subunits constitute core genes in these viruses and reflect a common origin. Previous studies showed a wide distribution of putative promoter motif in the IR of mimivirus, and half of the genes present the AAAATTGA in their upstream region. Similar results were described for marseilleviruses, and more than half of the genes demonstrated the presence of the motif promoter in its upstream regions (Suhre et al., 2005; Oliveira et al., 2017b). The analyses showed that the putative promoter motifs were found alone (TATTT or TATATA) or in pairs (TATTT/TATATA) in the same IR of faustovirus, kaumobavirus, and asfarvirus. As previously demonstrated for asfarvirus, these data may suggest that the motifs TATTT and TATATA can act simultaneously in a given IR of faustovirus and kaumobavirus (Rodríguez and Salas, 2013). The distribution analyses of the motifs TATTT and TATATA demonstrated a significantly higher occurrence of the TATTT and TATATA motifs in the genomic IR compared to CS for all of the analyzed viruses. Furthermore, the TATTT and TATATA motifs are located mainly at 0 to -100 base pairs upstream of ATG follow a similar promoter localization profile demonstrated for other organisms. The TATA Box is a classical promoter element of eukaryotes that are located in IRs approximately at -25 to -30 bp upstream of the transcription start site (Haberle and Lenhard, 2016). Bacterial genomes present short conserved motifs that are also rich in A/T, which are located approximately -10 and -35 bp upstream of the transcription start site (Browning and Busby, 2004). Regions rich in A/T at the 150 bp position upstream of ATG are predicted promoter sequences for other NCLDV members, such as poxviruses, asfarviruses, phycodnaviruses, iridoviruses, and for the mimiviruses, which are the first discovered amoebal giant viruses (García-Escudero and Viñuela, 2000; Suhre et al., 2005; Nalçacıoğlu et al., 2007; Fitzgerald et al., 2008; Salem et al., 2008; Legendre et al., 2010; Yang et al., 2011). Furthermore, the same localization profile

was also observed for marseillevirus, which is a giant virus that belongs to the NCLDV group (Oliveira et al., 2017b). Despite the fact that the importance of the specific positions of the motifs have already been demonstrated for asfarvirus gene expression, the role of the motifs in different IR positions for faustovirus and kaumobavirus should not be discarded. For this reason, we considered more localization possibilities in our analysis. In this study was showed that the IRs of the faustovirus, kaumobavirus, and asfarvirus display multiple repetitions of the TATTT and TATATA motifs, but it is not the first time that multiple copies of putative promoter motifs' have been described. A recent study suggested that the promoter sequence repetition in the marseillevirus genome can be associated with lateral-gene-transfer (LGT) events (Oliveira et al., 2017b). It has been suggested that viruses with large dsDNA genomes can evolve by gene acquisition from the genomes of cellular organisms and their hosts. Indeed, many genes of these viruses show high levels of sequence similarity to their cellular homologs, which is apparently indicative of relatively recent acquisition by the viral genomes (Bugert and Darai, 2000). Previous works suggest that LGT events are common among NCLDV (Boyer et al., 2009). In this way, it is noteworthy that both faustovirus and kaumobavirus exhibit a high level of genomic mosaicism that can be associated with LGT events (Reteno et al., 2015; Bajrai et al., 2016). Furthermore, paralogous genes represent 19% of the faustovirus gene complement and motif repetitions may be related to genetic duplications in the genome of these viruses.

The core genes' analysis revealed that most of the orthologous genes shared among faustovirus, kaumobavirus, and asfarvirus show the same predicted motif sequence. These data suggest that the motif here described sequences could be present in the ancestor of faustovirus, kaumobavirus, and asfarvirus. There is still much to learn about the structure of the promoters and the identity of transcription factors, which regulate the gene expression in giant viruses; however, with each new analysis, we can add a brick to this construction of knowledge.

AUTHOR CONTRIBUTIONS

GO, IdA, and AL performed the analyses. JA designed the study. GO, IdA, and JA wrote the manuscript. All authors approved the manuscript.

ACKNOWLEDGMENTS

We are grateful to our colleagues from the Laboratório de Vírus of Universidade Federal de Minas Gerais. In addition, we would like to thank PRPq-UFMG (Pró Reitoria de Pesquisa da Universidade Federal de Minas Gerais), PRPg-UFMG (Pró-Reitoria de Pós-Graduação da Universidade Federal de Minas Gerais), CNPq (Conselho Nacional de Desenvolvimento Científico e Tecnológico), CAPES (Coordenação de Aperfeiçoamento de Pessoal de Nível Superior), and FAPEMIG (Fundação de Amparo à Pesquisa do Estado de Minas Gerais). JA is a CNPq researcher.

REFERENCES

- Bajrai, L. H., Benamar, S., Azhar, E. I., Robert, C., Levasseur, A., Raoult, D., et al. (2016). Kaumoebavirus, a new virus that clusters with faustoviruses and *Asfarviridae*. *Viruses* 8:E278. doi: 10.3390/v8110278
- Benamar, S., Reteno, D. G., Bandaly, V., Labas, N., Raoult, D., and La Scola, B. (2016). Faustoviruses: comparative genomics of new *Megavirales* family members. *Front. Microbiol.* 7:3. doi: 10.3389/fmicb.2016.00003
- Boyer, M., Gimenez, G., Suzan-Monti, M., and Raoult, D. (2010). Classification and determination of possible origins of ORFans through analysis of nucleocytoplasmic large DNA viruses. *Intervirology* 53, 310–320. doi: 10.1159/000312916
- Boyer, M., Yutin, N., Pagnier, I., Barrassi, L., Fournous, G., Espinosa, L., et al. (2009). Giant Marseillevirus highlights the role of amoebae as a melting pot in emergence of chimeric microorganisms. *Proc. Natl. Acad. Sci. U.S.A.* 106, 21848–21853. doi: 10.1073/pnas.0911354106
- Browning, D. F., and Busby, S. J. (2004). The regulation of bacterial transcription initiation. *Nat. Rev. Microbiol.* 2, 57–65. doi: 10.1038/nrmicro787
- Bugert, J. J., and Darai, G. (2000). Poxvirus homologues of cellular genes. *Virus Genes* 21, 111–133. doi: 10.1023/A:1008140615106
- Edgar, R. C. (2004). MUSCLE: a multiple sequence alignment method with reduced time and space complexity. *BMC Bioinformatics* 5:113. doi: 10.1186/1471-2105-5-113
- Fitzgerald, L. A., Boucher, P. T., Yanai-Balser, G. M., Suhre, K., Graves, M. V., and Van Etten, J. L. (2008). Putative gene promoter sequences in the chlorella viruses. *Virology* 380, 388–393. doi: 10.1016/j.virol.2008.07.025
- García-Escudero, R., and Viñuela, E. (2000). Structure of African swine fever virus Late Promoters: requirement of a TATA sequence at the initiation region. *J. Virol.* 74, 8176–8182. doi: 10.1128/JVI.74.17.8176-8182.2000
- Haberle, V., and Lenhard, B. (2016). Promoter architectures and developmental gene regulation. *Semin. Cell Dev. Biol.* 57, 11–23. doi: 10.1016/j.semcdb.2016.01.0144
- Jones, D. T., Taylor, W. R., and Thornton, J. M. (1992). The rapid generation of mutation data matrices from protein sequences. *Comput. Appl. Biosci.* 8, 275–282. doi: 10.1093/bioinformatics/8.3.275
- Klose, T., Reteno, D. G., Benamar, S., Hollerbach, A., Colson, P., La Scola, B., et al. (2016). Structure of faustovirus, a large dsDNA virus. *Proc. Natl. Acad. Sci. U.S.A.* 113, 6206–6211. doi: 10.1073/pnas.1523999113
- Kumar, S., Stecher, G., and Tamura, K. (2016). MEGA7: molecular evolutionary genetics analysis version 7.0 for bigger datasets. *Mol. Biol. Evol.* 33, 1870–1874. doi: 10.1093/molbev/msw054
- Kuznar, J., Salas, M. L., and Vinuela, E. (1980). DNA-dependent RNA polymerase in African swine fever virus. *Virology* 101, 169–175. doi: 10.1016/0042-6822(80)90493-6
- La Scola, B., Audic, S., Robert, C., Jungang, L., de Lamballerie, X., Drancourt, M., et al. (2003). A giant virus in amoebas. *Science* 299:2033. doi: 10.1126/science.1081867
- Lechner, M., Findeiss, S., Steiner, L., Marz, M., Stadler, P. F., and Prohaska, S. J. (2011). Proteinortho: detection of (co-)orthologs in large-scale analysis. *BMC Bioinformatics* 12:124. doi: 10.1186/1471-2105-12-124
- Legendre, M., Audic, S., Poirot, O., Hingamp, P., Seltzer, V., Byrne, D., et al. (2010). mRNA deep sequencing reveals 75 new genes and a complex transcriptional landscape in Mimivirus. *Genome Res.* 20, 664–674. doi: 10.1101/gr.102582.109
- Legendre, M., Bartoli, J., Shmakova, L., Jeudy, S., Labadie, K., Adrait, A., et al. (2014). Thirty-thousand-year-old distant relative of giant icosahedral DNA viruses with a pandoravirus morphology. *Proc. Natl. Acad. Sci. U.S.A.* 111, 4274–4279. doi: 10.1073/pnas.1320670111
- Legendre, M., Lartigue, A., Bertaux, L., Jeudy, S., Bartoli, J., Lescot, M., et al. (2015). In-depth study of *Mollivirus sibericum*, a new 30,000-y-old giant virus infecting *Acanthamoeba*. *Proc. Natl. Acad. Sci. U.S.A.* 112, E5327–E5335. doi: 10.1073/pnas.1510795112
- Louazani, A., Andreani, J., Ouahache, M., Aherfi, S., Baptiste, E., Levasseur, A., et al. (2017). Genome sequences of new Faustovirus strains ST1 and LC9, isolated from the south of France. *Genome Announc.* 5:e00613-17. doi: 10.1128/genomeA.00613-17
- Nałcacioglu, R., Ince, I. A., Vlak, J. M., Demirbag, Z., and van Oers, M. M. (2007). The Chilo iridescent virus DNA polymerase promoter contains an essential AAAAT motif. *J. Gen. Virol.* 88, 2488–2494. doi: 10.1099/vir.0.82947-0
- Oliveira, G., Andrade, A., Rodrigues, R., Arantes, T., Boratto, P., Silva, L., et al. (2017a). Promoter motifs in NCLDVs: an evolutionary perspective. *Viruses* 9, E16–E32. doi: 10.3390/v9010016
- Oliveira, G., Lima, M., Arantes, T., Assis, F., Rodrigues, R., da Fonseca, F. G., et al. (2017b). The investigation of promoter sequences of marseilleviruses highlights a remarkable abundance of the AAATATTT motif in intergenic regions. *J. Virol.* 21:e1088-17. doi: 10.1128/JVI.01088-17
- Pagnier, I., Reteno, D. G., Saadi, H., Boughalmi, M., Gaia, M., Slimani, M., et al. (2013). A decade of improvements in Mimiviridae and Marseilleviridae isolation from amoeba. *Intervirology* 56, 354–363. doi: 10.1159/000354556
- Philippe, N., Legendre, M., Doutre, G., Coute, Y., Poirot, O., Lescot, M., et al. (2013). Pandoraviruses: amoeba viruses with genomes up to 2.5 Mb reaching that of parasitic eukaryotes. *Science* 341, 281–286. doi: 10.1126/science.1239181
- Reteno, D. G., Benamar, S., Khalil, J. B., Andreani, J., Armstrong, N., Klose, T., et al. (2015). Faustovirus, an asfarvirus related new lineage of giant viruses infecting amoebae. *J. Virol.* 89, 6585–6594. doi: 10.1128/JVI.00115-15
- Rinke, C., Schwientek, P., Sczyrba, A., Ivanova, N. N., Anderson, I. J., Cheng, J. F., et al. (2013). Insights into the phylogeny and coding potential of microbial dark matter. *Nature* 499, 431–437. doi: 10.1038/nature12352
- Rodriguez, J. M., and Salas, M. L. (2013). African swine fever virus transcription. *Virus Res.* 173, 15–28. doi: 10.1016/j.virusres.2012.09.014
- Rodriguez, J. M., Salas, M. L., and Viñuela, E. (1996). Intermediate class of mRNAs in African swine fever virus. *J. Virol.* 70, 8584–8589.
- Rutherford, K., Parkhill, J., Crook, J., Horsnell, T., Rice, P., and Rajandream, M. A. (2000). Artemis: sequence visualization and annotation. *Bioinformatics* 16, 944–945. doi: 10.1093/bioinformatics/16.10.944
- Salas, J., Salas, M. L., and Vinuela, E. (1988). Effect of inhibitors of the host cell RNA polymerase II on African swine fever virus multiplication. *Virology* 164, 280–283. doi: 10.1016/0042-6822(88)90646-0
- Salem, T. Z., Turney, C. M., Wang, L., Xue, J., Wan, X. F., and Cheng, X. W. (2008). Transcriptional analysis of a major capsid protein gene from *Spodoptera exigua* ascovirus 5a. *Arch. Virol.* 153, 149–162. doi: 10.1007/s00705-007-1081-3
- Suhre, K., Audic, S., and Claverie, J. M. (2005). Mimivirus gene promoters exhibit an unprecedented conservation among all eukaryotes. *Proc. Natl. Acad. Sci. U.S.A.* 102, 14689–14693. doi: 10.1073/pnas.0506465102
- Temmam, S., Montel-Bouchard, S., Sambou, M., Aubadie-Ladrix, M., Azza, S., Decloquement, P., et al. (2015). Faustovirus-like Asfarvirus in hematophagous biting midges and their vertebrate hosts. *Front. Microbiol.* 6:1406. doi: 10.3389/fmicb.2015.01406
- Tulman, E. R., Delhon, G. A., Ku, B. K., and Rock, D. L. (2009). African swine fever virus. *Curr. Top. Microbiol. Immunol.* 328, 43–87. doi: 10.1007/978-3-540-68618-7_2
- Yáñez, R. J., Rodríguez, J. M., Nogal, M. L., Yuste, L., Enríquez, C., Rodríguez, J. F., et al. (1995). Analysis of the complete nucleotide sequence of African swine fever virus. *Virology* 208, 249–278. doi: 10.1006/viro.1995.1149
- Yang, Z., Reynolds, S. E., Martens, C. A., Bruno, D. P., Porcella, S. F., and Moss, B. (2011). Expression profiling of the intermediate and late stages of poxvirus replication. *J. Virol.* 85, 9899–9908. doi: 10.1128/JVI.05446-11

Conflict of Interest Statement: The authors declare that the research was conducted in the absence of any commercial or financial relationships that could be construed as a potential conflict of interest.

Copyright © 2018 Oliveira, de Aquino, Luiz and Abrahão. This is an open-access article distributed under the terms of the Creative Commons Attribution License (CC BY). The use, distribution or reproduction in other forums is permitted, provided the original author(s) and the copyright owner are credited and that the original publication in this journal is cited, in accordance with accepted academic practice. No use, distribution or reproduction is permitted which does not comply with these terms.

4.4. ARTIGO 4: Tupanvirus-infected amoebas are induced to aggregate with uninfected cells promoting viral dissemination

Este artigo está em fase final de revisão pelos coautores e será submetido ao periódico Scientific Reports após as modificações que serão feitas seguindo as sugestões fornecidas pela banca avaliadora.

Nos últimos anos a descoberta de vírus gigantes tem impressionado a comunidade científica principalmente devido ao tamanho das suas partículas e à complexidade dos seus genomas. Entre essas descobertas, o nosso grupo de pesquisa descreveu recentemente o tupanvírus, cujas partículas apresentam uma cauda longa e o genoma contém o conjunto mais completo de genes relacionados à tradução já descritos na virosfera conhecida. Aqui nós descrevemos um novo tipo de interação vírus-hospedeiro, envolvendo o tupanvírus. Observamos que amebas infectadas por tupanvírus são induzidas a se agregarem a células não infectadas, promovendo a disseminação viral e formando cachos de células. Em seguida hipotetizamos que a interação entre células infectadas e não infectadas poderia ser promovida pela expressão de um gene que codifica uma proteína ligadora de manose presente na ameba e que interessantemente foi também aqui demonstrado ser codificado pelo tupanvírus. A fim de investigar essa hipótese, nós analisamos a expressão dos genes codificadores do receptor de manose viral e celular, na presença e ausência de manose livre, bem como a formação dos cachos. Nossas investigações demonstraram que a manose livre inibiu a formação de cachos, de maneira dependente da concentração, sugerindo que a formação de cachos no ciclo de multiplicação do tupanvírus correlaciona com a expressão dos genes que codifica a proteína ligadora de manose tanto viral quanto celular. Ao induzir a expressão desses genes, o tupanvírus promove a formação de grandes grupos de células infectadas e não infectadas. Deste modo, as células infectadas agem como “zumbis” controlados por tupanvírus, interagindo e ligando-se a células não infectadas, melhorando as chances de a recém-formada progênie viral encontrar uma nova célula hospedeira para se propagar.

Classification: Biological Sciences – Microbiology

Title: Tupanvirus-infected amoebas are induced to aggregate with uninfected cells promoting viral dissemination

Authors: Grazielle Pereira Oliveira^a, Lorena Christine Ferreira da Silva^a, Thiago Leão^a, Said Mougari^b, Flávio Guimarães da Fonseca^a; Erna Geessien Kroon^a, Bernard La Scola^b, Jônatas Santos Abrahão^{a*}

Authors affiliation: ^a*Departamento de Microbiologia, Instituto de Ciências Biológicas, Universidade Federal de Minas Gerais, Belo Horizonte, Minas Gerais, Brazil- postal code 31270-901;* ^b *URMITE, Aix Marseille Université, UM63, CNRS 7278, IRD 198, INSERM 1095, IHU - Méditerranée Infection, AP-HM, 19-21 boulevard Jean Moulin, 13005 Marseille, France*

***Corresponding author:** Jônatas Santos Abrahão, Departamento de Microbiologia, Universidade Federal de Minas Gerais, Belo Horizonte, Minas Gerais, Brazil, postal code 31270-901, +55 31 3409-3002, jonatas.abrahao@gmail.com.

Abstract

The discovery of giant viruses in the last years has fascinated the scientific community due to virus particles size and genome complexity. Among such fantastic discoveries, we have recently described tupanviruses, which particles present a long tail, and has a genome that contains the most complete set of translation-related genes ever reported in the known virosphere. Here we describe a new kind of virus-host interaction involving tupanvirus. We observed that tupanvirus-infected amoebas were induced to aggregate with uninfected cells, promoting viral dissemination and forming giant host cell bunches. Even after mechanical breakdown of bunches, amoebas reaggregated within a few minutes. This remarkable interaction between infected and uninfected cells seems to be promoted by the expression of a mannose receptor gene. Our investigations demonstrate that the pre-treatment of amoebas with free mannose inhibits the formation of bunches, in a concentration-dependent manner, suggesting that amoebal-bunch formation correlates with mannose receptor gene expression. Finally, our data suggest that bunch-forming cells are able to interact with uninfected cells promoting the dissemination and increase of tupanvirus progeny.

Keywords

Tupanviruses, cytopathic effect, bunches, mannose, mannose-binding protein.

Significance Statement

One of the most important challenges for viruses in nature is to find their permissive hosts. The infection of free-living amoebas by giant viruses, for example, is depending on a random encounter between cells and viruses. Here we describe a mechanism developed by tupanviruses (a giant virus) to keep permissive hosts available and around to a cell infected by them. Tupanviruses induces the expression of cellular and viral mannose receptor genes, which are well known for promote amoebas adhesion to other cells. By inducing those genes, tupanvirus promotes the formation of large bunches of infected and non-infected cells. In this way, infected cells act like “zombies” controlled by tupanviruses, attaching to uninfected cells, improving the chances of the just formed viral progeny to find a new host cell to propagate.

Introduction

The recent discovery of tupanvirus, one of the largest and most complex viruses isolated to date, has reinforced the structural and genomic complexity of the giant viruses (Abrahão JS, et al., 2018). Tupanviruses strains has been isolated from soda lakes, known as the most extreme aquatic environments, and from ocean sediments collected at a depth of 3000m (Sorokin DY, et al.,2014; Abrahão JS, et al., 2018). Phylogenetic analyzes showed the clustering of the tupanvirus with members of the family *Mimiviridae*. However, there are many peculiarities that make the tupanviruses unique entities in the known virosphere. Since its first observation tupanvirus proved to be a virus with unimaginable morphological characteristics since it had an optically visible particles average size about 1.2 μ m that can reach lengths up to 2.3 μ m due plasticity of a long tail attached to the capsid (Abrahão JS, et al., 2018). Tupanvirus has the largest host range described among amoebal-infecting giant viruses so far and can causes a shutdown of host rRNA likely related to host-nucleolus degradation (La Scola B, et al., 2003; Boyer M, et al., 2009; Philippe N, et al., 2013; Legendre M, et al., 2014; Legendre M, et al., 2015; Reteno DG, et al., 2015; Andreani, J. et al. 2016; Abrahão, JS et al., 2018). The tupanviruses replication cycle is similar to demonstrated to other mimiviruses, in which viral particles attach to the host-cell surface and enter through phagocytosis. Then the viral inner membrane fuses with the phagosome membrane, releasing the genome and a viral factory (VF) is then formed where particle

morphogenesis occurs ending by cell lysis and the release of viruses (Andrade, AC et al., 2017 ; Abrahão, JS et al., 2018). The study of its genome further aroused the interest of virologists not only due of its large size (~1.5Mb) but mainly because these viruses shows the largest translational apparatus described that is composed by up to 70 tRNA, 20 aaRS, 11 factors associated to translation, and factors related to tRNA/mRNA maturation and ribosome protein modification, lacking only the ribosome in gene set related to translation (Abrahão, JS et al., 2018). In addition to the robust translation apparatus, tupanvirus presents a gene encoding mannose-specific lectin, also called mannose-binding protein (MBP) (Abrahão, JS et al., 2018). Interestingly, previous studies revealed that *Acanthamoeba castellanii* express an MBP and that mannose sugar can inhibit the adhesion of *A. castellanii* to surfaces, suggesting that the MBP plays a role in the pathogenesis of *Acanthamoeba* infection (Allen PG, Dawidowicz EA, 1990; Yang Z, et al., 1997; Cao Z, et al., 1998; Garate M, et al., 2004, Garate M, et al., 2005; Kim JH, et al., 2012). In this work, we describe a mechanism developed by tupanviruses to keep permissive hosts available and around to a cell infected by them. Tupanviruses induces the expression of cellular and viral mannose receptor genes, which are well known for promote amoebas adhesion to other cells. Tupanvirus promotes the formation of large bunches of infected and non-infected cells. In this context, infected cells act like “zombies” controlled by tupanviruses, searching and attaching to uninfected cells, improving the chances of the just formed viral progeny to find a new host cell to propagate.

Results and discussion

Characterization of the tupanvirus cytopathic effect: a giant virus inducing cell aggregation

In order to characterize the cytopathic effect (CPE) triggered by tupanvirus, *A. castellanii* cells were infected and observed up to 72 h.p.i (Fig. 1).

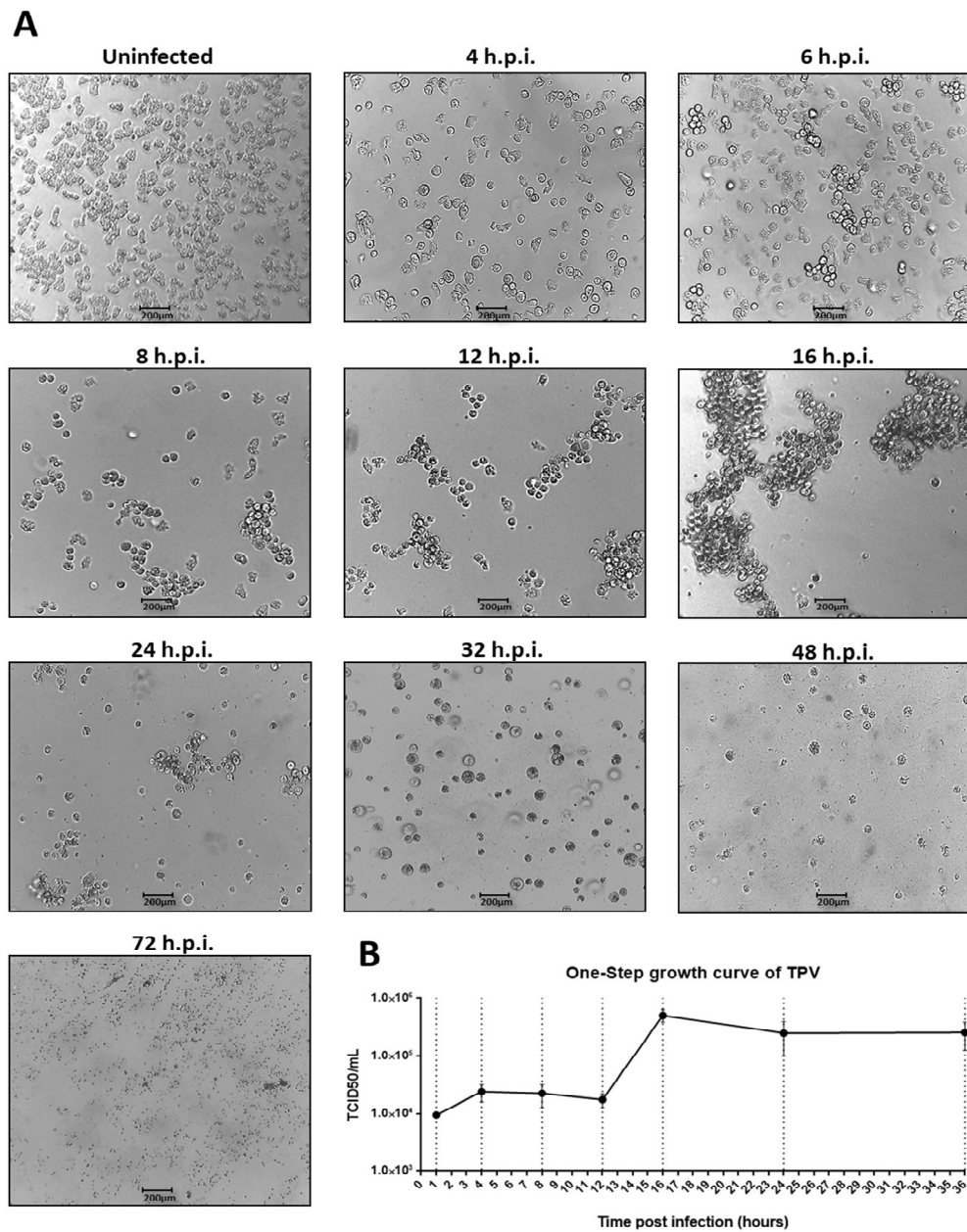


Fig. 1. Characterization of tupanvirus' cytopathic effect. Tupanvirus inducing cytopathic effects (CPEs) in an *A. castellanii* monolayer visualized by light microscopy. The CPEs was manifested by cell rounding approximately 4 h after the inoculation of *A. castellanii* monolayer. Approximately 6h after tupanvirus inoculation was observed the agglomeration of cells culminating in the formation of a characteristic effect referred as "bunches". The presence of bunches becomes more evident in 8, 12 and 16 h.p.i (when almost all the cells are clustered forming large bunches). The Cell lysis becomes more evident at 24 h.p.i. Around 32 h.p.i was observed a disaggregation of bunches. The end times are characterized by cell lysis (48 h.p.i) and a large amount of particles dispersed in the medium (72 h.p.i). (Scale bar, 200µm) (A). The one-step growth curve was constructed at an M.O.I of 10 in duplicate. The infected amoebae were collected and tittered. Error bars indicate SDs (B).

The cells became rounded and lost their adherence and this effect becomes more evident at 4 h.p.i as showed in figure 1. Interestingly, unlike of the other mimivirus as well as other known amoebal infecting-giant viruses, tupanvirus exhibits a peculiar CPE characterized by amoebae aggregation called "bunches". The formation of the "bunches" starts approximately at 6 h.p.i and becomes more evident at 8, 12 and 16 h.p.i (when almost all the cells are seen incorporated to large bunches) (Fig. 1A). Bunches that were formed up to 16 h.p.i were named here as early bunches. From 24 h.p.i., despite the presence of (late) bunches, cell lysis can be observed, concomitant with the reduction of bunches size. At 32 h.p.i., it was observed the complete disaggregation of bunches and at 48-72 h.p.i the majority of amoebae were lysed (Fig. 1A).

In order to better understand how viral infection develops into cells belonging to the "bunches", different times of infection (at an M.O.I. of 10) were selected for immunofluorescence assay (IF) (using anti-tupan antibody) and transmission/scanning electron microscopy (TEM and SEM). IF assays revealed that at times 0 and 1h.p.i. tupanvirus particles appear attached to amoebas (Fig. 2), even after cell washing step, suggesting that the virion fibrils could be important to early interaction to host-cells, as demonstrated to mimiviruses (Rodrigues RA, et al., 2015).

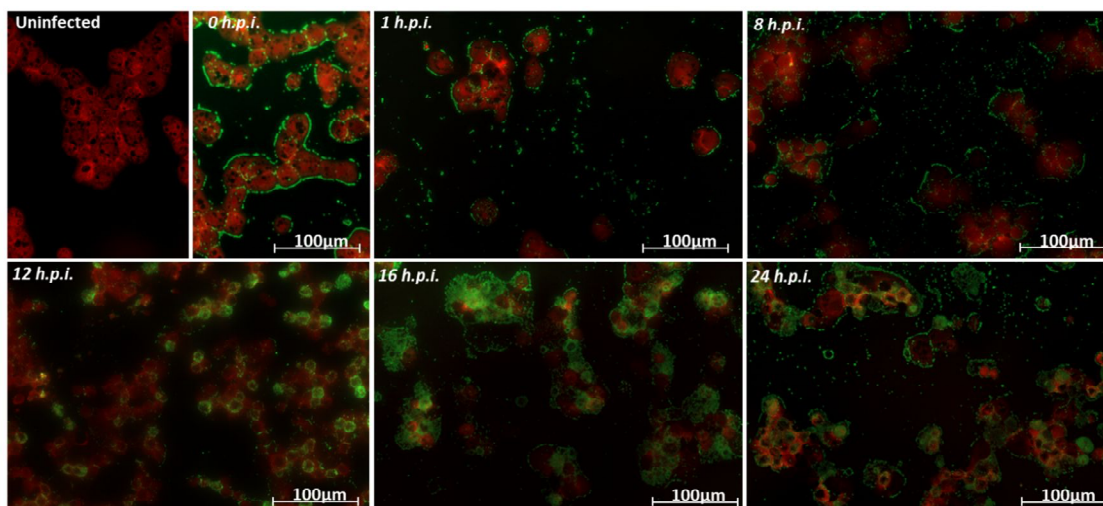


Fig. 2. Characterization of tupanvirus cycle in *A. castellanii* visualized by immunofluorescence. Tupanvirus particles are shown on the amoebae surface. The viral factory is formed between 8 and 12 h.p.i. At 16 and 24 h.p.i the *A. castellanii* cytoplasm is filled of the viral particles and cell lysis is observed at 24 h.p.i. The viral particles in green detected by anti-tupan particle antibody and amoeba cytoskeleton in red detected by evans blue. Scale bar, 100 μ m.

A long eclipse phase (Fig 1B and 2) was observed, and viral factories start to be detected by IF into amoebas` cytoplasm at 12h.p.i. Curiously, even at high multiplicity of infection (M.O.I.) it was not possible to observe a synchronous infection of all cells, being one more peculiarity related to tupanvirus that needs further investigation. Remarkably, we observed by IF at 12 h.p.i, 16 h.p.i and 24 h.p.i amoebas with or without viral factory/particles into cytoplasm, suggesting that bunches are formed by the association of uninfected cells and cells infected under different stages of the viral cycle (Fig. 2). This data was confirmed by SEM (Fig. 3A) and TEM(Fig. 3B), in which it was possible to observe bunches of amoebas presenting cells fulfilled/releasing tupanvirus particles associated to cells presenting intact plasmatic membrane and few particles inside of them (Fig. 3). This experiment was also performed at low M.O.I. (0.01) and the bunches formation was also observed, although presenting temporal differences in bunches appearance (Suppl. Fig 1).

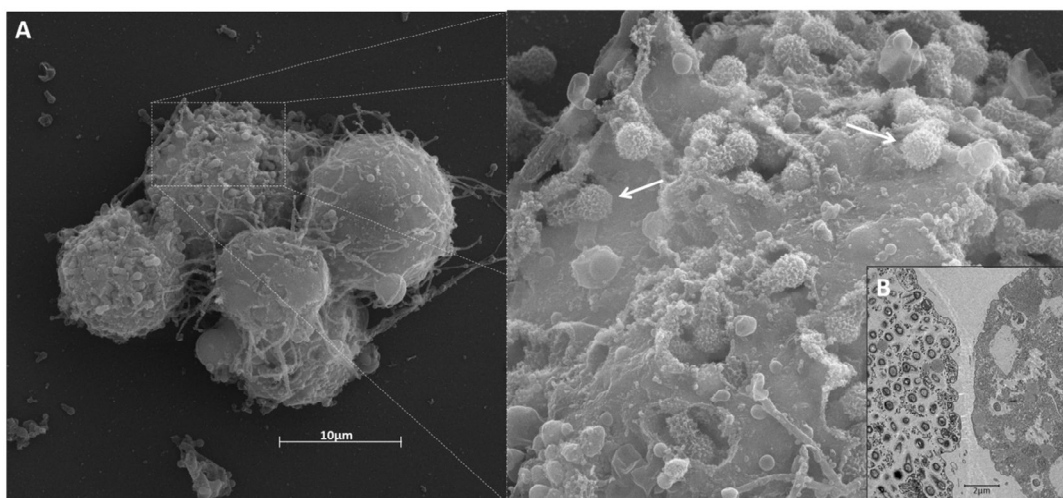
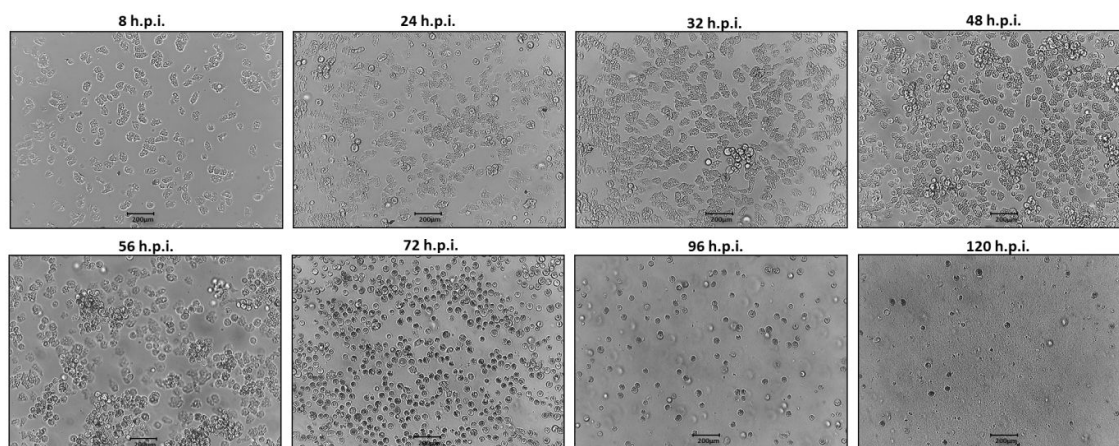


Fig. 3. Electron microscopy images of bunches. Scanning electron microscopy (A) and transmission electron microscopy (B) images of bunches formed by tupanvirus showing *A. castellanii* cells at different stages of infection. White arrows indicate the tupanvirus particles being released from amoebas. Scale bars, 2 µm and 10 µm.



Suppl. Fig 1. Characterization of tupanvirus' cytopathic effect at low M.O.I. *Acanthamoeba castellanii* infected at an M.O.I 0.01 shows rounding approximately 24 h.p.i. Approximately 32 h.p.i the bunches were observed and becomes more evident in 48 and 56 h.p.i. Around 72 h.p.i was observed a disaggregation of bunches. The end times are characterized by cell lysis (96 h.p.i) and a large amount of particles dispersed in the medium (120 h.p.i) (Scale bar, 200 µm).

Amoebal “early-bunches” reform after mechanical separation of cells

Another phenomenon that draw our attention was the occurrence of bunch reformation after its mechanical breakdown (Fig. 4). Initially, we observed that early and late bunches can be easily disaggregated by homogenization using a pipette or by vortexing. However, it was possible to observe that, 30 minutes after disaggregation, cells from early bunches (12h.p.i.) attract to each other, forming large clusters of cells and assuming a similar appearance as early bunches before separation of cells. In contrast, the reformation of the late bunches (24 h.p.i) was not observed. In addition, at light microscopy, a cell belonging to late bunches presented increased volumes, especially after the disaggregation procedure (Fig. 4).

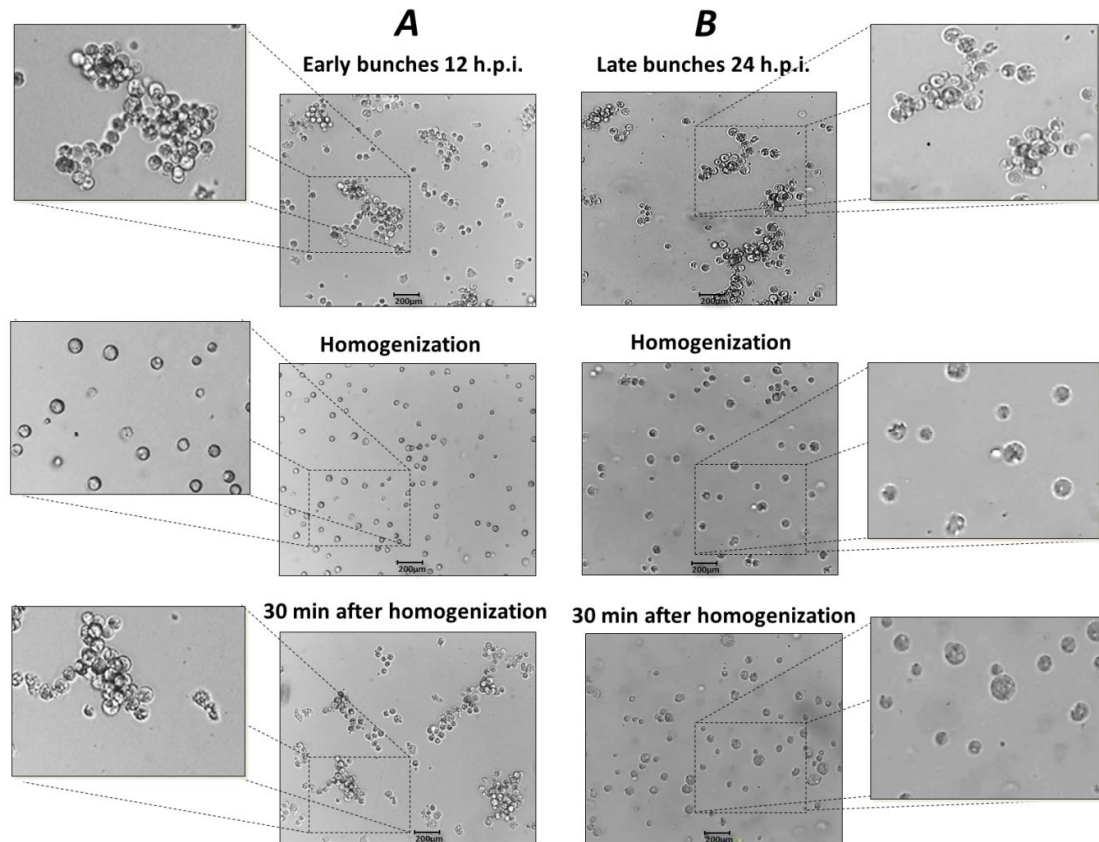


Fig. 4. Bunches re-aggregation profile. Re-aggregation of the early bunches 30 min after disassociation (A). Re-aggregation of late bunches was not observed (B). Scale bar, 200μm.

The lack of bunch reformation of cell at late times indicates that at 24h.p.i. cells are already dead by viral infection, and a simple homogenization would be able to permanently disaggregate the cells attached in late bunches. To confirm this hypothesis, we performed SEM of late bunches (24h.p.i.). Interestingly, we observed cells presenting plasmatic membrane almost completely degraded and fulfilled with an intricate network of tupanvirus particles and cell debris (Fig. 5).

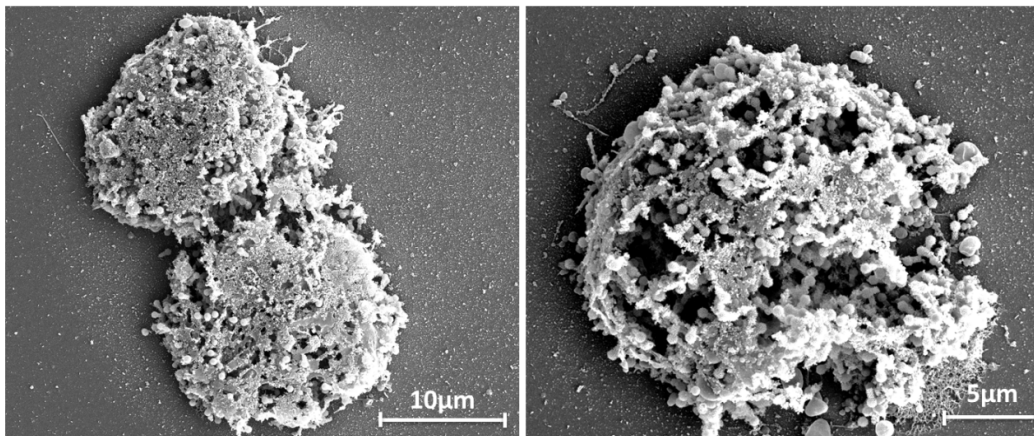


Fig. 5. *A. castellanii* cells intensely damaged at 24 h.p.i. (Scale bars, 5 µm and 10µm).

Taken together, our data demonstrated that tupanvirus promotes the formation of large aggregations of amoebas, containing infected and non-infected cells, whose are able to re-aggregate as long as cells are still alive. These remarkable findings motivated us to investigate a possible factor that may interfere in “bunches” formation and the possible biological relevance of “bunches” promoted by tupanvirus infection.

Amoebal-bunches formation correlates with viral and cellular mannose receptor genes expression

Acanthamoeba spp. is widely distributed in the environment and can cause human diseases associated mainly with immunocompromised patients and contact lenses wearers. Furthermore, *Acanthamoeba* spp. has a relevant role in ecosystems associated with its ability to act as host for microbial pathogens (Niederhorn JY, 1999; Marciano-Cabral F and Cabral G., 2003; Khan NA., 2006; Siddiqui R, Khan NA., 2012). Mannose receptor genes are well known for promote amoebas interaction to other cells. In this way, previous studies revealed that a mannose-binding protein (MBP) present on the surface of *Acanthamoeba* is one of the major virulence proteins and may be essential for pathogenesis and invasion in host cells (Allen PG, Dawidowicz EA, 1990; Garate M, et al., 2005). Garate et al, 2006 demonstrated that the potential of *Acanthamoeba* pathogenicity is directly dependent on the level of MBP, which is expressed on the surface of the amoeba (Garate M, et al., 2006). In addition, previous studies showed that *A. castellanii* treated with mannose had its adhesion and cytotoxicity reduced strongly suggesting that its pathogenicity is associated with the MBP (Allen PG, Dawidowicz EA, 1990; Yoo KT et al., 2012).

Interestingly, after an in-depth analysis of tupanvirus SL genome, we found that this virus presents an MBP gene that presents 525bp. The domain contains a three-fold internal repeat and the consensus sequence motif QXDXNXVXY is involved in mannose recognition. A previous study has shown that the sub domains QDN may be essential for the functionality of the protein. In addition, it was demonstrated the importance of subdomain Y in MBP-mannose interaction (Barre A, et al., 1997). This finding led us to investigate the MBP viral and cellular expression during the multiplication of tupanvirus and the possible implications of the free mannose on bunches formation. The analyses of MBP in uninfected *A. castellanii* cells showed a basal level of MBP transcript expression, since it is essential for cellular processes (Fig. 6A). However, during tupanvirus infection, the expression levels of cellular MBP transcripts significantly increased (P value: 0.0001) at earlier times of infection (1h.p.i; 2h.p.i and 4h.p.i.), suggesting that cellular MBP gene expression induced by tupanvirus precedes in few hours bunches formation (6h.p.i.) (Fig. 1A and 6A). Regarding tupanvirus encoding MBP, we observed a gradual increasing (or accumulation) of transcripts through

infection time-course. High levels of viral MBP transcripts could be observed from 4h.p.i. until 8h.p.i (Fig. 6B). Therefore, our data indicate that the expression of both cellular and the viral MBP genes is induced during tupanvirus infection, suggesting a possible relevance of this gene in the viral replication cycle (Fig. 6).

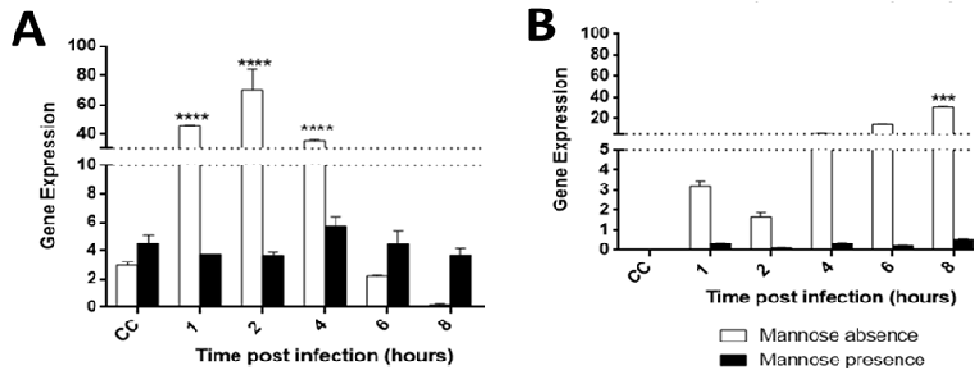
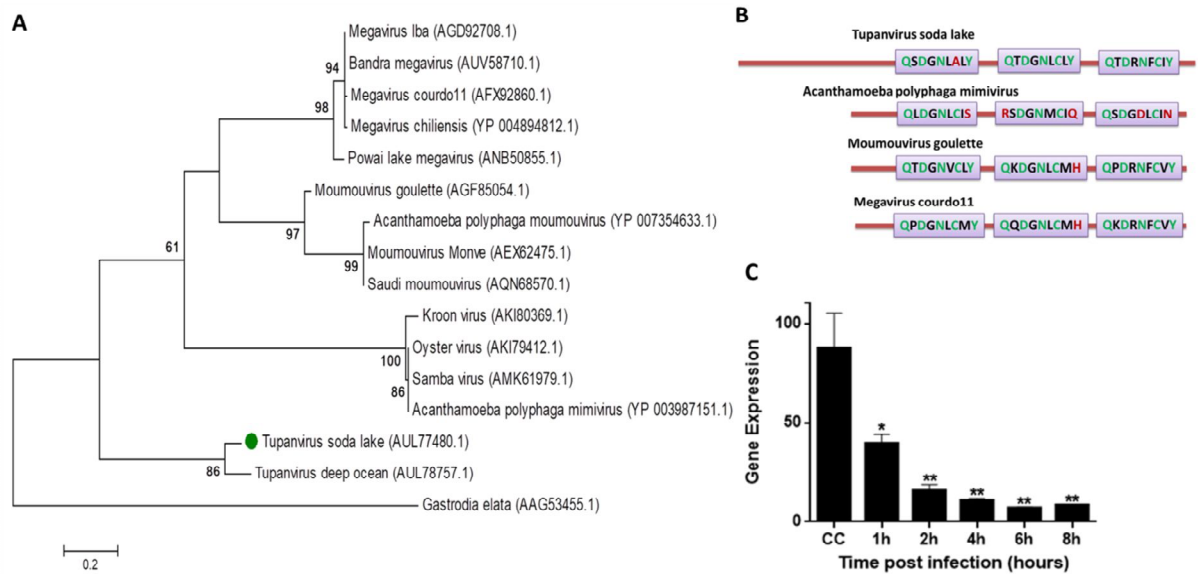


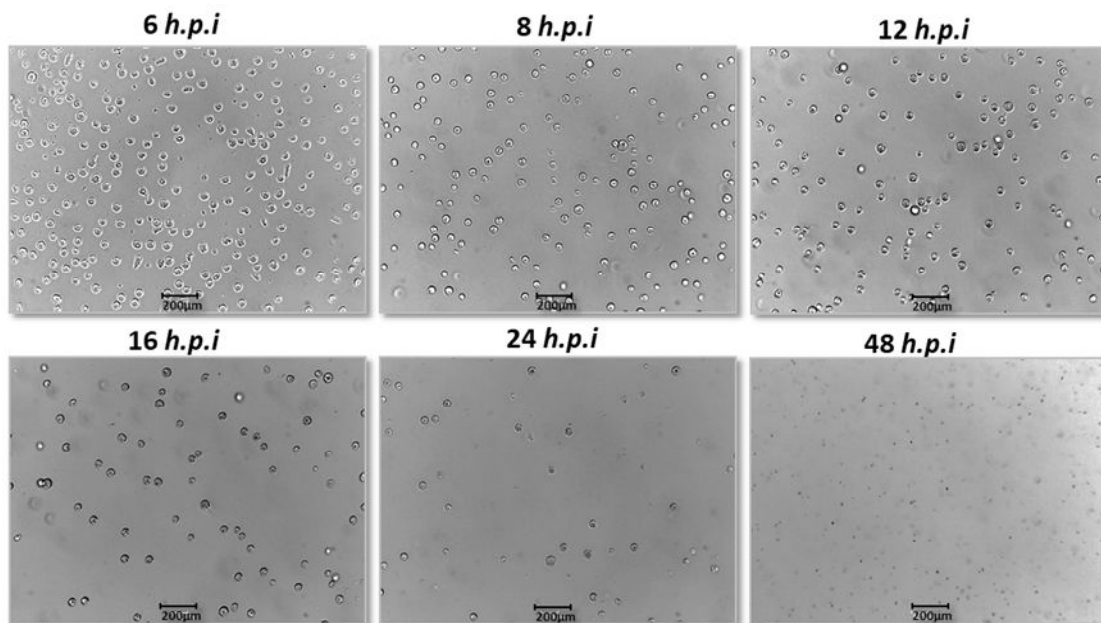
Fig. 6. Transcript analyses of the mannose binding protein. Mannose binding protein cellular (A) and viral (B). A. *castellanii* cells were infected and collected at 1h, 2h, 4h, 6h, 8h post-infection and mannose binding protein transcripts was measured by qPCR. The data were calculated using the $2^{-\Delta\Delta Ct}$ method and were represented as the standard deviation of two independent biological assays. Error bars indicate SDs. The statistical significance was given by a two-tailed 2 way ANOVA test, Tukey's range test ****, $P < 0.0001$, performed using GraphPad Prism software.

Although MBP gene has been found in the genome of other members of the *Mimiviridae* family, such as in the prototype *acanthamoeba polyphaga* mimivirus (APMV) (Suppl. Fig 2A), it has been observed that APMV displays modifications in QDN subdomains, that were associated with loss of MBP function in a previous study (Suppl. Fig 2B). Variations in subdomain Y have also been shown to be important for the MBP-mannose interaction and here was demonstrate that only tupanvirus presents these conserved subdomains (Suppl. Fig 2B) (Barre A, *et al.*, 1997). The analysis of similarity shows that the initial portion of tupanvirus MBP presented low similarity when comparing to other representative members of the *Mimiviridae* family (Suppl. Fig 2B). In addition, we demonstrated that APMV inhibits the cellular MBP gene expression, unlike that observed for tupanvirus (Suppl. Fig 2C).



Suppl. Fig 2. Phylogenetic tree and domains comparison of the MBP (A-B) and transcript expression analyses of the cellular MBP in APMV replication cycle (C). The phylogenetic analyses using the maximum likelihood method and based on the MBP amino acid sequences from tupanvirus and other representative members of the *Mimiviridae* family. The accession numbers are shown in the tree. A. castellanii cells were infected and collected at 1h, 2h, 4h, 6h, 8h post-infection and mannose binding protein transcripts was measured by qPCR. The data were calculated using the $2^{-\Delta\Delta Ct}$ method and were represented as the standard deviation of two independent biological assays. Error bars indicate SDs. The statistical significance was given by a two-tailed 2 way ANOVA test, Tukey's range test **, $P < 0.01$, performed using GraphPad Prism software.

Considering that APMV does not induce the bunches formation during its multiplication cycle (Suppl. Fig 3), these data reinforce the possible role of the MBP gene in bunches formation in tupanvirus multiplication cycle.



Suppl. Fig 3. Characterization of *Acanthamoeba polyphaga mimivirus*' cytopathic effect. *Acanthamoeba polyphaga mimivirus* infecting *Acanthamoeba castellanii* at an M.O.I 10 shows rounding and cell lysis. (Scale bar, 200μm).

Previous works had demonstrated that free-mannose negatively affects *Acanthamoeba* adhesion to surfaces and interferes with amoeba pathogenicity (Kim JH, et al., 2012; Yoo KT et al., 2012). Therefore, we decided to evaluate the impact of free-mannose in cellular and viral MBP gene expression, in uninfected and tupanvirus-infected cells. We observed that free mannose affects negatively the expression of cellular MBP gene, maintaining it close to basal levels (Fig. 6A). The same negative effect was observed in relation to the expression of the tupanvirus MBP gene (Fig. 6B). Considering these results, we decided to evaluate the effect of free mannose on the cytopathic effect of tupanvirus. Interestingly, when free mannose is added to culture medium at time 0 h.p.i., there is inhibition of bunches formation in dose-dependent way (Fig. 7), suggesting that no amoebal-bunches formation correlates with the suppression of the expression of viral and cellular MBP genes.

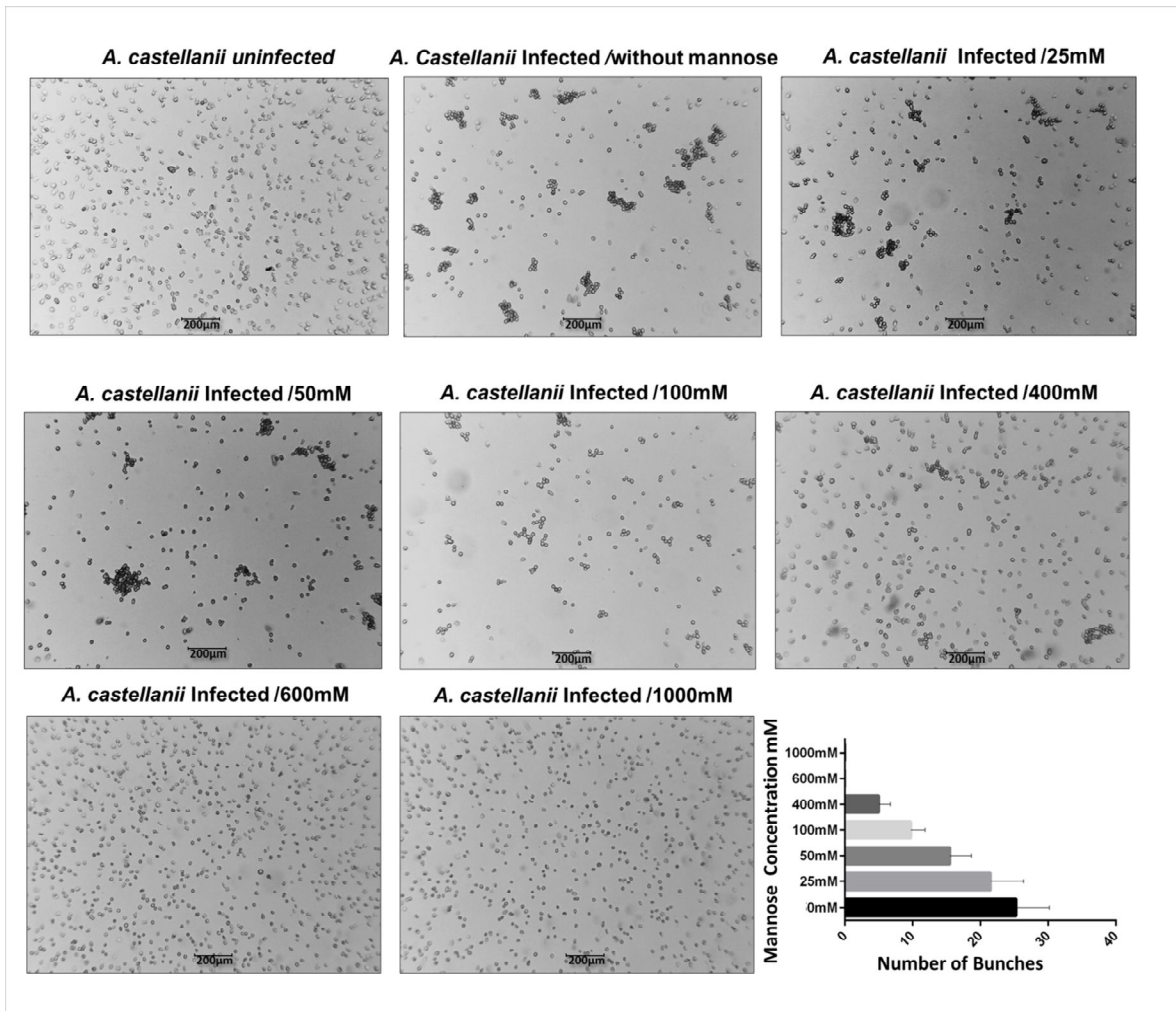
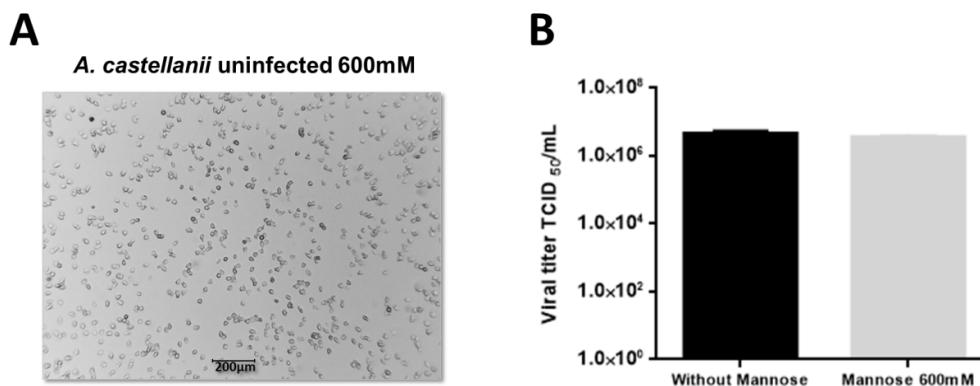


Fig. 7. Effect of mannose in tupanvirus' cytopathic effect. Tupanvirus' cytopathic effect in PAS medium contained mannose at concentrations ranging from 25 to 1000mM. The *A. castellanii* cells were observed under an optical microscope and visualized at 8 h.p.i. *A. castellanii* cells cultivated in PAS medium without mannose and containing mannose (600mM) but uninfected was used as the negative control. The bar graphs represent the number of bunches in different concentrations of mannose. Error bars indicate SDs. (Scale bar, 200µm).

Despite inhibiting the formation of amoebal bunches, the treatment of amoebas with 600nM mannose did not affect the replication of tupanviruses in amoebas (Suppl. Fig 4B). To date, no visible cytotoxic effects were observed in uninfected *A. castellanii* treated with 600mM mannose (Suppl. Fig 4A).



Suppl. Fig 4. Lack of cytotoxic effects and viral replication in *A. castellanii* treated with mannose. No visible cytotoxic effects were observed in uninfected *A. castellanii* treated with 600mM mannose (A). The treatment of amoebas with 600mM mannose did not affect the replication of tupanviruses (B) (Scale bar, 200µm). The statistical significance was given by a two-tailed Student's t-test, performed using GraphPad Prism software. Error bars indicate SDs.

Previous studies have shown that *Acanthamoeba* MBP is itself a glycoprotein containing mannose (Garate M, et al., 2005) that may be one of the factors that explains the formation of the bunches in cells infected by tupanvirus, since it induces the expression of cellular and viral MBP. Thus, the induction of mannose receptor gene expression in the tupanvirus cycle may be important for optimize the formation of bunches since the interaction between amoebas may occur through interaction between their receptors. In this way, with the inhibition of mannose receptor expression the amoebae cells have a lower potential for interaction among them.

Tupanvirus-infected amoebas are induced to aggregate to uninfected cells contributing to viral fitness

As previously characterized in this study, the formation of the "bunches" starts approximately at 6 h.p.i and persists until at least 24 h.p.i. At 16 h.p.i almost all the cells are clustered forming large bunches (Fig. 1A) and interestingly we observed that bunches are composed by amoebae at different stages of infection (Fig. 2; Fig.3). These findings led us to design an experiment for in order evaluate if the cell bunches were able to interact with uninfected cells (Fig.8A). For this, *A. castellanii* cells were infected with tupanviruses and 16 h.p.i bunches were collected and inoculated in uninfected *A. castellanii* cells in suspension. After incubation the non-adhered cells together with bunches were removed and the cells that remained adhered were counted to evaluate if the bunches were able to interact with the uninfected amoebas and were consequently removed due interacting with bunches. A control without bunches was realized in order to compare the amount of cells that remained adhered in the presence and absence of bunches (Fig. 8B). The supernatant were then submitted to immunofluorescence (Suppl. Fig 5) and to scanning electron microscopy images (Fig. 9). Interestingly, was observed that the number of amoebas that re-adhered after contact with bunches was lower when compared to the number of amoebas that re-adhered in the absence of bunches which shows that bunches were able to interact with uninfected cells (Fig. 8B). In addition, the evaluation of bunches appearance that were removed revealed the presence of a large number of infected and uninfected cells interacting as showed in the microscopy images (Fig. 9; Suppl. Fig 5).

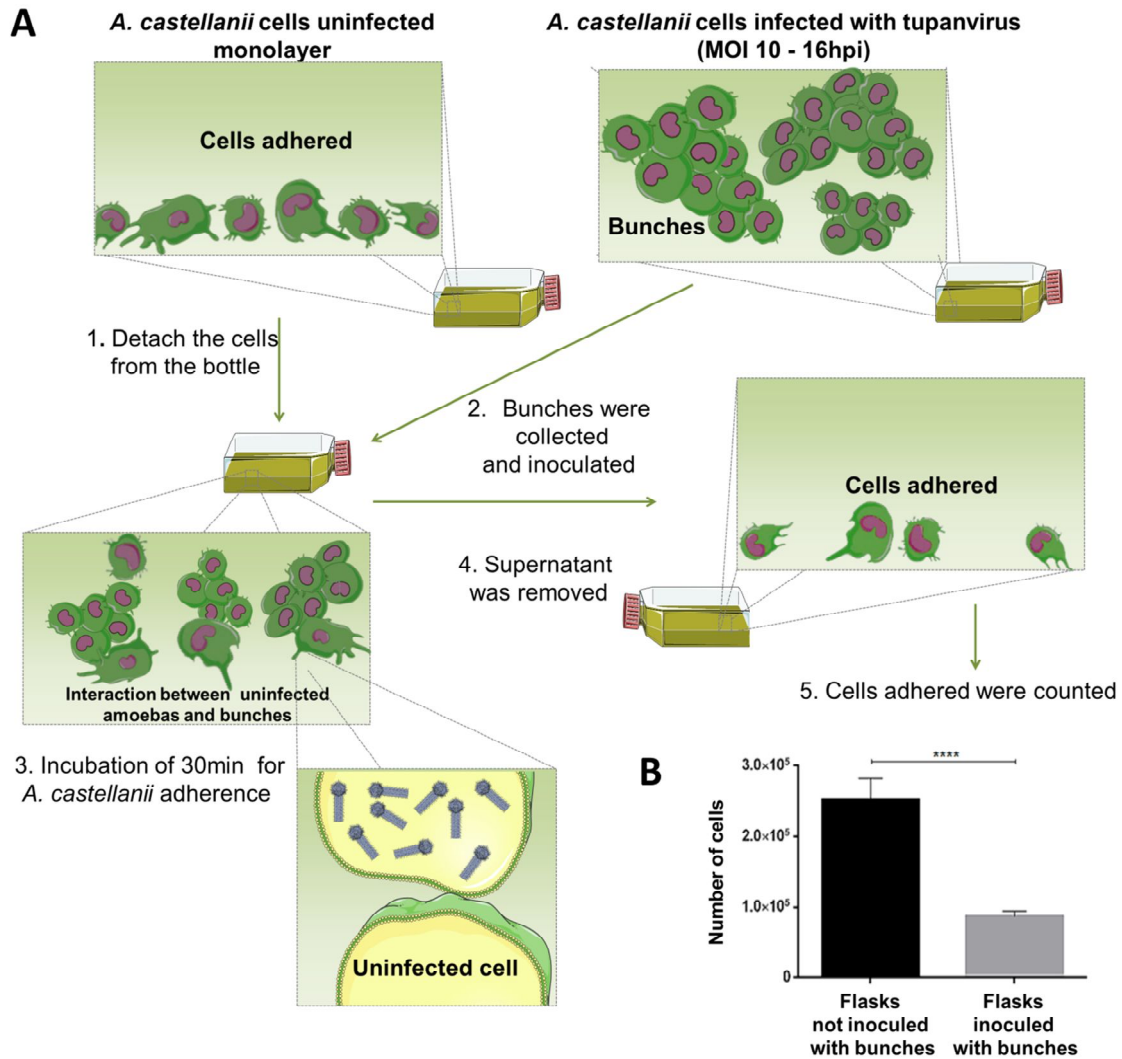


Fig.8. Bunches may contribute to the attraction of uninfected cells. Experimental design for evaluate if the bunches were able to interact with uninfected cells (A). *A. castellanii* cells were infected with tupanvirus and 16 h.p.i bunches were collected and inoculated in uninfected *A. castellanii* cells. After 30 min of incubation the non-adhered cells were removed and the cells that remained adhered were counted and plotted in a bar graph (B). The statistical significance was given by a two-tailed Student's t-test ***, $P < 0.001$, performed using GraphPad Prism software. Error bars indicate SDs.

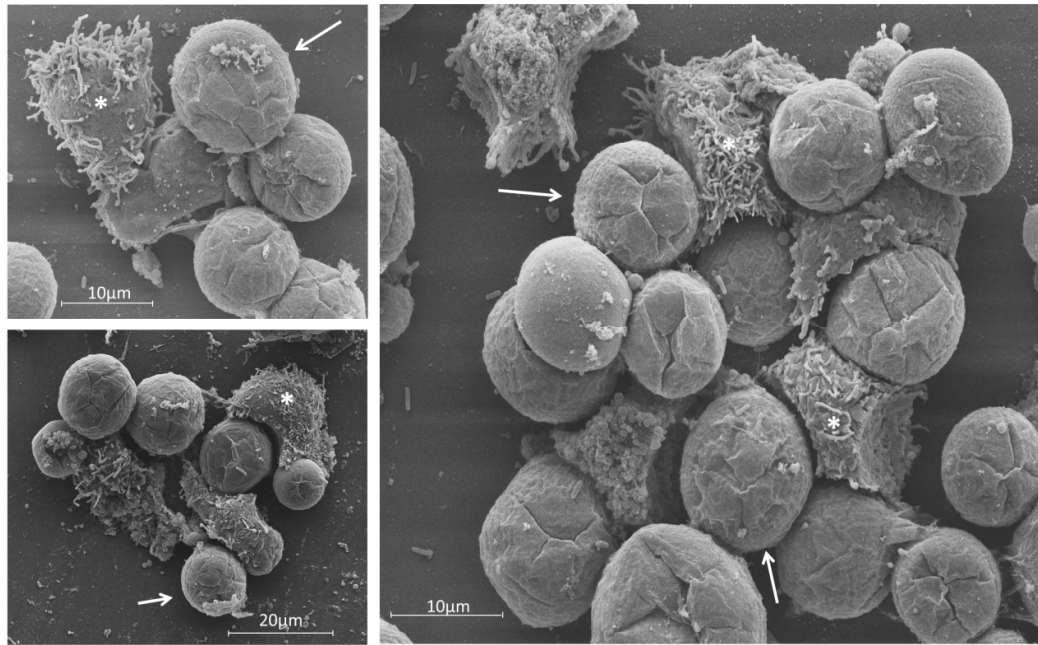
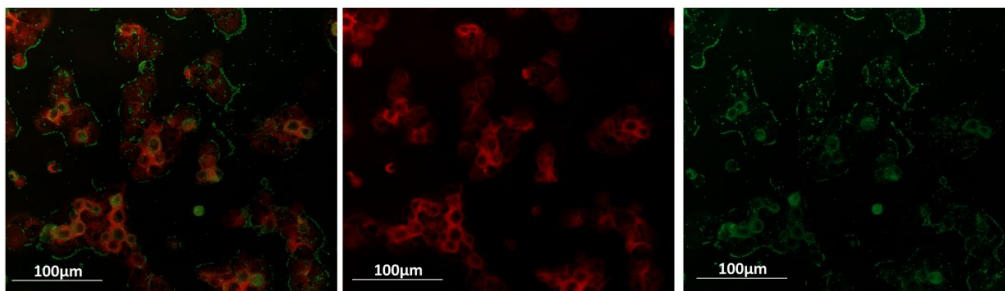


Fig. 9. Interaction between uninfected *A. castellanii* cells and bunches. Scanning electron microscopy images of the uninfected cells that interacted with bunches and were carried by them. Scale bars, 10µm, 20µm. Arrows indicate *A. castellanii* cells infected and asterisks indicate *A. castellanii* cells uninfected.



Suppl. Fig 5. Infected and uninfected *A. castellanii* cells interaction. Immunofluorescence images of the *A. castellanii* collected from assay showed in figure 8A. Scale bar: 100µm.

Thus, this set of data has led us to suggest that bunches may interact with uninfected cells keeping permissive hosts around to the amoebal infected by them. Tupanviruses shows the broadest host spectrum described among the giants viruses (Abrahão JS, et al., 2018). While the most of the giant viruses such as cedratvirus, marseilleviruses, mollivirus, pandoraviruses, mimivirus, faustovirus and kaumoebavirus were able to replicate only in single amoeba genus, tupanviruses were able to replicate in *A. castellanii*, *A. polyphaga*, *A. sp E4*, *A. griffini*, *V. vermiformis*, *Dysctiostelium discoideum*, and *Willartia magna* (Philippe N, et al., 2013; Aherfi S, et al., 2014; Legendre M, et al., 2014; Legendre M, et al., 2015; Reteno DG, et al., 2015; Andreani J, et al., 2016; Bajrai LH, et al., 2016; Abrahão JS, et al., 2018). The generalist profile displayed by tupanviruses may be related to aquatic extreme environments where they were isolated (high salinity, pH and depths) since that in inhospitable environments there is a less species richness and abundance, and the more hosts would facilitate the encounter between viral particles and their host (Sergeev VN, et al., 2002). In this some way, the bunches formation promoted by tupanvirus may be important to recruitment of cells improving the chances of the viral progenie to find a new host cell that may be scarce in those environments. Beside that the bunches formation can reduce the dilution effect in the aquatic environment thereby releasing more particles near the host, which could also facilitate the encounter between viral particles and their host. In addition, as previously mentioned, unexpectedly at 32 h.p.i at high M.O.I and 72 h.p.i at low M.O.I was observed the disaggregation of bunches (Fig. 1A; Suppl. Fig 1). Given the ability of bunches in recruitment of uninfected cells, we suggested that a possible explanation for this occurrence is that in this stage of infection when the cells are already infected and in the lysis process becomes less important the bunches presence in the absence of uninfected cells being the bunches broken. On the other hand we can consider the possibility that the cells at this stage of the infection are damaged so that it is not possible to maintain the interaction between the amoebas. Finally, in view of the importance of bunches in the interaction with uninfected cells, we decided to evaluate the possible impact of bunches during viral multiplication. For this, *A. castellanii* cells were infected using bunches (16 h.p.i) and after 36 h.p.i the supernatants were collected and titrated (Fig. 10).

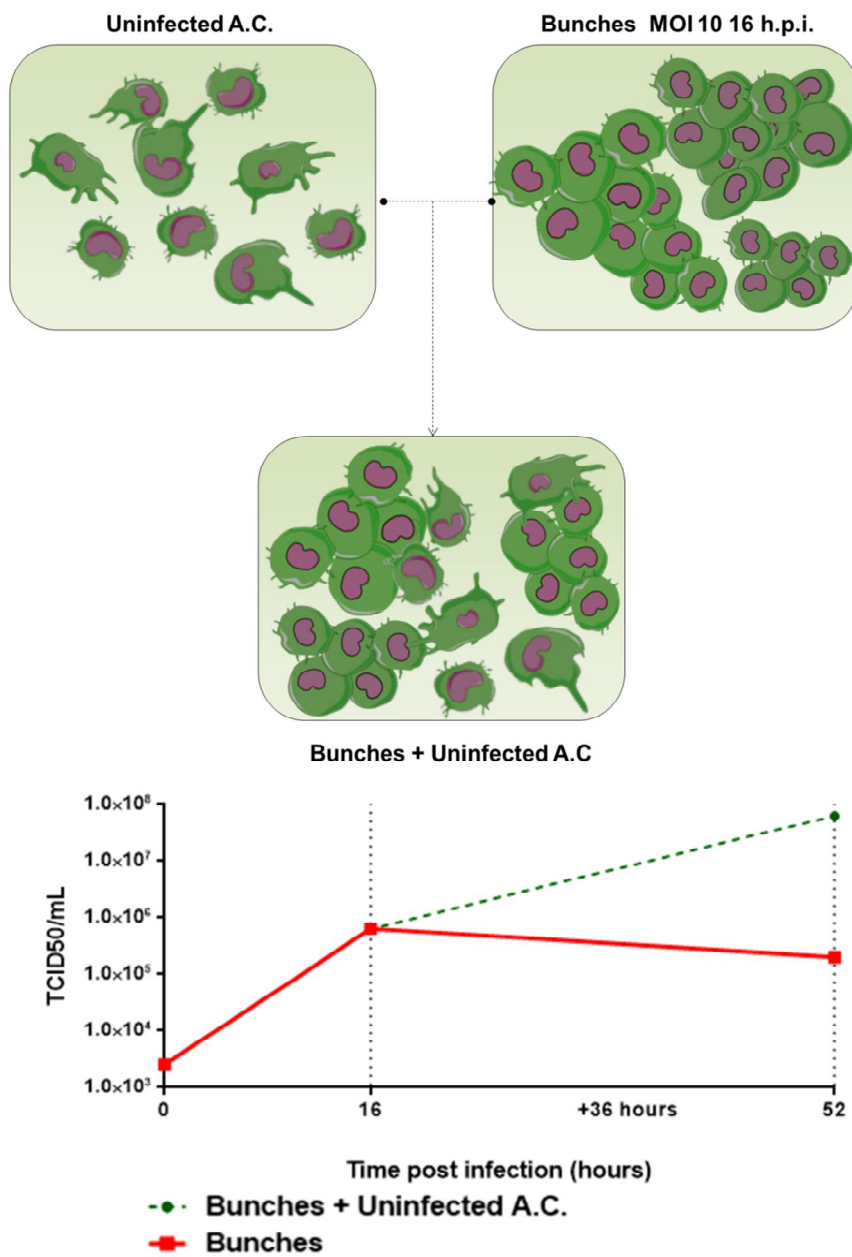


Fig. 10. Interaction between bunches and uninfected increased viral titer contributing to viral fitness. *A. castellanii* cells were infected by bunches and 36 h.p.i it was collected and titrated. Graph was constructed using GraphPad Prism version 7.00 (GraphPad Software).

The results revealed that the interaction between uninfected amoebas and bunches had a considerable importance in the increase of viral titer which was not observed in the absence of this interaction (Fig. 10). Taken together, these data suggest that bunches promoted by tupanvirus infection seem to be important for the improvement of tupanvirus fitness.

Concluding Remarks

Here we described a new virus-host interaction mechanism in which tupanvirus-infected amoebas are induced to aggregate with uninfected cells, forming bunches that can increase tupanvirus progeny. In addition, our results demonstrated that mannose reduced the transcript levels of cellular and viral mannose receptor genes, as well as inhibited bunch formation in a concentration-dependent manner, suggesting that amoebal-bunch formation correlates with MBP gene expression. Taken together, our results provide insights into the ecology of these intriguing viruses.

Materials and methods

Cell culture, viral production and titration

Acanthamoeba castellanii culture (ATCC 30010) was cultivated in Peptone-yeast extract with glucose (PYG) medium supplemented with 25 mg/ml amphotericin B (Fungizone; Cristalia, São Paulo, Brazil), 500 U/ml penicillin (Schering-Plough, Brazil) and 50 mg/ml gentamicin (Schering-Plough, Brazil). 175cm² cell culture flasks containing 7×10^6 *Acanthamoeba castellanii* cells were infected with tupanvirus or isolated from samples collected in soda lakes at an M.O.I of 0.1 and incubated at 32 °C. After the appearance of a cytopathic effect and the cell lysis was already evident, the cells and supernatants were collected, and the viruses were purified through ultracentrifugation with a 22% sucrose cushion at 36,000 g for 30min. After viral purification, the virus titer was determined using the endpoint method (Reed LJ, Muench H., 1938; Abrahão JS., 2016).

Cytopathic effect and cycle characterization

Oliveira, GP.

To investigate the cytopathic effect of tupanvirus in *A. castellanii* cells by optical microscopy, 25 cm² cell culture flasks containing 1×10^6 *A. castellanii* cells were infected with tupanvirus at an M.O.I of 0.01 and 10, incubated at 32°C and observed at different times post-infection for 72 hours. The *A. castellanii* cells were viewed under an optical microscopy at 0, 1, 2, 3, 4, 6, 8, 10, 12, 14, 16, 24, 32, 48 and 72 h.p.i and the more relevant times were demonstrated. For APMV the same conditions were used at an MOI of 10. A negative control containing only *A. castellanii* cells was used. The one-step growth curve was constructed using flasks (25cm²) in duplicate at an M.O.I of 10 (Fig. 1B). After different time points the infected *A. castellanii* cells and supernatants were collected and tittered using the endpoint method (Reed LJ, Muench H.,1938). For immunofluorescence, *A. castellanii* cells were infected by tupanvirus at an M.O.I 10 and at 0 (immediately after contact between tupanvirus and *A. castellanii*), 1, 8, 12, 16 and 24h, approximately 2×10^5 cells were collected and centrifuged at $800 \times g$ for 10min, the pellet was resuspended in 50µL of Page's Amoebae Saline (PAS), submitted to cytospin and the cells were fixed in methanol for 15min. After fixation, cells were incubated with 3% bovine serum albumin (BSA)-PAS for 30min, followed by rinsing with PAS-Tween 0,1% three times. Cells were then stained for 1h at 37°C with polyclonal anti-tupanvirus antibody produced in mouse (1:400 diluted in 3%BSA-PAS), followed by rinsing with PAS-Tween 0,1% three times. After incubation with an anti-mouse secondary antibody (1:400 diluted in 3%BSA-PAS) for 1h was added one drop of the Evans Blue (Sigma) 0,01% sufficient to cover the cells and incubated more 15min at 37°C, followed by rinsing with PAS-Tween 0,1% three times. The uninfected cells control were fixed and prepared as described. Fluorescently labeled cells were viewed using a microscope Axio Imager Z2-Apotome 2 (Zeiss). The software zen lite from zeiss microscopy was used for image processing. For transmission electron microscopy (TEM), the cells were pelleted for 10 min at 800 g. The pellet was washed twice with 0.1 M phosphate buffer (pH 7.4) and fixed with 2.5% glutaraldehyde in 0.1 M phosphate buffer for 1 h at room temperature. The pellet was then washed twice with 0.1 M phosphate buffer and resuspended in the same buffer. After, the amoebas were embedded in Epon resin by using a standard method, as follows: 2 h of fixation in 2% osmium tetroxide, five washes in distilled water, overnight incubation in uranyl acetate 2% at 2–8 °C, two washes in distilled water, 10 min dehydration in increasing ethanol concentrations (35%, 50%, 70%, 85%, 95% and 100% ethanol), 20 min incubation in acetone and embedding in EPON resin. Ultrathin sections were subsequently analyzed under transmission electron microscopy (TEM; Spirit Biotwin FEI-120 kV). For scanning electron

microscopy assays, 50 μ L of this supernatant were added to round glass coverslips covered with poly-L-lysine and fixed with 2.5% glutaraldehyde in 0.1 M cacodylate buffer for 1 h at room temperature. The samples were washed three times with 0.1 M cacodylate buffer and post-fixed with 1.0% osmium tetroxide for 1 h at room temperature. After a second fixation, the samples were washed three times with 0.1 M cacodylate buffer and immersed in 0.1% tannic acid for 20 min. The samples were then washed in cacodylate buffer and 10 min dehydrated by serial passages in ethanol solutions (35%, 50%, 70%, 85%, 95% and 100%). Samples were subsequently subjected to critical point drying using CO₂, placed in stubs and metalized with a 5 nm gold layer. The analyses were completed using scanning electron microscopy (FEG Quanta 200 FEI).

Mannose binding protein transcripts analyses and mannose assays

To evaluate the effect of mannose during tupanvirus infection, 1×10^6 cells were infected by tupanvirus at an M.O.I of 10 in PAS medium contained different concentrations of mannose (25mM, 50mM, 100mM, 400mM, 600mM and 1000mM) and incubated at 32°C. The *A. castellanii* cells were observed under an optical microscopy and visualized at 8 h.p.i. In addition the culture flasks were divided (2.5cm²/field) and the counting of bunches was made under an optical microscopy. Cells infected by tupanvirus in PAS medium without mannose and PAS medium with 600mM of mannose were titrated at 24 h.p.i. Uninfected *A. castellanii* cells cultivated in PAS medium without mannose and uninfected *A. castellanii* cells cultivated in PAS medium containing mannose (600mM) was used as control. To understand the role of the mannose in the expression pattern of the *A. castellanii* and tupanvirus mannose binding protein gene, total RNA was purified from 5×10^5 *A. castellanii* cells infected with tupanvirus (M.O.I:10) in the presence or absence of mannose (600mM) at 1h, 2h, 4h, 6h, 8h post-infection using RNeasy Mini Kit (Qiagen). To evaluate the expression of cellular mannose binding protein in amoebae infected with APMV total RNA was purified from 5×10^5 *A. castellanii* cells infected with APMV (M.O.I:10) at 1h, 2h, 4h, 6h, 8h post-infection. The samples were previously treated with DNase (Invitrogen) and reverse transcribed using M-MLV Reverse Transcriptase (200 U/L) - Thermo Fisher Scientific, according to the manufacturer's instructions. The resulting cDNAs were used as a template in a StepOne™ thermocycler (Applied Biosystems) quantitative polymerase chain reaction assay to target the

mannose receptor gene of the *A. castellanii* and tupanvirus. The thermal cycling conditions used were: one cycle at 95°C for 10 min, 40 cycles at 95°C for 10 s and 60°C for 40 s; a melting curve analysis at 95°C for 15 s and 58°C for 15 s and a final cycle was completed at 95°C for 15 s. The results were applied in $2^{-(\Delta Ct)}$ method and analyzed by StepOne software. The assays were carried out in biological duplicate. The graphs were completed using GraphPad Prism version 7.00 for Windows (GraphPad Software).

Evaluation of the interaction between uninfected amoebas and bunches

For evaluate if the bunches were able to interact with uninfected cells, 1×10^6 *A. castellanii* cells in 25cm² culture flasks were infected with tupanvirus (M.O.I 10) and 16 h.p.i the bunches were collected and inoculated in 25cm² culture flasks containing uninfected *A. castellanii* cells in suspension. After incubation for 30min at 32°C the non-adhered cells were removed from the culture flasks and the cells that remained adhered were counted. Was performed a negative control wherein only medium was added to uninfected *A. castellanii* cells. The experiment was performed in triplicate. The results were plotted in a column graph, and the statistical significance was given by a two-tailed Student's t test, performed using Graph Pad Prism software. In addition, the uninfected cells that interacted with bunches and were carried by them were subjected to immunofluorescence and scanning electron microscopy as previously described. To evaluate the importance of the brunches in the multiplication of the tupanvirus 7×10^6 *Acanthamoeba castellanii* cells were infected (M.O.I:10) and 16 h.p.i the medium was removed and the bunches and washed and used to infect *A. castellanii* cells and (for control) the bunches were added to a flask containing fresh medium. After 36 h.p.i the supernatants was collected and subjected to titration as previously described. Graphs were constructed using GraphPad Prism version 7.00 for Windows (GraphPad Software).

Acknowledgments

We are grateful to our colleagues from Laboratório de Vírus of Universidade Federal de Minas Gerais. In addition, we thank CNPq (Conselho Nacional de Desenvolvimento Científico e Tecnológico), CAPES (Coordenação de Aperfeiçoamento de Pessoal de Nível Superior), and FAPEMIG (Fundação de Amparo à Pesquisa do estado de Minas Gerais). E.G.K, J.S.A and F.G.F. are CNPq researchers. E.G.K.; B.L.S. and J.S.A. are members of a CAPES-COFECUB project.

References

1. Abrahão JS, et al. (2018) Tailed giant Tupanvirus possesses the most complete translational apparatus of the known virosphere. *Nat. Commun* 9, 749.
2. Sorokin DY, et al. (2014) Microbial diversity and biogeochemical cycling in soda lakes. *Extremophiles* 18: 791–809.
3. La Scola B, et al. (2003) A giant virus in amoebae. *Science (80)* 299 (5615): 2033.
4. Boyer M, et al. (2009) Giant Marseillevirus highlights the role of amoebae as a melting pot in emergence of chimeric microorganisms. *Proc Natl Acad Sci USA* 106(51):21848–21853.
5. Philippe N, et al. (2013) Pandoraviruses: amoeba viruses with genomes up to 2.5 Mb reaching that of parasitic eukaryotes. *Science* 341: 281–286
6. Legendre M, et al. (2014). Thirty-thousand-year-old distant relative of giant icosahedral DNA viruses with a pandoravirus morphology. *Proc. Natl. Acad. Sci. USA* 111: 4274–4279
7. Legendre M, et al. (2015) In-depth study of Mollivirus sibericum, a new 30,000-y-old giant virus infecting Acanthamoeba. *Proc. Natl. Acad. Sci. USA* 112: E5327–E5335
8. Reteno DG, et al.(2015) Faustovirus, an asfarvirus-related new lineage of giant viruses infecting amoebae. *J. Virol* 89: 6585–6594.
9. Andreani J, et al. (2016). Cedratvirus, a double-cork structured giant virus, is a distant relative of pithoviruses. *Viruses* 8, 1–11.

10. Andrade AC, et al. (2017) Filling gaps about mimivirus entry, uncoating and morphogenesis. *J. Virol* 91:e01335-17.
11. Allen PG, Dawidowicz EA. (1990) Phagocytosis in *Acanthamoeba*: I. A mannose receptor is responsible for the binding and phagocytosis of yeast. *J Cell Physiol* 145(3):508–513.
12. Yang Z, Cao Z, Panjwani N. (1997) Pathogenesis of *Acanthamoeba* keratitis: carbohydrate-mediated host-parasite interactions. *Infect Immun* 65:439–445.
13. Cao Z, Jefferson DM, Panjwani N. (1998) Role of carbohydrate-mediated adherence in cytopathogenic mechanisms of *Acanthamoeba*. *J Biol Chem* 273:15838–15845.
14. Garate M, et al. (2004) Cloning and characterization of a novel mannose-binding protein of *Acanthamoeba*. *J Biol Chem* 279: 29849–29856.
15. Garate M et al. (2005) Biochemical characterization and functional studies of *Acanthamoeba* mannose-binding protein. *Infect Immun* 73(9):5775-81.
16. Kim JH, et al. (2012) Functional roles of mannose-binding protein in the adhesion, cytotoxicity and phagocytosis of *Acanthamoeba castellanii*. *Exp Parasitol* 132(2):287-92.
17. Rodrigues RA, et al. (2015) Mimivirus Fibrils Are Important for Viral Attachment to the Microbial World by a Diverse Glycoside Interaction Repertoire. *J Virol*. 89(23):11812-9.
18. Niederkorn JY, et al. (1999) The pathogenesis of *Acanthamoeba* keratitis. *Microbes Infect* 1(6):437–443
19. Marciano-Cabral F, Cabral G. (2003) *Acanthamoeba* spp. as agents of disease in humans. *Clin Microbiol Rev* 16: 273-307.
20. Khan NA. (2006) *Acanthamoeba*: biology and increasing importance in human health. *FEMS Microbiol Rev* 30: 564-595.
21. Siddiqui R, Khan NA. (2012) Biology and pathogenesis of *Acanthamoeba*. *Parasit Vectors* 5: 6.

22. Garate M, et al. (2006) In vitro pathogenicity of *Acanthamoeba* is associated with the expression of the mannose-binding protein. *Invest Ophthalmol Vis Sci* 47: 1056-1062.
23. Yoo KT, Jung SY. (2012) Effects of Mannose on Pathogenesis of *Acanthamoeba castellanii*. *Korean J Parasitol* 50(4):365-9.
24. Barre A, et al. (1997) Curculin, a sweet-tasting and taste-modifying protein, is a non-functional mannose-binding lectin. *Plant Molecular Biology* 33: 691–698.
25. Aherfi S, et al. (2014). The expanding family Marseilleviridae. *Virology* 466–467, 27–37.
26. Bajrai LH, et al. (2016) Kaumobavirus, a new virus that clusters with Faustoviruses and Asfarviridae. *Viruses* 8 (11).
27. Sergeev VN, Gerasimenko LM, Zavarzin GA (2002). The Proterozoic history and present state of cyanobacteria. *Microbiology* 71(6):725-40.
28. Reed LJ, Muench H (1938) A simple method of estimating fifty per cent endpoints. *Am Journal Hyg* 27(3):493–497
29. Abrahão JS, et al. (2016) Mimiviruses: Replication, Purification, and Quantification. *Curr Protoc Microbiol* 6, 41:14G.1.1-14G.1.13.

5. DISCUSSÃO

A complexidade genômica e estrutural encontrada nos vírus gigantes têm surpreendido os virologistas e consequentemente fez emergir um novo e intrigante campo de estudo ainda pouco explorado. O estabelecimento de uma interação vírus-hospedeiro eficiente é um dos maiores desafios encontrados pelos vírus para sua manutenção na natureza. Nesse contexto merece destaque a regulação da expressão gênica e a disseminação viral que constitui os principais alvos de estudo do trabalho aqui apresentado.

Nesse trabalho foi inicialmente realizada uma breve revisão da regulação dos processos transcricionais em eucariotos e procariotos seguida de uma revisão detalhada do perfil de expressão gênica e sequências promotoras presentes nos vírus que compõem o grupo NCLDV. Sequências ricas em A/T foram previamente descritas atuando como promotores em vírus das famílias *Poxviridae*, *Iridoviridae*, *Phycodnaviridae*, *Ascoviridae* e *Asfarviridae* (Davison *et al.*, 1989; Garcia-Escudero *et al.*, 2000; Jakob *et al.*, 2001; Kang *et al.*, 2004; Kawasaki *et al.*, 2004; Nalcacioglu *et al.*, 2007; Salem *et al.*, 2008; Yang *et al.*, 2011). Dentre os vírus gigantes destaco a descrição de uma possível sequência promotora em vírus da família *Mimiviridae* (Suhre *et al.*, 2005). Em 2005, Suhre e colaboradores identificaram uma sequência composta de oito bases (AAAATTGA) associada a 45% dos genes de APMV, o que constitui um perfil de conservação elevado. Além disso, em outro vírus da família *Mimiviridae* tais como cafeteria roenbergensis virus e tupanvírus, a mesma sequência foi identificada (Fischer *et al.*, 2010; Abrahão *et al.*, 2018).

A descoberta do padrão diferencial de conservação de motivos promotores entre vírus da família *Mimiviridae* e as questões evolutivas levantadas acerca das sequências promotoras entre os NCLDVs reforçou nosso interesse na busca por motivos promotores entre outros vírus gigantes tais como entre os vírus da família *Marseilleviridae*. A busca por motivos promotores no genoma de vírus pertencentes as quatro linhagens da família *Marseilleviridae* resultou na descoberta de uma sequência composta por oito bases (AAATATTT) que está associada a 55% dos genes de marseillevirus marseillevirus e conservado em todas as linhagens da família *Marseilleviridae*. Mais de 80% dos motivos encontrados estão presentes nas regiões intergênicas do genoma dos marseillevírus analisados se comparado a sua presença na região codificadora. O que reforça que a presença desses motivos na região intergênica não ocorre provavelmente de forma randômica. Outro ponto considerado em relação a possível função promotora do motivo predito foi a distância em relação ao ATG. Observamos que os motivos se encontram preferencialmente distribuídos entre -1 e -100 pares

de bases a montante do início da tradução. Esse perfil de distribuição é consistente com os padrões de distância de sequências promotoras anteriormente descritas para outros vírus pertencentes ao grupo NCLDV, além de procariotos e eucariotos, tal como revisado nesse trabalho.

As fortes evidências de que o motivo AAATATTT poderia funcionar como sequência promotora em marseillevírus nos levou a investigar se essa sequência bem como variações pontuais na mesma poderia ter uma relevância biológica na expressão do gene que codifica GFP que foi inserido em um plasmídeo e posteriormente analisado sua transcrição e expressão. Os resultados de qPCR e análises de imunofluorescência confirmaram a relevância do motivo na transcrição e expressão do gene que codifica GFP uma vez que plasmídeos contendo a sequência predita (AAATATTT) demonstrou presença de transcritos e da proteína nos tempos de 1h.p.i, 2h.p.i e 3h.p.i. Em oposição, as células transfectadas com o plasmídeo contendo uma sequência controle (GCGCGCGC) não foi observada a presença de transcritos ou expressão do gene inserido. Para os demais plasmídeos contendo variações da sequência predita foram detectados níveis reduzidos de expressão ou em alguns casos completa abolição da expressão. Esse conjunto de dados corrobora que o motivo predito nesse trabalho pode atuar como promotor na expressão de genes em marseillevírus.

Outro ponto que despertou nossa atenção durante o estudo do motivo promotor de marseillevírus foi o grande número de repetições nas regiões intergênicas do seu genoma. Foram encontradas duas ou mais cópias do motivo em mais de 50% das regiões intergênicas do genoma de vírus de todas as linhagens de marseillevírus. Esse achado despertou nosso interesse em investigar e lançar hipóteses acerca da importância bem como das implicações dessas repetições dos motivos promotores no genoma dos marseillevírus.

Uma das características mais estudadas em relação ao genoma dos marseillevírus se refere ao seu mosaicismo (Boyer *et al.*, 2009). Estudos anteriores revelaram que o genoma dos marseillevírus é composto por genes provenientes de diferentes organismos e esse grande número de genes exógenos foi associado a eventos de TGL. Por análises dos genes transferidos por TGL nos hospedeiros doadores associado à busca por similaridade em relação a sequências intergênicas de marseillevírus nós sugerimos que os motivos presentes nas regiões intergênicas que antecedem os genes provenientes de TGL não foram adquiridos a partir do organismo doador/receptor durante o evento de TGL. É importante ressaltar também que nós identificamos que um grande número de motivos não estão imediatamente associados a genes em todas as linhagens de marseillevírus.

Com base na presença de genes provenientes de TGL associado à demonstração de que os motivos não são adquiridos por TGL, nós propusemos que os promotores não associados a genes poderiam funcionar como regiões propícias a incorporação e consequente fixação de novos genes o que ajudaria a explicar a manutenção dos genes adquiridos por TGL com consequente expansão do genoma dos marseillevírus.

Além da busca de promotores em marseillevírus, esse trabalho teve como alvo a investigação de motivos promotores no genoma de faustovírus e kaumoebavírus. A relação filogenética entre faustovírus, kaumoebavírus e asfarvírus (Reteno *et al.*, 2015; Bajrai *et al.*, 2016) nos levou a hipotetizar que as sequências que atuam como promotores previamente descritas no genoma de asfarvírus (TATTT e TATATA) poderiam estar presentes nos genomas de faustovírus e kaumoebavírus. A busca por esses motivos no genoma de faustovírus e kaumoebavírus corroborou nossa hipótese uma vez que ambos os motivos foram encontrados em abundância no genoma desses vírus. Além disso, a análise desses motivos foi também feita em asfarvírus visando confirmar sua distribuição no genoma desses vírus. Ambos os motivos demonstraram um perfil de distribuição prevalente nas regiões intergênicas se comparado à região codificadora e localização principalmente até -100 pares de bases a montante do ATG. Essas características seguem um perfil similar ao demonstrado para motivos promotores bem caracterizados reforçando que as sequências previamente descritas para asfarvírus podem atuar como promotores também em faustovírus e kaumoebavírus. Além disso, sequências promotoras ricas em A/T são comumente encontradas em outros NCLDV's bem como outros organismos. Outra observação digna de nota foi o grande número de repetições do motivo encontrado nas regiões intergênicas do genoma desses vírus tal como previamente demonstrado nesse trabalho para marseillevírus. Desta forma, vale ressaltar que faustovírus e kaumoebavírus também exibem um alto nível de mosaicismo genômico que podem estar associados a eventos de TGL (Reteno *et al.*, 2015; Bajrai *et al.*, 2016). Além disso, os genes parálogos representam cerca de 20% do conjunto gênico de faustovírus e a repetição de motivos pode estar relacionada a duplicações genéticas no genoma desses vírus. A busca pelos motivos aqui preditos nos genes compartilhados entre faustovírus, kaumoebavírus e asfarvírus revelou que a maioria dos genes compartilhados entre esses vírus (12 de 18) apresentou o motivo predito. Esses dados sugerem que os motivos promotores poderiam estar presentes no ancestral de faustovírus, kaumoebavírus e asfarvírus o que reforça sua relação filogenética. Estudos biológicos visando confirmar o papel na expressão gênica dos motivos TATTT e TATATA em faustovírus e kaumoebavírus ainda precisam ser realizados, no entanto fortes foram os indícios aqui obtidos para levantar essa hipótese.

Dentre os vírus mais complexos descobertos atualmente destaca-se o tupanvírus. O tupanvírus foi descoberto pelo nosso grupo de pesquisa e sua notável complexidade genômica despertou o interesse no estudo de sua interação com seus hospedeiros. Arantes observou que tupanvírus apresentava um efeito citopático peculiar em cultura de *Acanthamoeba castellanii* caracterizado pela presença de agregados celulares que foi denominado “cachos” (Arantes, 2018). Inicialmente nesse trabalho nós caracterizamos temporalmente a formação dos cachos ao longo do ciclo de multiplicação de tupanvírus. Foi demonstrado que os cachos iniciam aproximadamente 6.h.p.i e se tornam mais evidentes nos tempos de 8 h.p.i, 12 h.p.i e 16 h.p.i sendo que nesse momento da infecção quase todas as células se encontram incorporadas a grandes cachos. Foi possível observar ainda que aproximadamente 32 h.p.i ocorre a desagregação dos cachos e nos tempos entre 48 h.p.i e 72 h.p.i a maioria das amebas já se encontram lisadas. O perfil diferenciado do efeito citopático de tupanvírus, uma vez que essa foi a primeira descrição de um vírus gigante levando a formação de cachos, nos levou a investigar os fatores que poderiam estar envolvidos nesse efeito citopático bem como as possíveis implicações no valor adaptativo conferido por esse efeito ao vírus. Análises de microscopia eletrônica e imunofluorescência revelaram que os cachos são compostos por amebas em diferentes estágios de infecção. Estudos anteriores demonstraram que uma proteína de ligação a manose presente na superfície de *Acanthamoeba* spp exerce um papel fundamental na patogênese, uma vez que está relacionado à interação entre amebas e seus hospedeiros (Allen PG, Dawidowicz EA, 1990; Garate M, *et al.*, 2005). Nesse trabalho nós observamos a presença de um gene que codifica uma proteína ligadora de manose no genoma de tupanvírus e avaliamos sua expressão. Observamos que tupanvírus não só é capaz de expressar sua própria proteína ligadora de manose como é capaz de induzir a expressão do gene que codifica a proteína ligadora de manose amebiana durante a sua multiplicação, sugerindo uma possível relevância desse gene na multiplicação do tupanvírus. Estudos anteriores revelaram que a adição de manose afeta a patogenicidade de amebas do gênero *Acanthamoeba* (Kim JH, *et al.*, 2012; Yoo KT, *et al.*, 2012). Aqui nós demonstramos que a presença de manose no meio inibe a formação do cacho de maneira concentração dependente além de reduzir significativamente os níveis de transcritos do gene que codifica a proteína ligadora de manose viral e celular. Esses dados sugerem que a formação de cachos e a expressão da proteína ligadora de manose podem estar correlacionados. Considerando que a proteína ligadora de manose é uma glicoproteína contendo manose (Garate M, *et al.*, 2005) sugerimos que esse pode ser um dos fatores que explica a formação dos cachos em células infectadas por tupanvírus. Embora um gene que codifica a proteína ligadora de manose tenha

sido encontrado em outros membros da família *Mimiviridae*, modificações nos domínios de ligação a manose dessa proteína foram observadas. Nós demonstramos que APMV apresenta modificações em seus subdomínios de ligação a manose (QDN) que foram associados à perda de função em estudo prévio, o que sugere que a proteína ligadora de manose de APMV pode não exercer a mesma função como sugerido para tupanvírus (Barre A, *et al.*, 1997). O subdomínio Y também foi sugerido ser importante no reconhecimento da manose e nós demonstramos que apenas o tupanvírus apresenta esses subdomínios conservados. Além disso, a infecção por APMV levou a inibição do gene que codifica a proteína ligadora de manose, em oposição ao observado para tupanvírus. Considerando que APMV não induz a formação de cachos durante seu ciclo de multiplicação esses dados reforçam um possível papel da proteína ligadora de manose na formação dos cachos.

Assim, nós hipotetizamos que a indução da expressão gênica do receptor de manose no ciclo de tupanvírus pode ser importante para a formação dos cachos, uma vez que a interação entre as amebas pode ocorrer por meio da interação entre suas proteínas ligadoras de manose. Dessa forma, com a adição de manose no meio pode ocorrer saturação dos domínios de ligação à manose com conseqüente não formação dos cachos.

Como mencionado anteriormente, os cachos formados por tupanvírus apresentam células em diferentes estágios de infecção. Utilizando um desenho experimental aqui desenvolvido nós revelamos que os cachos formados durante a multiplicação do tupanvírus são capazes de interagir com amebas não infectadas o que poderia exercer um papel na disseminação viral. Dentre os vírus gigantes, tupanvírus é até o momento o que apresenta o maior espectro de hospedeiros, uma vez que a maioria dos vírus gigantes descritos até o momento são capazes de infectar apenas um gênero de amebas e o tupanvírus é capaz de multiplicar em amebas de pelo menos quatro gêneros diferentes (Philippe N, *et al.*, 2013; Aherfi S, *et al.*, 2014; Legendre M, *et al.*, 2014; Legendre M, *et al.*, 2015; Reteno DG, *et al.*, 2015; Andreani J, *et al.*, 2016; Bajrai LH, *et al.*, 2016; Abrahão JS, *et al.*, 2018). Esse perfil generalista pode ser associado aos ambientes extremos nos quais tupanvírus foram isolados uma vez que em ambientes inóspitos a riqueza e abundância de hospedeiros são reduzidas (Sergeev VN, *et al.*, 2002). Nesse contexto, a formação de cachos também poderia ser associada a essa necessidade de recrutamento de novos hospedeiros o que aumentaria a chance do encontro entre a progênie viral recém-formada e seus hospedeiros nesses ambientes em que a presença de amebas pode ser mais escassa. Além disso, a formação de cachos poderia reduzir o efeito diluidor no ambiente aquático liberando maior número de partículas próximo ao seu hospedeiro. Por fim, nós demonstramos ainda que a interação entre cachos e

amebas não infectadas levou a um aumento do título viral sugerindo que os cachos podem exercer um papel importante para o fitness viral.

Nesse trabalho nós inserimos novos dados ao universo inexplorado dos vírus gigantes e demonstramos que sua complexidade vai além da grandeza de seus genomas e partículas, uma vez que descrevemos aqui características biológicas e moleculares nunca antes descritas entre os vírus.

6. CONCLUSÕES

- Foi descrito pela primeira vez uma sequência (AAATATTT) que pode atuar como promotor em vírus da família *Marseilleviridae* relacionada com mais de 50% dos genes de marseillevirus marseillevirus, demonstrando um alto de nível de conservação.
- A sequência AAATATTT está preferencialmente distribuída nas regiões intergênicas do genoma na região entre -10 e -100 pares de bases a montante do códon de iniciação, seguindo um perfil semelhante ao de outros promotores descritos entre os NCLDV's.
- Variações na sequência AAATATTT causou um efeito negativo na expressão gênica em marseillevirus marseillevirus, sugerindo a importância biológica do octâmero.
- A distribuição homogênea e repetições do motivo AAATATTT nas regiões intergênicas do genoma de marseillevirus, conjuntamente com a observação de que as regiões intergênicas parecem não ter sido adquiridas a partir do organismo doador durante eventos de TGL, nos levou a propor que esses promotores não associados a genes estariam livres para regular genes recém-adquiridos por TGL podendo ser um dos fatores que explicam o mosaicism e plasticidade genômica dos vírus dessa família.
- Os motivos TATTT e TATATA que atuam como promotores em vírus da família *Asfarviridae* estão presentes em abundância no genoma de faustovirus e kaumoebavirus, reforçando sua relação filogenética.
- Os motivos TATTT e TATATA estão predominantemente distribuídos nas regiões intergênicas entre -0 e -100 pares de bases a montante do códon de iniciação do genes de asfarvirus, faustovirus e kaumoebavirus.
- A presença dos motivos promotores preditos nos genes compartilhados entre faustovirus, kaumoebavirus e asfarvirus sugere que os motivos já poderiam estar presentes no ancestral desses vírus antes da irradiação deste grupo.
- O tupanvirus é capaz de induzir a formação de cachos em cultura de *Acanthamoeba castellanii*, nos quais foi demonstrada a presença de amebas em diferentes estágios de infecção.

- Após a desagregação mecânica dos cachos precoces as amebas agregam-se novamente, enquanto os cachos tardios não reagregam.
- Amebas infectadas por tupanvírus tem aumento dos níveis de transcritos do gene que codifica a proteína ligadora de manose viral e celular, sugerindo um papel da proteína ligadora de manose no ciclo de multiplicação do tupanvírus.
- A adição de manose livre ao meio de cultura levou a supressão do aumento da expressão do gene que codifica a proteína ligadora de manose viral e celular e a inibição da formação do cacho em amebas infectadas por tupanvírus de uma maneira concentração dependente, sugerindo que a formação de cachos em tupanvírus correlaciona com a expressão do gene que codifica a proteína ligadora de manose.
- A infecção por acanthamoeba polyphaga mimivirus não levou a formação de cachos além de inibir a expressão do gene que codifica a proteína ligadora de manose celular, reforçando a importância da proteína ligadora de manose na formação dos cachos.
- Os cachos formados durante a multiplicação de tupanvírus são capazes de interagir com células não infectadas, o que pode exercer um impacto sobre o fitness viral.

7. REFERÊNCIAS BIBLIOGRÁFICAS

ABERGEL, C; RUDINGER-THIRION J.; GIEGÉ R.; CLAVERIE JM.(2007) Virus-Encoded Aminoacyl-tRNA Synthetases: Structural and Functional Characterization of Mimivirus TyrRS and MetRS. *Journal of Virology*, v. 81, n. 22, p. 12406–12417.

ABRAHÃO, J. S, ARAÚJO R, COLSON P, LA SCOLA B. (2017) The analysis of translation-related gene set boosts debates around origin and evolution of mimiviruses. *PLOS Genetics*, v. 13, n. 2, p. e1006532.

ABRAHÃO, J.; SILVA, L.; SILVA, L.S.; KHALIL, J.Y.B.; RODRIGUES, R.; ARANTES, T.; ASSIS, F.; BORATTO, P.; ANDRADE, M.; KROON, E.G.; RIBEIRO, B.; BERGIER, I.; SELIGMANN, H.; GHIGO, E.; COLSON, P.; LEVASSEUR, A.; KROEMER, G.; RAOULT, D.; LA SCOLA, B. (2018). Tailed giant Tupanvirus possesses the most complete translational apparatus of the known virosphere. *Nat Commun* v.9(1), p.749.

AHERFI, S.; PAGNIER, I.; FOURNOUS, G.; RAOULT, D.; LA SCOLA, B.; COLSON, P. (2013). Complete genome sequence of Cannes 8 virus, a new member of the proposed family "Marseilleviridae". *Virus Genes*, v.47, n.3, p.550-5.

AHERFI, S.; BOUGHALMI, M.; PAGNIER, I.; FOURNOUS, G.; LA SCOLA, B.; RAOULT, D.; COLSON, P. (2014a). Complete genome sequence of Tunisvirus, a new member of the proposed family Marseilleviridae. *Arch Virol*. v.159(9), p.2349-58.

AHERFI, S.; LA SCOLA, B.; PAGNIER, I.; RAOULT, D.; COLSON, P. (2014b). The expanding family *Marseilleviridae*. *Virology*. v.466, n.467, p.27-37.

ALLEN, P.G.; DAWIDOWICZ, E.A.; (1990). Phagocytosis in *Acanthamoeba*: I. A mannose receptor is responsible for the binding and phagocytosis of yeast. *J Cell Physiol* 145(3):508–513.

ANDRADE, A.C.D.S.P.; ARANTES, T.S.; RODRIGUES, R.A.L.; MACHADO, T.B.; DORNAS, F.P.; LANDELL, M.F.; FURST, C.; BORGES, L.G.A.; DUTRA, L.A.L.; ALMEIDA, G.; TRINDADE, G.S.; BERGIER, I.; ABRAHÃO, W.; BORGES, I.A.;

CORTINES, J.R.; DE OLIVEIRA, D.B.; KROON, E.G.; ABRAHÃO, J.S. (2018). Ubiquitous giants: a plethora of giant viruses found in Brazil and Antarctica. *Virology*. v.24, n.15(1), p.22.

ANDREANI, J.; AHERFI, S.; BOU KHALIL, J.Y.; DI PINTO, F.; BITAM, I.; RAOULT, D.; COLSON, P.; LA SCOLA, B. (2016). Cedratvirus, a Double-Cork Structured Giant Virus, is a Distant Relative of Pithoviruses. *Viruses*. v.3;8(11). 2016.

ANDERSSON JO (2009). Gene transfer and diversification of microbial eukaryotes. *Annu Rev Microbiol* 63:177–193. 448 32.

ANDREANI, J.; KHALIL, J.Y.B.; SEVVANA, M.; BENAMAR, S.; DI PINTO, F.; BITAM, I.; COLSON, P.; KLOSE, T.; ROSSMANN, M.G.; RAOULT, D.; LA SCOLA, B. (2017). Pacmanvirus, a New Giant Icosahedral Virus at the Crossroads between Asfarviridae and Faustoviruses. *J Virol*. ;91(14). pii: e00212-17.

ANDREANI, J.; KHALIL, J.Y.B.; BAPTISTE, E.; HASNI, I.; MICHELLE, C.; RAOULT, D.; LEVASSEUR, A.; LA SCOLA, B. (2018). Orpheovirus IHUMI-LCC2: A New Virus among the Giant Viruses. *Front Microbiol*. 22;8:2643.

ARANTES, T.S.; Isolamento de vírus gigantes de *Acanthamoeba* e caracterização do ciclo de multiplicação dos marseillevírus. Tese de Doutorado. Programa de Pós-Graduação em Microbiologia. UFMG. 2018.

BAJRAI, L.H.; BENAMAR, S.; AZHAR, E.I.; ROBERT, C.; LEVASSEUR, A.; RAOULT, D.; LA SCOLA, B. (2016). Kaumoebavirus, a New Virus That Clusters with Faustoviruses and Asfarviridae. *Viruses*. v.8 (11). p. 278. 2016.

BARRE A.; VAN DAMME, E.J.M.; PEUMANS. W.J.; ROUGE, P. (1997) Curculin, a sweet-tasting and taste-modifying protein, is a non-functional mannose-binding lectin. *Plant Molecular Biology* 33: 691–698.

BOYER, M.; YUTIN, N.; PAGNIER, I.; BARRASSI, L.; FOURNOUS, G.; ESPINOSA, L.; ROBERT C.; AZZA, S.; SUN, S.; ROSSMANN, M.G.; SUZANMONTI, M.; LA SCOLA, B.; KOONIN, E.V.; RAOULT, D. (2009). Giant Marseillevirus highlights the role of amoebae as a melting pot in emergence of chimeric microorganisms. *PNAS*, v.106, n.51, p. 21848–21853.

CLARKE M.; LOHAN AJ.; LIU B.; LAGKOUVARDOS I.; ROY S.; ZAFAR N.; BERTELLI C.; SCHILDE C.; KIANIANMOMENI A.; BÜRGLIN TR, FRECH C.; TURCOTTE B.; KOPEC KO.; SYNNOTT JM.; CHOO C.; PAPONOV I.; FINKLER A.; HENG TAN CS.; HUTCHINS AP.; WEINMEIER T.; RATTEI T.; CHU JS.; GIMENEZ G.; IRIMIA M.; RIGDEN DJ.; FITZPATRICK DA.; LORENZO-MORALES J.; BATEMAN A.; CHIU CH.; TANG P.; HEGEMANN P.; FROMM H.; RAOULT D.; GREUB G.; MIRANDA-SAAVEDRA D.; CHEN N.; NASH P.; GINGER ML.; HORN M.; SCHAAP P.; CALER L.; LOFTUS BJ. (2013) Genome of *Acanthamoeba castellanii* highlights extensive lateral gene transfer and early evolution of tyrosine kinase signaling. *Genome Biol* 14(2):R11.

CLAVERIE, J.M.; OGATA, H.; AUDIC, S.; ABERGEL, C.; SUHRE, K.; FOURNIER, P.E. (2006). Mimivirus and the emerging concept of "giant" virus. *VirusesResearch*, v. 117, n. 1, p.133-44.

COLSON, P.; PAGNIER, I.; YOOSUF, N.; FOURNOUS, G.; LA SCOLA, B.; RAOULT, D. (2013c). „Marseilleviridae“, a new family of giant viruses infecting amoebae. *Archives of virology, Áustria*, v. 158, n.4, p. 915-20.

DAVISON, A.J.; MOSS, B. The structure of vaccinia virus early promoters. (1989) *J. Mol. Biol.*, 210, 749–769.).

DORNAS, F.P.; ASSIS, F.L.; AHERFI, S.; ARANTES, T.; ABRAHÃO, J.S.; COLSON, P.; LA SCOLA, B. (2016). A Brazilian Marseillevirus Is the Founding Member of a Lineage in Family Marseilleviridae. *Viruses*, v. 8, n.3, p. 76.

DOS SANTOS, R.N.; CAMPOS, F.S.; MEDEIROS DE ALBUQUERQUE, N.R.; FINOKETTI, F.; CÔRREA, R.A.; CANO-ORTIZ, L.; ASSIS, F.L.; ARANTES, T.S; ROEHE, P.M.; FRANCO, A.C. (2016). A new marseillevirus isolated in Southern Brazil from *Limnoperna fortunei*. *Sci Rep.* v.6, p.35237.

DOUTRE, G.; PHILIPPE, N.; ABERGEL, C.; CLAVERIE, J. M. (2014). Genome analysis of the first Marseilleviridae representative from Australia indicates that most of its genes contribute to virus fitness. *J. Virol*, v. 88, n.24, p.14340– 14349.

FISCHER, M.G.; ALLEN, M.J.; WILSON, W.H.; SUTTLE, C.A. (2010) Giant virus with a remarkable complement of genes infects marine zooplankton. *Proc. Natl. Acad. Sci. USA* 2010, 9, 19508–19513.

FILÉE, J.; POUGET, N.; CHANDLER, M. (2008). Phylogenetic evidence for extensive lateral acquisition of cellular genes by Nucleocytoplasmic large DNA viruses. *BMC Evol Biol.* v. 8. p320. doi: 10.1186/1471-2148-8-320.

FILÉE, J.; CHANDLER, M (2010). Gene exchange and the origin of giant viruses. *Intervirology.* v.53(5), p.354-61.

GARATE M.; CUBILLOS, I.; MARCHANT, J.; PANJWANI, N (2005). Biochemical characterization and functional studies of *Acanthamoeba* mannose-binding protein. *Infect Immun* 73(9):5775-81.

GARCIA-ESCUADERO, R.; VINUELA, E. Structure of African swine fever virus late promoters: Requirement of a TATA sequence at the initiation region. *J. Virol.* 2000, 74, 8176–8182.

JAKOB, N.J.; MULLER, K.; BAHR, U.; DARAI, G.(2001) Analysis of the first complete DNA sequence of an invertebrate iridovirus: Coding strategy of the genome of Chilo iridescent virus. *Virology*, 286, 182–196.

JEUDY, S.; ABERGEL C.; CLAVERIE JM.; LEGENDRE M.(2012) Translation in Giant Viruses: A Unique Mixture of Bacterial and Eukaryotic Termination Schemes. *PLoS Genetics*, v. 8, n. 12.

KANG, M.; GRAVES, M.; MEHMEL, M.; MORONI, A.; GAZZARRINI, S.; THIEL, G.; GURNON, J.R.; VAN ETTEN, J.L. (2004) Genetic diversity in chlorella viruses flanking *kcv*, a gene that encodes a potassium ion channel protein. *Virology*, 326, 150–159.

KAWASAKI, T.; TANAKA, M.; FUJIE, M.; USAMI, S.; YAMADA, T. (2004) Immediate early genes expressed in chlorovirus infections. *Virology*, 318, 214– 223

KIM, J.H.; MATIN, A.; SHIN, H.J.; PARK, H.; YOO, K.T.; YUAN, X.Z.; KIM, K.S.; JUNG, S.Y. (2012). Functional roles of mannose-binding protein in the adhesion, cytotoxicity and phagocytosis of *Acanthamoeba castellanii*. *Exp Parasitol* 132(2):287-92.

LA SCOLA, B.; AUDIC, S.; ROBERT, C.; JUNGANG, L.; DE LAMBALLERIE, X.; DRANCOURT, M.; BIRTLES, R.; CLAVERIE, J.M.; RAOULT, D. (2003). A giant virus in amoebae. *Science*. v. 299, n. 5615, p. 2033.

LA SCOLA, B.; CAMPOCASSO, A.; N'DONG, R.; FOURNOUS, G.; BARRASSI, L.; FLAUDROPS, C.; RAOULT, D. (2010). Tentative characterization of new environmental giant viruses by MALDI-TOF mass spectrometry. *Intervirology*, Suíça, v. 53, n. 5, p. 344-53.

LAGIER, J. C.; ARMOUGOM, F.; MILLION, M.; HUGON, P.; PAGNIER, I.; OBERT, C.; BITTAR, F.; FOURNOUS, G.; GIMENEZ, G.; MARANINCHI, M.; TRAPE, J.F.; KOONIN, E.V.; LA SCOLA, B.; RAOULT, D. (2012). Microbial culturomics: paradigm shift in the human gut microbiome study. *Clin.Microbiol. Infect*, v. 18, n.12, p. 1185–1193.

LEGENDRE, M.; AUDIC, S.; POIROT, O.; HINGAMP, P.; SELTZER, V.; BYRNE, D.; LARTIGUE, A.; LESCOT, M.; BERNADAC, A.; POULAIN, J. (2010) mRNA deep sequencing reveals 75 new genes and a complex transcriptional landscape in Mimivirus. *Genome Res*. 20, 664–674.

LEGENDRE, M.; BARTOLI, J.; SHMAKOVA, L.; JEUDY, S.; LABADIE, K.; ADRAIT, A.; LESCOT, M.; POIROT, O.; BERTAUX, L.; BRULEY, C.; COUTÉ, Y.; RIVKINA, E.; ABERGEL, C.; CLAVERIE, J.M. (2014). Thirty-thousand-year old distant relative of giant icosahedral DNA viruses with a pandoravirus morphology. *PNAS, E.U.A*, v.111, n.11, p. 4274-9.

LEGENDRE, M.; LARTIGUE, A.; BERTAUX, L.; JEUDY, S.; BARTOLI, J.; LESCOT, M.; ALEMPIC, J.M.; RAMUS, C.; BRULEY, C.; LABADIE, K.; SHMAKOVA, L.; RIVKINA, E.; COUTÉ, Y.; ABERGEL, C.; CLAVERIE, J.M. (2015). In-depth study of Mollivirus sibericum, a new 30,000-y-old giant virus infecting *Acanthamoeba*. *PNAS*, v.112, n.38:E5327-35.

LWOFF, A. (1957). The concept of virus. *J Gen Microbiol.* v.17(2). p.239-53.

NALCACIOGLU, R.; INCE, I.A.; VLAK, J.M.; DEMIRBAG, Z.; VAN OERS, M.M. (2007) The Chilo iridescent virus DNA polymerase promoter contains an essential AAAAT motif. *J. Gen. Virol*, 88, 2488–2494).

PHILIPPE, N.; LEGENDRE, M.; DOUTRE, G.; COUTÉ, Y.; POIROT, O.; J.; CLAVERIE, J.M.; ABERGEL, C. (2013). Pandoraviruses: amoeba viruses with genomes up to 2.5 Mb reaching that of parasitic eukaryotes. *Science, E.U.A.*, v. 341, n. 6143, p. 281-6.

POPGEORGIEV, N.; BOYER, M.; FANCELLO, L.; MONTEIL, S.; ROBERT, C.; RIVET, R.; NAPPEZ, C.; AZZA, S.; CHIARONI, J.; RAOULT, D.; DESNUES, C. (2013a). Marseillevirus-like virus recovered from blood donated by asymptomatic humans. *The Journal of infectious diseases, United States*, v.208, n.7, p.1024-1050.

RETENO, D.G.; BENAMAR, S.; KHALIL, J.B.; ANDREANI, J.; ARMSTRONG, N.; KLOSE, T.; ROSSMANN, M.; COLSON, P.; RAOULT, D.; LA SCOLA, B. (2015) Faustovirus, an asfarvirus-related new lineage of giant viruses infecting amoebae. *J Virol*, v.89, n.13, p.6585-94.

SALEM, T.Z.; TURNEY, C.M.; WANG, L.; XUE, J.; WAN, X.-F.; CHENG, X.-W. ranscriptional analysis of a major capsid protein gene from *Spodoptera exigua* aascovirus^a (2008) *Arch. Virol*, 153, 149–162.

SCHULZ F.; YUTIN N.; IVANOVA NN.; ORTEGA DR.; LEE TK .; VIERHEILIG J ; DAIMS H.; HORN M.; WAGNER M.; JENSEN GJ.; KYRPIDES NC.; KOONIN EV.; WOYKE T.; (2017) Giant viruses with an expanded complement of translation system components. *Science*. 356(6333):82-85.

SUHRE, K.; AUDIC, S.; CLAVERIE, J.M (2005). Mimivirus gene promoters exhibit an unprecedented conservation among all eukaryotes. *PNAS, E.U.A.*, v. 102, n. 41, p. 14689-93, 2005.

TAKEMURA, M. (2016). Draft Genome Sequence of Tokyovirus, a Member of the Family Marseilleviridae Isolated from the Arakawa River of Tokyo, Japan. *Genome Announc*, v.9, n.4, e00429-16.

THOMAS, V.; BERTELLI, C.; COLLYN, F.; CASSON, N.; TELENTI, A.; GOESMANN, A.; CROXATTO, A.; GREUB, G. (2011). Lausannevirus, a giant amoebal virus encoding histone doublets. *Environ Microbiol.* v.13(6), p.1454-66.

WILLIAMS, T.; BARBOSA-SOLOMIEU, V.; CHINCHAR, V.G. A decade of advances in Iridovirus research. *Adv. Virus Res.* 2005, 65, 174–248.

YANG, Z.; REYNOLDS, S.E.; MARTENS, C.A.; BRUNO, D.P.; PORCELLA, S.F.; MOSS, B. (2011) Expression profiling of the intermediate and late stages of poxvirus replication. *J. Virol.* 85, 9899–9908.

YOO, K.T.; JUNG, S.Y. (2012). Effects of Mannose on Pathogenesis of *Acanthamoeba castellanii*. *Korean J Parasitol* 50(4):365-9.

YUTIN, N.; WOLF, Y.I.; RAOULT, D.; KOONIN, E.V. (2009). Eukaryotic large nucleocytoplasmic DNA viruses: clusters of orthologous genes and reconstruction of viral genome evolution. *Virology Journal*, Inglaterra, v. 6, n. 223, p. 01-13.

8. EVENTOS CIENTÍFICOS E PRODUÇÕES

8.1 Participações em eventos científicos

- II Simpósio de Microbiologia da UFMG - Microbiologia translacional: do ambiente natural às aplicações biotecnológicas. Período: 05 e 06 de outubro de 2015. Belo Horizonte, MG, Brasil.
- III Simpósio de Microbiologia da UFMG - Doenças microbianas emergentes. Período: 05 e 06 de setembro de 2016. Belo Horizonte, MG, Brasil.
- IV Simpósio de Microbiologia da UFMG - Metabolismo Microbiano: Saúde, Ambiente e Biotecnologia. Período: 02 e 03 de outubro de 2017. Belo Horizonte, MG, Brasil.
- II Encontro Científico do Laboratório de Vírus – Comemoração dos 55 anos. Período: 05 de setembro de 2017. Belo Horizonte, MG, Brasil/Palestrante como discente representante do laboratório de vírus.
- XXVI Brazilian Congress of Virology and X Mercosur Meeting of Virology. Período: 11 a 14 de outubro de 2015. Florianópolis, SC, Brasil.
- XXVIII Brazilian Congress of Virology and X Mercosur Meeting of Virology. Período: 06 a 10 de setembro de 2017. Belo Horizonte, MG, Brasil.

8.2 Organização de evento científico

- II Simpósio de Microbiologia da UFMG - Microbiologia translacional: do ambiente natural às aplicações biotecnológicas. Período: 05 e 06 de outubro de 2015. Belo Horizonte, MG, Brasil.

8.3 Artigos científicos publicados

1. **OLIVEIRA, GRAZIELE**; ASSIS, FELIPE ; ALMEIDA, GABRIEL ; ALBARNAZ, JONAS ; LIMA, MAURÍCIO ; ANDRADE, ANA ; CALIXTO, RAFAEL ; OLIVEIRA, CAIRO ; DIOMEDES NETO, JOSÉ ; TRINDADE, GILIANE ; FERREIRA, PAULO ; KROON, ERNA ; ABRAHÃO, JÔNATAS . From Lesions to Viral Clones: Biological and Molecular Diversity amongst Autochthonous Brazilian Vaccinia Virus. *Viruses*, v. 7, p. 1218-1237, 2015.

2. LIMA MT, ANDRADE AC, **OLIVEIRA GP**, CALIXTO RS, OLIVEIRA DB, SOUZA EL, TRINDADE GS, NICOLI JR, KROON EG, MARTINS FS, ABRAHÃO JS. Microbiota is an essential element for mice to initiate a protective immunity against Vaccinia virus. *FEMS Microbiol Ecol.* 2016 Feb; 92(2). pii: fiv147. doi: 10.1093/femsec/fiv147. Epub 2015 Nov 25.

3. SANTOS ABRAHÃO, J. ; DE SOUZA TRINDADE, G. ; **PEREIRA-OLIVEIRA, G.** ; DE OLIVEIRA FIGUEIREDO, P. ; COSTA, G. ; MOREIRA FRANCO-LUIZ, A. P. ; LOPES ASSIS, F. ; DE OLIVEIRA, D. BRETAS ; MATTOS PAIM, L. R. ; DE ARAÚJO OLIVEIRA, C. E. ; LEMOS MAIA NETO, A. ; GEESIEN KROON, E. . Detection of Vaccinia virus during an outbreak of exanthemous oral lesions in Brazilian equids. *Equine Veterinary Journal*, v. 8, p. n/a-n/a, 2016.

4. DUTRA, LARA AMBROSIO LEAL ; DE FREITAS ALMEIDA, GABRIEL MAGNO ; **OLIVEIRA, GRAZIELE PEREIRA** ; ABRAHÃO, JÔNATAS SANTOS ; KROON, ERNA GEESIEN ; TRINDADE, GILIANE DE SOUZA . Molecular evidence of Orthopoxvirus DNA in capybara (*Hydrochoerus hydrochaeris*) stool samples. *Archives of Virology*, v. 162, p. 1-10, 2016 .

5. DOS SANTOS PEREIRA ANDRADE, A.C. ; LIMA, M. TEIXEIRA ; **OLIVEIRA, G. PEREIRA** ; CALIXTO, R. SILVA ; DE SALES E SOUZA, É.LORENNA ; DA GLÓRIA DE SOUZA, D. ; DE ALMEIDA LEITE, C.M. ; FERREIRA, J.M. SIQUEIRA ; KROON, E.G. ; DE OLIVEIRA, D. BRETAS ; DOS

SANTOS MARTINS, F. ; Abrahão, J.S. . Daily ingestion of the probiotic *Lactobacillus paracasei* ST11 decreases Vaccinia virus dissemination and lethality in a mouse model. *Beneficial Microbes*, v. 7, p. 1-8, 2016.

6. ASSIS, FELIPE L. ; FRANCO-LUIZ, ANA PAULA M. ; PAIM, LUIS M. ; **OLIVEIRA, GRAZIELE P.** ; PEREIRA, ALEXANDRE F. ; DE ALMEIDA, GABRIEL M. F. ; FIGUEIREDO, LEANDRA B. ; TANUS, ADRIANO ; TRINDADE, GILIANE S. ; FERREIRA, PAULO P. ; KROON, ERNA G. ; ABRAHÃO, JÔNATAS S. . Horizontal study of vaccinia virus infections in an endemic area: epidemiologic, phylogenetic and economic aspects. *Archives of Virology*, v. 160, p. 2703-2708, 2015.

7. ARANTES, THALITA SOUZA; RODRIGUES, RODRIGO ARAÚJO LIMA; SILVA, LUDMILA KAREN DOS SANTOS; **OLIVEIRA, GRAZIELE PEREIRA**; DE SOUZA, HELTON LUÍS; B. KHALIL, JACQUES Y.; OLIVEIRA, DANILO BRETAS DE; TORRES, ALICE ABREU; DA SILVA, LUIS LAMBERTI; COLSON, PHILIPPE; KROON, ERNA GEESIEN; DA FONSECA, FLÁVIO GUIMARÃES; BONJARDIM, CLÁUDIO ANTÔNIO; LA SCOLA, BERNARD; ABRAHÃO, JÔNATAS SANTOS. The large marseillevirus explores different entry pathways by forming giant infectious vesicles. *Journal of Virology (Print)*, v. 90, p. JVI.00177-16, 2016.

8. BORATTO, PAULO VICTOR MIRANDA ; DORNAS, FÁBIO PIO ; DA SILVA, LORENA CHRISTINE FERREIRA ; RODRIGUES, RODRIGO ARAÚJO LIMA ; **OLIVEIRA, GRAZIELE PEREIRA** ; CORTINES, JULIANA REIS ; DRUMOND, BETÂNIA PAIVA ; ABRAHÃO, JÔNATAS SANTOS . The analysis of KV mimivirus major capsid gene and its transcript highlights a distinct pattern of gene evolution and splicing among mimiviruses. *JOURNAL OF VIROLOGY*, v. 92, p. JVI.01782-17, 2017.

9. **OLIVEIRA, GRAZIELE**; RODRIGUES, RODRIGO ; LIMA, MAURÍCIO ; DRUMOND, BETÂNIA ; ABRAHÃO, JÔNATAS . Poxvirus Host Range Genes and Virus-Host Spectrum: A Critical Review. *Viruses-Basel*, v. 9, p. 331, 2017.

10. ANDRADE, ANA CLÁUDIA DOS SANTOS PEREIRA ; RODRIGUES, RODRIGO ARAÚJO LIMA ; **OLIVEIRA, GRAZIELE PEREIRA** ; ANDRADE, KÉTYLLEN REIS ; BONJARDIM, CLÁUDIO ANTÔNIO ; LA SCOLA, BERNARD ; KROON, ERNA GEESIEN ; ABRAHÃO, JÔNATAS SANTOS . Filling gaps about mimivirus entry, uncoating and morphogenesis. JOURNAL OF VIROLOGY, v. 91, p. JVI.01335-17, 2017.

11. **OLIVEIRA, GRAZIELE PEREIRA**; LIMA, MAURÍCIO TEIXEIRA ; ARANTES, THALITA SOUZA ; ASSIS, FELIPE LOPES ; RODRIGUES, RODRIGO ARAÚJO LIMA ; DA FONSECA, FLÁVIO GUIMARÃES ; BONJARDIM, CLÁUDIO ANTÔNIO ; KROON, ERNA GEESIEN ; COLSON, PHILIPPE ; LA SCOLA, BERNARD ; ABRAHÃO, JÔNATAS SANTOS . The Investigation of Promoter Sequences of Marseilleviruses Highlights a Remarkable Abundance of AAATATTT motif in Intergenic Regions. JOURNAL OF VIROLOGY, v. 91, p. JVI.01088-17, 2017.

12. **OLIVEIRA, GRAZIELE**; ANDRADE, ANA ; RODRIGUES, RODRIGO ; ARANTES, THALITA ; BORATTO, PAULO ; SILVA, LUDMILA ; DORNAS, FÁBIO ; TRINDADE, GILIANE ; DRUMOND, BETÂNIA ; LA SCOLA, BERNARD ; KROON, ERNA ; ABRAHÃO, JÔNATAS . Promoter Motifs in NCLDVs: An Evolutionary Perspective. Viruses-Basel, v. 9, p. 16, 2017.

13. **OLIVEIRA, GRAZIELE P.**; DE AQUINO, ISABELLA L. M. ; LUIZ, ANA P. M. F. ; ABRAHÃO, JÔNATAS S. . Putative Promoter Motif Analyses Reinforce the Evolutionary Relationships Among Faustoviruses, Kaumoebavirus, and Asfarvirus. Frontiers in Microbiology, v. 9, p. 1-8, 2018.

14. PERES, MARINA ; BACCHIEGA, THAIS ; APPOLINÁRIO, CAMILA ; VICENTE, ACÁCIA ; MIONI, MATEUS ; RIBEIRO, BRUNA ; FONSECA, CLÓVIS ; PELÍCIA, VANESSA ; FERREIRA, FERNANDO ; **OLIVEIRA, GRAZIELE** ; Abrahão, Jonatas ; MEGID, JANE . Vaccinia Virus in Blood Samples of Humans, Domestic and Wild Mammals in Brazil. Viruses-Basel, v. 10, p. 42, 2018.

15. CALIXTO, RAFAEL ; **OLIVEIRA, GRAZIELE** ; LIMA, MAURÍCIO ; ANDRADE, ANA ; TRINDADE, GILIANE ; DE OLIVEIRA, DANILO ; KROON, ERNA . A Model to Detect Autochthonous Group 1 and 2 Brazilian Vaccinia virus Coinfections: Development of a qPCR Tool for Diagnosis and Pathogenesis Studies. *Viruses-Basel*, v. 10, p. 15-25, 2018.

16. LIMA, MAURÍCIO TEIXEIRA ; **OLIVEIRA, GRAZIELE PEREIRA** ; ASSIS, FELIPE LOPES ; BRETAS DE OLIVEIRA, DANILO ; VAZ, SIDINER MESQUITA ; TRINDADE, GILIANE DE SOUZA ; ABRAHÃO, JÔNATAS SANTOS ; KROON, ERNA GEESIEN . Ocular Vaccinia Infection in Dairy Worker, Brazil. *Emerging infectious diseases*, v. 24, p. 161-162, 2018.

8.4 Capítulos de livros publicados

1. ABRAHAO, J. S. ; **OLIVEIRA, GRAZIELE** ; SILVA, L. C. F. ; SILVA, L. K. S. ; KROON, E. G. ; LA SCOLA, B. . Mimiviruses: Replication, Purification, and Quantification. UNIT 14G.1 Mimiviruses: Replication, Purification, and Quantification. 1ed.: John Wiley & Sons, Inc., 2016, v. , p. 1-.

2. KROON, ERNA G. ; ABRAHÃO, JÔNATAS S. ; TRINDADE, GILIANE S. ; **OLIVEIRA, GRAZIELE P.** ; FRANCO-LUIZ, ANA PAULA M. ; COSTA, GALILEU B. ; LIMA, MAURÍCIO T. ; CALIXTO, RAFAEL S. ; OLIVEIRA, DANILO B. ; DRUMOND, BETÂNIA P. Natural Vaccinia Virus Infection: Diagnosis, Isolation, and Characterization. *Natural Vaccinia Virus Infection: Diagnosis, Isolation, and Characterization*. 0ed.: , 2016, v. , p. 1-.

3. **OLIVEIRA, GRAZIELE**; COSTA, GALILEU ; ASSIS, FELIPE ; FRANCO-LUIZ, ANA ; TRINDADE, GILIANE ; KROON, ERNA ; TURRINI, FILIPPO ; ABRAHÃO, JONATAS . Parapoxvirus. Molecular Detection of Animal Viral Pathogens. 1ed.: CRC Press, 2016, v. , p. 881-890.

8.5 Artigos em processo de revisão

1. RODRIGO ARAÚJO LIMA RODRIGUES; THALITA SOUZA ARANTES; **GRAZIELE PEREIRA OLIVEIRA**; LUDMILA KAREN DOS SANTOS SILVA; JÔNATAS SANTOS ABRAHÃO (2018). The complex nature of tupanviruses. **Submitted: Advances in Virus Research.**
2. MATEUS SÁ MAGALHÃES SERAFIM, STEFÂNIA NEIVA LAVORATO, THALES KRONENBERGER, YAMARA VIANA SOUSA, **GRAZIELE PEREIRA OLIVEIRA**, SIMONE GONÇALVES DOS SANTOS, ERNA GEESIEN KROON, VINÍCIUS GONÇALVES MALTAROLLO, RICARDO JOSÉ ALVES, BRUNO FERNANDES MOTA (2018). Antimicrobial activity of synthetic 1,3-bis(aryloxy)propan-2-amines against Gram-positive bacteria. **Submitted: Frontiers in Microbiology.**

9. ANEXOS_OUTROS ARTIGOS PUBLICADOS DURANTE O DOUTORADO

ANEXOS

Article

From Lesions to Viral Clones: Biological and Molecular Diversity amongst Autochthonous Brazilian *Vaccinia Virus*

Graziele Oliveira ¹, Felipe Assis ¹, Gabriel Almeida ², Jonas Albarnaz ¹, Maurício Lima ¹, Ana Cláudia Andrade ¹, Rafael Calixto ¹, Cairo Oliveira ³, José Diomedes Neto ⁴, Giliane Trindade ¹, Paulo César Ferreira ¹, Erna Geessien Kroon ¹ and Jônatas Abrahão ^{1,*}

¹ Laboratório de Vírus, Departamento de Microbiologia, Universidade Federal de Minas Gerais, Belo Horizonte, Minas Gerais 31270-901, Brazil; E-Mails: graziufmg@yahoo.com.br (G.O.); felipelopeassis@gmail.com (F.A.); jonasalbarnaz@yahoo.com.br (J.A.); maurili15@hotmail.com (M.L.); ana.andrade2008@hotmail.com (A.C.A.); calixtomicro@yahoo.com.br (R.C.); gitrindade@yahoo.com.br (G.T.); peregrinopcp@hotmail.com (P.C.F.); ernagkroon@gmail.com (E.G.K.)

² (AQUACEN) Laboratório Nacional Oficial de Referência de Doenças de Animais Aquáticos, Universidade Federal de Minas Gerais, Belo Horizonte, Minas Gerais 31270-901, Brazil; E-Mail: gabriel.magno@gmail.com

³ Laboratório de Retrovírus, Departamento de Medicina Veterinária Preventiva, Escola de Veterinária da Universidade Federal de Minas Gerais, Belo Horizonte, Minas Gerais 31270-901, Brazil; E-Mail: cairo_henrique@yahoo.com.br

⁴ Centro Agropecuário, Departamento de Ciência Animal, Universidade Federal do Pará, Pará 66075-110, Brazil; E-Mail: diomedes@ufpa.br

* Author to whom correspondence should be addressed; E-Mail: jonatas.abrahao@gmail.com; Tel.: +55-31-3409-2539.

Academic Editors: Elliot J. Lefkowitz and Chris Upton

Received: 17 December 2014 / Accepted: 9 March 2015 / Published: 16 March 2015

Abstract: *Vaccinia virus* (VACV) has had an important role for humanity because of its use during the smallpox eradication campaign. VACV is the etiologic agent of the bovine vaccinia (BV), an emerging zoonosis that has been associated with economic, social, veterinary and public health problems, mainly in Brazil and India. Despite the current and historical VACV importance, there is little information about its circulation, prevalence, origins and maintenance in the environment, natural reservoirs and diversity. Brazilian VACV (VACV-BR) are grouped into at least two groups based on genetic and biological

diversity: group 1 (G1) and group 2 (G2). In this study, we went to the field and investigated VACV clonal diversity directly from exanthemous lesions, during BV outbreaks. Our results demonstrate that the G1 VACV-BR were more frequently isolated. Furthermore, we were able to co-detect the two variants (G1 and G2) in the same sample. Molecular and biological analysis corroborated previous reports and confirmed the co-circulation of two VACV-BR lineages. The detected G2 clones presented exclusive genetic and biological markers, distinct to reference isolates, including VACV-Western Reserve. Two clones presented a mosaic profile, with both G1 and G2 features based on the molecular analysis of A56R, A26L and C23L genes. Indeed, some SNPs and INDELs in A56R nucleotide sequences were observed among clones of the same virus population, maybe as a result of an increased mutation rate in a mixed population. These results provide information about the diversity profile in VACV populations, highlighting its importance to VACV evolution and maintenance in the environment.

Keywords: *Vaccinia virus*; clones; diversity; evolution

1. Introduction

Vaccinia virus (VACV) has had an important role in human history due to its use as a vaccine during the smallpox vaccination campaign, resulting in the eradication of this deadly disease in 1980 [1]. More recently, VACV has been widely used as a vector for recombinant vaccines [2–4]. Following Smallpox eradication, other zoonotic orthopoxviruses (OPV) have emerged worldwide, such as *Cowpox virus* (CPXV), in Europe, *Monkeypox virus* (MPXV), endemic in many African countries and recently introduced in the USA, and finally VACV, endemic in Brazil and India [5–13]. VACV is the causative agent of bovine vaccinia (BV), an exanthemous disease responsible for outbreaks that affect both bovines and humans, causing public health impacts and economic losses in South America and India [10–12,14,15]. The clinical prognosis of BV includes the appearance of papules that progress to vesicles and growing scabs mainly on the teats and udder of infected bovines. In humans, the lesions occur primarily on milkers' hands and arms. Other symptoms, such as fever, myalgia, headache, arthralgia and lymphadenopathy are also frequently reported [11,16]. During outbreaks, direct contact with infected animals is the main transmission route to humans, but it may also occur by contact with contaminated fomites. Furthermore, reports have suggested a possible human-to-human transmission of VACV [16–18].

In Brazil, VACV was first isolated from rodents in the 1960s and since 1999 BV outbreaks have been consistently reported [10,12,15,19–24]. Some reports have shown a great genetic and biologic heterogeneity among Brazilian VACV (VACV-BR) isolates. This variability allowed clustering of VACV-BR into at least two distinct groups (Group 1—G1 and Group 2—G2), demonstrating a dichotomy supported by evidence of molecular and biological diversity such as virulence in BALB/c mouse model and plaque phenotype in BSC-40 cells. Group 2 strains display higher plaque sizes and are virulent to mice, unlike Group 1 [24–28]. Moreover, polymorphisms observed in specific VACV genes, such as hemagglutinin gene (A56R), A-type inclusion body gene (A26L), and chemokine binding

protein gene (C23L), have been used in phylogenetic studies and further confirmed the dichotomy between G1 and G2 VACV-BR [22,27,29,30].

The VACV-BR G2 comprises of viral isolates Guarani P1 virus (GP1V), Pelotas 1 virus (P1V), Belo Horizonte virus (VBH), the newest isolate Serro human virus 2 (SH2V) and others, while G1, the group most frequently reported during BV outbreaks, includes isolates of Araçatuba virus (ARAV), Cantagalo virus (CTGV), Mariana virus (MARV), Guarani P2 virus (GP2V), Pelotas 2 virus (P2V) and others [22–24,26,28,31,32]. It is worth mentioning that the GP1V and GP2V were isolated during the same outbreak (co-circulation), while P1V and P2V were isolated from the same clinical sample (co-infection) [26,28].

Several studies have demonstrated genetic and biological diversity among isolates of the same species of a given OPV, including *Variola virus* (VARV), CPXV and MPXV. Diversity studies among MPXV isolates have revealed the existence of a dichotomy supported by differences in epidemiological and clinical features, while CPXV is clustered in four or more groups. Furthermore, studies on VARV variability have demonstrated the existence of at least two groups with distinct virulence profiles: *variola major* and *variola minor*. Taken together, these studies showed a great biological and genetic diversity amongst isolates from different OPV species [33–40].

Osborne and colleagues in 2007 reported high genetic variability among clones of the smallpox vaccine Dryvax [41]. Moreover, other studies reveal that old vaccines were a complex mixture of viruses with a large number of single-nucleotide polymorphisms (SNPs) besides insertions and deletions (INDELs), resulting in genetically and phenotypically distinct clones [42–45]. Besides, recombination events can occur among OPVs since it has been observed in VACV co-cultures and between VARV and CPXV [46–48]. Together, these studies suggest that poxviruses from the same species exist as distinct genetical groups and can recombine inside co-infected hosts, which increases the importance of studying the genetic variability among strains and clones of poxviruses circulating in the environment. Even though studies using vaccine strains clones show that VACV can recombine, there is an absence of data concerning VACV clones from field samples. This work aims to contribute to the understanding about the biological and genetic variability among field VACV clones by using genetic and biological analyses to study the diversity of VACV populations isolated during BV outbreaks.

2. Materials and Methods

2.1. Ethics Approval

The study was approved by the Committee of Ethics in Animal Use from the Universidade Federal de Minas Gerais (CEUA/UFMG). The animals were anesthetized by intraperitoneal injection of ketamine (Vetnil, São Paulo, Brazil) and xylazine (União Química, São Paulo, Brazil) before the infection and those ones that had lost more than 25% of their initial body weight were euthanized with an overdose of anesthetics.

2.2. Cells and Viruses

African green monkey kidney BSC-40 and VERO cells (American type cell culture—ATCC) were maintained in 5% CO₂ atmosphere at 37 °C in Eagle's Minimum Essential Medium (MEM) (Gibco

BRL, Invitrogen, Carlsbad, CA, USA) supplemented with 5% fetal bovine serum (FBS) (Cultilab, Brazil), 25 µg/mL fungizone (Amphotericin B) (Cristália, São Paulo, Brazil), 500 U/mL penicillin (Cristália, São Paulo, São Paulo, Brazil) and 50 µg/mL gentamicin (Schering-Plough, São Paulo, Brazil). VERO cells were used for viral isolation from clinical specimens and growth. The BSC-40 cells were used for viral clones purification, plaque phenotype, comet phenotype and growth curve assays. Only typical poxviruses cytopathic effects were visualized after inoculation of clinical samples in both cell systems. The VACV Western Reserve (VACV-WR) was gently provided by Dr C. Jungwirth (Universität Würzburg, Würzburg, Germany) and was used as a virulent control in mice assays.

2.3. Clinical Samples

Clinical samples, consisting of swabs of vesicular fluids and scabs obtained from cattle's teats and milkers' hands, were collected during BV outbreaks that occurred between 2005 and 2011 in five Brazilian states: Minas Gerais, Bahia, Goiás, Espírito Santo and Pará. Sample collection procedures were performed by veterinarians, following institutional recommendations. Two viruses were isolated from human samples, obtained in Bahia and Minas Gerais states; and eight viruses were isolated from bovine samples, two obtained from Bahia state, two from Para state, two from Goiás state, one from Minas Gerais state and one from Espírito Santo state. The counties and states where the samples were isolated are shown in Table 1 and Figure 1.

Table 1. Identification of viral clones isolated from clinical samples.

VACV-BR isolates (abbreviation)	Isolated clones	Source	Isolation state	Isolation year
VACV-BABV	VACV-BABV Clone 1 to Clone 5	<i>Bos taurus</i>	Bahia	2011
VACV-BAB2V	VACV-BAB2V Clone 1 to Clone 5	<i>Bos taurus</i>	Bahia	2011
VACV-BAHV	VACV-BAHV Clone 1 to Clone 5	<i>Homo sapiens</i>	Bahia	2011
VACV-GOBV	VACV-GOBV Clone 1 to Clone 5	<i>Bos taurus</i>	Goiás	2011
VACV-GOB2V	VACV-GOB2V Clone 1 to Clone 5	<i>Bos taurus</i>	Goiás	2011
VACV-ESBV	VACV-ESBV Clone 1 to Clone 5	<i>Bos taurus</i>	Espírito Santo	2008
VACV-MGBV	VACV-MGBV Clone 1 to Clone 4	<i>Bos taurus</i>	Minas Gerais	2005
VACV-MGHV	VACV-MGHV Clone 1 to Clone 5	<i>Homo sapiens</i>	Minas Gerais	2011
VACV-PABV	VACV-PABV Clone 1 to Clone 5	<i>Bos taurus</i>	Pará	2011
VACV-PAB2V	VACV-PAB2V Clone 1 to Clone 4	<i>Bos taurus</i>	Pará	2010

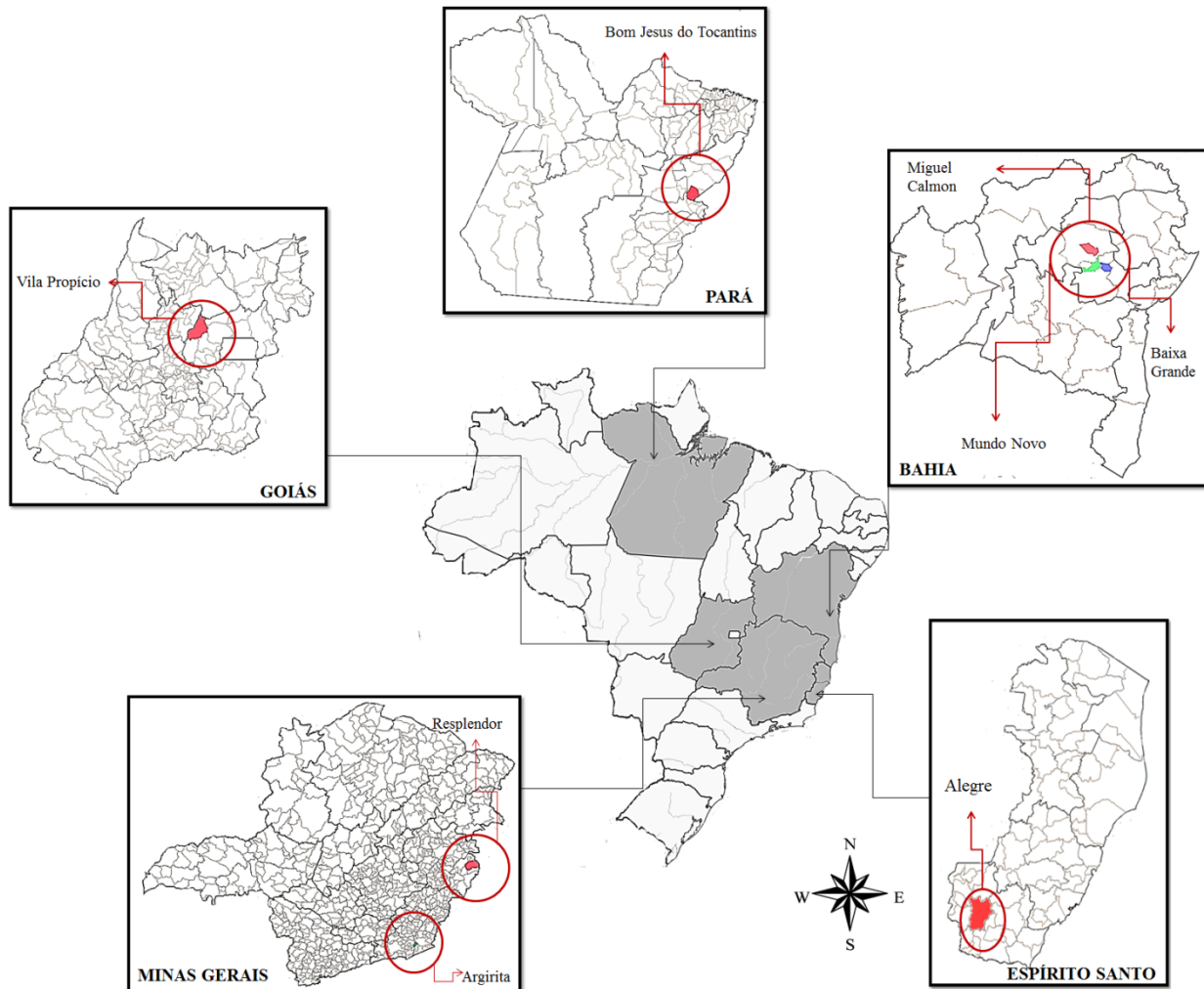


Figure 1. Map displaying Brazilian states and counties from which the clinical samples used for *Vaccinia virus* clone isolation were collected. The red circles indicate the counties where the samples were collected: Miguel Calmon, Baía Grande and Mundo Novo counties localized in Bahia state, Vila Propício county localized in Goiás state, Bom Jesus do Tocantins county localized in Pará state, Resplendor and Argirita counties localized in Minas Gerais States and Alegre county in Espírito Santo state.

2.4. Sample Processing and Virus Isolation

Scabs were macerated using a homogenizer (Polytron, Lucerne, Switzerland) in phosphate buffer saline (PBS) (0.1 g scab/0.9 mL PBS) containing 200 U/mL penicillin, 4 µg/mL amphotericin B and 100 µg/mL gentamicin, and then clarified by centrifugation at 2000× *g* for 3 min (min). To the swabs, 200 µL of PBS was added, followed by a centrifugation at 2000× *g* for 3 min [32]. For virus isolation, 200 µL of supernatant was added to VERO cells monolayers which were incubated after adsorption at 37 °C for 72 h or until detection of cytopathic effect (CPE).

2.5. Viral Clone Plaque Purification

BSC-40 cells were used for viral plaque purification as described elsewhere [49]. After isolation, each virus isolate was serially diluted (log₁₀) and inoculated into BSC-40 cells monolayers cultured in 6-well plates for clone selection and viral plaque purification. After 1 h of incubation (at 37 °C, 5%CO₂), culture medium was removed, cell monolayers were washed twice with PBS and solid medium (MEM supplemented with 1% FBS + agarose 1%—Gibco, São Paulo, Brazil) was added. After 48 hours, five viral plaques from each sample were collected and purified in BSC40 cells with solid medium. The criteria used to choose the clones was the plaque size: after measurement, small and large viral plaques were collected from each sample. Individual clones were then isolated by serial plaque-purifications in three passages in BSC40 cells using 1% agarose overlay. The resulting clones were propagated in Vero cells monolayers, purified and titrated as described [49,50]. Isolated VACV strains and clones are shown in Table 1. Two clones, from two distinct clinical samples, were not able to grow after some steps of clone plaque purification (Table 1). After clone plaque purification, clones were manipulated separately to avoid cross-contamination.

2.6. Biological Assays

2.6.1. Plaque Phenotype

For plaque phenotype assays, BSC40 cells seeded in 6-well plates at 90%–95% confluence were infected with specific clones. After 1 h of adsorption (37 °C, 5%CO₂), monolayers were washed twice with PBS and overlaid with solid medium prepared by mixing equal proportion of 1% agarose and 2× Eagle's minimum essential medium (MEM) (Gibco, São Paulo, Brazil) supplemented with 2% FBS (Gibco, São Paulo, Brazil). After 48 h of incubation (37 °C, 5% CO₂), cells were fixed with formaldehyde and stained with crystal violet for plaque size analysis.

2.6.2. Comet Phenotype Assay

For comet phenotype assays, BSC40 cells seeded in 6-well plates at 90%–95% confluence were infected with the large plaque clones. After 1 h of adsorption (37 °C, 5% CO₂), the medium was removed, monolayers were washed twice with PBS and fresh MEM supplemented with 1% FBS was added. After 48 h of incubation (37 °C, 5% CO₂), the cells were fixed with paraformaldehyde and stained with crystal violet.

2.6.3. Growth Curve Assays

BSC-40 cells were grown in 24-well plates and infected with VACV clones in biological duplicates. Infection was carried out at a MOI (multiplicity of infection) of 0.01 for 0, 12, 24 and 48 h post infection (hpi). Infected monolayers were then harvested, frozen (−70 °C) and thawed (37 °C) three times and titrated in BSC-40 cells as described. The analysis was performed with GraphPad Prism software (Version 5.00, GraphPad Software, San Diego, CA, USA, 2012).

2.7. Virulence in BALB/c Mice

To compare the virulence profile of these new clonal VACV isolates, five clones were selected for virulence assays. Mice were housed in filter-top microisolator cages and provided with commercial mouse food and water *ad libitum*. All the animal experiments were carried out in accordance with regulations and guidelines of the Committee of Ethics in Animal Use of the Universidade Federal de Minas Gerais/Brazil. BALB/c mice were anesthetized by intraperitoneal injection of ketamine and xylazine (3.2 mg and 0.16 mg/mice in 0.9% PBS, respectively) before the procedure (dose: 80–120 mg/kg per animal). Groups of four-week old male BALB/c mice ($n = 4$) were inoculated intranasally with 10 μ L of viral suspensions containing 10^6 plaque forming units (pfu) VACV-WR was used as positive control, given its virulence for mice, and the negative control group was inoculated with 10 μ L of PBS as described in [25]. Mice were weighed daily, and clinical signs were recorded for 10 days post infection (dpi) [25]. Mice that lost more than 25% of their initial weight were euthanized.

2.8. Molecular Assays

Amplification of A56R, A26L and C23L Genes and Phylogenetic Analyses

For the clones' molecular characterization, DNA extractions were carried out using phenol-chloroform-isoamyl alcohol (PCI) [51] and used as template for Polymerase chain reaction (PCR) amplification of the viral genes A56R (hemagglutinin), C23L (chemokine binding protein) and A26L (A-type inclusion body). These genes are traditionally used for OPV phylogenetic studies, including Brazilian VACV strains [27,29,30].

Two different reactions were made for C23L: reaction 1 was made using the primer pair 5'GCGTGTCCCCAGGACAAGGT3' 5' ATGTCGCTGTCTTTCTCTTCTTCGC 3', amplifying a 124 base pairs (bp) DNA fragment found in both VACV-BR groups. Reaction 2 was made with the primer pair 5'GCGTGTCCCCAGGACAAGGT3' and 5'CTGGATGGGTCTTG3', amplifying a 138 bp DNA fragment of VACV-BR Group 2 viruses but not from VACV-BR Group 1 viruses. This is possible since the reverse primer anneals to a region present on group 2 but deleted in group 1. PCR conditions were 94 °C for 10 min, 30 cycles of 94 °C for 30 s, 50 °C for 30 s and 72 °C for 30 s, followed by 72 °C for 10 min. A semi-nested PCR was made for A26L, using the primer pair 5'ACCACGTCTACTACTCGGCGA3' and 5'TGCATCGAGAGCGGAGGAGGA3' for the first reaction and the primer pair 5'ACCACGTCTACTACTCGGCGA3' and 5'CGATGCCAAGTACATCGACGA3' for the second reaction. Amplicon sizes are 750 bp and 160 bp respectively, and reaction conditions were: 95 °C for 10 min, 30 cycles of 95 °C for 1 min, 60 °C for 1 min and 72 °C for 1 min, followed by 72 °C for 10 min. Reactions were carried out using 10–50 ng of DNA as template with 0.4 mM of each primer; 0.1 M tris-HCl (pH 8.4); 0.5M KCl; 2.5 mM MgCl₂; 10 mM of each dNTPs and 2U Taq DNA polymerase to a final volume of 20 μ L. Brazilian isolates GP1V and GP2V were used as positive controls. Reactions for the A56R gene were made as previously described [52]. PCR products were electrophoresed in 8%-PAGE and silver stained [51].

For sequencing, the A56R gene was amplified with primers and conditions described elsewhere [53], resulting in amplicons of approximately 900 bp. The A56R fragments were sequenced in both orientations and in duplicate in an automated DNA sequencer (ABI PRISM, Applied Biosystems, São Paulo, Brazil).

The sequences were aligned with previously published OPV sequences from GenBank (accession numbers can be found in the figures) using MEGA software version 6.1 (Arizona State University, Phoenix, AZ, USA, 2014). The phylogenetic tree based on the A56R gene sequences was constructed by the Maximum Likelihood method based on the Tamura-Nei model implemented in MEGA6.1 (Arizona State University, Phoenix, AZ, USA, 2014). A56R sequences from clonal VACV-BR obtained in this study were deposited in GenBank. (BAB2V-Clone 1: KP282618; BAB2V-Clone 2: KP282619; BAB2V-Clone 3: KP282620; BAB2V Clone 4: KP282621; BAB2V-Clone 5: KP282622; MGHV-Clone 1: KP282623; MGHV-Clone 2: KP282624; MGHV-Clone 3: KP282625; MGHV-Clone 4: KP282626; MGHV-Clone 5: KP282627; BAHV-Clone 1: KP282628; BAHV-Clone 2: KP282629; BAHV-Clone 3: KP282630; BAHV-Clone 4: KP282631; BAHV-Clone 5: KP282632; ESBV-Clone 1: KP282633; ESBV-Clone 2: KP282634; ESBV-Clone 3: KP282635; ESBV-Clone 4: KP282636; ESBV-Clone 5: KP282637; GOB2V-Clone 1: KP282638; GOB2V-Clone 2: KP282639; GOB2V-Clone 3: KP282640; GOB2V-Clone 4: KP282641; GOB2V-Clone 5: KP282642; MGBV-Clone 1: KP282643; MGBV-Clone 2: KP282644; MGBV-Clone 3: KP282645; MGBV-Clone 4: KP282646; PAB2V-Clone 1: KP282647; PAB2V-Clone 2: KP282648; PAB2V-Clone 3: KP282649; PAB2V-Clone 4: KP282650; BABV-Clone 1: KP282651; BABV-Clone 2: KP282652; BABV-Clone 3: KP282653; BABV-Clone 4: KP282654; BABV-Clone 5: KP282655; GOBV-Clone 1: KP282656; GOBV-Clone 2: KP282657; GOBV-Clone 3: KP282658; GOBV-Clone 4: KP282659; GOBV-Clone 5: KP282660; PABV-Clone 1: KP282661; PABV-Clone 2: KP282662; PABV-Clone 3: KP282663; PABV-Clone 4: KP282664; PABV-Clone 5: KP282665).

3. Results

3.1. Viral Clone Isolation and Biological Assays

Upon inoculation onto Vero cells, the 10 clinical samples presented typical OPV CPEs, such as lytic plaques, cell agglomerates and formation of vacuoles were observed. No changes were observed in negative control cells. Then, a total of 48 viral clones from the 10 clinical samples were selected. It is important to emphasize that a higher prevalence of small plaques was observed during plaque selection. After three rounds of plaque purification, the selected clones were expanded and purified in sucrose cushion. Biological assays such as plaque phenotype, comet phenotype and growth curve assays were performed to compare the isolated clones. Plaque phenotype assays showed that the clones produced distinct plaques size (Figure 2 and Supplementary Figure S1). The VACV-BABV and VACV-GOBV revealed interesting results. Three clones isolated from the VACV-BABV (BABV-Clone 2, BABV-Clone 3 and BABV-Clone 4) showed a large-plaque profile, while two other clones (BABV-Clone 1 and BABV-Clone 5) presented a small-plaque profile; and the VACV-GOBV showed a single clone (GOBV-Clone 2) with a large-plaque profile and four clones (GOBV-Clone 1, GOBV-Clone 3, GOBV-Clone 4 and GOBV-Clone 5) with the small-plaque profile. These results demonstrate the co-circulation of VACV with at least two distinct plaque-size phenotypes in the same VACV population. The clones obtained from the other isolations showed only small plaque phenotype.

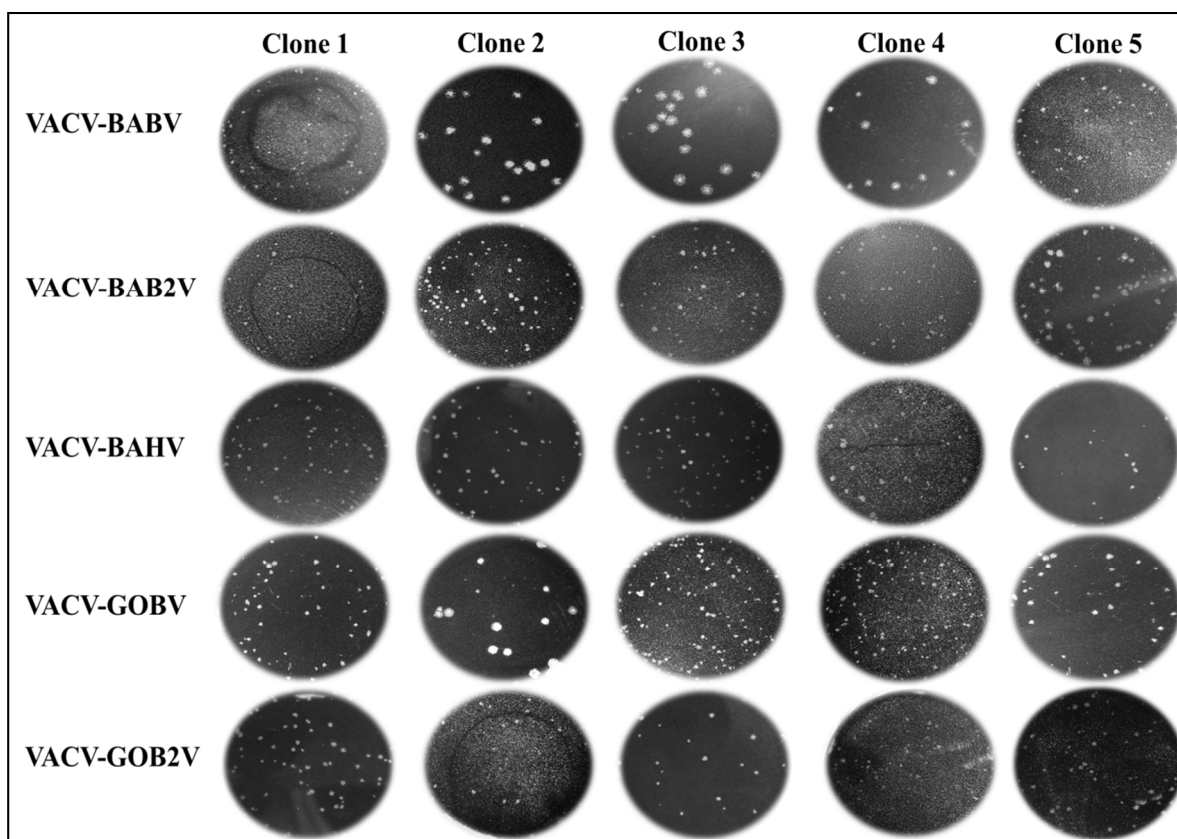


Figure 2. Viral clone plaque phenotype assays. BSC40 cells were cultured in a 6-well dish and then infected with VACV clones. Infection was carried out in the presence of 0.5% agarose for 48 h, followed by fixation and staining. All clones of the VACV-BAB2V, VACV-BAHV and VACV-GOB2V presented only small plaques, while VACV-BABV and VACV-GOBV strains presented small plaque clones as well as large plaque clones. VACV-BABV presented two small plaque clones (Clone 1 and 5) and three large plaque clones (Clone 2, 3 and 4). VACV-GOBV presented four small plaque clones (Clone 1, 3, 4 and 5) and one large plaque clone (Clone 2).

To proceed with the biological characterization, the comet phenotype assays for clones were carried out. Prominent comets were observed only in the four large plaque clones (data not shown). In order to compare the growth of VACV clones, we performed a growth curve assay showing that small-plaque clones presented a similar replication profile, but distinct from that observed for large plaque clones, that exhibited an increase of 2–4 logs when compared to the small plaque clones (Figure 3). Thereby, plaque phenotype and growth curve assays showed that large plaque clones display higher replication capacity when compared to small plaque clones and that those different profiles can be found in clones of a same sample.

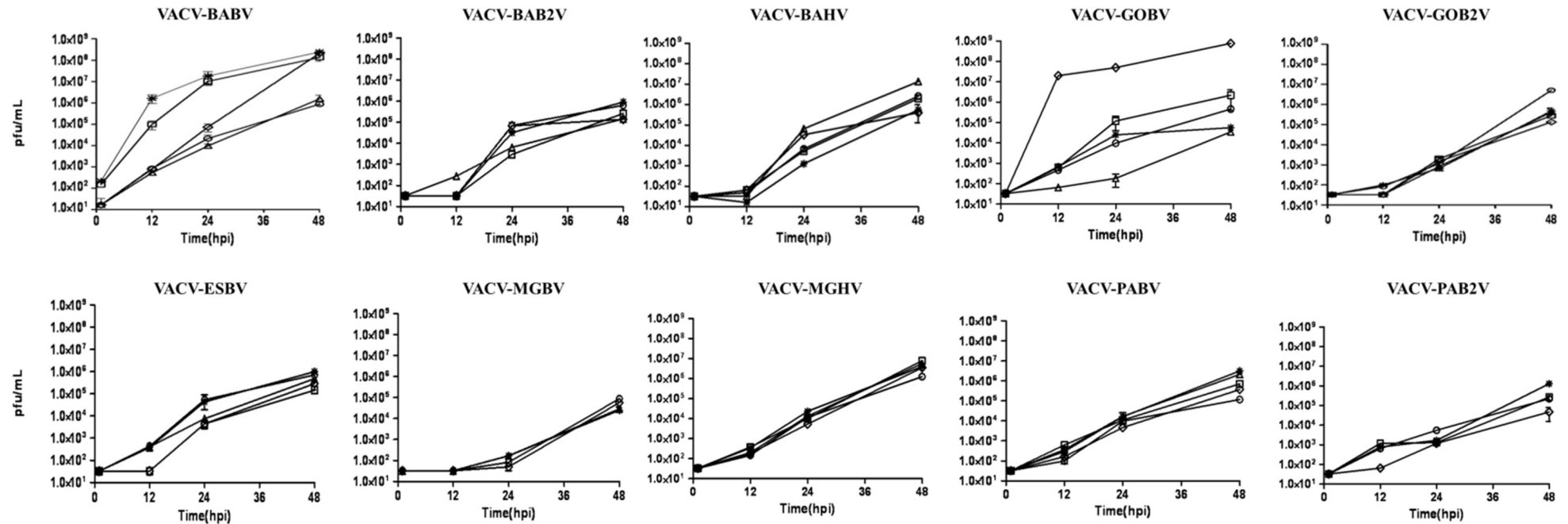


Figure 3. Growth curves assay of VACV-BR clones in BSC-40 cells. Cells were infected at an MOI of 0.01. Viral replication was determined by measuring the viral titer at 0, 12, 24 and 48 h after viral adsorption. The legend is the same for all the graphics: clone 1 (O), clone 2 (◇), clone 3 (*), clone 4 (□), and clone 5 (△) when present. Each data point represents the average of two independent experiments. The analysis was performed using GraphPad Prism 6.0 software (Version 5.00, GraphPad Software, San Diego, CA, USA, 2012).

3.2. Virulence of VACV-Clones in Balb/c Mice

For virulence assays, we selected the large plaque clones 2 and 3, and the small plaque clone 1 from VACV-BABV, and the large plaque clone 2 and small plaque clone 3 from VACV-GOBV. This selection was based on previous studies that correlated VACV plaque size and virulence in Balb/c mice [25]. Four-week-old BALB/c mice ($n = 4$) were intranasally infected with 1×10^6 pfu of each VACV clone and observed during 10 days for weight change, survival rate and clinical signs. The VACV-WR and PBS were used as virulence-positive and negative controls, respectively. We observed clinical signs, such as ruffling fur and arching back in mice inoculated with large plaque clones and VACV-WR within 3–7 dpi, similar to what has been previously reported for the virulent G2 VACV-BR [25]. However, some clinical signs, such as balanopostitis and periocular alopecia, were only observed in animals infected with VACV-WR (Figure 4C). Survival rates of mice inoculated with large plaque clones ranged from 0% (BABV-clone 2) to 50% (VACV-BABV-clone 3 and VACV-GOBV-clone 2), showing a variation in survival rate among virulent clones (Figure 4A). All mice inoculated with large plaque clones lost weight, while mice inoculated with small-plaque clones and with PBS gained weight over the 10-day experiment (Figure 4B). Moreover, mice inoculated with small-plaque clones, as well as the negative control group, did not present clinical signs and stayed alive during the 10 days of observation similar to what has been previously reported for the non-virulent VACV-BR group 1 [25].

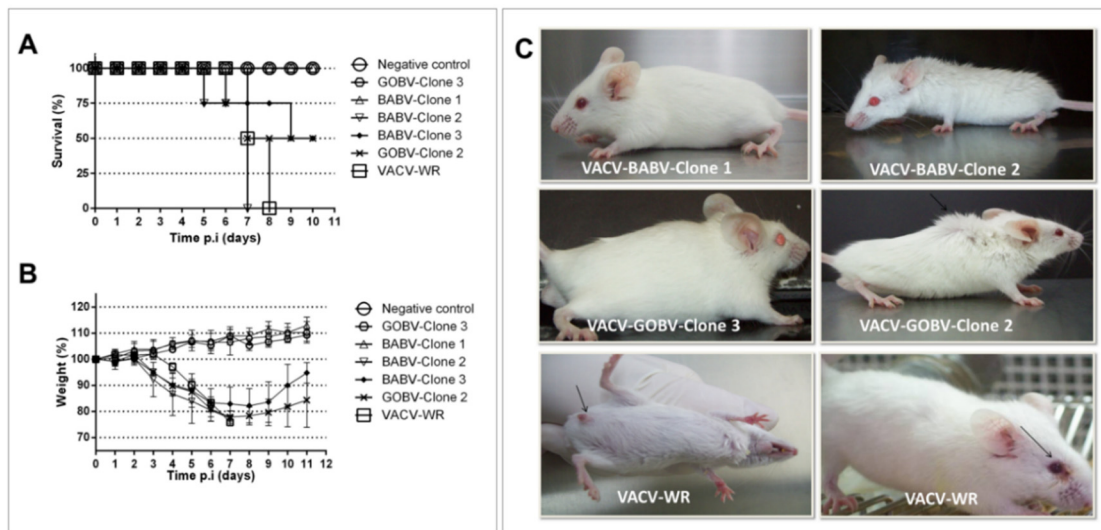


Figure 4. Virulence assays in a BALB/c mice model. Groups of four-week-old mice ($n = 4$) were inoculated by intranasal route with 10^6 PFU/ $10 \mu\text{L}$ of VACV-BABV strain clones 2 and 3 (large-plaque) and clone 1 (small plaque), and VACV-GOBV clone 2 (large plaque) and clone 3 (small plaque). VACV-WR was used as virulent control, and the negative control group was inoculated with PBS. No mice infected with small plaque clones died while the mice infected with large plaque clones had survival rates of 0% and 50%, showing variations in survival rates between the clones (A); Uninfected mice (negative control) and animals infected with small plaque clones gained weight, while mice infected with large plaque clones lost weight similarly to mice infected with virulent control VACV-WR (B). Ruffling fur and arching back were observed in mice infected with large plaque clones on day 4 p.i.

No clinical signals were observed in mice infected with small plaque clones from the same strain. Balanopostitis and periocular alopecia were observed only in mice infected with virulent control VACV-WR on day 3 p.i. No clinical signals were observed in control mice inoculated with PBS.

3.3. Phylogeny

For molecular comparison of the clones, the A56R, C23L, and A26L genes were amplified. Large plaque clones presented a typical G2 VACV-BR profile while the small plaque clones presented a profile similar to G1, which was corroborated by our biological data. However, two exceptions were found: large plaque clone 2 from VACV-BABV showed a G2 VACV-BR profile for the A56R and C23L genes and G1 profile for the A26L gene, and the small plaque clone 2 from the VACV-MGHV strain showed a G1 VACV-BR profile for the A56R and A26L genes and G2 profile to C23L gene. Table 2 summarizes these results. For phylogeny, we sequenced a partial fragment (900 bp) of the A56R gene of all VACV clones and the obtained sequences were compared to other VACV sequences available at NCBI nucleotide database. Phylogenetic analyses clustered the large plaque clones into G2 VACV-BR branch, while the small plaque clones were branched with G1 VACV-BR, further confirming the biological data (Figure 5). The branches were statistically supported by high bootstrap values, mainly due the presence of a molecular signature of 18-bp deletion in A56R gene from G1 of VACV-BR (Figure 6). Moreover, small plaque clones sequences showed specific polymorphisms that reflected the separation of some clones into different branches within this group (Figure 5 and Supplementary Figure S2).

Table 2. VACV-BR group 1 or 2 profile of the isolated clones based on A56R, A26L and C23L genes. Bold font indicates clones with mixed profile (Group 1 and 2).

Clones	Genes			Clones	Genes		
	A56R	A26L	C23L		A56R	A26L	C23L
BABV-Clone 1	Group 1	Group 1	Group 1	GOB2V-Clone 1	Group 1	Group 1	Group 1
BABV-Clone 2	Group 2	Group 1	Group 2	GOB2V-Clone 2	Group 1	Group 1	Group 1
BABV-Clone 3	Group 2	Group 2	Group 2	GOB2V-Clone 3	Group 1	Group 1	Group 1
BABV-Clone 4	Group 2	Group 2	Group 2	GOB2V-Clone 4	Group 1	Group 1	Group 1
BABV-Clone 5	Group 1	Group 1	Group 1	GOB2V-Clone 5	Group 1	Group 1	Group 1
BAB2V-Clone 1	Group 1	Group 1	Group 1	ESBV-Clone 1	Group 1	Group 1	Group 1
BAB2V-Clone 2	Group 1	Group 1	Group 1	ESBV-Clone 2	Group 1	Group 1	Group 1
BAB2V-Clone 3	Group 1	Group 1	Group 1	ESBV-Clone 3	Group 1	Group 1	Group 1
BAB2V-Clone 4	Group 1	Group 1	Group 1	ESBV-Clone 4	Group 1	Group 1	Group 1
BAB2V-Clone 5	Group 1	Group 1	Group 1	ESBV-Clone 5	Group 1	Group 1	Group 1
BAHV-Clone 1	Group 1	Group 1	Group 1	MGHV-Clone 1	Group 1	Group 1	Group 1
BAHV-Clone 2	Group 1	Group 1	Group 1	MGHV-Clone 2	Group 1	Group 1	Group 2
BAHV-Clone 3	Group 1	Group 1	Group 1	MGHV-Clone 3	Group 1	Group 1	Group 1
BAHV-Clone 4	Group 1	Group 1	Group 1	MGHV-Clone 4	Group 1	Group 1	Group 1
BAHV-Clone 5	Group 1	Group 1	Group 1	MGHV-Clone 5	Group 1	Group 1	Group 1

Table 2. Cont.

Clones	Genes			Clones	Genes		
	A56R	A26L	C23L		A56R	A26L	C23L
GOBV-Clone 1	Group 1	Group 1	Group 1	PABV-Clone 1	Group 1	Group 1	Group 1
GOBV-Clone 2	Group 2	Group 2	Group 2	PABV-Clone 2	Group 1	Group 1	Group 1
GOBV-Clone 3	Group 1	Group 1	Group 1	PABV-Clone 3	Group 1	Group 1	Group 1
GOBV-Clone 4	Group 1	Group 1	Group 1	PABV-Clone 4	Group 1	Group 1	Group 1
GOBV-Clone 5	Group 1	Group 1	Group 1	PABV-Clone 5	Group 1	Group 1	Group 1
MGBV-Clone 1	Group 1	Group 1	Group 1	PAB2V-Clone 1	Group 1	Group 1	Group 1
MGBV-Clone 2	Group 1	Group 1	Group 1	PAB2V-Clone 2	Group 1	Group 1	Group 1
MGBV-Clone 3	Group 1	Group 1	Group 1	PAB2V-Clone 3	Group 1	Group 1	Group 1
MGBV-Clone 4	Group 1	Group 1	Group 1	PAB2V-Clone 4	Group 1	Group 1	Group 1

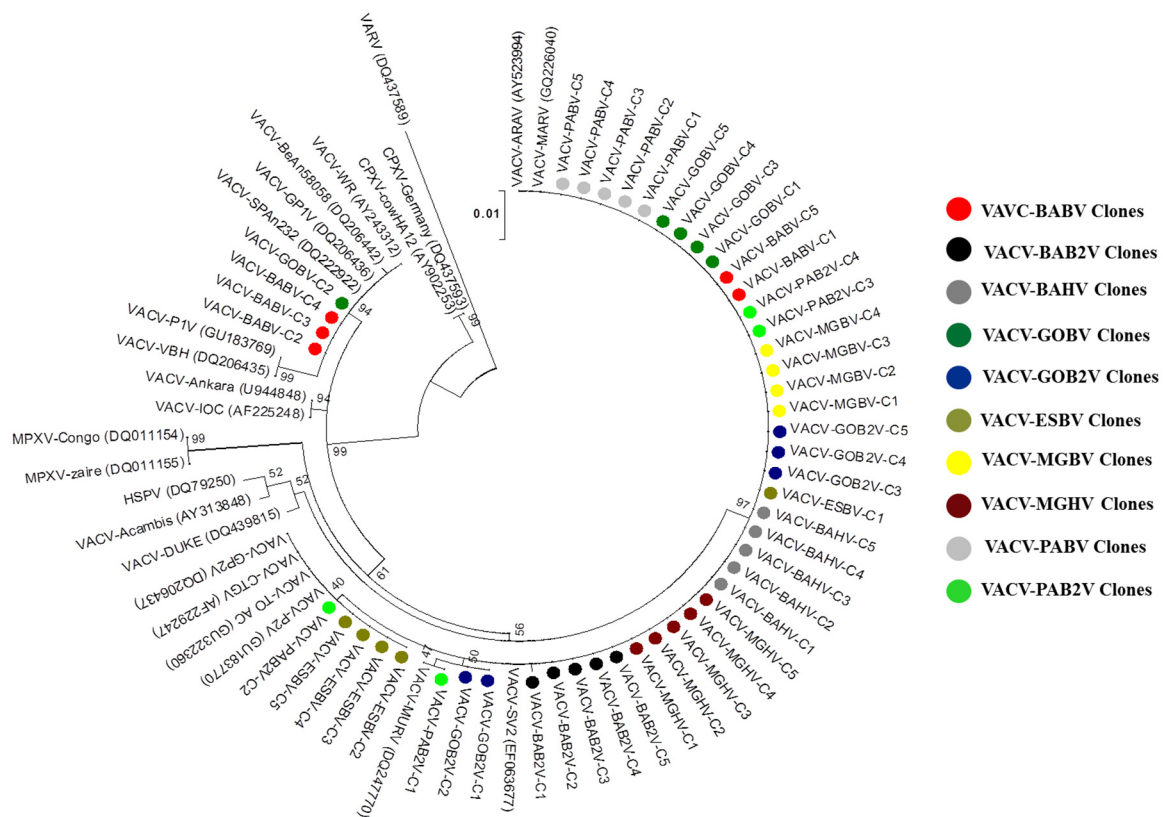


Figure 5. Phylogenetic analysis of viral clones based on the nucleotide sequences of *Orthopoxvirus* A56R gene. The tree was constructed by the Maximum Likelihood method with 1000 bootstrap replicates based in Tamura-Nei model implemented in MEGA6.1 software program (Arizona State University, Phoenix, AZ, USA, 2014) (www.megasoftware.net). Bootstrap confidence intervals are shown on branches. Nucleotide sequences were obtained from GenBank. Distinct colors indicate a strain and its clones as shown in the legend. Clones isolated from the same clinical sample were grouped in separate branches (Groups 1 and 2). Most of the clones were grouped in G1 and subgroups within the G1 were observed.

```

VACV-MARV_(GQ226040)   TTA ACC ACC GAT GAT GCG GAT CTT TAT --- --- --- --- --- GAT --- --- ACA GTA CCA CCA ACT ACT GTA GGC
VACV-BABV-C1          .C. .... .C. .... .C. .... .C. .... .C. .... .C. .... .C. .... .C. .... .C. .... .C. .... .C. .... .C. ....
VACV-BABV-C2          .C. .... .C. .... .C. .... .C. .... .C. .... .C. .... .C. .... .C. .... .C. .... .C. .... .C. .... .C. ....
VACV-BABV-C3          .C. .... .C. .... .C. .... .C. .... .C. .... .C. .... .C. .... .C. .... .C. .... .C. .... .C. .... .C. ....
VACV-BABV-C4          .C. .... .C. .... .C. .... .C. .... .C. .... .C. .... .C. .... .C. .... .C. .... .C. .... .C. .... .C. ....
VACV-BABV-C5          .C. .... .C. .... .C. .... .C. .... .C. .... .C. .... .C. .... .C. .... .C. .... .C. .... .C. .... .C. ....
VACV-BAB2V           .C. .... .C. .... .C. .... .C. .... .C. .... .C. .... .C. .... .C. .... .C. .... .C. .... .C. .... .C. ....
VACV-BAHV            .C. .... .C. .... .C. .... .C. .... .C. .... .C. .... .C. .... .C. .... .C. .... .C. .... .C. .... .C. ....
VACV-GOBV-C1         .C. .... .C. .... .C. .... .C. .... .C. .... .C. .... .C. .... .C. .... .C. .... .C. .... .C. .... .C. ....
VACV-GOBV-C2         .C. .... .C. .... .C. .... .C. .... .C. .... .C. .... .C. .... .C. .... .C. .... .C. .... .C. .... .C. ....
VACV-GOBV-C3         .C. .... .C. .... .C. .... .C. .... .C. .... .C. .... .C. .... .C. .... .C. .... .C. .... .C. .... .C. ....
VACV-GOBV-C4         .C. .... .C. .... .C. .... .C. .... .C. .... .C. .... .C. .... .C. .... .C. .... .C. .... .C. .... .C. ....
VACV-GOBV-C5         .C. .... .C. .... .C. .... .C. .... .C. .... .C. .... .C. .... .C. .... .C. .... .C. .... .C. .... .C. ....
VACV-GOB2V          .C. .... .C. .... .C. .... .C. .... .C. .... .C. .... .C. .... .C. .... .C. .... .C. .... .C. .... .C. ....
VACV-ESBV           .C. .... .C. .... .C. .... .C. .... .C. .... .C. .... .C. .... .C. .... .C. .... .C. .... .C. .... .C. ....
VACV-MGBV           .C. .... .C. .... .C. .... .C. .... .C. .... .C. .... .C. .... .C. .... .C. .... .C. .... .C. .... .C. ....
VACV-MGHV           .C. .... .C. .... .C. .... .C. .... .C. .... .C. .... .C. .... .C. .... .C. .... .C. .... .C. .... .C. ....
VACV-PABV           .C. .... .C. .... .C. .... .C. .... .C. .... .C. .... .C. .... .C. .... .C. .... .C. .... .C. .... .C. ....
VACV-PAB2V          .C. .... .C. .... .C. .... .C. .... .C. .... .C. .... .C. .... .C. .... .C. .... .C. .... .C. .... .C. ....
VACV-BeAn58058_(DQ206442) .C. .... .C. .... .C. .... .C. .... .C. .... .C. .... .C. .... .C. .... .C. .... .C. .... .C. .... .C. ....
VACV-GP1V_(DQ206436) .C. .... .C. .... .C. .... .C. .... .C. .... .C. .... .C. .... .C. .... .C. .... .C. .... .C. .... .C. ....
VACV-P1V_(GU183769) .C. .... .C. .... .C. .... .C. .... .C. .... .C. .... .C. .... .C. .... .C. .... .C. .... .C. .... .C. ....
VACV-VBH_(DQ206435) .C. .... .C. .... .C. .... .C. .... .C. .... .C. .... .C. .... .C. .... .C. .... .C. .... .C. .... .C. ....
VACV-SPAn232_(DQ222922) .C. .... .C. .... .C. .... .C. .... .C. .... .C. .... .C. .... .C. .... .C. .... .C. .... .C. .... .C. ....
VACV-Ankara_(U944848) .C. .... .C. .... .C. .... .C. .... .C. .... .C. .... .C. .... .C. .... .C. .... .C. .... .C. .... .C. ....
VACV-CTGV_(AF229247) .C. .... .C. .... .C. .... .C. .... .C. .... .C. .... .C. .... .C. .... .C. .... .C. .... .C. .... .C. ....
VACV-GP2V_(DQ206437) .C. .... .C. .... .C. .... .C. .... .C. .... .C. .... .C. .... .C. .... .C. .... .C. .... .C. .... .C. ....
VACV-MURV_(DQ247770) .C. .... .C. .... .C. .... .C. .... .C. .... .C. .... .C. .... .C. .... .C. .... .C. .... .C. .... .C. ....
VACV-ARAV_(AY523994) .C. .... .C. .... .C. .... .C. .... .C. .... .C. .... .C. .... .C. .... .C. .... .C. .... .C. .... .C. ....
VACV-P2V_(GU183770) .C. .... .C. .... .C. .... .C. .... .C. .... .C. .... .C. .... .C. .... .C. .... .C. .... .C. .... .C. ....
VACV-IOC_(AF225248) .C. .... .C. .... .C. .... .C. .... .C. .... .C. .... .C. .... .C. .... .C. .... .C. .... .C. .... .C. ....
VACV-SV2_(EF063677) .C. .... .C. .... .C. .... .C. .... .C. .... .C. .... .C. .... .C. .... .C. .... .C. .... .C. .... .C. ....
VACV-TO_AC_(GU322360) .C. .... .C. .... .C. .... .C. .... .C. .... .C. .... .C. .... .C. .... .C. .... .C. .... .C. .... .C. ....
VACV-WR_(AY243312) .C. .... .C. .... .C. .... .C. .... .C. .... .C. .... .C. .... .C. .... .C. .... .C. .... .C. .... .C. ....
MPXV-Congo_(DQ011154) .C. .... .C. .... .C. .... .C. .... .C. .... .C. .... .C. .... .C. .... .C. .... .C. .... .C. .... .C. ....
CPXV-Germany_(DQ437593) .C. .... .C. .... .C. .... .C. .... .C. .... .C. .... .C. .... .C. .... .C. .... .C. .... .C. .... .C. ....
VARV_(DQ437589) .C. ... G.. A.. .C. .... .C. .... .C. .... .C. .... .C. .... .C. .... .C. .... .C. .... .C. .... .C. .... .C. ....

```

Figure 6. Alignment of a fragment of viral clones A56R gene nucleotide sequences with other *Orthopoxvirus* sequences. The sequences were obtained from GenBank and aligned using the standard parameters of CLUSTAL W. Nucleotide positions are shown according to the VACV-MARV (G1 VACV-BR isolate). (.) indicates identity and (-) indicates deletion of nucleotides. The box highlights significant variations among clones from the same sample in which the clones 1 and 5 from the VACV-BABV showed a deletion of the 18 nucleotides observed in the A56R gene sequence of G1 VACV-BR, while clones 2, 3 and 4 from the same clinical sample did not show this deletion (G2). This alignment displays only representative clones from each sample, except for VACV-BABV and VACV-GOBV, in which all clones are represented.

4. Discussion

Bovine vaccinia outbreaks have been increasingly reported in Brazil since 1999 causing economic, social, veterinary and public health problems [11]. Despite the current and historical importance of VACV, little information is available about its circulation, prevalence, origins, maintenance in environment and natural reservoirs.

In this study, we were able to demonstrate the genetic and biologic variability among VACV and even among clones isolated from the same sample. Previous studies have demonstrated the genetic variability present in vaccine preparations of VACV, but in this study we observed the same profile among viruses isolated during BV outbreaks. Our study reinforced the circulation of the two groups (G1 and 2) of VACV-BR, as previously reported [24,26–28]. In addition, our data demonstrate the

co-circulation of mixed VACV populations in the same sample, as well as a great genetic diversity among VACV-BR G1 clones in the same sample. In addition, we isolated two clones (VACV-BABV-clone 2 and VACV-MGHV clone 2) that presented a mosaic profile, with both G1 and G2 features based on the molecular analysis of A56R, A26L and C23L genes. These clones may have arisen as product of a recombination event.

Previous studies have shown a high recombination rate during a poxvirus co-infection [46–48]. Co-circulation of the genetically different clones in the same sample as shown here may favor the recombination generating new genetic variants which can also have influence in virus evolution and pathogenesis. Moreover, genetic changes can favor adaptation to new hosts, such as described for other viruses of the same genus contributing to expand its circulation and host range [5].

Despite the existence of two VACV groups circulating in Brazil, generally G1 viruses has been more frequently isolated when compared to G2 viruses, including this study in which 92% of the isolated clones were grouped in VACV-BR-G1 while only 8% were grouped in VACV-BR-G2 were based on A56R gene. However, we believe that in addition to the higher prevalence of G1 VACV-BR there is a laboratory filter that favors the isolation and characterization of G1 VACV-BR, since the cellular systems commonly used in isolation and characterization, like embryonated chicken eggs and Vero cells, are unable to highlight differences between G1 and 2 such as plaque size variations. Probably, in a mixed sample (which has G1 and 2 viruses), the prevalence of G2 may be lower as was demonstrated in the case of VACV-GOBV sample, which would not allow the identification of the G2 viruses if the sample is directly processed and characterized by conducting PCR from VACV without previous plaque purification in an appropriate cellular system for the identification of both groups. Thus, we suggest that the viruses that have been isolated represent a small part of the diversity of VACV present in the natural environment. Our findings raise more discussions about the origin of VACV in Brazil, reinforcing the notion that VACV-BR viruses may have more than one origin [54].

We confirmed the virulence differences between large plaque and small plaque viruses as demonstrated previously [25,28]. While small plaque viral clones did not cause weight loss or death during infection in BALB/c mice, large plaque clones caused weight loss, clinical signs and death of infected BALB/C mice, showing that virulent and no virulent clones may be present in the same sample.

Here, we also showed that the replication rates varies among clones of the same sample with large plaque clones showing a higher replication rates when compared to small plaque clones isolated from the same sample in BSC40 cells. The importance of the higher replication rates for VACV evolution and maintenance in the environment needs further studies.

Taken together, data regarding G2 clones show exclusive biological and molecular features (including genes profiles, plaque phenotype and mouse clinical signs) distinct to other known large plaque reference samples, including VACV-Western Reserve.

In summary, our study demonstrated the genetic and biological variability between clones isolated from natural circulating VACV-BR in BV outbreaks, evidencing that VACV can contain viral clone subpopulations. These results raise new questions about the diversity and origin of VACV circulating in Brazilian natural and rural environments. Nevertheless, the real implications of different VACV clones' co-circulation are unknown but we can emphasize the significance in the evolution and maintenance of these viruses in the environment.

Acknowledgments

We thank colleagues from Laboratório de Vírus (ICB-UFMG). For assistance in collection of clinical specimens we thank Instituto Mineiro de Agropecuária (IMA), Laboratório de Virologia Animal da Escola de Medicina Veterinária of UFMG and Empresa Brasileira de Pesquisa Agropecuária.

(EMBRAPA). We thank Juliano Leal de Paula from Núcleo de Análise de Genoma e Expressão Gênica (NAGE)-Departamento de Bioquímica e Imunologia (ICB—UFMG). We thank Pró-Reitoria de Pesquisa da Universidade Federal de Minas Gerais (PRPq-UFMG) and support agencies (CNPq, CAPES and FAPEMIG) for the financial support.

Author Contributions

Conceived and designed the experiments: G.O., F.A., G.A., G.T., E.K., J.A. Performed the experiments: G.O., M.L., A.C.A., R.C. Analyzed the data: G.O., J.A., J.A. Contributed reagents/materials/analysis tools: F.A., P.C.F., E.K. Wrote the paper: G.O., J.A. All authors read and approved final manuscript.

Conflicts of Interest

The authors declare no conflict of interest.

References and Notes

1. Fenner, F.; Henderson, D.A.; Arita, I.; Jezek, A.; Ladnyi, I.D. *Smallpox and Its Eradication*; World Health Organization Press: Geneva, Switzerland, 1988.
2. Chen, H.; Chuai, X.; Deng, Y.; Wen, B.; Wang, W.; Xiong, S.; Ruan, L.; Tan, W. Optimisation of prime-boost immunization in mice using novel protein-based and recombinant vaccinia (Tiantan)-based HBV vaccine. *PLoS One* **2012**, *7*, e43730.
3. Deng, Y.; Zhang, K.; Tan, W.; Wang, Y.; Chen, H.; Wu, X.; Ruan, L. A recombinant DNA and vaccinia virus prime-boost regimen induces potent long-term T-cell responses to HCV in BALB/c mice. *Vaccine* **2009**, *27*, 2085–2088.
4. Liu, C.; Du, S.; Li, C.; Wang, Y.; Wang, M.; Li, Y.; Yin, R.; Li, X.; Ren, D.; Qin, Y.; *et al.* Immunogenicity analysis following human immunodeficiency virus recombinant DNA and recombinant vaccinia virus Tian Tan prime-boost immunization. *Sci. China Life Sci.* **2013**, *56*, 531–540.
5. Reynolds, M.G.; Carroll, D.S.; Karem, K.L. Factors affecting the likelihood of monkeypox's emergence and spread in the post-smallpox era. *Curr. Opin. Virol.* **2012**, *2*, 335–343.
6. Pahlitzsch, R.; Hammarin, A.L.; Widell, A. A case of facial cellulitis and necrotizing lymphadenitis due to cowpox virus infection. *Clin. Infect. Dis.* **2006**, *43*, 737–742.
7. Karem, K.L.; Reynolds, M.; Braden, Z.; Lou, G.; Bernard, N.; Patton, J.; Damon, I.K. Characterization of acute-phase humoral immunity to monkeypox: Use of immunoglobulin M enzyme-linked immunosorbent assay for detection of monkeypox infection during the 2003 North American outbreak. *Clin. Diagn. Lab. Immunol.* **2005**, *12*, 867–872.

8. Rimoin, A.W.; Mulembakani, P.M.; Johnston, S.C.; Lloyd Smith, J.O.; Kisalu, N.K.; Kinkela, T.L.; Blumberg, S.; Thomassen, H.A.; Pike, B.L.; Fair, J.N.; *et al.* Major increase in human monkeypox incidence 30 years after smallpox vaccination campaigns cease in the Democratic Republic of Congo. *Proc. Natl. Acad. Sci. USA* **2010**, *107*, 16262–16267.
9. Singh, R.K.; Hosamani, M.; Balamurugan, V.; Bhanuprakash, V.; Rasool, T.J.; Yadav, M.P. Buffalopox: An emerging and re-emerging zoonosis. *Anim. Health Res. Rev.* **2007**, *8*, 105–114.
10. Trindade, G.S.; Guedes, M.I.; Drumond, B.P.; Mota, B.E.; Abrahao, J.S.; Lobato, Z.I.; Gomes, J.A.; Corrêa-Oliveira, R.; Nogueira, M.L.; Kroon, E.G.; *et al.* Zoonotic vaccinia virus: Clinical and immunological characteristics in a naturally infected patient. *Clin. Infect. Dis.* **2009**, *48*, 37–40.
11. Kroon, E.G.; Mota, B.E.; Abrahão, J.S.; da Fonseca, F.G.; de Souza Trindade, G. Zoonotic Brazilian Vaccinia virus: from field to therapy. *Antivir. Res.* **2011**, *92*, 150–163.
12. Oliveira, D.B.; Assis, F.L.; Ferreira, P.C.; Bonjardim, C.A.; de Souza Trindade, G.; Kroon, E.G.; Abrahão, J.S. Short Report: Group 1 Vaccinia virus Zoonotic Outbreak in Maranhão State, Brazil. *Am. J. Trop. Med. Hyg.* **2013**, *89*, 1142–1145.
13. Kalthoff, D.; Bock, W.I.; Hühn, F.; Beer, M.; Hoffmann, B. Fatal cowpox virus infection in cotton-top tamarins (*Saguinus oedipus*) in Germany. *Vector Borne Zoonotic Dis.* **2014**, *14*, 303–305.
14. Fernandes, A.T.; Travassos, C.E.; Ferreira, J.M.; Abrahao, J.S.; Rocha, E.S.; Ferreira, F.V.; dos Santos, J.R.; Bonjardim, C.A.; Ferreira, P.C.; Kroon, E.G. Natural human infections with Vaccinia virus during bovine vaccinia outbreaks. *J. Clin. Virol.* **2009**, *44*, 308–313.
15. Megid, J.; Appolinário, C.M.; Langoni, H.; Pituco, E.M.; Okuda, L.H. Vaccinia virus in humans and cattle in southwest region of Sao Paulo state, Brazil. *Am. J. Trop. Med. Hyg.* **2008**, *79*, 647–665.
16. Damon, I.K.; Poxviruses. In *Fields Virology*, 6th ed.; Knipe, D.M., Howley, P.M., Eds.; Lippincott, Williams and Wilkins: Philadelphia, PA, USA, 2014; Volume 2, p. 2160.
17. Batista, V.H.; Scremin, J.; Aguiar, L.M.; Schatzmayr, H.G. Vulvar infection and possible human-to-human transmission of bovine poxvirus disease. *Virus Res.* **2009**, *14*, 1–10.
18. Oliveira, G.P.; Fernandes, A.T.; Assis, F.L.; Alves, P.A.; Franco Luiz, A.P.M.; Figueiredo, L.B.; Costa de Almeida, C.M.; Travassos, C.E.P.F.; Trindade, G.S.; Abrahão, J.S.; *et al.* Intrafamilial transmission of Vaccinia virus during a bovine Vaccinia outbreak in Brazil: A new insight in viral transmission chain. *Am. J. Trop. Med. Hyg.* **2014**, *90*, 1021–1023.
19. Lopes, O.S.; Lacerda, J.P.; Fonseca, I.E.; Castro, D.P.; Forattini, O.P.; Rabello, E.X. CotiaVirus: A New Agent Isolated from Sentinel Mice in Sao Paulo, Brazil. *Am. J. Trop. Med. Hyg.* **1965**, *14*, 156–157.
20. Fonseca, F.G.; Lanna, M.C.; Campos, M.A.; Kitajima, E.W.; Peres, J.N.; Golgher, R.R.; Ferreira, P.C.; Kroon, E.G. Morphological and molecular characterization of the poxvirus BeAn 58058. *Arch. Virol.* **1998**, *143*, 1171–1186.
21. Fonseca, F.G.; Trindade, G.S.; Silva, R.L.; Bonjardim, C.A.; Ferreira, P.C.; Kroon, E.G. Characterization of a vaccinia-like virus isolated in a Brazilian forest. *J. Gen. Virol.* **2002**, *83*, 223–228.

22. Damaso, C.R.; Esposito, J.J.; Condit, R.C.; Moussatche, N. An emergent poxvirus from humans and cattle in Rio de Janeiro State: Cantagalo virus may derive from Brazilian smallpox vaccine. *Virology* **2000**, *277*, 439–449.
23. Trindade, G.S.; da Fonseca, F.G.; Marques, J.T.; Diniz, S.; Leite, J.A.; de Bodt, S.; van der Peer, Y.; Bonjardim, C.A.; Ferreira, P.C.; Kroon, E.G. Belo Horizonte virus: a vaccinia-like virus lacking the A-type inclusion body gene isolated from infected mice. *J. Gen. Virol.* **2004**, *85*, 2015–2021.
24. Assis, F.L.; Borges, I.A.; Ferreira, P.C.; Bonjardim, C.A.; Trindade, G.S.; Lobato, Z.I.; Guedes, M.I.; Mesquita, V.; Kroon, E.G.; Abrahão, J.S. Group 2 vaccinia virus, Brazil. *Emerg. Infect. Dis.* **2012**, *18*, 2035–2038.
25. Ferreira, J.M.; Drumond, B.P.; Guedes, M.I.; Pascoal-Xavier, M.A.; Almeida-Leite, C.M.; Arantes, R.M.; Mota, B.E.; Abrahão, J.S.; Alves, P.A.; Oliveira, F.M.; *et al.* Virulence in Murine Model Shows the Existence of Two Distinct Populations of Brazilian Vaccinia virus Strains. *PLoS One* **2008**, *3*, e3043.
26. Trindade, G.S.; Lobato, Z.I.; Drumond, B.P.; Leite, J.A.; Trigueiro, R.C.; Guedes, M.I.; Fonseca, F.G.; Santos, J.R.; Bonjardim, C.A.; Ferreira, P.C.; Kroon, E.G. Shortreport: Isolation of two vaccinia virus strains from a single bovine vaccinia outbreak in rural area from Brazil: Implications on the emergence of zoonotic orthopoxviruses. *Am. J. Trop. Med. Hyg.* **2006**, *75*, 486–490.
27. Drumond, B.P.; Leite, J.A.; da Fonseca, F.G.; Bonjardim, C.A.; Ferreira, P.C.; Kroon, E.G. Brazilian Vaccinia virus strains are genetically divergent and differ from the Lister vaccine strain. *Microbes Infect.* **2008**, *10*, 185–197.
28. Campos, R.K.; Brum, M.C.; Nogueira, C.E.; Drumond, B.P.; Alves, P.A.; Siqueira-Lima, L.; Assis, F.L.; Trindade, G.S.; Bonjardim, C.A.; Ferreira, P.C.; *et al.* Assessing the variability of Brazilian Vaccinia virus isolates from a horse exanthematic lesion: Coinfection with distinct viruses. *Arch. Virol.* **2011**, *156*, 275–283.
29. Leite, J.A.; Drumond, B.P.; de Souza Trindade, G.; Bonjardim, C.A.; Ferreira, P.C.; Kroon, E.G. Brazilian Vaccinia virus strains show genetic polymorphism at the *ati* gene. *Virus Genes* **2007**, *35*, 531–539.
30. Assis, F.L.; Almeida, G.M.; Oliveira, D.B.; Franco-Luiz, A.P.; Campos, R.K.; Guedes, M.I.; Fonseca, F.G.; Trindade, G.S.; Drumond, B.P.; Kroon, E.G.; *et al.* Characterization of a new Vaccinia virus isolate reveals the C23L gene as a putative genetic marker for autochthonous Group 1 Brazilian Vaccinia virus. *PLoS One* **2012**, *11*, e50413.
31. Trindade, G.S.; da Fonseca, F.G.; Marques, J.T.; Nogueira, M.L.; Mendes, L.C.; Borges, A.S.; Peiró, J.R.; Pituco, E.M.; Bonjardim, C.A.; Ferreira, P.C.; *et al.* Araçatuba virus: A vaccinia-like virus associated with infection in humans and cattle. *Emerg. Infect. Dis.* **2003**, *9*, 155–160.
32. Abrahão, J.S.; Guedes, M.I.; Trindade, G.S.; Fonseca, F.G.; Campos, R.K.; Mota, B.F.; Lobato, Z.I.; Fernandes, A.T.; Rodrigues, G.O.; Lima, L.S.; *et al.* One more piece in the VACV ecological puzzle: Could peridomestic rodents be the link between wildlife and bovine vaccinia outbreaks in Brazil? *PLoS One* **2009**, *19*, e7428.
33. Reed, K.D.; Melski, J.W.; Graham, M.B.; Regnery, R.L.; Sotir, M.J.; Wegner, M.V.; Kazmierczak, J.J.; Stratman, E.J.; Li, Y.; Fairley, J.A.; *et al.* The detection of monkeypox in humans in the Western Hemisphere. *N. Engl. J. Med.* **2004**, *350*, 342–350.

34. Gubser, C.; Hue, S.; Kellam, P.; Smith, G.L. Poxvirus genomes: A phylogenetic analysis. *J. Gen. Virol.* **2004**, *85*, 105–117.
35. Chen, N.; Li, G.; Liszewski, M.K.; Atkinson, J.P.; Jahrling, P.B.; Feng, Z.; Schriewer, J.; Buck, C.; Wang, C.; Lefkowitz, E.J.; *et al.* Virulence differences between monkeypox virus isolates from West Africa and the Congo basin. *Virology* **2005**, *340*, 46–63.
36. Esposito, J.J.; Sammons, S.A.; Frace, A.M.; Osborne, J.D.; Olsen-Rasmussen, M.; Zhang, M.; Govil, D.; Damon, I.K.; Kline, R.; Laker, M.; *et al.* Genome sequence diversity and clues to the evolution of variola (smallpox) virus. *Science* **2006**, *313*, 807–812.
37. Emerson, G.L.; Li, Y.; Frace, M.A.; Olsen-Rasmussen, M.A.; Khristova, M.L.; Govil, D.; Sammons, S.A.; Regnery, R.L.; Karem, K.L.; Damon, I.K.; *et al.* The phylogenetics and ecology of the orthopoxviruses endemic to North America. *PLoS One* **2009**, *4*, e7666.
38. Gubser, C.; Hue, S.; Kellam, P.; Smith, G.L.; Hendrickson, R.C.; Wang, C.; Hatcher, E.L.; Lefkowitz, E.J. Orthopoxvirus genome evolution: The role of gene loss. *Viruses* **2010**, *2*, 1933–1967.
39. Kugelman, J.R.; Johnston, S.C.; Mulembakani, P.M.; Kisalu, N.; Lee, M.S.; Koroleva, G.; McCarthy, S.E.; Gestole, M.C.; Wolfe, N.D.; Fair, J.N.; *et al.* Genomic variability of monkeypox virus among humans, Democratic Republic of the Congo. *Emerg. Infect. Dis.* **2014**, *20*, 232–239.
40. Okeke, M.I.; Okoli, A.S.; Nilssen, Ø.; Moens, U.; Tryland, M.; Bøhn, T.; Traavik, T. Molecular characterization and phylogenetics of Fennoscandian cowpox virus isolates based on the p4c and atip genes. *Virol. J.* **2014**, *11*, 119–120.
41. Osborne, J.D.; Da Silva, M.; Frace, A.M.; Sammons, S.A.; Olsen-Rasmussen, M.; Upton, C.; Buller, R.M.; Chen, N.; Feng, Z.; Roper, R.L.; *et al.* Genomic differences of Vaccinia virus clones from Dryvax smallpox vaccine: The Dryvax-like ACAM2000 and the mouse neurovirulent Clone-3. *Vaccine* **2007**, *25*, 8807–8832.
42. Garcel, A.; Perino, J.; Crance, J.M.; Drillien, R.; Garin, D.; Favier, A.L. Phenotypic and genetic diversity of the traditional Lister smallpox vaccine. *Vaccine* **2009**, *27*, 708–717.
43. Morikawa, S.; Sakiyama, T.; Hasegawa, H.; Saijo, M.; Maeda, A.; Kurane, I.; Maeno, G.; Kimura, J.; Hirama, C.; Yoshida, T.; *et al.* An attenuated LC16m8 smallpox vaccine: Analysis of full genome sequence and induction of immune protection. *J. Virol.* **2005**, *79*, 11873–11891.
44. Qin, L.; Upton, C.; Hazes, B.; Evans, D.H. Genomic analysis of the vaccinia virus strain variants found in Dryvax vaccine. *J. Virol.* **2011**, *85*, 13049–13060.
45. Qin, L.; Liang, M.; Evans, D.H. Genomic analysis of vaccinia virus strain TianTan provides new insights into the evolution and evolutionary relationships between Orthopoxviruses. *Virology* **2013**, *442*, 59–66.
46. Fenner, F.; Comben, B.M. Genetic studies with mammalian poxviruses. I. Demonstration of recombination between two strains of vaccinia virus. *Virology* **1958**, *5*, 530–548.
47. Bedson, H.S.; Dumbell, K.R. Hybrids Derived from the Viruses of Variola Major and Cowpox. *J. Hyg.* **1964**, *62*, 147–158.
48. Qin, L.; Evans, D.H. Genome scale patterns of recombination between coinfecting vaccinia viruses. *J. Virol.* **2014**, *88*, 5277–5286.
49. Campos, M.A.S.; Kroon, E.G. Critical period for reversible block of vaccinia virus replication. *Rev. Braz. Microbiol.* **1993**, *24*, 104–110.

50. Joklik, W.K. The purification of four strains of poxvirus. *Virology* **1962**, *18*, 9–18.
51. Sambrook, J.; Russell, D.W. *Molecular Cloning: A Laboratory Manual*, 3rd ed.; Nolan, C., Ford, N., Eds.; Cold Spring Harbor Laboratory Press: New York, NY, USA, 2001.
52. Trindade, G.S.; Li, Y.; Olson, V.A.; Emerson, G.; Regnery, R.L.; da Fonseca, F.G.; Kroon, E.G.; Damon, I.K. Real-time PCR assay to identify variants of Vaccinia virus: Implications for the diagnosis of bovine vaccinia in Brazil. *J. Virol. Methods* **2008**, *152*, 63–71.
53. Ropp, S.L.; Jin, Q.; Knight, J.C.; Massung, R.F.; Esposito, J.J. PCR strategy for identification and differentiation of small pox and other *Orthopoxviruses*. *J. Clin. Microbiol.* **1995**, *33*, 2069–2076.
54. Trindade, G.S.; Emerson, G.L.; Carroll, D.S.; Kroon, E.G.; Damon, I.K. Brazilian Vaccinia Viruses and Their Origins. *Emerg. Infect. Dis.* **2007**, *13*, 965–972.

© 2015 by the authors; licensee MDPI, Basel, Switzerland. This article is an open access article distributed under the terms and conditions of the Creative Commons Attribution license (<http://creativecommons.org/licenses/by/4.0/>).

Horizontal study of vaccinia virus infections in an endemic area: epidemiologic, phylogenetic and economic aspects

Felipe L. Assis¹ · Ana Paula M. Franco-Luiz¹ · Luis M. Paim² ·
Graziele P. Oliveira¹ · Alexandre F. Pereira¹ · Gabriel M. F. de Almeida¹ ·
Leandra B. Figueiredo¹ · Adriano Tanus² · Giliane S. Trindade¹ ·
Paulo P. Ferreira¹ · Erna G. Kroon¹ · Jônatas S. Abrahão¹

Received: 26 January 2015 / Accepted: 21 July 2015 / Published online: 5 August 2015
© Springer-Verlag Wien 2015

Abstract Vaccinia virus (VACV), the etiological agent of bovine vaccinia (BV), is widespread in Brazil and present in most of the milk-producing regions. We conducted a horizontal study of BV in Bahia, a state of Brazil in which the production of milk is increasing. During 2011, human and bovine clinical samples were collected during outbreaks for BV diagnosis, virus isolation and molecular analysis. We collected data for epidemiological inferences. Vaccinia virus was detected in 87.7 % of the analyzed outbreaks, highlighting the effective circulation of VACV in Bahia. The molecular data showed the spreading of group 1 Brazilian VACV to Bahia. We observed a seasonal profile of BV, with its peak in the drier and cooler season. Manual milking was observed in 96 % of the visited properties, showing its importance to viral spread in herds. Under-notification of BV, ineffective animal trade surveillance, and bad milking practices have contributed to the spread of VACV in Brazil.

Introduction

Vaccinia virus (VACV) is a member the family *Poxviridae*, genus *Orthopoxvirus*, which includes other zoonotic agents, such as monkeypox virus (endemic in Africa) and cowpox virus (endemic in Europe). Furthermore, this genus also includes the exclusively human-associated pathogen variola virus (worldwide), which is the etiological agent of smallpox, one of the most maleficent pathogens in human history, which was eradicated in the 1980s [1–3]. Like other orthopoxviruses (OPVs), VACV is a double-stranded DNA virus (194,711 bp (VACV-WR [AY243312])), that encodes several structural proteins in addition to immunomodulatory and regulatory proteins that subvert the cellular environment [3]. VACV has been associated with bovine vaccinia (BV) outbreaks in Brazil, causing ulcerative lesions in cattle and humans, economic losses and social effects [4]. Although VACV had been isolated from Brazilian rain forests during the 1960s and 1970s, this virus became a public-health problem in Brazil in 1999, when frequent exanthematous outbreaks were reported [5]. Since then, great efforts have been made to uncover unknown features of VACV, such as its origin(s), host range, environmental maintenance and spread, as well as the epidemiology and phylogeny of Brazilian VACV (VACV-BR) isolates [6–9]. Some reports have shown great genetic and biological heterogeneity among VACV-BR isolates. This variability allowed clustering of VACV-BR into at least two distinct groups (group 1 [G1] and group 2 [G2]), demonstrating a dichotomy supported by evidence of molecular and biological diversity such as virulence in a BALB/c mouse model and a plaque phenotype in BSC-40 cells. Group 2 strains display larger plaque sizes and are virulent to mice, unlike group 1 [4]. Moreover, polymorphisms observed in specific VACV genes, such as the

F. L. Assis and A. P. M. Franco-Luiz contributed equally to this work

Electronic supplementary material The online version of this article (doi:10.1007/s00705-015-2549-1) contains supplementary material, which is available to authorized users.

✉ Jônatas S. Abrahão
jonatas.abraha@gmail.com

¹ Laboratório de Vírus, Departamento de Microbiologia, Instituto de Ciências Biológicas, Universidade Federal de Minas Gerais, Av. Antônio Carlos 6627, Caixa Postal 486, Belo Horizonte, MG 31270-901, Brazil

² Animal Defense Division, Agência Estadual de Defesa Agropecuária da Bahia, 481, Barão do Rio Branco street, Salvador 46830-000, Bahia, Brazil

hemagglutinin gene (A56R), A-type inclusion body gene (A26L, or A25L in the Copenhagen strain), and chemokine-binding protein gene (C23L), have been used in phylogenetic studies and further confirmed the dichotomy between G1 and G2 VACV-BR [4]. In Bahia, Brazil, VACV-like outbreaks have been reported since 2002 (unpublished); however, in these cases, no investigation has been conducted to confirm the involvement of VACV, such as biological and genetic features. In this work, we horizontally evaluated the epidemiological data collected during BV-like outbreaks in Bahia, in northeast Brazil, from January to December 2011. We conducted a phylogenetic study comparing viruses isolated in those outbreaks to other recent VACV-BR isolates from Brazil. Our data reinforce the hypothesis that BV outbreaks are influenced by weather conditions and raise new questions regarding VACV origins in this state.

Materials and methods

Case description

This work was conducted in association with the Agência de Defesa Agropecuária of Bahia State (Veterinary Surveillance Organ) (ADAB) and the Laboratório de Vírus of Universidade Federal de Minas Gerais (LV-UFGM). The epidemiological data were collected during active foot-and-mouth disease (FMD) surveillance conducted by the ADAB in 2011. After reports of exanthemas, veterinarians visited farms to perform clinical and epidemiological investigations (forms of disease research [FDR]), sample collection and advise farms regarding disease management.

During the study period from January to December, 2011, 57 BV-like outbreaks from 22 counties in Bahia were reported to the ADAB. Bovine samples of sera, scabs, swabs and vesicular fluid, in addition to samples from affected farm workers, were collected and stored at -70°C until they reached their destination. The collected samples were routed to LV-UFGM and diagnosed by serological (ELISA or PRNT) and/or molecular (PCR) methods. Based on the information and laboratory results of the FDR, some epidemiological inferences were made. In addition, we conducted viral isolation, sequencing and phylogenetic characterization.

Serological diagnosis

For ELISA, purified and inactivated VACV-WR was diluted to optimized concentrations in 0.01 M carbonate buffer at pH 9.6 and added to each well of 96-well ELISA plates (NUNC Maxisorb, USA); the plates were incubated

at 4°C for 18 h. The plates were washed with phosphate buffer containing 0.05 % Tween 20 (PBS-T) and then blocked with 5 % nonfat dried milk for 2 hours. After the washing procedures, the serum samples at a dilution of 1:100 were added to each well. After 60 minutes at 37°C , the plates were washed again, and rabbit anti-cow IgG peroxidase conjugate (Sigma-Aldrich, Germany) diluted 1:10,000 in PBS-T was added per well and incubated at 37°C for 30 minutes. Then, the plates were washed four times, and the substrate (0.1 M citrate buffer, pH 5.0, containing 0.3 mg of *ortho*-phenylenediamine (OPD) per mL and 0.03 % hydrogen peroxide) was added and incubated in the dark for 10 minutes. The reaction was stopped by the addition of a 2 N sulfuric acid, and the optical densities were measured at 492 nm [10].

For the plaque-reduction neutralization test (PRNT), the samples were inactivated at 56°C for 30 minutes, diluted 1:20 in minimum essential medium and incubated at 37°C for 16 hours with the same volume of minimum essential medium containing 10^2 PFU of VACV-WR per mL. Simultaneously, the viral suspension was incubated with a 1:20 dilution of fetal calf serum (FCS) in minimum essential medium to serve as a virus control. After that, 0.4 mL of this mixture was added to BSC-40 cell monolayers in 6-well plates and incubated for one hour at 37°C in a 5 % CO_2 atmosphere. Then, 2 mL of medium was added to each well, and the plate was incubated under the same conditions for 48 hours. The cells were then stained with a solution of crystal violet for 20 minutes, and the viral plaques were counted [11]. The results were expressed as the serum dilution that was able to neutralize at least 50 % (PRNT₅₀) of the viral plaques compared with negative controls. Bovine serum samples were used as positive and negative controls. The specificity (98.4 %) and sensitivity (93.5 %) of the OPV-PRNT were confirmed using receiver-operating characteristic analysis as described previously [10].

Molecular diagnosis

Sera and scab samples were diluted in phosphate-buffered saline (PBS) (137 mM NaCl, 7 mM KCl, 1.4 mM Na_2HPO_4 , pH 7.2) (0.1 mL serum/0.9 mL PBS). The scabs were macerated using a homogenizer (Politron, Littau, Switzerland) in PBS, which contained 200 U of penicillin, 4 μg of amphotericin B, and 100 μg of gentamicin per mL (0.1 g scab/0.9 mL PBS), and clarified by centrifugation at $2000\times g$ for 3 min [13]. The supernatants from scabs and diluted sera were used for diagnostic purposes, viral isolation, and molecular assays. The diluted samples were used as a template for a nested PCR that targeted a portion of the C11R (viral growth factor, *vgf*) gene. This gene is routinely used as an OPV diagnostic tool by our group. The

reactions were performed by adding 2 μ L of the template to 18 μ L of a PCR reaction containing 0.4 mM *vgf* primers as described previously. The PCR products were electrophoresed in 8 %-PAGE gels and silver stained [12, 13].

Virus isolation and phylogenetic analysis

For viral isolation, 200 μ L of the positive *vgf* samples was added to BSC-40 cell monolayers that were grown in a six-well plate and incubated at 37°C for 72 hours or until detection of a cytopathic effect (CPE) [13]. For molecular characterization, the viral genes A56R (hemagglutinin) and A26L (A-type inclusion body), which are traditionally used genes for this purpose, were amplified and sequenced [14–16]. The PCR fragments obtained in this study were sequenced directly in both orientations and in triplicate using a Mega-BACE 1000 sequencer (GE Healthcare, Buckinghamshire, UK). The sequences were aligned with previously published OPV sequences from GenBank using the ClustalW method, and the alignments were manually checked with MEGA version 4.0 software (Arizona State University, Phoenix, AZ, USA). The accession numbers for the analyzed sequences are given in the respective figures. Phylogenetic trees were constructed by the neighbor-joining method using the Tamura-Nei model of nucleotide substitutions and 1,000 bootstrap replicates, as implemented in the MEGA 4.0 program.

Results

Throughout the study period, we visited 57 outbreak areas in 22 counties of Bahia (Supplementary Table 1). The episodes were primarily reported in northern Bahia, with some isolated focus points in the south and southeast as well as one focus point in the west. During the outbreaks, VACV-like exanthematous umbilicated lesions were frequently observed on the teats and udder of dairy cows as well as on the workers' fingers, hands and forearms (Fig. 1). The outbreaks occurred predominantly in the drier and cooler season, from July to September (Supplementary Figure 1). VACV circulation was serologically or molecularly detected in 87.7 % (50/57) of the studied properties. Only 8.7 % (5/57) of the studied properties were free of circulation of the virus. Sampling was not performed for 2 of the 57 properties because of technical problems (Fig. 2A). The majority of the outbreaks were reported as third-party complaints (53 %), e.g., by neighboring farmers and autonomous milkers, followed by the farmers of the affected farms (28 %) and active surveillance (19 %) (Fig. 2B). In 81 % of the visited properties, humans and bovines were affected. In the remaining cases, only the cattle became sick (Fig. 2C). Regarding the origin of the

animals in the herds, 34/57 (59.6 %) of the properties were reported to have only native cattle in their herds, whereas the remaining 14 % (8/57) of the farmers reported having native and imported animals, predominantly from Minas Gerais State, which has a high incidence of VACV outbreaks. From 26.3 % of the properties (15/57) no information regarding the animal's origin was reported (Fig. 2D). Among the studied herds, 76 % comprised only dairy cattle, 19 % comprised dairy and beef cattle, and 5 % comprised only beef cattle (Fig. 2E). The predominant category of cattle observed among the affected properties was weaning (59.6 %) (Fig. 2F). Manual milking was observed in 96 % of the properties (Fig. 2G).

The clinical samples sent to the LV-UFMG comprised bovine (172/183) and human (11/183) samples. The bovine samples comprised sera (137/172), scabs (25/172) and swabs (10/172). The human samples comprised sera (4/11), scabs (5/11) and swabs (2/11). The samples sent to the LV-UFMG were molecularly and serologically diagnosed (see Materials and methods). PCR amplification of a conserved OPV gene (C11R – viral growth factor) was achieved with 73 of 183 (40 %) samples (19/73 scabs [5 human and 14 bovine], 43/73 sera [only bovine] and 11/73 swabs [2 human and 9 bovine]). Serological analysis performed on 141 (4 human and 137 bovine) serum samples revealed a positivity rate of 85.8 % (3 human and 118 bovine sample).

Additionally, we were able to perform virus isolation from a human sample scab from Mundo Novo, the county most affected by VACV outbreaks during the studied period (Supplementary Table 1). We amplified fragments of the *ha* and *ati* genes (728 bp and 1537 bp, respectively) for molecular analysis. The sequences were deposited in the GenBank database (accession nos. JQ361135.1 and JQ361144.1 for *ha* and *ati*, respectively). Alignment with other viral sequences available in the database revealed deletion signatures in the *ha* and *ati* genes (deletion of 18 nt and 21 nt, respectively). These molecular signatures are present in VACV sequences from VACV-BR isolates in group 1 (VACV-BR-G1) (Supplementary Figure 2). We constructed a phylogenetic tree from the alignment of the obtained sequences. As suggested by the previous molecular analysis, this virus isolate, mundo novo virus (MUNV), was grouped with the other VACV-BR-G1 isolate in the HA and ATI trees (Fig. 3).

Discussion

We conducted a horizontal study of VACV circulation in Bahia during 2011. During this period, we investigated 57 BV-like outbreaks in 22 counties. These episodes were reported predominantly during the drier and cooler season (July–September), although some reports occurred



Fig. 1 Lesions caused by VACV. (A, B) Exanthematic lesions on the hands, finger and forearm of the study patients, which were acquired after contact with VACV-infected dairy cattle. (C-E) Dairy cattle teats and calf muzzle with several umbilicated pustules and ulcerated lesions

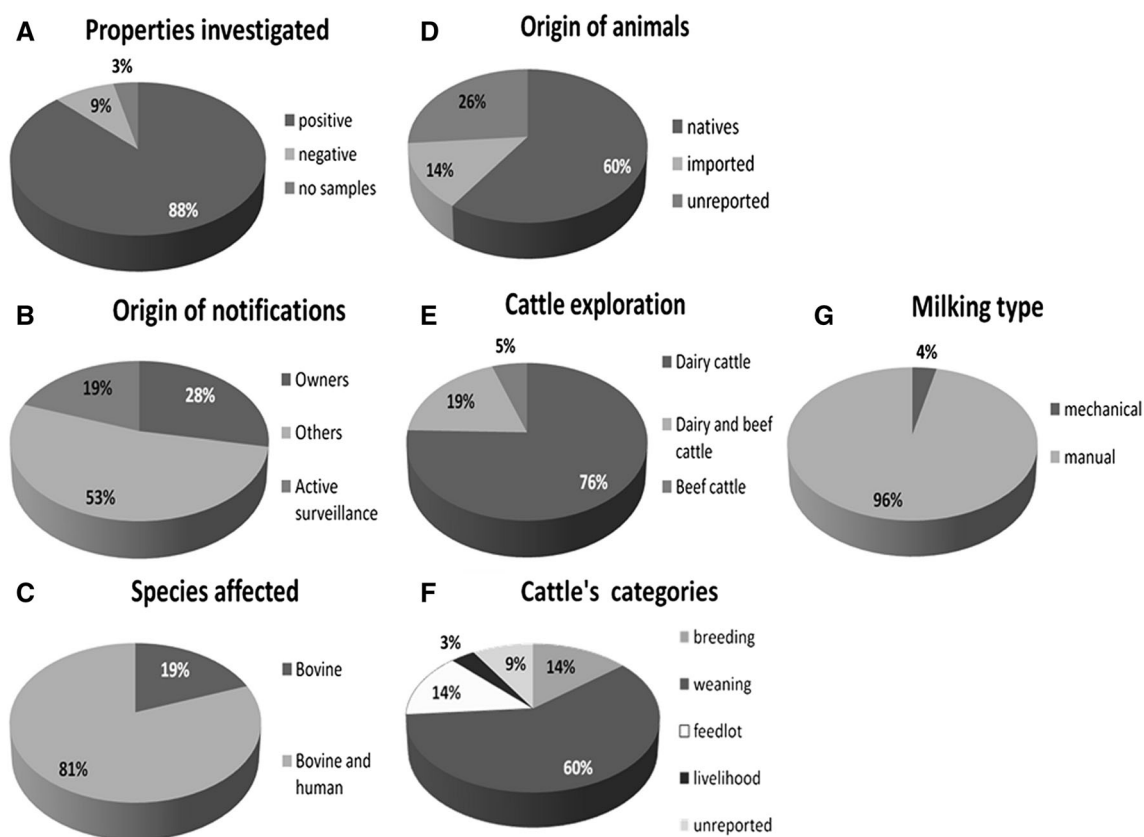


Fig. 2 Epidemiological information. (A) The positive/negative index of the VACV circulation at the visited properties; (B) the origin of the VACV outbreak notifications; (C) the human and/or bovine index affected in the outbreak episodes; (D) the origin of the animals at the

investigated properties. The majority of the imported animals originated in Minas Gerais State. (E) The profile of the cattle investigation in the visited farms; (F) the category index of the cattle at the farms; (G) the milking technology used at the visited farms

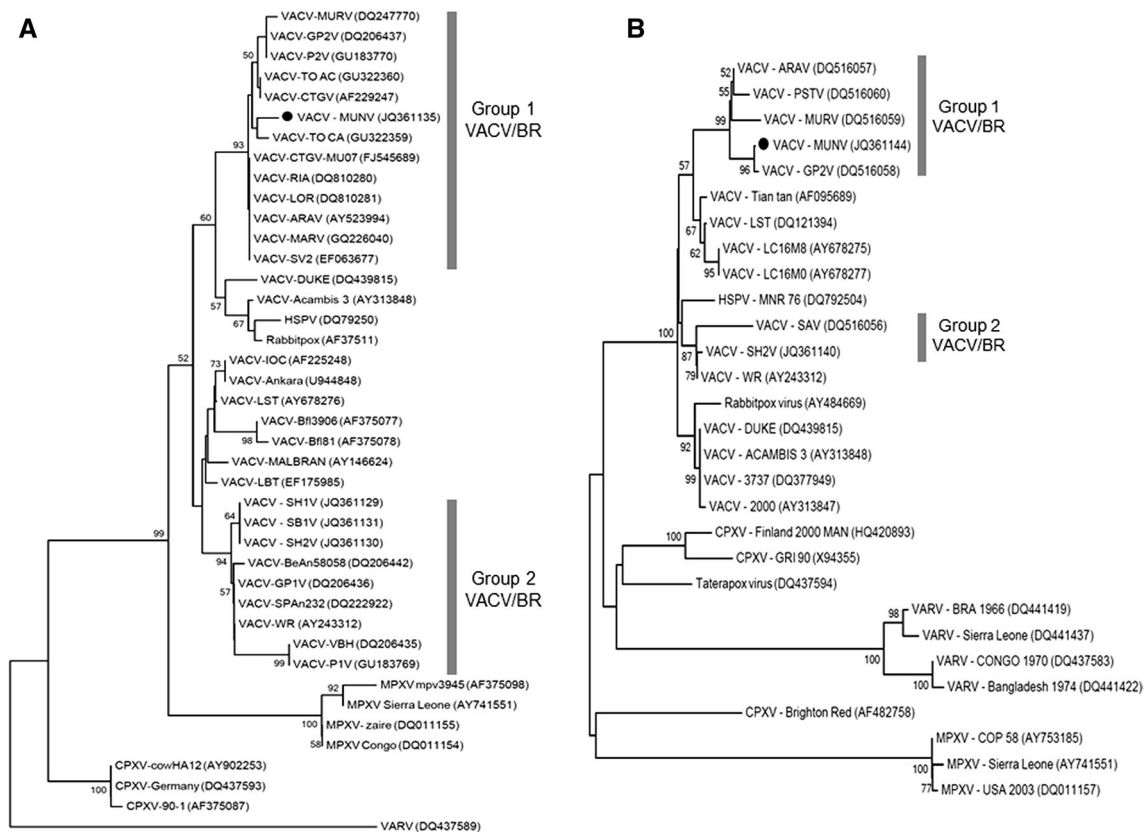


Fig. 3 Phylogenetic trees based on the nucleotide sequences of the A56R (A) and A26L (B) genes. In both phylogenetic trees, the MUNV isolate (black dot) was grouped into VACV/BR group 1, which includes most of the Brazilian VACV isolates. The trees were

constructed using the neighbor-joining method using the Tamura-Nei model of nucleotide substitutions and bootstrapping of 1,000 replicates in MEGA 4.0

throughout the study period. Some previous studies have implicated rats and mice as important agents in the VACV transmission chain when they are in constant contact with wildlife, humans and farm animals [8]. During the dry and cold season, these rodents are frequently sighted on BV-affected farms at the same places where cows and calves feed. During the sampling for this study, rodents were frequently observed in barns and silos. During dry and cold seasons, virus infection might be facilitated by frequently observed lesions on a cow's teats because of the climate conditions and wounds caused by dry grass.

The VACV serologic and/or molecular diagnosis pointed to viral circulation in 87.7 % of the visited properties, suggesting active circulation and/or introduction of VACV in Bahia. VACV spread to other Brazilian states, such as Rondônia, Maranhão, Rio Grande do Sul, has been reported previously [15–17]. However, the mechanisms of the spread of VACV are not completely understood. Effective BV surveillance might be hampered by a lack of awareness of the disease by farmers in rural areas. Some farmers do not report BV outbreaks for fear of trade embargoes. In our study, 53 % of the cases were reported as third-party

complaints. This finding represents the main obstacle for effective surveillance of BV in Brazil.

The origin of the affected animals is another important issue. Approximately 40 % of the visited properties harbored animals from Minas Gerais, an endemic area for VACV circulation, or from an unknown source, suggesting unregulated trade, which could contribute to VACV introduction in some herds. Minas Gerais and other Bahia border states have reported VAVC outbreaks. Previous studies have shown that a unique animal source is sufficient to rapidly initiate a VACV outbreak (Carangola). Therefore, the inadvertent introduction of a sick animal to Bahia's dairy herd might have been the cause of the current spread of VACV. However, the involvement of wildlife in this scenario cannot be ruled out and needs to be explored.

A high rate of human and cattle infection at the same farm (81 %) indicates that after viral introduction into the herd, regardless of the source, manual contact during the milking appears to be the main mechanism of BV outbreaks. Additionally, we observed that in 96 % of the visited properties, milking was performed manually without any protection or disinfection. Additionally, outbreaks

appear to predominantly affect dairy cattle because infection was not observed on beef cattle farms. The role of these animals in a mixed herd has not been established.

The molecular diagnosis revealed a low presence of viral DNA in the sera samples (30.5 %) and a higher presence in scabs (63.3 %) and swabs (91.6 %). This was to be expected, because skin tissue cells are the main sites of infection and the virus is multiplied. We compared the *ha* and *ati* gene sequences of the MUNV isolate with other VACV-BR isolates and observed the deletion signatures found in the sequences from the isolates of VACV-BR-C1, the most prevalent group circulating in Brazil, which is involved in BV outbreaks in states neighboring Bahia. The identification of this new isolate indicates the spread of members of this viral group to Bahia, affecting humans, cattle and, possibly, wildlife.

Acknowledgments We thank our colleagues from the Laboratório de Vírus for their excellent technical support. Financial support was provided by the Conselho Nacional de Desenvolvimento Científico e Tecnológico (CNPq), Coordenação de Aperfeiçoamento de Pessoal de Nível Superior (CAPES), Fundação de Amparo à Pesquisa do Estado de Minas Gerais (FAPEMIG), Ministério da Agricultura, Pecuária e Abastecimento (MAPA), and Pro-Reitoria de Pesquisa da Universidade Federal de Minas Gerais (PRPq-UFMG). E.G. Kroon, G.S. Trindade and P.C.P. Ferreira are researchers from CNPq.

Compliance with ethical standards

Conflict of interest The authors declare no potential conflicts of interest with respect to the research, authorship, and/or publication of this article.

References

- ICTVdB Management (2013) 00.058.1.01.001. Vaccinia virus. In: Buchen-Osmond C (ed) ICTVdB—The Universal Virus Database, version 4. Columbia University, New York, USA
- McFadden G (2005) Poxvirus tropism. *Nat Rev* 3:201–213
- Moss B (2007) Poxviridae: the viruses and their replication. In: Fields BN, Knipe DM, Howley PM (eds) *Fields virology*, 5th edn. Lippincott Williams & Wilkins, Philadelphia v 2, pp 2906–2945
- Kroon EG, Mota BEF, Abrahão JS, Fonseca FG, Trindade GS (2010) Zoonotic Brazilian vaccinia virus: from field to therapy. *Antivir Res* 92:150–163
- Damaso CRA, Joseph JE, Richard CC, Nissin M (2000) An emergent poxvirus from humans and cattle in Rio de Janeiro State: Cantagalo virus may derive from Brazilian smallpox vaccine. *Virology* 277:439–449
- Lobato ZI, Drumond BP, Leite JA, Trigueiro RC, Guedes MI, da Fonseca FG, dos Santos JR, Bonjardim CA, Ferreira PC, Kroon EG (2006) Short report: isolation of two *Vaccinia virus* strain from a single bovine vaccinia outbreak in rural area from Brazil: implications on the emergence of zoonotic Orthopoxviruses. *Am J Trop Med Hyg* 75:486–490
- Trindade GS, Ginny LE, Darin SC, Erna GK, Inger KD (2007) Brazilian vaccinia viruses and their origins. *Emerg Infect Dis* 13(7):965–972
- Abrahão JS, Guedes MI, Trindade GS, Fonseca FG, Campos R, Mota BF, Lobato ZIP, Silva-Fernandes AT, Rodrigues GOL, Lima LS, Ferreira PPF, Bonjardim CA, Kroon EK (2009) One more piece in the VACV ecological puzzle: could peridomestic rodents be the link between wildlife and bovine vaccinia outbreaks in Brazil? *PLoS One* 4(10):1–7
- Assis FL, Borges IA, Ferreira PCP, Bonjardim CA, Trindade GS, Lobato ZIP, Guedes MIM, Vaz M, Kroon EG, Abrahão JS (2012) Group 2 vaccinia virus, Brazil. *Emerg Infect Dis* 18:2035–2038
- Silva-Fernandes AT, Travassos CE, Ferreira JM, Abrahão JS, Rocha ES, Viana-Ferreira F, dos Santos JR, Bonjardim CA, Ferreira PC, Kroon EG (2009) Natural human infections with Vaccinia virus during bovine vaccinia outbreaks. *J Clin Virol* 44:308–313
- O'Brien TC, Martin GM, Nicola MT (1971) Kinetics of the vaccinia virus plaque neutralization test. *Appl Microbiol* 21:968–970
- Fonseca FG, Lanna MC, Campos MAS, Kitajima EW, Peres JN, Golgher RR, Ferreira PCP, Kroon EG (1998) Morphological and molecular characterization of the poxvirus BeAn 58058. *Arch Virol* 143:1171–1186
- Abrahão JS, Larissa SL, Assis FL, Alves PA, Silva-Fernandes AT, Cota MMG, Ferreira VM, Campos RK, Mansur C, Lobato ZIP, Trindade GS, Kroon EG (2009) Nested-multiplex PCR detection of *Orthopoxvirus* and *Parapoxvirus* directly from exanthematic clinical samples. *J Virol*. 140:1–5
- Ropp SL, Jin QI, Knight JC, Massung RF, Esposito JJ (1995) PCR strategy for identification and differentiation of smallpox and other orthopoxviruses. *J Clin Microbiol* 33:2069–2076
- Brum MCS, dos Anjos BL, Nogueira CEW, Amaral LA, Rudi W, Flores EF (2010) An outbreak of orthopoxvirus-associated disease in horses in southern Brazil. *J Vet Diagn Invest* 22:143–147
- Meyer H, Roop SL, Esposito JJ (1997) Gene for A-type inclusion body protein is useful for a polymerase chain reaction assay to differentiate orthopoxvirus. *J Virol Methods* 64:217–221
- Quixabeira-Santos JC, Medaglia MLG, Pescador CA, Damaso CR (2011) Animal movement and establishment of vaccinia virus Cantagalo strain in Amazon biome, Brazil. *Emerg Infect Dis* 17:726–729

Molecular evidence of Orthopoxvirus DNA in capybara (*Hydrochoerus hydrochaeris*) stool samples

Lara Ambrosio Leal Dutra^{1,2} · Gabriel Magno de Freitas Almeida^{1,2} ·
Graziele Pereira Oliveira¹ · Jônatas Santos Abrahão¹ · Erna Geessien Kroon¹ ·
Giliane de Souza Trindade¹

Received: 26 September 2016 / Accepted: 13 October 2016 / Published online: 22 October 2016
© Springer-Verlag Wien 2016

Abstract Vaccinia virus (VACV) is responsible for outbreaks in Brazil and has immense potential as an emerging virus. VACV can be found naturally circulating in India, Pakistan and South America, where it causes infections characterised by exanthematic lesions in buffaloes, cattle and humans. The transmission cycle of Brazilian VACV has still not been fully characterised; one of the most important gaps in knowledge being the role of wild animals. Capybaras, which are restricted to the Americas, are the world's largest rodents and have peculiar characteristics that make them possible candidates for being part of a natural VACV reservoir. Here, we developed a method for detecting orthopoxvirus DNA in capybara stool samples, and have described for the first time the detection of orthopoxvirus DNA in capybaras samples from three different regions in Brazil. These findings strongly suggest that capybaras might be involved in the natural transmission cycle of VACV and furthermore represent a public health problem, when associated with Brazilian bovine vaccinia outbreaks. This makes infected animals an important factor to be considered when predicting and managing Brazilian VACV outbreaks.

Introduction

Vaccinia virus (VACV) is a large DNA virus that is classified in the genus *Orthopoxvirus* of the family *Poxviridae* [1]. Even though it is the genus prototype and has been successfully used in the past as a vaccine against smallpox, there is little information regarding its origin, natural host and reservoir [2–6]. In the decades following smallpox eradication, orthopoxviruses (OPV) have become a serious threat as emergent viruses worldwide. VACV can be found naturally circulating in India, Pakistan and South America, where it causes infections in buffaloes, cattle and humans characterised by exanthematic lesions [6–9]. In Brazil the disease caused by VACV infections is known as Bovine Vaccinia (BV) and mainly affects dairy cattle and humans that manipulate these animals, leading to both economic losses and public health concerns. Since the late 1990s BV outbreaks have become more frequent in Brazil but little is known regarding viral dynamics in the environment and the role of sylvatic reservoirs [2, 10]. Several studies have suggested that small rodents might play a role in the natural BV cycle; reinforced by the isolation of virus from a peri-domestic rodent, a cow and a human during an outbreak on the same farm [2, 11, 12]. These findings led to the formation of a hypothetical model, where peri-domestic rodents could be infected by direct or indirect contact with wild animals near farms and, upon returning, transmit virus to farm animals and, in turn, to humans [2]. So far, however, there is very little information about the participation of other wild animals in the VACV natural cycle [3], but capybaras (*Hydrochoerus hydrochaeris*) could fit into the proposed model for VACV circulation in Brazil.

Capybaras, the world's largest rodents, which occur only in the Americas, have peculiar ecological features that support their presence in, or near, human modified

L. A. L. Dutra and G. M. de Freitas Almeida contributed equally to this work.

✉ Giliane de Souza Trindade
giliane@icb.ufmg.br

¹ Laboratório de Vírus, Departamento de Microbiologia, Instituto de Ciências Biológicas, Universidade Federal de Minas Gerais, Av. Antonio Carlos 6627, Pampulha, Belo Horizonte, Minas Gerais, Brasil

² Present Address: Department of Biological and Environmental Sciences, University of Jyväskylä, Jyväskylä, Finland

landscapes such as farms [13]. These animals live socially in groups of 4 to 40 individuals, led by an alpha male [14]. They are herbivorous animals that feed on grass and can inhabit different environments, as long as they are close to water bodies like rivers or lagoons. Capybaras can easily adapt to landscape changes promoted by humans because these changes often result in an environment with reduced natural predators but rich in food resources and water for most of the year. As a result they are commonly seen in, or near, farms [13, 15–17]. In the past hunting represented a threat to capybaras, which were sought after for their meat and grease, but since 1967 Brazilian legislation has forbidden this activity. Nowadays, the major conflicts between humans and capybaras are because of their population growth around farms and cities, which leads to crop destruction and the risk of disease transmission [18]. Capybaras are well established reservoirs for *Rickettsia rickettsii*, the aetiological agent of Brazilian spotted fever in Brazil, a tick-borne disease [19, 20]. The role of capybaras as vectors or reservoirs for other infectious diseases is still obscure, but a study published in 1955 demonstrated that viable VACV particles could be recovered from an experimentally infected capybara, showing that the virus can multiply in this animal [21]. A recent serological investigation found positive samples among free living capybaras captured near farms with no previous official outbreaks, suggesting contact between these animals and VACV in the wild [22].

Considering that: a) capybaras are large rodents that live between human settlements and wild environments; b) these animals are growing in number and are frequently in contact with humans due to landscape changes; and finally, c) it has been shown that capybaras are susceptible to VACV infections, the initial aim of this work was to develop a qPCR (quantitative, real-time, polymerase chain reaction)-based technique to detect OPV in capybara stool samples in order to clarify the role of this rodent in the natural life-cycle of VACV. Our decision to work with faecal samples was based on a study performed in experimentally infected mice that revealed that viable VACV particles could still be found in mouse faeces 20 days after environmental exposure, while viral DNA could be found for up to 60 days [23, 24]. This points to faecal transmission by small rodents being an important infection route for BV outbreaks [23, 25] and could be even more important for a species with coprophagous behaviour like capybaras. In addition stool sampling is an easy and cheap method for sample collection, dispenses the need for capturing animals, and interferes as little as possible with the animal's behaviour and natural environment. To our surprise, during the development of our method, we found molecular evidence of OPV in one of our capybara stool samples. We also validated our test with field samples, whereupon we

found two more positive faecal samples. To confirm this finding, we proceeded with the detection of several VACV gene targets and confirmed that our samples contained natural OPV DNA. In conclusion, in this study we not only describe a reliable qPCR-based method for OPV detection from capybaras stool samples, but we also present strong evidence that links this rodent to the natural life-cycle of Brazilian VACV for the first time.

Methodology

Sample collection and processing

Stool samples for standardisation tests were collected at Lagoa da Pampulha (19° 51' 4" S, 43° 58' 46" W), a lagoon and green area surrounded by the city of Belo Horizonte, in December of 2012. This area was chosen due its proximity to the university where the tests were performed, and the absence of an evident link to wild environments, supporting our hypothesis that no VACV was circulating in it. Twenty two samples were collected, each consisting of five pellets from a unique stack, and were analysed to characterise stool size and weight. Mean weight was 1.95 ± 1.06 grams, mean length was 23 ± 4.5 mm and mean width was 14.69 ± 2.80 mm.

To validate the test, field samples were collected in three regions with distinct landscapes and human interaction patterns: (a) Serro (MG), a habitat in the Cerrado biome where the main economic activity is dairy production and the contact between humans and cattle is direct and intense, and where VACV outbreaks have been notified since 2005; (b) Serra do Cipó National Park, a protected rocky field vegetation area with touristic activities that shelter several wild mammal species and where cattle graze free; (c) Mato Grosso do Sul along the Pantanal wetland, a region of intense livestock activity with little to no direct contact between humans and cattle due to extensive farming practices, and with large herds of wild capybaras and other mammals. The date of sample collection and geo-referencing can be found in Table 1 and Figure 1A.

Sample processing was started by a tenfold dilution (w/v) in sterile water and clarification by centrifugation (500g, 30 sec) in order to separate the fibrous part from the aqueous phase, which was kept as our stock dilution. From this stock, we prepared further dilutions for the tests described below.

Experimental contamination of diluted samples and DNA extraction

To determine the minimum non-inhibitory dilution and the limit of viral detection in our samples, serially diluted

Table 1 Data on the collection of fecal samples

Sample ID	Collection date	Georeference data	Collection region	Water content of faecal pellets
CAP1	Dec/12	19°20'45.7"S, 43°34'0.08"W	Serra do Cipó NP	Dry
CAP2	Dec/12	19°20'45.7"S, 43°34'0.08"W	Serra do Cipó NP	Dry
CAP3	Dec/12	19°20'45.7"S, 43°34'0.08"W	Serra do Cipó NP	Dry
CAP4	Dec/12	19°20'41.8"S, 43°36'58.8"W	Serra do Cipó NP	Humid
CAP5	Dec/12	19°20'42.7"S, 43°36'37.4"W	Serra do Cipó NP	Humid
CAP6	Dec/12	19°20'42.8"S, 43°36'36.1"W	Serra do Cipó NP	Humid
CAP7	Dec/12	19°20'45.7"S, 43°34'0.08"W	Serra do Cipó NP	Dry
CAP8	Dec/12	19°20'45.7"S, 43°34'0.08"W	Serra do Cipó NP	Dry
CAP9	Dec/12	19°20'44.4"S, 43°37'0.08"W	Serra do Cipó NP	Humid
CAP10	Dec/12	19°20'45.7"S, 43°37'0.08"W	Serra do Cipó NP	Dry
CAP11	Aug/12	18°34'53.4"S, 43°21'28.1"W	Serro (MG)	Humid
CAP12	May/13	17°56'54.4"S, 56°28'57.6"W	Pantanal	Dry
CAP13	May/13	18°57'21.3"S, 56°32'43.4"W	Pantanal	Humid
CAP14	May/13	18°41'31.6"S, 55°35'40.5"W	Pantanal	Humid
CAP15	May/13	18°51'59.9"S, 56°14'01.3"W	Pantanal	Dry
CAP16	May/13	18°58'17.4"S, 56°35'23.9"W	Pantanal	Dry
PAMP	Dec/12	19° 51' 4" S, 43° 58' 46" W	Lagoa da Pampulha	Humid

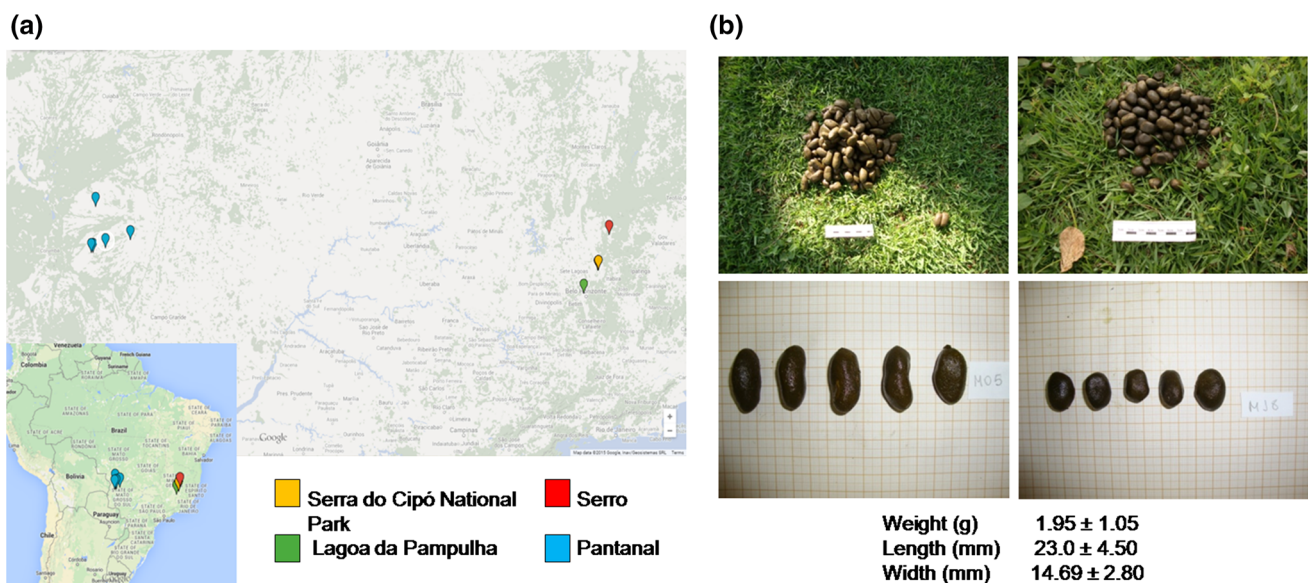


Fig. 1 Site of collection and morphology of capybara stool samples. Samples were collected in three regions of Brazil and a green area inside Belo Horizonte city. A) A map pointing to where the samples were obtained. B) An example of a capybara stool stack (up) and of

individual faecal pellets (down), showing their unique morphology and mean weight, length and width ($n = 22$). Each large square on the paper represents one square centimetre

samples were experimentally contaminated with VACV-WR at 10^4 pfu/ μ L or with a range from 10^4 pfu/ μ L to 1 pfu/ μ L, respectively. By measuring total viral particles instead of viable viral particles, as described by Joklik [26, 27], the dilution range used is approximately 5×10^5 to 50 total particles/ μ L. One μ L of this material (10^4 to 1 pfu, equivalent to 5×10^5 to 50 total particles) was then used directly as

a template for qPCR reactions. Alternatively, 500 μ l of the contaminated samples were subjected to DNA extraction, total DNA was resuspended in 50 μ l, and then 1 μ L of the extracted DNA was used as a template. DNA extraction was performed using the phenol:chloroform technique [28] or with the QIAamp DNA Stool Mini kit (Qiagen®) for additional tests on positive samples.

PCRs and sequencing

Initial tests were performed using a qPCR assay designed to detect the C11R gene, using 0.8 mM of each primer and Sybr Green® (Applied Biosystems) mix on the StepOne® Applied Biosystems platform. We also used similar qPCR reactions for detection of the C23L, B18R, A56R and E3L genes. The cycling conditions were as follows: an initial step of 10' at 95 °C, followed by 40 cycles of 15" at 95 °C and 1' at 60 °C, finished with a dissociation step. Conventional PCRs were used for amplification of the A26L, C11R, A56R and VH1 genes. Reactions were carried out with 0.4 mM of each primer, 0.4 mM dNTPs, 2.0 mM MgCl₂, 100 ng/μL of Bovine Serum Albumin (BSA) and 2 U of Taq DNA polymerase in the appropriate buffer. A26L, A56R and C11L are gene targets commonly used for OPV detection [2, 3, 7, 9, 24] while the other gene targets were selected to extend our results through detection of different targets. A compilation of information related to these PCRs can be found in Table 2. PCR amplicons were purified using the MinElute® PCR Purification kit (Qiagen®) and sequenced on the ABI3130 sequencing platform. The sequences were aligned with previously published OPV sequences from GenBank using MEGA, software version 6.1 (Arizona State University, Phoenix, AZ, USA, 2014).

The primers used for unpublished reactions were: A26L fwd ACCACGTCTACTCTCGGCGA; A26L rev TGCATCGAGAGCGGAGGAGGA (first reaction) or CGATGCCAAGTACATCGACGA (second reaction); C11L fwd CGCTACAACAGATATTCCAGCTATCAG; C11L rev AGCGTGGATACAGTCACCGTGTA, VH1fwd: GCGGGAGTAAATAGAAGCGGGGC; VH1 rev: TGCGCCTCTCAAGTCCCTCA; E3Lfwd: TGCTATGGTGTACAG

CTCCGACG; E3Lrev:ATCCGGCTTATCCGCCTCCGT; B19Rfwd: CCAGCATGTATGTTTCGGAGGCACA; B19Rrev: AGGACACTTTGCGCTGAATGGCT; and C23L fwd: GCGTGTCCCCAGGACAAGGT; C23Lrev:ATGTCGCTGTCTTTCTCTTCTTCGC.

Viral isolation and virus production

Vero cells and BHK-21 cells obtained from ATCC were grown at 37 °C in Dulbecco's modified Eagle's medium (DMEM) supplemented with 2 mM glutamine, 5 % foetal calf serum and antibiotics. *Vaccinia virus* WR was kindly donated by Dr. C. Jungwirth (Wurzburg, Germany). Viral stocks were made by infecting Vero cells at a MOI of 0.001, harvesting these cells after 48 hours and purifying the viruses using a 36 % sucrose cushion [2]. For viral isolation attempts, stool samples clarified by centrifugation were filtered (Millipore 1.2 μm) for sterilisation and then submitted to a tenfold dilution (10²–10⁶). Each dilution was added to wells containing confluent Vero or BHK-21 cells in duplicates, and after an adsorption step, the wells were covered in culture media and observed daily for the formation of cytopathic effect. Isolation attempts were made three times, in two independent experiments, in each cell line used.

Results

Sample collection

Samples collected for standardization tests varied in size, weight and water content, probably due to exposure time in the environment and variation in the animal size and age

Table 2 Summary of the qPCR and PCR reactions used in this study

Gene*	Platform used	Amplicon size**	References	PAMP results	CAP5 results	CAP13 results
C11R	qPCR	82 bp	***	Positive	Positive	Positive
B18R	qPCR	72 bp	***	Positive	Positive	Not tested
C23L	qPCR	124 bp	***	Positive	Positive	Positive
E3L	qPCR	70 bp	***	Negative	Negative	Not tested
A56R	qPCR	184 bp	[32]	Positive	Positive	Positive
VH1	PCR	120 bp	***	Negative	N/A	N/A
C11R	Nested PCR	381 bp (1 st reaction) 180 bp (2 nd reaction)	[29]	Positive	Positive	Positive
A26L	PCR	1596 bp	[30]	Positive	Not tested	Not tested
A26L	Semi-nested PCR	787 bp (1 st reaction) 166 bp (2 nd reaction)	***	Positive	Not tested	Not tested
A56R	PCR	948 bp	[31]	Positive†	Positive†	Positive†

Footnotes: * Gene nomenclature based on VACV Copenhagen; ** Amplicon size is based on VACV-WR sequence. *** Unpublished data. † Amplicon of unusual size. PAMP >1 kb, CAP5 <500 bp, CAP13 ≈ 500 bp

group. Faecal pellet lengths ranged from 15 to 33.1 mm, while the width ranged from 8.8 to 18.6 mm and the weight ranged from 0.57 to 4.11 g. The aspects of two stool stacks, and of five individual pellets from each, are shown in Figure 1B. The morphology and colour of the faecal pellets and their stacks is unique amongst Brazilian animals, making it unlikely for them to be mistaken for any other animal faeces [13]. Pellets were collected from the top or from the middle of the stacks, using sterile equipment, to avoid cross contamination and contamination from the soil. A total of 16 samples were collected on the three chosen study areas for our validation tests. Locale and time (month and year) were registered for each sample, and other features were recorded whenever possible (Table 1).

Determining the optimal conditions for VACV DNA detection by qPCR in capybara stool samples

Stool samples contain PCR inhibitors [33], so in order to determine the minimum non-inhibitory dilution of capybara samples, we further diluted our stock dilutions (from 20 to 2500 fold) and then contaminated them experimentally with 10^4 pfu/ μ L of VACV-WR. Part of these contaminated dilutions were used directly as templates in qPCR reactions for the detection of the C11R gene, while part was used for DNA extractions before being analysed. This experiment was performed with different faecal pellets, and the threshold cycle (C_t) and melting temperature (T_m) means of all replicates were calculated (Table 3). A representative result (for samples used directly as templates) is shown in Figure 2A, while a representative result (for the DNA extracted samples) is shown in Figure 2B. Taking all our experiments into account, the 200-fold dilution was the dilution that permitted VACV DNA detection without PCR inhibition, when the sample was used directly as a template. When DNA was extracted, however, the amplification was detected even at a 20-fold dilution.

Determining the sensitivity of VACV DNA detection in capybara stool samples

To determine the virus detection limit of our reactions, faecal samples were diluted 200-fold and contaminated with dilutions of VACV-WR, ranging from 10^4 to 1 pfu/ μ L. A part of these samples was used directly as a template in qPCR for the detection of the C11R gene, as described earlier, while another part was used for extraction of total DNA. This experiment was also performed with different faecal pellets, and the C_t and T_m means of all replicates were calculated (Table 4). A representative result for samples used directly as templates is shown in Figure 2C, while a representative result from the samples that

Table 3 The experiments performed to determine the minimum non-inhibitory dilution of capybara stool samples for C11R gene detection

Sample dilution	C_t mean \pm SD	T_m mean	Replicates
20	28.97 \pm 1.38	75.07	3/6
100	26.55 \pm 2.66	75.62	9/12
200	28.40 \pm 5.29	75.55	14/15
300	25.67 \pm 3.15	75.47	9/9
400	24.88 \pm 3.64	75.56	9/9
500	24.78 \pm 3.26	75.80	12/12
1000	22.26 \pm 0.50	75.68	6/6
2500	25.33 \pm 0.07	76.25	3/3
20*	27.10 \pm 0.18	75.61	3/3
100*	26.14 \pm 1.90	75.64	9/9
200*	26.64 \pm 3.41	75.61	15/15
300*	26.30 \pm 2.59	75.72	9/9
400*	26.06 \pm 2.53	75.66	9/9
500*	25.97 \pm 2.30	75.78	9/9
1000*	25.97 \pm 1.47	75.81	6/6
2500*	-	-	-

Footnotes: * Indicates samples used after DNA extraction

underwent DNA extraction is shown in Figure 2D. The PCR sensitivity using samples directly as templates was up to 1 pfu/ μ L. When DNA extraction was performed on the samples the sensitivity of DNA detection was 100 pfu/ μ L, 100 times lower than without extraction.

Detection of OPV DNA in a capybara stool sample

During the standardisation experiments described above, we found a stool sample with a peculiar characteristic. This specific sample (PAMP) was not experimentally contaminated since it was used as a negative faecal matrix control; however, amplification of the C11R-target-gene was detected. To confirm this finding and rule out accidental contamination this sample was tested in triplicate or duplicate in seven independent assays for C11R detection. This was performed using new dilutions made carefully from our original stock dilution and never handled simultaneously with viruses, virus containing samples, viral DNA or PCR amplicons. Amplification of the C11R gene in this PAMP sample was seen in 18 of the 20 replicates tested, with a T_m distinct from the one expected for the VACV-WR DNA (positive control) (Figure 3A). When samples from other locations were tested, two more positive samples were detected: one collected at Serra do Cipó (CAP5) and another from Pantanal (CAP13) (Figure 3B and 3C).

To confirm that these three DNA samples were indeed from an *Orthopoxvirus*, qPCRs and PCRs for other viral

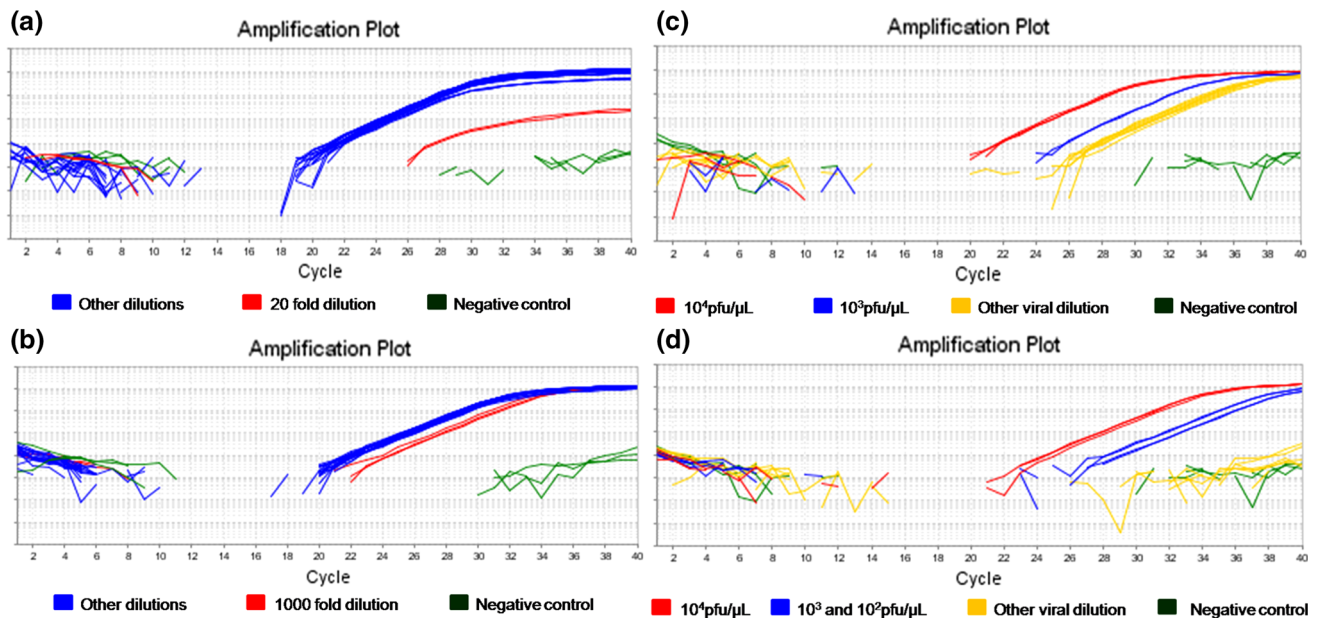


Fig. 2 Quantitative PCR amplification plots of VACV DNA in diluted capybara stool samples. Capybara stool samples were diluted, experimentally contaminated with VACV-WR and used, either directly for C11R gene-specific qPCR, or the DNA extracted and used. a) Results from samples diluted 20- to 2500-fold and experimentally contaminated with 10^4 pfu/ μ L used directly. b) Results from samples diluted 20- to 2500-fold, experimentally contaminated with 10^4 pfu/ μ L and subsequently DNA extracted

before being analysed by qPCR. c) Results from samples diluted 200-fold, experimentally contaminated with 10^4 to 1 pfu/ μ L and used directly. d) Results from samples diluted 200-fold, experimentally contaminated with 10^4 to 1 pfu/ μ L and subsequently DNA extracted before being analysed by qPCR. The x axis represents cycle number while the y axis represents the delta Rn value (SYBR green fluorescent signal normalised to the passive reference signal)

Table 4 The experiments performed to determine the C11R gene-specific detection range in capybara stool samples

Virus dilution	C_t mean \pm SD	T_m mean	Replicates
10^4 pfu/ μ L	26.42 ± 2.63	75.75	6/6
10^3 pfu/ μ L	29.85 ± 2.60	75.58	6/6
10^2 pfu/ μ L	32.91 ± 2.16	75.45	6/6
10^1 pfu/ μ L	35.95 ± 1.17	74.73	6/6
10^0 pfu/ μ L	34.93 ± 0.08	74.47	5/6
10^4 pfu/ μ L*	29.19 ± 3.06	75.68	6/6
10^3 pfu/ μ L*	32.88 ± 3.80	75.45	4/6
10^2 pfu/ μ L*	32.92 ± 2.55	75.51	5/6
10^1 pfu/ μ L*	-	-	0/6
10^0 pfu/ μ L*	-	-	0/6

Footnotes: * Indicates samples used after DNA extraction

gene targets were performed (Table 2). Viral DNA was detected using a qPCR assay targeting the C23L and A56R genes in all samples. Separately the B18R gene was detected in samples CAP5 and PAMP. A PCR targeting a large portion of the A56R gene resulted in fragments of different sizes for each sample (>1 kb for PAMP, <500 bp for CAP5, and \approx 500 bp for CAP13), all of them different from the \approx 900 bp expected for VACV-WR (control). The PCR test for C11R gene amplified fragments of the

expected size, about 180 bp, for all three samples. In addition other PCR amplifications were attempted targeting a large portion of the A26L gene. A 500 bp fragment, instead of the >1 Kb expected fragment seen in the control, was amplified from the PAMP sample. However, a semi-nested PCR targeting the same gene amplified a fragment similar to that amplified for the control. PCR reactions targeting the VH1 and E3L were also attempted, but no amplification was detected.

Partial DNA sequences were obtained from the amplified DNA of the C11R gene (192 bp) for all three positive samples and analysis revealed that they are highly similar to BR-VACV samples, with CAP5 being the most distant (Figure 4A). Partial sequence from the A26L (127 bp) gene was also obtained for PAMP, revealing that this sequence is also similar to BR-VACV samples (Figure 4B). Another sequence (82 bp) from the A26L gene sequence was also obtained for the PAMP and CAP13 sequences. This showed that these two samples possess a genetic marker found in group I BR-VACV but not in group II viruses nor in VACV-WR (Figure 4C). Taken together, these data confirm the presence of OPV in our samples, with a profile similar, but not identical, to VACV-WR, our positive control. Viral isolation was attempted twice in Vero cells, in independent experiments and in several replicates, however this was not successful (data not shown).

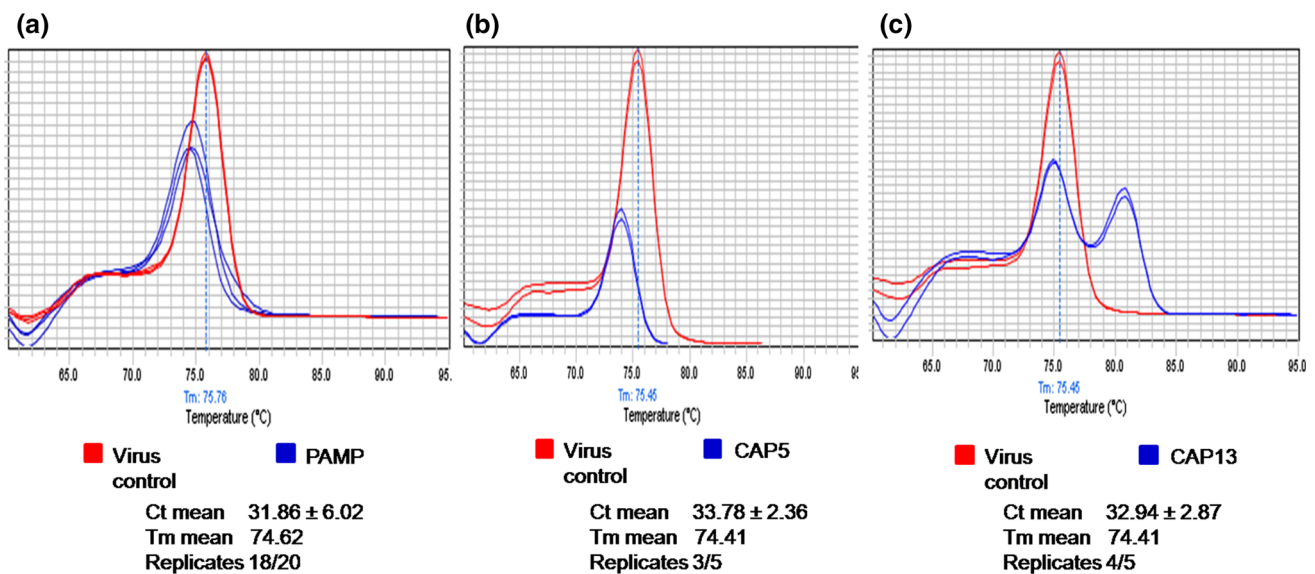


Fig. 3 Detection of VACV DNA in capybaras stool samples by qPCR. Capybara stool samples were processed and used as template for a qPCR targeting the C11R gene. The amplification plots were performed in Step One Software. a) A positive sample from Lagoa da

Pampulha (PAMP). b) A positive sample from Serra do Cipó (CAP5). c) A positive sample from Pantanal (CAP13). Fluorescence (negative derivative) is shown on the y axis while temperature is shown on the x axis

Discussion

In the decades following smallpox eradication, the emergence of other OPV became an important public health concern, especially due to the cessation of vaccination and the threat posed by viruses that could fill the empty niche left by *Variola virus*. In Brazil, this concern is focused on VACV emergence, a virus that has been increasingly the cause of outbreaks with important economical and public health outcomes. The VACV transmission cycle and sylvatic reservoirs remain a mystery; however, the role of small rodents in viral dissemination and as a link between wild and rural areas is becoming more apparent [2, 10]. Capybaras are wild rodents with unique features, including an increasing population and a preference for living in anthropised environments [14, 15]. The ecological position and habits of these animals highlights them as possible key components in the BR-VACV transmission cycle; however, so far no in depth study has considered this hypothesis.

Aiming to elucidate the role of capybaras in the VACV natural cycle, this study presents a well-established technique to detect OPV DNA in stool samples. Stool samples were chosen because it has already been shown that VACV can be found in stool samples from experimentally infected mice and cattle several days after exposure and even after the disappearance of skin lesions [24, 34]. In addition faecal shedding might be common among OPV, since black-tailed prairie dogs have been shown to shed monkeypox virus in their faeces whilst monkeypox virus was

detected in the rectal swabs of African pouched rats [35, 36].

We have shown that it is possible to detect VACV DNA (equivalent to at least 1 pfu/ μ L) when stool samples are diluted 200-fold and used directly as templates for qPCR reactions. Samples where the total DNA was extracted prior to qPCR permitted the use of lower dilutions; however, they also had lower sensitivity. Our preference was therefore to use samples without DNA extraction, due to this higher sensitivity and to avoid excessive sample manipulation. This method was revealed to be a simple, easy and relatively cheap way to screen for the presence of OPV DNA in this type of sample, and therefore has the potential to be expanded to other viral targets.

This study also presents, for the first time, molecular evidence for the presence of an OPV in capybaras. Stool samples obtained from four different Brazilian habitats were tested and from those three were found to be positive for an OPV using our screening method. These samples were further characterised by the amplification of other gene targets by PCR, and sequence analysis of the C11R and A26L gene confirmed that those viruses are indeed VACV. A polymorphism in the A26L gene shows that the three positive samples may resemble BR-VACV from group I, which are non-virulent in murine models and most commonly isolated from BV outbreaks. However, more genetic markers must be investigated before assigning these putative new viruses to a BR-VACV group. Unfortunately we were not able to isolate viruses from any of these samples, probably due to the composition of the

(a)

	WR	PAMP	CAP5	CAP13	MARV	ARAV	PSTV	DMTV	GP1V	GP2V	Lister	Cantagalo	IOC
WR	ID												
PAMP	1	ID											
CAP5	0.943	0.943	ID										
CAP13	1	1	0.943	ID									
MARV	0.994	0.994	0.938	0.994	ID								
ARAV	0.994	0.994	0.938	0.994	1	ID							
PSTV	1	1	0.943	1	0.994	0.994	ID						
DMTV	1	1	0.943	1	0.994	0.994	1	ID					
GP1V	1	1	0.943	1	0.994	0.994	1	1	ID				
GP2V	1	1	0.943	1	0.994	0.994	1	1	1	ID			
Lister	1	1	0.943	1	0.994	0.994	1	1	1	1	ID		
Cantagalo	1	1	0.943	1	0.994	0.994	1	1	1	1	1	ID	
IOC	1	1	0.943	1	0.994	0.994	1	1	1	1	1	1	ID

(b)

	WR	PAMP	ARAV	SH2V	PSTV	GOV1	Muriae	GP2	Cantagalo	IOC
WR	ID									
PAMP	0.934	ID								
ARAV	1	0.934	ID							
SH2V	1	0.934	1	ID						
PSTV	1	0.934	1	1	ID					
GOV1	0.99	0.925	0.99	0.99	0.99	ID				
Muriae	0.99	0.925	0.99	0.99	0.99	0.981	ID			
GP2	0.99	0.925	0.99	0.99	0.99	1	0.981	ID		
Cantagalo	1	0.934	1	1	1	0.99	0.99	0.99	ID	
IOC	1	0.934	1	1	1	0.99	0.99	0.99	1	ID

(c)

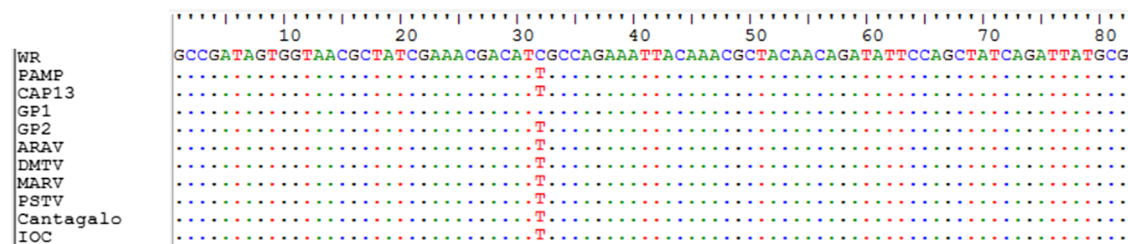


Fig. 4 Molecular analysis of VACV DNA amplified from capybara stool samples. PCR amplified fragments were sequenced and analysed for further characterization (using the Mega 6.0 software). a) Sequence identity matrix for a partial region inside the C11R gene. b) Sequence identity matrix for a partial region inside A26L gene. c) Alignment of a small portion of the A26L gene showing a genetic marker found in BR-VACV. The following abbreviations are used: WR (Vaccinia virus-Western Reserve strain), PAMP (Vaccinia virus-Pampulha sample), CAP 13 (Vaccinia virus-Capybara 13 sample), CAP 5 (Vaccinia virus-Capybara 5 sample), GP1 (Vaccinia virus-Guarani P1 virus), GP2 (Vaccinia virus-Guarani P2 virus), ARAV (Vaccinia virus-Araçatubavirus), DMTV (Vaccinia virus-Diamantina virus), MARV (Vaccinia virus - Mariana virus), PSTV (Vaccinia virus - Passatempo virus), Cantagalo (Cantagalo virus), IOC (Vaccinia virus- Instituto Oswaldo Cruz), SH2V (Vaccinia virus - Serro humano 2 virus), GOV1 (Vaccinia virus - Goiás virus 1), Muriae (Vaccinia virus - Muriae virus 1), and Lister (Vaccinia virus -Lister strain)

faecal sample or host range factors. Some studies have shown that viral DNA can be detected from mice and cow faecal samples several days after infection, while the recovery of live viruses has a smaller time window, showing that it is indeed easier to detect DNA than to isolate viruses from faecal samples [24, 34]. Our findings suggest that capybaras may be included as putative participants in the natural BR-VACV transmission cycle, thus increasing awareness regarding the presence of these animals in farms and even urban areas. In this scenario, capybaras could be a link between domestic and wild environments. Theoretically, they could bring virus from sylvatic habitats to domestic animals whilst grazing in the same area as cattle, or could take the virus from domestic habitats to sylvatic ones when returning to the wild.

The detection of an OPV positive sample in a supposedly complete urban environment (Lagoa da Pampulha, Belo Horizonte) was also an important observation. However, it is not possible to exclude factors such as the introduction of capybaras from other regions in the site where the standardization samples were collected. Besides, it is not uncommon to find smaller rodents, horses or cattle near the site, and these animals might also be considered as a source of infection for the capybara group. Finally, the lagoon used by these animals receives water from other streams carrying sewage water from miles away, so contaminated water can also be considered as a source for the infection. It is still difficult to determine how this virus ended up in this particular capybara herd, but once one individual is infected we speculate that it could spread the virus through its faeces, infecting other animals and even re-infecting itself through coprophagy. The two other positive samples were found in natural environments where wild animals and cattle coexist, therefore capybaras may also be an important link between these animals. The geographical distance between the samples shows that this

virus is probably spread among different capybara herds, and larger sampling in the future will help to better understand its epidemiology and occurrence.

Further studies are necessary to completely explain the capybara's role in the VACV transmission cycle, but the results shown in this paper are an important starting point. In the future serological analysis and active searching for typical VACV-lesions and viral isolation will be important. In addition, detailed ecological data associated with these laboratory results will make it much easier to understand how these animals participate and impact upon VACV circulation in Brazil.

Acknowledgments This work was supported by research grants from Fundação de Amparo a Pesquisado Estado de Minas Gerais (FAPEMIG), Conselho Nacional de Desenvolvimento Científico e Tecnológico (CNPq) and Coordenadoria de Aperfeiçoamento de Pessoal de Nível Superior (CAPES). From April, 2016 onwards LALD was funded by European Research Council (ERC) [EU FP7/2007-2013 (Micro-RIP 2014-2019, project #615146)]. From March 2016 onwards GMFA was funded by the Finnish Centre of Excellence Program of the Academy of Finland (CoE in Biological Interactions 2012–2017, project #252411). We would like to thank Ana Paula Moreira for obtaining the samples from Pantanal and Juliano Leal de Paula from Núcleo de Análise de Genoma e Expressão Gênica (NAGE)-Departamento de Bioquímica e Imunologia (ICB—UFMG). GST, JSA and EGK are researchers from CNPq.

References

- Moss B (2007) Poxviridae: The viruses and their replication. In: Fields BN, Knipe DM, Howley PM (eds) Fields virology, 5th edn. Lippincott Williams & Wilkins, Philadelphia, pp 2905–2946
- Abrahão JS, Guedes MI, Trindade GS, Fonseca FG, Campos RK, Mota BF, Lobato ZI, Silva-Fernandes AT, Rodrigues GO, Lima LS, Ferreira PC, Bonjardim CA, Kroon EG (2009) One more piece in the VACV ecological puzzle: could peridomestic rodents be the link between wildlife and bovine vaccinia outbreaks in Brazil? *PLoS One* 4:e7428
- Abrahão JS, Silva-Fernandes AT, Lima LS, Campos RK, Guedes MI, Cota MM, Assis FL, Borges IA, Souza-Júnior MF, Lobato ZI, Bonjardim CA, Ferreira PC, Trindade GS, Kroon EG (2010) Vaccinia virus infection in monkeys, Brazilian Amazon. *Emerg Infect Dis* 16:976–979
- Peres MG, Bacchiega TS, Appolinário CM, Vicente AF, Allendorf SD, Antunes JM, Moreira SA, Legatti E, Fonseca CR, Pituco EM, Okuda LH, Pantoja JC, Ferreira F, Megid J (2013) Serological study of vaccinia virus reservoirs in areas with and without official reports of outbreaks in cattle and humans in São Paulo, Brazil. *Arch Virol* 158:2433–2441
- Damon IK (2007) Poxviruses. In: Fields BN, Knipe DM, Howley PM (eds) Fields virology, 5th edn. Lippincott Williams & Wilkins, Philadelphia, pp 2947–2976
- Essbauer S, Pfeffer M, Meyer H (2010) Zoonotic poxviruses. *Vet Microbiol* 140:229–236
- Damaso CR, Esposito JJ, Condit RC, Moussatché N (2000) An emergent poxvirus from humans and cattle in Rio de Janeiro State: Cantagalo virus may derive from Brazilian smallpox vaccine. *Virology* 277:439–449
- Bhanuprakash V, Venkatesan G, Balamurugan V, Hosamani M, Yogisharadha R, Gandhale P, Reddy KV, Damle AS, Kher HN,

- Chandel BS, Chauhan HC, Singh RK (2010) Zoonotic infections of buffalopox in India. *Zoonoses Public Health* 57:e149–e155
9. Franco-Luiz AP, Fagundes-Pereira A, Costa GB, Alves PA, Oliveira DB, Bonjardim CA, Ferreira PC, GeS Trindade, Panei CJ, Galosi CM, Abrahão JS, Kroon EG (2014) Spread of vaccinia virus to cattle herds, Argentina, 2011. *Emerg Infect Dis* 20:1576–1578
 10. Trindade GS, Emerson GL, Carroll DS, Kroon EG, Damon IK (2007) Brazilian vaccinia viruses and their origins. *Emerg Infect Dis* 13:965–972
 11. Fonseca FG, Lanna MC, Campos MA, Kitajima EW, Peres JN, Golgher RR, Ferreira PC, Kroon EG (1998) Morphological and molecular characterization of the poxvirus BeAn 58058. *Arch Virol* 143:1171–1186
 12. da Fonseca FG, Trindade GS, Silva RL, Bonjardim CA, Ferreira PC, Kroon EG (2002) Characterization of a vaccinia-like virus isolated in a Brazilian forest. *J Gen Virol* 83:223–228
 13. Mones A, Ojasti J (1986) *Hydrochoerus hydrochaeris*. *Mamm Species* 264:1–7
 14. Herrera EA, Macdonald DW (1989) Resource utilization and territorially in group-living capybaras (*Hydrochoerus hydrochaeris*). *J Anim Ecol* 58:667–679
 15. Ferraz KMPMB, Ferraz SFB, Moreira JR, Couto HTZ, Verdade LM (2007) Capybara (*Hydrochoerus hydrochaeris*) distribution in agroecosystems: a cross scale habitat analysis. *J Biogeogr* 34:223–230
 16. Ferraz KMPMB, Manly B, Verdade LM (2010) The influence of environmental variables on capybara (*Hydrochoerus hydrochaeris*: Rodentia, Hydrochoeridae) detectability in anthropogenic environments of southeastern Brazil. *Popul Ecol* 52:263–270
 17. Ferraz KMPMB, Peterson AT, Scachetti-Pereira R, Vettorazzi CA, Verdade LM (2009) Distribution of capybaras in an agroecosystem, southeastern Brazil, based on ecological niche modeling. *J Mammal* 90:189–194
 18. Ferraz KMPMB, Lechevalier M, Couto HTZ, Verdade LM (2003) Damage caused by capybaras in a corn field. *Sci Agricola* 60:191–194
 19. Embrapa Pantanal (2007) Capybara diseases. Embrapa Pantanal, Brazil, p 74
 20. Krawczak FS, Nieri-Bastos FA, Nunes FP, Soares JF, Moraes-Filho J, Labruna MB (2014) Rickettsial infection in *Amblyomma cajennense* ticks and capybaras (*Hydrochoerus hydrochaeris*) in a Brazilian spotted fever-endemic area. *Parasit Vectors* 7:7
 21. Moreira CA (1955) Notes on the vaccinia virus evolution in wild animals from the Brazilian fauna. *Memórias do Instituto Oswaldo Cruz, Brazil*
 22. Barbosa AV, Medaglia ML, Soares HS, Quixabeira-Santos JC, Gennari SM, Damaso CR (2014) Presence of neutralizing antibodies to orthopoxvirus in capybaras (*Hydrochoerus hydrochaeris*) in Brazil. *J Infect Dev Ctries* 8:1646–1649
 23. Ferreira JM, Abrahão JS, Drumond BP, Oliveira FM, Alves PA, Pascoal-Xavier MA, Lobato ZI, Bonjardim CA, Ferreira PC, Kroon EG (2008) Vaccinia virus: shedding and horizontal transmission in a murine model. *J Gen Virol* 89:2986–2991
 24. Abrahão JS, GeS Trindade, Ferreira JM, Campos RK, Bonjardim CA, Ferreira PC, Kroon EG (2009) Long-lasting stability of Vaccinia virus strains in murine feces: implications for virus circulation and environmental maintenance. *Arch Virol* 154:1551–1553
 25. D'Anuniação L, Guedes MI, Oliveira TL, Rehfeld I, Bonjardim CA, Ferreira PP, GeS Trindade, Lobato ZP, Kroon EG, Abrahão JS (2012) Filling one more gap: experimental evidence of horizontal transmission of Vaccinia virus between bovines and rodents. *Vector Borne Zoonotic Dis* 12:61–64
 26. Joklik WK (1962) Some properties of poxvirus DNA. *J Mol Biol* 5(3):265–274
 27. Joklik WK, Becker Y (1964) The replication and coating of vaccinia DNA. *J Mol Biol* 10(3):452–474
 28. Sambrook J, Fritsch EF, Maniatis T (eds) (1989) *Molecular cloning: a laboratory manual*, 2nd edn. Cold Spring Harbor Laboratory Press, New York
 29. Abrahão JS, Lima LS, Assis FL, Alves PA, Silva-Fernandes AT, Cota MM, Ferreira VM, Campos RK, Mazur C, Lobato ZI, Trindade GS, Kroon EG (2009) Nested-multiplex PCR detection of orthopoxvirus and parapoxvirus directly from exanthematic clinical samples. *Virol J* 6:140
 30. Meyer H, Pfeffer M, Rziha HJ (1994) Sequence alterations within and downstream of the A-type inclusion protein genes allow differentiation of Orthopoxvirus species by polymerase chain reaction. *J Gen Virol* 75(Pt 8):1975–1981
 31. Ropp SL, Jin Q, Knight JC, Massung RF, Esposito JJ (1995) PCR strategy for identification and differentiation of small pox and other orthopoxviruses. *J Clin Microbiol* 33:2069–2076
 32. de Souza Trindade G, Li Y, Olson VA, Emerson G, Regnery RL, da Fonseca FG, Kroon EG, Damon I (2008) Real-time PCR assay to identify variants of vaccinia virus: implications for the diagnosis of bovine vaccinia in Brazil. *J Virol Methods* 152:63–71
 33. Schrader C, Schielke A, Ellerbroek L, Johne R (2012) PCR inhibitors—occurrence, properties and removal. *J Appl Microbiol* 113(5):1014–1026
 34. Rivetti AV Jr, Guedes MIMC, Rehfeld IS, Oliveira TML, Matos ACD, Abrahão JS, Kroon EG, Lobato ZIP (2013) Bovine vaccinia, a systemic infection: evidence of fecal shedding, viremia and detection in lymphoid organs. *Vet Microbiol* 162(1):103–111
 35. Hutson C, Olson V, Carroll D, Abel J, Hughes C, Braden Z, Weiss S, Self J, Osorio J, Hudson P, Dillon M, Karem K, Damon I, Regnery R (2009) A prairie dog animal model of systemic orthopoxvirus disease using West African and Congo Basin strains of monkeypox virus. *J Gen Virol* 90(2):323–333
 36. Hutson CL, Nakazawa YJ, Self J, Olson VA, Regnery RL et al (2015) Laboratory investigations of African pouched rats (*Cricetomys gambianus*) as a potential reservoir host species for monkeypox virus. *PLoS Negl Trop Dis* 9(10):e0004013



Detection of *Vaccinia virus* during an outbreak of exanthemous oral lesions in Brazilian equids

J. S. ABRAHÃO*, G. DE SOUZA TRINDADE, G. PEREIRA-OLIVEIRA, P. DE OLIVEIRA FIGUEIREDO, G. COSTA, A. P. MOREIRA FRANCO-LUIZ, F. LOPES ASSIS, D. BRETAS DE OLIVEIRA, L. R. MATTOS PAIM†, C. E. DE ARAÚJO OLIVEIRA†, A. LEMOS MAIA NETO† and E. GEESIEN KROON

Laboratório de Vírus, Universidade Federal de Minas Gerais, Minas Gerais, Brazil

†ADAB - Agência Estadual de Defesa Agropecuária da Bahia, Salvador, Brazil.

*Correspondence email: jonatas.abrahao@gmail.com; Received: 22.10.15; Accepted: 06.02.16

Summary

Reasons for performing study: In August 2014, an outbreak of oral exanthematous disease in equids was reported in Brazil, affecting 11 donkeys and 3 mules.

Objectives: To investigate if *Vaccinia virus* (VACV) was the aetiological agent in this outbreak.

Study design: Investigation of clinical cases using serological, molecular and phylogenetic approaches.

Methods: To analyse the presence of neutralising antibodies against VACV, samples were submitted in triplicate to a plaque-reduction neutralisation test (PRNT_{50%}). On the basis of previous studies which detected VACV DNA in sera, we submitted extracted DNA samples to different polymerase chain reaction (PCR) platforms targeting *Orthopoxvirus* (OPV) genes (C11R, A56R and A26L). The PCR products were directly sequenced in both orientations using specific primers and capillary electrophoresis. The alignment and phylogenetic analysis of the A26L and A56R nucleotide sequences (maximum likelihood) were prepared with the obtained nucleotide fragments.

Results: Serological and molecular data suggested VACV as the aetiological agent. The neutralising antibodies against OPV were detected in 5 (55.5%) of the equids, with titres ≥ 40 neutralising u/ml. Based on the results obtained from all PCR platforms, all samples were positive for OPV: 9 (100%) for A56R, 4 (44.4%) for C11R and 3 (33.3%) for A26L. The alignment of the nucleotide sequences of the A26L and A56R fragments revealed that the samples were highly similar to the homologous genes from other Brazilian VACV Group 1 isolates (98.8% identity on average). Furthermore, both the A26L and A56R sequences showed signature deletions also present in the sequences of Group 1 VACV isolates from Brazil.

Conclusions: Our data raises questions about the role of equids in the chain of VACV epidemiology. The surveillance of equids in VACV-affected areas worldwide is relevant.

The Summary is available in Chinese – see Supporting information.

Keywords: Horse; *Vaccinia virus*; orthopoxvirus; emerging infectious disease

Introduction

Since 1999, several *Vaccinia virus* (VACV) zoonotic outbreaks have been reported in cattle and man in rural areas of South America and Asia. *Vaccinia virus* causes exanthematous lesions in cows and milkers and affects the milk industry and public health services [1,2]. Although VACV had been isolated from Brazilian rain forests during the 1960s and 70s, this virus has been a public health problem in Brazil since 1999, when frequent exanthematous outbreaks have been reported [1,2]. Although VACV has been detected in wild animals [3,4], most cases of VACV are associated with infections in cattle and man [1,2]. Equids are important in farming and may associate directly with infected bovines; however, there have been few reported cases of equid vaccinia [5,6].

Materials and methods

Animals

An outbreak of severe exanthematous signs was reported in equids in Itiuba county in August 2014 (10°41'30"S/39°51'13"W), Bahia State, Brazil (Fig 1a). *Vaccinia* cases in cattle and man had occurred in this region in previous years. Together, the 2 affected properties had 108 milking cows, 4 horses, 11 donkeys and 30 mules. Clinical details and serum samples ($n = 9$) were collected (Day 4 post lesions appearance) from 9 equids.

Serological assays

To analyse the presence of neutralising antibodies against orthopoxvirus (OPV), a plaque-reduction neutralisation test (PRNT_{50%}) was performed, in

triplicate, as previously described [3,4]. Briefly, serum samples were inactivated by heating at 56°C for 30 min and anti-OPV PRNT performed. Inactivated samples were diluted 1:20–1:1640 \times in minimal essential medium and tested in BSC-40 by using the VACV-Western Reserve strain in the PRNT. Bovine samples positive for antibodies to OPV obtained during bovine vaccinia outbreaks [1] were used as positive controls; samples negative for these antibodies were used as negative controls. Serum titre was defined as the highest dilution that inhibited >50% of viral plaques compared with negative controls and OPV PRNT specificity (97.4%) and sensitivity (93.5%) were confirmed by using receiver-operating characteristic analysis [3].

Molecular assays

On the basis of previous studies that have detected OPV DNA in sera [3,7], extracted DNA samples were examined with PCR platforms targeting OPV genes: 1) Nested PCR to amplify the highly conserved OPV *vaccinia growth factor* (C11R) gene [8], 2) real-time PCR to amplify the haemagglutinin gene (A56R) [9] and 3) nested PCR targeting the a-type-inclusion-body (A26L) gene (F.L. Assis, unpublished data). Bovine VACV DNA-positive and DNA-negative serum samples obtained during bovine vaccinia outbreaks [1] were used as positive and negative controls, respectively. The A26L (~600 bp) and A56R (~90 bp) PCR products were directly sequenced in both orientations using specific primers and capillary electrophoresis (ABI3130 Applied Biosystems[®]). The alignment of the A26L and A56R nucleotide sequences (maximum likelihood, Tamura–Nei, 1000 bootstrap) was prepared with the obtained nucleotide fragments using ClustalW-MEGA5[®].

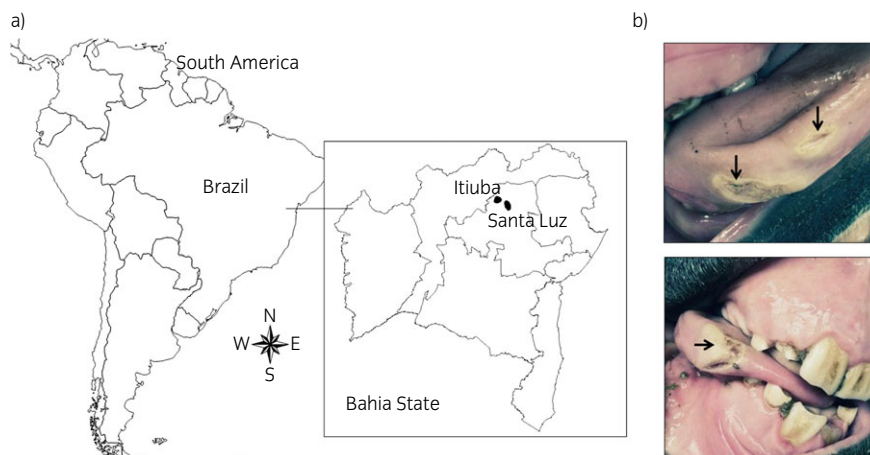


Fig 1: a) Map of Brazil, highlighting Bahia State and counties where collections were made. b) Exanthematous lesions on the tongue of an equid; vesicles and ulcers are indicated with black arrows.

Results

Eleven donkeys (100% of donkeys on the 2 premises) and 3 mules (10.0%) were affected, presenting with exanthematous lesions on their mouths and tongues (Fig 1b). The lesions began as small macules that evolved to papules, vesicles and ulcers and healed after 8–12 days (Fig 1b). The infected animals were inappetent with reduced fitness.

Neutralising antibodies against OPV were detected in 5 (55.5%) of the 9 equids sampled, with titres ≥ 40 neutralising u/ml (Table 1). Based on the results obtained from all PCR platforms (Table 1), all equid samples were positive for OPV: 9 (100%) for A56R, 4 (44.4%) for C11R and 3 (33.3%) for A26L. The samples were highly similar to the homologous genes from other Brazilian VACV Group 1 isolates (98.8% identity on average). Furthermore, both the A26L (Fig 2) and A56R sequences showed signature deletions also present in the sequences of Group 1 VACV isolates from Brazil. Because all of the obtained sequences from the equid outbreak were identical, we named them VACV-EquidBA2014. Considering all of the obtained sequences, VACV-EquidBA2014 showed a unique nucleotide sequence profile. In the phylogenetic tree constructed based on the A26L nucleotide sequences, VACV-EquidBA2014 clustered with several Group 1 VACVs isolated during outbreaks in Brazil (Fig 2a). Finally, we tried to isolate viruses from blood samples in BSC-40 cells but it was not possible.

Discussion

Here, we describe an exanthematous disease outbreak in equids, likely caused by VACV. The increased frequency of reports of VACV hosts may not only be a consequence of VACV spreading to farm and/or wild species, but may also be the result of increasing research efforts worldwide to

understand VACV circulation and the host range [1,2,4,6,10,11]. At least 3 origins are possible in this outbreak: 1) A donkey with no apparent clinical signs had recently been imported from Santa Luz county (~80 km) (Fig 1a), 2) some of the infected equids had been at auctions or fairs some weeks before the outbreak and 3) introduction of the virus from wildlife cannot be eliminated, since prior outbreaks in cattle and man were described in the region.

Because VACV lesions usually occur inside the mouth of equids, the circulation of VACV among horses, donkeys, mules and other equids may have been previously overlooked. An earlier description of VACV infection in horses in Brazil [6] described proliferative skin lesions, with little involvement of the oral cavity other than the lips; however, we believe that clinical cases like that may not be common, which can prevent diagnosis of the disease. Taken together, our data not only reinforce the notion that equids can be zoonotic sources of VACV but also raise questions about the need for the surveillance of these animals in areas affected by VACV throughout the world.

Authors' declaration of interests

No competing interests have been declared.

Ethical animal research

Research ethics committee oversight not currently required by this journal: procedures were performed as part of clinical investigations. Owners gave informed consent for their animals' inclusion in the study.

Source of funding

Financially supported by CNPq, CAPES, and FAPEMIG. JSA, GST and EGK are CNPq researchers.

Acknowledgements

We thank all our colleagues from Laboratório de Vírus (ICB-UFMG) and ADAB for their technical support. Financial support was provided by CNPq, Pro-Reitoria de Pesquisa da UFMG (PRPq-UFMG), CAPES, FAPEMIG and MAPA.

Authorship

J. Santos Abrahão and G. de Souza Trindade contributed equally to this work. J. Santos Abrahão, G. de Souza Trindade and E. Geessien Kroon were responsible for the study design, data interpretation, supply of reagents

TABLE 1: Results of serological and molecular assays for orthopoxvirus in 9 equids with exanthematic oral lesions

Sample	PRNT ₅₀ /titre	PCR		
		A56R	C11R	A26L
Donkey 1	+/1:40	+	+	-
Donkey 2	-	+	-	-
Donkey 3	+/1:40	+	+	+
Donkey 4	+/1:80	+	+	+
Donkey 5	+/1:40	+	-	-
Donkey 6	-	+	-	+
Donkey 7	-	+	-	-
Mule 1	+/1:80	+	+	-
Mule 2	-	+	-	-

+ = positive, - = negative, PRNT = plaque-reduction neutralising test.

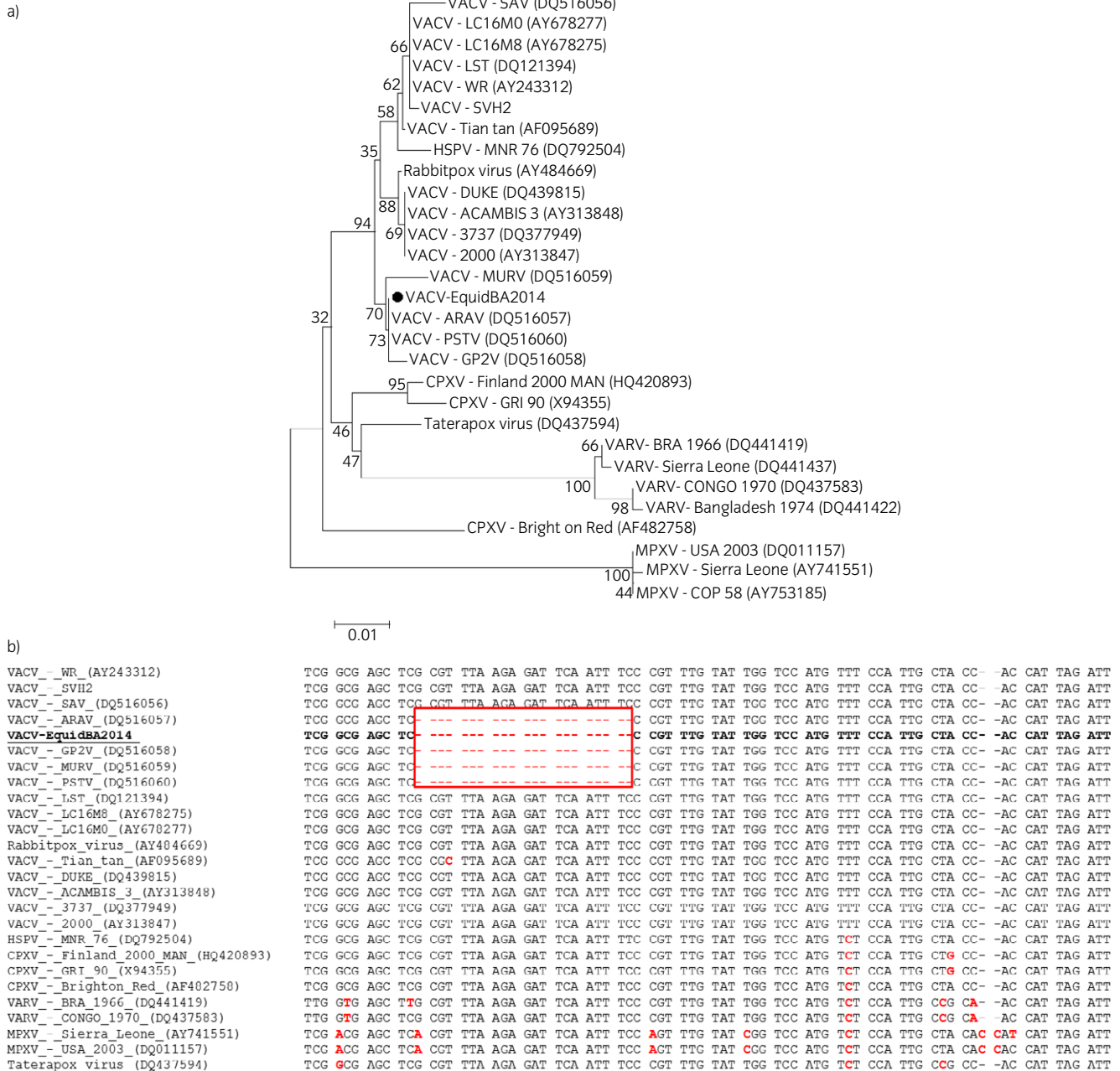


Fig 2: a) Consensus bootstrap phylogenetic tree based on the partial nucleotide sequences of the OPV A26L gene (correspondent from 135,675 to 135,750 VACV-WR genome). The trees were constructed using the maximum likelihood, Tamura-Nei, 1000 bootstrap replicates in MEGA version 5. Bootstrap values >30% are shown. The nucleotide sequences were obtained from GenBank. The black dot indicates VACV-EquidBA2014. b) Nucleotide sequence of the VACV-EquidBA2014 A26L gene and comparison with the homologous sequences of several OPV genes. A 21-nt deletion present in several Brazilian VACV Group 1 is highlighted in red. Polymorphisms are highlighted in red.

and manuscript preparation. G. Pereira-Oliveira and D. Bretas de Oliveira performed PCRs and sequencing, P. de Oliveira Figueiredo, G. Costa and A.P. Moreira Franco-Luiz performed cell culture and serological assays, F. Lopes Assis performed phylogenetic analysis, L.R. Mattos Paim, C.E. de Araújo Oliveira and A. Lemos Maia Neto collected samples and epidemiological data. All authors gave their final approval of the manuscript.

Manufacturers' addresses

^aApplied Biosystems, Foster City, California, USA.
^bClustalW- MEGA5, Phoenix, Arizona, USA.

References

1. Kroon, E.G., Mota, B.E.F., Abrahão, J.S., Fonseca, F.G. and Trindade, G.S. (2011) Zoonotic Brazilian Vaccinia virus: From field to therapy. *Antiviral Res.* **92**, 150-163.
2. Singh, R.K., Hosamani, M., Balamurugan, V., Bhanuprakash, V., Rasool, T.J. and Yadav, M.P. (2007) Buffalopox: an emerging and re-emerging zoonosis. *Anim. Health Res. Rev.* **8**, 105-114.
3. Abrahão, J.S., Silva-Fernandes, A.T., Lima, L.S., Campos, R.K., Guedes, M.I., Cota, M.M., Assis, F.L., Borges, I.A., Souza-Júnior, M.F., Lobato, Z.I.P., Bonjardim, C.A., Ferreira, P.C.P., Trindade, G.S. and Kroon, E.G. (2010)

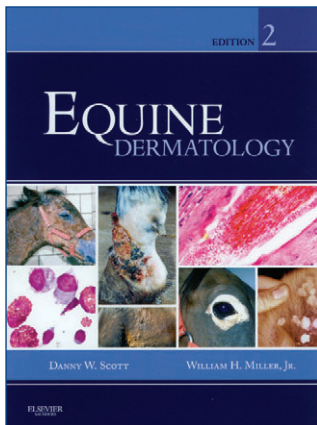
- Vaccinia virus infection in monkeys, Brazilian Amazon. *Emerg. Infect. Dis.* **16**, 976-979.
4. Peres, M.G., Bacchiega, T.S., Appolinário, C.M., Vicente, A.F., Allendorf, S.D., Antunes, J.M., Moreira, S.A., Legatti, E., Fonseca, C.R., Pituco, E.M., Okuda, L.H., Pantoja, J.C., Ferreira, F. and Megid, J. (2013) Serological study of vaccinia virus reservoirs in areas with and without official reports of outbreaks in cattle and humans in São Paulo, Brazil. *Arch. Virol.* **158**, 2433-2441.
 5. Campos, R.K., Brum, M.C., Nogueira, C.E., Drumond, B.P., Alves, P.A., Siqueira-Lima, L., Assis, F.L., Trindade, G.S., Bonjardim, C.A., Ferreira, P.C., Weiblen, R., Flores, E.F., Kroon, E.G. and Abrahão, J.S. (2011) Assessing the variability of Brazilian Vaccinia virus isolates from a horse exanthematic lesion: coinfection with distinct viruses. *Arch. Virol.* **156**, 275-283.
 6. Brum, M.C., Anjos, B.L., Nogueira, C.E., Amaral, L.A., Weiblen, R. and Flores, E.F. (2010) An outbreak of orthopoxvirus-associated disease in horses in southern Brazil. *J. Vet. Diagn. Invest.* **22**, 143-147.
 7. de Assis, F.L., Pereira, G., Oliveira, C., Rodrigues, G.O., Cotta, M.M., Silva-Fernandes, A.T., Peregrino Ferreira, P.C., Bonjardim, C.A., Trindade, G.S., Kroon, E.G. and Abrahão, J.S. (2012) Serologic evidence of orthopoxvirus infection in buffaloes. *Brazil. Emerg. Infect. Dis.* **18**, 698-700.
 8. Abrahão, J.S., Lima, L.S., Assis, F.L., Alves, P.A., Silva-Fernandes, A.T., Cota, M.M., Ferreira, V.M., Campos, R.K., Mazur, C., Lobato, Z.I., Trindade, G.S. and Kroon, E.G. (2009) Nested-multiplex PCR detection of Orthopoxvirus and Parapoxvirus directly from exanthematic clinical samples. *Virology* **11**, 140.
 9. de Souza Trindade, G., Li, Y., Olson, V.A., Emerson, G., Regnery, R.L., da Fonseca, F.G., Kroon, E.G. and Damon, I. (2008) Real-time PCR assay to identify variants of Vaccinia virus: Implications for the diagnosis of bovine vaccinia in Brazil. *J. Virol. Methods* **152**, 63-71.
 10. Damaso, C.R., Esposito, J.J., Condit, R.C. and Moussatché, N. (2000) An emergent poxvirus from humans and cattle in Rio de Janeiro State: Cantagalo virus may derive from Brazilian smallpox vaccine. *Virology* **277**, 439-449.
 11. Rivetti, A.V. Jr, Guedes, M.I., Rehfeld, I.S., Oliveira, T.M., Matos, A.C., Abrahão, J.S., Kroon, E.G. and Lobato, Z.I. (2013) Bovine vaccinia, a systemic infection: evidence of fecal shedding, viremia and detection in lymphoid organs. *Vet. Microbiol.* **162**, 103-111.

Supporting Information

Additional Supporting Information may be found in the online version of this article at the publisher's website:

Summary in Chinese

EVJ BOOKSHOP



Equine Dermatology, 2nd edition

Editors: Danny W. Scott and William H. Miller, Jr.

Publisher: Elsevier Saunders, December 2010 • Hardbound, 552 Pages

Diagnose, treat and manage equine skin disorders with the most comprehensive reference available! With 900 full-colour photos, *Equine Dermatology* covers skin diseases ranging from those that merely annoy the horse to others that interfere with the horse's ability to function in riding, working or show. Thorough coverage includes essential basics and practical diagnostic methods, therapies and specific abnormalities and defects. The book describes the structure and function of the skin, and discusses disorders including bacterial, fungal, parasitic, viral, protozoal, allergic, immune-mediated, endocrine, metabolic and nutritional diseases. It also covers congenital and hereditary defects, pigmentation abnormalities, keratinisation defects, environmental skin diseases and skin tumours. Written by renowned equine dermatologists Danny Scott and Bill Miller, this all-inclusive resource covers the latest dermatological topics and the newest therapies.

BEVA member:

£90.00

Non-member:

£100.00

EVJ Bookshop, Mulberry House, 31 Market Street, Fordham, Ely, Cambs. CB7 5LQ, UK
Tel: 01638 723555 ♦ Fax: 01638 724043 ♦ Email: bookshop@evj.co.uk ♦ www.beva.org.uk

RESEARCH ARTICLE

Microbiota is an essential element for mice to initiate a protective immunity against *Vaccinia virus*

Maurício T. Lima[†], Ana C. S. P. Andrade[†], Grazielle P. Oliveira, Rafael S. Calixto, Danilo B. Oliveira, Éricka L. S. Souza, Giliane S. Trindade, Jacques R. Nicoli, Erna G. Kroon, Flaviano S. Martins and Jônatas S. Abrahão*

Department of Microbiology, Universidade Federal de Minas Gerais, Brazil Belo Horizonte, MG, Brazil

*Corresponding author: Universidade Federal de Minas Gerais, Instituto de Ciências Biológicas, Laboratório de Vírus, Avenida Antônio Carlos, 6627, Caixa Postal 486, Bloco F4, Sala 258, 31270-901 Belo Horizonte, Minas Gerais, Brazil. Tel: + 55 31 3409 2539; E-mail: jonatas.abrahao@gmail.com

[†]These authors contributed equally to this work.

One sentence summary: The microbiota is essential for the effective immune response of mice against *Vaccinia virus* in intranasal inoculation and to control the virus at the primary site of infection.

Editor: Julian Marchesi

ABSTRACT

The gastrointestinal tract of vertebrates harbors one of the most complex ecosystems known in microbial ecology and this indigenous microbiota almost always has a profound influence on host–parasite relationships, which can enhance or reduce the pathology of the infection. In this context, the impact of the microbiota during the infection of several viral groups remains poorly studied, including the family *Poxviridae*. *Vaccinia virus* (VACV) is a member of this family and is the causative agent of bovine vaccinia, responsible for outbreaks that affect bovines and humans. To determine the influence of the microbiota in the development of the disease caused by VACV, a comparative study using a murine model was performed. Germ-free and conventional, 6- to 7-week-old Swiss NIH mice were infected by tail scarification and intranasally with VACV. Moreover, immunosuppression and microbiota reposition were performed, to establish the interactions among the host's immune system, microbiota and VACV. The data demonstrate that the microbiota is essential for the effective immune response of mice against VACV in intranasal inoculation and to control the virus at the primary site of infection. Furthermore, this study is the first to show that Swiss conventional mice are refractory to the intranasal infection of VACV.

Keywords: microbiota; *Vaccinia virus*; virus–microbiota interactions; germ-free mice

INTRODUCTION

The human gastrointestinal tract harbors one of the most complex ecosystems known in microbial ecology, with bacterial populations reaching 10^{10} – 10^{12} viable cells per gram of contents in its lower portions. In healthy hosts, the presence of this microbiota has a very large impact on various aspects of function and metabolism, such as metabolic rate, gastrointestinal function, specific and quantitative aspects of immune function, and the many aspects of biochemical homeostasis. Only the predomi-

nant species have population levels that are sufficient to be considered responsible for the three main functions of the intestinal microbiota that are particularly important for host health: (i) colonization resistance, (ii) immunomodulation, and (iii) a nutritional contribution to the host (Sekirov et al. 2010; Conlon and Bird 2014; Marietta et al. 2015).

Currently available data also indicate that this indigenous microbiota almost always has a profound influence on host–parasite relationships during bacterial and protozoan infections (Stecher and Hardt 2008). As examples, it is well known that

the presence of the indigenous microbiota is essential for the pathogenicity of some protozoa and helminthes (Phillips and Wolfe 1959; Wescott and Todd 1964; Wescott 1968; Przyjalkowski and Wescott 1969; Visco and Barnes 1972; Johnson and Reid 1973; Owen 1975; Rutter and Beer 1975; Gouet et al. 1984; Vieira et al. 1987; Torres et al. 2000). In contrast, the microbiota can reduce the pathological consequences of other infectious diseases, as described for experimental infections with protozoa, fungi and helminthes (Salkowski et al. 1987; Silva et al. 1987; Martins et al. 2000) and almost all enteropathogenic bacteria (Wilson 1995). There are very few cases where the indigenous microbiota has no influence on the course of an infectious disease (Reide and Botero 1967; Harleman and Meyer 1984).

The interrelationships between virus, indigenous microbiota and the host immune system show differences in relation to those observed with bacteria and protozoa (Wilks et al. 2013). Where viruses come into contact with the local microbiota at the beginning of their infectious processes on the host mucosal surfaces, these microbial communities can modulate the viral infection. However, information concerning the influence of the indigenous microbiota on viral infections is scarce. Viruses and commensal bacteria have co-evolved and some viruses are dependent on the presence of the microbiota or its products. For example, the host's microbiota facilitates viral replication and pathogenesis in poliovirus (*Enterovirus C*), *Murine leukemia virus* and *Mouse mammary tumor virus* infections. (Kouttab and Jutila 1972; Isaak, Bartizal and Caulfield 1988; Kane et al. 2011; Kuss et al. 2011). Conversely, as described above for pathogenic bacteria, fungi and protozoa, the microbiota can play a protective role against viral replication and virally induced disease, as observed for the influenza virus (Ichinohe et al. 2011; Abt et al. 2012). Additionally, *Murine norovirus*, a common murine enteric virus, can replace the maturing function of commensal bacteria when introduced into germ-free (GF) mice, reverting intestinal morphology and lymphocyte function to phenotypes similar to those observed in conventional (CV) animals (Kernbauer, Ding and Cadwell 2014). These data exemplify the different relationships between the host microbiota and diverse viral clades. The study of the interaction between viruses, microbiota and the host immunity system is an important field of research, which might lead to the discovery of improved treatments and the prevention of infectious diseases. Nevertheless, the impact of the microbiota on infection by several viral groups, such as the *Poxviridae* family, remains unknown.

Smallpox is a severe infectious disease caused by the *Variola virus* (VARV), a member of the *Orthopoxvirus* (OPV) genus (Fenner et al. 1988; Damon 2013). Considering only the 18th century, smallpox caused the death of more than 400 000 people annually in Europe. This highly lethal and contagious disease was declared to have been eradicated in 1980, after an intensive vaccination campaign promoted by the World Health Organization (WHO) (Fenner et al. 1988). *Vaccinia virus* (VACV), a virus closely related to VARV that also belongs to the OPV genus and can induce serological cross-reactivity against other OPV members, was used in the WHO campaign (Fenner et al. 1988; Damon 2013). Currently, species of the OPV genus have a great impact on human and veterinary health, due to emerging and re-emerging zoonotic agents around the world, such as *Cowpox virus* (Kalthoff et al. 2014) in Europe, *Monkeypox virus* primarily in Africa (Reynolds, Carroll and Karem 2012), and VACV in Asia and South America (Trindade et al. 2003; Singh et al. 2007; Franco-Luiz et al. 2014; Kroon et al. 2011).

Vaccinia virus is the causative agent of bovine vaccinia (BV), which is responsible for outbreaks that primarily affect bovines

and humans and cause economic losses and public health problems. This exanthematous disease starts with erythema, which evolves to vesicles, papules and pustules, and finally forms scabs. In cattle, these lesions occur primarily on the teats of cows and on the nose and mouth of calves (Trindade et al. 2003; Kroon et al. 2011). In humans, VACV infection is characterized by the development of skin lesions, principally on the hands, and systemic signs include headache, myalgia, fever and lymphadenopathy (Trindade et al. 2003; Kroon et al. 2011; Damon 2013). Virulence studies in a murine model using Balb/c showed the existence of two distinct populations of Brazilian VACV; one group caused disease and death, but the other did not cause any clinical symptoms or death in infected mice (Ferreira et al. 2008).

Despite the eradication of smallpox, bioterrorism and the emergence of OPVs are concerns for the population worldwide. Given the social and economic impact of the diseases caused by OPV viruses and the unknown relationships between the host microbiota and these pathogens, we evaluated the importance of the host's microbiota in VACV infection.

MATERIALS AND METHODS

Cells and viruses

African green monkey kidney BSC-40 (ATCC-CRL-2761) and Vero cells (ATCC-CCL-81) were maintained in a 5% CO₂ atmosphere at 37°C in Eagle's minimum essential medium (MEM) (Gibco BRL, Invitrogen, Carlsbad, CA, USA) supplemented with 5% fetal bovine serum (Cultilab, Brazil), 25 µg/mL fungizone (Amphotericin B) (Cristália, São Paulo, Brazil), 500 U/mL penicillin (Cristália) and 50 µg/mL gentamicin (Schering-Plough, São Paulo, Brazil). Vero cells were used for viral replication. The BSC-40 cells were used for titration assays. The VACV Western Reserve (VACV-WR) virus was kindly provided by Dr C. Jungwirth (Universität Würzburg, Würzburg, Germany) and was used for mice assays. The virus was purified on a sucrose gradient as described elsewhere (Joklik 1962).

Animal assays

Ethical aspects

The present study was approved by the Animal Ethics Committee (Comitê de Ética no Uso Animal; CEUA), of the Universidade Federal de Minas Gerais (UFMG), Brazil, protocol number 207/2011.

Germ-free and conventional mice

Six-week-old germ-free (GF) NIH Swiss mice were obtained from Taconic Farms (Germantown, NY, USA) and were maintained in flexible plastic isolators (Standard Safety Equipment, McHenry, MD, USA) using classical gnotobiology techniques (Pleasant 1974). Conventional (CV) NIH Swiss mice are derived from GF matrices and are considered to be CV only two generations after conventionalization. Water and a commercial autoclavable diet (Nuvilab, Nuvital, Curitiba, PR, Brazil) were sterilized by steam and administered *ad libitum*. For experiments, animals were maintained in micro-isolators (UNO Roestvaststaal, The Netherlands) located in a ventilated animal caging system (Alesco Ltd, Campinas, SP, Brazil) with controlled lighting (12 h light–12 h dark), humidity (60–80%) and temperature (22 ± 1°C).

Immunosuppression

For immunosuppression experiments, dexamethasone (Decadron, ACHÉ Laboratorios LTDA, Guarulhos, SP, Brazil)

was administered intraperitoneally (i.p.) at a dose of 10 mg/kg/day, for 15 days in CV mice.

Conventionalization

Conventionalization was performed both by intragastric inoculation of diluted feces from CV donors (Day 0) and co-housing with CV mice for 21 days, as previously described (Pleasant 1974). Conventionalized (CVZ) animals were maintained in the same conditions as described above. After 21 days, CVZ animals were submitted to intranasal VACV infection or phosphate-buffered saline (PBS) inoculation, as described below. To assess whether microbiota colonization had occurred, a thioglycollate test was performed on feces from CVZ mice.

VACV infection by intranasal inoculation

The mice of all groups were anesthetized by i.p. injection of ketamine and xylazine (3.2 mg and 0.16 mg per mouse, respectively, in 0.9% PBS) before the procedure (dose: 80–120 mg/kg). The mice were inoculated intranasally with 10 μ L of viral suspension containing 10⁶ plaque-forming units (pfu) of VACV and the negative control group was inoculated with 10 μ L of PBS as previously described (Ferreira et al. 2008). Mice were weighed daily, and other clinical signs were recorded for 10 days post-infection (p.i.). Mice were sacrificed on Day 10 p.i.

VACV infection by tail scarification

Mice were anesthetized as described above, and 10 scarifications were made with a 26 G syringe, 1 cm from the base of the tail, avoiding bleeding, as previously described (Melamed et al. 2007). Then, 10 μ L of PBS containing 10⁶ pfu VACV was spotted onto the area; PBS was inoculated in the same way for the control group after scarification.

Bronchoalveolar lavage

For bronchoalveolar lavage (BAL), mice were sacrificed with an overdose of ketamine–xylazine solution. Subsequently, a 1.7 mm catheter was inserted into the trachea and 1 mL PBS was inserted into the lungs and then re-aspired three times.

Tissue collection and processing, and viral titration

On Day 10 after VACV infection, three mice per group (GF, CV, CVZ) were sacrificed, and the spleen, lungs, ileum and blood were collected in pre-weighed 2.0-mL tubes (Axygen, USA). The tubes were weighed again to determine tissue weight and were then frozen at -80°C . On the day of processing, the tissues were thawed and macerated in MEM (Gibco, USA) and centrifuged at 20 000 g for 3 min, at 4°C . Supernatant fluids from macerated organs were collected and the virus titer (pfu/g) was determined by a plaque-forming assay in BSC-40 (Campos and Kroon 1993).

Plaque reduction neutralization test

For the plaque reduction neutralization test (PRNT), serum samples were heat-inactivated at 56°C for 30 min, serially diluted in a 1:20 ratio in MEM and incubated at 37°C for 16 h with the same volume of MEM containing 150 pfu of VACV-WR. At the same time, the viral suspension was also incubated with a 1:20 dilution of MEM to serve as a virus control. Following this, 400 μ L of this mixture was added to BSC-40 cells seeded in six-well plates, which were incubated for 1 h at 37°C and 5% CO_2 atmosphere. Then, 2 mL of the medium was added to each well and it was further incubated in the same conditions for 48 h. The cells were then stained with a solution of crystal violet for 20 min and

the viral plaques were counted. The results are expressed as the highest serum dilution that was able to neutralize at least 50% of viral plaques (PRNT₅₀).

Molecular assays

The BAL was tested using an OPV-specific PCR reaction that amplified the C11R gene, which encodes the viral growth factor (*vgf*). The PCR conditions were 94°C for 10 min, 30 cycles of 94°C for 30 s, 50°C for 30 s and 72°C for 30 s, followed by 72°C for 10 min.

Statistical analysis

All results were plotted using GraphPad Prism (GraphPad Software, La Jolla, CA, USA) and compared using Student's two-tailed t-test, one-way ANOVA, two-way ANOVA using the Bonferroni method and the Logrank test. In all tests, *P* values <0.05 were considered statistically significant.

RESULTS

Effect of microbiota determined by comparing CV and GF mice infected with VACV by intranasal inoculation

To determine the effect of the indigenous microbiota on VACV infection, CV mice and GF mice were infected with 10⁶ pfu of VACV via an intranasal route. These animals were monitored for 10 days p.i. to evaluate clinical symptoms and survival rates (Fig. 1). All GF animals presented clinical symptoms and 60% of the animals died on the eighth day p.i. (Fig. 1A). Initial clinical symptoms, such as periocular alopecia and closed inflamed eyes, appeared in all animals on Day 5 p.i. (Fig. 1E), followed by the ruffling of fur, an arched back and labored breathing on Day 7 p.i. The infection in these animals was associated with severe weight loss starting on the fifth day p.i. (Fig. 1B). No clinical symptoms or death was observed in CV or control mice. All animals were sacrificed on the 10th day p.i. and their organs were collected, to investigate viral tropisms. Viral infectious particles were detected only in the lungs and spleen from GF mice. In these organs, viral titers were approximately 10⁴ pfu/g (Fig. 1C and D). No viral infectious particles were detected in organs collected from CV and control mice (Fig. 1C and D). Blood was collected on the 10th day p.i. and sera were used to perform PRNT. Serum neutralizing activity was only detected in sera collected from the GF group (titers $>1/40$). Viral inoculation in CV animals was confirmed after viral DNA detection by qPCR performed in BAL collected from these animals (data not shown).

Effect of microbiota by comparing CV and GF mice infected with VACV by tail scarification

To investigate whether CV mice remained refractory by another route of infection, CV and GF mice were infected with 10⁶ pfu VACV by tail scarification. These animals were monitored 10 days p.i. to evaluate clinical symptoms, survival rates and lesions. All animals presented lesions at the inoculation site, but no systemic clinical symptoms such as fur ruffling, an arched back or periocular alopecia were observed (Fig. 2A and B). All mice survived to infection, and no significant difference in weight was observed between the analyzed groups (Fig. 2C). However, the lesions at the inoculation site showed differences in appearance and were more inflamed in CV than in GF mice on Day 10 p.i. No clinical signals or weight loss was observed in CV

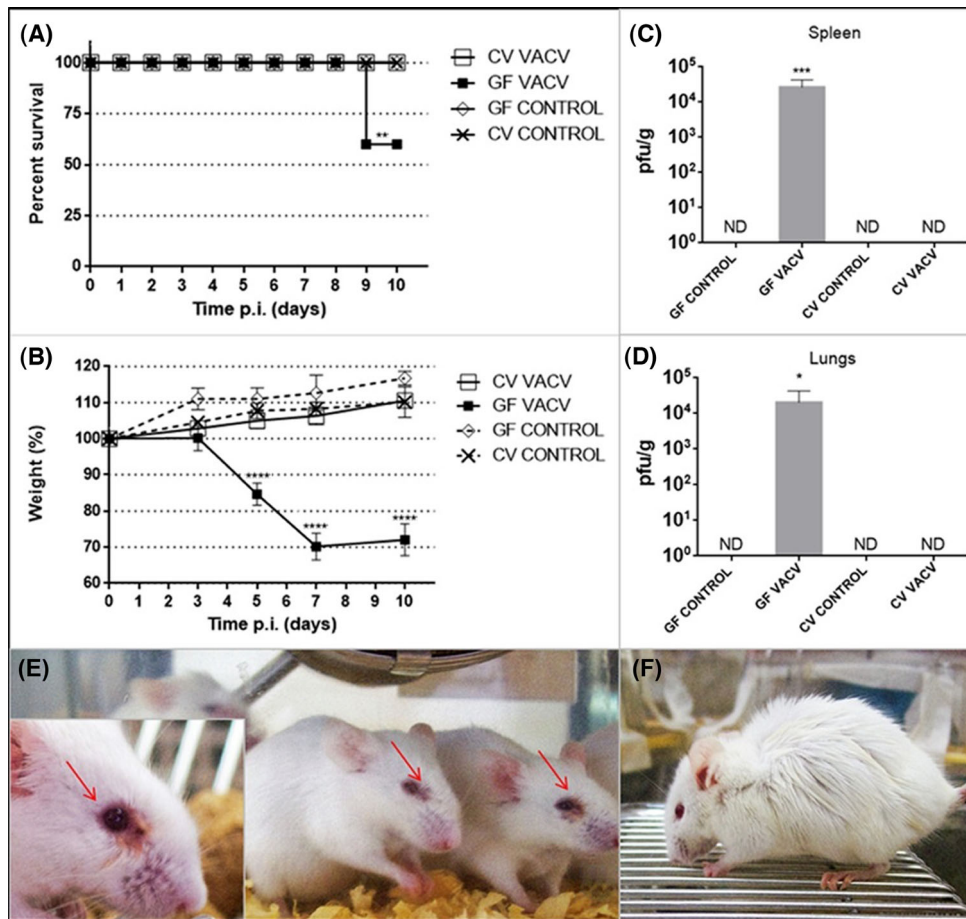


Figure 1. Intranasal infection of germ-free and conventional mice with Vaccinia virus. (A–D) Survival (A), relative mean weight (B) and viral titers in the spleen (C) and lungs (D) of the experimental and control groups ($n = 10$) of CV and GF mice inoculated with 10^6 pfu of VACV or PBS, respectively, via an intranasal route. The error bars indicate the standard deviations. For viral titers in lungs and spleens, organs ($n = 3$) were collected on Day 10 p.i. and were titrated. (E) Clinical aspects of mice on Day 5 p.i. (F) Facial edema and periocular alopecia (red arrows) were observed on Day 10 p.i., as well as fur ruffling and arching of the back. CV: conventional; GF: germ-free; ND: not detected; PBS: phosphate-buffered saline; VACV: Vaccinia virus. Asterisks indicate a statistically significant difference: * $P < 0.05$, ** $P < 0.01$, *** $P < 0.001$ and **** $P < 0.0001$.

or GF mice inoculated with PBS. The viral titers in lesions were similar for CV and GF groups 10 days p.i. ($\sim 10^6$ pfu/g) (Fig. 2D). Sera collected by Day 10 p.i. from CV and GF mice infected with VACV and submitted to PRNT were able to neutralize at least 50% of viral plaques (titers $> 1/40$).

Effect of immunosuppression on the resistance of CV mice to VACV infection

To evaluate the role of the immune system in the resistance of CV mice to VACV infection, 10 animals were submitted to immunosuppression by using dexamethasone (DEX) for 5 days at a dose of 10 mg/kg/d. An equal number of mice received PBS in the same period as a control group. After this treatment, animals were infected with 10^6 pfu of VACV and continued to receive the respective treatment with DEX and PBS until the end of the experiment. These mice were monitored for 10 days p.i. to evaluate clinical symptoms and survival rates (Fig. 3). Clinical symptoms such as fur ruffling, arching of the back and labored breathing were observed in all DEX-treated animals inoculated with VACV at 5 days p.i. (Fig. 3D). Two mice died on Day 8 p.i. and a severe weight loss was observed on Days 5 and 6 p.i. (Fig. 3A

and C). In contrast, no clinical symptoms were observed in the control groups. All animals were sacrificed on Day 10 p.i. and their organs were collected for viral tropism analysis. Viral infectious particles were detected in the lungs of all animals and in the spleen of two mice from the immunosuppressed group inoculated with VACV. In these lungs, viral titers were $\sim 10^4$ pfu/g (Fig. 3B), whereas in spleens, the titers ranged from 10^2 to 10^3 pfu/g. No viral infectious particles were detected in any of the organs from mice of the control groups.

Effect of conventionalization of GF mice on the susceptibility to VACV infection

To confirm the influence of the indigenous microbiota on the susceptibility to VACV infection, GF mice were conventionalized both by intragastric inoculation of diluted feces of CV donors (Day 0) and by co-housing with CV mice for 21 days, with the aim of acquiring the skin and mucosal microbiota. The CVZ mice were then infected with 10^6 pfu VACV via an intranasal route. These mice were monitored for an additional 10 days p.i. to evaluate clinical signs and survival rates (Fig. 4). All animals inoculated with VACV presented clinical symptoms, but as

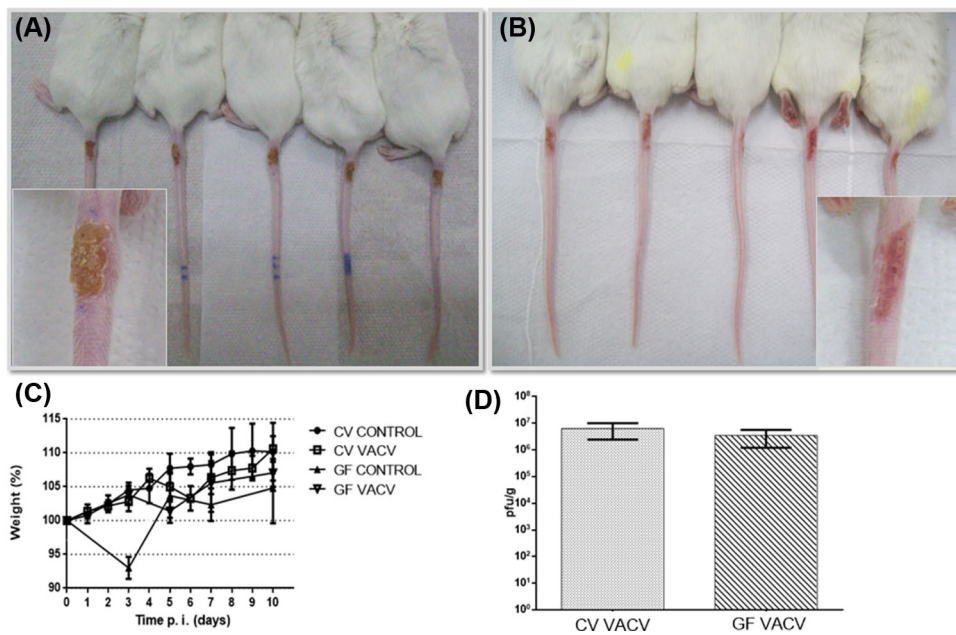


Figure 2. Tail scarification infection of germ-free and conventional mice with *Vaccinia virus*. Clinical aspects of CV (A) and GF (B) mice, relative mean weights (C) and viral titers in lesions (D) on Day 10 p.i. of CV and GF mouse groups ($n = 5$) inoculated with 10^6 pfu of VACV or PBS, respectively, by tail scarification. For viral titers in lesions, samples ($n = 5$) were collected on Day 10 p.i. and were titrated. CV: conventional; GF: germ-free; PBS: phosphate-buffered saline; VACV: *Vaccinia virus*. There were no significant differences in (C) and (D).

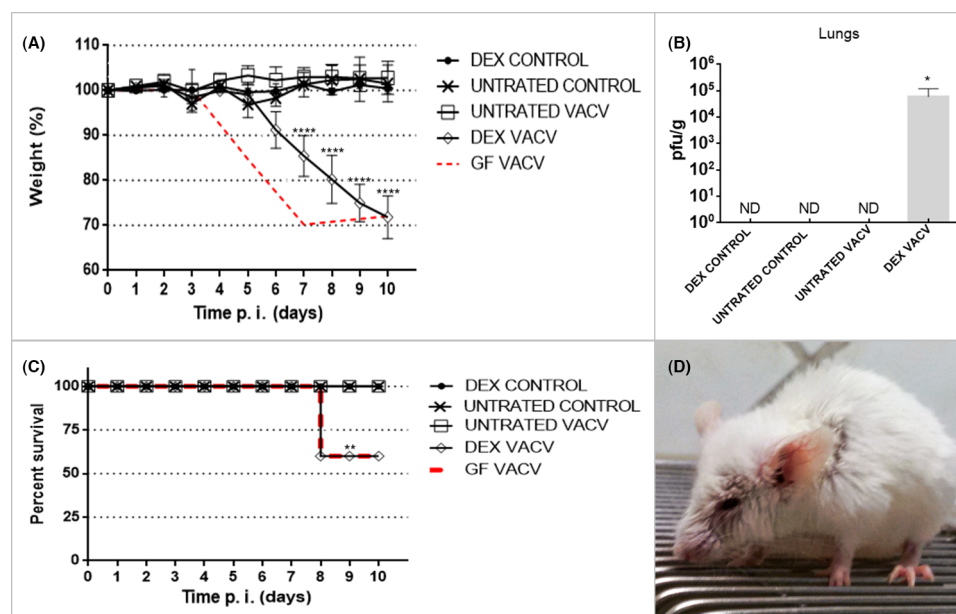


Figure 3. Intranasal infection of conventional immunosuppressed mice with *Vaccinia virus*. Relative mean weights (A), survival (B), viral titers in lungs (C) and clinical aspects (D) of experimental and control groups ($n = 5-10$) of CV immunosuppressed mice inoculated with 10^6 pfu of VACV or PBS, respectively, via an intranasal route. Mice were immunosuppressed by daily dexamethasone administration for 15 days. The control group was treated with PBS. For viral titers in lungs, organs ($n = 5$) were collected on Day 10 p.i. and were titrated. In red, data from Fig. 1 for GF mice intranasally infected with VACV are shown. Asterisks indicate a statistically significant difference: * $P < 0.05$, ** $P < 0.01$ and **** $P < 0.0001$. CV: conventional; DEX: dexamethasone; GF: germ-free; PBS: phosphate-buffered saline; VACV: *Vaccinia virus*.

expected, the lethality rate was lower in CVZ (12.5%) than GF mice (40%). All animals were sacrificed on Day 10 p.i. and their organs were collected for viral tropism analysis. Viral particles were detected in lungs from only two CVZ mice (ranging from 10^2 to 10^3 pfu/g), whereas all GF animals contained $\sim 10^4$ pfu/g VACV in their lungs. No viral infectious particles were detected in the organs of animals from the control group.

DISCUSSION

Previous studies have established varied interactions between the host's immune system, microbiota and viruses (Wilks et al. 2013). Similar to pathogenic bacteria and protozoa, the microbiota can potentially facilitate or hinder viral infections (Wilks et al. 2013), and each different virus studied to date shows diverse interactions with the host microbiota (Kouttab and Jutila

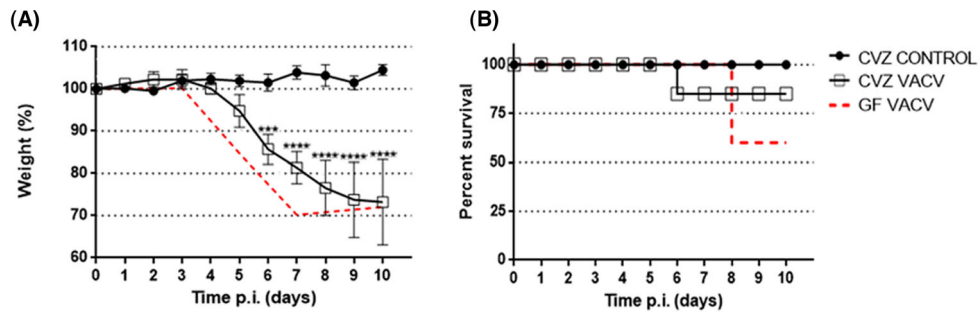


Figure 4. Intranasal infection of conventionalized mice with Vaccinia virus. Relative mean weights (A) and survival (B) of experimental and control groups ($n = 5-10$) of CVZ mice inoculated with 10^6 pfu of VACV-WR or PBS, respectively, via an intranasal route. In red, data from Fig. 1 for GF mice intranasally infected with VACV are shown. CVZ: conventionalized; GF: germ-free; PBS: phosphate-buffered saline; VACV: Vaccinia virus. Asterisks indicate a statistically significant difference: *** $P < 0.001$ and **** $P < 0.0001$. There were no significant differences in the survival curves in (B).

1972; Isaak, Bartizal and Caulfield 1988; Kane et al. 2011; Kuss et al. 2011; Ichinohe et al. 2011; Abt et al. 2012; Wilks and Golovkina 2012; Wilks et al. 2013; Kernbauer, Ding and Cadwell 2014). However, such correlations between commensal bacteria and many viral families such as the *Poxviridae* remain unknown. For this reason, the effect of the indigenous microbiota on VACV infection in this study was evaluated by using and comparing CV and GF mouse models. Additionally, the influence of two different routes of VACV administration (intranasal inoculation and tail scarification) was evaluated, bearing in mind that the intranasal route is considered the primary route of smallpox transmission in humans and the secondary route of transmission for monkeypox (Damon 2013). It has been already described that the intranasal inoculation of VACV causes systemic infections and lethality, which vary according to the dose and mouse lineage (Turner 1967; Hayasaka, Ennis and Terajima 2007; Ferreira et al. 2008). In this study, CV NIH Swiss mice were totally resistant to VACV administration, whereas this viral infection has been demonstrated to be lethal for Balb/c mice in another report (Turner 1967). No clinical signals or viral titers were observed in organs of these mice. On the other hand, all GF mice displayed expressive clinical symptoms and only 60% survived. Moreover, high viral titers were found in the lungs and spleen (10^4 pfu/g) of these animals. These results suggest an influence of the indigenous microbiota on VACV infection in NIH Swiss mice. Although NIH Swiss is not the standard breed used for OPV infections, this refractory model made clear the differences caused by absence of the microbiota. This role of the microbiota on the susceptibility of mice to VACV infection might occur by direct interactions between components of the microbiota and the virus or by an indirect effect via the immune system; indeed, it is well known that GF animals have immature secondary lymphoid tissues (Wilks et al. 2013). The intestinal mucosa of GF animals is characterized by fewer intra-epithelial lymphocytes (IELs) and lamina propria lymphocytes. Furthermore, Peyer's patches are less developed and lack a fully developed germinal center. The indigenous microbiota has also been shown to influence the development of $CD4^+CD8^+\alpha^+$ IELs by an extra-thymic pathway. Moreover, both α - β and γ - δ IELs from GF mice showed a lower proliferation rate than that of CV animals (Kamada and Núñez 2014).

Since CV and GF mice exhibited a different response via the intranasal route, tail scarification was used to evaluate the effects of VACV infection by another route. Infection via tail scarification in mice provides a useful model of VACV inoculation,

since it simulates the immunological and virological parameters of human smallpox vaccination (Melamed et al. 2007; Mota et al. 2011). In the present study, the cutaneous lesions showed differences in appearance and inflammation level between GF and CV mice, which can be associated with a microbiota-dependent regulation of inflammatory responses (Souza et al. 2004). However, PRNT and viral titers in the lesions showed similarities between GF and CV mice. Furthermore, these results showed that contrary to intranasal inoculation, CV mice are not refractory to VACV infection through the tail scarification route.

To confirm the importance of the immune system in the NIH Swiss murine strain infected by VACV, CV animals were immunosuppressed using daily DEX doses. In these animals, the clinical symptoms, lethality rate and viral titers in the lungs were similar to those observed in GF mice, even if the spleen presented slightly lower viral titers (10^2 pfu/g and 10^3 pfu/g) than those of GF mice. However, considerable DEX-induced changes in lymphocytes from the spleen might explain this variation (Ahmed and Sriranganathan 1994). These results demonstrate a similarity between the immature and the suppressed immunological systems of GF and DEX-treated murine models, respectively, and reinforce the indirect influence of the indigenous microbiota on VACV infection in Swiss NIH animals.

To determine whether conventionalization of GF mice could restore resistance to VACV, probably by maturing the immune response, CVZ animals were intranasally inoculated with VACV. The CVZ animals showed a lower lethality rate (12.5%) than GF mice infected with VACV, but all showed clinical symptoms, with substantial variations among the infected animals in the group. This might be due to an incorrect maturation of the immune system due to a conventionalization that occurred at an adult stage instead of soon after birth, as occurs naturally. The results obtained from GF mice conventionalized in adulthood showed failures in immune maturation compared with animals colonized at birth. Therefore, a time window exists (soon after delivery) for an effective immune modulator effect due to microbiota colonization (El Aidy et al. 2013).

In conclusion, data from the present study demonstrate that the microbiota is essential to mice to instigate an effective immune response against VACV in a model of systemic infection (intranasal). This response includes controlling the virus at the initial site of infection (lung) and the generation of an immune memory. These results raise new questions concerning how variations in the microbiota between individuals or during episodes of dysbiosis might influence OPV infections.

ACKNOWLEDGEMENTS

This work was supported by the grants Pró-Reitoria de Pesquisa da Universidade Federal de Minas Gerais (PRPq-UFGM) and by the support agencies Conselho Nacional de Desenvolvimento Científico e Tecnológico (CNPq), Coordenação de Aperfeiçoamento de Pessoal de Nível Superior (CAPES) and Fundação de Amparo à Pesquisa do estado de Minas Gerais (FAPEMIG).

Conflict of interest. None declared.

REFERENCES

- Abt MC, Osborne LC, Monticelli LA et al. Commensal bacteria calibrate the activation threshold of innate antiviral immunity. *Immunity* 2012;**37**:158–70.
- Ahmed SA, Sriranganathan N. Differential effects of dexamethasone on the thymus and spleen: alterations in programmed cell death, lymphocyte subsets and activation of T cells. *Immunopharmacology* 1994;**28**:55–66.
- Campos MAS, Kroon EG. Critical period for irreversible block of Vaccinia virus replication. *Rev Microbiol* 1993;**24**:104–10.
- Conlon MA, Bird AR. The impact of diet and lifestyle on gut microbiota and human health. *Nutrients* 2014;**7**:17–44.
- Damon I. Poxviridae and their replication. *Fields Virology* 2013;**6**:2160–84.
- de Souza Trindade G, da Fonseca FG, Marques JT et al. Araçatuba virus: a vaccinia like virus associated with infection in humans and cattle. *Emerg Infect Dis* 2003;**9**:155–60.
- El Aidy S, Hooiveld G, Tremaroli V et al. The gut microbiota and mucosal homeostasis: colonized at birth or at adulthood, does it matter? *Gut Microbes* 2013;**4**:118–24.
- Fenner F, Henderson DA, Arita I et al. *Smallpox and its Eradication*. Geneva: World Health Organization Press, 1988.
- Ferreira JM, Drumond BP, Guedes MI et al. Virulence in murine model shows the existence of two distinct populations of Brazilian Vaccinia virus strains. *PLoS One* 2008;**3**:e3043.
- Franco-Luiz AP, Fagundes-Pereira A, Costa GB et al. Spread of vaccinia virus to cattle herds, Argentina, 2011. *Emerg Infect Dis* 2014;**20**:1576–8.
- Gouet P, Yvone P, Naciri M et al. Influence of digestive microflora on parasite development and the pathogenic effect of *Eimeria ovinoidalis* in the axenic, gnotoxenic and conventional lamb. *Res Vet Sci* 1984;**36**:21–3.
- Harleman JH, Meyer RC. Life cycle of *Isospora suis* in gnotobiotic and conventionalized piglets. *Vet Parasitol* 1984;**17**:27–39.
- Hayasaka D, Ennis FA, Terajima M. Pathogenesis of respiratory infections with virulent and attenuated vaccinia viruses. *Virology* 2007;**4**:22.
- Ichinohe T, Pang IK, Kumamoto Y et al. Microbiota regulates immune defense against respiratory tract influenza A virus infection. *Proc Natl Acad Sci U S A* 2011;**108**:5354–9.
- Isaak DD, Bartizal KF, Caulfield MJ. Decreased pathogenicity of murine leukemia virus-Moloney in gnotobiotic mice. *Leukemia* 1988;**2**:540–4.
- Johnson J, Reid WM. *Ascaridia galli* (Nematoda): development and survival in gnotobiotic chickens. *Exp Parasitol* 1973;**33**:95–9.
- Joklik WK. The purification of four strains of poxvirus. *Virology* 1962;**18**:9–18.
- Kalthoff D, Bock WI, Hühn F et al. Fatal cowpox virus infection in cotton-top tamarins (*Saguinus oedipus*) in Germany. *Vector Borne Zoonotic Dis* 2014;**14**:303–5.
- Kamada N, Núñez G. Regulation of the immune system by the resident intestinal bacteria. *Gastroenterology* 2014;**146**:1477–88.
- Kane M, Case LK, Kopaskie K et al. Successful transmission of a retrovirus depends on the commensal microbiota. *Science* 2011;**334**:245–9.
- Kernbauer E, Ding Y, Cadwell K. An enteric virus can replace the beneficial function of commensal bacteria. *Nature* 2014;**516**:94–8.
- Kouttab NM, Jutila JW. Friend leukemia virus infection in germfree mice following antigen stimulation. *J Immunol* 1972;**108**:591–5.
- Kroon EG, Mota BE, Abrahão JS et al. Zoonotic Brazilian Vaccinia virus: from field to therapy. *Antiviral Res* 2011;**92**:150–63.
- Kuss SK, Best GT, Etheredge CA et al. Intestinal microbiota promote enteric virus replication and systemic pathogenesis. *Science* 2011;**334**:249–52.
- Marietta E, Rishi A, Taneja V. Immunogenetic control of the intestinal microbiota. *Immunology* 2015;**145**:313–22.
- Martins WA, Melo AL, Nicoli JR et al. A method of decontaminating *Strongyloides venezuelensis* larvae for the study of strongyloidiasis in germ-free and conventional mice. *J Med Microbiol* 2000;**49**:387–90.
- Melamed S, Sharon M, Paran N et al. Tail scarification with Vaccinia virus Lister as a model for evaluation of smallpox vaccine potency in mice. *Vaccine* 2007;**25**:7743–53.
- Mota BE, Gallardo-Romero N, Trindade G et al. Adverse events post smallpox-vaccination: insights from tail scarification infection in mice with Vaccinia virus. *PLoS One* 2011;**6**:e18924.
- Owen D. *Eimeria falciformis* (Eimer, 1870) in specific pathogen free and gnotobiotic mice. *Parasitology* 1975;**71**:293–303.
- Phillips BP, Wolfe PA. The use of germfree guinea pigs in studies on the microbial interrelationships in amoebiasis. *Ann N Y Acad Sci* 1959;**78**:308–14.
- Pleasant JR. Gnotobiotics. In Melby EC, Jr, Altman NH (eds). *Handbook of Laboratory Animal Science*, vol. I. Cleveland, OH: CRC Press 1974, 119–74.
- Przyjalkowski ZW, Wescott RB. *Trichinella spiralis*: establishment in gnotobiotic mice affected by *Bacillus mesentericus*, *B. subtilis*, and *Pseudomonas aeruginosa*. *Exp Parasitol* 1969;**25**:8–12.
- Reid WM, Botero H. Growth of the cestode *Raillietina cesticillus* in bacteria-free chickens. *Exp Parasitol* 1967;**21**:149–53.
- Reynolds MG, Carroll DS, Karem KL. Factors affecting the likelihood of monkeypox's emergence and spread in the post-smallpox era. *Curr Opin Virol* 2012;**2**:335–43.
- Rutter JM, Beer RJ. Synergism between *Trichuris suis* and the microbial flora of the large intestine causing dysentery in pigs. *Infect Immun* 1975;**11**:395–404.
- Salkowski CA, Bartizal KF, Balish MJ et al. Colonization and pathogenesis of *Cryptococcus neoformans* in gnotobiotic mice. *Infect Immun* 1987;**55**:2000–5.
- Sekirov I, Russell SL, Antunes LC et al. Gut microbiota in health and disease. *Physiol Rev* 2010;**90**:859–904.
- Silva ME, Evangelista EA, Nicoli JR et al. American trypanosomiasis (Chagas' disease) in conventional and germfree rats and mice. *Rev Inst Med Trop Sao Paulo* 1987;**29**:284–8.
- Singh RK, Hosamani M, Balamurugan V et al. Buffalopox: an emerging and re-emerging zoonosis. *Anim Health Res Rev* 2007;**8**:105–14.
- Souza DG, Vieira AT, Soares AC et al. The essential role of the intestinal microbiota in facilitating acute inflammatory responses. *J Immunol* 2004;**173**:4137–46.

- Stecher B, Hardt WD. The role of microbiota in infectious disease. *Trends Microbiol* 2008;**16**:107–14.
- Torres MF, Uetanabaro AP, Costa AF et al. Influence of bacteria from the duodenal microbiota of patients with symptomatic giardiasis on the pathogenicity of *Giardia duodenalis* in gnotoxenic mice. *J Med Microbiol* 2000;**49**:209–15.
- Turner GS. Respiratory infection of mice with vaccinia virus. *J Gen Virol* 1967;**1**:399–402.
- Vieira EC, Nicoli JR, Moraes-Santos T et al. Cutaneous leishmaniasis in germfree, gnotobiotic, and conventional mice. *Rev Inst Med Trop Sao Paulo* 1987;**29**:385–7.
- Visco RJ, Burns WC. *Eimeria tenella* in bacteria-free and conventionalized chicks. *J Parasitol* 1972;**58**:323–31.
- Wescott RB. Experimental *Nematospiroides dubius* infection in germfree and conventional mice. *Exp Parasitol* 1968;**22**:245–9.
- Wescott RB, Todd AC. A comparison of the development of *nippostrongylus brasiliensis* in germ-free and conventional mice. *J Parasitol* 1964;**50**:138–43.
- Wilks J, Beilinson H, Golovkina TV. Dual role of commensal bacteria in viral infections. *Immunol Rev* 2013;**255**:222–9.
- Wilks J, Golovkina T. Influence of microbiota on viral infections. *PLoS Pathog* 2012;**8**:e1002681.
- Wilson KH. Ecological concepts in the control of pathogens. In: Roth JA (ed.). *Virulence Mechanisms of Bacterial Pathogens*, Washington, DC: American Society for Microbiology 1995, 245–56.

Daily ingestion of the probiotic *Lactobacillus paracasei* ST11 decreases Vaccinia virus dissemination and lethality in a mouse model

A.C. dos Santos Pereira Andrade^{1#}, M. Teixeira Lima^{1#}, G. Pereira Oliveira¹, R. Silva Calixto¹, É. Loreнна de Sales e Souza¹, D. da Glória de Souza¹, C.M. de Almeida Leite², J.M. Siqueira Ferreira³, E.G. Kroon¹, D. Bretas de Oliveira¹, F. dos Santos Martins¹ and J.S. Abrahão^{1*}

¹Departamento de Microbiologia, Instituto de Ciências Biológicas, Universidade Federal de Minas Gerais, Av. Antônio Carlos 6627, 31270-901 Belo Horizonte, MG, Brazil; ²Departamento de Morfologia, Instituto de Ciências Biológicas, Universidade Federal de Minas Gerais, Av. Antônio Carlos 6627, 31270-901 Belo Horizonte, MG, Brazil; ³Laboratório de Microbiologia, Universidade Federal de São João del-Rei, Av. Sebastião Gonçalves Coelho 400, 35501-296 Divinópolis, MG, Brazil; jonatas.abrahao@gmail.com; #These authors contributed equally to this work

Received: 15 April 2016 / Accepted: 12 September 2016
© 2016 Wageningen Academic Publishers

RESEARCH ARTICLE

Abstract

Vaccinia virus (VACV) is an important pathogen. Although studies have shown relationships between probiotics and viruses, the effect of probiotics on VACV infection is unknown. Therefore, this work aims to investigate the probiotics effects on VACV infection. Mice were divided into four groups, two non-infected groups, one receiving the probiotic, the other one not receiving it, and two groups infected intranasally with VACV Western Reserve (VACV-WR) receiving or not receiving the probiotic. Viral titres in organs and cytokine production in the lungs were analysed. Lung samples were also subjected to histological analysis. The intake of probiotic results in reduction in viral spread with a significant decrease of VACV titer on lung, liver and brain of treated group. In addition, treatment with the probiotic results in attenuated mice lung inflammation showing fewer lesions on histological findings and decreased lethality in mice infected with VACV. The ingestion of *Lactobacillus paracasei* ST11 (LPST11) after VACV infection resulted in 2/9 animal lethality compared with 4/9 in the VACV group. This is the first study on probiotics and VACV interactions, providing not only information about this interaction, but also proposing a model for future studies involving probiotics and other poxvirus.

Keywords: probiotics, virus, inflammation, *Orthopoxvirus*

1. Introduction

The genus *Orthopoxvirus* (OPV) consists of important pathogens causing diseases including the smallpox, a severe infectious disease caused by Variola virus (Damon, 2013; ICTV, 2014). This highly contagious disease was the cause of death of more than 400,000 people annually in Europe, during the 18th century. Smallpox was declared eradicated in 1980 by World Health Organization (WHO), after global vaccination campaign (Fenner *et al.*, 1988). Despite smallpox eradication, other emerging and re-emerging zoonotic OPV are involved in outbreaks worldwide, such as *Monkeypox virus* in Africa (Reynolds *et al.*, 2012), *Cowpox virus* (Kalthoff *et al.*, 2014) in Europe and Vaccinia virus

(VACV) in South America and Asia (Franco-Luiz *et al.*, 2014; Kroon *et al.*, 2011; Singh *et al.*, 2007; Trindade *et al.*, 2003).

Bovine vaccinia (BV) is an exanthematous disease that starts with erythema, which evolves to vesicles, papules and pustules, and finally forms scabs. VACV affects commonly milking cows and dairy workers. In cattle, these lesions appear primarily on the teats of cows and on the nose and mouth of calves (Kroon *et al.*, 2011; Trindade *et al.*, 2003). In humans, the infection is characterised by the development of skin lesions, mainly on the hands, and systemic signs include fever, myalgia, headache, and lymphadenopathy (Damon, 2013; Kroon *et al.*, 2011; Trindade *et al.*, 2003). The

transmission also can occur by contact with contaminated fomites and by human-to-human transmission (Damon, 2013; Oliveira *et al.*, 2014). VACV infection has also been detected in a wide host range besides cattle and humans, such as rodents, horses and monkeys (Abrahão *et al.*, 2009, 2010, in press; Campos *et al.*, 2011). BV presents public health impacts and cause economical losses (Kroon *et al.*, 2011).

Despite the impact of these outbreaks in public health and economy, few therapeutic options are commercially available for the treatment of OPV infections (Kroon *et al.*, 2011). In recent years, probiotics have been proposed as a new therapeutic approach to viral disease control. Probiotics are defined as live microorganisms that promote a health benefit on the host (FAO/WHO, 2002). Manifold studies both *in vitro* and *in vivo* demonstrated that several strains of probiotics showing notorious protection against viral infections (Galán *et al.*, 2016; Hori *et al.*, 2001; Tomosada *et al.*, 2013). Several mechanisms of antiviral responses promoted by probiotics remain inaccurately. Possibly, these mechanisms may include hinder the adsorption and cell internalisation of the virus as well as the production of metabolites with a direct antiviral effect and also the immunomodulation of host (Lehtoranta *et al.*, 2014).

Among the probiotic microorganisms that exhibit antiviral activity, species belonging to the genus *Lactobacillus* are of particular interest (Kassaa *et al.*, 2014). The probiotic *Lactobacillus paracasei* ST11 (LPST11) was selected on the basis of its industrial properties yield, stability, safety and its immunomodulation profile, both *in vitro* and *in vivo*. LPST11 showed anti-inflammatory properties in previous studies (Guéniche *et al.*, 2010; Oliveira *et al.*, 2011) and considering that many symptoms generated during infection with VACV result from a systemic inflammatory response (Damon, 2013). Given the social and economic impact of the zoonosis caused by VACV and the unknown effects of probiotic therapy to VACV infection control, we evaluated the effects of LPST11 on VACV infection mice model.

2. Materials and methods

Cells and viruses

African green monkey kidney BSC-40 (ATCC-CRL-2761) and Vero cells (ATCC-CCL-81) were maintained in a 5% CO₂ atmosphere at 37 °C in Eagle's minimum essential medium (MEM) (Gibco BRL, Invitrogen, Carlsbad, CA, USA) supplemented with 5% foetal bovine serum (Cultilab, Campinas, Brazil), 25 µg/ml fungizone (Amphotericin B) (Cristalia, São Paulo, Brazil), 500 U/ml penicillin (Cristalia) and 50 µg/ml gentamicin (Schering-Plough, São Paulo, Brazil). Verocells were used for viral replication. The BSC-40 cells were used for titration assays. The VACV-WR virus was kindly provided by Dr C. Jungwirth (Universität Würzburg, Würzburg, Germany) and was used for mice

assays. The virus was purified on a sucrose gradient as described elsewhere (Joklik, 1962).

Animal assays

The present study was approved by the Animal Ethics Committee ('Comitê de Ética no Uso Animal', CEUA), of Universidade Federal de Minas Gerais (UFMG), Brazil, protocol number 207/2011. Seven-weeks male Balb/C mice previously dewormed were intranasally infected with 10⁶ plaque forming units (pfu) of VACV-WR as previously described (Ferreira *et al.*, 2008) and at the same day of infection, daily inoculation with LPST11 by gavage feeding was started. Mice were randomly separated into four groups which received phosphate buffered saline 0.9% (PBS) (Group PBS) (n=8); 10⁸ cfu live probiotic (Group LPST11) (n=9); PBS before and after infection (Group VACV) (n=9); and 10⁸ cfu of live probiotic following infection (Group LPST11-VACV) (n=9). The PBS and LPST11 groups were non-infected groups inoculated with PBS only. Mice were weighed daily, and clinical signs were recorded for nine days post infection (dpi).

Survival tests

Two survival assays were performed. In the first, five mice were used per group and in the second, three were used for PBS group and four animals for the remaining groups.

Tissue collection and processing, and viral titration

On day 9 after VACV infection, the mice were sacrificed, and the lungs, liver and brain were collected in pre-weighed 2.0-ml tubes (Axygen, Union City, CA, USA). The tubes were weighed again to determine tissue weight and were then frozen at -80 °C. On the day of processing, the tissues were thawed and macerated in MEM (Gibco, Waltham, MA, USA) and centrifuged at 20,000×g for 3 min, at 4 °C. Supernatant fluids from macerated organs were collected and the virus titer (pfu/g) was determined by a plaque-forming assay in BSC-40 (Campos and Kroon, 1993).

Cytokines analyses

Cytokines, including tumour necrosis factor alpha (TNF-α), interleukin 17 (IL-17) and interferon (IFN)-γ, were measured in the lungs (n=4) at 9 dpi using commercially available Enzyme-Linked Immunosorbent Assay (ELISA) assays, in accordance with the manufacturer's instructions (R&D Systems, Minneapolis, MN, USA). The expression of IFN-α₂, IFN-β, IFN-λ_{2/3} and interferon stimulated genes (ISGs), protein kinase RNA-activated (PKR) and 2'-5'-oligoadenylate synthetase 1 (OAS1a) in the lungs (n=3) were measured by quantitative PCR (qPCR). RNA was extracted using the RNeasy kit (Qiagen, Hilden, Germany) according to the manufacturer's recommendations. qPCR reactions were

performed as previously described (Barbosa *et al.*, 2014), whereby SYBR Green Master Mix (Applied Biosystems, Santa Clara, CA, USA), primers described in Table 1, and a Step One apparatus (100 Applied Biosystems) were used. Results were analysed based on the delta CT (cycle threshold) method, as previously described (Livak and Schmittgen, 2001). For histological analysis, mouse lungs collected (n=3) on 9 dpi were fixed and paraffin embedded.

Histological analyses

Histological sections (4 μ m) were stained with haematoxylin and eosin (HE), examined, and classified according to lesion extent and severity as mild, moderate, or severe as previously described (Duniho *et al.*, 2002).

Table 1. Primers used for qRT-PCR.

Oligonucleotides	Sequence forward	Sequence reverse	References
Beta actin	AAATCGTGCGTGACATCAAAGA	GCCATCTCCTGCTCGAAGTC	This work
IFN/ α 2	GGACAGGCAGGACTTTGGATT	GCCTTCTGGATCTGCTGGTTA	This work
IFN/ β	ACACCAGCCTGGCTTCCATCA	AGGGCTGTCGTGGTGGAGAAGCAC	Barbosa <i>et al.</i> , 2014
IFN/ λ 2/3	ACCCTGAAGGTCTGGGAGAAC	AAGAGCTGGCCAGGAT	Barbosa <i>et al.</i> , 2014
OAS1a	CCACACTCAAGGGCAAGTCA	CAAAGCTGGTGAATTGTTAAGA	This work
PKR	CCTCCTCAGTCTCCGAACA	TGCTCGCTGGCAATCTCA	This work

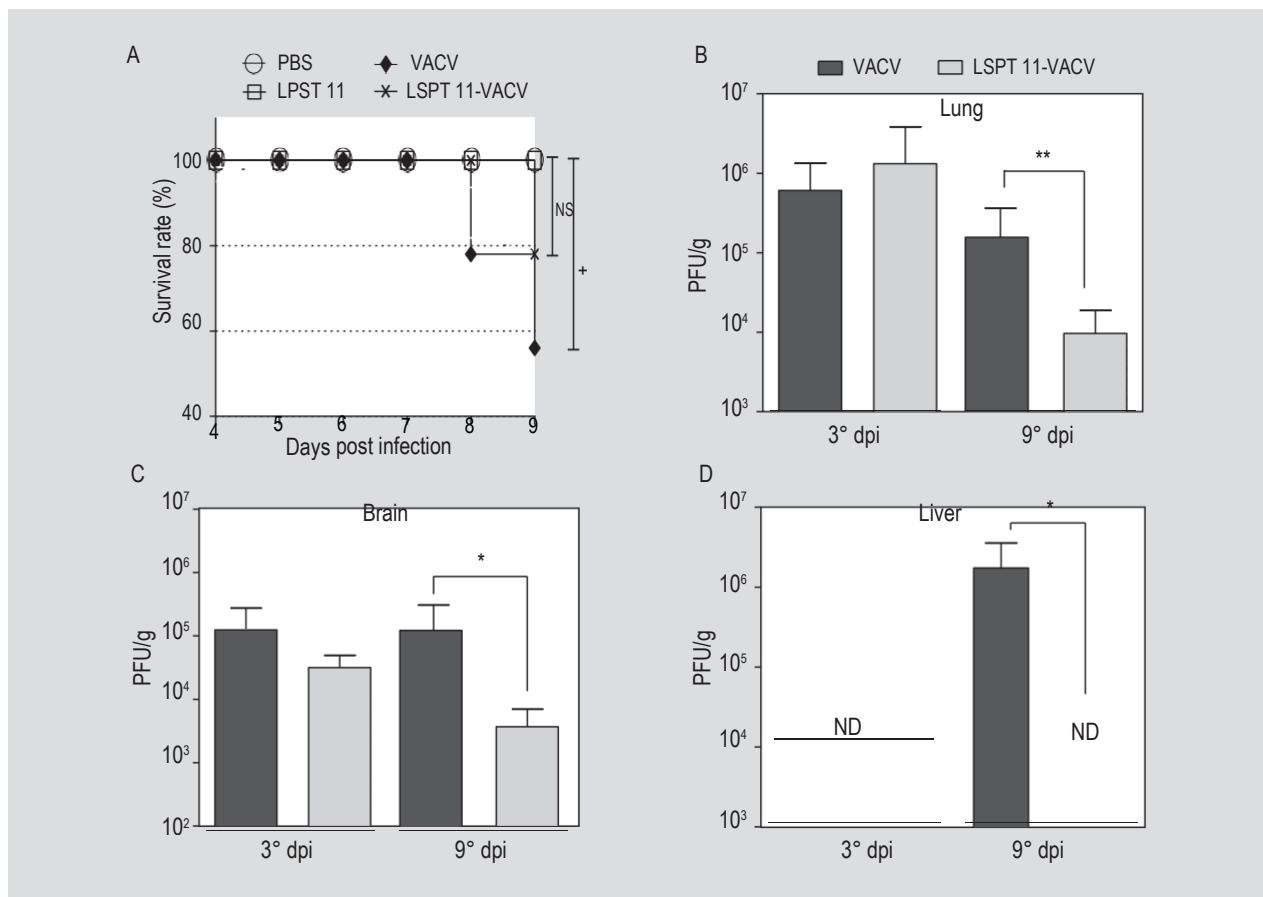


Figure 1. Impact of *Lactobacillus paracasei* ST11 (LPST11) on Vaccinia virus (VACV) infection in a mouse model. (A) Survival rate (n=9). (B-D) viral titration in BSC-40 of VACV infected mice organs (n=5) and comparison to LPST11-treated mice organs: (B) lung, (C) brain and (D) liver. ND = not detected. * $P < 0.05$, ** $P < 0.001$ (Student's t test and Log-rank test). The bars indicate standard deviations.

Statistical analysis

All results were plotted using the Log-Rank test, Student's t test and One-way ANOVA using Newman-Keuls test in GraphPadPrism (GraphPad Software, La Jolla, CA, USA). In all tests, P -values <0.05 were considered statistically significant.

3. Results

Survival and weight loss

Considering the survival experiments, results showed that ingestion of LPST11 after VACV infection resulted in 7/9 animal survival compared with 5/9 in the VACV group (Figure 1A), although treatment did not prevent any weight loss of infected groups (Figure 2).

Viral dissemination

Viral dissemination analysis showed that ingestion of LPST11 was able to significantly reduce the titres of VACV in the lungs (Figure 1B), brain (Figure 1C), and liver (Figure 1D). Titration of organs collected on 3 dpi showed that LPST11 did not prevent viral spread (Figure 1B-D) at early stages of infection, but did decrease viral spread to the lung, brain and liver at 9 dpi (Figure 1B-D).

Cytokines profile

TNF- α levels measured in the lungs of the LPST11-VACV group were significantly reduced (Figure 3A). In addition to TNF- α , the ingestion of LPST11 also reduced the expression of other inflammatory cytokines, such as IFN- γ and IL-17 (Figure 3A). The decreased production of IFN- γ occurred simultaneously with the boosted of messenger RNA (mRNA) expression levels of antiviral cytokines, such as

IFN- α , IFN- β , and IFN- λ in addition to ISGs, OAS, and PKR in the treated group (Figure 3B).

Histological findings

To investigate whether the decrease in pro-inflammatory cytokines demonstrated in the LPST11-VACV group resulted in a decreased inflammatory response in the lung, histological analyses were performed. VACV-infected mice showed severe lung lesions, with inter-alveolar septal thickening and interstitial inflammation, alveolar collapse due to oedema, fibrin, haemorrhage, and inflammatory cell infiltrate. Scattered degeneration and necrosis of bronchiolar epithelium were also detected in VACV-infected mice. The LPST11-VACV group showed lungs with moderate or mild lesions. Pulmonary lesions were focal, with less prominent inter-alveolar septal thickening and interstitial inflammation, and partial preservation of alveolar air spaces (Figure 4). The non-infected (PBS/LPST11) groups showed normal histological findings.

5. Discussion and conclusions

Probiotics have been proposed as a new therapeutic approach to the control of various viral diseases (Kassaa *et al.*, 2014). However, studies regarding probiotics and poxvirus interactions have not been described yet. To evaluate the role of LPST11 during the infection of VACV, mice were infected with the virus and treated with the probiotic. All infected mice showed clinical signs of VACV infection according to previously described (Ferreira *et al.*, 2008). However, the ingestion of LPST11 after VACV infection resulted in an increase of survival rate. Similar reductions in mortality were also described in previous studies with *Lactobacillus pentosus* b240 and *Lactobacillus rhamnosus* ingestion in influenza virus-infected mice (Kiso *et al.*, 2013; Lee *et al.*, 2013).

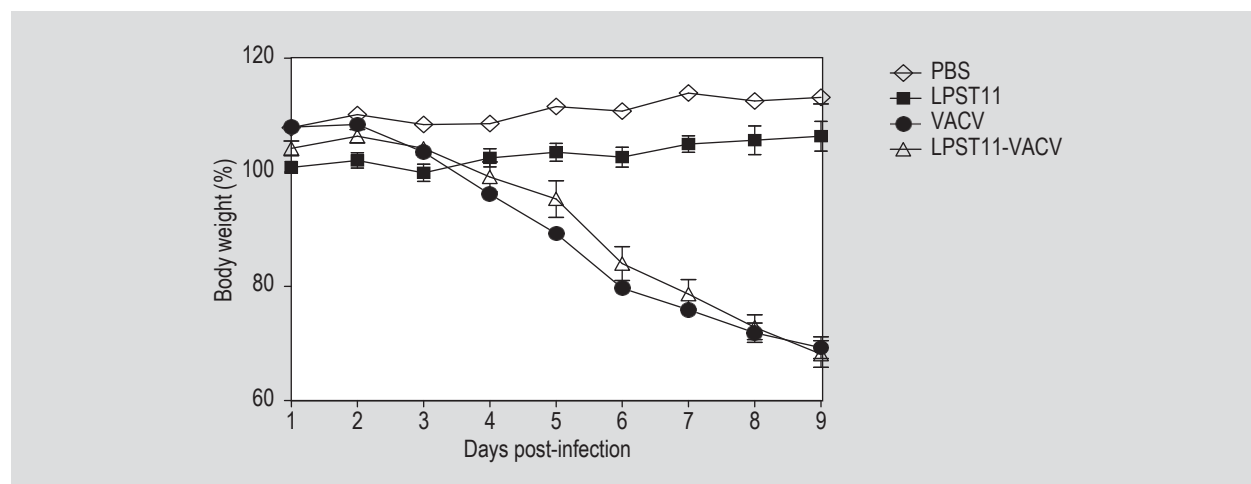


Figure 2. Impact of *Lactobacillus paracasei* ST11 (LPST11) on body weight of mice infected with Vaccinia virus (VACV) (n=9). The bars indicate standard deviation.

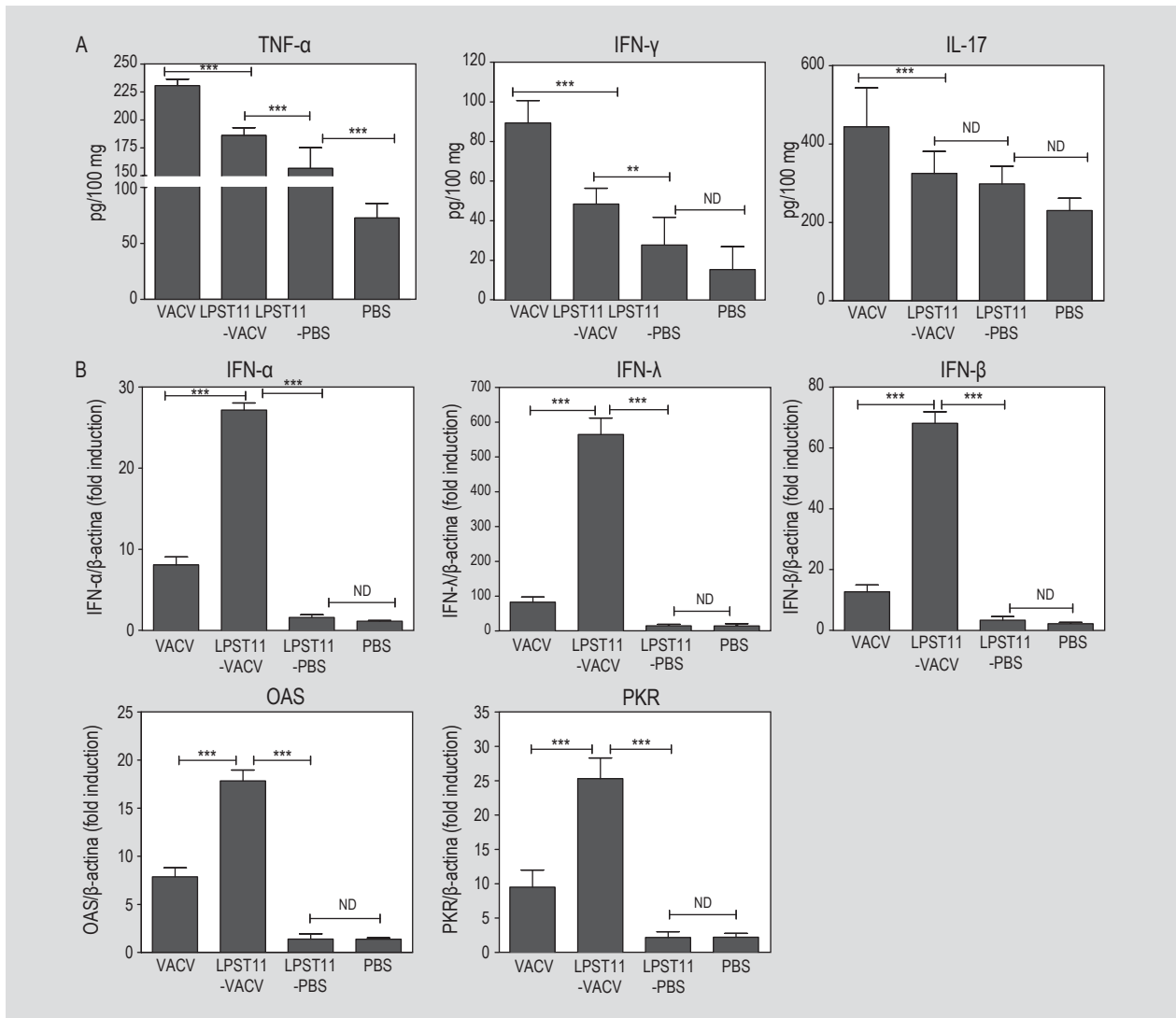


Figure 3. Inflammatory response analyses and interferons (IFNs) and interferon stimulated genes (ISGs) mRNA levels in Vaccinia virus (VACV) infection in lungs (n=3) of mice treated with *Lactobacillus paracasei* ST11 (LPST11). (A) Cytokines IFN- γ , tumour necrosis factor α (TNF- α) and interleukin-17 (IL-17) in mouse lungs were measured by ELISA. (B) IFN- α , IFN- β , IFN- λ , protein kinase RNA-activated (PKR) and 2'-5'-oligoadenylate synthetase (OAS) mRNA levels were measured by qPCR. (n=3) * $P < 0.05$, ** $P < 0.001$, * $P < 0.0001$ (One-way ANOVA using Newman-Keuls test). The bars indicate standard deviations.**

The decrease of viral replication in the lung, liver, and brain indicate systemic nature of probiotic action. Furthermore, the ingestion of LPST11 reduced the expression of inflammatory cytokines, such as TNF- α , IFN- γ and IL-17 in the lungs of the LPST11-VACV group. Previous studies have also shown that LPST11 inhibited symptoms of substance P induced cutaneous inflammation and production of the proinflammatory cytokine, TNF- α (Guéniche *et al.*, 2010) and decreased inflammatory mediators and allergy symptoms in patients with allergic rhinitis the mouse and human respiratory systems (Perrin *et al.*, 2014; Wassenberg *et al.*, 2011), and highlighted their anti-inflammatory properties (Oliveira *et al.*, 2011). IL-17 reduction may be related to decreased lethality and viral dissemination, since increased IL-17 is associated with

increased susceptibility to severe infection with VACV (Oyoshi *et al.*, 2009). Although IFN- γ production has an important role in VACV elimination (Xu *et al.*, 2004), there was a reduction in levels of this cytokine in lungs of the LPST11-VACV group, which showed decreased lethality.

Little information is available about how the *L. paracasei* ST11 strain regulates inflammatory cytokines expression. Guéniche and colleagues in 2010 reported that *L. paracasei* ST11 is able to inhibit inflammatory symptoms and TNF- α production *in vitro*. Our data suggested that LPST11 probiotic inhibits the TNF production during infection. However, in the absence of VACV infection it is able to induce the expression of this cytokine. We believe that new

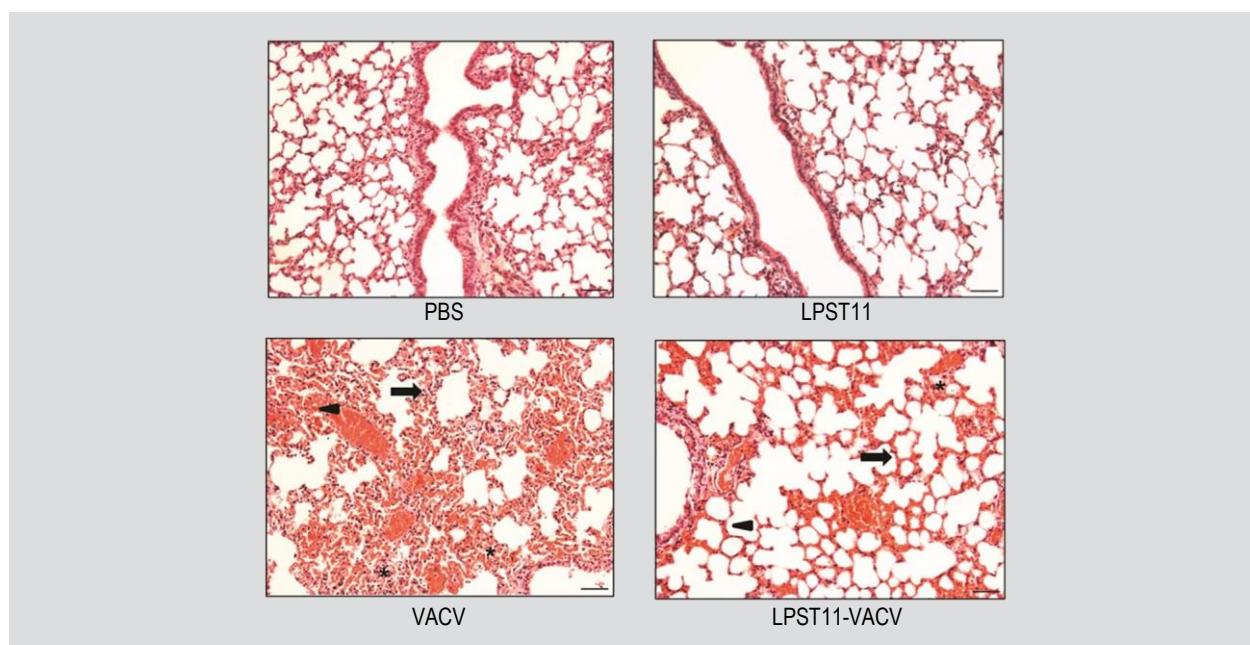


Figure 4. Lung histological analyses by HE staining. Severe pulmonary lesions in the Vaccinia virus (VACV) group showing interalveolar septal thickening (arrow) and interstitial inflammation (*), alveolar collapse (arrowhead) due to oedema, fibrin, haemorrhage, and inflammatory cell infiltrate. In the LPST11-VACV group, preserved interalveolar septa (arrow), less prominent interstitial inflammation (*), and preservation of alveolar air spaces (arrowhead) were observed. Bar = 50 µm. * $P < 0.05$.

studies are needed to clarify the cytokines modulation by LPST11 probiotic.

Interferons have important antiviral functions. Three classes of IFN, designated types I to III have been described. All types of IFN described induce expression of ISGs. Among these ISGs OAS and PKR ISGs are directly implicated in instigating the antiviral state. OAS proteins activate the latent form of RNaseL, which can then mediate RNA degradation. In this way, OAS and RNaseL constitutes an antiviral RNA decay pathway. PKR protein kinase regulate protein synthesis and allows the cell to reconfigure gene expression (Sadler and Williams, 2008).

Antiviral cytokines profile showed that gene expression levels of cytokines IFN- α , IFN- β , IFN- λ and ISGs OAS, and PKR was increased in the treated group. This antiviral activity may have been responsible for a reduction of more than a log in the viral titre in lungs and brain, at the late phase of infection. Control of virus replication could reduce the need for intense inflammatory activity mediated by IFN- γ . This balance is positively related to reduced tissue damage and better infection control (Chiu and Openshaw, 2014).

Other studies already showed that *Lactobacillus plantarum* and *L. rhamnosus* have beneficial activities against acute viral infections caused by influenza viruses when the probiotic is administered for 16 days before infection in mice (Kiso *et al.*, 2013; Lee *et al.*, 2013). Our data suggest

that similar studies could be done in the future for ST11 and VACV.

During survival tests, nine animals were used in VACV and LPST11-VACV groups. Four animals of VACV group died due to the natural course of infection during this test. The lungs of these mice became unviable for use in ELISA and qPCR assays, because the cytokines IFN- γ , TNF- α and IL-17, as well as the mRNA encoding the IFN- α cytokines, IFN- β , IFN- λ and ISGs are easily degradable. Therefore, we considered an n-value of 5. The lungs collected from these 5 animals were used in 3 different tests: viral titer, qPCR and ELISA. Therefore, the last assay, i.e. dosage of IFN- α mRNA expression, IFN- β , IFN- λ and ISGs, was not possible to use the same number of animals of the other assays. For histological analysis, an n=3 was considered sufficient because it is a qualitative analysis.

This study presents a pilot trial using a low sample size with evidence of a beneficial activity exerted by LPST11 during the infection by VACV. Many aspects of the interaction between the probiotic and the host's immune system during a viral infection remain unknown. Thus, this data represent the beginning of new studies for a better understanding of how is the interaction of probiotics with poxviruses.

Taken together, the results of this pilot study indicate that daily ingestion of *L. paracasei* ST11 may decrease the magnitude of viral replication in organs, attenuates lung inflammation and reduces lethality in mice infected

with VACV. These outcomes are possibly the result of a positive balance between immune mediators and virus multiplication. The increase in antiviral cytokines and decrease in proinflammatory cytokines seems to lead to a better control of virus dissemination. More studies concerning the use of probiotics during VACV infection can contribute to the search for alternative treatments, which can minimise the damage caused by these infections. In addition, this is the first study on probiotics and VACV interactions, providing not only information about this interaction, but also proposing a model for future studies involving probiotics and other poxvirus.

Acknowledgements

We would like to thank Pró-Reitoria de Pesquisa da Universidade Federal de Minas Gerais (PRPq-UFMG) and Conselho Nacional de Desenvolvimento Científico e Tecnológico (CNPq), Coordenação de Aperfeiçoamento de Pessoal de Nível Superior (CAPES) and Fundação de Amparo à Pesquisa do estado de Minas Gerais (FAPEMIG). EGK, GST, DGS, FM and JSA are CNPq researchers.

References

- Abrahão, J.S., Oliveira, T.M.L., Campos, R.K., Madureira, M.C., Kroon, E.G. and Lobato, Z.I.P., 2009. Bovine Vaccinia outbreaks: detection and isolation of Vaccinia virus in milk samples. *Foodborne Pathogens and Disease* 6: 1141-1146.
- Abrahão, J.S., Silva-Fernandes, A.T., Lima, L.S., Campos, R.K., Guedes, M.I.M.C., Cota, M.M.G., Assis, F.L., Borges, I.A., Souza Jr., M.F., Lobato, Z.I.P., Bonjardim, C.A., Ferreira, P.C.P., Trindade, G.S. and Kroon, E.G. 2010. Vaccinia virus infection in monkeys, Brazilian Amazon. *Emerging Infectious Diseases* 16: 976-979.
- Abrahão, J.S., Trindade, G.S., Oliveira, G.P., Figueiredo, P.O., Costa, G., Franco-Luiz, A.P.M., Assis, F.L., Oliveira, D.B., Paim, L.R.M., Oliveira, C.E.A., Neto, A.L.M. and Kroon, E.G., in press. Detection of Vaccinia virus during an outbreak of exanthemous oral lesions in Brazilian equids. *Equine Veterinary Journal*. DOI: <https://doi.org/10.1111/evj.12571>.
- Barbosa, R.P.A., Salgado, A.P.C., Garcia, C.C., Filho, B.G., Gonçalves, A.P.F., Lima, B.H.F., Lopes, G.A.O., Rachid, M.A., Peixoto, A.C.C., Oliveira, D.B., Ataíde, M.A., Zirke, C.A., Cotrim, T.M., Costa, E.A., Almeida, G.M.F., Russo, R.C., Gazzinelli, R.T. and Machado A.M.V., 2014. Protective immunity and safety of a genetically modified influenza virus vaccine. *PLoS ONE* 9: 98685.
- Campos, M.A.S. and Kroon, E.G. 1993. Critical period of irreversible block of VACV replication. *Revista de Microbiologia* 28: 474-483.
- Campos, R.K., Brum, M.C.S., Nogueira, C.E.W., Drumond, B.P., Alves, P.A., Siqueira-Lima, L., Assis, F.L., Trindade, G.S., Bonjardim, C.A., Ferreira, P.C., Weiblen, R., Flores, E.F., Kroon, E.G. and Abrahão, J.S., 2011. Assessing the variability of Brazilian Vaccinia virus isolates from a horse exanthematic lesion: coinfection with distinct viruses. *Archives of Virology* 156: 275-283.
- Chiu, C. and Openshaw, P.J., 2014. Antiviral B cell and T cell immunity in the lungs. *Nature Immunology* 16: 18-26.
- Damon, I.K., 2013. Poxviruses. In: Knipe, D.M., Howley, P.M., Griffin, D.E., Lamb, R.A., Martin, M.A. and Roizman, B. (eds.) *Fields virology*, Vol. 2, 5th edition. Lippincott Williams and Wilkins, Philadelphia, PA, pp. 2947-2975.
- Duniho, S.M., Jeffrey, M., Forster, S., Cascio, M.B., Moran, T.S., Carpin, L.B. and Sciuto, A.M., 2002. Acute changes in lung histopathology and bronchoalveolar lavage parameters in mice exposed to the choking agent gas phosgene. *Toxicologic Pathology* 30: 339-349.
- Fenner, F., Henderson, D.A., Arita, I., Jezek, Z. and Ladnyi, I.D., 1988. *Smallpox and its eradication*. World Health Organization Press, Geneva, Switzerland.
- Ferreira, J.M., Drumond, B.P., Guedes, M.I.M.C., Pascoal-Xavier, M.A., Almeida-Leite, C.M., Arantes, R.M.E., Mota, B.E.F., Abrahão, J.S., Alves, P.A., Oliveira, F.M., Ferreira, P.C.P., Bonjardim, C.A., Lobato, Z.I.P. and Kroon, E.G. 2008. Virulence in murine model shows the existence of two distinct populations of Brazilian Vaccinia virus strains. *PLoS ONE* 26: 3043-3050.
- Food and Agriculture Organization of the United Nations/World Health Organization (FAO/WHO), 2002. Guidelines for the evaluation of probiotics in food. Report of a joint FAO/WHO working group on drafting guidelines for the evaluation of probiotics in food. Available at: <http://tinyurl.com/ou88oa2>.
- Franco-Luiz, A.P., Fagundes-Pereira, A., Costa, G.B., Alves, P.A., Oliveira, D.B., Bonjardim, C.A., Ferreira, P.C.P., Trindade, G.S., Panei, C.J., Galosi, C.M., Abrahão, J.S. and Kroon, E.G. 2014. Spread of Vaccinia virus to cattle herds, Argentina, 2011. *Emerging Infectious Diseases* 20: 1576-1578.
- Galán, N.N.O., Rubiano, J.C.U., Reyes, F.A.V., Duarte, K.P.F., Cárdenas, S.P.S. and Fernandez, M.F.G., 2016. *In vitro* antiviral activity of *Lactobacillus casei* and *Bifidobacterium adolescentis* against rotavirus infection monitored by NSP4 protein production. *Journal of Applied Microbiology* 120: 1041-1051.
- Guéniche, A., Benyacoub, J., Philippe, D., Kusy, N., Breton, L., Blum, S. and Castiel-Higounenc, I., 2010. *Lactobacillus paracasei* CNCM I-2116 (ST11) inhibits substance P-induced skin inflammation and accelerates skin barrier function recovery *in vitro*. *European Journal of Dermatology* 20: 731-737.
- Hori, T., Kiyoshima, J., Shida, K. and Yasui, H., 2001. Effect of intranasal administration of *Lactobacillus casei* Shirota on influenza virus infection of upper respiratory tract in mice. *Clinical and Diagnostic Laboratory Immunology* 8: 593-597.
- International Committee on Taxonomy of Viruses (ICTV). Available at: <http://tinyurl.com/cz69k2>.
- Joklik, W.K., 1962. The purification of four strains of poxvirus. *Virology* 18: 9-18.
- Kalthoff, D., Bock, W.I., Hühn, F., Beer, M. and Hoffmann, B., 2014. Fatal cowpox virus infection in cotton-top tamarins (*Saguinus oedipus*) in Germany. *Vector Borne Zoonotic Diseases* 14: 303-305.
- Kassaa, A.I., Hober, D., Hamze, M., Chihib, N.E. and Drider, D., 2014. Antiviral potential of lactic acid bacteria and their bacteriocins. *Probiotics Antimicrobial Proteins* 6: 177-185.
- Kiso, M., Takano, R. and Sakabe, S., 2013. Protective efficacy of orally administered, heat-killed *Lactobacillus pentosus* b240 against influenza A virus. *Nature Scientific Reports* 3: 1-8.

- Kroon, E.G. Mota, B.E., Abrahão, J.S., Da Fonseca, F.G. and Trindade, G.S., 2011. Zoonotic Brazilian vaccinia virus: from field to therapy. *Antiviral Research* 92: 150-163.
- Lee, Y., Youn, H., Kwon, J., Lee, D.H., Park, J.K., Yuk, S.S., Erdene-Ochir, T.O., Kim, K.T., Lee, J.B., Park, S.Y., Choi, I.S. and Song, C.S., 2013. Sublingual administration of *Lactobacillus rhamnosus* affects respiratory immune responses and facilitates protection against influenza virus infection in mice. *Antiviral Research* 98: 284-290.
- Lehtoranta, L., Pitkäranta, A. and Korpela, R., 2014. Probiotics in respiratory virus infections. *European Journal of Clinical Microbiology and Infectious Diseases* 33: 1289-1302.
- Livak, K.J. and Schmittgen, T.D., 2001. Analysis of relative gene expression data using real-time quantitative PCR and the 2(-Delta Delta C(T)) method. *Methods* 25: 402-408.
- Oliveira, G.P., Fernandes, A.T.S., Assis, F.L., Alves, P.A., Franco Luiz, A.P.M., Figueiredo, L.B., Almeida, C.M.C., Pires Travassos, C.E.P.F., Trindade, G.S., Abrahão, J.S. and Kroon, E.G., 2014. Intrafamilial transmission of vaccinia virus during a bovine vaccinia outbreak in Brazil: a new insight in viral transmission chain. *American Journal of Tropical Medicine and Hygiene* 90: 1021-1023.
- Oliveira, M., Bosco, N., Perruisseau, G., Nicolas, J., Segura-Roggero, I., Duboux, S., Briand, M., Blum, S., Benyacoub, J., 2011. *Lactobacillus paracasei* reduces intestinal inflammation in adoptive transfer mouse model of experimental colitis. *Clinical and Developmental Immunology* 11: 1-13.
- Oyoshi, M.K., Elkhali, A., Kumar, L., Scott, J.E., Koduru, S., He, R., Leung, D.Y., Howell, M.D., Oettgen, H.C., Murphy, G.F. and Geha, R.S., 2009. Vaccinia virus inoculation in sites of allergic skin inflammation elicits a vigorous cutaneous IL-17 response. *Proceedings of the National Academy of Sciences of the USA* 106: 14954-14959.
- Perrin, Y., Nutten, S., Audran, R., Berger, B., Bibiloni, R., Wassenberg, J., Barbier, N., Aubert, V., Moulin, J., Singh, A., Magliola, C., Mercenier, A. and Spertini, F., 2014. Comparison of two oral probiotic preparations in a randomized crossover trial highlights a potentially beneficial effect of *Lactobacillus paracasei* NCC2461 in patients with allergic rhinitis. *Clinical Translational Allergy* 4: 1-12.
- Reynolds, M.G., Carroll, D.S. and Karem, K.L., 2012. Factors affecting the likelihood of monkeypox's emergence and spread in the post smallpox era. *Current Opinion in Virology* 2: 335-343.
- Sadler, A.J. and Williams, B.R.G., 2008. Interferon-inducible antiviral effectors. *Nature Reviews Immunology* 8: 559-568.
- Singh, R.K., Hosamani, M., Balamurugan, V., Prabhu, M., Yogisharadha, R., Bora, D.P., Gandhale, P.N., Sankar, M.S., Kulkarni, A.M., Singh, R.K. and Bhanuprakash, V., 2007. Buffalopox: an emerging and re-emerging zoonosis. *Animal Health Research Reviews* 8: 105-114.
- Tomosada, Y., Chiba, E., Zelaya, H., Takahashi, T., Tsukida, K., Kitazawa, H., Alvarez, S. and Villena, J., 2013. Nasally administered *Lactobacillus rhamnosus* strains differentially modulate respiratory antiviral immune responses and induce protection against respiratory syncytial virus infection. *BMC Immunology* 14: 40.
- Trindade, G.S., Fonseca, F.G., Marques, J.T., Nogueira, M.L., Mendes, L.C., Borges, A.S., Peiró, J.R., Pituco, E.M., Bonjardim, C.A., Ferreira, P.C. and Kroon, E.G. 2003. Araçatubavirus: a vaccinia like virus associated with infection in humans and cattle. *Emerging Infectious Diseases* 9: 155-160.
- Xu, R., Johnson, A.J., Liggitt, D. and Bevan, M.J., 2004. Cellular and humoral immunity against Vaccinia virus infection of mice. *Journal of Immunology* 172: 6265-6271.
- Wassenberg, J., Nutten, S., Audran, R., Barbier, N., Aubert, V., Moulin, J., Mercenier, A. and Spertini, F., 2011. Effect of *Lactobacillus paracasei* ST11 on a nasal provocation test with grass pollen in allergic rhinitis. *Clinical and Experimental Allergy* 41: 565-573.

The Large Marseillevirus Explores Different Entry Pathways by Forming Giant Infectious Vesicles

Thalita Souza Arantes,^a Rodrigo Araújo Lima Rodrigues,^a Ludmila Karen dos Santos Silva,^a Grazielle Pereira Oliveira,^a Helton Luís de Souza,^a Jacques Y. B. Khalil,^c Danilo Bretas de Oliveira,^a Alice Abreu Torres,^a Luis Lamberti da Silva,^b Philippe Colson,^c Erna Geessien Kroon,^a Flávio Guimarães da Fonseca,^a Cláudio Antônio Bonjardim,^a Bernard La Scola,^c Jônatas Santos Abrahão^a

Department of Microbiology, Institute of Biological Sciences, Universidade Federal de Minas Gerais, Belo Horizonte, Minas Gerais, Brazil^a; Department of Cell and Molecular Biology, Ribeirão Preto Medical School, Universidade de São Paulo, Ribeirão Preto, São Paulo, Brazil^b; URMITE CNRS UMR 6236-IRD 3R198, Aix Marseille Université, Marseille, France^c

ABSTRACT

Triggering the amoebal phagocytosis process is a *sine qua non* condition for most giant viruses to initiate their replication cycle and consequently to promote their progeny formation. It is well known that the amoebal phagocytosis process requires the recognition of particles of >500 nm, and most amoebal giant viruses meet this requirement, such as mimivirus, pandoravirus, pithovirus, and mollivirus. However, in the context of the discovery of amoebal giant viruses in the last decade, *Marseillevirus marseillevirus* (MsV) has drawn our attention, because despite its ability to successfully replicate in *Acanthamoeba*, remarkably it does not fulfill the >500-nm condition, since it presents an ~250-nm icosahedrally shaped capsid. We deeply investigated the MsV cycle by using a set of methods, including virological, molecular, and microscopic (immunofluorescence, scanning electron microscopy, and transmission electron microscopy) assays. Our results revealed that MsV is able to form giant vesicles containing dozens to thousands of viral particles wrapped by membranes derived from amoebal endoplasmic reticulum. Remarkably, our results strongly suggested that these giant vesicles are able to stimulate amoebal phagocytosis and to trigger the MsV replication cycle by an acidification-independent process. Also, we observed that MsV entry may occur by the phagocytosis of grouped particles (without surrounding membranes) and by an endosome-stimulated pathway triggered by single particles. Taken together, not only do our data deeply describe the main features of MsV replication cycle, but this is the first time, to our knowledge, that the formation of giant infective vesicles related to a DNA virus has been described.

IMPORTANCE

Triggering the amoebal phagocytosis process is a *sine qua non* condition required by most giant viruses to initiate their replication cycle. This process requires the recognition of particles of >500 nm, and many giant viruses meet this requirement. However, MsV is unusual, as despite having particles of ~250 nm it is able to replicate in *Acanthamoeba*. Our results revealed that MsV is able to form giant vesicles, containing dozens to thousands of viral particles, wrapped in membranes derived from amoebal endoplasmic reticulum. Remarkably, our results strongly suggest that these giant vesicles are able to stimulate phagocytosis using an acidification-independent process. Our work not only describes the main features of the MsV replication cycle but also describes, for the first time to our knowledge, the formation of huge infective vesicles in a large DNA viruses.

The discovery of the amoebal giant virus *Acanthamoeba polyphaga mimivirus* (APMV) in 2003 (1) raised new and exciting questions regarding the virosphere and boosted the hunt for new giant viruses. Owing to these efforts, an increasing number of remarkable giant viruses have been described (2–6).

Recent data suggest that giant viruses initiate their replication cycles after being phagocytosed by amoebas or other phagocytic cells (1, 7). This conclusion is well supported by classical studies which show that the phagocytosis process is triggered in *Acanthamoeba* by particles of >500 nm (8). Therefore, most of the giant viruses, such as mimivirus, pandoravirus, pithovirus, and mollivirus, meet this requirement (1–3, 5). *Marseillevirus marseillevirus* (MsV) particles, on the other hand, are formed by 250-nm icosahedral capsids that do not reach the 500-nm size threshold (6). Nonetheless, MsV still is able to successfully replicate in *Acanthamoeba*, raising the question of how the virus enters its host cell. After entry, a large and diffuse viral factory is assembled (2 to 4 h), wherein genome replication and virion morphogenesis occurs (6 to 8 h), and the virions are released from the cell within 24 h. Just

like the mimivirus, MsV has fibers with globular ends on the surface, although they are shorter in length (~12 nm compared to ~125 nm of mimiviruses), and both have an internal membrane surrounding the nucleocapsid (6). However, the origins of the MsV inner membrane remain unknown (6). The first marseillevirus was isolated from a water sample collected from a cooling

Received 28 January 2016 Accepted 10 March 2016

Accepted manuscript posted online 16 March 2016

Citation Arantes TS, Rodrigues RAL, dos Santos Silva LK, Oliveira GP, de Souza HL, Khalil JYB, de Oliveira DB, Torres AA, da Silva LL, Colson P, Kroon EG, da Fonseca FG, Bonjardim CA, La Scola B, Abrahão JS. 2016. The large marseillevirus explores different entry pathways by forming giant infectious vesicles. *J Virol* 90:5246–5255. doi:10.1128/JVI.00177-16.

Editor: G. McFadden

Address correspondence to Bernard La Scola, bernard.la-scola@univ-amu.fr, or Jônatas Santos Abrahão, jonatas.abrahao@gmail.com.

Copyright © 2016, American Society for Microbiology. All Rights Reserved.

tower in Paris, France, by culturing *Acanthamoeba castellanii* cells. Since then, marseillevirus-like organisms have been isolated from several environmental samples, with representatives from France, Tunisia, Senegal, Australia, and Brazil (6, 9–13).

Although these viruses were discovered almost a decade ago, little is known regarding their replication cycle. Thus, our objective was to perform a detailed study on the steps of the MsV replication cycle, specifically focusing on two fundamental questions: does MsV enter its amoeba host by phagocytosis, and if so, how does it stimulate the phagocytosis process while being smaller than 500 nm in size? Interestingly, our findings reveal that MsV is able to form giant vesicles containing dozens to thousands of viral particles. Using several approaches, it was possible to track the origins of these vesicles, as well as their important role in MsV biology and the maintenance of these viruses in the environment. Our results strongly suggest that these giant vesicles are remarkably able to stimulate amoeba phagocytosis by an acidification-independent process, successfully initiating the MsV replication cycle. Also, we observed that MsV entry may occur by phagocytosis of grouped particles (without surrounding membranes) or by an endosome-mediated pathway triggered by single particles. Taken together, our data not only thoroughly describe the main features of the MsV replication cycle but also provide the first report, to our knowledge, of the formation of giant infective vesicles as a way to boost the replicative success of a large DNA virus.

MATERIALS AND METHODS

Virus production, purification, and replication cycle analysis. *Acanthamoeba castellanii* cells (ATCC 30010) were cultivated in PYG medium supplemented with 7% fetal calf serum (FCS; Cultilab, Brazil), 25 mg/ml amphotericin B (Fungizone; Cristalia, São Paulo, Brazil), 500 U/ml penicillin, and 50 mg/ml gentamicin (Schering-Plough, Brazil). A total of 7×10^6 cells were infected with MsV at a multiplicity of infection (MOI) of 0.01 and incubated at 32°C. After the appearance of cytopathic effect, the cells and supernatant were collected and the viruses were then purified through ultracentrifugation with a 25% sucrose cushion at $36,000 \times g$ for 2 h. After purification, the amoeba cells were infected with purified viruses at MOIs of 0.01 and 10 to evaluate the MsV replication cycle. Infected cells were fixed with 2.5% glutaraldehyde in a 0.1 M sodium phosphate buffer for 1 h at room temperature at various times postinfection. The amoebas were postfixed with 2% osmium tetroxide and embedded in EPON resin. Ultrathin sections then were analyzed under transmission electron microscopy (TEM; Spirit Biotwin FEI-120 kV).

Purification of vesicles. For the purification of the vesicles, the supernatant obtained from *A. castellanii* cells infected with MsV at an MOI of 0.01 was submitted to ultracentrifugation at $20,000 \times g$ for 5 min. The pellet containing vesicles was collected and the supernatant containing only naked particles was discarded. After this purification, the samples were prepared for analysis by scanning electron microscopy (SEM), as previously described (14). Furthermore, we also evaluated if these vesicles could be phagocytosed by amoebas. This analysis was conducted under TEM. For the infection, 1×10^6 50% tissue culture infective doses (TCID₅₀) (15) of purified vesicles were added to a culture flask containing 7×10^6 cells of *A. castellanii*. One hour postadsorption the cells were fixed with 2.5% glutaraldehyde in a sodium phosphate buffer, 0.1 M, and analyzed by TEM as described above.

Entry assays. In this set of experiments, we evaluated different entry pathways that MsV explores in order to infect amoeba cells. First, we evaluated the endocytic pathway using chloroquine treatment. For this experiment, *A. castellanii* cells were infected with single particles of MsV or vesicles at an MOI of 10, plus chloroquine (Sigma) at a concentration of 50 µg/ml. Twenty-four hours postinfection, the treated and untreated cells were titrated using TCID₅₀ methods. In addition, we evaluated

whether the inhibition of actin filaments and microtubules (related to phagocytosis) could decrease the viral titer. For this, *A. castellanii* cells were infected with particles of the MsV or vesicles at an MOI of 10 and further treated with cytochalasin D (Sigma) at a concentration of 2 µM. Twenty-four hours postinfection, the treated and untreated cells were titrated by TCID₅₀ methods.

In order to verify the impact of membrane transportation on the viral replication cycle, *A. castellanii* cells were infected with MsV at an MOI of 10 and treated with 10 µg/ml of brefeldin A (BFA). We observed four different infection periods, 1, 2, 4, and 8 h, that correspond to four different stages of the MsV replication cycle, namely, entry, membrane recruitment, early viral factory formation, and mature viral factories. The amoebas were then transferred to 96-well microplates containing 100 µl of PYG medium and maintained at 32°C for 24 h before being further titrated by TCID₅₀.

Biological properties of the vesicles. *A. castellanii* cells were infected with MsV at an MOI of 0.01. Forty-eight hours postinfection, the vesicles were purified as described above. A portion of the purified vesicles was treated with a lysis buffer at a ratio of 1:1 for 10 min for the release of viral particles present in the vesicles. The vesicles containing the viruses, and also the single particles, then were titrated using the TCID₅₀ method. After titration, 1×10^5 TCID₅₀ of each was used to infect new *A. castellanii* cells. The cells were observed daily, and 100 µl was collected after 24, 48, and 72 h. In addition, we evaluated the temperature resistance of vesicles and single particles. For this, we used 1×10^5 TCID₅₀ vesicles or single particles and submitted them to 70°C for 1, 3, 5, 7, and 10 min using an Eppendorf Thermomixer comfort apparatus. Seventy degrees was chosen due to previous data from our laboratory that indicated this temperature is a good choice for performing heat resistance assays of large/giant viruses. It is important to highlight that at room temperature (25°C), both MsV naked particles and vesicles remain infective for at least 2 months (data not published). The samples then were titrated in *A. castellanii* using TCID₅₀.

The origins of the internal membrane and the giant vesicles. To investigate the origins of the internal membrane and the giant vesicles formed by marseilleviruses, immunofluorescence microscopy and an immunoblotting assay were performed.

(i) Immunofluorescence microscopy. *A. castellanii* cells were grown on coverslips and infected with MsV (MOI of 10) for 1.5 and 4 h for endosome, endoplasmic reticulum (ER), and Golgi analysis. After infection, the cells were rinsed in cold phosphate-buffered saline (PBS) and fixed with 4% paraformaldehyde (PFA) in PBS for 10 min at room temperature (RT). After fixation, the cells were permeabilized with 0.2% Triton X-100 in 3% bovine serum albumin (BSA)–PBS for 5 min, followed by a rinse with 3% BSA–PBS three times. The cells then were stained for 1 h at room temperature with four specific primary antibodies: rabbit polyclonal anti-sorting nexin 2 (SNX2) (Santa Cruz Technology, USA) (16), goat polyclonal anti-GRP 78 (N-20) (Santa Cruz Technology, USA), mouse monoclonal anti-GM130 (BD Biosciences, USA), and mouse polyclonal anti-MsV (17). After incubation with secondary antibodies, fluorescently labeled cells were visualized using a Zeiss (LSM 510 META) microscope. The images were processed with LSM Image Browser and Adobe Photoshop (version 7.0) software.

(ii) Immunoblotting assay. Briefly, for protein extraction, electrophoresis, and immunoblotting of the infected cells, vesicles, and purified single particles (described above), the samples were disrupted on ice with a lysis buffer and centrifuged at $18,000 \times g$ for 15 min at 4°C. The protein concentration was determined using Bio-Rad protein assay dye reagent concentrate number 5000006. Thirty micrograms of protein per sample was separated by electrophoresis on a 10% SDS polyacrylamide gel and transferred to polyvinylidene difluoride membranes. The membranes were incubated overnight at 4°C with anti-sorting nexin 2 (1:1,000), anti-GRP 78 (1:1,000), and anti-GM130 (1:1,000) antibodies. After washing, the membranes were incubated with peroxidase-conjugated anti-rabbit (1:5,000) and anti-goat (1:5,000) secondary antibodies. Immunoreactive

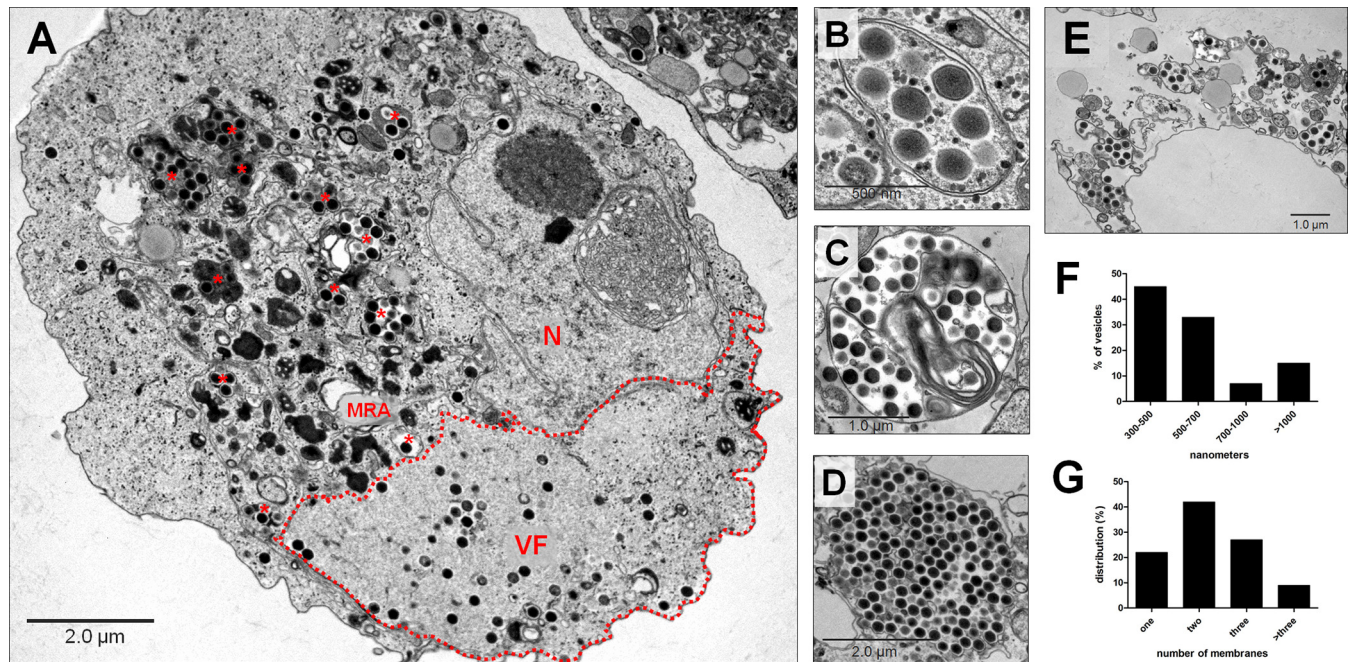


FIG 1 MsV forms a large viral factory and produces giant vesicles. (A) A TEM image of an *A. castellanii* cell infected with MsV exhibiting a large viral factory surrounded by membranes and vesicles (asterisks), with several viral particles, both inside and outside, often being found in vesicles. The dotted red line surrounds the viral factory. (B to D) TEM images demonstrating that the vesicles may contain one or more membranes and variable numbers of viruses. (E) A TEM image demonstrating a cell undergoing lysis, releasing a number of MsV vesicles. (F) Analyses of the size of the vesicles, in nanometers, found in the cytoplasm of an *A. castellanii* cell. (G) The distribution of the number of membranes present in the vesicles. For panels F and G, a total of 200 circular vesicles were considered. *, viral particles in vesicles; VF, viral factory; MRA, membrane-rich area; N, nucleus. All of the images were obtained 24 h postinfection at low MOI (0.01).

bands were visualized using a Luminata Forte Western horseradish peroxidase (HRP) substrate.

RESULTS

MsV viral factory observations. It was possible to clarify the various stages of the MsV replication cycle, which had so far remained poorly understood, through observations of *A. castellanii* cells at different times postinfection using transmission electron microscopy (TEM). Around 3 to 4 h postinfection we observed large viral factories, occupying 1/3 to 1/2 of the amoeba cytoplasm, all containing MsV particles in different stages of morphogenesis (Fig. 1A). At the edge of the viral factories it was possible to observe membrane-rich areas (MRA) (Fig. 1A) in which most of the mature viral particles were wrapped into large vesicles. These vesicles varied widely in terms of size and number of membranes (Fig. 1B, C, and D). By means of TEM, we also could observe some cells undergoing lysis, releasing a number of MsV vesicles (Fig. 1E). We noticed that the vesicles could measure from 300 nm up to >1,000 nm in diameter, depending on the amount of virus found within them. Most vesicles had an approximate size of 300 to 500 nm, representing 45% of the produced vesicles (Fig. 1F). Interestingly, we observed that the vesicles consisted of various numbers of membranes. By performing an analysis of infected amoebas containing vesicles, we evaluated the number of membranes present in each one. There were vesicles with only one membrane but also vesicles with three or more membranes. Vesicles with two membranes were the most prevalent, making up around 40% of the total (Fig. 1G).

The origins of vesicle membranes and their impact on viral replication. During the replication of MsV, we observed the re-

cruitment and rearranging of cell membranes toward vesicle formation. In addition, we noted that the vesicles could consist of one or several membranes. In order to investigate the origins of these membranes, we performed immunofluorescence (IF) assays targeting three distinct parts of cellular membranes, namely, endoplasmic reticulum (ER; anti-GRP78), Golgi complex (anti-GM130), and endosome (anti-SNX2), as these structures have been described as being involved in the morphogenesis of a number of other viruses. We also used an anti-MsV polyclonal antibody. *A. castellanii* cells were infected with MsV. Three hours postinfection we could observe colocalization between the anti-GRP78 and anti-MsV targets, suggesting that the membranes of the vesicles originated from the ER (Fig. 2A). The colocalization between MsV vesicles and other analyzed cellular targets was not observed (data not shown). Only structures outside the particles were targeted, as we believe that the immunofluorescence permeabilization process is not efficient enough to allow the binding of antibodies to membranes inside the viral particle (to answer this question, we performed immunoblotting assays of purified particles as described below). It is also clear from Fig. 2A that vesicle formation is polarized within the cell, coinciding with the polarization of ER membranes at this specific moment of infection. The formation of ER membrane-rich areas during MsV infection could be further visualized by TEM (Fig. 2B).

After we confirmed the origins of the vesicle membranes, we evaluated the influence of BFA, a membrane transport inhibitor, during the MsV replication cycle and vesicle formation. A decrease of ~2 logs in viral titer was observed in treated cells compared to untreated cells (Fig. 2C). In addition, using TEM images,

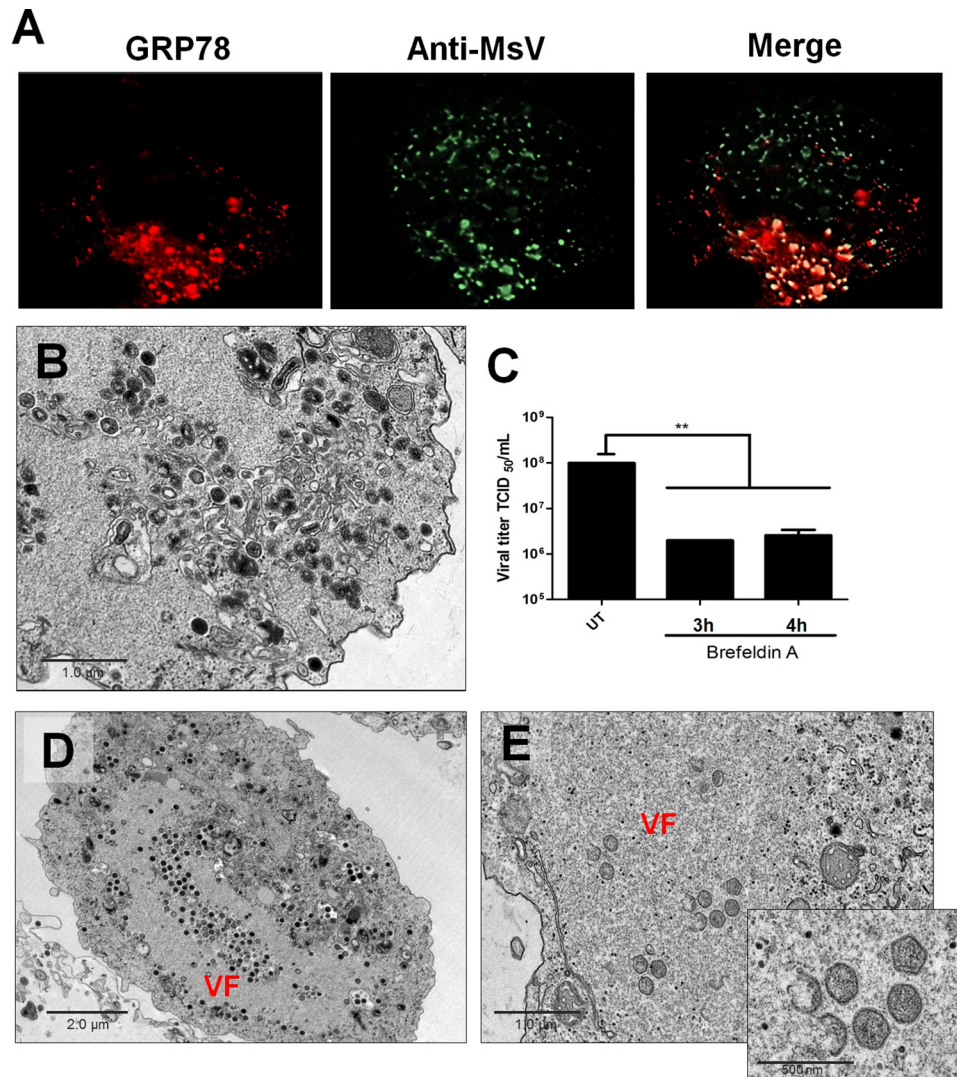


FIG 2 Membranes of MsV giant vesicles likely originate from ER. (A) Immunofluorescence microscopy showing the colocalization between anti-GRP78 and anti-MsV targets, suggesting that the membranes of the vesicles originate from the ER. (B) A TEM image of an *A. castellanii* cell 3 h postinfection, demonstrating an ER-rich area. (C) The impact of BFA on viral replication. After infected *A. castellanii* cells were treated with BFA, an ~ 2 log reduction in the viral titer was observed relative to untreated cells. The experiment was performed twice in duplicate. (D) TEM image of a cell not treated with brefeldin A, evidencing many viral particles within the viral factory. (E) TEM image of brefeldin A-treated cells (3 h of treatment) exhibiting a decrease in or absence of membranes around the viral factories as well as a significant reduction in the number of particles being assembled. **, $P < 0.001$; VF, viral factory.

we observed that treated cells exhibited a decrease/absence of membranes around the viral factories, as well as a significant reduction in the number of particles being assembled compared to untreated cells (Fig. 2D), suggesting that membranes are important not only to vesicle formation but also to particle morphogenesis (Fig. 2E).

Vesicle attachment and entry into amoebas. After establishing the origin of the vesicles, we then evaluated whether MsV vesicles could attach to and be phagocytosed by amoebas. Initially, to demonstrate that the viruses could be released within vesicles, we performed a scanning electron microscopy (SEM) analysis of these structures after they were purified from amoebas infected with MsV. The SEM images corroborated the existence of the extracellular vesicles (Fig. 3A). In addition, the results also demonstrated the efficacy of the purification method used. Considering that MsV particles are icosahedral and that most of the vesicles

are spherical, we estimated the number of virus particles present within the vesicles, as they varied in size (300 to $>1,000$ nm in diameter). Using a mathematical model, we sought to obtain the most probable number of viral particles present in each vesicle. A logarithmic profile was achieved, and it was possible to estimate that $>1,000$ viral particles could exist inside a vesicle (Fig. 3B). A vesicle 1,100 nm in diameter hypothetically could contain ~ 100 MsV particles, for example (Fig. 3B).

In order to verify that the vesicles were able to attach to the host surface and stimulate phagocytosis, purified vesicles were incubated with *A. castellanii* cells for 10 min and further analyzed by SEM. The images demonstrated that an interaction between vesicles of different sizes and amoebae occurred (Fig. 3C to E). TEM analysis of the vesicles after 30 min of incubation with *A. castellanii* cells also was performed. It was possible to observe intact vesicles and many viruses spread throughout the cell cytoplasm (Fig. 3F

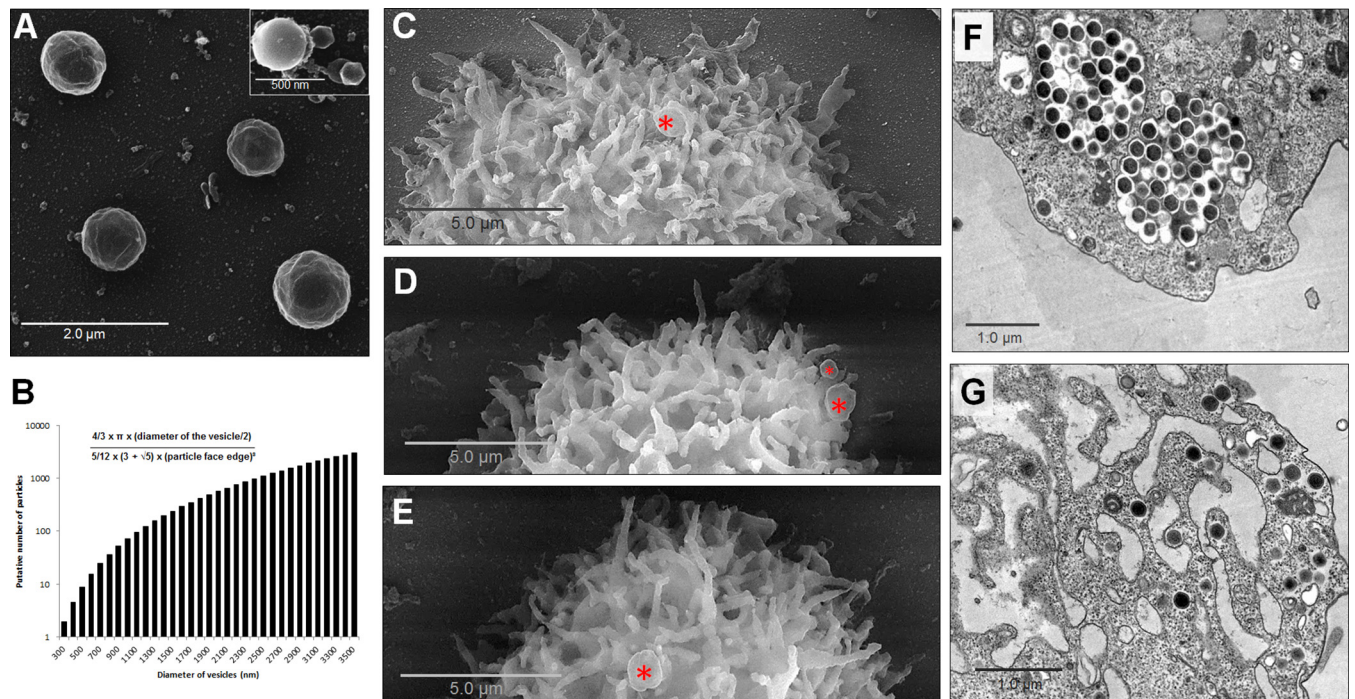


FIG 3 Giant vesicles contain several viral particles and promote phagocytosis. (A) SEM images of purified giant vesicles produced by MsV during its replication cycle. (Top right) Details of some particles close to a small vesicle. (B) A putative amount of viral particles inside vesicles of different sizes. Using a mathematical model, the number of particles per vesicle with diameters ranging from 300 to 3,500 nm was estimated. (C to E) Vesicles of different sizes attached to the surface of an *A. castellanii* cell. (F) A TEM image of intact giant vesicles inside an *A. castellanii* cell directly after penetration. The vesicles had more than one membrane. The external layer fused with the cell membrane, releasing the viruses surrounded by the inner membrane of the vesicles. (G) A TEM image of several dispersed viral particles inside an *A. castellanii* cell directly after penetration of a giant vesicle. In contrast to results shown in panel F, the giant vesicle likely had only one membrane that fused with the cell membrane, releasing the viruses directly into the cytoplasm of the cell. An asterisk indicates vesicles attached to amoebal pseudopods; in panels C and E it is possible to see amoebal pseudopods attached to the vesicles. Both TEM images were obtained 1 h postinfection with the large vesicles.

and G). We believe that when a vesicle has only one membrane, it merges with the phagosome membrane and releases the viruses inside the cytoplasm of the amoeba (Fig. 3G). However, when a vesicle has several membranes, only the outer membrane merges with the phagosome membrane and the internal membranes remain intact, keeping the viruses inside the vesicle (Fig. 3F).

The origins of the inner membrane of MsV. Considering the results described above, a rational next step would be to perform immunoblotting assays of purified vesicles to confirm their origins. However, Boyer and colleagues (6) have previously hypothesized the existence of an MsV inner membrane. Therefore, to design this assay we would have to consider the possibility that this inner membrane has a different origin from that described for the membranes of the giant vesicles. Indeed, as described previously (6), during MsV morphogenesis we observed the incorporation of structures resembling membranes (Fig. 4A).

In order to confirm the origins of the giant vesicles and to investigate the origins of the MsV inner membrane, we performed immunoblotting assays of vesicles (membrane and particles), of particles released from vesicles (after detergent treatment), and of membranes purified from vesicles. Distinct parts of the cellular membranes were probed (ER, Golgi complex, and endosome). As expected, purified vesicle membranes were recognized only by the anti-ER marker antibody (GRP78). Remarkably, purified particles were recognized only by the anti-endosome marker antibody (SNX2). Finally, vesicles containing MsV particles (and the *A.*

castellanii protein extract-positive control) were recognized both by anti-ER and anti-endosome antibodies. The anti-Golgi antibody (anti-GM130) only recognized the positive control (Fig. 4B). Therefore, these data suggest that the origin of the MsV inner membrane is endosomal.

Endosomes are recruited to early viral factories. To investigate how endosome membranes are incorporated in the viral factory, we infected *A. castellanii* cells with MsV, and after 90 min we performed IF assays using antibodies against MsV (anti-MsV) and an endosome marker (anti-SNX2). The colocalization between anti-SNX2 and anti-MsV reinforced our previous results and suggests that endosomes are recruited to the MsV viral factory during the early stages of infection (Fig. 4C).

Since the endosome participates in the formation of MsV particles, we performed TEM of infected cells in order to observe its location and participation in the MsV multiplication cycle. During the early stages (1, 2, and 3 h) of infection, we observed many endosomal vacuoles in the cytoplasm of the host cell surrounding an early membrane-rich viral factory (Fig. 4D, E, and F). Since these vacuoles are found near the viral factory region, they probably contribute to the morphogenesis of the viruses, likely contributing to the formation of the particle internal membrane, corroborating our previous data.

Vesicles versus particles: biological properties. Our next step was to evaluate if MsV giant vesicles confer any advantage compared to single viral particles. In order to measure the efficacy of

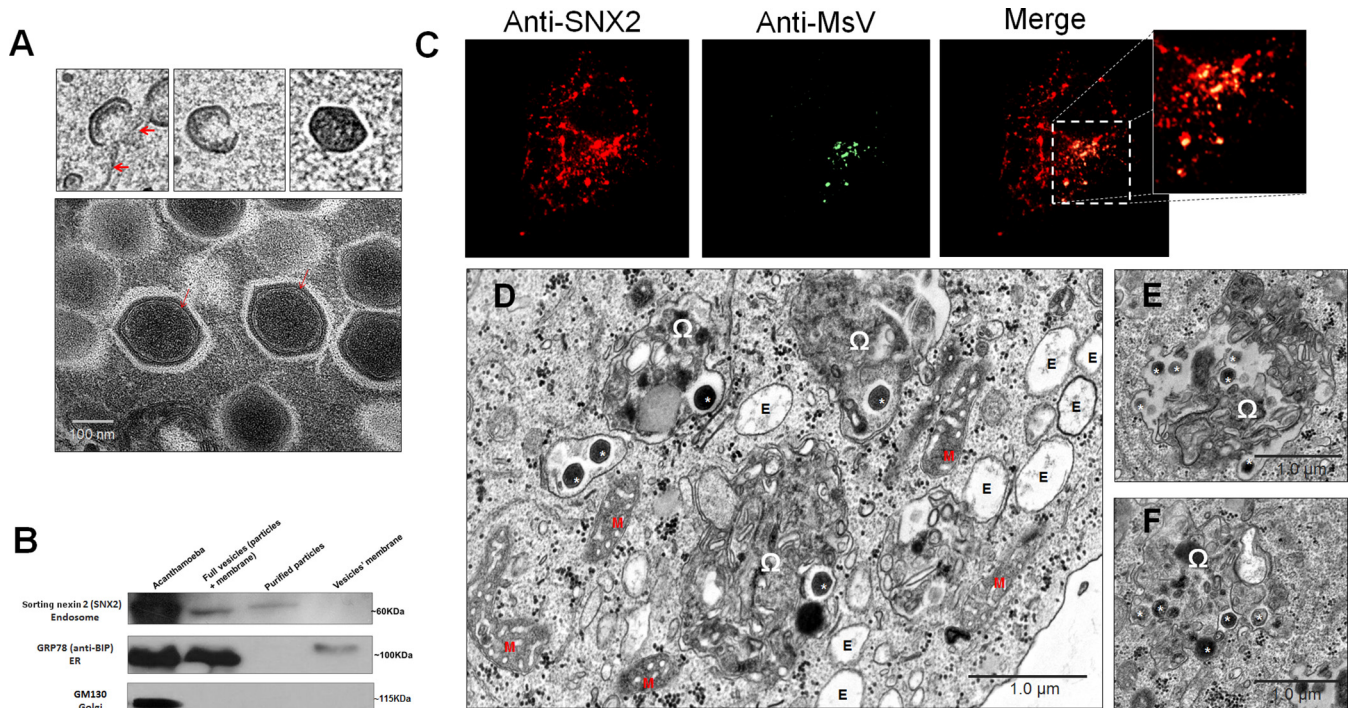


FIG 4 Marseilleviruses have an internal membrane that likely originates from the endosome. (A) TEM images of immature (inset) and mature MsV particles showing the crescent structure of the viral particles and the internal membrane surrounding the nucleocapsid (arrows). (B) The internal membrane originates from the endosome, while the giant vesicles originate from the ER. A specific endosome antibody (SNX2) recognized the full vesicles and the purified particles but not the vesicles' membrane, indicating that endosomal components are present only when the viral particles are present (60 kDa). Otherwise, a specific antibody to ER (GRP78) recognized the full vesicles and the vesicles' membrane but not the purified particles, demonstrating the ER origins of giant vesicles (100 kDa). Both antibodies recognized the *A. castellanii* structures. The anti-Golgi antibody (anti-GM130) recognized only the positive control. (C) Immunofluorescence microscopy corroborates the Western blotting data once MsV colocalizes with the endosomal components. (D) A TEM image of an *A. castellanii* cell infected with MsV, showing the presence of several endosomes (some containing viruses) and some membrane-rich areas containing viruses, probably originating from the endosome. (E and F) TEM images showing different membrane-rich areas containing viral particles. *, viral particles; M, mitochondria; E, endosome; Ω , membrane-rich area. TEM images were obtained 3 h postinfection.

vesicles and single particles in infecting *A. castellanii*, 1×10^5 TCID₅₀ of each (full vesicles and viruses, previously normalized as infectious entities) was incubated with *A. castellanii* cells. The cells were observed daily and collected 24, 48, and 72 h postinfection for further titration. It was possible to observe that the vesicles have a higher efficacy in terms of infection than the isolated viruses. For each evaluated time point the vesicles reached significantly higher titers. After 72 h the titer of the vesicles increased by ~ 2 logs, while the particles exhibited a lower increase of ~ 1.5 logs (Fig. 5A).

In order to investigate if giant vesicles confer any physical advantage to MsV compared to isolated particles, we simulated an extreme heat condition. After exposure to 70°C on multiple occasions, our findings showed the giant vesicles were significantly more resistant to this physical stress than the particles. Exposure to 70°C for 7 and 10 min completely eliminated the infectivity of isolated particles of MsV; however, some vesicles remained infectious under the same conditions, reaching $\sim 1 \times 10^2$ TCID₅₀ (Fig. 5B). This result strongly suggests that giant vesicles confer a physical advantage to MsV.

Vesicles versus particles: entry. Based on our findings (Fig. 3C to G), i.e., the discovery of giant vesicles, we raised an interesting question regarding MsV entry: would vesicles be able to stimulate phagocytosis? To address this question, we designed additional

experiments and compared the MsV entry pathways of giant vesicles and isolated particles.

Thus, *A. castellanii* cells were treated with chloroquine or with cytochalasin D and then infected with giant vesicles or isolated particles. Twenty-four hours postinfection the infected and treated cells were collected and the MsV titer determined. Chloroquine is a 9-aminoquinoline that prevents the acidification of the endosome and has a negative impact on the replication of some viruses that depend on this pathway (18). Cytochalasin D is a mycotoxin that promotes a variety of changes in cellular functions, including the destabilization of the cytoskeleton, and has been associated with the inhibition of phagocytosis (19).

Our results showed that treatment with chloroquine significantly impacted the titers of isolated particles ($P < 0.001$) but not (significantly) those of giant vesicles (Fig. 5C). On the other hand, cytochalasin D significantly decreased ($P < 0.01$) the titers of the cells infected with giant vesicles but not (significantly) those infected with isolated particles (Fig. 5D). Together, these results indicate that while isolated particles use an endosomal acidification-dependent entry pathway, giant vesicle entry is mediated via phagocytosis.

In addition, TEM images from amoebas infected with MsV corroborated our hypothesis that particle entry into the amoeba occurs via the endosome. It was possible to observe the viral par-

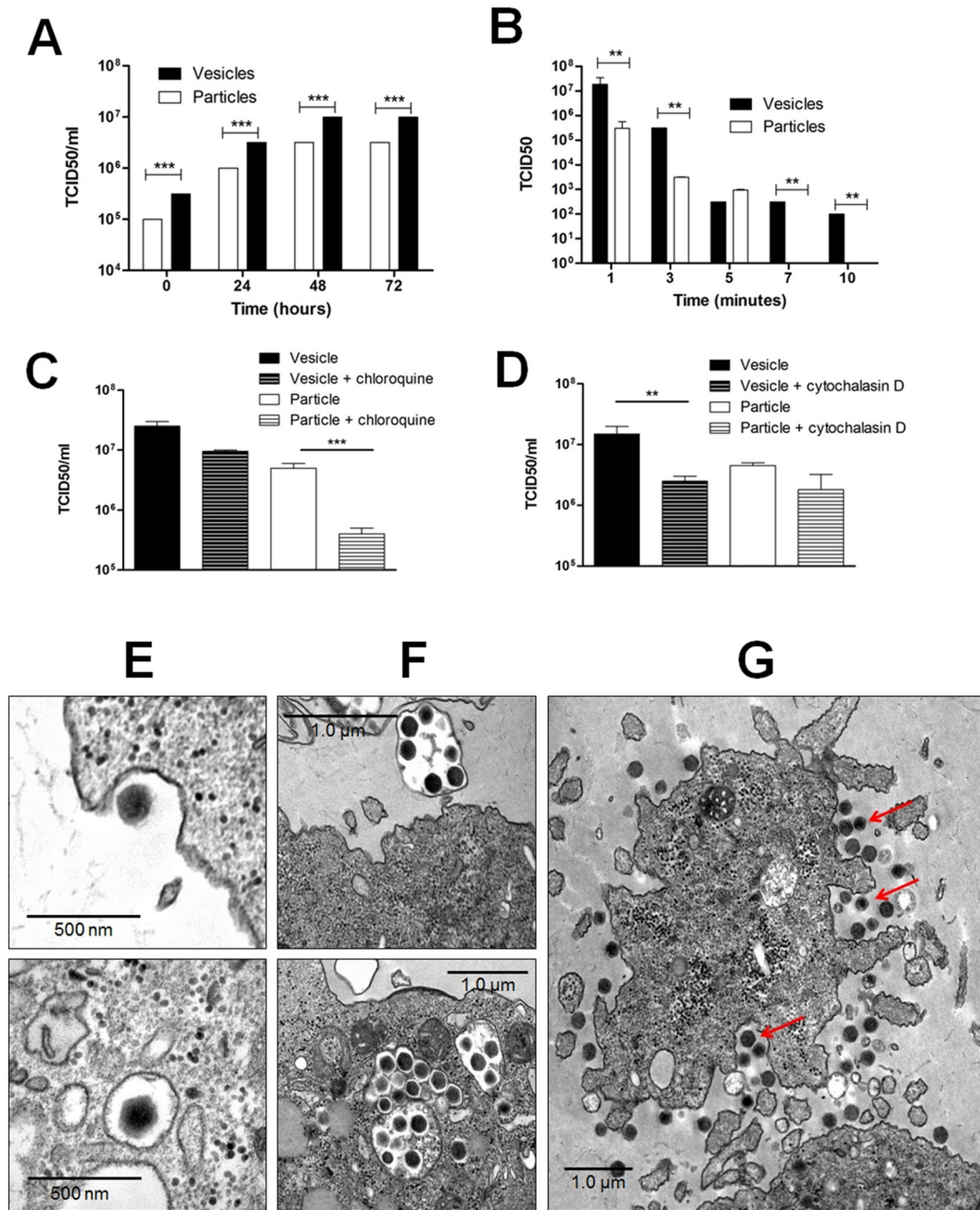


FIG 5 MsV entry into the host cell through different pathways. (A) Vesicles containing viruses provide a faster beginning to the replication cycle than single particles. (B) Vesicles confer longer-duration temperature resistance to MsV than single particles. (C and D) The effects of chloroquine and cytochalasin D on viral replication when viruses are isolated or found within vesicles. (E) TEM images of the MsV penetrating an *A. castellanii* cell using the endocytic pathway. (F) TEM images of giant vesicles penetrating an *A. castellanii* cell by phagocytosis. (G) A TEM image of grouped viral particles being engulfed by *A. castellanii* (arrows). The experiments were performed twice in duplicate. **, $P < 0.001$; ***, $P < 0.0001$. TEM images were obtained 1 h postinfection.

ticle interacting with the surface of the amoebae (Fig. 5E), and such interaction might occur through the short viral fibers found on the viral capsid. Moreover, after entry there were particles within the amoeba cytoplasm (Fig. 5E). Also, the TEM images corroborated the results from the cytochalasin D condition that vesicles can enter via phagocytosis, as it was possible to observe them both outside and inside the cell (Fig. 5F). Furthermore, it was possible to observe an aggregate of viral particles being en-

gulfed by the cell, suggesting that phagocytosis of grouped particles is another virus entry route (Fig. 5G).

DISCUSSION

In 2013, Feng and colleagues described a pathogenic picornavirus able to acquire an envelope by hijacking cellular membranes (20). This represented a breakthrough in virology as, until then, a virus was considered either enveloped or nonenveloped, without the

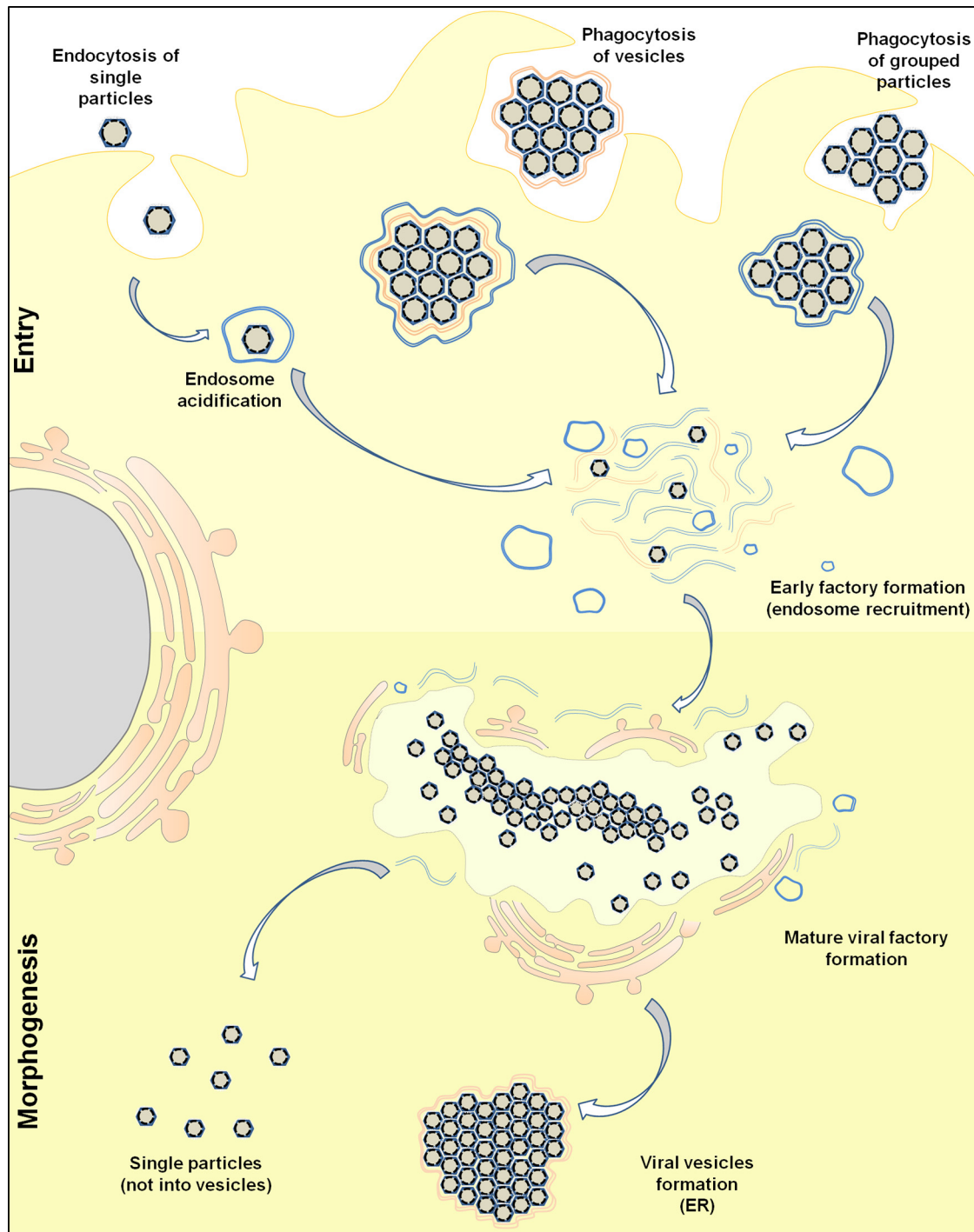


FIG 6 Models of MsV cycle replication. This model summarizes the replication cycle of MsV in *Acanthamoeba* cells. MsV can enter into the cell by different pathways, including endocytosis of single particles, phagocytosis of giant vesicles, and phagocytosis of grouped particles.

possibility of interchangeable states by the acquisition of membranes by the virus. A few other RNA viruses also are able to form infectious vesicles, which act mainly as a mechanism for escape from host immunity (21). Here, we describe for the first time, to our knowledge, a DNA virus, marseillevirus, that is able to induce the formation of giant vesicles while replicating within amoebas, its natural host.

Acanthamoeba species are unicellular protozoans that obtain nutrients through phagocytosis of microorganisms, including giant viruses (1, 22). Here, we have demonstrated that MsV, which is different from other amoebal viruses where a single particle can penetrate by phagocytosis, has developed an alternative mechanism to trigger this process, the formation of giant vesicles. The dispersion of pathogenic RNA viruses by vesicles was described as

useful in repelling specific antibodies, thus providing an important advantage to those viruses within their hosts (20, 21). Given the natural hosts of marseilleviruses, this does not seem to be applicable, as amoebas do not possess an adaptive immune system. However, this could be important if humans were their hosts, since marseilleviruses have already been described as putative human pathogens (17, 23). In addition, our results suggest that infection through vesicles evolved as a powerful mechanism to boost the replicative success of this virus within its natural hosts and/or its survival in the environment where they coexist. Indeed, we have demonstrated here that being wrapped inside vesicles may confer to the virus a number of advantages, including a greater efficiency of infection and the ability to stimulate phagocytosis. Therefore, these vesicles can facilitate the spread of the virus to other susceptible cells by collectively transferring multiple viral genomes into the cytoplasm (21). Also, we demonstrated that the vesicles confer to MsV resistance to high temperature. Considering the vesicle as an infectious entity and that each viral particle has the same heat stability, being wrapped within a membranous structure is an advantage for the species (in the case of MsV as the infectious agent), since more particles will remain infectious and grouped even under harsh conditions. In addition, the vesicle membranes could confer more resistance to wrapped particles. The giant vesicles observed in this study seem to have originated from the ER and can contain one or more membranes (Fig. 1) and up to 1,000 viral particles (Fig. 3). It seems that MsV modulates these membranes for the host cell in order to delimit a large viral factory where the vesicles are produced. The number of membrane layers in the vesicles can influence the entry of the virus into the cell. When the vesicles have only one layer, they can fuse with the cell membrane, releasing the viruses directly into the cytoplasm of the amoeba in a disorganized way. When more than one layer is present, fusion also occurs but the internal membranes remain intact, preserving the viruses within them. The large size of the vesicles makes them appropriate for phagocytosis. According to a study by Korn and Weisman, which evaluated the phagocytosis capacity of *Acanthamoeba* using latex beads of different sizes, particles smaller than 500 nm, such as those of MsV, were not phagocytosed unless they formed vesicles or particle agglomerations around the amoeba surface (8). Generally, giant viruses, such as mimivirus, pandoravirus, and pithovirus, enter into the host cell via phagocytosis, since they range in size from 750 nm to 1.5 μm (1–3). However, despite the relatively small size of marseilleviruses, they are able to enter into their host via phagocytosis using a mechanism never described before for large DNA viruses (Fig. 6).

In addition to the phagocytic pathway, marseilleviruses can enter into their host via endocytosis (Fig. 6). Macropinocytosis might be involved as well, but this should be investigated further (Fig. 5G and 6). A similar mechanism was observed in vaccinia virus (VACV), which can penetrate the cell in different ways, e.g., membrane fusion, macropinocytosis, or a low-pH-dependent endocytic route (24, 25). Another similarity between VACV and MsV is the presence of an inner membrane. In this study, we suggested that the inner membrane of MsV is acquired from the endosomes, although we believe that other sources cannot be ruled out. After penetration, it was possible to observe the accumulation of endosomal vacuoles near the viral factories (Fig. 4); therefore, when the particle was formed a membrane layer was incorporated into the viral capsid. Other large DNA viruses, such

as *Paramecium bursaria* chlorella virus, African swine fever virus, and APMV, also acquire their inner membranes during the morphogenesis step, but these membranes have different origins (26). Altogether, our results fill in some of the gaps regarding the replication cycle of the marseilleviruses, providing some important biological information about these large viruses. Using several different approaches, we have demonstrated that MsV either can interact with the cell surface and enter through endocytosis or can be found inside giant vesicles that stimulate the phagocytosis mechanism. Finally, the discovery of giant viruses not only has brought to light their genomic complexity, with hundreds of new genes/proteins that are able to perform activities never before attributable to a virus, but also allowed us a glimpse into a microcosm of ecological interactions, where viruses are able, for example, to actively seek new hosts and habitats by adsorbing into other, more complex life forms, such as fungi and arthropods (14). Here, we have identified yet another possible ecological strategy for the release of a giant virus from its last host in vesicles that have the potential to boost its entry into another host, as well as to help it endure in the environment during an “interhost” period. Although rare, we can trace a parallel between this strategy and the type B inclusion body of cowpox virus, which also may represent a similar method of enhancing interhost resistance and infectivity (27). The investigation and discovery of new giant viruses is fundamental to uncovering new information about the biology of these amazing viruses and to better understand their biological interactions, both cellular and molecular, with their hosts.

ACKNOWLEDGMENTS

We thank our colleagues from Gepvig, Laboratório de Vírus, Centro de Microscopia da UFMG, and Aix Marseille Université for their excellent technical support.

We also thank the CAPES, FAPEMIG, and CNPq for their financial support.

We have no conflicts of interest to declare.

FUNDING INFORMATION

This work, including the efforts of Jonas Santos Abrahao, was funded by MCTI | Conselho Nacional de Desenvolvimento Científico e Tecnológico (CNPq) (470645/2011-3).

REFERENCES

1. La Scola B, Audic S, Robert C, Jungang L, de Lamballerie X, Drancourt M, Birtles R, Claverie JM, Raoult D. 2003. A giant virus in amoebae. *Science* 299:2033. <http://dx.doi.org/10.1126/science.1081867>.
2. Philippe N, Legendre M, Doutré G, Couté Y, Poirot O, Lescot M, Arslan D, Seltzer V, Bertaux L, Bruley C, Garin J, Claverie JM, Abergel C. 2013. Pandoraviruses: amoeba viruses with genomes up to 2.5 Mb reaching that of parasitic eukaryotes. *Science* 341:281–286. <http://dx.doi.org/10.1126/science.1239181>.
3. Legendre M, Bartoli J, Shmakova L, Jeudy S, Labadie K, Adrait A, Lescot M, Poirot O, Bertaux L, Bruley C, Couté Y, Rivkina E, Abergel C, Claverie JM. 2014. Thirty-thousand-year-old distant relative of giant icosahedral DNA viruses with a pandoravirus morphology. *Proc Natl Acad Sci U S A* 111:4274–4279. <http://dx.doi.org/10.1073/pnas.1320670111>.
4. Reteno DG, Benamar S, Khalil JB, Andreani J, Armstrong N, Klose T, Rossmann M, Colson P, Raoult D, La Scola B. 2015. Faustovirus, an asfarvirus-related new line age of giant viruses infecting amoebae. *J Virol* 89:6585–6594. <http://dx.doi.org/10.1128/JVI.00115-15>.
5. Legendre M, Lartigue A, Bertaux L, Jeudy S, Bartoli J, Lescot M, Alempic JM, Ramus C, Bruley C, Labadie K, Shmakova L, Rivkina E, Couté Y, Abergel C, Claverie JM. 2015. In-depth study of Mollivirus sibericum, a new 30,000-y-old giant virus infecting *Acanthamoeba*. *Proc*

- Natl Acad Sci U S A 112:E5327–E5335. <http://dx.doi.org/10.1073/pnas.1510795112>.
6. Boyer M, Yutin N, Pagnier I, Barrassi L, Fournous G, Espinosa L, Robert C, Azza S, Sun S, Rossmann MG, Suzan-Monti M, La Scola B, Koonin EV, Raoult D. 2009. Giant marseillevirus highlights the role of amoebae as a melting pot in emergence of chimeric microorganisms. *Proc Natl Acad Sci U S A* 106:21848–21853. <http://dx.doi.org/10.1073/pnas.0911354106>.
 7. Ghigo E, Kartenbeck J, Lien P, Pelkmans L, Capo C, Mege JL, Raoult D. 2008. Ameobal pathogen mimivirus infects macrophages through phagocytosis. *PLoS Pathog* 4:e1000087. <http://dx.doi.org/10.1371/journal.ppat.1000087>.
 8. Weisman RA, Korn ED. 1967. Phagocytosis of latex beads by *Acanthamoeba*. I. Biochemical properties. *Biochemistry* 6:485–497.
 9. Thomas V, Bertelli C, Collyn F, Casson N, Telenti A, Goesmann A, Croxatto A, Greub G. 2011. Lausannevirus, a giant amoebal virus encoding histone doublets. *Environ Microbiol* 13:1454–1466. <http://dx.doi.org/10.1111/j.1462-2920.2011.02446.x>.
 10. Aherfi S, Boughalmi M, Pagnier I, Fournous G, La Scola B, Raoult D, Colson P. 2014. Complete genome sequence of Tunisivirus, a new member of the proposed family Marseilleviridae. *Arch Virol* 159:2349–2358. <http://dx.doi.org/10.1007/s00705-014-2023-5>.
 11. Lagier JC, Armougom F, Million M, Hugon P, Pagnier I, Robert C, Bittar F, Fournous G, Gimenez G, Maraninchi M, Trape JF, Koonin EV, La Scola B, Raoult D. 2012. Microbial culturomics: paradigm shift in the human gut microbiome study. *Clin Microbiol Infect* 18:1185–1193. <http://dx.doi.org/10.1111/1469-0691.12023>.
 12. Doutre G, Philippe N, Abergel C, Claverie JM. 2014. Genome analysis of the first Marseilleviridae representative from Australia indicates that most of its genes contribute to virus fitness. *J Virol* 88:14340–14349. <http://dx.doi.org/10.1128/JVI.02414-14>.
 13. Dornas FP, Khalil JY, Pagnier I, Raoult D, Abrahão J, La Scola B. 2015. Isolation of new Brazilian giant viruses from environmental samples using a panel of protozoa. *Front Microbiol* 6:1086.
 14. Rodrigues RA, Dos Santos Silva LK, Dornas FP, de Oliveira DB, Magalhães TF, Santos DA, Costa AO, de Macêdo Farias L, Magalhães PP, Bonjardim CA, Kroon EG, La Scola B, Cortines JR, Abrahão JSA. 2015. Mimivirus fibrils are important for viral attachment to the microbial world by a diverse glycoside interaction repertoire. *J Virol* 89:11812–11819. <http://dx.doi.org/10.1128/JVI.01976-15>.
 15. Reed LJ, Muench H. 1938. A simple method of estimating fifty percent endpoints. *Am J Hyg* 27:493–497.
 16. Haft CR, de la Luz Sierra M, Barr VA, Haft DH, Taylor SI. 1998. Identification of a family of sorting nexin molecules and characterization of their association with receptors. *Mol Cell Biol* 18:7278–72787. <http://dx.doi.org/10.1128/MCB.18.12.7278>.
 17. Popgeorgiev N, Michel G, Lepidi H, Raoult D, Desnues C. 2013. Marseillevirus adenitis in an 11-month-old child. *J Clin Microbiol* 51:4102–4105. <http://dx.doi.org/10.1128/JCM.01918-13>.
 18. Savarino A, Boelaert JR, Cassone A, Majori G, Cauda R. 2003. Effects of chloroquine on viral infections: an old drug against today's diseases? *Lancet Infect Dis* 3:722–727. [http://dx.doi.org/10.1016/S1473-3099\(03\)00806-5](http://dx.doi.org/10.1016/S1473-3099(03)00806-5).
 19. Koch G, Koch F. 1978. The use of cytochalasins in studies on the molecular biology of virus-host cell interactions. *Front Biol* 46:475–498.
 20. Feng Z, Hensley L, McKnight KL, Hu F, Madden V, Ping L, Jeong SH, Walker C, Lanford RE, Lemon SM. 2013. A pathogenic picornavirus acquires an envelope by hijacking cellular membranes. *Nature* 496:367–371. <http://dx.doi.org/10.1038/nature12029>.
 21. Altan-Bonnet G, Chen YH. 2015. Intercellular transmission of viral populations with vesicles. *J Virol* 89:12242–12244.
 22. Visvesvara GS, Moura H, Schuster FL. 2007. Pathogenic and opportunistic free-living amoebae: *Acanthamoeba* spp., *Balamuthia mandrillaris*, *Naegleria fowleri*, and *Sappinia diploidea*. *FEMS Immunol Med Microbiol* 50:1–26. <http://dx.doi.org/10.1111/j.1574-695X.2007.00232.x>.
 23. Popgeorgiev N, Boyer M, Fancello L, Monteil S, Robert C, Rivet R, Nappez C, Azza S, Chiaroni J, Raoult D, Desnues C. 2013. Marseillevirus-like virus recovered from blood donated by asymptomatic humans. *J Infect Dis* 208:1042–1050. <http://dx.doi.org/10.1093/infdis/jit292>.
 24. Senkevich TG, Ojeda S, Townsley A, Nelson GE, Moss B. 2005. Poxvirus multiprotein entry-fusion complex. *Proc Natl Acad Sci U S A* 102:18572–18577. <http://dx.doi.org/10.1073/pnas.0509239102>.
 25. Townsley AC, Weisberg AS, Wagenaar TR, Moss B. 2006. Vaccinia virus entry into cells via a low-pH-dependent endosomal pathway. *J Virol* 80:8899–8908. <http://dx.doi.org/10.1128/JVI.01053-06>.
 26. Milrot E, Mutsafi Y, Fridmann-Sirkis Y, Shimoni E, Rechav K, Gurnon JR, Van Etten JL, Minsky A. 2016. Virus-host interactions: insights from the replication cycle of the large *Paramecium bursaria* chlorella virus. *Cell Microbiol* 18:3–16. <http://dx.doi.org/10.1111/cmi.12486>.
 27. Kato S, Takahashi M, Kameyama S, Kamahora J. 1959. A study of the morphological and cyto-immunological relationship between the inclusions of vaccinia, rabbitpox, vaccinia (variola origin) and vaccinia IHD and a consideration of the term “Guarnieri body.” *Biken's J* 2:343–363.

1 **Title: The analysis of KV mimivirus major capsid gene and its**
2 **transcript highlights a distinct pattern of gene evolution and**
3 **splicing among mimiviruses**

4
5 **Running title: KV mimivirus major capsid analysis**

6
7 **Authors and Affiliations**

8
9 Paulo Victor Miranda Boratto¹, Fábio Pio Dornas¹, Lorena Christine Ferreira da
10 Silva¹, Rodrigo Araújo Lima Rodrigues¹, Grazielle Pereira Oliveira¹, Juliana Reis
11 Cortines², Betânia Paiva Drumond¹, Jônatas Santos Abrahão^{1*}

12
13 1. Laboratório de Vírus, Departamento de Microbiologia, Instituto de Ciências
14 Biológicas, Universidade Federal de Minas Gerais, Belo Horizonte, MG, Brazil

15 2. Instituto de Microbiologia Paulo de Góes, Departamento de Virologia –
16 Centro de Ciências da Saúde, Cidade Universitária, Ilha do Fundão, Rio de Janeiro, RJ,
17 Brazil

18
19
20
21 Jônatas Santos Abrahão

22
23 jonatas.abrahao@gmail.com

33

34 Abstract

35 The inclusion of *Mimiviridae* members in the putative monophyletic NCLDV
36 group is based on genomic and phylogenomic patterns. This shows that, along with
37 other viral families, they share a set of genes known as core or “hallmark genes”,
38 including the major capsid protein (MCP). Although previous studies have suggested
39 that the maturation of mimivirus MCP transcripts is dependent on splicing, there is little
40 information about the processing of this transcript in other mimivirus isolates. In this
41 work, we report the characterization of a new mimivirus isolate, called KV mimivirus.
42 Analysis of the structure, syntheny and phylogenetic relationships of the MCP gene in
43 many mimivirus isolates revealed a remarkable variation at position and types of
44 intronic and exonic regions, even for mimiviruses belonging to the same lineage. In
45 addition, sequencing of KV and APMV MCP transcripts has shown that, inside the
46 family, even related giant viruses may present different ways to process the MCP
47 mRNA. These results contribute to the understanding of the genetic organization and
48 evolution of the MCP gene in mimiviruses.

49

50 Importance

51 Mimivirus isolates have been obtained by prospecting studies since 2003. Based
52 on genomic and phylogenomic studies of conserved genes, these viruses have been
53 clustered together with members of six other viral families. Although being an
54 important part of the so called “hallmark genes”, there is little information about the
55 processing and structure of the major capsid protein (MCP) gene in many mimivirus
56 isolates. In this work, we have analyzed the structure, syntheny and phylogenetic
57 relationships of the MCP gene in many mimivirus isolates, showing remarkable
58 variation at position and types of intronic and exonic regions, even for mimiviruses
59 belonging to the same lineage. These results contribute to the understanding of the
60 genetic organization and evolution of the MCP gene in mimiviruses.

61

62 **Keywords:** KV, Mimivirus, Megavirales, giant virus, isolation, capsid.

63

64 Introduction

65

66 The term *virus* is used to define a group of biological entities united under a set
67 of generic and polythetic features (1). Among these features, the viruses can be linked
68 together primarily by their dependence on the host biosynthetic machinery and also by
69 their intracellular parasitic character. The fact that there is no a single gene uniting all of
70 the viruses in a separated phylogenetic clade can means that these organisms are
71 considered a polyphyletic group, in which the different viral species emerged from
72 distinct ancestors (2-4). However, there are some specific subgroups of viruses in which
73 a set of genes, called as “core/hallmark genes”, are present in all the members,
74 suggesting a probable common ancestry between them (4). The nucleocytoplasmic large
75 DNA viruses (NCLDVs) comprise one of those subgroups which is composed of seven
76 different viral families: *Ascoviridae*, *Asfarviridae*, *Iridoviridae*, *Marseilleviridae*,
77 *Mimiviridae*, *Phycodnaviridae* and *Poxviridae* (5, 6). These viral families share a
78 common set of core genes that are generally related to the replication of the viral
79 genome and also to the composition of the viral particle structure, encoding the major
80 capsid protein, a primase-helicase, a family B DNA polymerase, a packaging ATPase
81 and a transcription factor (5, 6).

82 Amoeba giant viruses belonging to the *Mimivirus* genus (*Mimiviridae* family)
83 were first described in 2003, during a characterization study of a pathogenic amoeba-
84 associated microorganism that was related to outbreaks of nosocomial pneumonia in a
85 hospital in Bradford, England (7). Since then a large diversity of related viruses has
86 been isolated from many different places (8-13). As new giant viruses were being
87 described, these organisms started to be phylogenetically classified based on the
88 sequence of the gene related to DNA polymerase B. This gene is conserved between
89 different viral members, but presents sufficient differences to separate them in three
90 different lineages (A, B and C) (14). Other genes that form part of the group of hallmark
91 genes have not been as well explored in the literature when it comes to the phylogenetic
92 relationships between mimiviruses. One example is that related to the synthesis of the
93 major capsid protein (MCP). This gene plays a key role in the formation of the viral
94 particle structure, representing the most abundant glycoprotein in *Acanthamoeba*
95 *polyphaga mimivirus* (APMV) (15). In a previous study, Azza and colleagues
96 interestingly observed that the APMV MCP gene is structured in five different regions,
97 with three exons separated by two intronic sites (16). The idea of a gene undergoing
98 splicing in giant viruses has also been shown in another study which confirmed that the
99 transcript of the APMV capsid gene is composed of three exonic regions (17). As

100 observed for DNA polymerase B, the MCP gene also presents high homology rates in
101 other members of the genus *Mimivirus*. However, there is not much information on how
102 this gene is structured in different *Mimivirus* members.

103 In this work, we report the characterization of Kroon virus (KV), a new
104 mimivirus belonging to lineage A. Here, we analyze the structure, synteny and
105 phylogenetic relationships of the major capsid gene (a hypothetically conserved gene
106 shared by the *Mimiviridae* members) in different giant virus isolates, including
107 mimivirus KV. By using phylogenetic analyses and comparing the order of the intronic
108 and exonic regions that compose the MCP gene of these giant viruses, we observed a
109 distinct pattern of genetic organization and gene evolution involving KV and other
110 mimiviruses, even among members of lineage A, to which KV belongs. These
111 differences are also reflected by the way in which the MCP mRNA is spliced. By
112 sequencing the mature transcripts of the MCP gene in both APMV (type-species among
113 mimiviruses and member of the lineage A) and KV, we have observed many differences
114 in terms of content and organization, suggesting that this gene is processed in a different
115 form in KV. Taken together, our results enabled us to highlight the MCP gene as a new
116 marker that could also help in future studies involving the characterization of
117 mimiviruses.

118

119 **Results**

120

121 *Virus isolation*

122 In 2012, in an attempt to isolate novel strains of giant viruses, we decided to
123 collect water samples from several urban lakes located in different cities of Brazil. A
124 total of 14 water samples were collected at equidistant points around an urban lagoon
125 located in the city of Lagoa Santa, Brazil (Figure 1A). Inoculation of these samples in
126 *Acanthamoeba castellanii* monolayers prompted us to isolate a new amoebal-associated
127 microorganism, initially characterized by the observation of cytopathic effects (CPEs)
128 in these cell cultures after 3-4 days after infection. The CPEs were characteristic of the
129 isolation of other giant viruses, including cell rounding, the absence of vacuoles and cell
130 lysis at later times of viral infection.

131

132 *Virus characterization*

133 With this new microorganism, we started to investigate any resemblance with
134 other mimivirus isolates by using transmission electron microscopy, morphometric
135 analysis and the analysis of genomic amplification by qPCR. First, we have linked our
136 new isolated virus to members of the family *Mimiviridae* since an amplification of the
137 conserved RNA helicase gene was detected.

138 Electron microscopy and morphometric assays enabled us to observe a great
139 number of viral particles, with a pseudo-icosahedral symmetry, fibrils surrounding the
140 capsid and a size that is comparable to that which has been observed for other studies
141 involving mimivirus isolation (7, 8, 11-13). These mimivirus-like particles presented an
142 average size of 673.43 nm in total, fibers of about 128.9 nm and a capsid size of 433.2,
143 spread along the *Acanthamoeba* cytoplasm [Figure 1B and C]. KV also presents several
144 characteristics that resemble steps of mimivirus replication, as we could observe (i) the
145 initial process of viral penetration, in which the viral particles start to be surrounded by
146 *Acanthamoeba* pseudopods, (ii) the presence of electron-dense regions in the amoebal
147 cytoplasm called viral factories, where the giant virus particles start to be assembled,
148 and (iii) the release of mature particles by cell lysis [Figure 2A-C]. By performing one-
149 step-growth-curve assays, we observed that our isolate reaches the plateau for viral
150 production at around 8-10 hours post-infection (the same as described for other
151 mimiviruses), but with viral titers exceeding the production of APMV particles in about
152 2.5 logs [Figure 2D]. Finally, the phylogenetic characterization of our isolate, both for
153 the RNA helicase and DNA polymerase genes, have clustered it with members of the
154 lineage A from *Mimiviridae*, that includes *Acanthamoeba castellanii* mamavirus,
155 Mimivirus terra2, Niemeyer virus, Samba virus, and Oyster virus, among others (8, 9,
156 13, 18) [Figure 3A and 3B].

157

158 ***MCP gene layout***

159 We then started to become more interested in a specific gene that is present
160 among members that compose the family *Mimiviridae*. This gene encodes the major
161 capsid protein (MCP). In APMV, it has been demonstrated that the MCP gene is
162 responsible for producing a spliced mRNA, with a structure that is composed of three
163 exons separated by two untranscribed regions (16, 17). In another giant virus, the
164 *Acanthamoeba castellanii* mamavirus, this gene was found to be lacking the two
165 intronic regions, but presented its own type of untranscribed sequence (10). As far as we
166 know, no other studies have investigated how the capsid gene is arranged and

167 phylogenetically related in members of the family *Mimiviridae*. After extensive analysis
168 of the mimivirus MCP gene, we have seen that the MCP gene of those viruses can
169 present different layouts. The first layout is slightly more complex than the others, being
170 present in most members of lineage A. It is composed of three exons (called here *e1*, *e2*
171 and *e3*), separated by two intronic regions that are specific for members of this lineage
172 (called here *iA1* and *iA2*) [Figure 4]. Interestingly, not all the members from lineage A
173 share this same structure. KV, as well as three other analyzed members of lineage A
174 (*Hirudovirus*, *Mamavirus* and *Mimivirus terra2*), have a different layout for their MCP
175 genes. In these viruses, the MCP gene has the described structure: (i) a fraction of the
176 region corresponding to exon *e1* in APMV, followed by (ii) a specific untranscribed
177 region (called *iA3* here), and finally by (iii) another specific region (called exon *eX*
178 here), which is followed by a sequence homologue to exon *e3* in APMV [Figure 4]. The
179 third layout is most closely related to members of lineage C. In these viruses, the same
180 transcribed regions composed of exons *e1* and *e3* are separated by two adjacent and
181 specific intronic regions called *iC1* and *iC2* (the exception is Powai lake megavirus,
182 which has the *e1* and *e3* regions separated only by *iC1*). As for the mimiviruses
183 belonging to lineage B, the small number of isolate sequences deposited in NCBI have
184 imposed some difficulties to better analyze the group. From what we can see, two
185 members from this lineage, *Moumouvirus goulette* and *Moumouvirus moumouvirus*,
186 have considerably diverged when we consider how their MCP gene is structured, with
187 the first one resembling the structure of mimiviruses from lineage C and the latter
188 resembling the layout observed for KV virus, with some differences related to the
189 absence of *e1* and *eX*, in addition to the inclusion of two short intronic regions (*iB1* and
190 *iB2*) [Figure 4].

191

192 ***Major capsid gene phylogenetic analysis***

193 Structural differences involving the capsid gene, as described above for several
194 mimiviruses, may reflect the way in which evolution has affected the diverse
195 relationships between members of the family *Mimiviridae* for such a conserved gene.
196 To get an idea of these relationships, we have constructed phylogenetic trees that
197 covered either the entire sequence of the MCP gene or just the sequence related to exon
198 *e3* (the largest and most conserved of the exons described above). Interestingly, the
199 constructed phylogenetic trees almost reflected the profile which was previously
200 described in the structural composition of MCP for the different giant viruses. When the

201 capsid gene of these viruses was analyzed, considering either the whole gene or just the
202 *e3* fragment, we observed a clear separation that divided the viral members into three
203 groups corresponding to the lineages A, B and C, as expected based on other hallmark
204 genes [Figure 5A-B]. The construction of phylogenetic trees containing members of
205 lineage A alone also matched the disposition of groups from trees that considered the
206 three lineages together [Figure 5C-D]. This is relevant because, in those trees, KV and
207 the other three viruses that share a distinct pattern of MCP organization (Hirudovirus,
208 Mamavirus and Mimivirus terra2) are represented as the viruses that were most
209 phylogenetically separated from the rest of the members in lineage A (the exception is
210 Oyster virus, which is also located on a separate branch in trees corresponding to the
211 analysis of exon 3) [Figure 5D]. The same occurred for Powai lake megavirus,
212 occupying a different branch to the members belonging to the lineage C [Figure 5A-B].
213 As for the *Moumouvirus goulette*, even with this MCP gene structure resembling
214 organization of the capsid gene in viruses of lineage C, the phylogenetic trees have
215 demonstrated that this virus has been grouped together with *Moumouvirus*
216 *moumouvirus*, the other member belonging to lineage B of mimiviruses [Figure 5A-B].

217

218 ***Analysis of the MCP gene transcript***

219 As structural differences in the MCP gene have been shown to influence viral
220 grouping in the phylogenetic trees described above, we chose to investigate whether
221 these differences could also determine major changes along the sequence of the mature
222 transcript related to this gene. For this test, we sequenced and analyzed the mRNA
223 encoding the MCP protein belonging to APMV and KV. For APMV, the sequences
224 corresponding to the three exons of MCP gene are conserved in the final transcript
225 [Figure 6A-B]. The gene, initially organized in a sequence of 3496 nucleotides, is
226 reduced after mRNA maturation in a sequence of 1782 nucleotides, with a query cover
227 of 51% and identity of 100% to the original gene. As observed in another study, the
228 transcript is processed as a sequence that excludes the two intronic regions present
229 originally in this gene. For KV however, the virus seems to use as its mature mRNA
230 only the region corresponding to the larger exon *e3* and the adjacent *exon X*, excluding
231 from the processed transcript both the region homologue to the exon *e1* in APMV and
232 the intronic region *iA3* [Figure 6A-B]. Curiously, analysis of the nucleotide sequence
233 from exon *eX* has shown this region as being a small fragment from the 53bp region
234 belonging to exon *e1* in the APMV-like viruses (data not shown). In addition, during

235 the transcription and formation of the mature mRNA, the regions corresponding to the
236 5'UTR and 3'UTR seem to be inverted from the observed in the original sequence. In
237 KV, the gene is initially present as a sequence of 2332 nucleotides, being reduced after
238 mRNA maturation to a sequence of 1716 nucleotides. The transcript has a query cover
239 of 73% and an identity of 100% with the original gene.

240

241 **Discussion**

242 Members of the family *Mimiviridae* have been isolated worldwide from an
243 increasing variety of samples (7, 8, 10, 12, 13). As demonstrated in other studies,
244 environments where there are high concentrations of organic matter seem to work as
245 hot-spots, marking the presence of a great diversity of mimiviruses, which is probably
246 related to the suitable habitat for their amoebal host to live (8, 19). Here, we have
247 managed to obtain another mimivirus isolate belonging to the lineage A of the family
248 *Mimiviridae*. To date, around a hundred mimivirus (and related viruses) isolates have
249 been obtained by many different strategies that use the culture of amoebal cells,
250 especially species that are included in the *Acanthamoeba* genus (12, 13, 20, 21). Despite
251 the considerable number of isolated giant viruses, the vast majority belong to lineage A
252 (19). This could be related to the fact that most of the platforms for mimivirus isolation
253 employ the use of *Acanthamoeba* organisms as the main type of cellular culture. The
254 use of this narrow host spectrum as cell support for mimivirus isolation may be filtering
255 away the discovery of other species of giant viruses that would potentially be present in
256 the samples.

257 Transmission electron microscopy has shown us that KV has a viral cycle typical of
258 other mimiviruses. Nevertheless, by undertaking a more detailed analysis of the cycle,
259 *one-step-growth curve* assays have demonstrated that this new isolate, under the same
260 conditions, produces a much larger number of mature viral particles than APMV,
261 highlighting that, even phylogenetically related, different mimivirus isolates may
262 present distinct replication profiles in *Acanthamoeba* sp

263 By analyzing the structural composition of the major capsid protein gene in
264 different members of the family *Mimiviridae*, we have reinforced a previous observation
265 which suggested that, for some genes, there is a certain level of dichotomy separating
266 mimiviruses inside lineage A (8). Here, we have observed that, for the capsid gene, KV,
267 Mamavirus, Hirudovirus and Mimivirus terra2 present a different genetic structure
268 (considering the intronic and exonic regions of the gene) when compared with

269 homologous regions in other members of the same lineage. This creates inside lineage
270 A an apparent separation with two existent groups, the one corresponding to the four
271 viruses mentioned above and the second group composed of other viruses analyzed in
272 this work: APMV, Mimivirus Shirakomae, Oyster virus, Mimivirus Bombay, Mimivirus
273 Kasaii, Niemeyer virus and Samba virus. This clear dichotomy gives us an important
274 clue, enabling the MCP gene to be considered to follow distinct evolutionary pathways
275 for each group of mimivirus isolates. This has also shown that these many giant viruses
276 harbor different structural variations for such a conserved gene as the MCP.

277 In addition to the structural results, the dichotomic event was also supported
278 when we considered phylogenetic trees associated with both the whole MCP gene, as
279 well as just for the region of exon 3, in the different mimiviruses. In those trees, the
280 giant viruses composed by KV, Mamavirus, Hirudovirus and Mimivirus terra2 have
281 remained at separate positions to others belonging to lineage A. The fact that this
282 pattern has been the same considering the two situations implies that if we take into
283 account the phylogenetic trees made for the MCP gene, the use of the region associated
284 with *e3* alone gives us an interesting biomarker that also serves to separate mimiviruses
285 in the current classification involving the three lineages. As stated before, interestingly,
286 this dichotomic phenomena has also already been seen for many other genes encoding
287 different aminoacyl-tRNA-synthetases, indicating that KV could represent a divergent
288 lineage A mimivirus (8).

289 Another interesting factor linked to the phylogenetic analysis that comprehends
290 the MCP gene is related to the position of Oyster virus in the evolutionary trees. As
291 observed, even with a gene structure that differs from that observed for KV, Mamavirus,
292 Hirudovirus and Mimivirus terra2, this giant virus is represented in the phylogenetic
293 trees in a position that is closer to the aforementioned viruses than to other members of
294 lineage A, also taking into consideration analyses that have been performed both for the
295 whole gene or just for the *e3* region. This result reinforces the importance that exonic
296 region 3 can contribute as a phylogenetic biomarker to characterize mimivirus strains.

297 Finally, by the analysis of sequences belonging to the MCP mRNA, we have
298 shown that while this sequence is processed in APMV in a way that both intronic
299 regions are spliced out, for KV, the MCP transcript is processed differently, before the
300 steps involving translation. In KV, the regions homologous to exon *e1* in APMV and
301 intronic region *iA3* are excluded. Taken together, our results indicate that in giant
302 viruses, even genes that are considered to be conserved among different species, may

303 present relevant differences that are related not only to the structural part of the gene but
304 also to how this element is processed after transcription.

305

306 **Material and Methods**

307

308 **Collection of environmental samples**

309 Water samples were collected at the Central lagoon, Lagoa Santa city, Minas
310 Gerais state, Brazil [Figure 1A]. The lagoon has a total area of 1.31 km², an
311 approximate perimeter of 6.5 km and maximum depth of between 6 and 7 meters (22).
312 It normally receives household waste water. A total of 14 water samples, 1ml each,
313 were collected along all its extension, at equidistant places, and stored at 4°C until
314 isolation procedures were performed. The samples were collected on the surface of the
315 water, near aquatic plants and areas that indicated the formation of biofilms.

316

317 **Amoebal culture procedures**

318 *Acanthamoeba castellanii* (ATCC 30010) were grown in 75 cm² cell culture
319 flasks (Nunc, USA), in PYG (peptone-yeast extract-glucose) medium supplemented
320 with 7% fetal calf serum (FCS, Cultilab, Brazil), 25 mg/ml Fungizone (amphotericin B,
321 Cristalia, São Paulo, Brazil), 500 U/ml penicillin and 50 mg/ml gentamicin (Schering-
322 Plough, Brazil).

323

324 **Enrichment protocol and isolation procedures**

325 Samples were initially submitted to an enrichment protocol adapted from Arslan
326 and collaborators (12, 23). Briefly, 500 µl of each sample was added to 4.5 ml of water-
327 rice medium (40 grains of rice per liter of water) and kept in the dark at room
328 temperature for 20 days. Following this incubation, an input of 5000 amoebas was
329 performed and the samples were incubated at the same conditions for more than 10
330 days. The samples were then filtered through 1.2 µm membranes (to retain impurities)
331 and then through 0.2 µm membranes (to retain potential giant viruses isolated in these
332 samples). The membranes were eluted in 500 µl of PBS and 100 µl of each eluate was
333 inoculated into amoebal monolayers, contained in 96-well plates in a total series of three
334 passages. Cytopathic effects (CPE) were evaluated daily.

335

336 **DNA Extraction and PCR assays**

337 Samples presenting CPE in amoebal monolayers were tested for mimivirus by a
338 qPCR targeting the conserved helicase gene (primers: 5'-
339 ACCTGATCCACATCCCATAACTAAA-3' and 5'-
340 GGCCTCATCAACAAATGGTTTCT-3'). The DNA was extracted by PCI and
341 quantified by nanodrop before the PCR assays. The qPCR was performed with a
342 commercial mix Power SYBr Green (Applied Biosystems, USA), primers (4 mM each)
343 and 1 ml sample in reaction of 10 ml final volume. All reactions were performed in a
344 StepOne thermocycler: 95°C (10 min), 40 cycles [95°C (15 s)/60°C (15 s)], followed by
345 a dissociation step (specific T_m = 73°C).

346 The whole genome of KV was obtained and partially analyzed as described in
347 another study (access number: KM982402.1) (24).

348

349 **Virus purification procedures**

350 The KV particles were isolated and purified from infected amoebae as
351 previously described (13). Briefly, after reaching confluence, the amoebas were infected
352 with the new isolated giant virus and incubated at 37°C until the appearance of CPE.
353 Virus-rich supernatants from the infected amoeba were collected and filtered through a
354 0.8-µm (Millipore, USA) filter to remove amoeba debris. The viruses were then purified
355 using a sucrose cushion suspended in PBS, stored at -80°C and titrated using the TCID₅₀
356 methodology (25).

357

358 **Transmission electron microscopy analyses**

359 For the transmission electron microscopy (TEM), *A. castellanii* cells were
360 infected with KV at an MOI of 0.01. Uninfected amoebae were used as controls. When
361 ~70% of the cells presented cytopathic effects, the amoeba monolayer was fixed with
362 2.5% glutaraldehyde (Merck, Germany) for 1 hour at room temperature in 0.1 M
363 sodium phosphate buffer. Amoebas were then post-fixed with 2% osmium tetroxide and
364 embedded in Epon resin, and ultrathin sections were examined under a Transmission
365 Electron Microscopy TECNAI G2-20 – SuperTwin FEI – 120 kV at the Center of
366 Microscopy, UFMG, Brazil.

367

368 **One-step-growth curve**

369 To evaluate the replication profile of the new giant virus isolate, six-well plates
370 containing 1×10^7 amoebas/well were infected with KV at m.o.i. of 10 and incubated at
371 32°C for 0, 0.5, 1, 2, 4, 6, 8, 12 and 24 hours. Infected cells were collected and
372 centrifuged, and the pellet was used for titration in amoebas. The viral titer was
373 determined using the TCID₅₀ method calculated with the Reed-Muench method (25).

374

375 Synteny analysis of the MCP gene

376 In this work we have also searched for differences in the layout of the major
377 capsid protein gene of several mimivirus samples. Given that APMV, as the type
378 species of the family *Mimiviridae*, has the best characterized genome among
379 mimiviruses, its nucleotide sequence was used as reference for MCP analyses. To do
380 that, for each gene feature belonging to APMV (*exons 1, 2, 3* and *introns 1, 2*), we
381 searched for similar sequences in other viruses using the BLAST tool from the NCBI
382 database (e-value of 10^{-3}). Sequences that were found to be homologous to APMV were
383 separated and then the final gene layouts were constructed based in the position and
384 orientation occupied by these different sequences. Specific MCP gene features found in
385 some viruses were also searched for in other mimivirus samples. A scheme of the MCP
386 gene was prepared including isolates from all mimivirus lineages (Figure 4).

387

388 MCP mRNA sequencing

389 Twenty-four-well plates containing 1×10^5 amoebas/well were infected with KV
390 or APMV at m.o.i. of 5 and incubated at 32°C . After 30 min and 6 hours, cells were
391 collected and centrifuged, and the pellet was homogenized used for total RNA
392 extraction, reverse transcription and conventional PCR for the MCP gene amplification.
393 The amplicons were examined by electrophoresis in a 1% agarose gel, TBE buffer and
394 run at 150V. The amplicon band was purified and sequenced in both orientations, in
395 triplicate (3730 DNA Analyzer; Thermo Fischer Scientific, Waltham, MA, USA). The
396 sequences were analyzed using the alignment tool available in the software MEGA 7.

397

398 Phylogenetic analyses

399 For the phylogenetic analyses, separated alignments for the major capsid protein,
400 DNA polymerase B subunit, RNA helicase genes and the *exon 3* region of the major
401 capsid gene were used. Strains of several viruses of the three mimivirus lineages (A, B
402 and C) were selected to assemble the dataset. The predicted nucleotide sequences were

403 obtained from NCBI GenBank and aligned using ClustalW in Mega 7.0 software. Trees
404 were constructed using maximum likelihood method and bootstrap of 1,000.

405

406 **Conflict of interest statement**

407 The authors declare no conflict of interest

408

409 **Acknowledgements**

410 We would like to thank colleagues from Gepvig, Laboratório de Vírus, Centro
411 de Microscopia da UFMG and Aix Marseille Université for their excellent support. Also,
412 we would like to thank Pro-reitoria de pesquisa da Universidade Federal de Minas
413 Gerais, CAPES, FAPEMIG, CNPq. JSA is a CNPq researcher.

414

415 **References**

- 416 1. **Lwoff A.** 1957. The concept of virus. *J Gen Microbiol* **17**:239-253.
- 417 2. **Koonin EV, Yutin N.** 2010. Origin and evolution of eukaryotic large nucleo-
418 cytoplasmic DNA viruses. *Intervirology* **53**:284-292.
- 419 3. **Moreira D, Lopez-Garcia P.** 2009. Ten reasons to exclude viruses from the
420 tree of life. *Nat Rev Microbiol* **7**:306-311.
- 421 4. **Koonin EV, Senkevich TG, Dolja VV.** 2006. The ancient Virus World and
422 evolution of cells. *Biol Direct* **1**:29.
- 423 5. **Iyer LM, Aravind L, Koonin EV.** 2001. Common origin of four diverse
424 families of large eukaryotic DNA viruses. *J Virol* **75**:11720-11734.
- 425 6. **Iyer LM, Balaji S, Koonin EV, Aravind L.** 2006. Evolutionary genomics of
426 nucleo-cytoplasmic large DNA viruses. *Virus Res* **117**:156-184.
- 427 7. **La Scola B, Audic S, Robert C, Jungang L, de Lamballerie X, Drancourt M,**
428 **Birtles R, Claverie JM, Raoult D.** 2003. A giant virus in amoebae. *Science*
429 **299**:2033.
- 430 8. **Boratto PV, Arantes TS, Silva LC, Assis FL, Kroon EG, La Scola B,**
431 **Abrahao JS.** 2015. Niemeyer Virus: A New Mimivirus Group A Isolate
432 Harboring a Set of Duplicated Aminoacyl-tRNA Synthetase Genes. *Front*
433 *Microbiol* **6**:1256.
- 434 9. **Andrade KR, Boratto PP, Rodrigues FP, Silva LC, Dornas FP, Pilotto MR,**
435 **La Scola B, Almeida GM, Kroon EG, Abrahao JS.** 2015. Oysters as hot spots
436 for mimivirus isolation. *Arch Virol* **160**:477-482.
- 437
438
439
440
441
442
443
444
445

- 446 10. **Colson P, Yutin N, Shabalina SA, Robert C, Fournous G, La Scola B,**
447 **Raoult D, Koonin EV.** 2011. Viruses with more than 1,000 genes: Mamavirus,
448 a new *Acanthamoeba polyphaga* mimivirus strain, and reannotation of
449 Mimivirus genes. *Genome Biol Evol* **3**:737-742.
450
- 451 11. **Yoosuf N, Yutin N, Colson P, Shabalina SA, Pagnier I, Robert C, Azza S,**
452 **Klose T, Wong J, Rossmann MG, La Scola B, Raoult D, Koonin EV.** 2012.
453 Related giant viruses in distant locations and different habitats: *Acanthamoeba*
454 *polyphaga* mousmouvirus represents a third lineage of the Mimiviridae that is
455 close to the megavirus lineage. *Genome Biol Evol* **4**:1324-1330.
456
- 457 12. **Arslan D, Legendre M, Seltzer V, Abergel C, Claverie JM.** 2011. Distant
458 Mimivirus relative with a larger genome highlights the fundamental features of
459 Megaviridae. *Proc Natl Acad Sci U S A* **108**:17486-17491.
460
- 461 13. **Campos RK, Boratto PV, Assis FL, Aguiar ER, Silva LC, Albarnaz JD,**
462 **Dornas FP, Trindade GS, Ferreira PP, Marques JT, Robert C, Raoult D,**
463 **Kroon EG, La Scola B, Abrahao JS.** 2014. Samba virus: a novel mimivirus
464 from a giant rain forest, the Brazilian Amazon. *Viol J* **11**:95.
465
- 466 14. **Yutin N, Colson P, Raoult D, Koonin EV.** 2013. Mimiviridae: clusters of
467 orthologous genes, reconstruction of gene repertoire evolution and proposed
468 expansion of the giant virus family. *Viol J* **10**:106.
469
- 470 15. **Renesto P, Abergel C, Decloquement P, Moinier D, Azza S, Ogata H,**
471 **Fourquet P, Gorvel JP, Claverie JM.** 2006. Mimivirus giant particles
472 incorporate a large fraction of anonymous and unique gene products. *J Virol*
473 **80**:11678-11685.
474
- 475 16. **Azza S, Cambillau C, Raoult D, Suzan-Monti M.** 2009. Revised Mimivirus
476 major capsid protein sequence reveals intron-containing gene structure and extra
477 domain. *BMC Mol Biol* **10**:39.
478
- 479 17. **Legendre M, Audic S, Poirot O, Hingamp P, Seltzer V, Byrne D, Lartigue**
480 **A, Lescot M, Bernadac A, Poulain J, Abergel C, Claverie JM.** 2010. mRNA
481 deep sequencing reveals 75 new genes and a complex transcriptional landscape
482 in Mimivirus. *Genome Res* **20**:664-674.
483
- 484 18. **Yoosuf N, Pagnier I, Fournous G, Robert C, Raoult D, La Scola B, Colson**
485 **P.** 2014. Draft genome sequences of Terra1 and Terra2 viruses, new members of
486 the family Mimiviridae isolated from soil. *Virology* **452-453**:125-132.
487
- 488 19. **Dornas FP, Khalil JY, Pagnier I, Raoult D, Abrahao J, La Scola B.** 2015.
489 Isolation of new Brazilian giant viruses from environmental samples using a
490 panel of protozoa. *Front Microbiol* **6**:1086.
491
- 492 20. **Khalil JY, Robert S, Reteno DG, Andreani J, Raoult D, La Scola B.** 2016.
493 High-Throughput Isolation of Giant Viruses in Liquid Medium Using
494 Automated Flow Cytometry and Fluorescence Staining. *Front Microbiol* **7**:26.
495

- 496 21. **Legendre M, Bartoli J, Shmakova L, Jeudy S, Labadie K, Adrait A, Lescot**
497 **M, Poirot O, Bertaux L, Bruley C, Coute Y, Rivkina E, Abergel C, Claverie**
498 **JM.** 2014. Thirty-thousand-year-old distant relative of giant icosahedral DNA
499 viruses with a pandoravirus morphology. *Proc Natl Acad Sci U S A* **111**:4274-
500 4279.
501
- 502 22. **Brighenti LS, Pinto-Coelho RM, Bezerra-Neto JF, Gonzaga AV.** 2011.
503 Parâmetros morfométricos da Lagoa Central (Lagoa Santa, Estado de Minas
504 Gerais): comparação de duas metodologias. . *Acta Scientiarum Biological*
505 *Sciences* **33**:7.
506
- 507 23. **Dornas FP, Silva LC, de Almeida GM, Campos RK, Boratto PV, Franco-**
508 **Luiz AP, La Scola B, Ferreira PC, Kroon EG, Abrahao JS.** 2014.
509 *Acanthamoeba polyphaga mimivirus* stability in environmental and clinical
510 substrates: implications for virus detection and isolation. *PLoS One* **9**:e87811.
511
- 512 24. **Assis FL, Bajrai L, Abrahao JS, Kroon EG, Dornas FP, Andrade KR,**
513 **Boratto PV, Pilotto MR, Robert C, Benamar S, Scola BL, Colson P.** 2015.
514 Pan-Genome Analysis of Brazilian Lineage A Amoebal Mimiviruses. *Viruses*
515 **7**:3483-3499.
516
- 517 25. **Reed LJ, Muench H.** 1938. A simple method of estimating fifty percent
518 endpoints. *The American Journal of Hygiene* **27**:493 - 497.
519

520 **Figures**

521 **Figure 1. KV mimivirus collection site, electron microscopy and**
522 **morphometric analysis.** (A) A map of the Central Lagoon, from where the samples
523 were collected. (B) An image of KV virus particle, observed from the transmission
524 electron microscopy assays. (C) Shows the size, in nanometers, of different components
525 of KV particle: only the capsid, only the fibers and the particle as a whole.
526

527 **Figure 2. KV replication cycle.** The major steps of KV life cycle are
528 highlighted by transmission electron microscopy and one-step-growth curve assays. In
529 (A) giant viral particles initiate the process of viral penetration by being phagocytosed
530 by *Acanthamoeba castellanii* cells. (B) Shows a later step, in which a KV viral factory,
531 located at the cytoplasm of an infected amoebal host, starts to produce and bud several
532 particles. (C) Demonstrates the last step of KV replication, in which the produced
533 mature particles start to be released by lysis of the amoebal cell. (D) Shows the general
534 replication cycle of KV in comparison with APMV by one-step-growth curve assays.
535 After 24h of infection, KV exceeds the production of APMV particles in about 2.5 logs.
536

537 **Figure 3. Phylogenetic reconstruction of mimiviruses.** Phylogenetic analyses
538 for many representatives of the different *Mimiviridae* lineages (A, B, and C) including
539 KV virus strain, based on the (A) RNA helicase and (B) DNA polymerase-B amino acid
540 sequences. For these analysis, we used MEGA7 software (maximum-likelihood method
541 and 1,000 bootstrap replicates). The different *Mimiviridae* lineages were highlighted
542 using different colored boxes (lineage A: blue, lineage B: green and lineage C: red) and
543 KV is shown by a yellow arrow, being clustered with other mimivirus isolates
544 belonging to lineage A. For each sequence, the gene identification numbers are
545 indicated.

546

547 **Figure 4. General scheme showing the structure of the MCP gene on**
548 **different *Mimiviridae* members.** This figure shows the structural layout of the MCP
549 gene belonging to several members of the *Mimiviridae* family. The different
550 *Mimiviridae* lineages were highlighted using different colored boxes (lineage A: blue,
551 lineage B: green and lineage C: red). Representatives from these lineages seems to
552 present distinct genetic structures for the gene. However, the general layout for this
553 conserved gene may also suffer variations inside members of the same lineage, as it is
554 observed for KV, Mamavirus, Hirudovirus and Mimivirus terra2 compared to other
555 members of lineage A.

556

557 **Figure 5. Phylogeny of the MCP gene for different *Mimiviridae***
558 **members.** Here, a phylogenetic analysis for many representatives of the different
559 *Mimiviridae* lineages is shown (A, B, and C), including for the new Brazilian mimivirus
560 isolate KV strain, based on the nucleotide sequences of the whole MCP gene or for just
561 the sequences corresponding to the *exon 3*. In (A), the rectangular tree layout represents
562 an analysis of the whole gene, considering members of the three different lineages,
563 highlighted by different colored boxes (lineage A: blue, lineage B: green and lineage C:
564 red). In (B), the same members are considered, but the phylogenetic relationships were
565 based on the nucleotide sequences of just the *exon 3*. Image (C) represents a radial tree,
566 corresponding to analysis of the whole MCP gene for members of the lineage A alone.
567 Finally, in (D), the phylogenetic relationships of members of lineage A are represented
568 by another radial tree, but this time considering only sequences belonging to the *exon 3*.
569 For these analysis, we have used MEGA7 software (maximum-likelihood method and

570 1,000 bootstrap replicates). For each sequence, the gene identification numbers are
571 indicated.

572

573 **Figure 6. General scheme representing the process of splicing for the MCP gene in**

574 **APMV and KV isolates.** (A) The APMV capsid transcript suffers a process of splicing

575 in which its processed form is composed by the sequences of *exon 1*, *exon 2* and *exon 3*.

576 KV, however, beyond its different MCP gene layout, uses as mature mRNA only the

577 regions corresponding to the exons *eX* and *e3*. (B) Alignment for the aminoacid

578 sequence produced by APMV and KV after translation of their respective MCP genes.

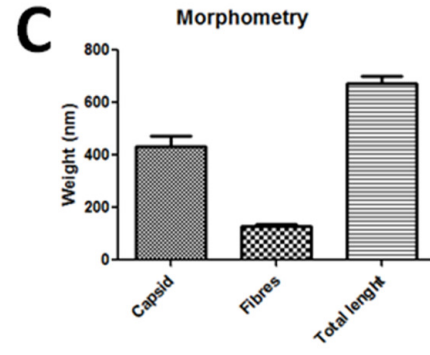
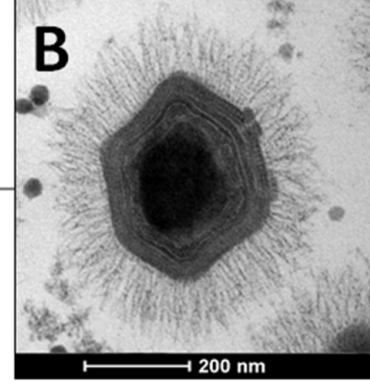
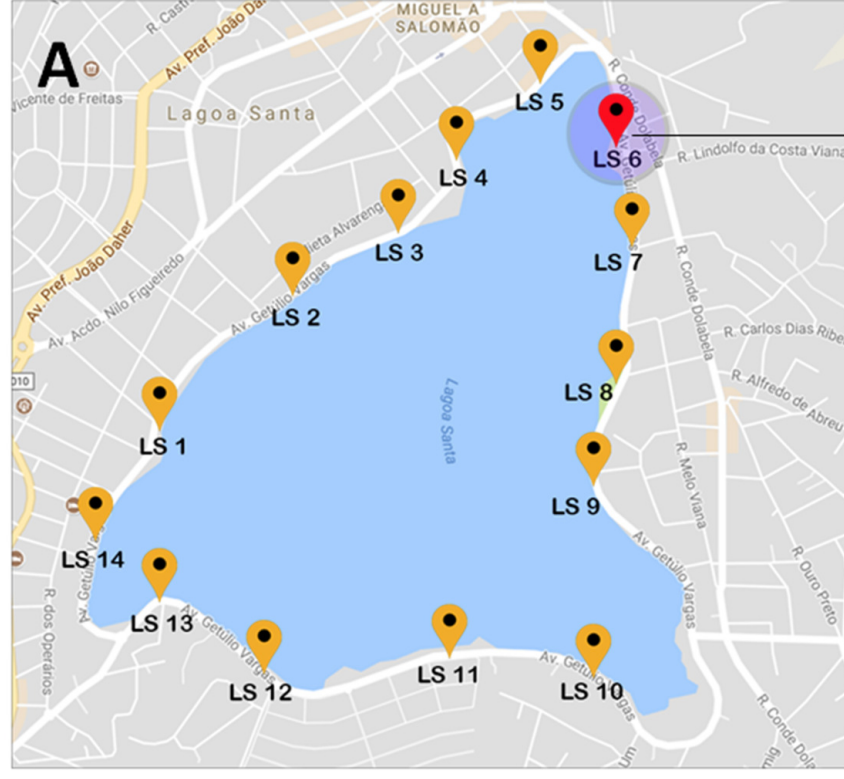
579 Arrow indicates mismatched amino acids.

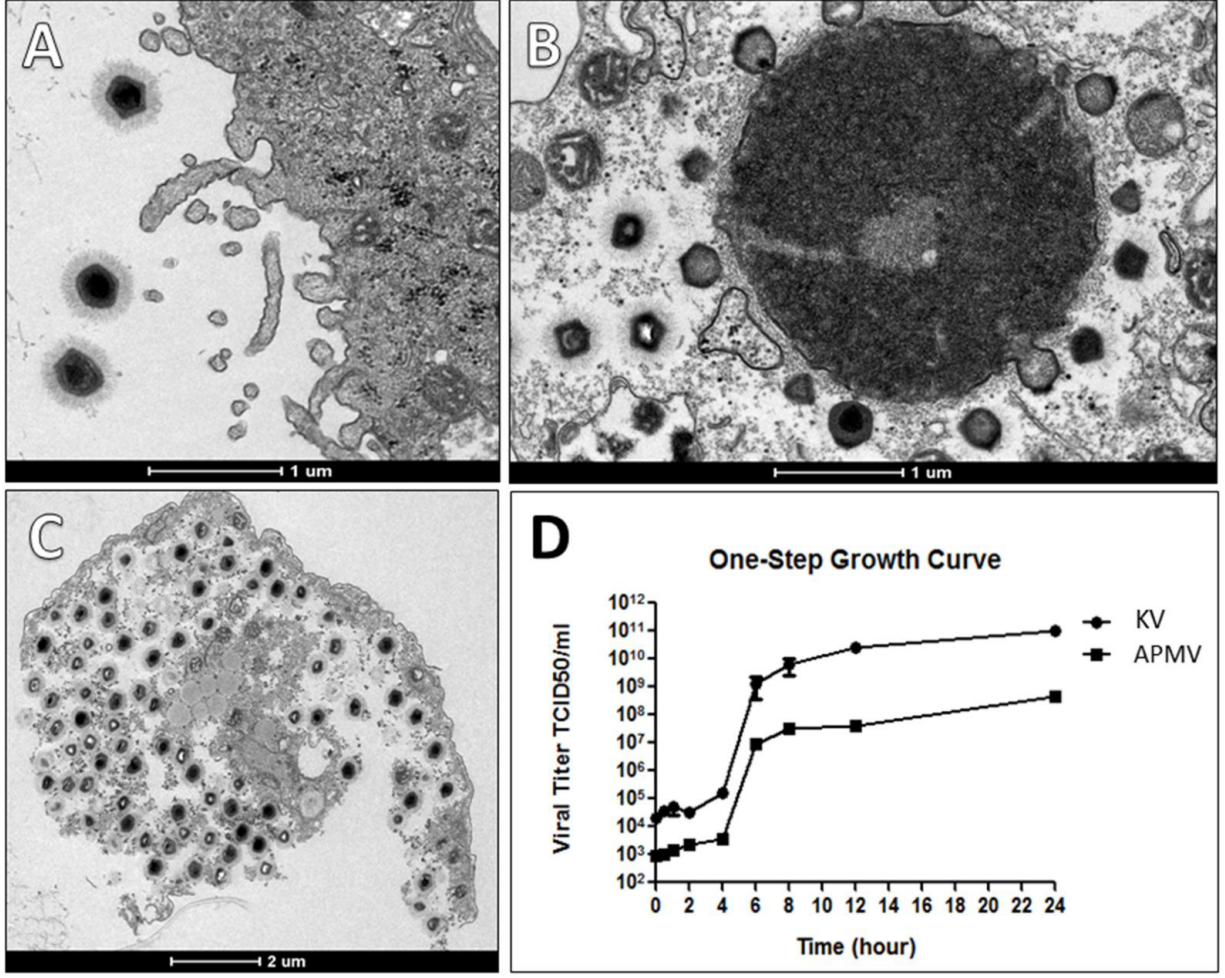
580

581

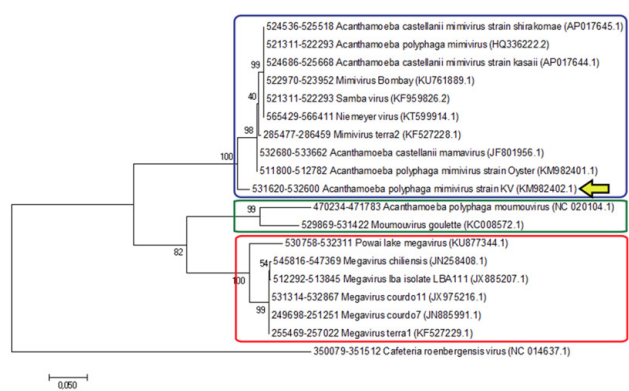
582

583

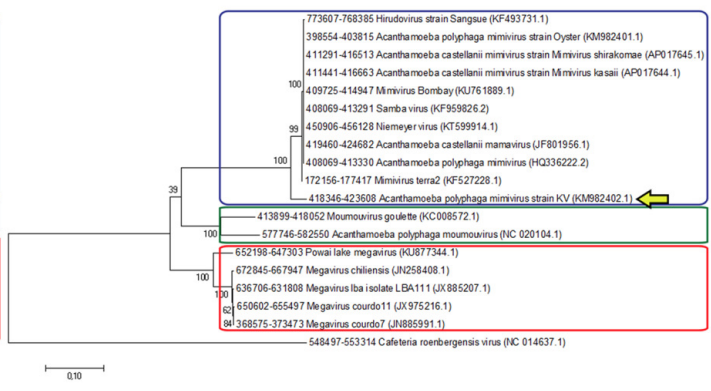


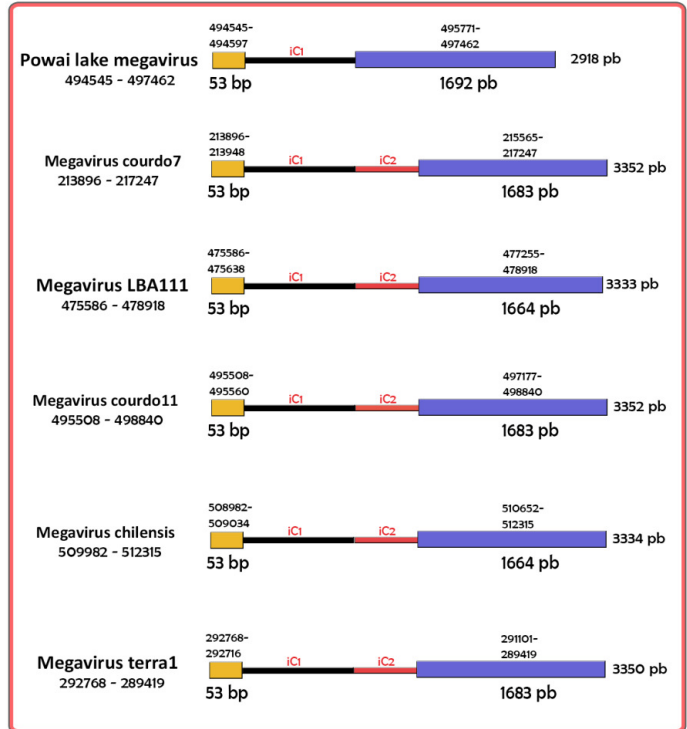
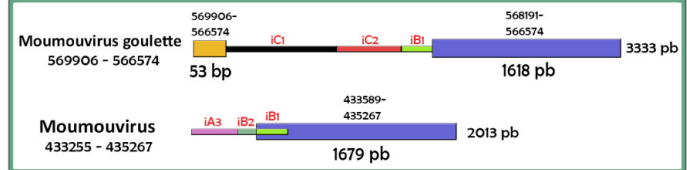
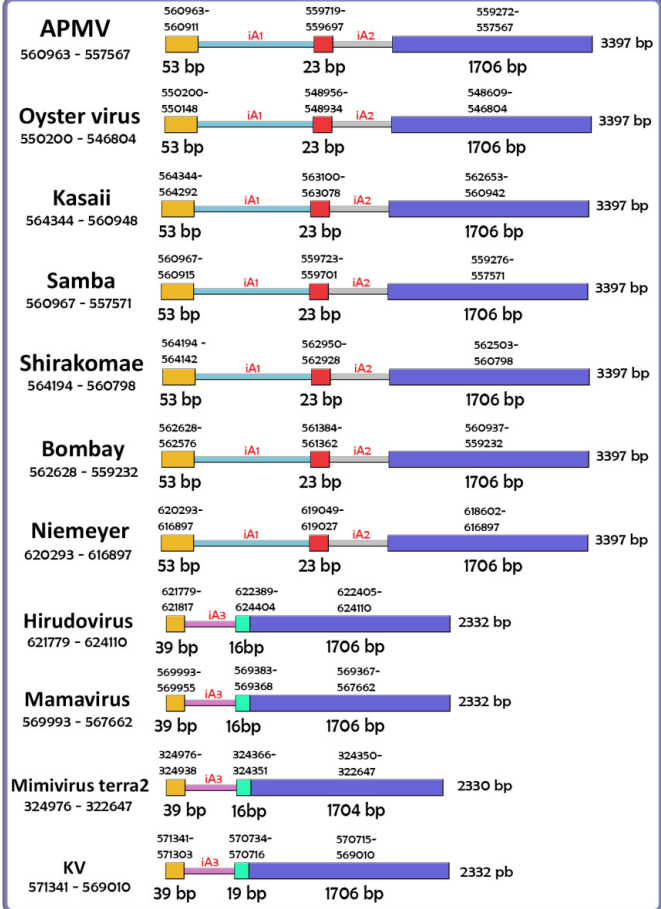


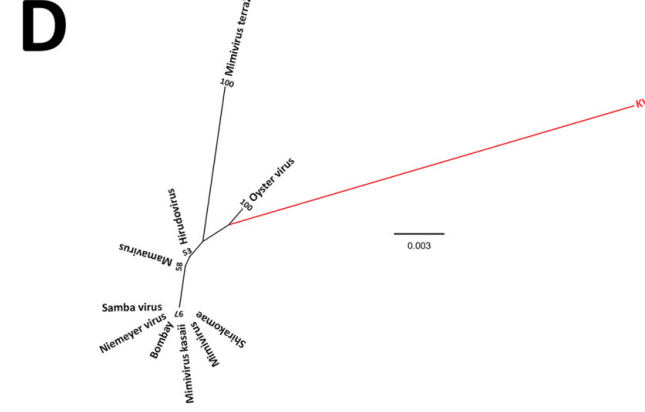
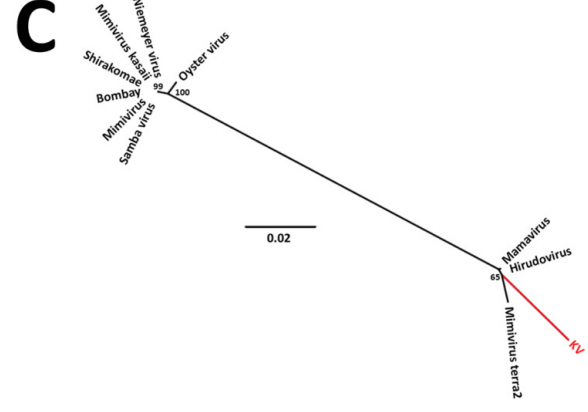
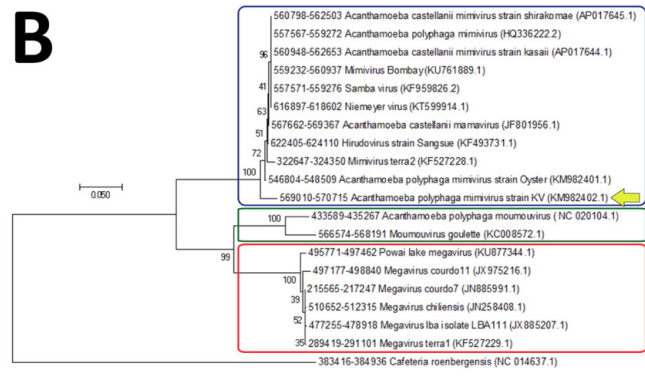
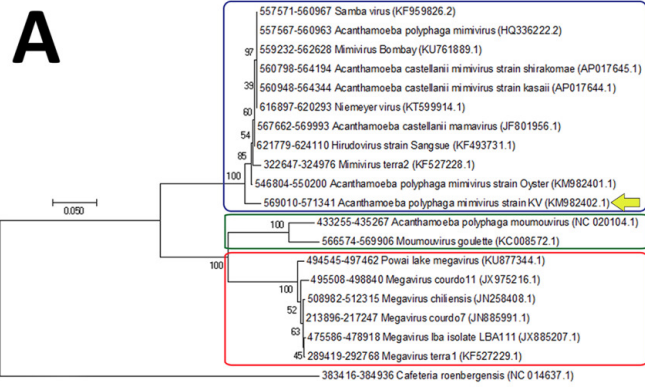
A



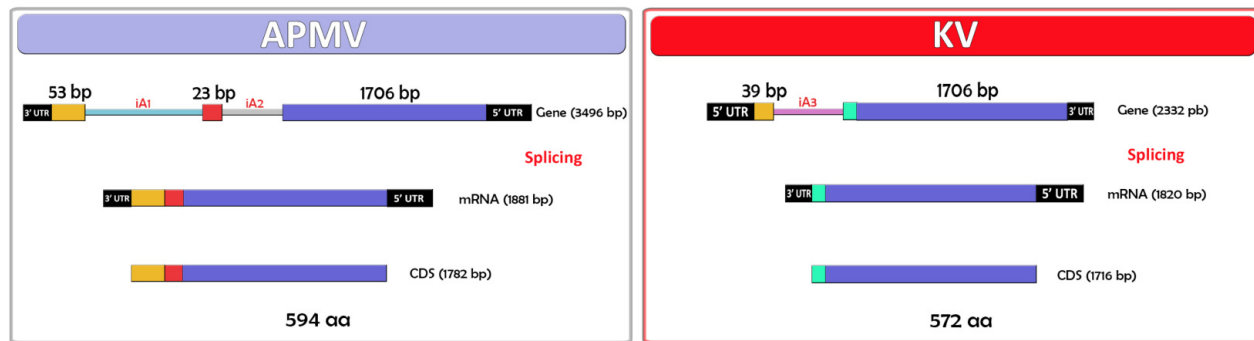
B







A



B

```

#AEMV  MAGGLQLWA YGAQDVYLTG NPMITFFKVV YRRHTNFAVE SIEQFFGGNL GFGKSSAEI NRSGLITQV FLKVTLPEVR YCGDFTNPGH VEFANVRNIG HAIVEETELE IGGSPIDKHY GDWLQIQQDV SSSKDHEKGL ARMLGDVPEL TSISTLSNDV
#KV    ----- --MITFFKVV YRRHTNFAVE SIEQFFGGNL GFGKSSAEI NRSGLITQV FLKVTLPEVR YCGDFTNPGH VEFANVRNIG HAIVEETELE IGGSPIDKHY GDWLQIQQDV SSSKDHEKGL ARMLGDVPEL TSISTLSNDV

#AEMV  PDNTVLKPSY TLYVPLQFYF NRNGLALPL IALQYHQVRI YVKFRQADQC YIASDAFKSG CGNLQLDDVS LYVNYVFLDT EERRRPAQVS HEYLIQLQF TGEESAGSSN SAKYKLNPNH PVKAIYWTK LQNYQGGKFM TYDPVCWENA RENAAKLLLL
#KV    PDNTVLKPSY TLYVPLQFYF NRNGLALPL IALQYHQVRI YVKFRQADQC YIASDAFKSG CGNLQLDDVS LYVNYVFLDT EERRRPAQVS HEYLIQLQY TGEESAGSSN SAKYKLNPNH PVKAIYWTK LQNYQGGKFM TYDPVCWENA RENAAKLLLL

#AEMV  AQYDLDDWGY FQEPGGYECE GNDGRSYVGD CGVQYTAVDP SNPSEEPSYI FNDTTAEAF DGSLIGLKA PCVPLKRNK DVLDKDKVEG IIRIHTDFEN DRMKYPEVEK ITRNDLTLHD LSVPIISKYDV DNRVDYIKKF DVTWQHNNF GLLIDGSGNF
#KV    AQYDLDDWGY FQEPGGYECE GNDGRSYVGD CGVQYTAVDP SNPSEEPSYI FNDTTAEAF DGSLIGLKA PCVPLKRNK DVLDKDKVEG IIRIHTDFEN DRMKYPEVEK ITRNDLTLHD LSVPIAKYDV DNRVDYIKKF DVTWQHNNF GLLIDGSGNF

#AEMV  THEAELQLNG QPRQSKRGGI WYDVTNPTVH HTKSPRDGVN VFSFALNPEE HQPSCTCNFS RIDTAQLNLW FQHTNHKFA DVFADNDNKV LIFAVNYNVL RMLSGMAGLA YSN*
#KV    THEAELQLNG QPRQSKRGGI WYDVTNPTVH HTKSPRDGVN VFSFALNPEE HQPSCTCNFS RIDTAQLNLW FQHTNHKFA DVFADNDNKV LIFAVNYNVL RMLSGMAGLA YSN*
    
```

Review

Poxvirus Host Range Genes and Virus–Host Spectrum: A Critical Review

Grazielle Pereira Oliveira [†], Rodrigo Araújo Lima Rodrigues [†], Maurício Teixeira Lima [†],
Betânia Paiva Drumond and Jônatas Santos Abrahão ^{*}

Laboratório de Vírus, Departamento de Microbiologia, Instituto de Ciências Biológicas,
Universidade Federal de Minas Gerais, Belo Horizonte, Minas Gerais 31270-901, Brazil;
graziufmg@yahoo.com.br (G.P.O.); rodriguesral07@gmail.com (R.A.L.R.);
maurili15@hotmail.com (M.T.L.); betaniadrmond@gmail.com (B.P.D.)

^{*} Correspondence: jonatas.abrahao@gmail.com; Tel.: +55-31-3409-2766

[†] These authors contributed equally to this work.

Received: 20 September 2017; Accepted: 6 November 2017; Published: 7 November 2017

Abstract: The *Poxviridae* family is comprised of double-stranded DNA viruses belonging to nucleocytoplasmic large DNA viruses (NCLDV). Among the NCLDV, poxviruses exhibit the widest known host range, which is likely observed because this viral family has been more heavily investigated. However, relative to each member of the *Poxviridae* family, the spectrum of the host is variable, where certain viruses can infect a large range of hosts, while others are restricted to only one host species. It has been suggested that the variability in host spectrum among poxviruses is linked with the presence or absence of some host range genes. Would it be possible to extrapolate the restriction of viral replication in a specific cell lineage to an animal, a far more complex organism? In this study, we compare and discuss the relationship between the host range of poxvirus species and the abundance/diversity of host range genes. We analyzed the sequences of 38 previously identified and putative homologs of poxvirus host range genes, and updated these data with deposited sequences of new poxvirus genomes. Overall, the term host range genes might not be the most appropriate for these genes, since no correlation between them and the viruses' host spectrum was observed, and a change in nomenclature should be considered. Finally, we analyzed the evolutionary history of these genes, and reaffirmed the occurrence of horizontal gene transfer (HGT) for certain elements, as previously suggested. Considering the data presented in this study, it is not possible to associate the diversity of host range factors with the amount of hosts of known poxviruses, and this traditional nomenclature creates misunderstandings.

Keywords: *Poxviridae*; network; host range genes; horizontal gene transfer; evolution

1. Introduction

Poxviruses are among the best known and most feared viruses. The *Poxviridae* family is currently divided in two subfamilies, named *Entomopoxvirinae* (insect-infecting viruses) and *Chordopoxvirinae* (vertebrate-infecting viruses), wherein the first is composed of three genera, and the latter contains 10 genera, in addition to two viral species that have yet to be classified into each subfamily [1]. While the entomopoxviruses have been poorly investigated over the years, the chordopoxviruses are among the most studied groups in virology, due to the medical and veterinary relevance of many of their members. Among the chordopoxviruses, the *Variola virus* (VARV_abbreviations are shown in Supplementary Table S1) is one of the most well-known species. VARV is the agent of smallpox, a disease that has plagued humanity for centuries, until it was considered eradicated by the World Health Organization in 1980 after a successful global vaccination and surveillance campaign [2–4]. Other chordopoxviruses, such as vaccinia virus (VACV), cowpox virus (CPXV) and monkeypox virus

(MPXV), are responsible for several outbreaks of exantematic diseases around the world, both in humans and other animals (e.g., bovines and equids), and are considered emergent zoonotic viral diseases [5,6]. Furthermore, studies with poxviruses have been pivotal for the advancement of other areas of knowledge, especially in cell biology, vaccinology, and virotherapy, where it was possible to elucidate many important metabolic pathways for immune response and the development of different strategies of immunization against infectious diseases [7–10].

The *Poxviridae* family consists of large double-stranded DNA viruses, which replicate entirely in the cytoplasm of host cells [11]. The poxviruses have a complex structure and an extensive linear genome ranging from 128 to 365 kbp (Genera *Parapoxvirus* and *Avipoxvirus*, respectively), which code for over 200 genes [12–14]. *Chordopoxvirinae* is divided in two clusters that are well-resolved phylogenetically. The first of the two clusters corresponds to the *Orthopoxvirus* (OPV) genus. The second cluster formed by the genera *Yatapoxvirus*, *Leporipoxvirus*, *Capripoxvirus*, *Cervidpoxvirus*, and *Suipoxvirus* forms a sister clade to orthopoxviruses, and the former can be classified as “clade II” poxviruses [15,16]. The origin and evolution of poxviruses are still blurred. Although there is some strong evidence suggesting that these viruses emerged thousands of years ago, their genome has evolved through the gain and loss of genes, especially through gene duplication and horizontal gene transfer (HGT) [15–17]. Many of the genes present in the poxvirus genome are not essential to viral replication in cell culture, but are important to the modulation of the host antiviral response, and thus are considered virulence genes [18,19]. Some of these genes impact viral replication only in a set of cell lineages that originated on different tissues or host species. These genes act on poxvirus-specific differences in tropism and host range, and have been referred to as host range genes [18–20]. All poxviruses are predicted to encode a unique collection of host range genes; however, only the genera *Orthopoxvirus* and *Leporipoxvirus* have been observed in many of the biological studies so far [13]. Known poxvirus host range genes are currently grouped into 12 distinct classes, some of which have only one gene (e.g., K3L, E3L, K1L, others), and others exhibiting many members (e.g., serpins, C7L family, TNFR2 family, others), which likely result from lineage duplication events [20]. Some of these factors were functionally characterized using in vitro models and gene knockout analysis, which is associated mostly with the manipulation of diverse cellular targets, including cellular kinases and phosphatases, apoptosis, and many antiviral pathways [19,21]. In the absence of these genes, viruses lose the ability to infect certain cell lineages, whereas infection is efficiently established in the presence of the genes. Several in vivo investigations showed that some factors impact viral pathogenicity, although the model animals were still infected [22–24].

Historically, these genes have been referred to as host range genes when considering only the cells as hosts, i.e., not considering the animals that are actually infected by the viruses [18–20]. Would it be possible to extrapolate the restriction of viral replication in a specific cell lineage in an animal, which is a far more complex organism? Some works have suggested a direct association between the diversity of host range factors and the amount of host species for different poxviruses, but this association is still under debate [18,19]. In view of these intriguing questions, we sought to establish the natural hosts for the poxviruses officially assigned to viral species and recognized by the International Committee on Taxonomy of Viruses (ICTV) [1]. Based on the available data so far, we performed an extensive search for different host range genes according to those that were described previously [20], reviewing the main features of each class of host range factors. In light of the data presented here, we could not associate a diversity of host range factors with the amount of hosts, which lead us to discuss the assertiveness of the term “host range genes”. Finally, we analyzed the evolutionary history of these genes, reaffirming the occurrence of HGT for some elements, as previously suggested [16,17,20].

Among the nucleocytoplasmic large DNA viruses (NCLDV), the poxviruses are those with the widest host range, which are able to infect different groups of insects and vertebrates [25]. However, when we look specifically at each member of the *Poxviridae* family, the host spectrum is variable, wherein some viruses can infect a large range of hosts [25–27], while others are restricted to only one host species [3,28,29]. To have a clear view of the host range of poxviruses, we performed an

extensive search to define the natural hosts for each member of the *Poxviridae* family, and we presented this relationship in a network graph. In this analysis, we searched only the hosts for viruses that are currently classified into viral species by the ICTV, since it presents the most up-to-date dataset of known viral species, and gathers and reflects the diversity of the circulating viruses in nature. We defined hosts as those organisms in which consistent evidence was available related to viral detection in a given species by isolation, serology, and molecular detection. In this view, we seek to associate hosts at the lowest possible taxonomical level.

The ICTV currently recognizes a total of 71 species of poxvirus, with 30 belonging to the *Entomopoxvirinae* subfamily, and 41 to the *Chordopoxvirinae* subfamily (Supplementary Table S2). The known entomopoxviruses infect Pterygota subclass members (winged insects) from the orders Diptera, Coleoptera, and Hymenoptera, but mainly Lepidoptera and Orthoptera (Figure 1).

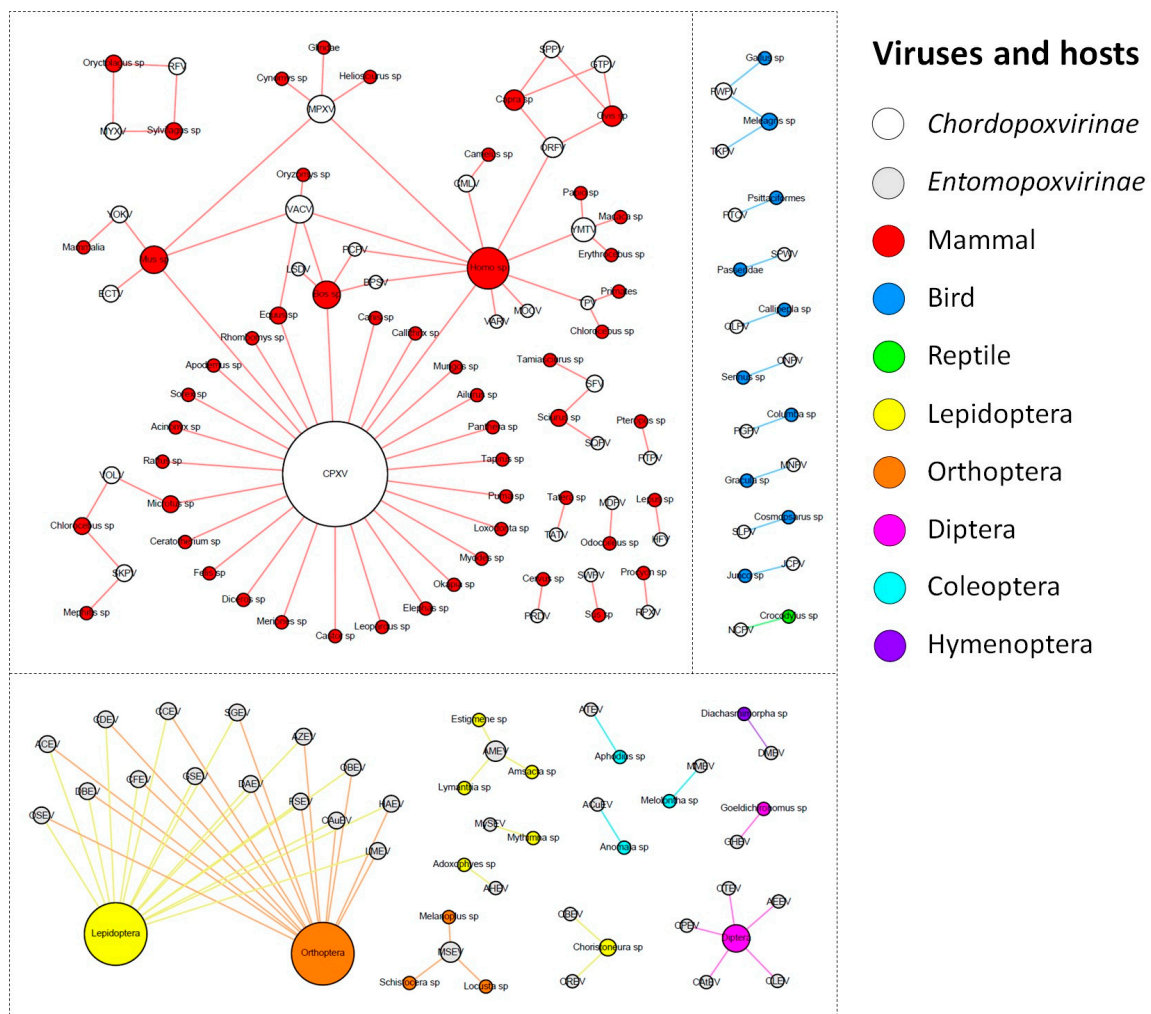


Figure 1. Poxvirus host network. The poxvirus species and their hosts (taxonomic level of genus or higher) are depicted in the graph. The network layout was generated by applying a force-based algorithm, followed by manual rearrangement of the nodes. The full names of the viral species are listed in Supplementary Table S1.

For most of the viral species of this group, it was not possible to determine the virus hosts beyond the order taxonomic level. For the remaining viral species, we determined the hosts at the genus or species level. Corroborating the previous descriptions in the literature, entomopoxviruses tend to exhibit a fairly narrow host range, but the species of *Betaentomopoxvirus* genus can infect

distant hosts, which suggests that large host shifts can occur. This view of entomopoxvirus hosts is likely a consequence of the lack of host range studies that have been performed on these viruses [30,31]. Recently, a study showed that genes involved in lateral gene transfer (LGT) events among entomopoxviruses species conferred a possible adaptation to both specific and distantly related hosts [32]. It is possible that with the advancement of metaviromic approaches, we will be able to move forward in our comprehension of the diversity and host range of entomopoxviruses, uncover new viruses in different and unexplored hosts, and therefore improve the network presented here [33].

In contrast, the chordopoxviruses are the targets of intense investigation because of the clinical relevance of many of its members to humans and domesticated animals of economic importance [34–38]. The known chordopoxviruses infect mammals (29 viral species), birds (10 viral species), and reptiles (one viral species), and viruses do not cross this host barrier, i.e., viruses infecting mammals do not infect birds, and vice versa (Figure 1). Interestingly, an avipoxvirus was isolated once from a terminally ill rhinoceros in 1969 and characterized as an atypical fowlpox virus, thus raising questions about the host restriction of avipoxviruses [39]. However, since it was an isolated case and there are no other descriptions of an avipoxvirus infecting a non-avian host, it is still uncertain whether these viruses can efficiently cross the host barrier. Differently from entomopoxviruses, there were only four chordopoxviruses for which we could not define the hosts at the genus or species level ($4/40 = 10\%$). One of these viruses is the yokapox virus (YOKV), a poxvirus isolated from a mosquito pool over 40 years ago whose natural host is probably a mammal. However, further investigation is required to better understand the biology of this virus [40]. Similar to YOKV, it is possible that other hosts are associated with known chordopoxviruses, but these relationships need to be further investigated. Most of the chordopoxviruses are associated with only one host genus ($25/40 = 62.5\%$), which suggests a restricted host range for these viruses (Figure 1). Interestingly, there is a trend among large DNA viruses to exhibit a narrow host range, but some viruses can infect a broader range of hosts, such as VACV and MPXV, which have been associated with outbreaks involving humans and cattle. For these viruses, it is likely that rodents act as reservoir hosts of these viruses [41–43]. The CPXV is the most prominent member in the group, since it presents by far the widest host spectrum among the poxviruses, being able to infect at least 27 different groups of hosts, including humans, cattle, equids, and felines (Figure 1). Recent data suggests that *Cowpox virus* is comprised of at least five different viral species [44]. Assuming this, it is likely that the hosts defined here of what we now consider as *Cowpox virus* are actually a host compilation of hosts for at least five distinct viral species.

After the eradication of smallpox in 1980, several poxvirus outbreaks have been reported around the world that are related to different viruses, driving a huge effort to identify these viruses and their possible natural and reservoir hosts [45–48]. At least 11 poxvirus species have been known to cause human infections to date: CPXV, VACV, MPXV, VARV, *Molluscum contagiosum virus* (MOCV), *Orf virus* (ORFV), *Camelpox virus* (CMLV), *Yaba monkey tumor virus* (YMTV), *Tanapox virus* (TPV), *Bovine papular stomatitis virus* (BPSV), and *Pseudocowpox virus* (PCPV) [49,50] (Figure 1). Among them, only VARV and MOCV have humans as the sole host, while the other poxviruses are emerging zoonoses that affect different groups of animals, such as cattle, rodents, primates, and others (Figure 1) [3,28]. The main clinical feature of poxvirus infection is skin lesions, which can vary from small pearly papules in MOCV infection to large crusts and generalized pustules in VARV infection. However, other symptoms are common, including fever, headache, and rash. Similar clinical signals are verified in other animals infected by these viruses. Cases of human infections by some poxviruses, such as VACV, CPXV, and MPXV, have been constantly reported [3,26,28,35,51]. Differently, skin lesions related to CMLV have only been observed during the last few years, which opens important questions regarding the expanding host range of this virus [52]. The *Parapoxvirus* genus comprises four viral species that are distributed worldwide and mainly infect domestic ruminants and a broader host range, which includes camels, seals, deer species, and humans [53]. In this context, it is possible that other known poxviruses might affect humans. An example of this is the isolation of a strain of *Ectromelia virus* (ECTV) from the throat swabs of an affected man in China during an outbreak of erythromelalgia [54]. It is still

uncertain whether this virus is a true human pathogen, since ECTV has only been found in *Mus* sp. (Figure 1), causing mousepox disease [55]. If this association is confirmed, it will be another example of host range expansion in poxviruses. Furthermore, one must have in mind that a virus can infect a host without causing any disease. Although the majority of poxviruses isolation reports are related to any clinical manifestation in a given host, some viruses have already been identified in known hosts without presenting any clinical manifestation, such as the group 1 of Brazilian VACV strains [41]. Moreover, there are descriptions of poxvirus detection in cattle, but the hosts had no clinical signals [56]. There is also a description of the isolation of a parapoxvirus from an apparently healthy red deer in the Bavarian Alps [57], which reinforces that poxviruses are related to hosts exhibiting no disease. In this context, we might expect that the network presented here is likely more interconnected, but more recurrent data regarding poxvirus' detection in healthy organisms will be needed.

Based on currently available data, it appears that certain poxviruses have a broad host range, such as VACV, MPXV, and CPXV. However, these viruses are the most studied within the *Poxviridae* family, which is the reason why we recognize more host species for them compared with other viruses, and especially compared with entomopoxviruses. In contrast, other viruses that are also the targets of intense research exhibit a very restricted host range, as is the case with VARV and MOCV (both infect only humans). The reason for such a difference is still a mystery, but some studies have suggested that the answer might lie in the genetic diversity between those viruses, namely, the diversity and abundance of the referred host range genes [18,19].

2. Diversity and Abundance of Host Range Factors Are Not Proportional to the Diversity of Hosts in *Poxviridae*

Host range genes are virulence genes of poxviruses, which code for factors that influence the virus' tropism for certain cell lineages [18]. Historically, the first of these genes to be described belonged to the serpin superfamily (serine protease inhibitors), which was initially found in the rabbitpox virus over 60 years ago, where it was verified in "white pock" mutants observed in the chorioallantoic membrane. It was associated with the viral loss of the ability to replicate in some cell lineages, and posteriorly mapped to the SPI-1 gene [58–62]. Thereafter, other genes that impacted the replication of poxviruses in some cell types were described, reiterating the definition of "host range genes" [21].

There are currently 12 groups of known host range factors. These factors are made up of a few dozen genes that are heterogeneously distributed within the *Poxviridae* family, and no single viral host range ortholog common to all poxvirus genomes has been identified [19–21]. Traditionally, the discovery of these genes has been the result of in vitro analysis, with targeted knockout genes in which mutant viruses exhibited deficiencies in replication in a subset of cells that are permissive to parental viruses [63,64]. In contrast, in vivo assays have shown that the absence of these genes does not impair viral infection in the animal model, but does affect the degree of pathogenicity of the virus, even though in vivo assays are lacking for the majority of the host range genes [65,66]. With the advancement of molecular techniques, some genes in different poxviruses have been suggested as host range genes due to their homology compared with other previously described genes, i.e., K3L, C7L and m63r, E3L, M11L/F1L, ANK-F-box CP77, and T5, but the function of the putative genes lacks experimental validation [20].

The function of some host range genes is already known, but some functions remain obscure. Generally speaking, the products of these genes interact with antiviral and/or anti-inflammatory host pathways, including the interferon (IFN), apoptosis, and inflammasome pathways [21]. Among the known and predicted host range genes found in poxviruses, the most studied are the E3L and K3L VACV genes. E3L encodes a protein that contains a C-terminal double-stranded RNA-binding domain, which acts as an inhibitor of protein kinase R (PKR) and 2'-5' oligoadenylate synthase, likely by preventing activation by dsRNA and induction by IFN [67–70]. Similar to E3L, the K3L protein also acts by inhibiting the PKR activity, since it is homologous to the S1 domain of the α subunit of eukaryotic translation initiation factor 2 (eIF2), therefore acting as a pseudosubstrate and competitive

inhibitor of the kinase protein [71–75]. Another well-known host range gene is SPI-1, but it is possible that other serpins also contribute to poxvirus host range genes, including *Orthopoxvirus* SPI-2/CrmA and SPI-3, three serpins in the *Leporipoxvirus* genus, and five serpins in the *Avipoxvirus* genus [76]. The serpins in the poxvirus counteract the host response to viral infection, acting on different targets of inflammation, coagulation, and complement activation pathways [76]. Some poxviruses also present genes coding for proteins containing short complement-like repeats (SCRs)—the B5R/VCP family—which interacts with a yet to be identified cellular surface molecule that leads to the activation of Src kinase, prompting actin polymerization and the enhancement of cell-to-cell virus spread [77,78].

Poxviruses have many proteins with ankyrin repeat domains (ANK), most of which contain an F-box domain at their carboxy-terminal region. A poxvirus ANK protein has been identified as a host range factor, named CP77 or CHOhr, since its absence in VACV led to a restriction of replication in a Chinese hamster ovary cell line [79]. At the molecular level, CP77 inhibits nuclear factor KB (NF-KB) activation, likely by the interaction with the ANK repeats in the p65 subunit of NF-KB and the F-box of the cellular SCF ligase complex [80]. Other ANK proteins might have similar functions, but further evidence is required. Similar to these, other genes/families of genes have already been identified as host range genes, but their molecular mechanism is not fully elucidated, such as p28/N1R, and the C7 family. The C7 family contains C7L and C4L, which were initially identified in the VACV genome, and other three C7L-related genes that were found in leporipoxviruses, M062R, M063R, and M064R [20,81].

Classes of host range genes were initially identified in leporipoxviruses, and their presence was further described in other poxviruses [21]. The T2 gene found in *Myxoma virus* (MYXV) is a homolog of tumor necrosis factor receptor II (TNFR2), in which the resulting protein acts by neutralizing the host TNF, thus impairing the inflammation response [82,83]. Homologs of T2 are found in some orthopoxviruses, in which they are called cytokine response modifiers (crm) [20,84], and comprise the TNFR2 family of host range genes. The T4 and M11L/F1L are families of genes that inhibit apoptosis and were initially described in MYXV and VACV, but the precise molecular mechanism is not completely clear [20,85]. Finally, the M13L gene found in MYXV contains an N-terminal pyrin domain, while the M1 in MYXV was shown to inhibit caspase-1 activation and thus the processing of mature IL-1 β and IL-18 in human THP-1 cells, impairing the inflammatory response [86].

We reviewed the complete genomic sequences available at the National Center for Biotechnology Information database (<https://www.ncbi.nlm.nih.gov>) for 38 identified and putative homologs of poxvirus host range genes, and updated this gene data with new deposited poxvirus sequences. The searches for poxvirus host range gene homologs were performed using Basic Local Alignments Search Tools—Protein (BLASTP, <https://blast.ncbi.nlm.nih.gov/Blast.cgi>). Protein sequences of previously identified host range genes were used as reference sequences for BLASTP analyses (Supplementary Table S3). For the analysis, putative homologs were considered inside of a fixed cutoff threshold for all genes (E-value ≤ 0.0001 ; Ident $\geq 30\%$; Coverage $\geq 40\%$). Using the obtained data, a circle plot was created (Figure 2), indicating the presence of homologous genes in different species and samples of poxviruses.

Analyzed homologs are found in the genera *Orthopoxvirus* (28), *Leporipoxvirus* (14), *Cervidpoxvirus* (13), *Suipoxvirus* (12), *Capripoxvirus* (11), *Centapoxvirus* (11), *Yatapoxvirus* (9), *Avipoxvirus* (3)—including Shearwater poxvirus (ShWPV) and Penguin poxvirus (PNGV)—in the unassigned species *Pteropoxvirus* (1), and in the unassigned samples NY_014 poxvirus (NY_014) (26), Murmansk poxvirus (MMPV) (17), Cotia virus (COTV) (13), Yaba-like disease virus (YLDV) (8), BeAn58058 (BeAn) (5) and Eptesipoxvirus (ETPV) (3). Within the estimated cut-offs, homologs were not found in the *Crocodylidpoxvirus*, *Molluscipoxvirus*, or *Parapoxvirus*, nor all of the entomopoxviruses genera. It is noteworthy that the CPXV species has up to 27 host range gene homologs; however, when we analyze the different isolates as separate clades, groups A (27), B (26), D (25), and E (25) have very close numbers of homologs, while group C (14) presented considerably fewer homologs. On the other hand, phylogenetic analyses of various host range genes show that different clades of CPXV are sometimes grouped with another

OPV species rather than each other. These data are in accordance with the current hypotheses about diversity within CPXV species (Figures 3–5, Supplementary Figures S1 and S2) [44]. The genes that have homologs with the highest range of species are E3L, C7L, and m62r (C7L Family) with 25, 24, and 19 viral species, respectively (Figure 2). One Ank-box homolog and the F1L are unique to the genus *Orthopoxvirus* (Figure 2). M11L and m63r (C7L Family) were found only in *Leporipoxvirus*. M11L and F1L-encoded proteins were related to the cellular, prosurvival Bcl-2 family, but there was not any primary sequence similarity in our searches and previous works [20]. Our data corroborates with the previously described literature concerning the distribution of host range families in poxvirus genera, since orthopoxviruses and clade II poxviruses contain the majority of homologs (Figure 3; Supplementary Figures S1 and S2) [17,20,21]. One factor that could influence this is the concentration of studies in the OPV and clade II viruses. Thus, the distantly related poxviruses likely contain different genes that are important for their host range, but have not yet been identified.

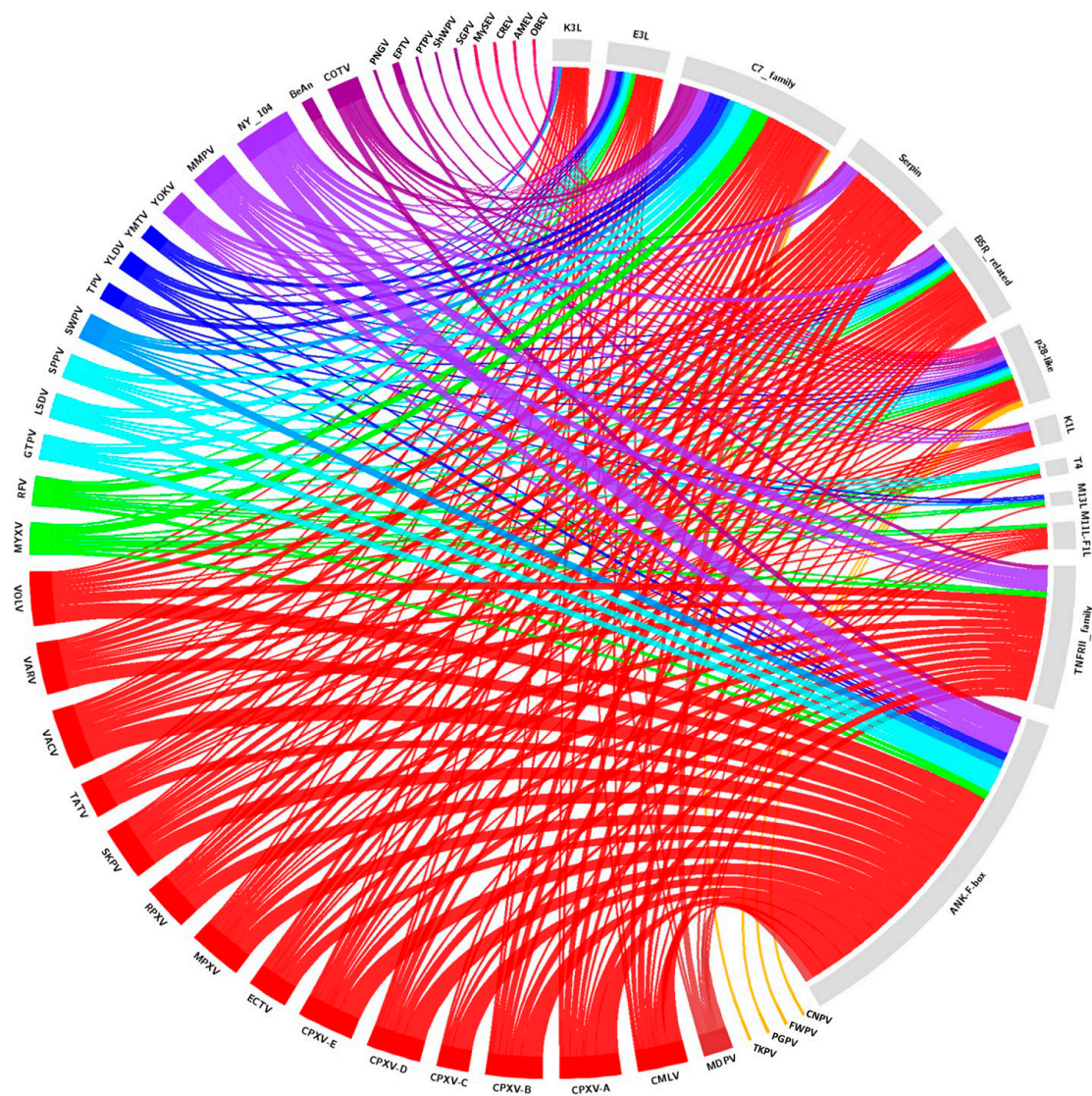


Figure 2. Circos plot representing the amount and diversity of host range genes among the poxviruses. Genomic information was available at the NCBI database, following the established criteria (E-value ≤ 0.0001 ; Ident $\geq 30\%$; Coverage $\geq 40\%$). The different colors stand for the genus of poxviruses and the family of host range genes. The full names of the viruses are listed in Supplementary Table S1.

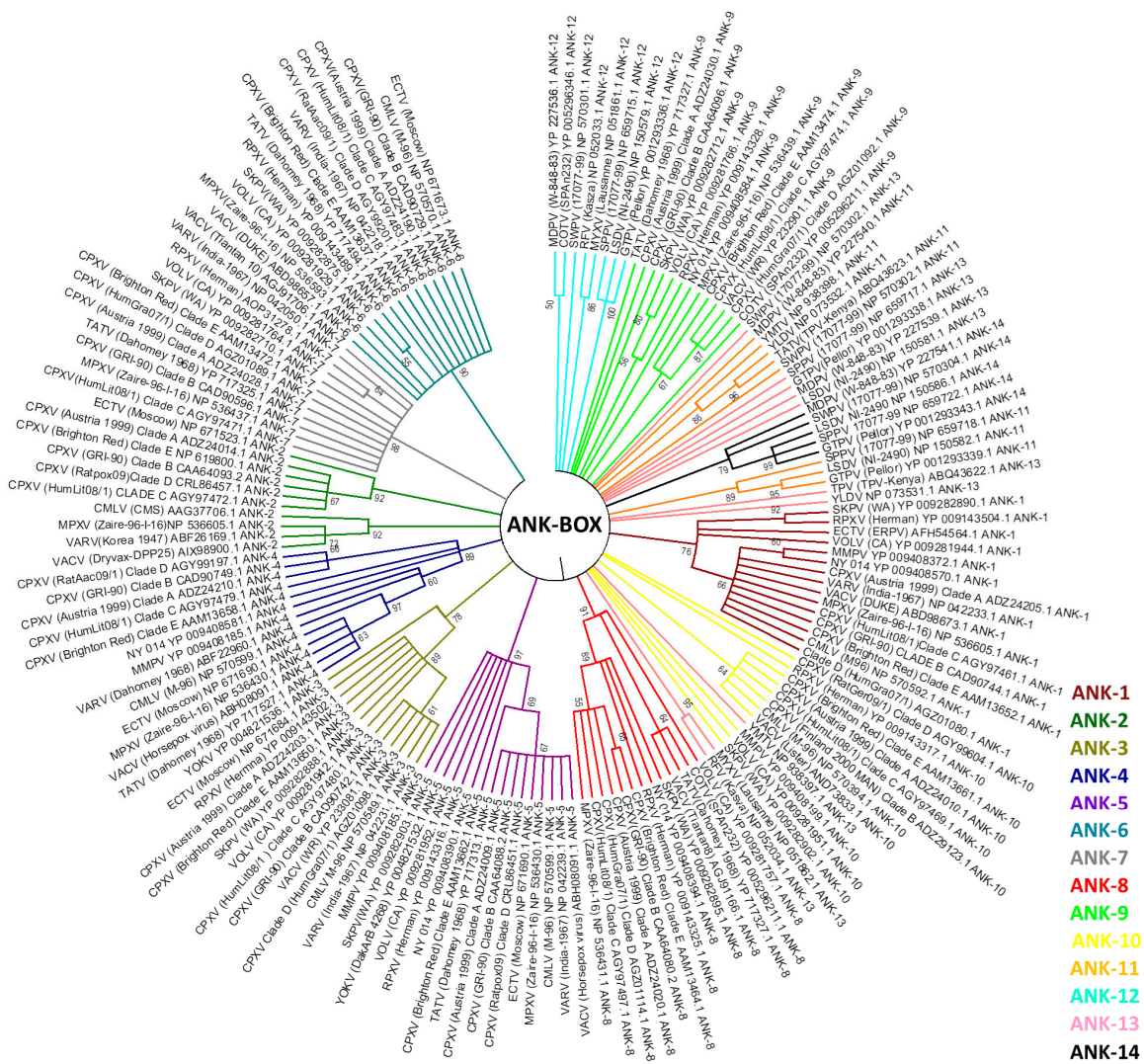


Figure 3. Presence of Ank-box host range gene projected onto a tree showing the phylogenetic relationships of representative poxvirus strains. The tree was generated from a multiple protein sequence alignment of the indicated sequences using the maximum likelihood method. A bootstrap of 1000 was used, and support >50 is indicated above the branches.

Another important point to be addressed is that no clear correlation was observed in the host range size versus the host range gene homologs’ diversity and quantity. For instance, *Parapoxvirus* (ORFV, PCPV, BPSV, *Parapoxvirus of red deer in New Zealand*—PRDV) is associated with a host range that is equal to or larger than other poxvirus groups, which have a wide range of host gene homologs (Figures 1 and 2). However, parapoxviruses have a strict range of permissive cells, including primary ovine and bovine fibroblasts [18]. Two other viruses that clearly show the absence of direct correlation between the host range and host range genes are MOCV and VARV. Both viruses have the narrowest tropism of any poxvirus, and use humans as exclusive natural hosts [18]. The MOCV genome lacks more than 80 genes common to most orthopoxviruses, including VARV [87]. These genes have a functional role in the suppression of the host response to viral infection, and their absence may be related to MOCV’s restricted replication in basal keratinocytes of the human epidermis [21,87]. In contrast, VARV’s replication range includes most mammalian cells [18]. Although the VARV host range is remarkably different from other OPVs—such as CPXV, VACV, and MPXV—in terms of their reservoir or zoonotic hosts, in tissue culture cells, these differences disappear, and the host range genes influence this homogeneity within the genus. Although MOCV and VARV only infect humans,

the presence or absence of different host range genes may be related to different means of evolution, and culminate in different pathogenesis, tropism, and immune regulation between both viruses. Ecological aspects of virus–host relationships such as host abundance, environmental influences on the transmission cycle, geographical distribution, and overlapping areas of species may be essential for the dynamics of the host spectrum of a virus. Take for example the globalized geographical aspect of myxomatosis in Australian rabbits, whereby a South American virus infects a European host in a new continent for both species, i.e., virus and host. Taking these aspects into account, the current view of the poxviruses' host range can be highly complex and could contain some biased points. There are plenty of unanswered questions relative to the host range genes and the host spectrum of poxviruses, and ecological and evolutionary perspectives may provide important insights about this.

3. Host Range Genes: An Evolutionary Perspective

The evolution of virulence genes for a certain host is probably influenced by the effectiveness and route of virus transmission, the immune status of the host species, the availability of additional reservoir hosts, intra- and inter-species competition with other viruses, and positive selection for hosts that are more resistant to virus infection [19,88]. The origin of viruses, or at least certain viral groups, is still a mystery. It is possible that some viral groups have a degree of monophyly. The NCLDV group, which includes the family *Poxviridae* as well as other large dsDNA viruses that infect eukaryotes, is a candidate for monophyly [89,90]. In phylogenetic analyses, there is evidence of an ancient origin provided by a topology in which all of the poxvirus homologs cluster together, apart from those of cellular organisms [16,91]. Certain viral-specific genes may be involved in poxvirus evolutionary processes, including some host range genes.

In this study, we review this evidence in three aspects of host range genes in poxvirus evolutionary biology: (1) the phylogeny of previously identified poxvirus host range genes; (2) possible lateral transfer of host range genes; and (3) evolutionary correlations with other viral groups. We used sequence alignments containing the homologous protein sequences of 38 identified host range genes. A total of 396 completely sequenced poxvirus genomes available in public databases were used to perform phylogenetic analyses. These sequences belong to genera *Avipoxvirus* (8), *Capripoxvirus* (15), *Centapoxvirus* (3), *Cervidpoxvirus* (2), *Crocodylidpoxvirus* (1), *Leporipoxvirus* (64), *Molluscipoxvirus* (5), *Orthopoxvirus* (262), *Parapoxvirus* (17), *Suipoxvirus* (1), *Yatapoxvirus* (4), entomopoxviruses (7), and also unassigned species and isolates (7). Most of the chordopoxviruses genomes are concentrated in the genera *Orthopoxvirus* and *Leporipoxvirus*, although at least one genome is available by genus. The sequence alignment was performed using ClustalW [92] to infer a maximum likelihood phylogenetic tree. In our phylogenetic analyses, the E3L, C7L, and Ank-Box host range genes supported the evolutionary correlation between OPV and clade II poxviruses (Figure 3; Supplementary Figures S1 and S2). Murmansk poxvirus and NY 014 poxvirus samples were closely related to YOKV, which are likely unclassified centapoxviruses [93]. The Cotia virus is grouped within poxvirus Clade II, as described above, and the unknown samples BeAn58058 follow this trend. In addition, ANK repeat proteins were highly abundant in various poxvirus genera. The OPV ANK-box homologs have similarities with those found in YOKV, NY 014 poxvirus, Murmansk poxvirus, and Cotia virus. Clade II Ank-box homologs are present in *Leporipoxvirus* (2 homologs), *Cervidpoxvirus* (4 homologs), *Suipoxvirus* (4 homologs), *Capripoxvirus* (4 homologs), *Yatapoxvirus* (2 homolog), Yaba-like disease virus (2) and Cotia virus (1) (Figure 3).

Between the 14 ANK/F-box homolog genes analyzed, none were similar to ANK, which was described in the literature for avipoxvirus and parapoxvirus. This indicated a distant correlation between these homologs and those of other poxviruses [20]. ANK/F-Box genes probably originated from multiple duplications in all poxviruses groups, and our data suggested that these duplications occurred after the radiation of orthopoxviruses and clade II poxviruses of another family of viruses [20].

The p28/N1R RING zinc finger protein is the most abundant gene family in poxviruses, and has also been identified in other NCLDVs, such as iridoviruses and mimiviruses [94,95]. In our analysis,

p28-like protein homologs are found in most members of the *Chordopoxvirinae* subfamily and in acanthamoeba polyphaga mimivirus (*Mimiviridae*), as previously described [96]. This fact may reinforce the common ancestry hypothesis between both families. The recently discovered chordopoxvirus Salmon gill poxvirus (SGPV), appears to be a distant chordopoxvirus [97]. The p28-like protein homologs of Cotia virus and BeAn58058 form a high bootstrap clade (Figure 4). Despite Eptesipox virus forming a well-supported clade with Pteropox virus, both viruses were isolated from bats, which could suggest an adaptation of p28 to the host [98,99]. However, p28-like protein homologs of entomopoxvirus and mimivirus formed an external clade (Figure 4). Even considering the ancestry of these groups, the sharing of such genes across distinct viral groups might in turn be explained by LGT events [97].

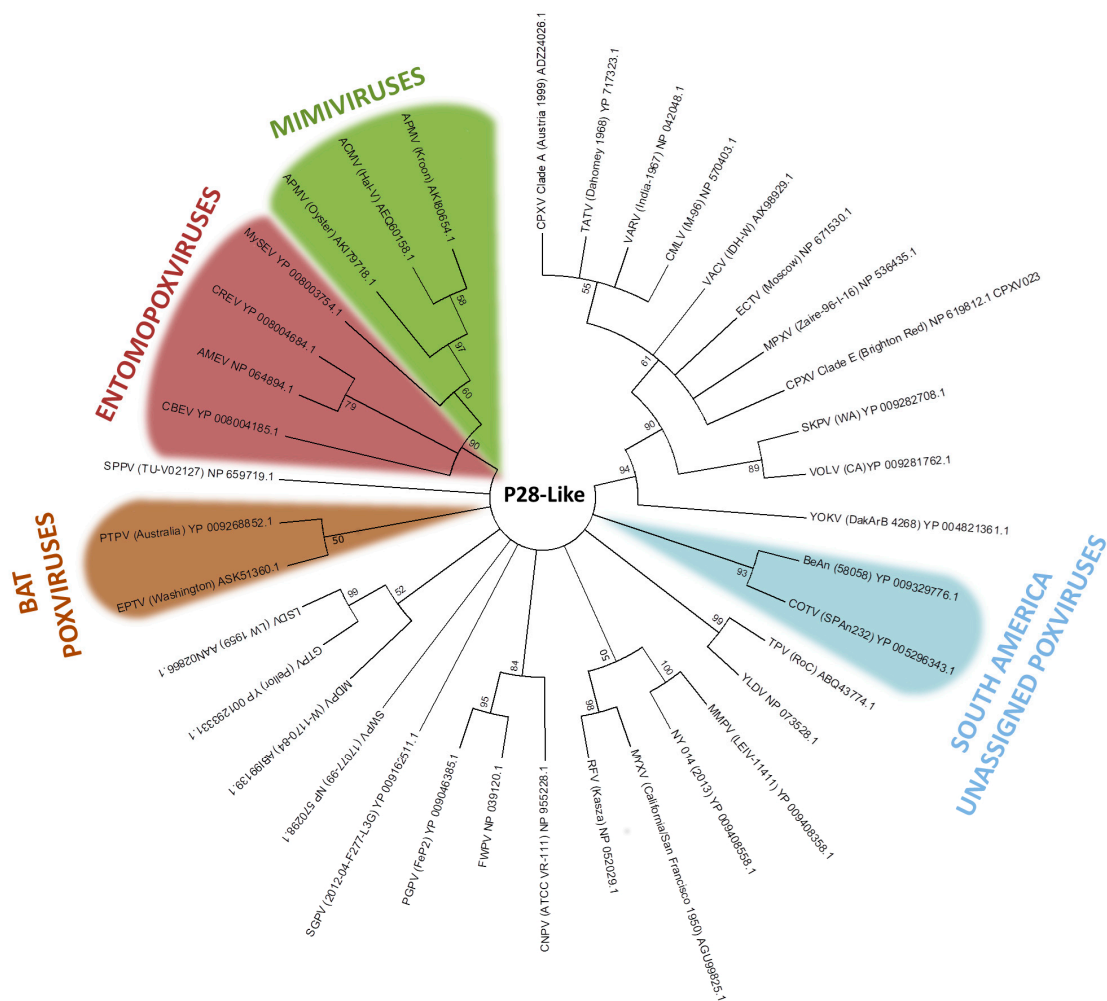


Figure 4. Phylogenetic relationship of p28-like genes. The tree was generated from a multiple protein sequence alignment of the indicated sequences using the maximum likelihood method. A bootstrap of 1000 was used, and support >50 is indicated above the branches.

LGT is an important process in viral evolution, and in pathogenic viruses, this process can often increase their virulence and fitness [16,17,96,100–103]. Poxviruses also express proteins homologous to the vertebrate immune system signaling molecules or receptors, which are encoded by genes that were probably incorporated from the host [91]. Among the host range genes, the serpin family members are potential candidates to LGT, as identified by PSI-BLAST search [15,104]. In addition, the B5R-related genes express CD46-like proteins (30–40% similar with mammal hosts) to control the host complement system [105,106]. Our analyses showed that the B5R-related genes are closely related with the homologs of several mammalian orders (Figure 5).

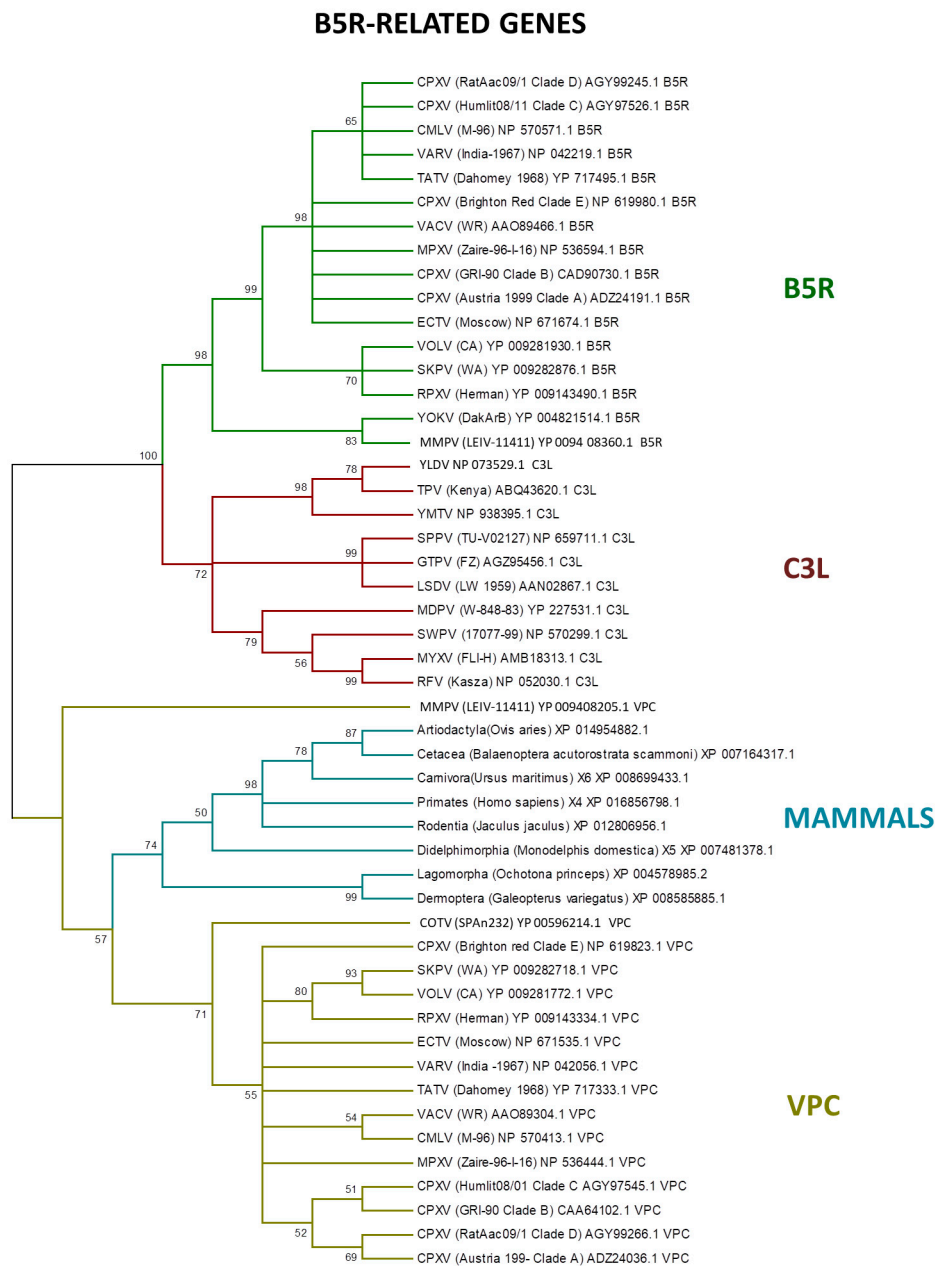


Figure 5. Phylogenetic relationship of poxvirus B5R-related proteins. The tree was generated from a multiple protein sequence alignment of the indicated sequences using the maximum likelihood method. A bootstrap of 1000 was used, and support > 50 is indicated above the branches.

Previous studies indicated that the ancestral B5R/C3L genes faced a duplication event early in orthopoxvirus evolution [20]. Indeed, the B5R gene retained the transmembrane domain, keeping the protein trapped in the external enveloped virion membrane, while the other homologs—VCP and C3L—are secreted, which is an example of neofunctionalization as a different virulence factor by inhibiting the host complement factors [78,107,108].

4. Future Directions

The poxviruses are one of the most intensively studied groups among the virosphere, especially because of their medicinal importance for humans and a large range of domesticated animals. These viruses have been isolated and identified in different groups of animals, both vertebrates and

invertebrates, and it has been tempting to correlate this host spectrum to the amount and diversity of the so-called host range genes [18–20]. Although some host range genes were described in viruses with numerous hosts, such as CPXV, no apparent correlations between the host organisms and the number and diversity of host range genes have been found. Furthermore, the high number of these genes described in VACV, CPXV, and MPXV may be directly related to the large number of studies about these viruses. In addition, viruses with the same host range, such as VARV and MOCV, do not share the same host range genes. On the other hand, the presence of host range genes is better viewed and characterized when referring to the range of cells permissive to viral replication, thus having little effect (if any) on the capacity of a virus to infect an animal host.

The evolutionary origins of poxviruses' host range gene families are likely diverse. Some genes are ancient, and remain conserved in several groups of NCLDV_s, while others probably evolved due to lineage-specific duplications. LGT events are also possible between different viruses and between viruses and their hosts. The description of new poxvirus samples, especially in previously unrelated hosts, such as those recently discovered in bats and fish, can bring new aspects of poxvirus biology and new host range genes. Other genes in these families are likely to possess host range functions that might impact the host spectrum of viruses at the organism level. These analyses will also provide valuable insights about the risk assessment for poxvirus emergence. In light of the data presented here, great effort must be taken to better elucidate the poxvirus host network, especially concerning the entomopoxviruses. Furthermore, it seems that the term 'host range genes' is not the most appropriate for these virulence genes, since there is no direct correlation between their presence and the host range of poxviruses, at least when considering animals as hosts, rather than cells. More in-depth investigation regarding the diversity of the poxvirus and their hosts, associated with *in silico*, *in vitro*, and *in vivo* assays about these virulence genes, will certainly bring more insights into this intriguing field of virus–host coevolution.

Supplementary Materials: The following are available online at www.mdpi.com/1999-4915/9/11/331/s1, Figure S1: Phylogenetic relationship of C7L gene. The tree was generated from a multiple protein sequence alignment of the indicated sequences using the maximum likelihood method. A bootstrap of 1000 was used, and support >50 is indicated above the branches. Branches in red represent the OPV clade, and branches in green represent clade II poxviruses; Figure S2: Phylogenetic relationship of E3L gene. The tree was generated from a multiple protein sequence alignment of the indicated sequences using the maximum likelihood method. A bootstrap of 1000 was used, and support >50 is indicated above the branches. Branches in red represent the OPV clade, and branches in green represent clade II poxviruses; Table S1: Names and abbreviations of the International Committee on Taxonomy of Viruses (ICTV) poxviruses species; Table S2: Poxvirus species and the associated hosts; Table S3: Protein sequences used as references for the BLASTP analyses.

Acknowledgments: We would like to thank our colleagues from GEPVIG (Grupo de Estudo and Prospecção de Vírus Gigantes) and Laboratório de Vírus of Universidade Federal de Minas Gerais. In addition, CNPq (Conselho Nacional de Desenvolvimento Científico and Tecnológico), CAPES (Coordenação de Aperfeiçoamento de Pessoal de Nível Superior) and FAPEMIG (Fundação de Amparo à Pesquisa do estado de Minas Gerais). Jônatas Santos Abrahão is a CNPq researcher.

Author Contributions: Rodrigo Araújo Lima Rodrigues, Grazielle Pereira Oliveira and Maurício Teixeira Lima performed the analysis and wrote the paper. Betânia Paiva Drumond and Jônatas Santos Abrahão designed the study and reviewed the final manuscript.

Conflicts of Interest: The authors declare no conflict of interest.

References

1. International Committee on Taxonomy of Viruses—Taxonomy. Available online: <https://talk.ictvonline.org/taxonomy/w/ictv-taxonomy> (accessed on 1 July 2017).
2. Fenner, F.; Henderson, D.A.; Arita, I.; Jezek, Z.; Ladnyi, I.D. *Smallpox and Its Eradication*, 1st ed.; World Health Organization: Geneva, Switzerland, 1988; pp. 1371–1409.
3. Thèves, C.; Biagini, P.; Crubézy, E. The rediscovery of smallpox. *Clin. Microbiol. Infect.* **2014**, *20*, 210–218. [[CrossRef](#)] [[PubMed](#)]
4. Henderson, D.A. The eradication of smallpox—An overview of the past, present, and future. *Vaccine* **2011**, *29*, 7–9. [[CrossRef](#)] [[PubMed](#)]

5. Essbauer, S.; Pfeffer, M.; Meyer, H. Zoonotic poxviruses. *Vet. Microbiol.* **2010**, *140*, 229–236. [[CrossRef](#)] [[PubMed](#)]
6. Kroon, E.G.; Mota, B.E.F.; Abrahão, J.S.; da Fonseca, F.G.; de Souza Trindade, G. Zoonotic Brazilian Vaccinia virus: From field to therapy. *Antivir. Res.* **2011**, *92*, 150–163. [[CrossRef](#)] [[PubMed](#)]
7. Stanford, M.M.; McFadden, G. The ‘supervirus’? Lessons from IL-4-expressing poxviruses. *Trends Immunol.* **2005**, *6*, 339–345. [[CrossRef](#)] [[PubMed](#)]
8. Castrucci, M.R.; Facchini, M.; Di Mario, G.; Garulli, B.; Sciaraffia, E.; Meola, M.; Fabiani, C.; De Marco, M.A.; Cordioli, P.; Siccardi, A.; et al. Modified vaccinia virus Ankara expressing the hemagglutinin of pandemic (H1N1) 2009 virus induces cross-protective immunity against Eurasian “avian-like” H1N1 swine viruses in mice. *Influenza Other Respir. Viruses* **2014**, *8*, 367–375. [[CrossRef](#)] [[PubMed](#)]
9. García-Arriaza, J.; Cepeda, V.; Hallengård, D.; Sorzano, C.Ó.; Kümmerer, B.M.; Liljestrom, P.; Esteban, M. A Novel Poxvirus-Based Vaccine, MVA-CHIKV, Is Highly Immunogenic and Protects Mice against Chikungunya Infection. *J. Virol.* **2014**, *88*, 3527–3547. [[CrossRef](#)] [[PubMed](#)]
10. Chan, W.M.; Rahman, M.M.; McFadden, G. Oncolytic myxoma virus: The path to clinic. *Vaccine* **2013**, *31*, 4252–4258. [[CrossRef](#)] [[PubMed](#)]
11. Moss, B. Poxvirus DNA Replication. *Cold Spring Harb. Perspect. Biol.* **2013**, *5*, a010199. [[CrossRef](#)] [[PubMed](#)]
12. Lefkowitz, E.J.; Wang, C.; Upton, C. Poxviruses: Past, present and future. *Virus Res.* **2006**, *117*, 105–118. [[CrossRef](#)] [[PubMed](#)]
13. Tulman, E.R.; Afonso, C.L.; Lu, Z.; Zsak, L.; Kutish, G.F.; Rock, D.L. The Genome of Canarypox Virus. *J. Virol.* **2004**, *78*, 353–366. [[CrossRef](#)] [[PubMed](#)]
14. Günther, T.; Haas, L.; Alawi, M.; Wohlsein, P.; Marks, J.; Grundhoff, A.; Becher, P.; Fischer, N. Recovery of the first full-length genome sequence of a parapoxvirus directly from a clinical sample. *Sci. Rep.* **2017**, *7*, 3734. [[CrossRef](#)] [[PubMed](#)]
15. Hughes, A.L.; Friedman, R. Poxvirus genome evolution by gene gain and loss. *Mol. Phylogenet. Evol.* **2005**, *35*, 186–195. [[CrossRef](#)] [[PubMed](#)]
16. Bratke, K.A.; McLysaght, A. Identification of multiple independent horizontal gene transfers into poxviruses using a comparative genomics approach. *BMC Evol. Biol.* **2008**, *8*, 67. [[CrossRef](#)] [[PubMed](#)]
17. McLysaght, A.; Baldi, P.F.; Gaut, B.S. Extensive gene gain associated with adaptive evolution of poxviruses. *Proc. Natl. Acad. Sci. USA* **2003**, *100*, 15655–15660. [[CrossRef](#)] [[PubMed](#)]
18. McFadden, G. Poxvirus tropism. *Nat. Rev. Microbiol.* **2005**, *3*, 201–213. [[CrossRef](#)] [[PubMed](#)]
19. Haller, S.L.; Peng, C.; McFadden, G.; Rothenburg, S. Poxviruses and the evolution of host range and virulence. *Infect. Genet. Evol.* **2014**, *21*, 15–40. [[CrossRef](#)] [[PubMed](#)]
20. Bratke, K.A.; McLysaght, A.; Rothenburg, S. A survey of host range genes in poxvirus genomes. *Infect. Genet. Evol.* **2013**, *14*, 406–425. [[CrossRef](#)] [[PubMed](#)]
21. Werden, S.J.; Rahman, M.M.; McFadden, G. Poxvirus Host Range Genes Chapter 3. *Adv. Virus Res.* **2008**, *71*, 135–171. [[PubMed](#)]
22. Chen, W.; Drillien, R.; Spehner, D.; Buller, R.M. In vitro and in vivo study of the ectromelia virus homolog of the vaccinia virus K1L host range gene. *Virology* **1993**, *196*, 682–693. [[CrossRef](#)] [[PubMed](#)]
23. Stern, R.J.; Thompson, J.P.; Moyer, R.W. Attenuation of B5R mutants of rabbitpox virus in vivo is related to impaired growth and not an enhanced host inflammatory response. *Virology* **1997**, *233*, 118–129. [[CrossRef](#)] [[PubMed](#)]
24. Liu, J.; Wennier, S.; Moussatche, N.; Reinhard, M.; Condit, R.; McFadden, G. Myxoma Virus M064 Is a Novel Member of the Poxvirus C7L Superfamily of Host Range Factors That Controls the Kinetics of Myxomatosis in European Rabbits. *J. Virol.* **2012**, *86*, 5371–5375. [[CrossRef](#)] [[PubMed](#)]
25. Damon, I.K. Poxviruses. In *Fields Virology*, 6th ed.; Knipe, D.M., Howley, P.M., Eds.; Lippincott, Williams and Wilkins: Philadelphia, PA, USA, 2014; Volume 2, p. 2160.
26. Trindade, G.S.; Emerson, G.L.; Sammons, S.; Frace, M.; Govil, D.; Mota, B.E.F.; Abrahão, J.S.; de Assis, F.L.; Olsen-Rasmussen, M.; Goldsmith, C.S.; et al. Serro 2 Virus Highlights the Fundamental Genomic and Biological Features of a Natural Vaccinia Virus Infecting Humans. *Viruses* **2016**, *8*, 328. [[CrossRef](#)] [[PubMed](#)]
27. Alzhanova, D.; Früh, K. Modulation of the host immune response by cowpox virus. *Microbes Infect.* **2010**, *12*, 900–909. [[CrossRef](#)] [[PubMed](#)]
28. Chen, X.; Anstey, A.V.; Bugert, J.J. Molluscum contagiosum virus infection. *Lancet Infect. Dis.* **2013**, *10*, 877–888. [[CrossRef](#)]

29. Fenner, F. Adventures with poxviruses of vertebrates. *FEMS Microbiol. Rev.* **2000**, *24*, 123–133. [[CrossRef](#)] [[PubMed](#)]
30. Afonso, C.L.; Tulman, E.R.; Lu, Z.; Oma, E.; Kutish, G.F.; Rock, D.L. The Genome of *Melanoplus sanguinipes* Entomopoxvirus. *J. Virol.* **1999**, *73*, 533–552. [[PubMed](#)]
31. Thézé, J.; Takatsuka, J.; Li, Z. New Insights into the Evolution of Entomopoxvirinae from the Complete Genome Sequences of Four Entomopoxviruses Infecting *Adoxophyes honmai*, *Choristoneura biennis*, *Choristoneura rosaceana*, and *Mythimna separata*. *J. Virol.* **2013**, *87*, 7992–8003. [[CrossRef](#)] [[PubMed](#)]
32. Thézé, J.; Takatsuka, J.; Nakai, M.; Arif, B.; Herniou, E.A. Gene Acquisition Convergence between Entomopoxviruses and Baculoviruses. *Viruses* **2015**, *7*, 1960–1974. [[CrossRef](#)] [[PubMed](#)]
33. Baker, K.S.; Leggett, R.M.; Bexfield, N.H.; Alston, M.; Daly, G.; Todd, S.; Tachedjian, M.; Holmes, C.E.; Crameri, S.; Wang, L.F. Metagenomic study of the viruses of African straw-coloured fruit bats: Detection of a chiropteran poxvirus and isolation of a novel adenovirus. *Virology* **2013**, *441*, 95–106. [[CrossRef](#)] [[PubMed](#)]
34. Abrahão, J.S.; Campos, R.K.; De Souza Trindade, G.; Da Fonseca, F.G.; Ferreira, P.C.P.; Kroon, E.G. Outbreak of severe zoonotic vaccinia virus infection, Southeastern Brazil. *Emerg. Infect. Dis.* **2015**, *21*, 695–698. [[CrossRef](#)] [[PubMed](#)]
35. Assis, F.L.; Borges, I.A.; Mesquita, V.S.; Ferreira, P.C.; Trindade, G.S.; Kroon, E.G.; Abrahão, J.S. Vaccinia virus in household environment during bovine vaccinia outbreak, Brazil. *Emerg. Infect. Dis.* **2013**, *19*, 2045–2047. [[CrossRef](#)] [[PubMed](#)]
36. Nolen, L.D.; Osadebe, L.; Katomba, J.; Likofata, J.; Mukadi, D.; Monroe, B.; Doty, J.; Hughes, C.M.; Kabamba, J.; Malekani, J. Extended human-to-human transmission during a monkeypox outbreak in the Democratic Republic of the Congo. *Emerg. Infect. Dis.* **2016**, *22*, 1014–1021. [[CrossRef](#)] [[PubMed](#)]
37. Campe, H.; Zimmermann, P.; Glos, K.; Bayer, M.; Bergemann, H.; Dreweck, C.; Graf, P.; Weber, B.K.; Meyer, H.; Büttner, M. Cowpox virus transmission from pet rats to humans, Germany. *Emerg. Infect. Dis.* **2009**, *15*, 777–780. [[CrossRef](#)] [[PubMed](#)]
38. Shchelkunov, S.N. An Increasing Danger of Zoonotic Orthopoxvirus Infections. *PLoS Pathog.* **2013**, *9*, 1–4. [[CrossRef](#)] [[PubMed](#)]
39. Mayr, A.; Mahnel, H. Characterization of a fowlpox virus isolated from a rhinoceros. *Arch. Gesamte Virusforsch.* **1970**, *31*, 51–60. [[CrossRef](#)] [[PubMed](#)]
40. Zhao, G.; Droit, L.; Tesh, R.B.; Popov, V.L.; Little, N.S.; Upton, C.; Virgin, H.W.; Wang, D. The Genome of Yoka Poxvirus. *J. Virol.* **2011**, *85*, 10230–10238. [[CrossRef](#)] [[PubMed](#)]
41. Abrahão, J.S.; Guedes, M.I.M.; Trindade, G.S.; Fonseca, F.G.; Campos, R.K.; Mota, B.F.; Lobato, Z.I.P.; Silva-Fernandes, A.T.; Rodrigues, G.O.L.; Lima, L.S. One more piece in the VACV ecological puzzle: Could peridomestic rodents be the link between wildlife and bovine vaccinia outbreaks in Brazil? *PLoS ONE* **2009**, *4*, 7428. [[CrossRef](#)] [[PubMed](#)]
42. Hutson, C.L.; Nakazawa, Y.J.; Self, J.; Olson, V.A.; Regnery, R.L.; Braden, Z.; Weiss, S.; Malekani, J.; Jackson, E.; Tate, M. Laboratory Investigations of African Pouched Rats (*Cricetomys gambianus*) as a Potential Reservoir Host Species for Monkeypox Virus. *PLoS Negl. Trop. Dis.* **2015**, *9*, 1–20. [[CrossRef](#)] [[PubMed](#)]
43. Villarreal, L.P.; Defilippis, V.R.; Gottlieb, K.A. Acute and persistent viral life strategies and their relationship to emerging diseases. *Virology* **2000**, *272*, 1–6. [[CrossRef](#)] [[PubMed](#)]
44. Mauldin, M.; Antwerpen, M.; Emerson, G.; Li, Y.; Zoeller, G.; Carroll, D.; Meyer, H. Cowpox virus: What's in a Name? *Viruses* **2017**, *9*, 101. [[CrossRef](#)] [[PubMed](#)]
45. Kroon, E.G.; Abrahão, J.S.; de Souza Trindade, G.; Oliveira, G.P.; Luiz, A.P.M.F.; Costa, G.B.; Lima, M.T.; Calixto, R.S.; Oliveira, D.B.; Drumond, B.P. Natural Vaccinia virus infection: Diagnosis, isolation, and characterization. *Curr. Protoc. Microbiol.* **2016**, *42*, 14A.5.1–14A.5.43.
46. Ninove, L.; Domart, Y.; Vervel, C.; Voinot, C.; Salez, N.; Raoult, D.; Meyer, H.; Capek, I.; Zandotti, C.; Charrel, R.N. Cowpox Virus Transmission from Pet Rats to Humans, France. *Emerg. Infect. Dis.* **2009**, *15*, 781–784. [[CrossRef](#)] [[PubMed](#)]
47. Reynolds, M.G.; Carroll, D.S.; Olson, V.A.; Hughes, C.; Galley, J.; Likos, A.; Montgomery, J.; Suu-Ire, R.; Kwasi, M.O.; Root, J.J. A silent enzootic of an orthopoxvirus in Ghana, West Africa: Evidence for multi-species involvement in the absence of widespread human disease. *Am. J. Trop. Med. Hyg.* **2010**, *82*, 746–754. [[CrossRef](#)] [[PubMed](#)]

48. Hutson, C.L.; Lee, K.N.; Abel, J.; Carroll, D.S.; Montgomery, J.M.; Olson, V.A.; Li, Y.; Davidson, W.; Hughes, C.; Dillon, M.; et al. Monkeypox zoonotic associations: Insights from laboratory evaluation of animals associated with the multi-state US outbreak. *Am. J. Trop. Med. Hyg.* **2007**, *76*, 757–768. [[PubMed](#)]
49. Bowman, K.F.; Barbery, R.T.; Swango, L.J.; Schnurrenberger, P.R. Cutaneous form of bovine papular stomatitis in man. *JAMA* **1981**, *246*, 2813–2818. [[CrossRef](#)] [[PubMed](#)]
50. Abrahão, J.S.; Silva-Fernandes, A.T.; Assis, F.L.; Guedes, M.I.; Drumond, B.P.; Leite, J.A.; Coelho, L.F.; Turrini, F.; Fonseca, F.G.; Lobato, Z.I. Human vaccinia virus and pseudocowpox virus co-infection: Clinical description and phylogenetic characterization. *J. Clin. Virol.* **2010**, *48*, 69–72. [[CrossRef](#)] [[PubMed](#)]
51. Leung, A.K.; Barankin, B.; Hon, K.L. Molluscum contagiosum: An update. *Recent Pat. Inflamm. Allergy Drug Discov.* **2017**, *10*, 2174. [[CrossRef](#)] [[PubMed](#)]
52. Balamurugan, V.; Venkatesan, G.; Bhanuprakash, V.; Singh, R.K. Camelpox, an emerging orthopox viral disease. *Indian J. Virol.* **2013**, *3*, 295–305. [[CrossRef](#)] [[PubMed](#)]
53. Oliveira, G.; Costa, G.; Assis, F.; Franco-Luiz, A.P.; Trindade, G.; Kroon, E.; Turrini, F.; Abrahão, J. Parapoxvirus. In *Molecular Detection of Animal Viral Pathogens*; Liu, D., Ed.; CRC Press: Boca Raton, FL, USA, 2016; pp. 881–890.
54. Mendez-Rios, J.D.; Martens, C.A.; Bruno, D.P.; Porcella, S.F.; Zheng, Z.M.; Moss, B. Genome Sequence of Erythromelalgia-Related Poxvirus Identifies it as an Ectromelia Virus Strain. *PLoS ONE* **2012**, *7*, 34604. [[CrossRef](#)] [[PubMed](#)]
55. Sigal, L.J. The pathogenesis and immunobiology of mousepox. *Adv. Immunol.* **2016**, *129*, 251–276. [[PubMed](#)]
56. Franco-Luiz, A.P.; Oliveira, D.B.; Pereira, A.F.; Gasparini, M.C.; Bonjardim, C.A.; Ferreira, P.C.; Trindade, G.S.; Puentes, R.; Furtado, A.; Abrahão, J.S.; et al. Detection of Vaccinia Virus in Dairy Cattle Serum Samples from 2009, Uruguay. *Emerg. Infect. Dis.* **2016**, *22*, 2174–2177. [[CrossRef](#)] [[PubMed](#)]
57. Friederichs, S.; Krebs, S.; Blum, H.; Lang, H.; Büttner, M. Parapoxvirus (PPV) of red deer reveals subclinical infection and confirms a unique species. *J. Gen. Virol.* **2015**, *96*, 1446–1462. [[CrossRef](#)] [[PubMed](#)]
58. Fenner, F. The biological characters of several strains of vaccinia, cowpox, and rabbitpox viruses. *Virology* **1958**, *5*, 502–529. [[CrossRef](#)]
59. Gemmell, A.; Cairns, J. Linkage in the genome of an animal virus. *Virology* **1959**, *8*, 381–383. [[CrossRef](#)]
60. Sambrook, J.F.; Padgett, B.L.; Tomkins, J.K. Conditional lethal mutants of rabbitpox virus. I. Isolation of host cell-dependent and temperature-dependent mutants. *Virology* **1966**, *28*, 592–599. [[CrossRef](#)]
61. Fenner, F.; Sambrook, J.F. Conditional lethal mutants of rabbitpox virus. II. Mutants (p) that fail to multiply in PK-2a cells. *Virology* **1966**, *28*, 600–609. [[CrossRef](#)]
62. Ali, A.N.; Turner, P.C.; Brooks, M.A.; Moyer, R.W. The SPI-1 gene of rabbitpox virus determines host range and is required for hemorrhagic pox formation. *Virology* **1994**, *202*, 305–314. [[CrossRef](#)] [[PubMed](#)]
63. McClain, M.E.; Greenland, R.M. Recombination between rabbitpox virus mutants in permissive and nonpermissive cells. *Virology* **1965**, *25*, 516–522. [[CrossRef](#)]
64. Beattie, E.; Paoletti, E.; Tartaglia, J. Distinct patterns of IFN sensitivity observed in cells infected with vaccinia K3L- and E3L-mutant viruses. *Virology* **1965**, *210*, 254–263. [[CrossRef](#)] [[PubMed](#)]
65. Barrett, J.W.; Shun Chang, C.; Wang, G.; Werden, S.J.; Shao, Z.; Barrett, C.; Gao, X.; Belsito, T.A.; Villeneuve, D.; McFadden, G. Myxoma virus M063R is a host range gene essential for virus replication in rabbit cells. *Virology* **2007**, *361*, 123–132. [[CrossRef](#)] [[PubMed](#)]
66. Legrand, F.A.; Verardi, P.H.; Jones, L.A.; Chan, K.S.; Peng, Y.; Yilma, T.D. Induction of potent humoral and cell-mediated immune responses by attenuated vaccinia virus vectors with deleted serpin genes. *J. Virol.* **2004**, *78*, 2770–2779. [[CrossRef](#)] [[PubMed](#)]
67. Chang, H.W.; Jacobs, B.L. Identification of a conserved motif that is necessary for binding of the vaccinia virus E3L gene products to double-stranded RNA. *Virology* **1993**, *194*, 537–547. [[CrossRef](#)] [[PubMed](#)]
68. Chang, H.W.; Watson, J.C.; Jacobs, B.L. The E3L gene of vaccinia virus encodes an inhibitor of the interferon-induced, double-stranded RNA-dependent protein kinase. *Proc. Natl. Acad. Sci. USA* **1992**, *89*, 4825–4829. [[CrossRef](#)] [[PubMed](#)]
69. Rivas, C.; Gil, J.; Melkova, Z.; Esteban, M.; Diaz-Guerra, M. Vaccinia virus E3L protein is an inhibitor of the interferon (i.f.n.)-induced 2–5A synthetase enzyme. *Virology* **1998**, *243*, 406–414. [[CrossRef](#)] [[PubMed](#)]
70. Langland, J.O.; Kash, J.C.; Carter, V.; Thomas, M.J.; Katze, M.G.; Jacobs, B.L. Suppression of proinflammatory signal transduction and gene expression by the dual nucleic acid binding domains of the vaccinia virus E3L proteins. *J. Virol.* **2006**, *80*, 10083–10095. [[CrossRef](#)] [[PubMed](#)]

71. Davies, M.V.; Elroy-Stein, O.; Jagus, R.; Moss, B.; Kaufman, R.J. The vaccinia virus K3L gene product potentiates translation by inhibiting double-stranded-RNA-activated protein kinase and phosphorylation of the alpha subunit of eukaryotic initiation factor 2. *J. Virol.* **1992**, *66*, 1943–1950. [[PubMed](#)]
72. Davies, M.V.; Chang, H.W.; Jacobs, B.L.; Kaufman, R.J. The E3L and K3L vacciniavirus gene products stimulate translation through inhibition of the double-stranded RNA-dependent protein kinase by different mechanisms. *J. Virol.* **1993**, *67*, 1688–1692. [[PubMed](#)]
73. Craig, A.W.; Cosentino, G.P.; Donze, O.; Sonenberg, N. The kinase insert domain of interferon-induced protein kinase PKR is required for activity but not for interaction with the pseudosubstrate K3L. *J. Biol. Chem.* **1996**, *271*, 24526–24533. [[CrossRef](#)] [[PubMed](#)]
74. Kawagishi-Kobayashi, M.; Silverman, J.B.; Ung, T.L.; Dever, T.E. Regulation of the protein kinase PKR by the vaccinia virus pseudosubstrate inhibitor K3L is dependent on residues conserved between the K3L protein and the PKR substrate eIF2alpha. *Mol. Cell. Biol.* **1997**, *17*, 4146–4158. [[CrossRef](#)] [[PubMed](#)]
75. Langland, J.O.; Jacobs, B.L. The role of the PKR-inhibitory genes, E3L and K3L, in determining vaccinia virus host range. *Virology* **2002**, *299*, 133–141. [[CrossRef](#)] [[PubMed](#)]
76. Silverman, G.A.; Bird, P.I.; Carrell, R.W.; Church, F.C.; Coughlin, P.B.; Gettins, P.G.; Irving, J.A.; Lomas, D.A.; Luke, C.J.; Moyer, R.W. The serpins are an expanding superfamily of structurally similar but functionally diverse proteins. Evolution, mechanism of inhibition, novel functions, and a revised nomenclature. *J. Biol. Chem.* **2001**, *276*, 33293–33296. [[CrossRef](#)] [[PubMed](#)]
77. Herrera, E.; Lorenzo, M.M.; Blasco, R.; Isaacs, S.N. Functional analysis of vaccinia virus B5R protein: Essential role in virus envelopment is independent of a large portion of the extracellular domain. *J. Virol.* **1998**, *72*, 294–302. [[PubMed](#)]
78. Rodger, G.; Smith, G.L. Replacing the SCR domains of vaccinia virus protein B5R with EGFP causes a reduction in plaque size and actin tail formation but enveloped virions are still transported to the cell surface. *J. Gen. Virol.* **2002**, *83*, 323–332. [[CrossRef](#)] [[PubMed](#)]
79. Spehner, D.; Gillard, S.; Drillien, R.; Kim, A. A cowpox virus gene required for multiplication in Chinese hamster ovary cells. *J. Virol.* **1988**, *62*, 1297–1304. [[PubMed](#)]
80. Chang, S.J.; Hsiao, J.C.; Sonnberg, S.; Chiang, C.T.; Yang, M.H.; Tzou, D.L.; Mercer, A.A.; Chang, W. Poxviral host range protein CP77 contains a F-box-like domain that is necessary to suppress NF- κ B activation by TNF- α but is independent of its host range function. *J. Virol.* **2009**, *83*, 4140–4152. [[CrossRef](#)] [[PubMed](#)]
81. Meng, X.; Chao, J.; Xiang, Y. Identification from diverse mammalian poxviruses of host-range regulatory genes functioning equivalently to vaccinia virus C7L. *Virology* **2008**, *372*, 372–383. [[CrossRef](#)] [[PubMed](#)]
82. Smith, C.A.; Davis, T.; Anderson, D.; Solam, L.; Beckmann, M.P.; Jerzy, R.; Dower, S.K.; Cosman, D.; Goodwin, R.G. A receptor for tumor necrosis factor defines an unusual family of cellular and viral proteins. *Science* **1990**, *248*, 1019–1023. [[CrossRef](#)] [[PubMed](#)]
83. Smith, C.A.; Davis, T.; Wignall, J.M.; Din, W.S.; Farrah, T.; Upton, C.; McFadden, G.; Goodwin, R.G. T2 open reading frame from the Shope fibroma virus encodes a soluble form of the TNF receptor. *Biochem. Biophys. Res. Commun.* **1991**, *176*, 335–342. [[CrossRef](#)]
84. Alejo, A.; Ruiz-Arguello, M.B.; Ho, Y.; Smith, V.P.; Saraiva, M.; Alcami, A. A chemokine-binding domain in the tumor necrosis factor receptor from variola (smallpox) virus. *Proc. Natl. Acad. Sci. USA* **2006**, *103*, 5995–6000. [[CrossRef](#)] [[PubMed](#)]
85. Douglas, A.E.; Corbett, K.D.; Berger, J.M.; McFadden, G.; Handel, T.M. Structure of M11L: A myxoma virus structural homolog of the apoptosis inhibitor, Bcl-2. *Protein Sci.* **2007**, *16*, 695–703. [[CrossRef](#)] [[PubMed](#)]
86. Johnston, J.B.; Barrett, J.W.; Nazarian, S.H.; Goodwin, M.; Ricciuto, D.; Wang, G.; McFadden, G. A poxvirus-encoded pyrin domain protein interacts with ASC-1 to inhibit host inflammatory and apoptotic responses to infection. *Immunity* **2005**, *23*, 587–598. [[CrossRef](#)] [[PubMed](#)]
87. Senkevich, T.G.; Koonin, E.V.; Bugert, J.J.; Darai, G.; Moss, B. The genome of molluscum contagiosum virus: Analysis and comparison with other poxviruses. *Virology* **1997**, *233*, 19–42. [[CrossRef](#)] [[PubMed](#)]
88. Hughes, A.L.; Irausquin, S.; Friedman, R. The evolutionary biology of poxviruses. *Infect. Genet. Evol.* **2010**, *10*, 50–59. [[CrossRef](#)] [[PubMed](#)]
89. Iyer, L.M.; Aravind, L.; Koonin, E.V. Common Origin of Four Diverse Families of Large Eukaryotic DNA Viruses. *J. Virol.* **2001**, *75*, 11720–11734. [[CrossRef](#)] [[PubMed](#)]

90. Boyer, M.; Gimenez, G.; Suzan-Monti, M.; Raoult, D. Classification and determination of possible origins of ORFans through analysis of nucleocytoplasmic large DNA viruses. *Intervirology* **2010**, *53*, 310–320. [[CrossRef](#)] [[PubMed](#)]
91. Hughes, A.L. Origin and evolution of viral interleukin-10 and other DNA virus genes with vertebrate homologues. *J. Mol. Evol.* **2002**, *54*, 90–101. [[CrossRef](#)] [[PubMed](#)]
92. Thompson, J.D.; Higgins, D.G.; Gibson, T.J. CLUSTAL W: Improving the sensitivity of progressive multiple sequence alignment through sequence weighting, position-specific gap penalties and weight matrix choice. *Nucleic Acids Res.* **1994**, *22*, 4673–4680. [[CrossRef](#)] [[PubMed](#)]
93. Smithson, C.; Meyer, H.; Gigante, C.M.; Gao, J.; Zhao, H.; Batra, D.; Damon, I.; Upton, C.; Li, Y. Two novel poxviruses with unusual genome rearrangements: NY_014 and Murmansk. *Virus Genes* **2017**. [[CrossRef](#)] [[PubMed](#)]
94. Wong, C.K.; Young, V.L.; Kleffmann, T.; Ward, V.K. Genomic and proteomic analysis of invertebrate iridovirus type 9. *J. Virol.* **2011**, *85*, 7900–7911. [[CrossRef](#)] [[PubMed](#)]
95. Legendre, M.; Santini, S.; Rico, A.; Abergel, C.; Claverie, J.M. Breaking the 1000-gene barrier for Mimivirus using ultra-deep genome and transcriptome sequencing. *Virol. J.* **2011**, *8*, 99. [[CrossRef](#)] [[PubMed](#)]
96. Odom, M.R.; Hendrickson, R.C.; Lefkowitz, E.J. Poxvirus protein evolution: Family-wide assessment of possible horizontal gene transfer events. *Virus Res.* **2009**, *144*, 233–249. [[CrossRef](#)] [[PubMed](#)]
97. Gjessing, M.C.; Yutin, N.; Tengs, T.; Senkevich, T.; Koonin, E.; Rønning, H.P.; Alarcon, M.; Ylving, S.; Lie, K.I.; Saure, B. Salmon Gill Poxvirus, the Deepest Representative of the Chordopoxvirinae. *J. Virol.* **2015**, *89*, 9348–9367. [[CrossRef](#)] [[PubMed](#)]
98. O’Dea, M.; Tu, S.-L.; Pang, S.; De Ridder, T.; Jackson, B.; Upton, C. Genomic characterization of a novel poxvirus from a flying fox: Evidence for a new genus? *J. Gen. Virol.* **2016**, *97*, 2363–2375. [[CrossRef](#)] [[PubMed](#)]
99. Tu, S.L.; Nakazawa, Y.; Gao, J.; Wilkins, K.; Gallardo-Romero, N.; Li, Y.; Emerson, G.L.; Carroll, D.S.; Upton, C. Characterization of Eptesipoxvirus, a novel poxvirus from a microchiropteran bat. *Virus Genes* **2017**. [[CrossRef](#)] [[PubMed](#)]
100. Koonin, E.V.; Senkevich, T.G.; Dolja, V.V. The ancient Virus World and evolution of cells. *Biol. Direct* **2006**, *1*, 29. [[CrossRef](#)] [[PubMed](#)]
101. Barry, M.; McFadden, G. Virus encoded cytokines and cytokine receptors. *Parasitology* **1997**, *115*, 89–100. [[CrossRef](#)]
102. Lawrence, J.G.; Ochman, H. Molecular archaeology of the *Escherichia coli* genome. *Proc. Natl. Acad. Sci. USA* **1998**, *95*, 9413–9417. [[CrossRef](#)] [[PubMed](#)]
103. Ochman, H.; Lawrence, J.G.; Groisman, E.A. Lateral gene transfer and the nature of bacterial innovation. *Nature* **2000**, *405*, 299–304. [[CrossRef](#)] [[PubMed](#)]
104. Upton, C.; McFadden, G. DNA sequence homology between the terminal inverted repeats of Shope fibroma virus and an endogenous cellular plasmid species. *Mol. Cell. Biol.* **1986**, *6*, 265–276. [[CrossRef](#)] [[PubMed](#)]
105. Liszewski, M.K.; Leung, M.K.; Hauhart, R.; Fang, C.J.; Bertram, P.; Atkinson, J.P. Smallpox inhibitor of complement enzymes (SPICE): Dissecting functional sites and abrogating activity. *J. Immunol.* **2009**, *183*, 3150–3159. [[CrossRef](#)] [[PubMed](#)]
106. Ojha, H.; Panwar, H.S.; Gorham, R.D.; Morikis, D.; Sahu, A. Viral regulators of complement activation: Structure, function and evolution. *Mol. Immunol.* **2014**, *61*, 89–99. [[CrossRef](#)] [[PubMed](#)]
107. Kotwal, G.J.; Moss, B. Analysis of a large cluster of nonessential genes deleted from a vaccinia virus terminal transposition mutant. *Virology* **1988**, *167*, 524–537. [[CrossRef](#)]
108. Kotwal, G.J.; Isaacs, S.N.; McKenzie, R.; Frank, M.M.; Moss, B. Inhibition of the complement cascade by the major secretory protein of vaccinia virus. *Science* **1990**, *250*, 827–830. [[CrossRef](#)] [[PubMed](#)]



1 **Title: Filling gaps about mimivirus entry, uncoating and morphogenesis**

2

3 **Running title: Updating mimiviruses' replication cycle**

4

5 **Authors:** Ana Cláudia dos Santos Pereira Andrade^{1†}; Rodrigo Araújo Lima
6 Rodrigues^{1†}; Grazielle Pereira Oliveira^{1†}; Kétyllen Reis Andrade²; Cláudio
7 Antônio Bonjardim¹, Bernard La Scola³; Erna Geessien Kroon¹; Jônatas Santos
8 Abrahão^{1*}.

9

10 **Authors affiliation:**

11 ¹Departamento de Microbiologia, Instituto de Ciências Biológicas, Universidade
12 Federal de Minas Gerais, Belo Horizonte, Minas Gerais, Brazil

13 ² Laboratório de Imunopatologia de Doenças Virais, Centro de Pesquisas René
14 Rachou / Fiocruz, Minas Gerais, Brazil

15 ³URMITE CNRS UMR 6236-IRD 3R198, Aix Marseille Université, Marseille,
16 France

17

18 † These authors contributed equally to this work

19 * jonatas.abrahao@gmail.com

20

21 **Keywords:** Mimivirus, electron microscopy, replication cycle, phagocytosis,
22 fibril acquisition area

23

24

25

26

27

28

29

30

31 **Abstract**

32

33 Since the discovery of mimivirus, its unusual structural and genomic features
34 have raised great interest in the study of its biology; however, many aspects
35 concerning its replication cycle remain uncertain. In this study, extensive
36 analyses of electron microscope images, as well as biological assays, shed light
37 on unclear points concerning the mimivirus replication cycle. Here, we
38 demonstrate that cytochalasin treatment, a phagocytosis inhibitor, impacts
39 negatively on the incorporation of mimivirus particles by *Acanthamoeba*
40 *castellanii*, causing a negative effect on viral growth in amoebae monolayers.
41 The treatment of amoebas with bafilomycin impacts significantly on mimivirus
42 uncoating and replication. In conjunction with microscopic analyses, these data
43 suggest that mimiviruses indeed depend on phagocytosis for entry into
44 amoebas, and particle uncoating (and stargate opening) appears to be
45 dependent on phagosome acidification. In depth analyses of particle
46 morphogenesis suggests that the mimivirus capsids are assembled from
47 growing lamellar structures. Despite proposals of previous studies that genome
48 acquisition occurs before the acquisition of fibrils, our results clearly
49 demonstrate that the genome and fibrils can be acquired simultaneously. Our
50 data suggest the existence of a specific area surrounding the core of the viral
51 factory, where particles acquire the surface fibrils. Furthermore, we reinforce
52 that defective particles can be formed even in the absence of virophages. Our
53 work provides new information about unexplored steps in the life cycle of
54 mimiviruses.

55

56

57 **Importance**

58

59 Investigating the viral life cycle is essential to a better understanding of viruses'
60 biology. The combination of biological assays and microscope images allows a
61 clear view of the biological features of viruses. Since the discovery of mimivirus,
62 many studies have been conducted to characterize its replication cycle, but
63 many gaps remain to be filled. In this study, we conducted a new examination of

64 the replication cycle of mimiviruses, providing new evidence concerning some
65 stages of the cycle which were previously unclear, mainly entry, uncoating and
66 morphogenesis. Furthermore, we demonstrated that atypical virion
67 morphologies can occur even in the absence of virophages. Our results, along
68 with previous data, lead us to present an ultimate model for the mimivirus
69 replication cycle.

70

71 Introduction

72

73 The giant *Acanthamoeba polyphaga* mimivirus (APMV), which is
74 associated with amoebas of *Acanthamoeba* genus, was isolated in 2003 and
75 astonished the scientific community with unusual structural and genomic
76 features within the virosphere (1, 2). In subsequent years, several mimi-like
77 viruses were uncovered in different parts of the world, thus expanding the
78 *Mimiviridae* family, especially the *Mimivirus* genus (3–7). These viruses have
79 some genetic differences which define three distinct lineages (A, B and C), but
80 they are structurally similar.

81 Mimiviruses have a particle with a pseudo-icosahedral symmetry of 750
82 nm in diameter and a genome of double-stranded DNA molecule of
83 approximately 1.2 Mb (2, 8). They have a capsid of 500 nm that is formed of
84 multiple protein layers and a lipid membrane, surrounding an inner
85 proteinaceous core which contains the genome. A star-shaped projection is
86 present on the capsid from which the viral genome is released into the host's
87 cytoplasm; this is referred to as the stargate and represents a unique feature of
88 mimiviruses (9). In addition, a dense layer of 125-nm long glycoproteic fibers
89 cover the viral surface, which is important for viral attachment to different
90 organisms, including amoebal hosts (10).

91 Given the large size of mimiviruses, it has been proposed and largely
92 accepted that the replication cycle of these viruses begins with phagocytosis of
93 viral particles by acanthamoeba cells (11, 12). The set of events that occurs
94 between virion entry and stargate opening lacks information. But there is
95 evidence demonstrating that after opening of the stargate, the virion inner lipid

96 membrane merges with that of the entry vesicle and releases the viral seed into
97 the cytoplasm. An atypical viral eclipse phase is then established during which
98 viral particles are not visible in the cell (11, 13). The viral seed releases the
99 DNA, promoting a reorganization of the host cytoplasm with further formation of
100 viral factories (VF), where virus genome is replicated, transcribed and new
101 particles are assembled (13, 14). Based on atomic force microscopy, Kuznetsov
102 and colleagues proposed a model for morphogenesis of mimivirus particles
103 (15). In this model, the capsid assembly occurs on VFs surface in a temporal-
104 fashion pattern, initiated by the formation of the stargate portal, followed by
105 thickening of the protein layer in its immediate vicinity. Before capsid formation
106 is complete, they are filled with DNA and other macromolecules through a
107 stargate distal portal. Once the genome is enclosed within the capsid, an
108 integument protein layer attaches to the capsid, on which a coating of fibrils
109 then adheres to the entire viral surface (15). The involvement of the nucleus
110 during the replication of these viruses is still unclear. Suzan-Mont and
111 colleagues (2007) suggest that APMV replication is nucleo-cytoplasmic,
112 although other studies argue that replication occurs exclusively in the host cell
113 cytoplasm (11, 13).

114 Mimiviruses have been studied for several years; nevertheless, some
115 aspects regarding their biology remain unclear. Based on biological assays in
116 conjunction with extensive electron microscopic analyses, we shed a new light
117 on the mimivirus replication cycle.

118

119 **Materials and methods**

120

121 **Cell culture and virus production, purification and titration**

122

123 *Acanthamoeba castellanii* (ATCC 30010) cells were cultivated in PYG
124 medium supplemented with 25 mg/ml amphotericin B (Fungizone; Cristalia, São
125 Paulo, Brazil), 500 U/ml penicillin and 50 mg/ml gentamicin (Schering-Plough,
126 Brazil). A total of 7×10^6 cells were infected with MsV at a multiplicity of
127 infection (MOI) of 0.01 and incubated at 32 °C. After the appearance of a

128 cytopathic effect, cells and supernatant were collected and viruses were then
129 purified through ultracentrifugation with a 25% sucrose cushion at 36,000 g for 2
130 h. After purification, amoeba cells were infected with purified viruses at MOI of
131 0.01. The viruses were serially diluted, and multiple replicate samples of each
132 dilution were inoculated into *A. castellanii* (ATCC 30234) monolayers. After 72–
133 96 h of incubation, the amoebae were analyzed to determine whether infection
134 had taken place. Based on these data, the virus titers were determined using
135 the endpoint method (16).

136

137 **Transmission electron microscopy**

138

139 The *Acanthamoeba castellanii* cells were infected as described in the
140 previous section at MOI of 0.01 and fixed at various times post-infection with
141 2.5% glutaraldehyde in a 0.1 M sodium phosphate buffer for 1 h at room
142 temperature. The amoebas were post-fixed with 2% osmium tetroxide and
143 embedded in EPON resin. Ultrathin sections then were analyzed under
144 transmission electron microscopy (TEM; Spirit Biotwin FEI-120 kV).

145

146 **Scanning electron microscopy**

147 The *Acanthamoeba castellanii* cells infected at MOI 0.01 were added to
148 round glass coverslips covered with poly-L-lysine and fixed with 2.5%
149 glutaraldehyde in 0.1 M cacodylate buffer for at least 1 h at room temperature.
150 The samples were then washed three times with 0.1 M cacodylate buffer and
151 post-fixed with 1.0% osmium tetroxide for 1 h at room temperature. After a
152 second fixation, the samples were washed three times with 0.1 M cacodylate
153 buffer and immersed in 0.1% tannic acid for 20 min. The samples were then
154 washed in cacodylate buffer and dehydrated by serial passages in ethanol
155 solutions at concentrations ranging from 35% to 100%. Samples were then
156 subjected to critical point drying using CO₂, placed in stubs and metalized with a
157 5-nm gold layer. The analyses were completed using scanning electronic
158 microscopy (FEG Quanta 200 FEI).

159 **Entry and uncoating assays**

160

161 In these experiments we evaluated whether blocking of phagocytosis and
162 phagosome acidification impacts on APMV entry and replication. A total of 10^6
163 *A. castellanii* cells were treated with 2 μ M of cytochalasine, a phagocytosis
164 inhibitor, in a total volume of 5 ml of PYG medium. After 1 h, supernatant was
165 removed and cells were infected with APMV at an MOI of 5. As a negative
166 control for the phagocytosis process, we used sonicated, purified particles of
167 marseillevirus marseillevirus (MsV) under the same conditions as described for
168 APMV. It was previously demonstrated that isolated particles of MsV enter
169 amoebas by endocytosis, not phagocytosis. Control groups of untreated,
170 infected amoebas were also used. Two hours post-infection, the supernatant
171 was collected to measure the remaining viral particles (non-phagocytized). The
172 supernatant was also collected immediately after infection (0 h post-infection).
173 The quantity of particles was calculated using flow cytometry as previously
174 described (17). The rate of particle incorporation was calculated taking into
175 consideration the variation in particle content of the supernatant between times
176 0 h and 2 h post-infection. An identical assay was performed in parallel, but
177 after infection the monolayer was washed with PAS, fresh medium was added
178 and at 8 h post-infection amoebas were collected and titrated. The aim of this
179 experiment was to estimate the impact of the blocking of phagocytosis on viral
180 replication. Finally, to investigate whether blocking of cell acidification impacts
181 on APMV and MsV replication, cells were treated with 5 nM of bafilomycin.
182 Eight hours post-infection, cells were collected and titrated. All the experiments
183 were performed three independent times, in duplicate. Graphs were constructed
184 using GraphPad Prism version 7.00 for Windows (GraphPad Software).

185

186 **Results**

187 **Biological assays suggest mimivirus entry into amoebas by phagocytosis**

188 Although mimiviruses have been known of for more than a decade, some
189 aspects of their replication cycle remain uncertain, such as their entry into
190 natural hosts. Due to its large size (~700 nm), it has been proposed and widely

191 accepted that mimivirus enters acanthamoeba cells by phagocytosis (11, 13).
192 However, to our knowledge there has been no biological demonstration of this
193 process. Here we confirm this hypothesis using experimental data.
194 Pretreatment of cells with cytochalasin D significantly decreased the titers and
195 particles incorporated into cells infected with APMV (Fig. 1A-B). The MsV titer
196 and particle incorporation were not reduced after this treatment, since isolated
197 purified particles exploit the endocytic pathway (18). Pretreatment with
198 bafilomycin also resulted in a significant reduction in APMV and MsV titers (Fig.
199 1C). Bafilomycin is a specific inhibitor of vacuolar-type H⁺/ATPase, preventing
200 phagosome and endosome acidification (19). Therefore, these results
201 demonstrate that APMV replication is dependent on the acidification of
202 phagosomes for the uncoating step. The acidification of the entry compartment
203 is also important for MsV (18). These results are corroborated by several TEM
204 images that show the occurrence phagosome-lysosome fusion, subsequent
205 stargate opening and release of the viral seed (Fig. 1D-L). Taken together,
206 these results support the view that APMV entry into acanthamoeba cells may
207 occur via phagocytosis.

208

209 **Capsids are assembled from growing lamellar structures**

210 After mimivirus enters amoeba cells and delivers the viral seed, early
211 DNA replication and transcription appears to take place exclusively in the host
212 cytoplasm, moments before the formation of a mature VF (13). Once a mature
213 VF is formed, the morphogenesis step is initiated. It has been proposed that the
214 formation of the mimivirus capsid begins with the formation of the stargate,
215 followed by thickening of the protein layer in its immediate vicinity (15).
216 However, it is not yet clear how expansion of this protein layer occurs.
217 Throughout analyses of TEM images of VFs at different time-points post-
218 infection, we observed the presence of several lamellar structures preceding
219 capsid formation, with different sizes in the inner part of the VF (Fig. 2A-C, 3A-
220 B). Mutsafi and colleagues (2013) showed the formation of multi-vesicular
221 bodies and membrane sheets from the endoplasmic reticulum (ER) in
222 outermost zone of the mimiviruses factories, called the membrane assembly
223 zone (20). Our TEM images provide evidence for the formation of lamellar

224 structures, not only on the periphery of the VF, but also in its interior (Fig. 2A-C;
225 3A-B), which is in accordance with the data of Mutsafi and colleagues. It is
226 noteworthy that after assembly of the complete particle in the later stages of
227 infection (~7 h post-infection), the crescents were no longer observed. These
228 lamellar structures, which began in an analogous way to crescents described in
229 poxviruses and marseilleviruses, increased in complexity until reaching the VF
230 periphery and moving to the next stages of virion morphogenesis (Fig. 2D-I),
231 incorporation of DNA and surface fibrils. In contrast to lamellar capsid forming
232 structures the main component of viral factory presents a globular aspect, likely
233 formed by DNA, membranes and enzymes (Fig 3 A-B).

234 **Dynamic acquisition of surface fibrils: fibrils acquisition area (FAA)**

235 The mature mimivirus particle is covered by fibrils with lengths ranging
236 from 125 nm to 140 nm (8). A previous study based on atomic force microscopy
237 proposed that the surface fibers are acquired by viral capsids when they pass
238 sequentially through a membrane embedded with integument protein and then
239 through a membrane containing surface fibers (15). In this model, layers of
240 integument and fibrils are acquired as an envelope involving the capsid. This
241 same study also suggested that the integument protein layer is acquired near
242 the VFs but the fibril layer is acquired near the cellular periphery, but the source
243 of these fibrils has not been demonstrated (15).

244 We noticed a very clear phenomenon regarding the dynamics of fibril
245 acquisition, leading us to make an overview of this step. In TEM images, it is
246 possible to observe at the periphery of the VFs a less electron-dense region of
247 apparent fibrillar nature, which we named the “fibrils acquisition area” (FAA)
248 (Fig. 4A-B). This arrangement is very clear and can be verified in almost all
249 VFs. During particle morphogenesis, newly formed capsids pass through this
250 region where the particles acquire the fibrils. This was evident when we
251 observed particles at the edge of the FAA, which had fibrils only in the upper
252 portion, suggesting that this fibrillar region provided the fibrils for these particles
253 (Fig. 5). In addition, the particles that had already passed through this region
254 had fibrils all over their surface (Fig. 5). In the stages where we found few viral
255 particles formed, the dimension of FAA was larger, and as long as the amount

256 of newly formed particles increased, this region was reduced in size (Fig. 4A-B;
257 5). This phenomenon suggests that, as viral particles are formed, the fibrillar
258 material that gives rise to fibrils is consumed. The TEM images of the VFs
259 showed the viral capsids being formed in blocks, growing in thickness and
260 complexity as they migrated to the outermost part of the VFs and acquiring
261 fibrils when they passed through the FAA (Fig 2; 4C). In the SEM image, it was
262 not possible to view the FAA and the particles were being assembled before
263 fibrils acquisition (Fig. 4D). Notably, all particles were without fibrils and
264 displayed a prominent stargate (Fig. 4D).

265 Altogether, the data presented here lead us to suggest that the fibrils are
266 acquired in FAA, not near the cellular periphery as was previously suggested
267 (15). This view is also supported by the presence of various viral particles with
268 fibrils in the cell cytoplasm. In addition, we did not observe the acquisition of the
269 fibril layer by passage through a membrane, as previously described (15). Our
270 images suggest that fibrils are acquired by the capsid when they pass through a
271 region presenting the preformed fibrils. The full composition of the FAA, as well
272 as the mechanisms of fibril binding in the protein capsid, still require further
273 investigation.

274

275 **Simultaneous occurrence of genome incorporation and fibrils acquisition**

276 The processes of release and packaging of the viral genome in
277 mimiviruses have been analyzed in previous studies (9, 13, 15). It has already
278 been demonstrated that genome delivery occurs through the stargate and
279 packaging through the opposite portal (9). This strategy is different to that of
280 other icosahedral viruses, where a single vertex-portal system plays a crucial
281 role in both genome release and packaging (9, 21). The viral genome is
282 acquired at the periphery of the VFs during the morphogenesis step (11, 13).
283 The particles that have already acquired a genome have a more electron-dense
284 region inside them, while those that have not yet acquired the genome do not
285 exhibit this feature (Fig. 2E-H; 5). It was previously proposed that the formation
286 of the capsid, acquisition of genome and acquisition of fibrils by mimivirus
287 particles occur sequentially in this order (15). According to this model, the

288 genome enters into the empty capsid, the nucleic acid condenses inside and
289 the entry portal is sealed, completing the assembly of the capsid. Subsequently,
290 upper structural layers of integument and fibrils are acquired to form a mature
291 particle (15).

292 Our data strongly suggest an alternative view of these events during
293 mimivirus morphogenesis. In transverse sections of the VF we could clearly
294 observe particles which were fully or partially covered by fibrils still acquiring the
295 genome (Fig. 4C; 5). Further TEM images showed particles that had already
296 passed through the fibrillar region, therefore were covered by fibrils, and were
297 acquiring the genome in the opposite region to the stargate (Fig. 4C; 5). It is
298 noteworthy that some viral particles were not fully covered by the fibrils (only
299 half of the particle has fibrils) and the genome was still being packaged (Fig. 5).
300 In contrast to what has been previously proposed, our data suggest that no
301 sequential order of events appears to occur in the final steps of mimivirus
302 morphogenesis concerning genome acquisition and fibril incorporation. It is
303 possible that fibrils attach to the some viral particles after genome fully
304 acquisition, but most of the images presented here lead us to support the
305 hypothesis that the acquisition of the genome occurs concomitantly with the
306 acquisition of the surface fibrils.

307

308 **Viral particles with unusual morphologies**

309 The particles of viral progeny were mostly well formed with a typical
310 morphology. However, particles with unusual structures were also observed.
311 TEM images showed unusual projections starting from the capsid or on its sides
312 and capsids with no typical symmetry (Fig. 6A-C). In addition, an assembled
313 empty capsid in the center of the VF was observed, an unexpected finding
314 considering the particular stage of the virus replication cycle (Fig. 6D). Particles
315 with altered fibril arrangement were also identified and SEM images showed
316 particles with non-uniform distribution of fibrils (Fig. 6E-F).

317 It has been shown that virophages affect the replication cycle of
318 mimiviruses, decreasing amoebal lysis and generating particles with abnormal

319 morphologies (22–24). Some particles showed capsid layers assymmetrically
320 accumulated on the viral particle or harbouring fibrils only in one part of the
321 capsid. The Sputnik was the first virophage to be described which infected a
322 strain of mimivirus (22). Since then, other virophages have been described, thus
323 reinforcing this new class of viruses (5, 24, 25). Virophages cannot replicate
324 alone in amoebas, but they can replicate in the mimiviral VFs. They have a
325 small diameter (50 nm) and an icosahedral capsid, but they can be visualized in
326 TEM images in VFs and even within viral particles (22, 24). However, none of
327 the images analyzed in this study exhibited signs of the presence of virophages,
328 even in those images in which defective particles were found. To date, our
329 APMV stocks have been tested by PCR for the presence of Sputniks and
330 Zamilon, but fail to amplify any virophage gene.

331 As previously demonstrated, different multiplicity of infections (MOI) used
332 for mimivirus production resulted in distinct proportions of infectious particles in
333 a newly formed progeny, whereas the most efficacious way to produce
334 infectious mimivirus' particles is using low MOI (26). Although we followed this
335 strategy during sample preparation for TEM analyses, multiple particles can
336 infect the same cell and saturate the cellular machinery, thus generating
337 defective particles. This is probably a usual phenomenon in nature, and the
338 formation of defective particles, even in the absence of virophages, may be
339 more frequent than previously thought (22, 26).

340

341 Discussion

342 A better comprehension of the biology of a virus is achieved with basic
343 investigations of its life cycle. Viruses are a highly heterogeneous group of
344 organisms and present different replication strategies. In general, DNA viruses
345 replicate in the host cell nucleus, while RNA viruses replicate within the cell
346 cytoplasm. However, there are some exceptions, such as some members of the
347 putative *Megavirales* order, poxviruses and iridoviruses for instance (27). These
348 dsDNA viruses replicate in the host cytoplasm, wherein they establish a
349 complex viral factory as an intracellular compartment in which both genome
350 replication and viral morphogenesis occur (28). The giant mimiviruses share this

351 same peculiarity. Studies have been conducting to better comprehend the
352 replication cycle of these viruses, wherein models to explain the viruses' life
353 cycle are constantly being updated (11, 13, 15, 20). In this study, we filled some
354 gaps in the data concerning mimiviruses and introduced some data relating to
355 entry, uncoating and morphogenesis in the mimivirus replication cycle.

356

357 Mimiviruses have a diameter of approximately 700 nm and infect free-
358 living amoebas from the *Acanthamoeba* genus, protists that feed by
359 phagocytosis (8, 29). The large size of mimiviruses associated with their host's
360 life style, along with electron microscopy images, led to the assumption that
361 these viruses entered host cells by phagocytosis, but until now there were no
362 biological data to validate these assumptions. Inhibition of phagocytosis with
363 cytochalasin D allowed us to observed a significant reduction in mimivirus entry,
364 which was not observed with marseilleviruses (viruses of ~200 nm diameter)
365 (Fig. 1A-B). Supported by TEM images, the data show that mimiviruses entered
366 amoeba cells by phagocytosis, while marseilleviruses explored alternative
367 pathways, as previously demonstrated (18). Furthermore, our data suggested a
368 possible importance of phagosome acidification for mimiviruses uncoating(Fig.
369 1C-L). In the presence of bafilomycin, viral replication was impaired. It is
370 possible that a decrease in pH after formation of phagolysosome was the
371 triggering factor to the opening of the mimiviruses' stargate, thus allowing the
372 release of viral seed into the host cytoplasm. Nevertheless, it remains uncertain
373 which pH value is ideal for triggering this process, or whether enzymes present
374 in the lysosomes are essential for this process.

375

376 After release of the viral seed, the DNA replication and transcription take
377 place into early VF (13). It is possible that nuclear factors are involved in this
378 step, but further evidence is needed (30). Assembly of new viral particles takes
379 place inside a mature VF. Previous studies have shown that membranes from
380 the endoplasmic reticulum (ER) migrate toward the edge of the VF and act as
381 scaffolding for the assembly of capsids, which would occur by acquisition of
382 individual pentameric units in sequence (15). Our data corroborate this theory,
383 demonstrating the existence and expansion of lamellar structures, in an
384 analogous way to crescents described for poxviruses and marseilleviruses (Fig.

385 2, 3) (18, 31). It is possible that membranes from ER migrate into the VF
386 wherein they act as scaffolding for protein blocks. These structures increase in
387 size by incorporation of proteins which move away from the core of the VF, until
388 they pass through a fibrillar-aspect area, which we named the fibril acquisition
389 area (FAA), wherein the new viral particles acquire surface fibrils (Fig. 4; 5).
390 This hypothesis was strengthened when we systematically observed the
391 reduction of the fibrillar area after release of viral particles from the VF,
392 suggesting that a fibrillar matrix is continuously consumed as the particles pass
393 through it. Curiously fibrils proteins were not detected by proteomic approaches
394 in isolated VF (14). It is possible that a large fraction of that region was lost
395 during the purification process of the factories, thus hampering the detection of
396 fibrils by this method. Our hypothesis for the acquisition of fibrils by mimiviruses
397 goes on a different or maybe complementary way to the proposal of Kuznetsov
398 and colleagues, who proposed that a layer containing the fibrils involves the
399 viral capsid in a region distant from the VF (15). Moreover, the authors
400 proposed that genome acquisition occurs before the acquisition of fibrils. Our
401 images clearly show that these events occur simultaneously (Fig. 4C; 5). It is
402 possible that some particles receive the genome while the capsid is assembled
403 and then the fibrils are attached as previously proposed, but we believe that, in
404 most cases, these events occur concomitantly.

405

406 The data presented in this study, along with previous published data
407 using atomic force microscopy, X-ray diffraction and fluorescence lead us to
408 present an updated model of the replication cycle of mimiviruses (Fig. 7).
409 Viruses enter amoeba cells by phagocytosis (0 h). After fusion of the
410 phagosome with the lysosome (1-2 h), the stargate is opened and the viral seed
411 is released (4 h). An early VF is established and viral proteins are synthesized
412 outside of the factory (4-6 h). In a mature VF, viral crescents increase in
413 complexity and acquire genome and fibrils simultaneously, as long as they
414 move from the core of VF to the FAA (8 h). Among the newly-formed viral
415 particles, some of them might not be infectious (defective particles), exhibiting
416 morphological features similar to those in the presence of virophages (22, 24).
417 Finally, the viral progeny is released by cell lysis. The comprehension of the
418 biology of mimiviruses is improving due to a combination of biological and

419 genetic data, along with increasingly illuminating images from different
420 microscopic techniques. Notwithstanding current developments, some aspects
421 regarding the replication cycle of mimiviruses remain uncertain, mainly
422 occurring at the molecular level. Future studies will further enhance the model
423 presented here and improve our understanding of the biology of these complex
424 viruses.

425

426 **Acknowledgements**

427

428 We thank our colleagues from Gepvig and the Laboratório de Vírus for their
429 excellent technical support. We also thank CNPq, CAPES and FAPEMIG for
430 scholarship and the Center of Microscopy of UFMG. JSA, CAB and EGK are
431 CNPq researchers. JSA, EGK, BLS are members of a CAPES-COFECUB
432 project.

433

434 **References**

435

- 436 1. La Scola B, Audic S, Robert C, Jungang L, de Lamballerie X, Drancourt
437 M, Birtles R, Claverie J-M, Raoult D. 2003. A giant virus in amoebae.
438 *Science* (80-) 299:2033.
- 439 2. Raoult D, Audic S, Robert C, Abergel C, Renesto P, Ogata H, Scola B La,
440 Suzan M, Claverie J-M. 2004. The 1.2-Megabase Genome Sequence of
441 Mimivirus. *Science* (80-) 306:1344–1350.
- 442 3. Yoosuf N, Yutin N, Colson P, Shabalina SA, Pagnier I, Robert C, Azza S,
443 Klose T, Wong J, Rossmann MG, La Scola B, Raoult D, Koonin E V.
444 2012. Related giant viruses in distant locations and different habitats:
445 *Acanthamoeba polyphaga* moumouvirus represents a third lineage of the
446 Mimiviridae that is close to the Megavirus lineage. *Genome Biol Evol*
447 4:1324–1330.
- 448 4. Arslan D, Legendre M, Seltzer V, Abergel C, Claverie J-M. 2011. Distant
449 Mimivirus relative with a larger genome highlights the fundamental
450 features of Megaviridae. *Proc Natl Acad Sci* 108:17486–17491.
- 451 5. Campos RK, Boratto P V, Assis FL, Aguiar ER, Silva LC, Albarnaz JD,
452 Dornas FP, Trindade GS, Ferreira PP, Marques JT, Robert C, Raoult D,

- 453 Kroon EG, La Scola B, Abrahão JS. 2014. Samba virus: a novel mimivirus
454 from a giant rain forest, the Brazilian Amazon. *Virology* 11:95.
- 455 6. Dornas FP, Khalil JYB, Pagnier I, Raoult D, Abrahão J, La Scola B.
456 2015. Isolation of new Brazilian giant viruses from environmental samples
457 using a panel of protozoa. *Front Microbiol* 6:1–9.
- 458 7. Saadi H, Reteno DGI, Colson P, Aherfi S, Minodier P, Pagnier I, Raoult D,
459 La Scola B. 2013. Shan virus: A new mimivirus isolated from the stool of a
460 tunisian patient with pneumonia. *Intervirology* 56:424–429.
- 461 8. Xiao C, Kuznetsov YG, Sun S, Hafenstein SL, Kostyuchenko VA, Chipman
462 PR, Suzan-Monti M, Raoult D, McPherson A, Rossmann MG. 2009.
463 Structural studies of the giant Mimivirus. *PLoS Biol* 7:0958–0966.
- 464 9. Zauberman N, Mutsafi Y, Halevy D Ben, Shimon E, Klein E, Xiao C, Sun
465 S, Minsky A. 2008. Distinct DNA exit and packaging portals in the virus
466 *Acanthamoeba polyphaga* mimivirus. *PLoS Biol* 6:1104–1114.
- 467 10. Rodrigues RAL, dos Santos Silva LK, Dornas FP, de Oliveira DB,
468 Magalhães TFF, Santos DA, Costa AO, de Macêdo Farias L, Magalhães
469 PP, Bonjardim CA, Kroon EG, La Scola B, Cortines JR, Abrahão JS.
470 2015. Mimivirus Fibrils Are Important for Viral Attachment to the Microbial
471 World by a Diverse Glycoside Interaction Repertoire. *J Virol* 89:11812–
472 11819.
- 473 11. Suzan-Monti M, La Scola B, Barrassi L, Espinosa L, Raoult D. 2007.
474 Ultrastructural characterization of the giant volcano-like virus factory of
475 *Acanthamoeba polyphaga* Mimivirus. *PLoS One* 2.
- 476 12. Abrahão JS, Dornas FP, Silva LC, Almeida GM, Boratto PV, Colson P, La
477 Scola B, Kroon EG. 2014. *Acanthamoeba polyphaga* mimivirus and other
478 giant viruses: an open field to outstanding discoveries. *Virology* 11:120.
- 479 13. Mutsafi Y, Zauberman N, Sabanay I, Minsky A. 2010. Vaccinia-like
480 cytoplasmic replication of the giant Mimivirus. *Proc Natl Acad Sci U S A*
481 107:5978–5982.
- 482 14. Fridmann-Sirkis Y, Milrot E, Mutsafi Y, Ben-Dor S, Levin Y, Savidor A,
483 Kartvelishvili E, Minsky A. 2016. Efficiency in Complexity: Composition
484 and Dynamic Nature of Mimivirus Replication Factories. *J Virol* 90:10039–
485 10047.
- 486 15. Kuznetsov YG, Klose T, Rossmann M, McPherson A. 2013.

- 487 Morphogenesis of Mimivirus and Its Viral Factories: an Atomic Force
488 Microscopy Study of Infected Cells. *J Virol* 87:11200–11213.
- 489 16. Reed LJ, Muench H. 1938. A simple method of estimating fifty per cent
490 endpoints. *Am Journal Hyg* 27:493–497.
- 491 17. Khalil JYB, Robert S, Reteno DG, Andreani J, Raoult D, La Scola B.
492 2016. High-throughput isolation of giant viruses in liquid medium using
493 automated flow cytometry and fluorescence staining. *Front Microbiol* 7:1–
494 9.
- 495 18. Arantes TS, Rodrigues RAL, dos Santos Silva LK, Oliveira GP, de Souza
496 HL, Khalil JYB, de Oliveira DB, Torres AA, da Silva LL, Colson P, Kroon
497 EG, da Fonseca FG, Bonjardim CA, La Scola B, Abrahão JS. 2016. The
498 Large Marseillevirus Explores Different Entry Pathways by Forming Giant
499 Infectious Vesicles. *J Virol* 90:5246–5255.
- 500 19. Yuan N, Song L, Zhang S, Lin W, Cao Y, Xu F, Fang Y, Wang Z, Zhang
501 H, Li X, Wang Z, Cai J, Wang J, Zhang Y, Mao X, Zhao W, Hu S, Chen S,
502 Wang J. 2015. Bafilomycin A1 targets both autophagy and apoptosis
503 pathways in pediatric B-cell acute lymphoblastic leukemia. *Haematologica*
504 100:345–356.
- 505 20. Mutsafi Y, Shimoni E, Shimon A, Minsky A. 2013. Membrane Assembly
506 during the Infection Cycle of the Giant Mimivirus. *PLoS Pathog* 9.
- 507 21. Cerritelli ME, Trus BL, Smith CS, Cheng N, Conway JF, Steven AC. 2003.
508 A second symmetry mismatch at the portal vertex of bacteriophage T7: 8-
509 Fold symmetry in the procapsid core. *J Mol Biol* 327:1–6.
- 510 22. La Scola B, Desnues C, Pagnier I, Robert C, Barrassi L, Fournous G,
511 Merchat M, Suzan-Monti M, Forterre P, Koonin E, Raoult D. 2008. The
512 virophage as a unique parasite of the giant mimivirus. *Nature* 455:100–
513 104.
- 514 23. Desnues C, Raoult D. 2012. Virophages question the existence of
515 satellites. *Nat Rev Microbiol* 10:234–234.
- 516 24. Gaia M, Benamar S, Boughalmi M, Pagnier I, Croce O, Colson P, Raoult
517 D, La Scola B. 2014. Zamilon, a novel virophage with Mimiviridae host
518 specificity. *PLoS One* 9.
- 519 25. Gong C, Zhang W, Zhou X, Wang H, Sun G, Xiao J, Pan Y, Yan S, Wang
520 Y. 2016. Novel virophages discovered in a freshwater lake in China. *Front*

- 521 Microbiol 7.
- 522 26. Abrahão JôS, Boratto P, Dornas FP, Silva LC, Campos RK, Almeida
523 GMF, Kroon EG, La Scola B. 2014. Growing a giant: Evaluation of the
524 virological parameters for mimivirus production. J Virol Methods 207:6–
525 11.
- 526 27. Colson P, De Lamballerie X, Fournous G, Raoult D. 2012.
527 Reclassification of giant viruses composing a fourth domain of life in the
528 new order Megavirales. Intervirology 55:321–332.
- 529 28. Netherton CL, Wileman T. 2011. Virus factories, double membrane
530 vesicles and viroplasm generated in animal cells. Curr Opin Virol 1:381–
531 387.
- 532 29. Siddiqui R, Khan N. 2012. Biology and pathogenesis of Acanthamoeba.
533 Parasit Vectors 5:6.
- 534 30. Suttle C a. 2007. Marine viruses--major players in the global ecosystem.
535 Nat Rev Microbiol 5:801–812.
- 536 31. Maruri-Avidal L, Domi A, Weisberg AS, Moss B. 2011. Participation of
537 Vaccinia Virus L2 Protein in the Formation of Crescent Membranes and
538 Immature Virions. J Virol 85:2504–2511.

539

540 **Figure legends**

541 **Fig 1. Mimivirus entry into the host cell by phagocytosis and uncoating**
542 **depends on acidification of phagosome.** (A-C) The impact of cytochalasin D
543 and bafilomycin on mimivirus replication. Treatment with cytochalasin D and
544 bafilomycin decreased the mimivirus titers and particle incorporation. The MsV
545 was used as a control and its titer was not reduced after the treatment with
546 cytochalasin D, but was reduced with treatment with bafilomycin. (D-L)
547 Transmission electron microscopy images of mimivirus particles entering cells
548 by phagocytosis (D-F), the phagosome-lysosome fusion (F-J), stargate opening
549 (K) and release of the viral seed (L). The inhibitory assays were performed in
550 triplicate. Error bars indicate SD. *, $P < 0.05$ (two-tailed Student's t test); UN:
551 untreated cells; T: treated cells. L: lysosome.

552

553 **Fig 2. Growing lamellar structures seem to be important to mimivirus**
554 **capsid assembly.** (A-C) Growing lamellar structures with different sizes in the
555 viral factory demonstrating the viral crescent-like structures in blue. The smaller
556 blocks are observed in interior of the viral factory and more complete particles
557 are shown in the periphery of the factory. (D-I) Transmission electron
558 microscopy images showing stages of mimivirus particle formation, growing in
559 thickness and complexity; viral crescent (D); particles without genome (E) and
560 fibrils (E,F), particles acquiring genome (red arrows) and fibrils (F-H) until
561 complete mimivirus particle formation (I).

562 **Fig. 3: Scanning microscopy of disrupted mimivirus viral factory.** (A)
563 Lamellar structures related to capsid morphogenesis. (B) In contrast to lamellar
564 capsid forming structures the main component of viral factory presents a
565 globular aspect, likely formed by DNA, membranes and enzymes.

566

567

568 **Fig. 4: Area of fibrils acquisition is present in the periphery of the viral**
569 **factory.** (A-C) Transmission electron microscopy images of the viral factory of
570 mimivirus with a less electron-dense area surrounding the periphery of the
571 factory that was decreased in the size during the particles morphogenesis. Fibril
572 acquisition area at early (A) and mature (B) viral factory (highlighted by blue
573 lines). (C) Mimivirus particles with fibrils in periphery of the viral factory and
574 particles without fibrils inside the factory before passing through the fibril
575 acquisition area. (D) Scanning electron microscopy image of viral factory with
576 particles without fibrils (before fibril acquisition) and prominent stargate.

577

578 **Fig. 5: Fibrils acquisition and genome incorporation can occur**
579 **simultaneously.** Transmission electron microscopy images of mature viral
580 factories indicating the genome incorporation (red arrows) simultaneously to the
581 acquisition of fibrils (purple arrow heads). Viral particles are not fully covered by
582 the fibrils (only half of the particle has fibrils) and the genome is still being

583 packaged. The image shows that the viral genome is acquired at the periphery
584 of the viral factory, at FAA.

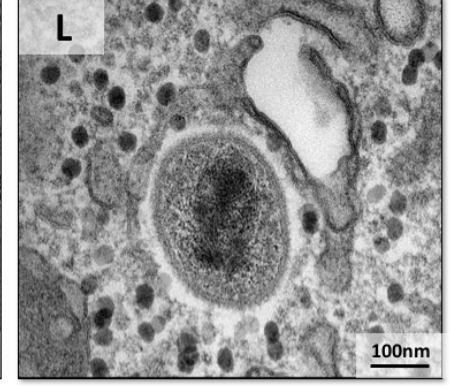
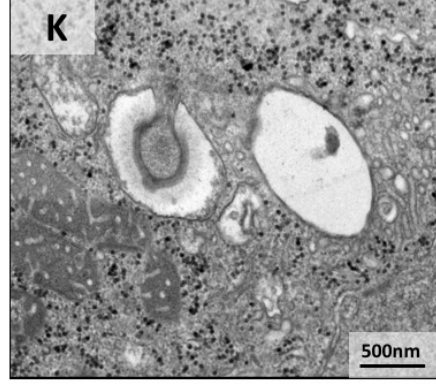
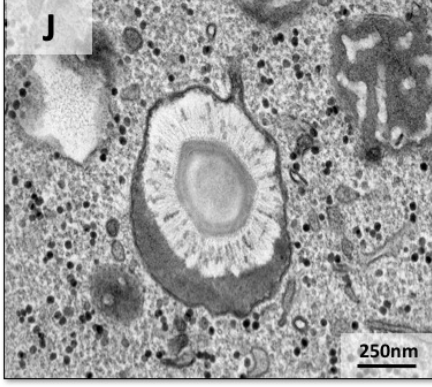
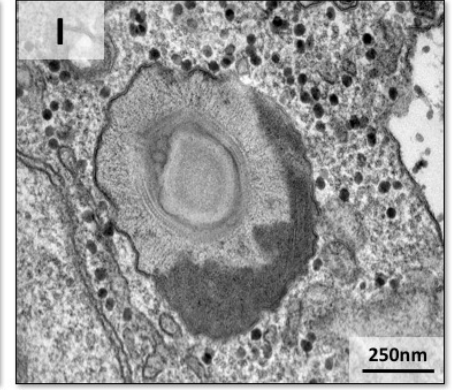
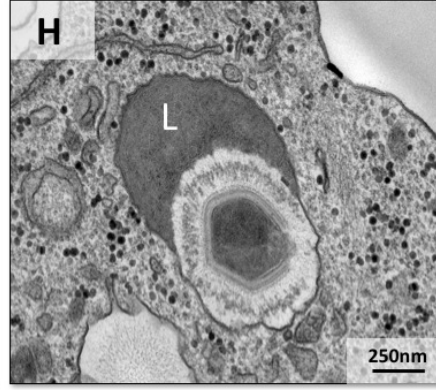
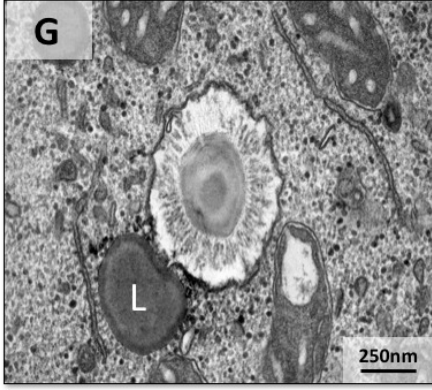
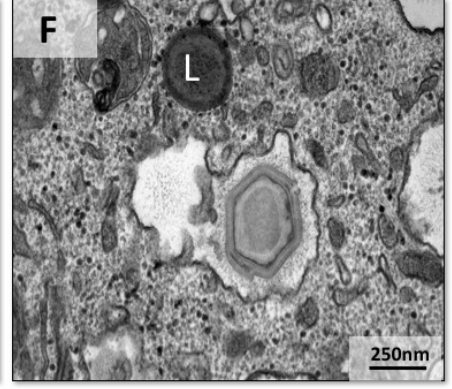
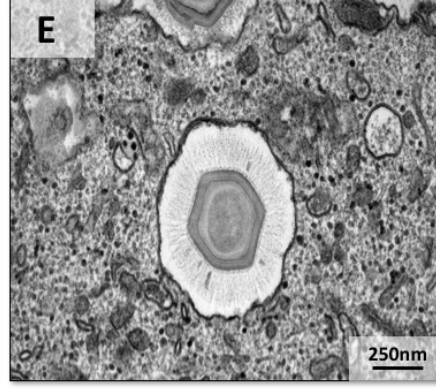
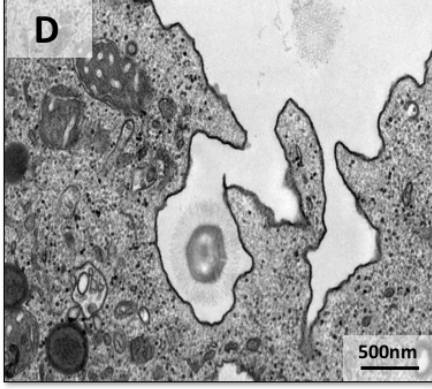
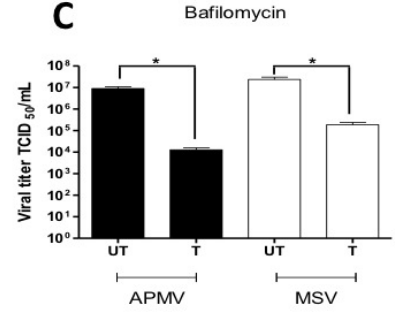
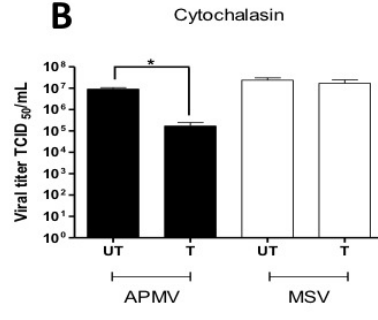
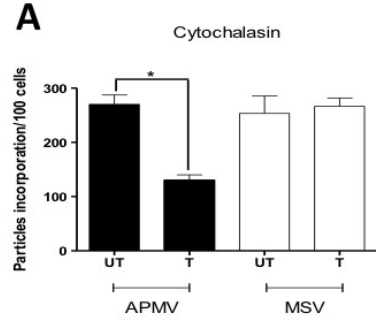
585

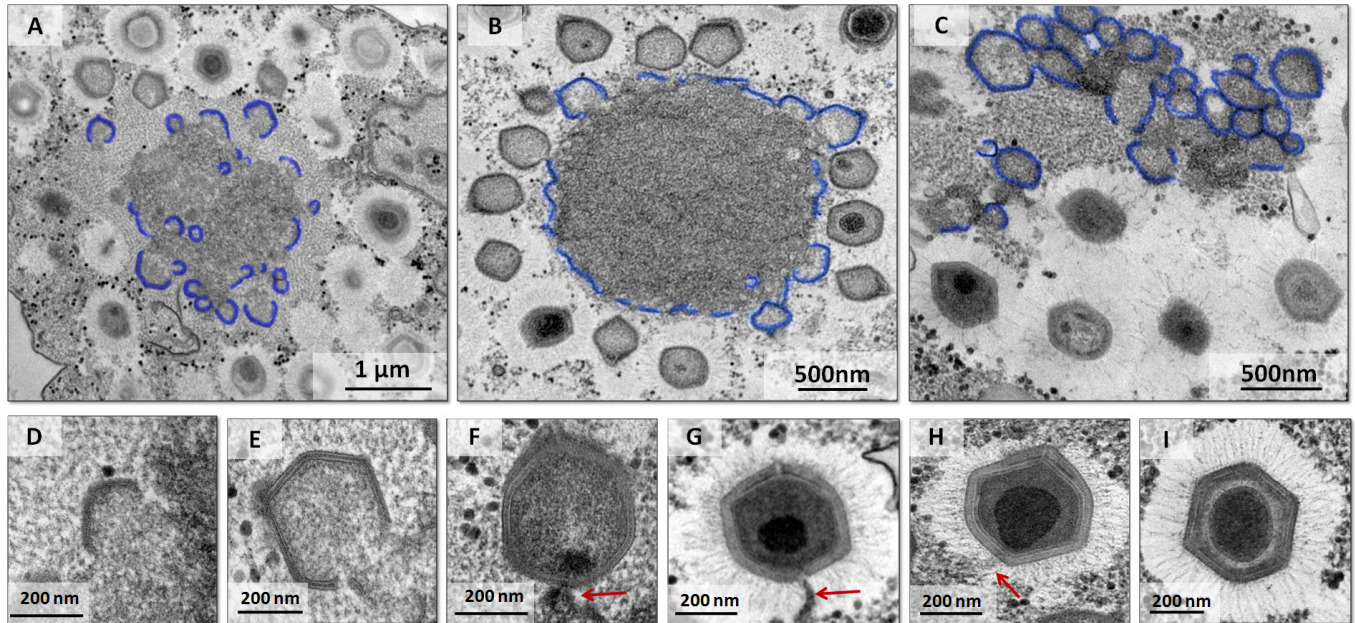
586 **Fig. 6. Defective particles in the mimivirus replication cycle in the absence**
587 **of virophages.** (A-C) Transmission electron microscopy images of mimivirus
588 particles with atypical morphology and (D) unusual localization of assembled
589 empty capsid in the center of the viral factory. (E,F) Scanning electron
590 microscopy images of the particles with non-uniform distribution of fibrils. Red
591 arrows point to unusual features.

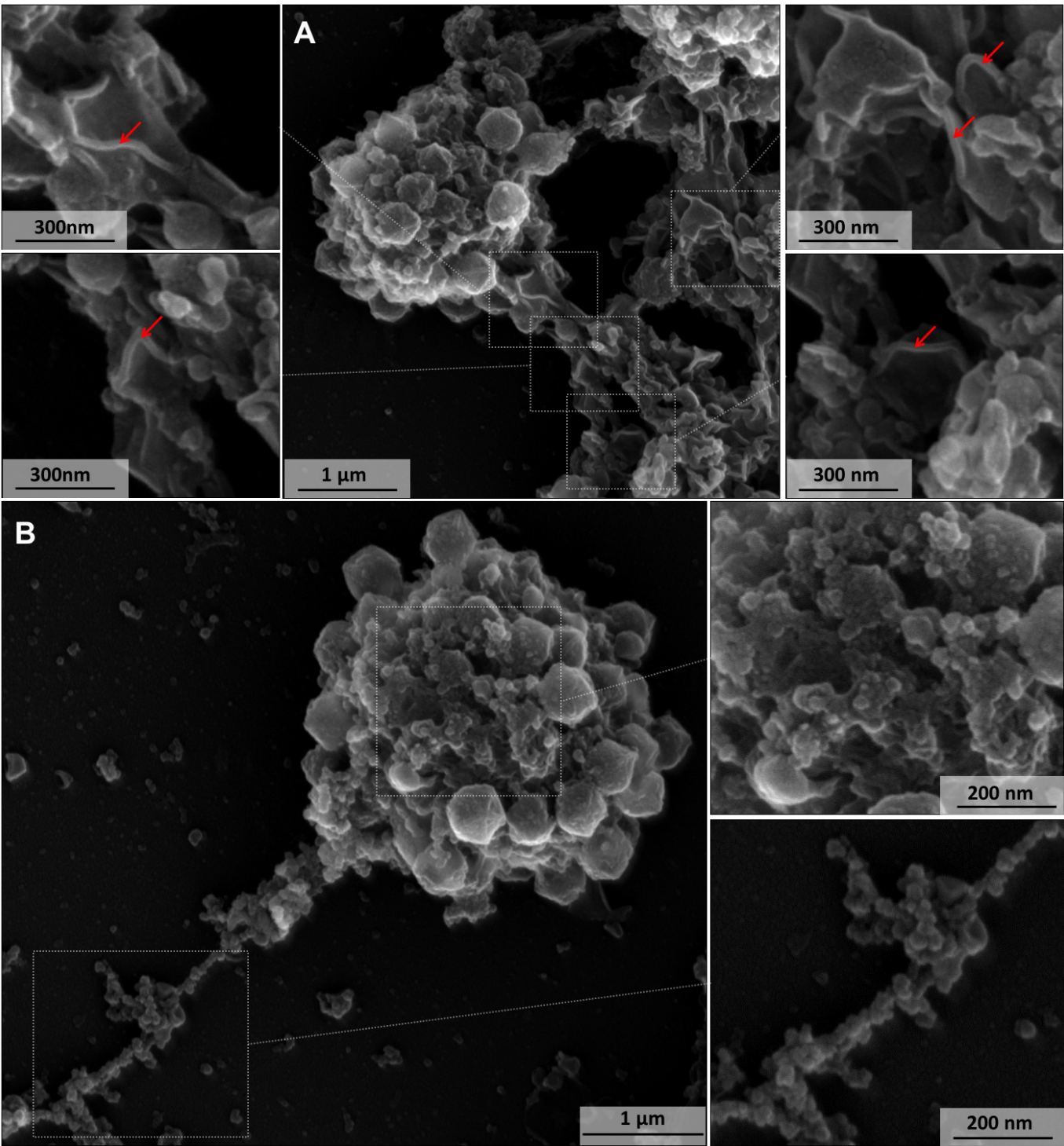
592

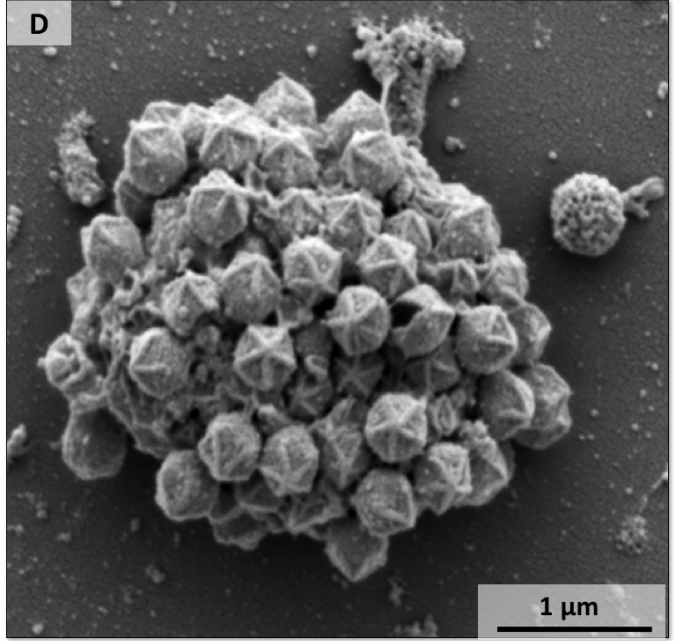
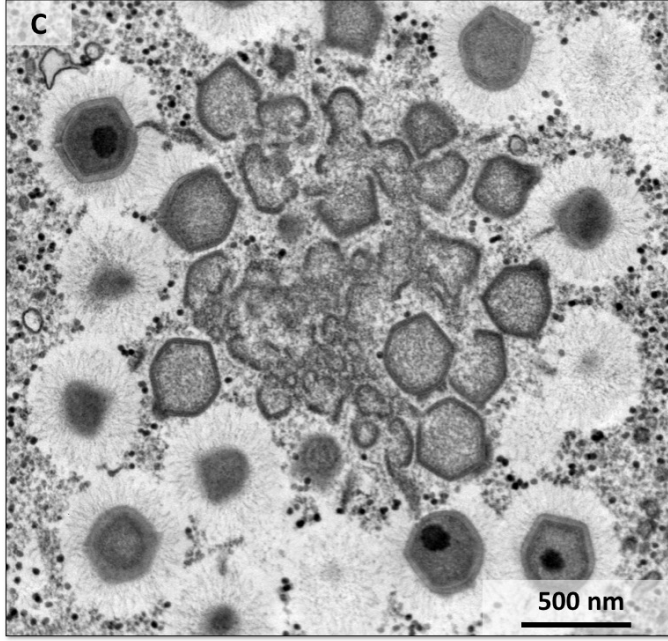
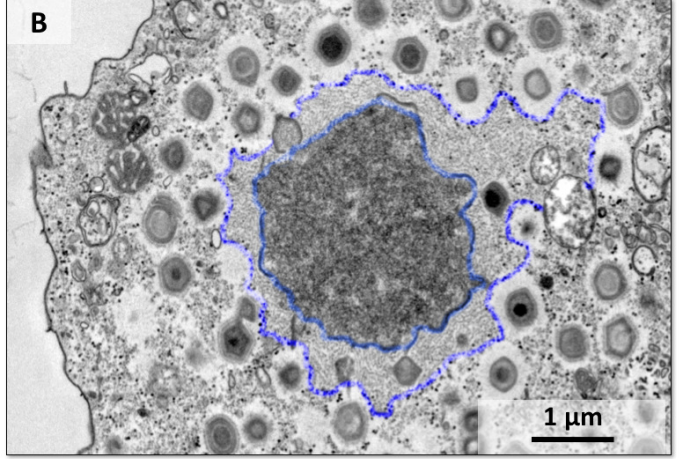
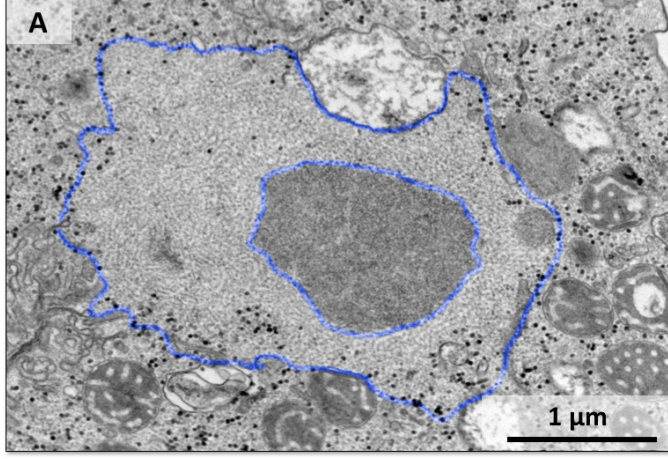
593 **Fig. 7. Representative scheme of the mimivirus replication cycle.** Infectious
594 mimivirus particles enter host cell by phagocytosis. Fusion of phagosome with
595 lysosome occurs and opening of the stargate, followed by release of the viral
596 seed. An early viral factory is established and viral proteins are synthesized
597 outside of the factory. It is uncertain whether the cell nucleus is involved in
598 mimivirus genome replication. The viral crescents increase in thickness and
599 complexity in the mature viral factory and might acquire genome and fibrils
600 simultaneously. The particles move from the core of the viral factory to the fibrils
601 acquisition area (FAA) where the particles incorporate the surface fibrils. Among
602 the newly-formed viral particles, some of them might not be infectious (defective
603 particles), presenting atypical morphology. The viral progeny is released by cell
604 lysis.

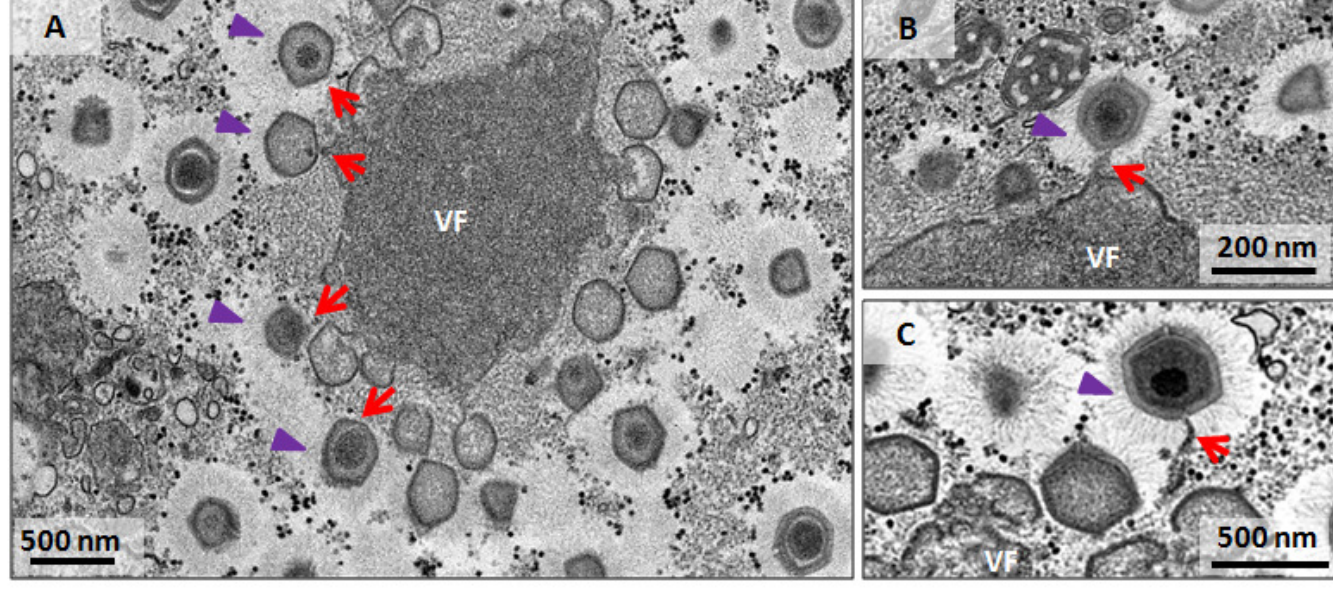
605

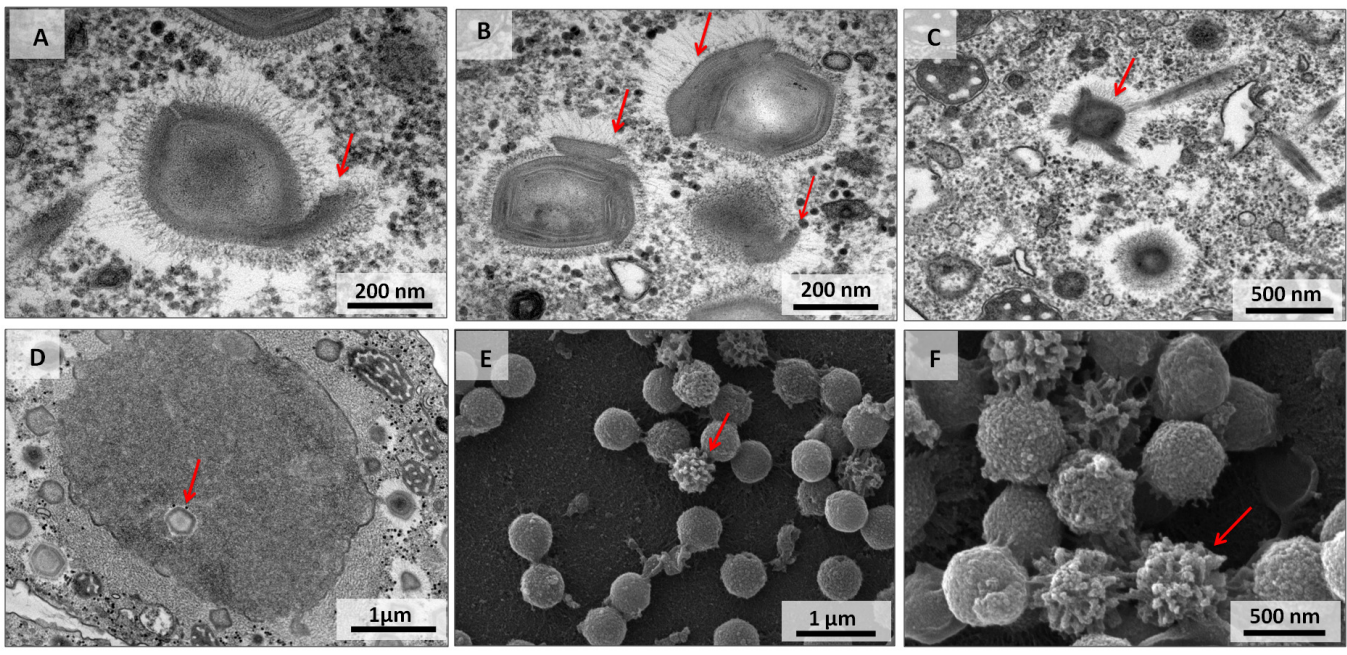


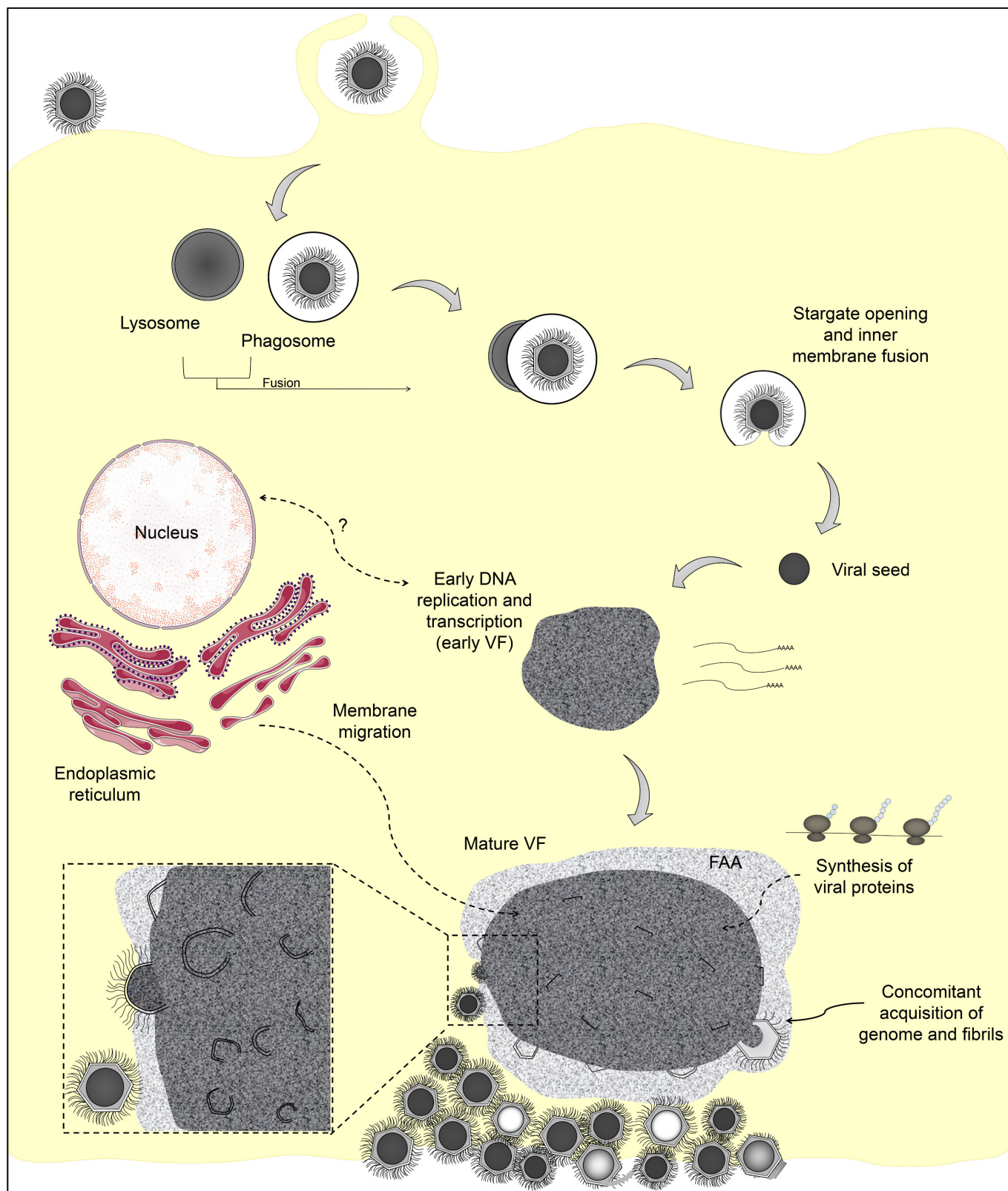













Article

Vaccinia Virus in Blood Samples of Humans, Domestic and Wild Mammals in Brazil

Marina G. Peres ¹, Thais S. Bacchiega ¹, Camila M. Appolinário ¹, Acácia F. Vicente ¹, Mateus de Souza Ribeiro Mioni ¹, Bruna L. D. Ribeiro ¹, Clóvis R. S. Fonseca ¹, Vanessa C. Pelícia ¹, Fernando Ferreira ², Grazielle P. Oliveira ³, Jonatas S. Abrahão ³ and Jane Megid ^{1,*} 

¹ Faculdade de Medicina Veterinária e Zootecnia, UNESP—Universidade Estadual Paulista, Botucatu CEP 18618-970, Brazil; marinageavet@yahoo.com.br (M.G.P.); tatabacch@hotmail.com (T.S.B.); camilaapp.vet@gmail.com (C.M.A.); acaciavicante@hotmail.com (A.F.V.); mateusmioni@yahoo.com.br (M.d.S.R.M.); brunadevider@gmail.com (B.L.D.R.); crsfonseca2@yahoo.com.br (C.R.S.F.); vcpelicia@yahoo.com.br (V.C.P.)

² Faculdade de Medicina Veterinária e Zootecnia, USP—Universidade de São Paulo, São Paulo CEP 05508-270, Brazil; fernando@vps.fmvz.usp.br

³ Instituto de Ciências Biológicas, UFMG—Universidade Federal de Minas Gerais, Belo Horizonte CEP 31270-901, Brazil; graziufmg@yahoo.com.br (G.P.O.); jonatas.abraha@gmail.com (J.S.A.)

* Correspondence: jane@fmvz.unesp.br; Tel.: +55-14-3884-2109

Received: 26 November 2017; Accepted: 17 January 2018; Published: 18 January 2018

Abstract: Outbreaks of Vaccinia virus (VACV) affecting cattle and humans have been reported in Brazil in the last 15 years, but the origin of outbreaks remains unknown. Although VACV DNA have been already detected in mice (*Mus musculus*), opossums (*Didelphis albiventris*) and dogs during VACV zoonotic outbreaks, no transmission to cattle or humans from any of these were reported during Brazilian outbreaks. In this work, we assessed the PCR positivity to VACV in blood samples of cows and other domestic mammals, wild rodents and other wild mammals, and humans from areas with or without VACV infection reports. Our results show the detection of VACV DNA in blood samples of cows, horse and opossums, raising important questions about VACV spread.

Keywords: Vaccinia virus; blood samples; humans; domestic mammals; wild mammals; public health; epidemiology; transmission

1. Introduction

The first official report of a Vaccinia virus (VACV) outbreak in cattle and humans in Brazil was recorded in 1999 at Cantagalo city, Rio de Janeiro State [1]. Since then, outbreaks have been described in several regions of the country [2–9]. It was believed that VACV reemergence in zoonotic outbreaks was related to the VACV vaccines strain used during campaigns of World Health Organization (WHO) against smallpox, and their possible adaptation to some wild host [10]. Now it is known that VACV isolated in Brazilian outbreaks is divergent from VACV vaccines strains, but the origin of outbreaks remains unknown [11,12].

In this way, a model of transmission has been proposed in which peridomestic rodents act as a link between domestic animals and wildlife [13]. In fact, peridomestic rodents like *Mus musculus*, *Rattus rattus* and *Rattus norvegicus* act as host reservoirs of cowpox virus in Europe [14]. Then the members of Rodentia order have been targeted of research looking for explaining its possible role in the VACV spread [15–18].

Despite VACV has once isolated from peritoneum and testicles samples of *Mus musculus*, and VACV DNA was once detected in blood samples of opossums (*Didelphis albiventris*) and dogs,

The minimum number of sampled cows was determined using the program HERDACC3.0[®] for each farm, assuming a PCR sensitivity of 80%, a specificity of 99.9%, and a proportion of infected animals in a positive herd of 20%. The minimum number of lactating cows that needed to be sampled to ensure a minimum sensitivity and specificity of 95% was 20 animals. In a cattle herd with more than 20 animals, only 20 lactating cows selected randomly were sampled, but in a herd with fewer than 20 animals, samples were collected from all animals. From other species (horse, sheep, swine, dogs and cats), one to five samples were collected.

Blood samples were collected from February to April 2011, by mammary vein puncture or jugular puncture from cows and by jugular puncture from other domestic species, and stored at $-20\text{ }^{\circ}\text{C}$ until the PCR test. All animals were examined to presence of characteristic clinical signs, as pustules and crusts.

Capture of wild mammals was conducted from May to September 2011 and was authorized by the Brazilian Institute of Environment and Natural Resource Renewable (IBAMA), the Chico Mendes Biodiversity Conservation Institute (ICM-Bio) by Biodiversity Information and Authorization System (SISBIO) under authorization number 23918-1.

Tomahawk traps with chicken bait were used for capture of wild mammals and pitfall and Sherman traps with a bait consisting of a mixture of peanut cream, canned sardine, cornmeal and oatmeal were used for wild rodents capture. Five traps nights in each farm were required to capture animals in native forest areas surrounding them (consisting of a transitional Atlantic Forest and Cerrado).

Wild mammals were anesthetized with tiletamine and zolazepan (Zoletil[®]) using the recommended dose for each species [23] and blood samples were collected by jugular puncture. Due to infectious agents related to rodents, like *Hantavirus* spp, all wild rodents procedure before, during and after blood samples collection, were performed with uses of personal protective equipment (EPP), as previously described [18]. All collected blood samples were stored at $-20\text{ }^{\circ}\text{C}$ until the PCR test. All animals were examined to presence of characteristic clinical signs, as pustules and crusts.

Blood samples of farmers, rural workers and their families were collected by nurses by cephalic vein puncture during October and November 2011, and stored at $-20\text{ }^{\circ}\text{C}$ until the PCR test.

Viral DNA was extracted using the Invisorb[®] Spin Blood Mini Kit (Strattec Molecular, Berlin, Germany). A nested PCR was used for the amplification of the Vaccinia growth factor (*vgf*) gene [24]. The nested PCR was carried out in a two-step reaction protocol. In the first step, were used the OPV primers (*vgfF*: CGCTGCTATGATAATCAGATCATT and *vgfR*: GATATGGTTGTGCCATAATTTTAT). In the nested step, the pair of internal OPV primers (*vgfF2*: ACACGGTGACTGTATCCA and *vgfR2*: CTAATACAAGCATAATAC) were used [24]. In the first step, 2 μL of template were added to 18 μL of the PCR reaction mixture containing 0.4 mM of OPV primers (VGF-F and VGF-R), 10 mM dNTPs, 2.0 mM MgCl_2 , 500 ng Bovine Serum Albumin (BSA) and 2 U of Taq DNA polymerase, using the manufacturer's supplied $10\times$ buffer. Reactions were performed using the following protocol: incubation at $95\text{ }^{\circ}\text{C}$ for 9 min; 30 cycles of denaturation ($94\text{ }^{\circ}\text{C}$, 1 min), annealing ($45\text{ }^{\circ}\text{C}$, 1 min) and extension ($72\text{ }^{\circ}\text{C}$, 1 min); final extension ($72\text{ }^{\circ}\text{C}$, 10 min). The nested PCR step was carried out using 1 μL of undiluted first PCR product as template. The same chemical and thermal conditions were used, but using internal OPV primers (*vgfF2* and *vgfR2*). PCR sensitivity was determined with decimal serial dilutions ranging from 10^4 to 1PFU of VACV-WR as templates and the sensitivity was defined by the highest viral dilution detected by PCR [24]. The *vgf* gene is a conserved *Orthopoxvirus* (OPV) gene, widely used as a PCR target, in diagnostic and phylogenetic of Brazilian VACV outbreaks [22,24,25]. The *vgf* PCR products were purified by uses of the Illustra[®] GFX PCR and Gel Band Purification Kit (GE Healthcare Life Science, Freiburg, Germany) and then, were submitted to cloning using the pGEM[®]-T Easy Vector System I (Promega, Madison, WI, USA) at Virus Laboratory of Bioscience Institute of the Federal University of Minas Gerais—UFMG. Cloned samples were submitted to gene sequencing and obtained sequences aligned with previously published VACV sequences from GenBank using the Clustal W method, and the alignments were manually checked with MEGA version 7.0 software (Arizona State University, Phoenix, AZ, USA). A phylogenetic tree was constructed using

the neighbor-joining method, the Tamura-3 model of nucleotide substitutions and a bootstrap of 1000 replicates.

3. Results

3.1. Missing Values

A total of 48 farms was randomly chosen for the study, however one farm from Torre de Pedra didn't authorize the study, resulting in a total of 47 farms sampled. A number of 138 wild rodents were captured but collection of blood samples were successfully performed in 103 animals, then results are shown only for these animals.

3.2. Samples Collected and Positivity

A total of 1331 blood samples—148 from humans, 688 from cows, 44 from sheep, 22 from swine, 117 from horses, 114 from dogs, 7 from cats, 57 from white-eared opossums (*Didelphis albiventris*), 16 from black-eared opossums (*Didelphis aurita*), 6 from Brazilian gracile opossums (*Gracilinanus microtarsus*), 4 from crab-eating foxes (*Cerdocyon thous*), 4 from coatis (*Nasua nasua*), 1 from ocelot (*Leopardus pardalis*), and 103 from wild rodents (4 *Akodon montensis*, 4 *Nectomys squamipes*, 4 *Calomys tener*, 13 *Sooretamys angouya*, 17 *Oligoryzomys flavescens*, 61 *Oligoryzomys nigripes*)—were collected (Table 1).

From collected samples, eight (0.6%) were positive for amplification of *vfg* gene in the PCR test. Positivity were observed in four cows (0.6% of sampled cows), one horse (0.8% of sampled horse), two black-eared opossums (12.5% of sampled *D. aurita*) and one white-eared opossum (1.7% of sampled *D. albiventris*) (Table 1). The positive animals were from Anhembi (0.7%) and Bofete (0.7%), and no positivity were detected in blood samples from Torre de Pedra (Table 2), where VACV zoonotic outbreaks were previously reported [3,6].

Table 1. Total of collected blood samples and PCR positivity among species.

Species	<i>n</i>	<i>p</i>	(%)
Human	148	0	(0,0)
Cow	688	4	(0,6)
Sheep	44	0	(0,0)
Swine	22	0	(0,0)
Horse	117	1	(0,8)
Dog	114	0	(0,0)
Cat	7	0	(0,0)
<i>Didelphis albiventris</i>	57	1	(1,7)
<i>Didelphis aurita</i>	16	2	(12,5)
<i>Gracilinanus microtarsus</i>	6	0	(0,0)
<i>Cerdocyon thous</i>	4	0	(0,0)
<i>Nasua nasua</i>	4	0	(0,0)
<i>Leopardus pardalis</i>	1	0	(0,0)
<i>Akodon montensis</i>	4	0	(0,0)
<i>Nectomys squamipes</i>	4	0	(0,0)
<i>Calomys tener</i>	4	0	(0,0)
<i>Sooretamys angouya</i>	13	0	(0,0)
<i>Oligoryzomys flavescens</i>	17	0	(0,0)
<i>Oligoryzomys nigripes</i>	61	0	(0,0)
TOTAL	1331	8	(0,6)

n = collected samples; *p* = positive samples; (%) = percentage of positives.

Table 2. Blood samples distribution among municipalities and proportion of PCR positives between different species.

Species	Anhembi		Bofete		Torre de Pedra	
	<i>n</i>	<i>p</i> (%)	<i>n</i>	<i>p</i> (%)	<i>n</i>	<i>p</i> (%)
Human	82	0 (0,0)	38	0 (0,0)	28	0 (0,0)
Cow	332	3 (0,9)	204	1 (0,5)	152	0 (0,0)
Sheep	33	0 (0,0)	9	0 (0,0)	2	0 (0,0)
Swine	9	0 (0,0)	12	0 (0,0)	1	0 (0,0)
Horse	71	1 (1,4)	23	0 (0,0)	23	0 (0,0)
Dog	56	0 (0,0)	35	0 (0,0)	23	0 (0,0)
Cat	3	0 (0,0)	2	0 (0,0)	2	0 (0,0)
<i>D. albiventris</i>	31	1 (3,2)	19	0 (0,0)	7	0 (0,0)
<i>D. aurita</i>	0	0 (0,0)	13	2 (15,4)	3	0 (0,0)
<i>G. microtarsus</i>	2	0 (0,0)	2	0 (0,0)	2	0 (0,0)
<i>C. thous</i>	3	0 (0,0)	1	0 (0,0)	0	0 (0,0)
<i>N. nasua</i>	3	0 (0,0)	1	0 (0,0)	0	0 (0,0)
<i>L. pardalis</i>	1	0 (0,0)	0	0 (0,0)	0	0 (0,0)
<i>A. montensis</i>	0	0 (0,0)	4	0 (0,0)	0	0 (0,0)
<i>N. squamipes</i>	3	0 (0,0)	1	0 (0,0)	0	0 (0,0)
<i>C. tener</i>	0	0 (0,0)	2	0 (0,0)	2	0 (0,0)
<i>S. angouya</i>	13	0 (0,0)	0	0 (0,0)	0	0 (0,0)
<i>O. flavescens</i>	11	0 (0,0)	3	0 (0,0)	3	0 (0,0)
<i>O. nigripes</i>	30	0 (0,0)	26	0 (0,0)	5	0 (0,0)
TOTAL	683	5 (0,7)	395	3 (0,7)	253	0 (0,0)

n = collected sampled; *p* = positive samples; (%) = percentage of positive samples.

Of the total analyzed samples, one animal from Bofete was simultaneously positive for the detection of DNA in the blood and neutralizing antibodies (titer equal to 16) against OPV in the serum respectively, while the other seven PCR positive samples were from seronegative animals (Table 3), and serological results previously published [18].

Table 3. Correlation between Vaccinia virus (VACV) DNA detection in blood samples by PCR test and detection of neutralizing antibodies in serum samples of the same sampled animals previously tested [18].

Serological Condition	PCR Positive (%)	PCR Negative (%)	Total (%)
Seropositive ¹	1 * (0,5)	185 (99,5)	186 (100)
Seronegative ¹	7 ** (0,6)	1138 (99,4)	1145 (100)
Total	8 (0,6)	1323 (99,4)	1331 (100)

* Cow both positive, PCR and serology (OPV neutralizing antibodies titer equal to 16); ** PCR positive but seronegative animals (three cows, one horse, one *D. albiventris*, two *D. aurita*); ¹ Data from previous serologic study [18].

The PCR positive animals were from six different milking farms, four located in Anhembi county and two from Bofete county, both counties without official reports of VACV outbreaks. PCR positivity in two animals (a cow and a horse) from the same farm were observed in one milking farm from Anhembi and other milking farm from Bofete (two *D. aurita*). The farms that presented the PCR-positive animals are those that had previous seropositivity to OPV in animals and humans (Table 4).

3.3. Sequencing and Analysis of the Sequences

Although all eight positive samples were sequenced just seven could be considered for the phylogenetic analysis due to low coverage of one of them. Thus, the sequencing and phylogenetic tree based on the seven orthopoxvirus nucleotide sequence of the *vgf* gene revealed that our strains (Sample 694, Sample 211, Sample 693, Sample 263, Sample 270, Sample 706) clustered with the Brazilian VACVs (i.e., TOa, TOb, Passatempo, MURV, GP1V, GP2V) and vaccine VACVs (i.e., Lc16m2, WR,

and Lister), which characterized it as a Vaccinia virus (Figure 2). The percentage of identity between the different samples is presented in the Table S1.

Table 4. Farms in which VACV DNA were detected by PCR in blood samples and previous seropositivity of animals and humans from these DNA positive farms.

Milking Farms	PCR Positive Animals	Previous Seropositive ¹			
		Species	p (%)	n	
Anhembi	A16 Opossum (<i>D. albiventris</i>)	Human	1 (25)	4	
		Domestic dog	1 (50)	2	
	A2	Cow	1 (5)	20	
	A23	Cow	1 (6,6)	15	
		Horse			
	A7	Cow	Human	1 (16,6)	6
			Cow	1 (5)	20
Domestic dog			2 (33,3)	6	
Wild rodent (<i>O. nigripes</i>)			1 (5,5)	18	
Bofete	B46 Cow *	Horse	1 (25)	4	
		Domestic dog	1 (16,6)	6	
	B47 Opossum (two <i>D. aurita</i>)	Cows	5 (25)	20	
		Human	1 (50)	2	
		Swine	2 (33,3)	6	

* Cow positive in both tests, PCR and Serology; ¹ Data from previous serologic study [18], p = number of previous seropositive; n = sampled individuals from each species; (%) = percentage of seropositives.

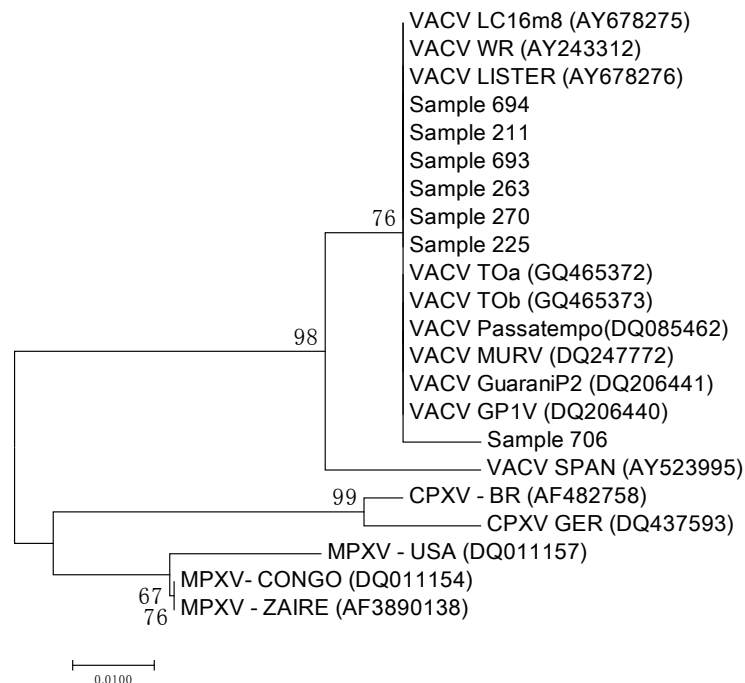


Figure 2. Phylogenetic tree based on the OPV nucleotide sequence of the *vgf* gene showing blood samples cluster (Sample 694, Sample 211, Sample 693, Sample 263, Sample 270, Sample 225, Sample 706). Sample 694 = blood sample of *Didelphis aurita*; Sample 211 = blood sample of cow; Sample 693 = blood sample of *Didelphis aurita*; Sample 263 = blood sample of cow; Sample 270 = blood sample of horse; Sample 225 = blood sample of cow; Sample 706 = blood sample of *Didelphis albiventris*.

4. Discussion

Vaccinia virus (VACV), as other *Orthopoxvirus* (OPV), exhibit a tropism for epithelial cells. During outbreaks, diagnoses are done preferably through the analysis of scabs [1–7]. In the present study, we assessed the presence of VACV in bovine herds and in other domestic and wild mammals, as well as in humans from milk farms located in areas with and without official reports of zoonotic outbreaks. Once the 47 milk farms were not in the proximity of a VACV outbreak, and considering that VACV DNA has been detected in blood samples of experimentally and naturally infected animals, even as in blood samples of naturally infected humans [15,17,19,20,22], we investigated the presence of VACV DNA in blood samples collected of healthy animals and humans from these properties.

Viral DNA could be detected in the blood samples of one horse, three opossums (one *Didelphis albiventris* and two *Didelphis aurita*) and four cows, all apparently healthy, from areas without official reports of VACV outbreaks (Anhembí and Bofete counties) in São Paulo State. To the best of our knowledge, this is the first time that VACV DNA is detected in blood samples of naturally infected cows, horse and *Didelphis aurita*.

All sampled animals and humans of the present study were previously tested for the presence of OPV neutralizing antibodies, and seropositivity was observed in humans, cows, horses, swine, dog, cat, opossums (*D. aurita*; *D. albiventris*), coati (*Nasua nasua*), and in wild rodents (*Oligoryzomys nigripes*, *Oligoryzomys flavescens*, *Sooretamys angouya*) [18]. In the present study, only one cow showed simultaneous detection of viral DNA and neutralizing antibodies, in blood and serum samples respectively, while the other three cows and the horse showed only the presence of viral DNA without detectable neutralizing antibodies. A similar situation was observed during a VACV zoonotic outbreak when serum samples of unaffected humans showed only viral DNA, or both, viral DNA and neutralizing antibodies [20]. The absence of clinical signs associated with the presence of viral DNA in the blood with or without simultaneous presence of neutralizing antibodies suggest a systemic and subclinical infection or an early stage of infection that could evolve to future clinical manifestation.

Apparently humans acquire clinical infection when in contact with viral particles disposed on bovine or human crusts [3,4,6,8], however subclinical human infections has been described with the detection of viral DNA in the blood, been related to other routes of infection, as fomites in the household or through the consume of raw milk and cheese [20]. In our study all human blood samples tested negative for the presence of viral DNA, however neutralizing antibodies were previously detected in 17% of them, and seropositivity was directly correlated with age, and higher in older persons [18]. Both possibilities were suggested, the smallpox vaccine memory or lifelong exposure of farmer to the circulating virus in domestic animals, especially cows [18], but considering that we had seropositive results in people that had never been vaccinated with smallpox vaccine [18], it is possible to suggest that the absence of viral DNA in the blood associated with neutralizing antibodies, may be due to constant contact with domestic animals clinically or sub-clinically infected once the seropositivity was observed in regions with and without VACV infection reported.

The opossums (*D. aurita*; *D. albiventris*) in which blood samples viral DNA were detected, were previously classified as seronegative. This classification was based on the amount of neutralizing antibodies presented by these animals that was insufficient to induce 50% or more of reduction of viral plaques [18]. However, the presence of viral DNA in the blood, associated with the low percentage (9% in *D. albiventris*; 13% and 14% respectively in both *D. aurita*) of reduction of viral plaques may suggest acute infection with initial production of neutralizing antibodies; these animals would present clinical signs in the future, but subclinical infection cannot be ruled out. In a previous report [19], *Didelphis albiventris*, apparently healthy, also showed the presence of viral DNA in their blood samples, during a VACV zoonotic outbreak and subclinical infection as well as their possible role as VACV reservoir was questioned.

Concerning the role of wild rodents in VACV spread, our results didn't show viral DNA in blood of sampled wild rodents from this sampling area, and low percentage of seropositivity were previously detected in these animals [18]. However, VACV DNA was detected in the feces of *O. flavescens*,

O. nigripes and *S. angouya*, as well as in urine of *O. flavescens* from the same area. The simultaneous detection of VACV DNA in feces and neutralizing antibodies in serum samples of two *O. flavescens* from Bofete were observed (unpublished work [18,26]). These animals were apparently healthy, and showed 54% and 59% of reduction in viral plaques being considered positives to OPV antibodies [18]. These finds together suggest acute infection with initial production of neutralizing antibodies in these animals that could lead them to develop or not clinical signs. In fact, sentinel mice exposed to feces of experimentally infected cows and mice didn't show any clinical sign but viral DNA could be detected in their blood, organs and feces samples suggesting subclinical infection [15,17].

Taking our findings together, we cannot rule out the possibility of these animals (DNA positive) eventually developing clinical signs, but considering that no VACV-like outbreaks were reported in the three sampled counties, from the initial period of samples collection until now, these animals (DNA positive) presumably subclinically infected, can sustain the viral circulation in the sampling area.

Accordingly, in Torre de Pedra, a county with two VACV zoonotic outbreaks registered in 2007 and 2010 [3,6], no viral DNA were detected in blood samples, neither in feces or urine samples of wild rodents (Peres et al., unpublished data). On the other hand, this county showed the greatest proportion of seropositivity for cows (39%) and horses (22%), while 10% opossum were seropositive and all wild rodents were seronegative [18]. Comparatively, Bofete showed detection of viral DNA in blood samples of one cow and two *D. aurita*, and in feces of two *O. flavescens* and one *O. nigripes* (unpublished work [26]). Bofete also showed the second highest seropositive rate of cows (14%) and horses (9%), 9% of opossums (*D. albiventris* and *D. aurita*) seropositive, and the highest seropositive rate in wild rodents (11%) [18]. In contrast, in Anhembi, VACV DNA in blood samples were detected in three cows, one horse and one *D. albiventris*, while viral DNA were detected in feces samples from one *O. nigripes* and two *S. angouya* and in urine samples from one *O. flavescens* (unpublished work [26]). In addition, Anhembi showed the lowest seropositive rate in cows (5%) and horses (3%), and opossums (6.5%) and the second highest rate in wild rodents, with 9% of seropositivity [18].

When considering our previous results of serology associated with the outbreak situation, counties localization, and viral DNA detection, we can observe that Torre de Pedra, which had a VACV outbreak, showed a high prevalence of neutralizing antibodies in domestic animals, followed by Bofete and Anhembi (lower percentage of seropositivity, but VACV DNA animals positive in both counties). This is compatible with the model of endemic infection known as the SIR model [27], where after the outbreaks in Torre de Pedra, the number of removals (R) increased due to long-term immunity promoted by VACV, resulting in reduction of susceptibles (S) and infectives (I), justifying viral DNA absence in sampled species. In contrast, the findings of Bofete and Anhembi suggests that there was still a large number of susceptibles (S = DNA negative and seronegative), which were acquired the infection (I = DNA positive), thus resulting in a progressive increase of removals (R = seropositive). In addition, this suggests the existence of a viral spread by contiguity, from Torre de Pedra to Bofete to Anhembi. It is possible that this viral circulation occurs in opossums and wild rodents, and these last animals eliminate low viral loads in their feces and urine (unpublished work [26]) contaminating the environment. The low viral loads in the environment can induce subclinical infections, which is evidenced by presence of viral DNA and neutralizing antibodies in blood of domestic and wild animals that are apparently healthy. Despite wild rodents eliminating the DNA virus in their feces, this was not evidenced in Torre de Pedra, probably due to small sample size in this county, or the average life span of these wild rodent species [28], also evidenced by the absence of positivity in both the PCR testing of blood and the Plaque Reduction Neutralizing Test (PRNT) in this county, suggesting that the virus is no longer circulating in this county.

Spread of infectious agents by contiguity is based on having a shared edge [29]. In these sense, Torre de Pedra, Bofete and Anhembi are neighboring municipalities (Figure 1). Most of the emerging infections usually originate in one geographic location and then disseminate to new places [30], so the origin could be the Torre de Pedra outbreaks. A factor that has been attributed to the spread of the VACV to other regions is the movement of bovine cattle, i.e., the buying and selling of animals

between neighboring municipalities, even among states [25,31,32]. Then, the movement of herds among municipalities can promote viral spread. In addition, if the reservoir host becomes more widely disseminated, the infectious agent can appear in new places [30]. Accordingly, both opossums (*D. albiventris* and *D. aurita*) and wild rodents (*O. nigripes*, *O. flavescens* and *S. agouya*) were the most sampled wild mammals (Table 2). The factors involved in the interaction between them are still unclear, but may include contact with feces, social interactions, and predation, among others, as previously suggested in the murine transmission model proposed by Abrahão et al. [13].

The possible role of rodents and opossums in the spread and environmental maintenance of VACV has been suggested [13,16,19], as well as the transmission of subclinical infection between sentinel mice exposed to feces of experimentally infected mice [15,17], which reinforces our suggestion of subclinical viral spread through the feces and urine of wild rodents.

In attempt to confirm our suggestion that the virus of Torre de Pedra outbreak is the same that is circulating as a subclinical infection in wild and domestic animals from the studied region, all blood samples that were positive in amplification of the *vgf* gene were submitted to the amplification of the gene that encodes viral hemagglutinin (*ha*) [33]. According to the amino acid deletion in the *ha* gene, it is possible to classify the Brazilian VACV into two groups [11,12], which allow us to infer the origin of our virus. All tested samples results were negative to amplification of *ha* gene, and we attribute this to the possible low viral load circulating in this animals as well as the *vgf* targeting PCR would be more sensitive than HA targeting PCR once *vgf* is duplicated at most of VACV genomes, which could improve its detection by PCR. The *ha* protocol is less sensitive and does not detect low viral loads, which reinforces our hypothesis of low viral loads circulating in animals with subclinical infections. As mentioned in materials and methods, all samples that resulted positive in *vgf* gene amplification were submitted to cloning because the DNA concentration was insufficient to allow the direct sequencing. This low DNA concentration in the *vgf* PCR products can be possible due to low viral load in the blood of subclinical infected animals.

In attempt to increase the viral load, and although not mentioned in materials and methods, all positive samples were submitted to virus isolation in Vero cell culture at Biologic Institute of São Paulo State, which would allow amplification and sequencing of *ha* gene. After six passages in Vero cell cultures, no cytopathic effect was observed in any inoculated sample. We justify this to the low viral load in the blood of apparently health animals, evidenced by the low DNA concentrations observed in PCR tests.

Accordingly, the presence of viral DNA in blood samples of apparently healthy animals, does not mean that viable viral particles are present in the blood. Previous reports demonstrated that persons vaccinated against smallpox with the Dryvax vaccin, had VACV DNA detected in the blood, while the infectious virus were not detected in viral isolation [21]. The authors also referred that the isolation of VACV in blood samples of vaccine recipients was only observed in persons with moderate or severe complications of Vaccinia vaccine [21]. Then it is possible that viable viral particles are not present in the blood during subclinical infections.

The second possibility is that viable viral particles are not detected in the blood with the same frequency at which the viral DNA is detected. Rivetti Jr et al. [22] showed that one from eight experimentally infected cows were positive in VACV isolation in cell culture only on the fourth day post-inoculation, during 70 days of blood samples collection and analysis while an intermittent detection of VACV DNA was observed between the 2nd and 15th days post-inoculation. The absence of viable viral particles and the low DNA detection in sampled blood samples could justify both of these results.

Despite our efforts to infer about the source of the VACV found in blood samples of domestic and wild mammals in the present study, it was not possible infer any similarity to the VACV previously detected in Torre de Pedra. However, the results of *vgf* gene analysis allowed us to characterize the virus detected in blood samples of domestic and wild mammals as a Vaccinia virus. Our results corroborate previous findings that the VACV induces systemic infection with viral DNA detection in the

blood [22], as well as subclinical infection in experimentally and naturally infected animals [15,17,19], and suggest that animals in the present study experience subclinical infection. Additionally, these data suggest that the virus may be circulating by contiguity in this region, but more studies are needed to confirm this.

Supplementary Materials: Supplementary materials can be found at www.mdpi.com/1999-4915/10/1/42/s1.

Acknowledgments: We thank Fundação de Amparo à Pesquisa do Estado de São Paulo (FAPESP) for financial support (Process:2013/07693-1).

Author Contributions: Jane Megid and Marina G. Peres conceived and designed the experiments, contributed reagents/materials/analysis tools; designed the experiments and wrote the paper; Marina G. Peres, Thais S. Bacchiega, Camila M. Appolinário, Acácia F. Vicente, Mateus S. R. Mioni, Bruna L. D. Ribeiro, Clóvis R. S. Fonseca and Vanessa C. Pelícia performed the experiments, Fernando Ferreira designed the experiments; Grazielle P. Oliveira and Jonas S. Abrahão performed part of the experiments, analyzed the data and wrote the paper.

Conflicts of Interest: The authors declare no conflicts of interest.

References

1. Damaso, C.R.A.; Esposito, J.J.; Condit, R.C.; Moussatche, N. An emergente poxvirus from humans and cattle in Rio de Janeiro State: Cantagalo Virus may derive from Brazilian Smallpox Vaccine. *Virology* **2000**, *277*, 439–449. [[CrossRef](#)] [[PubMed](#)]
2. Negasse-segahara, T.K.; Kisielius, J.J.; Ueda-Ito, M.; Curtis, S.P.; Figueiredo, C.A.; Cruz, A.S.; Silv, M.M.J.; Ramos, C.H.; Silva, M.C.C.; Sakurati, T.; et al. Human Vaccinia-like outbreaks in São Paulo and Goiás States, Brazil: Vírus detection, isolation and identification. *Rev. Inst. Med. Trop. São Paulo* **2004**, *46*, 315–322. [[CrossRef](#)]
3. Megid, J.; Appolinário, C.M.; Langoni, H.; Pituco, E.M.; Okuda, L.H. Short Report: Vaccinia virus in humans and cattle in southwest region of São Paulo State, Brazil. *Am. J. Trop. Med. Hyg.* **2008**, *79*, 647–651. [[PubMed](#)]
4. Abrahão, J.S.; Sival-Fernandes, A.T.; Assis, F.L.; Guedes, M.I.; Drumond, B.P.; Leite, J.A.; Coelho, L.F.L.; Turrini, F.; Fonseca, F.G.; Lobato, Z.I.P.; et al. Human Vaccinia vírus and Pseudocowpox viru co-infection: Clinical description and phylogenetic characterization. *J. Clin. Virol.* **2010**, *48*, 69–72. [[CrossRef](#)] [[PubMed](#)]
5. Brum, M.C.S.; Anjos, B.L.; Nogueira, C.E.W.; Amaral, L.A.; Wiblen, R.; Flores, E.F. An outbreak of orthopoxvirus-associated disease in horse in Southern Brazil. *J. Vet. Diagn. Investig.* **2010**, *22*, 143–147.
6. Megid, J.; Borges, I.A.; Abrahão, J.S.; Trindade, G.S.; Appolinário, C.M.; Ribeiro, M.G.; Allendorf, S.D.; Antunes, J.M.A.P.; Silva-Fernandes, A.T.; Kroon, E.G. Vaccinia Virus, Zoonotic Infection, São Paulo State, Brazil. *J. Emerg. Infect. Dis.* **2012**, *18*, 189–191. [[CrossRef](#)] [[PubMed](#)]
7. Assis, F.L.; Vinhote, W.M.; Barbosa, J.D.; Oliveira, C.H.S.; Oliveira, C.M.G.; Campos, K.F.; Silva, N.S.; Trindade, G.S.; Abrahão, J.S.; Kroon, E.G. Reemergence of Vaccinia vírus during zoonotic outbreak, Pará State, Brazil. *Emerg. Infect. Dis.* **2013**, *19*, 2017–2020. [[CrossRef](#)] [[PubMed](#)]
8. Oliveira, G.P.; Fernandes, A.T.S.; Assis, F.L.; Alves, P.A.; Luiz, A.P.M.F.; Figueiredo, L.B.; Almeida, C.M.C.; Travassos, C.E.P.F.; Trindade, G.S.; Abrahão, J.S.; et al. Short Report: Intrafamilial transmission of Vaccinia vírus during a bovine Vaccinia outbreak in Brazil: A New Insight in Viral Transmission Chain. *Am. J. Trop. Med. Hyg.* **2014**, *90*, 1021–1023. [[CrossRef](#)] [[PubMed](#)]
9. Abrahão, J.S.; Campos, R.K.; Trindade, G.S.; Fonseca, F.G.; Ferreira, P.C.P.; Kroon, E.G. Outbreak of severe zoonotic Vaccinia vírus infection, Southeastern Brazil. *Emerg. Infect. Dis.* **2015**, *21*, 695–698. [[CrossRef](#)] [[PubMed](#)]
10. Moussatche, N.; Damaso, C.R.; McFadden, G. When good vaccine go wild: Feral Orthopoxvirus in developing countries and beyond. *J. Infect. Dev. Ctries.* **2008**, *2*, 156–173. [[CrossRef](#)] [[PubMed](#)]
11. Trindade, G.S.; Emerson, G.L.; Carroli, D.S.; Kroon, E.G.; Damon, I.K. Brazilian Vaccinia virus and their origins. *Emerg. Infect. Dis.* **2007**, *13*, 965–972. [[CrossRef](#)] [[PubMed](#)]
12. Drumond, B.P.; Leite, J.A.; da Fonseca, F.G.; Bonjardim, C.A.; Ferreira, P.C.P.; Kroon, E.G. Brzilian Vaccinia vírus strains are genetically divergente and differ from the Lister vaccine strain. *Microb. Infect.* **2008**, *10*, 185–197. [[CrossRef](#)] [[PubMed](#)]

13. Abrahão, J.S.; Guedes, M.I.M.; Trindade, G.S.; Fonseca, F.G.; Campos, R.K.; Mota, B.F.; Lobato, Z.I.P.; Silva-Fernandes, A.T.; Rodrigues, G.O.L.; Lima, L.S.; et al. One more piece in the VACV ecological puzzle: Could peridomestic rodents be the link between wildlife and bovine Vaccinia outbreaks in Brazil? *PLoS ONE* **2009**, *4*, e7428. [[CrossRef](#)] [[PubMed](#)]
14. Essbauer, S.; Pfeffer, M.; Meyer, H. Zoonotic poxviruses. *Vet. Microbiol.* **2010**, *140*, 229–236. [[CrossRef](#)] [[PubMed](#)]
15. Ferreira, J.M.S.; Abrahão, J.S.; Drumond, B.P.; Oliveira, F.M.; Alves, P.A.; Pascoal-Xavier, M.A.; Lobato, Z.I.P.; Bonjardim, C.A.; Ferreira, P.C.P.; Kroon, E.G. Vaccinia vírus: Shedding and horizontal transmission in a murine model. *J. Gen. Virol.* **2008**, *89*, 2986–2991. [[CrossRef](#)] [[PubMed](#)]
16. Abrahão, J.S.; Trindade, G.S.; Ferreira, J.M.S.; Campos, R.K.; Bonjardim, C.A.; Ferreira, P.C.P.; Kroon, E.G. Long-lasting stability of Vaccinia virus strains in murine feces: Implications for virus circulation and environmental maintenance. *Arch. Virol.* **2009**, *154*, 1551–1553. [[CrossRef](#)] [[PubMed](#)]
17. D’Anunção, L.; Guedes, M.I.M.; Oliveira, T.L.; Rehfeld, I.; Bonjardim, C.A.; Ferreira, P.P.; Trindade, G.S.; Lobato, Z.P.; Kroon, E.G.; Abrahão, J.S. Filling one more gap: Experimental evidence of horizontal transmission of Vaccinia virus between bovines and rodents. *Vector Borne Zoonotic Dis.* **2012**, *12*, 61–64. [[CrossRef](#)] [[PubMed](#)]
18. Peres, M.G.; Bacchiega, T.S.; Appolinário, C.M.; Vicente, A.F.; Allendorf, S.D.; Antunes, J.M.A.P. Serological study of vaccinia virus reservoirs in areas with and without official reports of outbreaks in cattle and humans in São Paulo, Brazil. *Arch. Virol.* **2013**, *158*, 2433–2441. [[CrossRef](#)] [[PubMed](#)]
19. Peres, M.G.; Barros, C.B.; Appolinário, C.M.; Antunes, J.M.A.P.; Mioni, M.S.R.; Bacchiega, T.S.; Allendorf, S.D.; Vicente, A.F.; Fonseca, C.R.; Megid, J. Dogs and opossums positive for vaccinia virus during outbreak affecting cattle and humans, São Paulo State, Brazil. *J. Emerg. Infect. Dis.* **2016**, *22*, 271–273. [[CrossRef](#)] [[PubMed](#)]
20. Costa, G.B.; Borges, I.A.; Alves, P.A.; Miranda, J.B.; Luiz, A.P.M.F.; Ferreira, P.C.P.; Abrahão, J.S.; Moreno, E.C.; Kroon, E.G.; Trindade, G.S. Alternative routes of zoonotic Vaccinia virus transmission, Brazil. *Emerg. Infect. Dis.* **2015**, *15*, 12–14. [[CrossRef](#)] [[PubMed](#)]
21. Cohen, J.I.; Hohman, P.; Preuss, J.C.; Li, L.; Fischer, S.H.; Fedorko, D.P. Detection of Vaccinia virus DNA, but not infectious virus in the blood of smallpox vaccine recipients. *Vaccine* **2007**, *25*, 4571–4574. [[CrossRef](#)] [[PubMed](#)]
22. Rivetti, A.V., Jr.; Guedes, M.I.M.C.; Rehfeld, I.S.; Oliveira, T.M.L.; Matos, A.C.D.; Abrahão, J.S.; Kroon, E.G.; Lobato, Z.I.P. Bovine vaccinia, a systemic infection: Evidence of fecal shedding, viremia and detection in lymphoid organs. *Vet. Microbiol.* **2013**, *162*, 103–111. [[CrossRef](#)] [[PubMed](#)]
23. Nunes, A.L.V.; Cruz, M.L.; Cortopasso, S.R.G. *Anestesiologia*; Cubas, S.Z., Silva, I.C.R., Catão, J.L., Eds.; Tratado de Animais Selvagens: São Paulo, Brazil, 2006; pp. 1040–1067.
24. Abrahão, J.S.; Lima, L.S.; Assis, F.L.; Alves, P.A.; Silva-Fernandes, A.T.; Cota, M.M.G.; Ferreira, V.M.; Campos, R.K.; Mazur, C.; Lobato, Z.I.P.; et al. Nested-multiplex PCR detection of Orthopoxvirus and Parapoxvirus directly from exanthematic clinical samples. *Virol. J.* **2009**, *6*, 140. [[CrossRef](#)] [[PubMed](#)]
25. Assis, F.L.; Franco-Luiz, A.P.M.; Paim, L.M.; Oliveira, G.P.; Pereira, A.F.; Almeida, G.M.F.; Figueiredo, L.B.; Tanus, A.; Trindade, G.S.; Ferreira, P.P.; et al. Horizontal study of vaccinia virus infections in an endemic area: Epidemiologic, phylogenetic and economic aspects. *Arch. Virol.* **2015**, *160*, 2703–2708. [[CrossRef](#)] [[PubMed](#)]
26. Peres, M.G.; Bacchiega, T.S. Vaccinia virus in feces and urine of wild rodents from São Paulo State, Brazil. *Viruses* **2018**, in revision.
27. Kermack, W.O.; McKendrick, A.G. A contribution to the mathematical theory of epidemics. *R. Soc. Lond. Ser. A* **1927**, *115*, 700–721. [[CrossRef](#)]
28. Reis, N.L.; Perachi, A.L.; Pedro, W.A.; Lima, I.P. *Mamíferos do Brasil*; Universidade Estadual de Londrina: Londrina, Brazil, 2006; pp. 364–365.
29. Flood, J.S.; Prophyre, T.; Tindesley, M.J.; Wollhouse, M.E. The performance of approximations of farm contiguity compared to contiguity defined using detailed geographical information in two sample areas in Scotland: Implications for foot-and-mouth disease modelling. *Vet. Res.* **2013**, *9*, 2–13. [[CrossRef](#)] [[PubMed](#)]
30. Morse, S.S. Factor in the emergence of infectious diseases. *Emerg. Infect. Dis.* **1995**, *1*, 7–15. [[CrossRef](#)] [[PubMed](#)]

31. Medaglia, M.L.G.; Pessoa, L.C.G.D.; Sales, E.R.C.; Freitas, T.R.P.; Damaso, C.R. Spread of Cantagalo Vírus to Northern Brazil. *Emerg. Infect. Dis.* **2009**, *15*, 1142–1143. [[CrossRef](#)] [[PubMed](#)]
32. Quixabeira-Santos, J.C.; Medaglia, M.L.G.; Pescador, C.A.; Damaso, C.R. Animal movement and establishment of Vaccinia virus Cantagalo strain in Amazon Biome Brazil. *Emerg. Infect. Dis.* **2011**, *17*, 726–729. [[CrossRef](#)] [[PubMed](#)]
33. Damaso, C.R.A.; Reis, S.A.; Jesus, D.M.; Lima, P.S.F.; Moussatché, N. A PCR-based assay for detection of emerging vaccinia-like viroses isolated in Brazil. *Diagn. Microbiol. Infect. Dis.* **2007**, *57*, 39–46. [[CrossRef](#)] [[PubMed](#)]



© 2018 by the authors. Licensee MDPI, Basel, Switzerland. This article is an open access article distributed under the terms and conditions of the Creative Commons Attribution (CC BY) license (<http://creativecommons.org/licenses/by/4.0/>).

Article

A Model to Detect Autochthonous Group 1 and 2 Brazilian *Vaccinia virus* Coinfections: Development of a qPCR Tool for Diagnosis and Pathogenesis Studies

Rafael Calixto ¹, Grazielle Oliveira ¹, Maurício Lima ¹, Ana Cláudia Andrade ¹,
Giliane de Souza Trindade ¹, Danilo Bretas de Oliveira ^{1,2} and Erna Geessien Kroon ^{1,*}

¹ Laboratório de Vírus, Departamento de Microbiologia, Universidade Federal de Minas Gerais, Belo Horizonte 31270-901, Minas Gerais, Brazil; calixtomicro@yahoo.com.br (R.C.); graziufmg@yahoo.com.br (G.O.); maurili15@hotmail.com (M.L.); ana.andrade2008@hotmail.com (A.C.A.); gitrindade@yahoo.com.br (G.d.S.T.); danilobretas@yahoo.com.br (D.B.d.O.)

² Faculdade de Medicina de Diamantina, Universidade Federal dos Vales do Jequitinhonha e Mucuri, Dimantina 39100-000, Minas Gerais, Brazil

* Correspondence: kroone@icb.ufmg.br or ernagkroon@gmail.com; Tel.: +55-031-99949-1240

Received: 1 December 2017; Accepted: 29 December 2017; Published: 30 December 2017

Abstract: *Vaccinia virus* (VACV) is the etiological agent of bovine vaccinia (BV), an emerging zoonosis that has been associated with economic losses and social effects. Despite increasing reports of BV outbreaks in Brazil, little is known about the biological interactions of Brazilian VACV (VACV-BR) isolates during coinfections; furthermore, there are no tools for the diagnosis of these coinfections. In this study, a tool to co-detect two variants of VACV was developed to provide new information regarding the pathogenesis, virulence profile, and viral spread during coinfection with VACV-BR isolates. To test the quantitative polymerase chain reactions (qPCR) tool, groups of BALB/c mice were intranasally monoinfected with Pelotas virus 1—Group II (PV1-GII) and Pelotas virus 2—Group I (PV2-GI), or were coinfecting with PV1-GII and PV2-GI. Clinical signs of the mice were evaluated and the viral load in lung and spleen were detected using simultaneous polymerase chain reactions (PCR) targeting the *A56R* (*hemagglutinin*) gene of VACV. The results showed that qPCR for the quantification of viral load in coinfection was efficient and highly sensitive. Coinfected mice presented more severe disease and a higher frequency of VACV detection in lung and spleen, when compared to monoinfected groups. This study is the first description of PV1 and PV2 pathogenicity during coinfection in mice, and provides a new method to detect VACV-BR coinfections.

Keywords: *Vaccinia virus*; qPCR; coinfection; mice model

1. Introduction

Vaccinia virus (VACV) is a member of the family *Poxviridae*, genus *Orthopoxvirus*, which includes other members, such as *Variola virus*, *Cowpox virus* and *Monkeypox virus* [1,2]. *Variola virus* was one of the most terrible pathogens in human history, but it was declared eradicated in 1980 after an intensive vaccination campaign promoted by the World Health Organization (WHO) [3]. VACV can induce serological cross-reactivity against other orthopoxvirus (OPV) members and was used in the WHO campaign [1,3].

VACV is the etiological agent of bovine vaccinia (BV), an exanthematous disease that causes ulcerative lesions in cattle and humans, economic losses, and social effects in South America and Asia, especially in Brazil [4–8]. The clinical signs of BV range from papules and vesicles to scabs, mainly on the udder and teats of bovines. In humans, lesions occur primarily on the hands and arms, and other

symptoms, such as fever, myalgia, headache, arthralgia, and lymphadenopathy, have been described and there is a significant economic impact on rural workers [1,6].

The natural circulation of VACV in Brazil has been often reported since 1999, and is associated with exanthematous outbreaks [6,7,9–12]. Many studies have shown biological and genetic variations among Brazilian VACV (VACV-BR) isolates. This variability allowed VACV-BR clustering into two distinct groups: Group 1 (GI) and group 2 (GII). These two groups are supported by biological features, such as virulence in a BALB/c mouse model and plaque phenotype in BSC-40 cells. GII isolates display larger plaque sizes and are virulent to mice, unlike GI [4,12–16]. Furthermore, molecular diversity is observed in specific VACV genes, such as the *hemagglutinin* gene (*A56R*), *A-type inclusion body* gene (*A26L*), and *chemokine-binding protein* gene (*C23L*), and these genes have been used in phylogenetic studies and further confirmed the dichotomy between GI and GII VACV-BR. The *A56R* sequence contains a signature deletion of 18 nt, present in the sequences of GI isolates and absent of GII isolates, which is used as a “molecular marker” for VACV-BR group identification [9,13,16–18]. The circulation of the two VACV-BR groups was demonstrated in the same outbreak in 2006 [4] and in the same host as a coinfection was only identified later [15,16]. In 2008, a VACV outbreak, caused by viruses of the two VACV-BR groups, was described in horses from Pelotas City, Brazil. This coinfection presented hemorrhagic lesion and scabs in the muzzles and nostrils of animals [15,19]. The VACV isolates were named Pelotas virus 1—Group II (PV1-GII) and Pelotas virus 2—Group I (PV2-GI) and were used in this study [15]. Despite increasing reports of outbreaks related to VACV-BR, little is known about its biological relevance, virulence profile and viral spread during coinfections with VACV-BR of GI and GII. Moreover, until now, there have been no established tools for the diagnosis or pathogenesis studies of coinfections with VACV-BR of GI and GII. As the best well-characterized molecular difference of the two groups is the *A56R* sequence which contains a signature deletion of 18 nt for GI, it results in the difficulty of developing a test for direct quantification of this group.

In this study, a new tool for the detection and quantification of VACV isolates in coinfections was developed and could be used as a tool to provided new information regarding the diagnosis, pathogenicity, virulence profile, and viral spread during a coinfection with VACV-BR isolates. Our method aims to improve screening in outbreaks and consequently the study of VACV-BR GI/GII coinfections pathogenesis.

2. Materials and Methods

2.1. Ethical Statement

This study was approved by the Committee of Ethics in Animal Use from the Universidade Federal de Minas Gerais (CEUA/UFMG, Belo Horizonte, Brazil), protocol number 207/2010.

2.2. Cells and Viruses

African green monkey kidney BSC-40 (ATCC-CRL-2761) and VERO (ATCC-CCL-81) cells were maintained in a 5% CO₂ atmosphere at 37 °C, in Eagle’s Minimum Essential Medium (MEM) (Gibco BRL, Invitrogen, Carlsbad, CA, USA), supplemented with 5% fetal bovine serum (FBS) (Cultilab, Brazil), 25 µg/mL fungizone (Amphotericin B) (Cristália, São Paulo, Brazil), 500 U/mL penicillin and 50 µg/mL gentamicin (Schering-Plough, São Paulo, Brazil). VERO cells were used for viral replication and the BSC-40 cells were used for viral plaque phenotypes and titration. The VACV used in the study, PV1 and PV2, were isolated from clinical specimens of horses during an equine vaccinia outbreak [15,19].

2.3. Animal Experiments

For all animal experiments, five-week-old male Balb/c mice were used, and were maintained in micro-isolators located in a ventilated animal caging system (Alesco Ltd., Campinas, SP, Brazil), and were provided with commercial mouse food and water, ad libitum, in controlled lighting (12 h

light–12 h dark), humidity (60–80%) and temperature (22 ± 1 °C). The mice of all groups were anesthetized via intraperitoneal injection of 0.1 mg of ketamine and 0.01 mg of xylazine in 0.9% PBS, per gram of animal weight. The four groups of five mice were inoculated intranasally with 10 μ L of viral suspension: PV1-GII 1×10^6 p.f.u.; PV2-GI 1×10^6 p.f.u.; PV1-GII+ PV2-GI 5×10^5 p.f.u. of each sample; a negative control group was inoculated with 10 μ L of PBS, as previously described [14]. Mice were weighed daily, and other clinical signs were recorded for 30 days post infection (d.p.i.). To study viral tropism, the mice were euthanized with an overdose of anesthetics (three times the anesthetic solution) and were perfused with PBS-EDTA intracardiac and those animals had their spleens and lungs collected on 5 d.p.i. [14]. The collected organs were weighed and macerated with the Beadbeater 16 homogenizer in 500 μ L of PBS, with glass beads in the microtubes thread. Three cycles of freezing and thawing were performed in order to release the viral particles from the cells. The cells were then centrifuged at $425 \times g$ for 10 min at 4 °C and the supernatants were used for DNA extraction and plaque phenotype assays. For DNA extraction, the High Pure Viral Nucleic Acid Kit (Roche Diagnostics GmbH, Branchburg, NJ, USA) was used.

2.4. Plaque Phenotype

For plaque phenotype assays, BSC40 cells seeded in 6-well plates at 90–95% confluence were inoculated with the macerated tissues. After 1 h of adsorption (37 °C, 5% CO₂), monolayers were washed twice with PBS and overlaid with solid medium, prepared by mixing equal parts (1:2) of 1% agarose and twice the standard concentration Eagle’s minimum essential medium (MEM) supplemented with 2% FBS. After 48 h of incubation (37 °C, 5% CO₂), cells were fixed with formaldehyde and stained with crystal violet for plaque size analysis.

2.5. qPCR

The qPCR consisted of two simultaneous reactions, A and B, targeting the *hemagglutinin* gene [20]. DNA amplifications were carried out in duplicate in a StepOne™ thermocycler (Applied Biosystems, Foster City, CA, USA). qPCR took place in a total volume of 10 μ L, containing 5 μ L of Master Mix SYBR Green (Applied Biosystems, manufactured by Roche, Branchburg, NJ, USA), 200 nM of each of the forward and reverse primers (Table 1) and 10–50 ng of each DNA sample.

Table 1. Real-time PCR primers.

Reaction	Primers	Sequence (5′-3′)	Specificity
A	A56R-gen F A56R-gen R	AACCACCGATGATGCGGAT TGCCACGGCCGACAATATAA	Amplify all VACV Group I and II.
B	A56R-BVV-nDEL F A56R-generic R	GCGGATCTTTATGATACGTACAATG ACGGCCGACAATATAATTAATGC	Amplify all VACV that do not present the 18nt deletion Group II [20].

Figure 1 shows the target DNA regions for the primers used in this study. Thermal cycling conditions were as follows: one cycle at 95 °C for 10 min, followed by 40 cycles at 95 °C for 10 s, and 58 °C for 40 s; and a melting curve analysis, consisting of 95 °C for 15 s, 58 °C for 15 s, followed by increasing the temperature by 1 °C every 2 s until 95 °C was reached, and then 95 °C for 15 s. Standard curves were constructed by plotting four dilutions of each prototype DNA against the corresponding cycle threshold value (Ct); melting curves were used to ensure there were no non-specific amplifications.

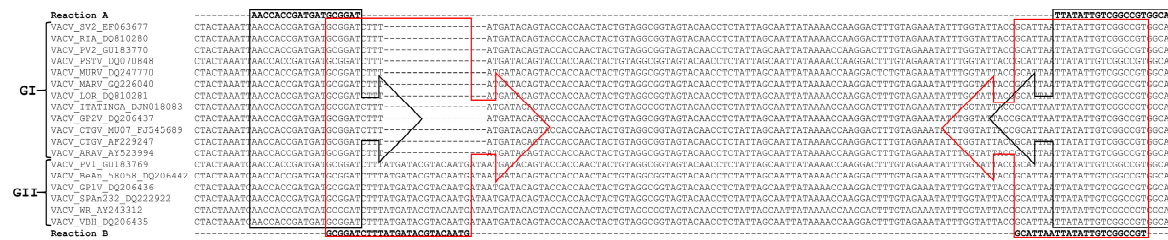


Figure 1. Alignment of the target DNA region within the *A56R* gene of the *Vaccinia virus* used for primer sequence design. The virus sequences were obtained from GenBank and the accession numbers are shown in the figure. The alignment was performed using the standard parameters of CLUSTAL W. The primers used in Reaction A (*A56R*-gen F and *A56R*-gen R) are outlined in black and, for Reaction B (*A56R*-BVV-nDEL F and *A56R*-generic R), are in red.

For standardization, a curve was made using lungs from uninfected Balb/c mice, spiked with 10^6 , 10^5 , 10^4 , 10^3 , 10^2 or 10^1 p.f.u. of PV1-GII and PV2-GI. For validation lungs from uninfected Balb/c mice were spiked with 10^5 p.f.u. of each sample (PV1-GII and PV2-GI). DNA was extracted and qPCR reactions A and B were performed. An equation for the differential viral load calculation was proposed:

$$\begin{aligned}
 [] \text{ VACV GI} &= [] \text{ VACV total (GI+GII)} - [] \text{ VACV GII} \\
 [] \text{ VACV GI} &= 3.38 \times 10^6 - 1.68 \times 10^6 \\
 [] \text{ VACV GI} &= 1.70 \times 10^6 \\
 \text{GI} &= 1.70 \times 10^6 \text{ and GII} = 1.68 \times 10^6
 \end{aligned}$$

2.6. Statistical Analyses

All results were plotted using GraphPad Prism (GraphPad Software, version 6.01, La Jolla, CA, USA) and compared using one-way ANOVA and Tukey’s multiple comparisons test, and two-way ANOVA using the Bonferroni method. In all tests, *p*-values < 0.05 were considered statistically significant.

3. Results

3.1. Development of qPCR Tool

The efficiency of primers developed for the *A56R* gene in *VACV* coinfection, for Reaction A, showed an efficiency of 96.6% and an R^2 value of 0.971; for Reaction B, an efficiency of 94.0% and a value of R^2 of 0.983 (Figure 2) were found. The detection limit of the assay was 2 p.f.u./mg of tissue and the reaction was efficient in different matrices such as lung, gut, and spleen.

The analysis of only one quantitative PCR (qPCR) peak fluorescence reaction was not able to distinguish the *VACV*-BR groups and to identify the presence of the deletion of 18 nt in *A56R* gene of GI viruses. In qPCR Reaction A, the fluorescence peaks were within 0.5 °C, making it difficult to rely on the melting (T_m) curve as a unique identifier for each PCR product (T_m GI: 75.8 °C and T_m GII: 76.3 °C). In Reaction B, GI is not amplified.

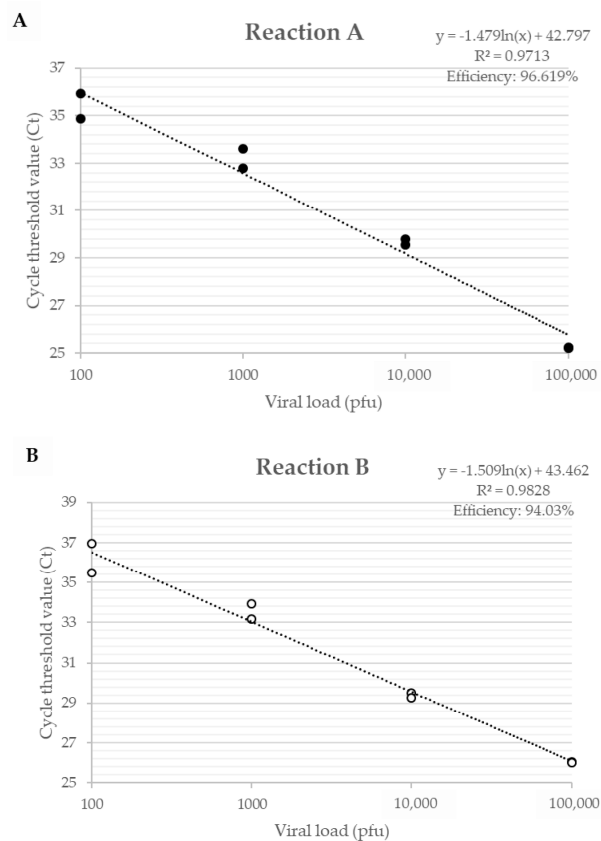


Figure 2. Efficiency curve of *A56R* gene qPCR in coinfection of PV1-GII and PV2-GI. Uninfected Balb/c mice lungs were spiked with 10^6 , 10^5 , 10^4 , 10^3 , 10^2 and 10^1 p.f.u. of PV1-GII and PV2-GI. (A) in Reaction A shown in black circles, primers *A56R*-gen F and *A56R*-gen R were used; and (B) in Reaction B shown in white circles, primers *A56R*-BVV-nDEL F and *A56R*-generic R were used.

3.2. *A56R* qPCR as a Tool to Study Pathogenesis and Viral Spread

3.2.1. Clinical Signs in Mice: Coinfected Versus Monoinfected

Mice that were inoculated with PV1-GII (1×10^6) and coinfecting (PV1-GII + PV2-GI with 5×10^5 of each) showed the first clinical signs, such as facial edema, fur ruffling, hunching of the back, dyspnea and severe weight loss from 4 to 15 d.p.i. The coinfecting mice presented a slightly longer clinical manifestation compared to the PV1-GII group, which was not significant with respect to percent weight loss (PV1-GII vs. PV1-GII + PV2-GI). In the PBS and PV2-GI groups, no clinical signs or weight loss were observed. The only significant differences were the weight variation of PV1-GII and the co-infected group compared to the PBS group (Figure 3).

3.2.2. Coinfected Mice Present Higher Frequency of VACV Detection in Lungs and Spleens than Monoinfected Groups

Using Reaction A, which amplifies all VACV, a positive qPCR was obtained in the lungs and spleen of 100% of the mice inoculated with PV1-GII and PV1-GII + PV2-GI and in 60% of the PV2-GI infected mice lungs and 80% of the spleens. Reaction B of qPCR, which amplifies only the GII *A56R* gene (inoculated with PV1), showed a high positivity (100%) in lungs and only 60% of positivity in spleen (Figure 4A). This was confirmed by plaque phenotype assays (Figure 4B) of the lungs of four mice that were coinfecting, which showed the presence of two viral populations (small plaques-PV2-GI and large plaques-PV1-GII).

3.2.3. Viral Load in Lung and Spleen

The analysis of the viral loads in the lungs of mice in the monoinfected group (PV1) revealed an average viral load of almost two logs higher than monoinfected group (PV2-GI) (Figure 5A). A significant difference was observed when the viral loads of both monoinfected groups (PV1-GII and PV2-GI) were compared with each sample in coinfection (PV1-GII with PV1-GII + PV2-GI and PV2-GI with PV1-GII + PV2-GI) (Figure 5A). Differences about one log for PV1-GII groups and almost three logs between PV2-GI mice groups were observed (Figure 5A).

The differences between the monoinfected groups (PV1-GII or PV2-GI) in the spleens were irrelevant, demonstrating a higher concentration of viral DNA of GI in this tissue (Figure 5B). The viral load in spleens of PV2-GI monoinfected was very similar to that of PV2-GI from the coinfecting group (PV1 + PV2) (Figure 5B). When the viral load of PV1-GII monoinfected with PV1-GI from the coinfecting group (PV1-GII + PV2-GI) was compared, it showed a decrease of about one log with statistical significance (Figure 5B).

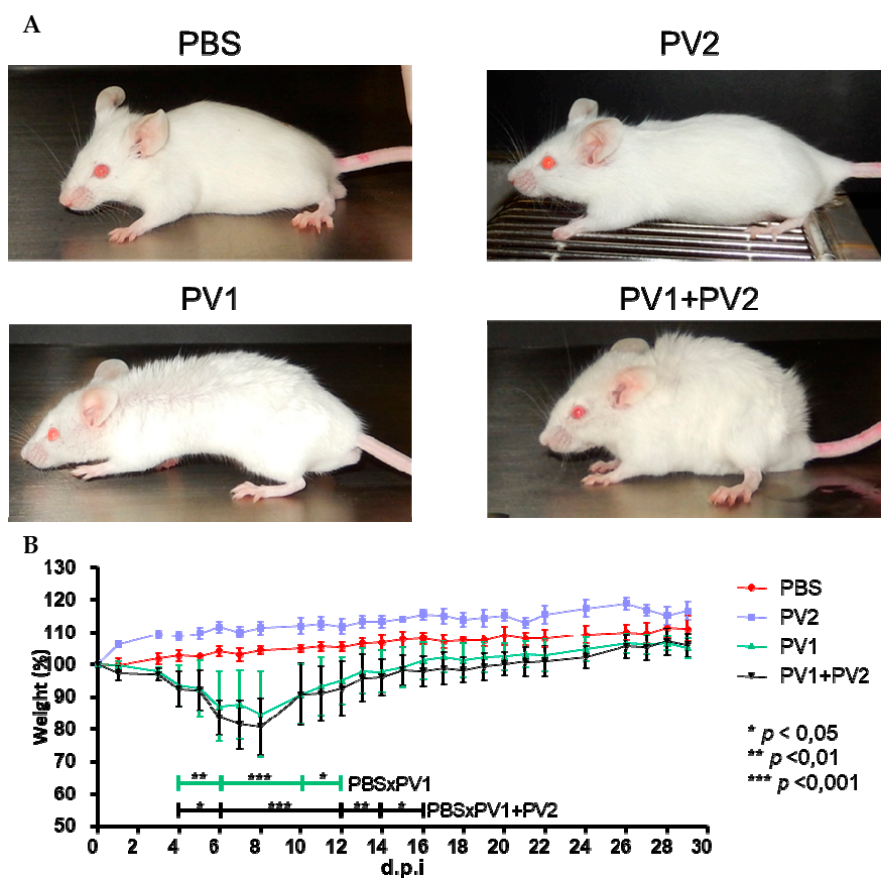


Figure 3. Clinical signs of Balb/c mice coinfecting and monoinfected with PV1-GII and PV2-GI. Five-week-old male Balb/c mice were intranasally inoculated with 10 μ L of viral suspension: PV1-GII 1×10^6 p.f.u.; PV2-GI 1×10^6 p.f.u.; PV1-GII + PV2-GI 5×10^5 p.f.u. of each sample; and a negative control group was inoculated with 10 μ L of PBS. Clinical signs were observed on day 5 p.i and were recorded for 30 days post infection (d.p.i.). (A) In PBS and PV2-GI groups, no clinical signals were observed. Mice monoinfected with PV1-GII and coinfecting (PV1-GII + PV2-GI) showed fur ruffling and hunching of the back. (B) The mice were daily weighed and relative mean weight was calculated. The error bars indicate standard deviations. PV1-GII: Pelotas virus 1 Group II; PV2-GI: Pelotas virus 2 Group I; PBS: phosphate-buffered saline. Asterisks indicate a statistically significant difference: * $p < 0.05$; ** $p < 0.01$; *** $p < 0.001$.

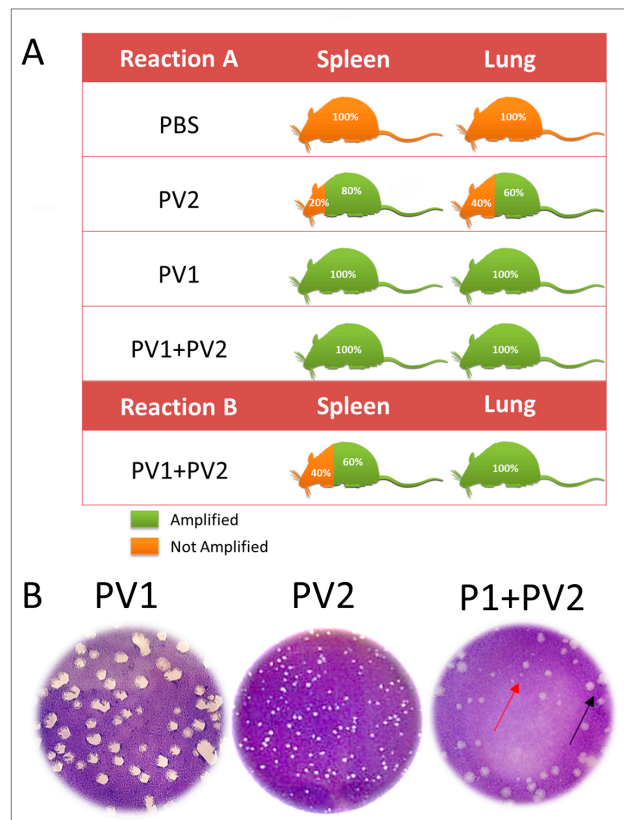


Figure 4. Detection of VAC-BR GI and GII in infected Balb/C mice: (A) qPCR detection of viral DNA from VACV A56R gene in mice spleen and lung samples. The results of Reaction A and Reaction B are represented. (B) Plaque phenotype assays of monoinfected (PV1-GII and PV2-GI) and coinfecting mice showed two viral populations: small plaques-PV2 (red arrows) and large plaques-PV1 (black arrows). PV1-GII: Pelotas virus 1; PV2-GI: Pelotas virus 2; PBS: phosphate-buffered saline.

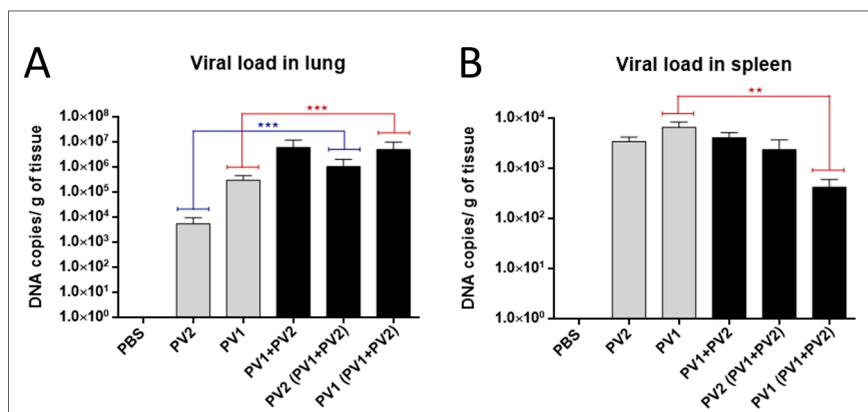


Figure 5. Viral load in mono or coinfecting PV1-GII and PV2-GI mice. Viral loads in: lungs (A); and spleen (B) of Balb/c mice monoinfected (grey columns) and coinfecting (black columns) with PV1-GII and PV2-GI were determined by qPCR. Comparisons between mono and coinfecting groups are highlighted in red (PV1-GII groups) and blue (PV2-GI groups). The error bars indicate standard deviations. The statistical tests used were One-Way ANOVA and Tukey’s multiple comparisons test. Asterisks indicate a statistically significant difference: ** $p < 0.01$; *** $p < 0.001$. PV1: Pelotas virus 1; PV2: Pelotas virus 2; PBS: phosphate-buffered saline.

4. Discussion

Notifications of natural cases of VACV infection have increased [4,15,16], but this increase may be due to the development and improvement of study and detection techniques. qPCR is a rapid diagnostic tool, and is more sensitive than standard PCR; in addition, it allows acquiring molecular quantifications. Currently, multiplex real-time PCR has been described as a simple, reliable, and rapid method for the detection, identification and quantification of many kinds of viral coinfections [21–23]. In this way, qPCR assays have been used to detect and identify parapoxviruses and orthopoxviruses [24–27]. Here, we developed a new tool for the detection and quantification of VACV-BR isolates belonging to GI and GII during coinfections. This method was standardized under controlled conditions in animal model. Although the detection limit of 2 p.f.u./mg make its efficiency possible for many types of clinical samples more studies are needed to better clarify the total applications of method.

The qPCR assay to measure the viral load in coinfection was efficient and highly sensitive for different specimens (lung and spleen), showing a detection limit of 2 p.f.u./mg of tissue. The developed qPCR assay was useful as a detection system and in establishing the total viral load or relative viral load of VACV-GI and -GII in coinfections. The viral load could be measured because the efficiencies between two reactions are very close (96% and 94%).

Previous studies have shown that isolates of VACV-BR GII are virulent in murine model Balb/c, with weight loss and severe clinical signs, differently from GI, which is avirulent in this model [14]. Corroborating these data, the VACV isolates used in this work, in the monoinfected groups, PV1-GII and PV2-GI, followed the same pattern of virulence that has been previously described [15]. However, in this study, clinical signals in coinfecting mice were evaluated and, unlike other studies conducted to date, this study evaluated animals until 30 d.p.i. when they had recovered from the infection [14–16]. Mice infected with the PV1-GII, a virulent representative of GII, and coinfecting with PV2-GI, showed similar clinical signs, such as facial edema, fur ruffling, hunching of the back, dyspnea and severe weight loss. The weight variation data were significant at several points in the curve when we compared the control group to the groups infected with PV1-GII and co-infected (we use the two-way ANOVA test and Bonferroni method post-test).

The viral spread could be analyzed using this developed tool demonstrating a higher number of positive spleens samples (80%), compared to lung samples (60%) which is the primary site of inoculation in mice infected with PV2-GI. Furthermore, this analysis demonstrated the first description of spread of VACV-BR samples of GI. Viral loads data and the spread of VACV-BR GI isolates have not yet been demonstrated in other studies, and these results demonstrate the tendency of a higher tropism for lungs of PV1-GII and PV2-GI in coinfections.

In primary infection site (lungs), the coinfections with both viruses have higher viral loads, contrasting with monoinfected groups. On the other hand, in spleen the viral load of the virulent group (PV1-GII) is low in case of coinfection compared with the group monoinfected by same virus. These results may suggest an intriguing interaction among host and viruses which could help to understand why these two VACV groups are found in coinfections on nature. It is too early to answer the many questions raised by these results and more studies are needed to generalize these characteristics for all VACV-BR GI and GII coinfections, or as exclusive of PV1-GII and PV2-GI isolates.

Studies have shown that plaque size phenotypes are one of the biological characteristics that make possible the differentiation of the two groups of VACV-BR GI, with a small plaque phenotype, and GII with a large plaque phenotype [10,15,16,28]. Confirming biological characteristics of the plaque phenotype, the two viral populations (GI and GII) were detected in lungs of coinfecting mice.

Using the developed tool of differential qPCR the first description of VACV-BR GI spread was possible. In previous studies, the GI virus could not be detected in mice lungs 5 d.p.i. [14]. Reports related to VACV-BR groups coinfections increases as well as the difficulty to detect both groups at the same time by methods of viral isolation and DNA sequencing. The main focus of this study was to develop an efficient tool to facilitate screening during outbreaks and consequently the study of coinfection, and also clarify its possible medical and veterinary importance.

Acknowledgments: We thank colleagues from Laboratório de Vírus (ICB-UFMG). This work was supported by research grants from Fundação de Amparo a Pesquisado Estado de Minas Gerais (FAPEMIG), Conselho Nacional de Desenvolvimento Científico e Tecnológico (CNPq) and Coordenadoria de Aperfeiçoamento de Pessoal de Nível Superior (CAPES). EGK and GST are researchers from CNPq.

Author Contributions: Conceived and designed the experiments: Rafael Calixto, Grazielle Oliveira, Giliane de Souza Trindade, Danilo Bretas de Oliveira, and Erna Geessien Kroon. Performed the experiments: Rafael Calixto, Grazielle Oliveira, Maurício Lima, and Ana Cláudia Andrade. Analyzed the data: Rafael Calixto, Danilo Bretas de Oliveira, and Erna Geessien Kroon. Contributed reagents/materials/analysis tools: Giliane de Souza Trindade and Erna Geessien Kroon. Wrote the paper: Rafael Calixto, Grazielle Oliveira, Danilo Bretas de Oliveira, and Erna Geessien Kroon. All authors read and approved final manuscript.

Conflicts of Interest: The authors declare no conflict of interest.

References

1. Damon, I.K. Poxviruses. In *Fields Virology*, 6th ed.; Knipe, D.M., Howley, P.M., Eds.; Lippincott, Williams and Wilkins: Philadelphia, PA, USA, 2014; Volume 2, pp. 2160–2184.
2. Moss, B. Poxviridae. In *Fields Virology*, 6th ed.; Knipe, D.M., Howley, P.M., Eds.; Lippincott, Williams and Wilkins: Philadelphia, PA, USA, 2014; Volume 2, pp. 2129–2159.
3. Fenner, F.; Henderson, D.A.; Arita, I.; Jezek, A.; Ladnyi, I.D. *Smallpox and Its Eradication*; World Health Organization Press: Geneva, Switzerland, 1988.
4. Trindade, G.S.; Lobato, Z.I.; Drumond, B.P.; Leite, J.A.; Trigueiro, R.C.; Guedes, M.I.; da Fonseca, F.G.; dos Santos, J.R.; Bonjardim, C.A.; Ferreira, P.C.; et al. Short report: Isolation of two vaccinia virus strains from a single bovine vaccinia outbreak in rural area from Brazil: Implications on the emergence of zoonotic orthopoxviruses. *Am. J. Trop. Med. Hyg.* **2006**, *75*, 486–490. [[PubMed](#)]
5. Singh, R.K.; Hosamani, M.; Balamurugan, V.; Bhanuprakash, V.; Rasool, T.J.; Yadav, M.P. Buffalopox: An emerging and re-emerging zoonosis. *Anim. Health Res. Rev.* **2007**, *8*, 105–114. [[CrossRef](#)] [[PubMed](#)]
6. Kroon, E.G.; Mota, B.E.; Abrahão, J.S.; da Fonseca, F.G.; de Souza Trindade, G. Zoonotic Brazilian Vaccinia virus: From field to therapy. *Antivir. Res.* **2011**, *92*, 150–163. [[CrossRef](#)] [[PubMed](#)]
7. Oliveira, D.B.; Assis, F.L.; Ferreira, P.C.; Bonjardim, C.A.; de Souza Trindade, G.; Kroon, E.G.; Abrahão, J.S. Group 1 Vaccinia virus zoonotic outbreak in Maranhao State, Brazil. *Am. J. Trop. Med. Hyg.* **2013**, *89*, 1142–1145. [[CrossRef](#)] [[PubMed](#)]
8. Franco-Luiz, A.P.; Fagundes-Pereira, A.; Costa, G.B.; Alves, P.A.; Oliveira, D.B.; Bonjardim, C.A.; Ferreira, P.C.; de Souza Trindade, G.; Panei, C.J.; Galosi, C.M.; et al. Spread of vaccinia virus to cattle herds, Argentina, 2011. *Emerg. Infect. Dis.* **2014**, *20*, 1576–1578. [[CrossRef](#)] [[PubMed](#)]
9. Damaso, C.R.; Esposito, J.J.; Condit, R.C.; Moussatché, N. An emergent poxvirus from humans and cattle in Rio de Janeiro State: Cantagalo virus may derive from Brazilian smallpox vaccine. *Virology* **2000**, *277*, 439–449. [[CrossRef](#)] [[PubMed](#)]
10. Trindade, G.S.; Emerson, G.L.; Carroll, D.S.; Kroon, E.G.; Damon, I.K. Brazilian vaccinia viruses and their origins. *Emerg. Infect. Dis.* **2007**, *13*, 965–972. [[CrossRef](#)] [[PubMed](#)]
11. Megid, J.; Appolinário, C.M.; Langoni, H.; Pituco, E.M.; Okuda, L.H. Vaccinia virus in humans and cattle in southwest region of Sao Paulo state, Brazil. *Am. J. Trop. Med. Hyg.* **2008**, *79*, 647–651. [[PubMed](#)]
12. Assis, F.L.; Almeida, G.M.; Oliveira, D.B.; Franco-Luiz, A.P.; Campos, R.K.; Guedes, M.I.; Fonseca, F.G.; Trindade, G.S.; Drumond, B.P.; Kroon, E.G.; et al. Characterization of a new Vaccinia virus isolate reveals the C23L gene as a putative genetic marker for autochthonous Group 1 Brazilian Vaccinia virus. *PLoS ONE* **2012**, *7*, e50413. [[CrossRef](#)] [[PubMed](#)]
13. Drumond, B.P.; Leite, J.A.; da Fonseca, F.G.; Bonjardim, C.A.; Ferreira, P.C.; Kroon, E.G. Brazilian Vaccinia virus strains are genetically divergent and differ from the Lister vaccine strain. *Microbes Infect.* **2008**, *10*, 185–197. [[CrossRef](#)] [[PubMed](#)]
14. Ferreira, J.M.; Drumond, B.P.; Guedes, M.I.; Pascoal-Xavier, M.A.; Almeida-Leite, C.M.; Arantes, R.M.; Mota, B.E.; Abrahão, J.S.; Alves, P.A.; Oliveira, F.M.; et al. Virulence in murine model shows the existence of two distinct populations of Brazilian Vaccinia virus strains. *PLoS ONE* **2008**, *3*, e3043. [[CrossRef](#)] [[PubMed](#)]

15. Campos, R.K.; Brum, M.C.; Nogueira, C.E.; Drumond, B.P.; Alves, P.A.; Siqueira-Lima, L.; Assis, F.L.; Trindade, G.S.; Bonjardim, C.A.; Ferreira, P.C.; et al. Assessing the variability of Brazilian Vaccinia virus isolates from a horse exanthematic lesion: Coinfection with distinct viruses. *Arch. Virol.* **2011**, *156*, 275–283. [[CrossRef](#)] [[PubMed](#)]
16. Oliveira, G.; Assis, F.; Almeida, G.; Albarnaz, J.; Lima, M.; Andrade, A.C.; Calixto, R.; Oliveira, C.; Diomedes Neto, J.; Trindade, G.; et al. From lesions to viral clones: Biological and molecular diversity amongst autochthonous Brazilian vaccinia virus. *Viruses* **2015**, *7*, 1218–1237. [[CrossRef](#)] [[PubMed](#)]
17. Leite, J.A.; Drumond, B.P.; de Souza Trindade, G.; Bonjardim, C.A.; Ferreira, P.C.; Kroon, E.G. Brazilian Vaccinia virus strains show genetic polymorphism at the *ati* gene. *Virus Genes* **2007**, *35*, 531–539. [[CrossRef](#)] [[PubMed](#)]
18. Assis, F.L.; Borges, I.A.; Ferreira, P.C.; Bonjardim, C.A.; de Souza Trindade, G.; Lobato, Z.I.; Guedes, M.I.; Mesquita, V.; Kroon, E.G.; Abrahão, J.S. Group 2 vaccinia virus, Brazil. *Emerg. Infect. Dis.* **2012**, *18*, 2035–2038. [[CrossRef](#)] [[PubMed](#)]
19. Brum, M.C.S.; Anjos, B.L.; Nogueira, C.E.W.; Amaral, L.A.; Weiblen, R.; Flores, E.F. An outbreak of orthopoxvirus-associated disease in horses in southern Brazil. *J. Vet. Diagn. Investig.* **2010**, *22*, 143–147.
20. Trindade, G.S.; Li, Y.; Olson, V.A.; Emerson, G.; Regnery, R.L.; da Fonseca, F.G.; Kroon, E.G.; Damon, I.K. Real-time PCR assay to identify variants of Vaccinia virus: Implications for the diagnosis of bovine vaccinia in Brazil. *J. Virol. Methods* **2008**, *152*, 63–71. [[CrossRef](#)] [[PubMed](#)]
21. Zheng, L.L.; Wang, Y.B.; Li, M.F.; Chen, H.Y.; Guo, X.P.; Geng, J.W.; Wang, Z.Y.; Wei, Z.Y.; Cui, B.A. Simultaneous detection of porcine parvovirus and porcine circovirus type 2 by duplex real-time PCR and amplicon melting curve analysis using SYBR Green. *J. Virol. Methods* **2013**, *187*, 15–19. [[CrossRef](#)] [[PubMed](#)]
22. Venkatesan, G.; Balamurugan, V.; Bhanuprakash, V. TaqMan based real-time duplex PCR for simultaneous detection and quantitation of capripox and orf virus genomes in clinical samples. *J. Virol. Methods* **2014**, *201*, 44–50. [[CrossRef](#)] [[PubMed](#)]
23. Balboni, A.; Dondi, F.; Prosperi, S.; Battilani, M. Development of a SYBR Green real-time PCR assay with melting curve analysis for simultaneous detection and differentiation of canine adenovirus type 1 and type 2. *J. Virol. Methods* **2015**, *222*, 34–40. [[CrossRef](#)] [[PubMed](#)]
24. Carletti, F.; di Caro, A.; Calcaterra, S.; Grolla, A.; Czub, M.; Ippolito, G.; Capobianchi, M.R.; Horejsh, D. Rapid, differential diagnosis of orthopox- and herpesviruses based upon real-time PCR product melting temperature and restriction enzyme analysis of amplicons. *J. Virol. Methods* **2005**, *129*, 97–100. [[CrossRef](#)] [[PubMed](#)]
25. Fedele, C.G.; Negredo, A.; Molero, F.; Sánchez-Seco, M.P.; Tenorio, A. Use of internally controlled real-time genome amplification for detection of variola virus and other orthopoxviruses infecting humans. *J. Clin. Microbiol.* **2006**, *44*, 4464–4470. [[CrossRef](#)] [[PubMed](#)]
26. Nitsche, A.; Büttner, M.; Wilhelm, S.; Pauli, G.; Meyer, H. Real-time PCR detection of parapoxvirus DNA. *Clin. Chem.* **2006**, *52*, 316–319. [[CrossRef](#)] [[PubMed](#)]
27. Li, Y.; Olson, V.A.; Laue, T.; Laker, M.T.; Damon, I.K. Detection of monkeypox virus with real-time PCR assays. *J. Clin. Virol.* **2006**, *36*, 194–203. [[CrossRef](#)] [[PubMed](#)]
28. Abrahão, J.S.; Guedes, M.I.; Trindade, G.S.; Fonseca, F.G.; Campos, R.K.; Mota, B.F.; Lobato, Z.I.; Silva-Fernandes, A.T.; Rodrigues, G.O.; Lima, L.S.; et al. One more piece in the VACV ecological puzzle: Could peridomestic rodents be the link between wildlife and bovine vaccinia outbreaks in Brazil? *PLoS ONE* **2009**, *4*, e7428. [[CrossRef](#)] [[PubMed](#)]



8. Killick-Kendrick R, Killick-Kendrick M, Tang Y. Anthroponotic cutaneous leishmaniasis in Kabul, Afghanistan: the low susceptibility of *Phlebotomus papatasi* to *Leishmania tropica*. *Trans R Soc Trop Med Hyg*. 1994;88:252–3. [http://dx.doi.org/10.1016/0035-9203\(94\)90320-4](http://dx.doi.org/10.1016/0035-9203(94)90320-4)
9. Khan NH, Bari AU, Hashim R, Khan I, Muneer A, Shah A, et al. Cutaneous leishmaniasis in Khyber Pakhtunkhwa province of Pakistan: clinical diversity and species-level diagnosis. *Am J Trop Med Hyg*. 2016;95:1106–14. <http://dx.doi.org/10.4269/ajtmh.16-0343>
10. van Thiel P-P, Leenstra T, de Vries HJ, van der Sluis A, van Gool T, Krull AC, et al. Cutaneous leishmaniasis (*Leishmania major* infection) in Dutch troops deployed in northern Afghanistan: epidemiology, clinical aspects, and treatment. *Am J Trop Med Hyg*. 2010;83:1295–300. <http://dx.doi.org/10.4269/ajtmh.2010.10-0143>

Address for correspondence: Shahzad Munir, Yunnan Agricultural University, Kunming 650201, China; email: shazid_10@yahoo.com

Ocular Vaccinia Infection in Dairy Worker, Brazil

Maurício Teixeira Lima, Grazielle Pereira Oliveira, Felipe Lopes Assis, Danilo Bretas de Oliveira, Sidiner Mesquita Vaz, Giliane de Souza Trindade, Jônatas Santos Abrahão, Erna Geessien Kroon

Author affiliation: Universidade Federal de Minas Gerais, Belo Horizonte, Brazil (M.T. Lima, G.P. Oliveira, F.L. Assis, D.B. de Oliveira, G. de Souza Trindade, J.S. Abrahão, E.G. Kroon); Casa de Caridade de Carangola, Carangola, Brazil (S.M. Vaz); Universidade Federal dos Vales do Jequitinhonha e Mucuri, Diamantina, Diamantina, Brazil (D.B. de Oliveira)

DOI: <https://doi.org/10.3201/eid2401.170430>

We studied a clinical case of vaccinia virus that caused an ocular manifestation in a dairy worker in Brazil. Biologic and molecular analyses identified a co-infection with 2 isolates from different Brazilian vaccinia virus phylogenetic groups.

Detection of co-infections for various viral pathogens recently has increased (1,2). However, the presence of ≥ 2 viral etiologic agents often is not considered (1). The range of pathogens that can present co-infections and the association of these infections with the occurrence and severity of disease remain unclear (1,2). Vaccinia virus (VACV), the prototype virus of the genus *Orthopoxvirus*, has been associated with exanthematic outbreaks in Asia and South America that affect mainly dairy cattle and rural workers (3,4). In Brazil, several Brazilian VACV (VACV-BR)

have been isolated and characterized biologically and phylogenetically. These studies demonstrated that circulating viruses belonged to at least 2 distinct genetic clusters (4–8). Previous studies have demonstrated the co-circulation of distinct VACV isolates during the same outbreak and VACV co-infecting horses and cattle (6–8).

We obtained 2 distinct VACV isolates from the same clinical sample from 1 eye of a rural worker. Our data show that the eye was co-infected with 2 VACV and demonstrates the detection and isolation of VACV from a natural case of ocular vaccinia infection.

In September 2015, an unvaccinated 45-year-old man who worked on a farm in Carangola County, Minas Gerais State, Brazil (20°44'06"S, 42°01'52"W), showed development of typical manifestations of vaccinia infection, including fever and painful vesiculopustular lesions (online Technical Appendix Figure, panel A, <https://wwwnc.cdc.gov/EID/article/24/1/17-0430-Techapp1.pdf>). He had lesions on the left hand, right arm, and nose and an atypical manifestation in the left eye with aches in the ocular globe and periorbital region. The clinical condition progressed to major visual acuity losses in the affected eye. He reported recent contact with sick cows on the farm during milking.

Dried swab specimens from his lesions were soaked in 200 μ L phosphate-buffered saline containing amphotericin B (4 μ g/mL), penicillin (200 U/mL), and streptomycin (100 μ g/mL); homogenized; and centrifuged at 3,000 $\times g$ for 5 min (4). The supernatants were used for molecular diagnosis using orthopoxvirus-specific PCR that targeted the C11R gene, which encodes viral growth factor, and the A56R gene, which encodes viral hemagglutinin protein (4). All samples were positive for both orthopoxvirus targets.

Vero cells were cultured in 25-cm² culture flasks and infected with the specimen supernatants to isolate the virus at 37°C until a cytopathic effect was detected (4). VACV was isolated from the hand, nose, and eye samples. These isolates were tested for their plaque phenotypes in BSC-40 cells incubated at 37°C for 48 h (4), which demonstrated the presence of at least 2 types of viral populations comprising small and large plaques in an estimated ratio 2:1. Two viral plaques (1 forming large and 1 forming small plaques) were obtained from the eye sample after 3 additional rounds of plaque purification in BSC-40 cells (online Technical Appendix Figure, panel B) (4). The viral plaques were propagated and titrated by plaque assay in Vero cells, and their DNA was extracted (4).

We obtained the complete genomes using the Illumina MiSeq instrument (Illumina, San Diego, CA, USA) with the paired-end application. The sequence reads were assembled de novo using ABYSS software (<http://www.bcgscc.ca/platform/bioinfo/software/abyss>), and the resulting contigs were ordered by the python-based CONTIGuator.py software (<http://contiguator.sourceforge.net>). The GenBank accession numbers are MG012795 (small) and MG012796 (large).

Analysis of the complete genome revealed 92% similarity between the 2 isolates, and some genes confirm a remarkable variability (online Technical Appendix Figure, panel C). We constructed a phylogenetic tree (online Technical Appendix Figure, panel D) using the A56R gene sequence by the maximum-likelihood method and 1,000 bootstrap replicates in MEGA 6.02 (<http://www.megasoftware.net>). The analysis demonstrated a co-infection with viruses from both VACV-BR groups, such that the large-plaque clone clustered with group 2 VACV-BR isolates and the small-plaque clone clustered with group 1 VACV-BR isolates. We named these isolates Carangola eye virus 1 (small) and Carangola eye virus 2 (large).

Our study demonstrated the genetic and phenotypic variability between 2 viruses isolated from the same sample in a natural human co-infection with VACV. The viruses belong to 2 distinct VACV-BR groups, reinforcing and expanding previous work with other hosts (6–8). These results raise new questions about how co-infections with these viruses might change the aspects of an infection and its signs and symptoms, such as development of ocular vaccinia. Although cases of ocular vaccinia have been reported after vaccination and accidental laboratory infection (9,10), we proved the association and isolate VACV samples from a natural ocular vaccinia infection. The effort to understand singular aspects of VACV-BR co-infections should be increased, and further molecular and biologic characterizations of these samples should be conducted to identify and better understand the natural dynamics and signs and symptoms caused by VACV-BR.

About the Author

Mr. Lima is a PhD candidate at the Laboratório de Vírus, Departamento de Microbiologia, Instituto de Ciências Biológicas, Universidade Federal de Minas Gerais. His primary research interest is the poxviruses.

References

1. Stefanska I, Romanowska M, Donevski S, Gawryluk D, Brydak LB. Co-infections with influenza and other respiratory viruses. *Adv Exp Med Biol*. 2013;756:291–301. http://dx.doi.org/10.1007/978-94-007-4549-0_36
2. Griffiths EC, Pedersen AB, Fenton A, Petchey OL. The nature and consequences of coinfection in humans. *J Infect*. 2011;63:200–6. <http://dx.doi.org/10.1016/j.jinf.2011.06.005>
3. Damon IK. Poxviruses. In: Knipe DM, Howley PM, Griffin DE, Lamb RA, Martin MA, Roizman B, et al., editors. *Fields virology*. Vol II. 5th ed. Philadelphia: Lippincott Williams and Wilkins; 2007. p. 2947–75.
4. Kroon E, Santos Abrahão J, de Souza Trindade G, Pereira Oliveira G, Moreira Franco Luiz AP, Barbosa Costa G, et al. Natural vaccinia virus infection: diagnosis, isolation, and characterization. *Curr Protoc Microbiol*. 2016;42:14A.5.1–14A.5.43. <http://dx.doi.org/10.1002/cpmc.13>
5. Damaso CR, Esposito JJ, Condit RC, Moussatché N. An emergent poxvirus from humans and cattle in Rio de Janeiro State: Cantagalo virus may derive from Brazilian smallpox vaccine. *Virology*. 2000;277:439–49. <http://dx.doi.org/10.1006/viro.2000.0603>
6. Trindade GS, Lobato ZI, Drumond BP, Leite JA, Trigueiro RC,

Guedes MI, et al. Short report: isolation of two vaccinia virus strains from a single bovine vaccinia outbreak in rural area from Brazil: implications on the emergence of zoonotic orthopoxviruses. *Am J Trop Med Hyg*. 2006;75:486–90.

7. Campos RK, Brum MC, Nogueira CE, Drumond BP, Alves PA, Siqueira-Lima L, et al. Assessing the variability of Brazilian vaccinia virus isolates from a horse exanthematic lesion: coinfection with distinct viruses. *Arch Virol*. 2011;156:275–83. <http://dx.doi.org/10.1007/s00705-010-0857-z>
8. Oliveira G, Assis F, Almeida G, Albarnaz J, Lima M, Andrade AC, et al. From lesions to viral clones: biological and molecular diversity amongst autochthonous Brazilian vaccinia virus. *Viruses*. 2015;7:1218–37. <http://dx.doi.org/10.3390/v7031218>
9. Lewis FMT, Chernak E, Goldman E, Li Y, Karem K, Damon IK, et al. Ocular vaccinia infection in laboratory worker, Philadelphia, 2004. *Emerg Infect Dis*. 2006;12:134–7. <http://dx.doi.org/10.3201/eid1201.051126>
10. Hu G, Wang MJ, Miller MJ, Holland GN, Bruckner DA, Civen R, et al. Ocular vaccinia following exposure to a smallpox vaccinee. *Am J Ophthalmol*. 2004;137:554–6. <http://dx.doi.org/10.1016/j.ajo.2003.09.013>

Address for correspondence: Maurício Teixeira Lima and Erna Geessien Kroon, Instituto de Ciências Biológicas, Universidade Federal de Minas Gerais, Dept Microbiologia, Lab de Vírus, bloco F4, sala 258, Av. Antonio Carlos 6627, 31270-901 Belo Horizonte, Minas Gerais, Brazil; emails: maurili15@hotmail.com and ernagkroon@gmail.com

Estimation of Undiagnosed *Naegleria fowleri* Primary Amebic Meningoencephalitis, United States¹

Almea Matanock, Jason M. Mehal, Lindy Liu, Diana M. Blau, Jennifer R. Cope

Author affiliation: Centers for Disease Control and Prevention, Atlanta, Georgia, USA

DOI: <https://doi.org/10.3201/eid2401.170545>

Primary amebic meningoencephalitis is an acute, rare, typically fatal disease. We used epidemiologic risk factors and multiple cause-of-death mortality data to estimate the number of deaths that fit the typical pattern for primary amebic meningoencephalitis; we estimated an annual average of 16 deaths (8 male, 8 female) in the United States.

¹Preliminary results of this study were presented at the Infectious Diseases Society of America Conference; October 8–12, 2014, Philadelphia, Pennsylvania, USA.

97 Parapoxvirus

Graziele Oliveira, Galileu Costa, Felipe Assis, Ana Paula Franco-Luiz, Giliane Trindade, Erna Kroon, Filippo Turrini, and Jonatas Abrahão

CONTENTS

97.1 Introduction	881
97.1.1 Classification, Morphology, and Genome Organization	881
97.1.2 Transmission, Clinical Features, and Pathogenesis.....	882
97.1.2.1 Orf Virus.....	882
97.1.2.2 Bovine Papular Stomatitis Virus	883
97.1.2.3 Pseudocowpox Virus	884
97.1.2.4 Parapoxvirus of Red Deer in New Zealand.....	884
97.1.3 Diagnosis	884
97.1.3.1 Conventional Techniques.....	884
97.1.3.2 Molecular Techniques.....	884
97.2 Methods	885
97.2.1 Sample Collection and Virus Isolation.....	885
97.2.2 Detection Procedures.....	885
97.2.2.1 DNA Extraction	885
97.2.2.2 qPCR Detection of PPV.....	885
97.2.2.3 Nested PCR Detection of PPV.....	886
97.2.3 Sequencing and Phylogeny of PPV.....	886
97.3 Conclusion	888
References.....	888

97.1 INTRODUCTION

The *Parapoxvirus* (PPV) genus of the *Poxviridae* family includes four worldwide-distributed viral species that mainly infect domestic and wild ruminants (e.g., sheep, goat, and cattle). PPV species are transmissible to humans and, for this reason, are considered zoonotic agents of veterinary and public health relevance [1,2]. The fact that PPV infection has been reported in an even broader host range (including camels, seals, and deer species) highlights the emerging importance of this genus [1,3,4]. PPVs are epitheliotropic viruses whose clinical manifestations include exanthematic lesions as painful pustules and vesicles. Clinical diagnosis of PPV infection is often made difficult by both the absence of pathognomonic signs and the great similarity in the symptoms to either different *Poxviridae* infections or unrelated exanthematic diseases, such as cutaneous anthrax, foot-and-mouth disease, blue tongue, and bovine viral diarrhea. In addition, subclinical infections have been recorded. Thus, improvement of molecular analyses and epidemiological studies is considered an urgent priority in order not only to avoid unnecessary treatment due to misdiagnosis but also to lessen the economical impact of PPV diseases and to implement strategies for the limitation of this infection. Clinical evidence and restriction analysis have been traditionally used to diagnose and

characterize PPV diseases. Nevertheless, the historical relevance of the *Poxviridae* family has increased the availability of genomic data in scientific databases. This further facilitates the use of the molecular diagnostic approach for improved diagnosis of PPV infection.

97.1.1 CLASSIFICATION, MORPHOLOGY, AND GENOME ORGANIZATION

The PPV genus belongs to the subfamily *Chordopoxvirinae* (ChPV), family *Poxviridae*. The genus comprises four zoonotic viral species that cause localized skin nodules mainly in domestic and wild ruminants: *Bovine papular stomatitis virus* (BPSV), *Pseudocowpox virus* (PCPV), the genus prototype species *Orf virus* (ORFV), and the newest characterized species *Parapoxvirus of red deer in New Zealand* (PVNZ) [5–7]. PPVs are primarily classified on their natural host range and viral DNA restriction enzyme analyses, while the extensive serological cross-reactivity makes neutralization tests and immunofluorescence useless to differentiate viral species [8].

Viral particles are large, enveloped, and oval shaped, with variable size ranging from 260 nm × 160 nm in ORFV to 300 nm × 190 nm in PCPV. Tubular filiform structures surround virions and can be used to discriminate PPV particle

from others poxviruses, such as orthopoxviruses (OPV) by electron microscopy (EM) [9,10]. PPV virions enclose a typical *Poxviridae* genome, consisting of linear double-stranded DNA of approximately 140 kb, composed by one central region and two flanking inverted terminal repeats (ITR) terminally linked by a hairpin structure that allows cross-hybridization between isolates of the same species. High intraspecific variability has been found at either genomic level, by viral DNA restriction pattern analyses, or protein level [8,11–16].

PPV genome contains approximately 130 open reading frames organized in a conserved central core and two external regions. ChPV conserved genes are essential for viral replication and morphogenesis and encode transcription and replication machineries. Nonessential variable genes, conversely located along ITRs, are mainly responsible for pathogenesis and virulence and, in some cases, are genus specific [10,17,18]. *B2L* gene encodes PPV major envelope antigen of approximately 42 kDa. This gene is the homologue of *F13L* gene of *Vaccinia virus* (VACV) and has been widely used in PPV diagnosis and characterization, as well as vascular endothelial growth factor gene (*VEGF*) and virus interferon resistance (*VIR*) genes, which are common targets of phylogenetic analyses. For differential diagnosis, a polymerase chain reaction (PCR) assay targeting the *A32L* gene, which encodes a 34 kDa ATPase protein involved in DNA packaging, has also been developed [19–26]. Like other poxviruses, PPV replicates in the cytoplasm of host cells, exploiting their own machinery for DNA transcription and replication. Notably, PPV shares with the *Molluscipoxvirus* genus the peculiar genome feature of high guanine and cytosine (G+C) content. In fact, conversely to a majority of other poxvirus genomes that enclose approximately 25%–35% of G+C, PPV genome contains about 65% of G+C [12,27,28].

97.1.2 TRANSMISSION, CLINICAL FEATURES, AND PATHOGENESIS

PPV infections occur primarily in ruminants such as sheep, goats, and cattle. Infections in wild species, such as grey seals, serows, cervids, and gazelle, have also been described. Furthermore, PPV infections have been reported in cats expanding the range of the identified hosts [6,29–34]. PPV infections are zoonoses, and their transmission is facilitated by contact with lesions or fomites. Zoonotic transmission to humans represents an occupational hazard that mainly affects either milkers or particular risk category workers like veterinarians, farmers, and butchers, who directly handle infected mammals. Additionally, transmission from wild animals is also possible at low frequency. Often, the presence of painful lesions impairs milking and breastfeeding, and the infected animals become unproductive resulting in economical losses in outbreak-affected farms [35–37]. Finally, the reported cases of human-to-human transmission have highlighted the importance of developing a thorough understanding of the chain of transmissional events [38–44].

The clinical outcome in human manifestations consists of painful lesions on hands and less frequently on the face [9,45,46], while the main clinical signs observed in infected animals are papular lesions around the mouth and in the oral mucosa, skin, and teats. Lesions in the esophagus, stomach, and intestine have been reported with less frequency. Lesion progression is characterized by formation of macules and papules, followed by vesicles and pustules. Disease progression and resolution generally occur over the course of 1–2 months concomitantly with an accumulation of neutrophils, T and B cells, and dendritic cells in proximity to infected epidermal cells. Keratinocytes are the major multiplication site that is characterized by eosinophilic cytoplasmic inclusions and irregularly shaped nuclei.

97.1.2.1 Orf Virus

ORFV is the prototype species of the PPV genus and the causative agent of contagious ecthyma (CE), also known as orf, a zoonosis that primarily affects domestic sheep and goats, although some cases have been also described in wild animals [34,47,48]. CE can decrease the fitness of infected hosts leading to severe economic losses, as well as public health problems, according to the zoonotic potential of this disease [49–52].

Since the first identification of a human ORFV by Newsom and Cross in 1934 [53], several human cases caused by occupational or household exposures have been reported [54–56]. CE is characterized by epidermal proliferative lesions (vesicles) mainly localized in the lips, mouth, nostrils, gums, and tongue. Less frequently, lesions can be observed in the esophagus, stomach, and intestine, while among sheep, the lesions are commonly localized at the teat and udder. Genital lesions have also been described. However, asymptomatic ORFV infections can occur. In addition, when lesions in the mouth, lips, and udders prevent infected animals from feeding, the consequences can be even more severe leading to a rapid weight loss and increased mortality rate [57]. Incubation period in sheep ranges from 3 to 14 days, while in humans is shorter (2–4 days). Based on the clinical symptoms only, CE can be frequently misdiagnosed, leading to unnecessary treatments. Furthermore, cases of coinfection between poxviruses of different genera have been reported, reinforcing the need to apply molecular assay for the differential diagnosis [36,48,52,58]. In human, ORFV causes skin lesions and occasionally malaise and lymphadenopathy, while immunodeficient individuals can develop even severe infection. In such cases, even though the treatment had resulted in successful outcome, no therapeutic options have been yet characterized [59–61]. Studies have shown that the mortality rate in kids can reach 93%; nevertheless, the disease is considered mild by some authors. ORFV transmission is typically associated to animal direct contact (Figure 97.1), and the importance of preventive measure (e.g., wearing gloves and appropriate hand hygiene) is pivotal in order to limit the zoonotic transmission of CE, especially in rural areas where the risk of human-to-human transmission can be very high.

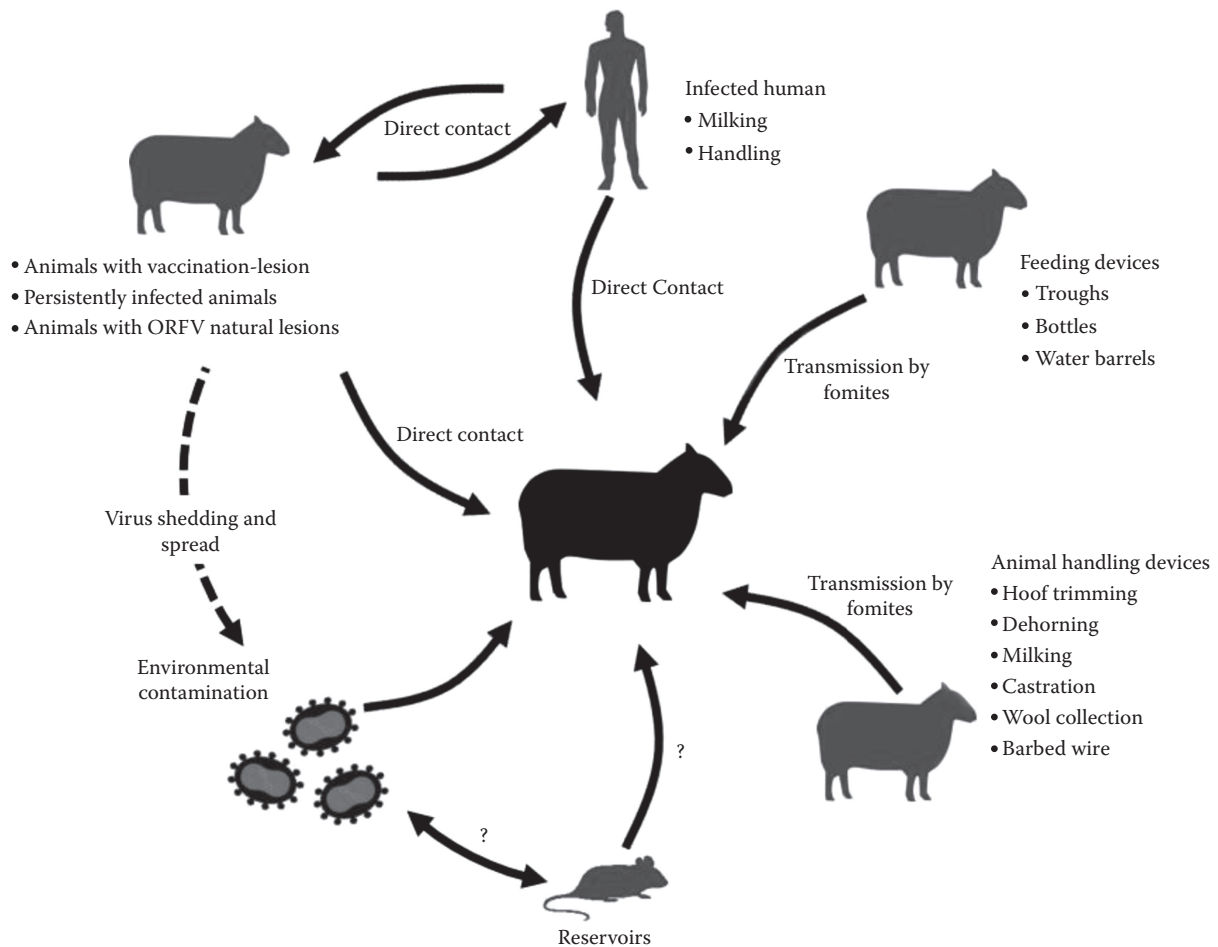


FIGURE 97.1 *Orf virus* hypothetical transmission cycle.

In human, lesions generally appear on the hands and face, but some patients develop ulcerating lesions on oral mucosa, in particular at the level of the upper lip [22,57,62–65]. A case of human-to-human transmission was reported from father to daughter via the common use of tweezers. Despite being uncommon, human-to-human infection reveals new questions concerning the transmissional chain of the ORFV [44]. Like other poxviruses, ORFV contains immune modulatory genes primarily located in terminus of the viral genome. Among them, granulocyte macrophage colony-stimulating factor (GM-CSF) inhibitory factor gene (*GIF*) encodes for an inhibitor of both GM-CSF and viral gene encoding an interferon resistance factor orf virus interferon-resistance gene (*OVIFNR*). These genes have been used in genetic variation studies of ORFV [66–69].

Immunohistological studies of the skin of infected sheep have shown that there is an accumulation of neutrophils, dendritic cells, and T cells. CD4+ are the predominant T cells in lesions. Re-infection can occur, but smaller lesions are observed, which resolve usually in 3 weeks. For this reason, the disease is most severe in those animals, such as lambs, that have never been exposed to the virus [66,70,71]. In some countries, vaccination with attenuated vaccine is practiced. The virus was attenuated through serial passages on primary chicken embryo fibroblast tissue cultures. A field study was

conducted to confirm the efficacy of the vaccine and demonstrated that vaccination was able to block the normal course of the disease and induce rapid recovery. Thus, the ORFV vaccine can limit the severity of the disease [72]. In short, CE is an emerging zoonosis, with an increasing number of outbreaks reported worldwide. It not only has a significant impact on livestock but also poses a public health threat. Further studies and epidemiologic surveys are warranted in order to improve our knowledge on this viral disease [51,63,73–75].

97.1.2.2 Bovine Papular Stomatitis Virus

BPSV infection is characterized by exanthematic lesions mainly localized on the muzzle, around the mouth, oral mucosa, and less frequently in the esophagus and forestomach of calves and udders of cows. In general, lesions begin with papules formation progressing to pustules and vesicles that regress approximately 12–16 days after the onset. Calves usually develop the classical disease outcome, whereas *BPSV* is the cause of severe esophagitis in adult bull [76–78]. The exanthematic lesions typically resemble those of foot-and-mouth disease, highlighting the importance of differential diagnosis. Commonly, acute forms of disease are described, but chronic forms of bovine papular stomatitis in young cattle have been also demonstrated [79]. Recently, a molecular

analysis has identified a new viral strain, revealing the existence of genetic variability in the BPSV envelope gene [80]. Reinfections by BPSV are commonly observed, indicating that this virus does not confer permanent immunity, as it has been shown for other viruses of the family, such as VACV, which cause repeated outbreaks of bovine vaccinia mainly in Brazil and ORFV in sheep and goats. BPSV has a worldwide distribution, and infection of calves and cows is of economical importance as it leads to a decrease in milk production [81–84]. Furthermore, since it is a zoonosis, human cases have a significant public health impact. Human transmission usually occurs by direct contact with lesions causing nodules and pustules on the hands and less frequently on the face; occasional cases may develop severe lesions [46]. In this way, milkers and other livestock workers are exposed to infection [41].

97.1.2.3 Pseudocowpox Virus

First isolation of PCPV, the causative agent of milker's nodule disease, dates back to 1963, and it was obtained from lesions of cows and calves [85]. Nowadays, PCPV infections are currently worldwide distributed affecting cows and calves and representing a zoonotic threat to human health [86–89]. Moreover, infection in hosts such as camels in the Arabian Peninsula, reindeers, and cats has also been described [90–92]. The virus is usually transmitted by direct contact with infected animals. Once infected, milking cows develop proliferative lesions on teats and udders in a clinical course of approximately 10–15 days. As observed for ORFV and BPSV, cases of reinfection can occur in herds. In addition, chronic lesions may occur. PCPV diagnosis is complicated not only by virion morphology but also by clinical symptoms, which are similar with other poxvirus infections that affect bovine, such as VACV and BPSV. Moreover, cases of PCPV human coinfection with different *Poxviridae* species have been described [93]. Therefore, the correct diagnosis of PCPV infection in cattle mainly relies upon the identification of the viral agent by molecular assays [94].

97.1.2.4 Parapoxvirus of Red Deer in New Zealand

PVNZ has been classified as new PPV species due to its distinct restriction enzyme patterns [5]. PPV in red deer have been firstly reported in New Zealand and, more recently, in Italy among wild ruminants. In red deer, the disease is characterized by lesions mainly located in the muzzle, lips, ears, and neck. Infections are more common in younger animals, with morbidity often reaching 100%. Diagnosis is generally made on clinical signs alone, but histology, EM, and molecular tests have also been used [95,96].

97.1.3 DIAGNOSIS

Diagnostic methods for PPV infection include clinical diagnosis based on the history of contact with animals and the clinical appearance of the lesion. However, PPV infections may be misdiagnosed due to the great similarity in symptoms with other vesicular–pustular diseases. In these cases, the diagnosis can be established by histopathology and EM;

serological methods, such as ELISA, immunofluorescence assay (IFA), agar gel immunodiffusion (AGID), and neutralization test (NT); viral growth in cell cultures and molecular assays as restriction fragment length polymorphism (RFLP); and conventional PCR, multiplex PCR, and real-time PCR (qPCR). Among the available methods, molecular approaches and nucleic acid sequence analysis are widely used for detection and identification of PPV infections.

97.1.3.1 Conventional Techniques

PPV infection can be identified by histopathological analysis that usually shows vascular degeneration of keratinocytes, the primary viral target [97]. PPV infection of keratinocytes is also characterized by eosinophilic cytoplasmic inclusions and irregularly shaped nuclei [34,97]. The diagnosis can be enhanced by negative-stain EM, which identifies the viral particles within infected cells, discriminating PPV genus from OPV [34,97]. However, EM requires morphologically intact clinical samples with high viral load (approximately 10^6 particles per mL), as well as trained personnel [98,99]. High viral load is usually obtained from fresh lesions and crusts of infected individuals and/or animals, whereas in case of low viral load or not correctly processed samples, EM may produce false-negative results with high probability. In this case, virus isolation can also be performed using primary ovine or bovine cell culture. Although once regarded as the gold standard method for detection of poxviruses, virus isolation is not attempted routinely in clinical laboratories [17,100–103].

Determination of serum titers during the acute and convalescent phase of disease is also useful. The presence of specific antibodies can be confirmed by AGID and IFA. In these techniques, Madin–Darby bovine kidney–infected, fetal bovine muscle–infected, and bovine fetal testicle–infected cells with known PPV strains can be used as antigen after lysis or sonication treatments [104–106]. Moreover, ELISA for IgM and IgG determination has also been employed, according to the direct correlation between fast healing of lesions and rise in antibody levels during the infection [58,104,105,107]. Furthermore, NT assays are also applied. Although neutralizing antibodies are associated with protective status, all PPV are immunologically related and cannot be distinguished in NT [108,109]. Western blot analysis is usually confirmatory and has demonstrated that the produced antibodies in response to infection are directed against the viral surface tubule protein [99,102].

97.1.3.2 Molecular Techniques

Traditional diagnostic laboratories rely on conventional culture and serological methods for the confirmation of several viral infections. The access to reliable diagnostic laboratory testing methods is limited, due to the requirement of well-qualified personnel, standard and automated products, and equipments. The identification and characterization of an already isolated viral pathogen is mainly assessed by molecular techniques that represent a rapid tool for the diagnosis of fresh clinical specimens. Indeed, molecular techniques generally in use for PPV diagnostic include RFLP, nucleic acid

hybridization, and, especially nowadays, conventional PCR and qPCR. These methods, and in particular PCR, are well recognized to be more rapid, sensitive, and specific than conventional techniques for the identification of target viruses.

In RFLP analysis, viral DNA is digested with one or more restriction enzymes (e.g., EcoRI, HindIII, BamHI), and the resulting restriction fragments are separated according to their size by electrophoresis, generating distinct restriction fragment profiles and allowing species and strains differentiation [5,15,34,80,110,111]. Multiplex PCR can be useful for clinical differential diagnosis as rapid approach for simultaneous detection of coinfections with different *Poxviridae* genera, such as PPV and OPV [112,113], and PPV and capripoxvirus [114].

The PCR assay that has traditionally provided the most valuable approach to identify PPV infections targets the conserved major envelope protein gene (*B2L*), which is the homologue of VACV envelope protein antigen-p37K [26]. Besides, *B2L* gene has been widely used in the molecular characterization and phylogenetic analysis, representing the main molecular marker for PPV genetic analysis. Other PPV-specific genes have been described as target of PCR amplification, such as interferon-resistant protein (*VIR*) [101,115], ATPase (*A32L*), dsRNA-binding protein (*E3L*) [116], and GM-CSF/interleukin-2 inhibitory factor (*GIF*) genes [111]. These genes have been extensively used for phylogenetic studies in order to investigate on epidemiology and evolution of PPVs [21,24,75,93,101,111,112,115,116].

Finally, qPCR assays have further improved the diagnosis of PPV infections due to their high efficiency and sensitivity. These features are required for the analysis of human clinical samples, which often have a low viral load and/or poor DNA quality. Different qPCR methods for PPV DNA detection in clinical specimens have been developed [23,116–118]. These methods target ORFV major envelope antigen *B2L* and can be used either in the diagnosis and quantification of ORFV [23,117] or in the diagnosis of several PPV species including PCPV and BPSV [23].

97.2 METHODS

97.2.1 SAMPLE COLLECTION AND VIRUS ISOLATION

Biopsies of lesions are the most frequent and suitable clinical samples collected for the diagnosis of PPV-associated infections. For virus isolation, 1%–10% (weight–volume) of biopsy suspension is prepared in pH 7.4 phosphate-buffered saline (PBS) or nuclease-free water, both supplemented with gentamycin to eliminate bacterial contamination, then clarified by centrifugation at 2000 × g for 3 min to eliminate larger debris. The supernatant is collected and submitted to DNA extraction [119] or, in order to isolate viruses, is directly used to infect cell cultures. There are some permissive cell lines useful for PPV isolation, such as ovine organotypic skin culture, ovine fetal turbinate (OFTu) cells, and Madin–Darby ovine kidney cells [120,121]. Besides, primary bovine lineage esophageal cells (KOP, cell culture collection Friedrich Loeffler Institute,

Riems, Germany), bovine lung, or kidney fibroblasts can be used. OFTu cells, which are the most frequently used for PPV isolation, are cultured in minimal essential medium (Hyclone) with 10% fetal bovine serum (Hyclone), 2 mM of L-glutamine, 100 U of penicillin, 100 µg of streptomycin, 20 µg of nystatin per mL at 37°C, and 5% of CO₂ [121]. In this system, the cytopathic effect (CPE) is usually detected 1–2 days postinfection, according to the starting viral load, and is characterized by cell rounding, pyknosis, and cell detachment. When 50%–75% of CPE is observed, cell cultures are subjected to one cycle of freeze–thawing. The virus-containing supernatants are then clarified by centrifugation, aliquoted, and frozen at –70°C [34,99].

97.2.2 DETECTION PROCEDURES

97.2.2.1 DNA Extraction

DNA from macerated sample supernatant, serum, and virus-infected cells is extracted by commercial kits and phenol–chloroform–isoamyl alcohol, or in some cases, samples can be submitted to PCR with no previous DNA extraction step [112].

97.2.2.2 qPCR Detection of PPV

One of the first diagnostic qPCR for PPV detection was developed by Nitsche and colleagues in 2006. Before that time, the diagnosis of PPV infections had been traditionally performed by EM and/or conventional PCR. The following protocol describes the qPCR currently used for detection of PPV. We have used this protocol in our lab successfully. To date, this assay is capable of specifically amplifying DNA from all PPV species. A conserved region into the major envelope protein gene (*B2L*) was chosen for the design of two primers and one 5-nuclease minor groove-binder (MGB) probe [23].

Primer	Target Gene	Sequence (5'–3')	Expected Product (bp)	Reference
PPV up	B2L	TCGATGCGGTGCAGCAC	95	[23]
PPV do		GCGGCGTATTCTTCTCGGAC		
PPV TMGB		GTCGTCCACGATGAGCAG		

The reaction is performed into a mix solution containing 1× PCR buffer, 5 mM of MgCl₂, 1 mM of deoxynucleotide triphosphate mixture with dUTP, 1 µM of ROX, 1 U of platinum Taq polymerase (Invitrogen), 7.5 pmol of each primers, 2.5 pmol of the MGB probe, and 5 µL of DNA template [23].

Cycle condition

Incubation at 95°C for 5 min

↓

40 cycles

Denaturation (95°C, 15 s)

Annealing (60°C, 30 s)

This reaction has a linear detection range from 10^6 to 10^1 copies per reaction, with a correlation (R^2) of 0.99 and an amplification efficiency of 97%. Its limit of detection is 4.7 copies per assay (95% confidence interval, 3.7–6.8 copies/reaction). The assay variability is <30% for yield close to the detection limit (10^2 copies) and <15% for higher DNA amount (10^4 and 10^6 copies). The assay specificity has been tested against several viral DNA, such as OPV (*vaccinia*, *cowpox*, *monkeypox*, *ectromelia*, and *camelpox virus*), *Molluscum contagiosum virus*, *Yaba-like disease virus*, human herpesviruses types 1–8, and adenoviruses, and no amplifications were detected [23].

In 2013, Zhao and colleagues have validated a new robust and specific qPCR assay, which amplifies the conserved RNA polymerase gene of all PPV species.

Primer	Target Gene	Sequence (5'–3')	Reference
Forward primer	PAPV J6R	CGCGGTCTGGTCCTTG	[118]
Reverse primer		CAGCATCAACCTCTCTACATCA	
Probe		CCACGAAGCTGCGCAGCAT	

PCR protocol is as follows.

Component	Concentration	Thermocycle
PPV primers	0.4 $\mu\text{mol/L}$	Incubation at 95°C for 2 min
FastStart TaqMan Universal PCR Master Mix (Applied Biosystems, Foster City, CA)	1 \times	45 cycles
TaqMan probe	200 nmol/L	Denaturation (95°C, 5 s)
Template	2 μL	Annealing (62.5°C, 20 s)
Total volume	25 μL	

97.2.2.3 Nested PCR Detection of PPV

Abrahão and colleagues in 2009 designed a nested–multiplex PCR to detect orthopox–parapox coinfections. In addition, the reaction was successfully used to specifically detect PPV, with high sensitivity. An adapted nested PCR protocol developed to detect exclusively PPV in scabs is as follows. Clinical sample is prepared by maceration of the scab in PBS (pH 7.4) (0.1 g scab/0.9 mL PBS) and clarification by centrifugation at $2000 \times g$ for 3 min. Supernatant is collected and directly amplified by PCR targeting the gene ORFV011–*B2L* gene (viral envelope antigen). As previously stated, the *B2L* gene is the most common target used for diagnosis and phylogenetic studies of PPV. The technique described in the following has been previously reported [24,26,75,93,112], and here, we proposed an adaptation. It is worth mentioning that all known PPV species are detected by this reaction.

Primer	Target Gene	Step	Sequence (5'–3')	Expected Product (bp)	References
OVB2LF1	B2L	First step	TCCCTGAA GCCCTATTA TTTTTGT	1206	[26]
OVB2LR1			GCTTGCG GGCG TTCGGA CCTTC		
PPP-1		Nested step	GTCGTCCAC GATGA GCAG	592	[24]
PPP-4			TACGTGGGA AGCGCC TCGCT		

Prepare the mix of the first step and perform the reaction in a thermal cycler following the protocol:

Component	Concentration	Thermocycle
PPV primers	0.8 mM	Incubation at 95°C for 9 min
dNTPs	10 mM	↓
MgCl ₂	2.0 mM	30 cycles
Bovine serum albumin (BSA)	500 ng	Denaturation (94°C, 1 min)
Taq DNA Polymerase (Promega, Madison, the United States)	2 U	Annealing (45°C, 1 min)
DEPC-treated water q.s	18 μL	Extension (72°C, 1 min)
Template	2 μL	↓
Total volume	20 μL	Final extension (72°C, 10 min)

Notes: For the nested step, the same chemical and thermal conditions must be used, but using internal PPV (PPP-1 and PPP-4–0.8 mM) primers. The final PCR products may be electrophoresed on 2% agarose or 8% PAGE gels in parallel with standard DNA, as described elsewhere [119].

97.2.3 SEQUENCING AND PHYLOGENY OF PPV

In order to discriminate the PPV species detected by PCR, the amplified products are usually sequenced and subjected to phylogenetic analysis. Sequencing is usually performed using the primers described earlier and those by Hosamani et al. [26] and Inoshima et al. [24]. In addition, other targets have been described for characterization as shown in the following:

Primer	Target Gene	Sequence (5'–3')	References
PPV011-F	ORF 011 (B2L)	GTG CGC GAA GGT GTC GTC CA	[103]
PPV011-R		ATGTGGCCGTTCTCTCCATC	
PPV032-F	ORF 032	CGA GCT TTA AAT AGT GGA AAC ACA GC	
PPV032-R		GCA CCA TCA TCC TGT ACT TCC TC	
D27F	VEGF	AAT GTA AAT WMT AAC GCC	[122]

(Continued)

11R		AAC CCA GAA ACG TCC CGC TAC	
D2R		CGT TTG GAT MTG CGG TCC	
VIR1	VIR	TTA GAA GCT GAT GCC GCA G	[34]
VIR2		ACA ATG GCC TGC GAG TG	
FP	A32L	GTG TTG ATC ATC GAA GAC TCG GTG	[123]
RP1		GTC GCC CTT GTC GCC CTT AGT CTC	
RP2		CCG CCG TCA GAG TCG ACG TCG CCC T	

^a VEGF, vascular endothelial growth factor;

^b W, A/T. M, A/C;

^c VIR, virus interferon resistance.

In 2014, Friederichs and colleagues developed a pan-PPV PCR reaction using primers that encompasses all PPV strains, designed on *B2L* gene [103]. They also described a further PCR protocol, targeting a more variable region within the ORF 032. For the ORF 032 gene, the same B2L-PCR protocol must be used, but the annealing temperature is set to 67°C. PCR conditions for B2L and ORF 032 are the following:

Component	Concentration	Thermocycle
PPV primers (B2L/ ORF 032)	0.5 µM	Incubation at 98°C for 30 s
dNTPs	200 µM	↓
Q5 reaction buffer	1×	35 cycles
Q5 high GC enhancer	1×	Denaturation (98°C, 10 s)
Q5 high fidelity DNA polymerase (New England Biolabs, MA)	1 U	Annealing for B2L (65°C, 30 s) Annealing for ORF 032 (67°C, 30 s)
DEPC-treated water q.s	49 µL	Extension (72°C, 30 s)
Template	1 µL	↓
Total volume	50 µL	Final extension (72°C, 2 min)

Other genes that encode nonstructural proteins—*VEGF* and *VIR*—have been previously described to characterize PPV isolates [122,124]. Worth of note, high variability in *VEGF* gene of PCPV has been reported, suggesting that particular attention is required in choosing this target for PCR diagnosis. PCR conditions for *VEGF* and *VIR* are the following:

Component	Concentration	Thermocycle
PPV primers VEGF/VIR	0.2 µM	Incubation at 95°C for 5 min
DNTpsmix	800 µM	↓
Tris-HCl (pH 8.3)	10 mM	35 cycles
KCl	50 mM	Denaturation (94°C, 30 s)
MgCl ₂	1.5 mM	Annealing for VEGF(40°C, 30 s)
AmpliQ Gold DNA polymerase (Applied Biosystems, CA)	1 U	Annealing for VIR (55°C, 30 s)
DEPC-treated water q.s	49 µL	Extension (72°C, 30 s)

(Continued)

Template	1 µL	↓
Total volume	50 µL	Final extension (72°C, 7 min)

The PPV strains can be genotyped using a differential PCR for the *A32L* gene, as described previously [123]. This process is based on the polymorphisms among PPV isolates, and the PCR conditions for the *A32L* are described as follows.

Component	Concentration	Thermocycle
FP primer	1 µM	Incubation at 95°C for 9 min
RP1 primer	0.4 µM	↓
RP2 primer	0.4 µM	35 cycles
dNTP mix	800 µM	Denaturation (94°C, 30 s)
Tris-HCl (pH 8.3)	10 mM	Annealing (63°C, 30 s)
KCl	50 mM	Extension (72°C, 30 s)
MgCl ₂	1.5 mM	↓
AmpliQ Gold DNA polymerase	1 U	Final extension (72°C, 7 min)
Extracted DNA	3 µL	
Total volume	50 µL	

The expected gene fragments are amplified by the protocols mentioned earlier and electrophoresed on 2% agarose gels. The amplicons are purified, cloned, and sequenced. The obtained sequences are compared with the available sequences in the National Center for Biotechnology Information GenBank database, The European Molecular Biology Laboratory, or DNA Data Bank of Japan.

With these results, phylogenetic and molecular evolutionary analyses have been performed. Several studies have traditionally inferred PPV phylogeny by amplification and sequencing of *B2L* gene [15,24,26,96]. However, Friederichs and colleagues recently proposed to include ORF 032 in phylogenetic analyses of PPV. ORFV phylogenetic tree based on *B2L* gene, as well as on ORF 032, shares a similar basic structure and reveals three distinct clusters with high bootstrap support, each representing one of the PPV species: ORFV, PCPV, and BPSV. In particular, ORF 032–derived phylogenetic tree shows a highly diversified branching and consequently provides an improvement in the analysis of PPV phylogeny [103].

As previously reported, *B2L* gene has been extensively used in phylogeny. In 2010, Inoshima and colleagues have reported a highly conservative profile among *B2L* sequences from Japanese's ORFs. Then, they have proposed additional analysis using three nonstructural protein genes, such as *VEGF*, *VIR*, and *A32L*. These additional analyses are suitable to phylogeny allowing the proper clustering of PPV isolates into regional clades [103]. Interestingly, *B2L*, *VIR*, and *VEGF* genes of Brazilian ORFV isolates have been recently analyzed, showing a high variation degree among them, indicating a multiple introduction source of ORFV in Brazil from different sources, such as European countries, Asia, North America, and/or Oceania. The cocirculation of allochthonous-derived isolates may have led to this polytomous phenomenon observed among Brazilian ORFV isolates [21].

Virus isolation, molecular detection, and whole genome sequencing are useful tools for the diagnosis of PPV infections. The genome-wide studies can support the understanding about the origins, evolution, and epidemiology of ORFVs. All of these concerns are of great importance in the veterinary, economy, and public health fields.

97.3 CONCLUSION

The emergence of zoonotic poxviruses has highlighted the importance of molecular techniques in the diagnosis of PPV infections. In recent years, improvement in molecular assays has enhanced the accuracy of pathogen identification and yielded insights into PPV genomic organization and phylogeny. Further refinement of molecular diagnostic techniques in relation to test turnaround time and automation will not only contribute to the discovery of new pathogens but also assist researchers and clinicians in the implementation of effective intervention (e.g., vaccines and drugs) and management strategies for PPV infections.

REFERENCES

- Buttner, M. and Rziha, H.J., Parapoxviruses: From the lesion to the viral genome, *J. Vet. Med. B Infect. Dis. Vet. Public Health*, 49, 7, 2002.
- MacNeil, A. et al., Diagnosis of bovine-associated parapoxvirus infections in humans: Molecular and epidemiological evidence, *Zoonoses Public Health*, 57, 161, 2010.
- Dashtseren, T. et al., Camel contagious ecthyma (pustular dermatitis), *Acta Virol.*, 28, 122, 1984.
- Sainsbury, A.W. and Gurnell, J., An investigation into the health and welfare of red squirrels, *Sciurus vulgaris*, involved in reintroduction studies, *Vet. Rec.*, 137, 367, 1995.
- Robinson, A.J. and Mercer, A.A., Parapoxvirus of red deer: Evidence for its inclusion as a new member in the genus *Parapoxvirus*, *Virology*, 208, 812, 1995.
- Damon, I., Poxviruses. In: Fields, B.N., Knipe, D.M., and Howley, P.M. (eds.), *Fields Virology*, 6th edn. Lippincott, Williams & Wilkins, Philadelphia, PA, p. 2173, 2013.
- King, A.M.Q. et al. (eds.), *Virus Taxonomy: Classification and Nomenclature of Viruses: Ninth Report of the International Committee on Taxonomy of Viruses*. Elsevier Academic Press, San Diego, CA, 2011.
- Wittek, R. et al., Genetic and antigenic heterogeneity of different parapoxvirus strains, *Intervirology*, 13, 33, 1980.
- Robinson, A.J. and Lyttle, D.J., Parapoxviruses: Their biology and potential as recombinant vaccines. In: Binns, M.M. and Smith, G.L. (eds.), *Recombinant Poxviruses*. CRC Press, Inc., Boca Raton, FL, p. 285, 1992.
- Moss, B., Poxviridae. In: Fields, B.N., Knipe, D.M., and Howley, P.M. (eds.), *Fields Virology*, 6th edn. Lippincott, Williams & Wilkins, Philadelphia, PA, p. 2129, 2013.
- Buddle, B.M., Dellers, R.W., and Schurig, G.G., Heterogeneity of contagious ecthyma virus isolates, *Am. J. Vet. Res.*, 45, 75, 1984.
- Gassmann, U., Wyler, R., and Wittek, R., Analysis of parapoxvirus genomes, *Arch. Virol.*, 83, 17, 1985.
- Robinson, A.J., Ellis, G., and Balassu, T., The genome of orf virus: Restriction endonuclease analysis of viral DNA isolated from lesions of orf in sheep, *Arch. Virol.*, 71, 43, 1982.
- Robinson, A.J. et al., Conservation and variation in orf virus genomes, *Virology*, 157, 13, 1987.
- Inoshima, Y. et al., Genetic heterogeneity among parapoxviruses isolated from sheep, cattle and Japanese serows (*Capricornis crispus*), *J. Gen. Virol.*, 82, 1215, 2001.
- Rziha, H.J. et al., Relatedness and heterogeneity at the near-terminal end of the genome of a parapoxvirus bovis 1 strain (B177) compared with parapoxvirus ovis (*Orf virus*), *J. Gen. Virol.*, 84, 1111, 2003.
- Delhon, G. et al., Genomes of the parapoxviruses orf virus and bovine Papular stomatitis virus, *J. Virol.*, 78, 168, 2004.
- Mercer, A.A. et al., The establishment of a genetic map of orf virus reveals a pattern of genomic organization that is highly conserved among divergent poxviruses, *Virology*, 212, 698, 1995.
- Koonin, E.V., Senkevich, T.G., and Chernos, V.I., Gene A32 product of vaccinia virus may be an ATPase involved in viral DNA packaging as indicated by sequence comparisons with other putative viral ATPases, *Virus Genes*, 7, 89, 1993.
- Sullivan, J.T. et al., Identification and characterization of an orf virus homologue of the vaccinia virus gene encoding the major envelope antigen p37 K, *Virology*, 202, 968, 1994.
- Abrahão, J.S. et al., Looking back: A genetic retrospective study of Brazilian *Orf virus* isolates, *Vet. Rec.*, 171, 476, 2012.
- Zhang, K. et al., Comparison and phylogenetic analysis based on the B2L gene of orf virus goats and sheep in China during 2009–2011, *Arch. Virol.*, 159, 1475, 2014.
- Nitsche, A. et al., Real-time PCR detection of parapoxvirus DNA, *Clin. Chem.*, 52, 316, 2006.
- Inoshima, Y., Morooka, A., and Sentsui, H., Detection and diagnosis of parapoxvirus by the polymerase chain reaction, *J. Virol. Methods*, 84, 201, 2000.
- Li, H. et al., Phylogenetic analysis of two Chinese orf virus isolates based on sequences of B2L and VIR genes, *Arch. Virol.*, 158, 1477, 2013.
- Hosamani, M. et al., Comparative sequence analysis of major envelope protein gene (B2L) of Indian orf viruses isolated from sheep and goats, *Vet. Microbiol.*, 116, 317, 2006.
- Lefkowitz, E.J., Wang, C., and Upton C., Poxviruses: Past, present and future, *Virus Res.*, 117, 105, 2006.
- Wittek, R., Kuenzle, C.C., and Wyler, R. High GC content in parapoxvirus DNA, *J. Gen. Virol.*, 43, 231, 1979.
- Yerulam, I., Nyska, A., and Abraham, A., Parapox infection in a gazelle kid (*Gazella gazella*), *J. Wildl. Dis.*, 30, 260, 1994.
- Simpson, V.R. et al., Parapox infection in grey seals (*Halichoerus grypus*) in Cornwall, *Vet. Rec.*, 134, 292, 1994.
- Suzuki, T. et al., Isolation and antibody prevalence of a parapoxvirus in wild Japanese serows (*Capricornis crispus*), *J. Wildl. Dis.*, 29, 384, 1993.
- Hamblet, C.N., Parapoxvirus in a cat, *Vet. Rec.*, 132, 144, 1993.
- Fairley, R.A. et al., Recurrent localized cutaneous parapoxvirus infection in three cats, *N. Z. Vet. J.*, 56, 196, 2008.
- Guo, J. et al., Genetic characterization of orf viruses isolated from various ruminant species of a zoo, *Vet. Microbiol.*, 99, 81, 2004.
- Okada, H., Matsukawa, K., and Chihaya, Y., Experimental transmission of contagious pustular dermatitis from a Japanese serow, *Capricornis crispus*, to a calf and goats, *J. Jpn. Vet. Med. Assoc.*, 39, 578, 1986.
- McKeever, D.J. et al., Studies of the pathogenesis of orf virus infection in sheep, *J. Comp. Pathol.*, 99, 317, 1988.

37. Jenkinson, D.M., Hutchison, G., and Reid, H.W., The B and T cell responses to orf virus infection of ovine skin, *Vet. Dermatol.*, 3, 57, 1992.
38. Almagro, M. et al., Milker's nodes: Transmission by fomites and virological identification, *Enferm. Infecc. Microbiol. Clin.*, 9, 286, 1991.
39. Smith, K.J. et al., Parapoxvirus infections acquired after exposure to wildlife, *Arch. Dermatol.*, 127, 79, 1991.
40. Schuler, G., Hönigsmann, H., and Wolff, K., The syndrome of milker's nodules in burn injury: Evidence for indirect viral transmission, *J. Am. Acad. Dermatol.*, 6, 334, 1982.
41. Carson, C.A. and Kerr, K.M., Bovine papular stomatitis with apparent transmission to man, *J. Am. Vet. Med.*, 151, 183, 1967.
42. Yirrell, D.L. and Vestey, J.P., Human orf infections, *J. Eur. Acad. Dermatol. Venereol.*, 3, 451, 1994.
43. Bayindir, Y. et al., Investigation and analysis of a human orf outbreak among people living on the same farm, *New Microbiol.*, 34, 37, 2011.
44. Ohashi, A. et al., A rare human-to-human transmission of orf, *Int. J. Dermatol.*, 53, 1, 2014.
45. Hosamani, M. et al., Orf: An update on current research and future prospective, *Expert Rev. Anti Infect.*, 7, 879, 2009.
46. Bowman, K.F. et al., Cutaneous form of bovine papular stomatitis in man, *JAMA*, 246, 2813, 1981.
47. Haig, D.M. and Mercer, A.A., Ovine diseases: Orf, *Vet. Res.*, 29, 311, 1998.
48. Nandi, S., De, U.K., and Chowdhury, S., Current status of contagious ecthyma or orf disease in goat and sheep—A global perspective, *Small Ruminant Res.*, 96, 73, 2011.
49. Mazur, C. and Machado, R.D., Detection of contagious pustular dermatitis virus of goats in a severe outbreak, *Vet. Rec.*, 125, 419, 1989.
50. Mazur, C. et al., Molecular characterization of Brazilian isolates of orf virus, *Vet. Microbiol.*, 73, 253, 2000.
51. Zhao, K. et al., Identification and phylogenetic analysis of an orf virus isolated from an outbreak in sheep in the Jilin province of China, *Vet. Microbiol.*, 142, 408, 2010.
52. Billinis, C. et al., Phylogenetic analysis of strains of *Orf virus* isolated from two outbreaks of the disease in sheep in Greece, *Virol. J.*, 9, 24, 2012.
53. Newsom, I.E. and Cross, F., Sore mouth in sheep transmissible to man, *J. Am. Vet. Med. Assoc.*, 84, 799, 1934.
54. Huminer, D., Alcalay, J., and Pitlik, S., Human orf in Israel: Report of three cases, *Isr. J. Med. Sci.*, 24, 54, 1988.
55. Khaled, A. et al., Orf of the hand, *Tunis. Med.*, 87, 352, 2009.
56. Al-Qattan, M.M., Orf infection of the hand, *J. Hand. Surg. Am.*, 36, 1855, 2011.
57. Lederman, E.R. et al., An investigation of a cluster of Parapoxvirus cases in Missouri, Feb–May 2006: Epidemiologic, clinical and molecular aspects, *Animals*, 3, 142, 2013.
58. Sant'Ana, F.J. et al., Coinfection by vaccinia virus and an orf virus-like parapoxvirus in an outbreak of vesicular disease in dairy cows in midwestern Brazil, *J. Vet. Diagn. Invest.*, 25, 267, 2013.
59. Lederman, E.R. et al., Progressive orf virus infection in a patient with lymphoma: Successful treatment using imiquimod, *Clin. Infect. Dis.*, 44, 100, 2007.
60. Geernick, K. et al., A case of human orf in an immunocompromised patient treated successfully with cidofovir cream, *J. Med. Virol.*, 64, 543, 2001.
61. Tan, S.T., Blake, G.B., and Chambers, S., Recurrent orf in an immunocompromised host, *Br. J. Plast. Surg.*, 44, 465, 1991.
62. Darbyshire, J.H., A fatal, ulcerative mucosal condition of sheep associated with the virus of contagious pustular dermatitis, *Br. Vet. J.*, 117, 97, 1961.
63. Scagliarini, A. et al., Orf in South Africa: Endemic but neglected, *Onderstepoort J. Vet. Res.*, 7, 79, 2012.
64. Meechan, J.G. and MacLeod, R.I., Human labial orf: A case report, *Br. Dent. J.*, 173, 343, 1992.
65. Nougairede, A. et al., Sheep-to-human transmission of orf virus during Eid al-Adha religious practices, France, *Emerg. Infect. Dis.*, 19, 102, 2013.
66. McInnes, C.J., Wood, A.R., and Mercer, A.A., Orf virus encodes a homolog of the vaccinia virus interferon resistance gene E3L, *Virus Genes*, 17, 107, 1998.
67. Haig, D.M. et al., The orf virus gene OV20.0L gene product is involved in interferon resistance and inhibits an interferon-inducible, double-stranded RNA-dependent kinase, *Immunology*, 93, 335, 1998.
68. Haig, D.M. and Fleming, S., Immunomodulation by virulence proteins of the parapoxvirus orf virus, *Vet. Immunol. Immunopathol.*, 15, 72, 1999.
69. Kottaridi, C. et al., Phylogenetic correlation of Greek and Italian orf virus isolates based on VIR gene, *Vet Microbiol.*, 116, 310, 2006.
70. Lyttle, D.J. et al., Homologs of vascular endothelial growth factor are encoded by the poxvirus orf virus, *J. Virol.*, 68, 84, 1994.
71. Haig, D.M. and McInnes, C.J., Immunity and counterimmunity during infection with the parapoxvirus orf virus, *Virus Res.*, 88, 3, 2002.
72. Mercante, M.T. et al., Production and efficacy of an attenuated live vaccine against contagious ovine ecthyma, *Vet. Ital.*, 44, 537, 2008.
73. Kumar, N. et al., Isolation and phylogenetic analysis of an orf virus from sheep in Makhdoom, India, *Virus Genes*, 48, 3012, 2014.
74. Chan, K.W. et al., Identification and phylogenetic analysis of orf virus from goats in Taiwan, *Virus Genes*, 35, 705, 2007.
75. Abrahão, J.S. et al., Detection and phylogenetic analysis of orf virus from sheep in Brazil: A case report, *Virol. J.*, 4, 47, 2009.
76. Mayr, A. and Buttner, M., Bovine papular stomatitis virus. In: Dinter, Z. and Morein, B. (eds.), *Virus Infections of Ruminants*. Elsevier, Amsterdam, the Netherlands. p. 23, 1990.
77. Leonard, D. et al., Unusual bovine papular stomatitis virus infection in a British dairy cow, *Vet. Rec.*, 164, 311, 2009.
78. Jeckel, S. et al., Severe oesophagitis in an adult bull caused by bovine papular stomatitis virus, *Vet. Rec.*, 169, 317, 2011.
79. Yeruham, I., Abraham, A., and Nyska, A., Clinical and pathological description of a chronic form of bovine papular stomatitis, *J. Comp. Pathol.*, 111, 279, 1994.
80. Yaegashi, G. et al., Molecular analysis of parapoxvirus detected in eight calves in Japan, *J. Vet. Med. Sci.*, 75, 1399, 2013.
81. Aguilar-Setién, A. et al., Bovine papular stomatitis, first report of the disease in Mexico, *Cornell Vet.*, 70, 10, 1980.
82. Inoshima, Y., Nakane, T., and Sentsui, H., Severe dermatitis on cattle teats caused by bovine papular stomatitis virus, *Vet. Rec.*, 164, 311, 2009.
83. Sant'Ana, F.J. et al., Bovine papular stomatitis affecting dairy cows and milkers in Midwestern Brazil, *J. Vet. Diagn. Invest.*, 24, 442, 2012.
84. Oem, J.K. et al., Bovine papular stomatitis virus (BPSV) infections in Korean native cattle, *J. Vet. Med. Sci.*, 75, 675, 2013.
85. Moscovici, C. et al., Isolation of a viral agent from pseudocowpox disease, *Science*, 141, 915, 1963.

86. Carter, M.E., Brookbanks, E.O., and Dickson, M.R., Demonstration of a pseudo-cowpox virus in New Zealand, *N. Z. Vet. J.*, 16, 105, 1968.
87. Cargnelutti, J.F. et al., An outbreak of pseudocowpox in fattening calves in southern Brazil, *J. Vet. Diagn. Invest.*, 24, 437, 2012.
88. Asagba, M.O., Recognition of pseudocowpox in Nigeria, *Trop. Anim. Health Prod.*, 14, 184, 1982.
89. Rossi, C.R., Kiesel, G.K., and Jong, M.H., A paravaccinia virus isolated from cattle, *Cornell Vet.*, 67, 72, 1977.
90. Abubakr, M.I. et al., Pseudocowpox virus: The etiological agent of contagious ecthyma (Auzdyk) in camels (*Camelus dromedarius*) in the Arabian Peninsula, *Vector Borne Zoonotic Dis.*, 7, 257, 2007.
91. Hautaniemi, M. et al., The genome of pseudocowpoxvirus: Comparison of a reindeer isolate and a reference strain, *J. Gen. Virol.*, 91, 1560, 2010.
92. Fairley, R.A. et al., Persistent pseudocowpox virus infection of the skin of a foot in a cat, *N. Z. Vet. J.*, 61, 242, 2013.
93. Abrahão, J.S. et al., Human vaccinia virus and pseudocowpox virus co-infection: Clinical description and phylogenetic characterization, *J. Clin. Virol.*, 48, 69, 2010.
94. Munz, E. and Dumbell, K., Pseudocowpox. In: Coetzer, J.A.W., Thomson, G.R., and Tustin, R.C. (eds.), *Infectious Disease of Livestock*. Oxford University Press, Oxford, U.K., vol. 1, p. 625, 1994.
95. Horner, G.W. et al., Parapoxvirus infections in New Zealand farmed red deer (*Cervus elaphus*), *N. Z. Vet. J.*, 35, 41, 1987.
96. Scagliarini, A. et al., Parapoxvirus infections of red deer, Italy, *Emerg. Infect. Dis.*, 17, 684, 2011.
97. Dal Pozzo, F. et al., Original findings associated with two cases of bovine papular stomatitis, *J. Clin. Microbiol.*, 49, 4397, 2011.
98. Hazelton, P.R. and Gelderblom, H.R., Electron microscopy for rapid diagnosis of infectious agents in emergent situations, *Emerg. Infect. Dis.*, 9, 294, 2003.
99. Guo, J. et al., Characterization of a North American orf virus isolated from a goat with persistent, proliferative dermatitis, *Virus Res.*, 93, 169, 2003.
100. McInnes, C.J. et al., Genomic comparison of an avirulent strain of orf virus with that of a virulent wild type isolate reveals that the orf virus G2L gene is non-essential for replication, *Virus Genes*, 22, 141, 2001.
101. Kottaridi, C. et al., Laboratory diagnosis of contagious ecthyma: Comparison of different PCR protocols with virus isolation in cell culture, *J. Virol. Methods*, 134, 119, 2006.
102. Li, W. et al., Isolation and phylogenetic analysis of orf virus from the sheep herd outbreak in northeast China, *BMC Vet. Res.*, 23, 229, 2012.
103. Friederichs, S. et al., Comparative and retrospective molecular analysis of Parapoxvirus (PPV) isolates, *Virus Res.*, 6, 11, 2014.
104. Inoshima, Y. et al., Serological survey of parapoxvirus infection in wild ruminants in Japan in 1996–1999, *Epidemiol. Infect.*, 126, 153, 2001.
105. Inoshima, Y. et al., Use of protein AG in an enzyme-linked immunosorbent assay for screening for antibodies against parapoxvirus in wild animals in Japan, *Clin. Diagn. Lab. Immunol.*, 6, 388, 1999.
106. Iketani, Y. et al., Persistent parapoxvirus infection in cattle, *Microbiol. Immunol.*, 46, 285, 2002.
107. Nollens, H.H. et al., Seroepidemiology of parapoxvirus infections in captive and free-ranging California sea lions *Zalophus californianus*, *Dis. Aquat. Organ.*, 6, 153, 2006.
108. Schütze, N. et al., Specific antibodies induced by inactivated parapoxvirus ovis potentially enhance oxidative burst in canine blood polymorphonuclear leukocytes and monocytes, *Vet. Microbiol.*, 6, 81, 2010.
109. Zhang, K. et al., Human infection with orf virus from goats in China, 2012, *Vector Borne Zoonotic Dis.*, 14, 365, 2014.
110. Klein, J. and Tryland, M., Characterisation of parapoxviruses isolated from Norwegian semi-domesticated reindeer (*Rangifer tarandus tarandus*), *Virol. J.*, 2, 79, 2005.
111. Hosamani, M. et al., Isolation and characterization of an Indian orf virus from goats, *Zoonoses Public Health*, 54, 204, 2007.
112. Abrahão, J.S. et al., Nested-multiplex PCR detection of Orthopoxvirus and Parapoxvirus directly from exanthematic clinical samples, *Virol. J.*, 6, 140, 2009.
113. Schroeder, K. and Nitsche, A., Multicolour, multiplex real-time PCR assay for the detection of human-pathogenic poxviruses, *Mol. Cell Probes*, 24, 110, 2010.
114. Venkatesan, G., Balamurugan, V., and Bhanuprakash, V., Multiplex PCR for simultaneous detection and differentiation of sheeppox, goatpox and orf viruses from clinical samples of sheep and goats, *J. Virol. Methods*, 195, 1, 2014.
115. de Oliveira, C.H. et al., Multifocal cutaneous orf virus infection in goats in the Amazon region, Brazil, *Vector Borne Zoonotic Dis.*, 12, 336, 2012.
116. Chan, K.W. et al., Phylogenetic analysis of parapoxviruses and the C-terminal heterogeneity of viral ATPase proteins, *Gene*, 432, 44, 2009.
117. Gallina, L. et al., A real time PCR assay for the detection and quantification of orf virus, *J. Virol. Methods*, 134, 140, 2006.
118. Zhao, H. et al., Specific qPCR assays for the detection of orf virus, pseudocowpox virus and bovine papular stomatitis virus, *J. Virol. Methods*, 194, 229, 2013.
119. Sambrook, J., Fritsch, E.F., and Maniatis, T. *Molecular Cloning: A Laboratory Manual*. Cold Spring Harbor University Press, Cold Spring Harbor, NY, 1989.
120. Scagliarini, A. et al., Ovine skin organotypic cultures applied to the ex vivo study of orf virus infection, *Vet. Res. Commun.*, 29, 245, 2005.
121. Gaili, W. et al., In vitro RNA interference targeting the DNA polymerase gene inhibits orf virus replication in primary ovine fetal turbinate cells, *Virology*, 159, 915, 2014.
122. Inoshima, Y., Ishiguro, N., Molecular and biological characterization of vascular endothelial growth factor of parapoxviruses isolated from wild Japanese serows (*Capricornis crispus*), *Vet. Microbiol.*, 140, 63, 2010.
123. Chan, K.W. et al., Differential diagnosis of orf viruses by a single-step PCR, *J. Virol. Methods*, 160, 85, 2009.
124. Inoshima, Y., Ito, M., and Ishiguro, N., Spatial and temporal genetic homogeneity of orf viruses infecting Japanese serows (*Capricornis crispus*), *J. Vet. Med. Sci.*, 72, 701, 2010.

Mimiviruses: Replication, Purification, and Quantification

Jônatas Santos Abrahão,^{1,3} Grazielle Pereira Oliveira,^{1,3}
Lorena Christine Ferreira da Silva,¹ Ludmila Karen dos Santos Silva,¹
Erna Geessen Kroon,¹ and Bernard La Scola²

¹Instituto de Ciências Biológicas, Departamento de Microbiologia, Laboratório de Vírus, Universidade Federal de Minas Gerais, Belo Horizonte-Minas Gerais, Brazil

²Unité de Recherche sur les Maladies Infectieuses et Tropicales Emergentes (URMITE), Aix-Marseille Université, Marseille, France

³These authors contributed equally to this work

The aim of this protocol is to describe the replication, purification, and titration of mimiviruses. These viruses belong to the *Mimiviridae* family, the first member of which was isolated in 1992 from a cooling tower water sample collected during an outbreak of pneumonia in a hospital in Bradford, England. In recent years, several new mimiviruses have been isolated from different environmental conditions. These giant viruses are easily replicated in amoeba of the *Acanthamoeba* genus, its natural host. Mimiviruses present peculiar features that make them unique viruses, such as the particle and genome size and the genome's complexity. The discovery of these viruses rekindled discussions about their origin and evolution, and the genetic and structural complexity opened up a new field of study. Here, we describe some methods utilized for mimiviruses replication, purification, and titration. © 2016 by John Wiley & Sons, Inc.

Keywords: mimiviruses • purification • replication • titration

How to cite this article:

Abrahão, J.S., Oliveira, G.P., Ferreira da Silva, L.C., dos Santos Silva, L.K., Kroon, E.G., and La Scola, B. 2016. Mimiviruses: replication, purification, and quantification. *Curr. Protoc. Microbiol.* 41:14G.1.1-14G.1.13.
doi: 10.1002/cpmc.2

INTRODUCTION

Mimiviruses are a group of recently discovered giant viruses that are distributed worldwide and infect amoeba of the *Acanthamoeba* genus and have been related to infections in a number of vertebrates. The first *Mimivirus* was isolated from a cooling tower water sample collected in a hospital in Bradford, England, during an outbreak of pneumonia in 1992 (La Scola et al., 2003). This isolate was named *Acanthamoeba polyphaga mimivirus* (APMV); due to its unique morphological and molecular features, it was included in a new viral family denominated *Mimiviridae*. The family *Mimiviridae* contains two genera: *Mimivirus* and *Cafeteriavirus* (King et al., 2012). Mimiviruses present peculiar features that make them unique viruses. One of the most notable characteristics is the 700-nm diameter particles; that size allows their retention on 0.2- μ m filters which are commonly used in virus studies. The mimivirus particles are constituted of a core, an inner membrane, a capsid with semi-icosahedral symmetry, and external fibrils (Xiao et al., 2005). Members of the *Mimiviridae* family are composed of a double-stranded DNA genome of



~1.2 Mb that encodes more than 900 proteins, thereby surpassing the coding capacity of some bacteria (La Scola et al., 2003; Raoult et al., 2004; Moreira and Brochier-Armanet, 2008).

The *Mimiviridae* family was grouped with other families of giant virus known as nucleocytoplasmic large DNA viruses (NCLDVs) which include *Poxviridae*, *Asfarviridae*, *Iridoviridae*, *Ascoviridae*, *Phycodnaviridae*, and *Marseilleviridae*, leading to the proposition of the putative order “Megavirales” to group these families (Arslan et al., 2011). In addition, phylogenetic studies resulted in an exclusive clade for the giant viruses, distinct from Eukarya, Bacteria, and Archaea, generating the proposition of a fourth domain of life composed of the giant viruses (Boyer et al., 2010).

Due to the unique structure and genetic complexity of the mimiviruses, a new field of study was opened, and subsequently rekindled several debates regarding the definition of viruses, and their evolution and origin (Raoult and Forterre, 2008; Yamada, 2011).

Amoebae of the *Acanthamoeba* genus are the natural hosts of mimiviruses (La Scola et al., 2003). The APMV was first isolated from *A. polyphaga* culture, but it is also able to replicate in *A. castellanii*, *A. griffin*, *A. lenticulata*, and *A. quina* (La Scola et al., 2003; Claverie et al., 2009). Nevertheless, there is increasing evidence that these viruses have a wider host range, since APMV is internalized by different phagocyte cells (including human cells) and it has been shown that this virus can interact with the human interferon system (Ghigo et al., 2008; Silva et al., 2013). Mimivirus DNA has been detected in primates and bovines (Dornas et al., 2014a). A number of studies proposed that APMV could be pathogenic to humans and mice, and described the presence of antibodies against mimivirus in patients with nosocomial pneumonia (Raoult et al., 2006; Khan et al., 2007; Bousbia et al., 2013). Furthermore, mimiviruses have been isolated from samples collected from patients with pneumonia (Colson et al., 2013; Saadi et al., 2013a,b). It was also found that environmental exposure to mimivirus represents a risk factor in triggering autoimmunity to collagens (Shah et al., 2013).

Viruses belonging to the *Mimiviridae* family have been isolated from environments such as soil, air, aquatic environments, sewage treatment systems, hospital environments, and systems of ventilation and air conditioning, suggesting that they represent a ubiquitous group. The isolation reports were from England, France, Tunisia, U.S., Chile, and Brazil and also from oceans (La Scola et al., 2003; Arslan et al., 2011; Boughalmi et al., 2012; Legendre et al., 2012; Campos et al., 2014; Andrade et al., 2015; Santos Silva et al., 2015). Furthermore, metagenomic studies showed the presence of mimivirus DNA in the Sargasso Sea and other oceanic samples (Ghedini and Claverie, 2005; Monier et al., 2008; Yamada, 2011; Williamson et al., 2012). Mimiviruses and other giant viruses are an outstanding research field, and the rate of publications related to these viruses has increased since their discovery (Abrahão et al., 2014a).

This unit describes the methods utilized for replication (Basic Protocol 1), purification (Basic Protocol 2), and titration (Basic Protocol 3) of mimiviruses. Furthermore, it provides a procedure for *Acanthamoeba* cell maintenance (Support Protocol). Although there is evidence of mimivirus replication in human phagocytes (Ghigo et al., 2008; Silva et al., 2013), the *Acanthamoeba* sp. cell, mainly *A. castellanii*, is the preferred choice for mimivirus replication in the laboratory. Mimivirus purification is performed using sucrose cushions, which successfully increase the viral titer by concentrating the viral stock and removing non-viral elements. Although sucrose gradient methodology is commonly used for virus purification, for most biological and molecular experiments involving mimiviruses, the level of purification and titer obtained by pelleting through

a 24% sucrose cushion is sufficient. Although it is also possible to titrate mimiviruses using a plaque-forming unit assay (depending on the *Acanthamoeba* strain used), here we describe an end-point dilution assay.

CAUTION: Mimiviruses have been studied for a few years and many of their relationships with the environment and other hosts remain unclear. Furthermore, mimiviruses were initially associated with outbreaks of pneumonia and several studies reinforced the hypothesis of their clinical relevance. Although the role of mimiviruses as etiological agents of pneumonia is still under investigation, it is recommended that assays are done using a Class II biological safety cabinet. In addition, it is important to inactivate the viruses by autoclaving lab material containing viral residue before they are discarded. To clean the working area, a 70% ethanol solution can be used. Amoebae of the *Acanthamoeba* genus are the host for mimivirus propagation and titration. Although ubiquitous, these protists can cause opportunistic infections. Therefore, it is important to take precautions, such as not wearing contact lenses when handling these amoebae (Marciano-Cabral and Cabral, 2003). Despite the mimivirus particles being very stable in environmental and clinical substrates (Dornas et al., 2014b), it is recommended that the virus solutions are kept on ice while working. Although mimivirus particles are very stable when stored at -20°C , we recommend storing the purified virus stock at -80°C to avoid viral titer decrease.

MIMIVIRUS PRODUCTION

Mimiviruses can be replicated in large amounts of *Acanthamoeba* sp. culture to increase the virus stock. Mimiviruses should be produced in culture flasks containing *Acanthamoeba* sp. cultivated in peptone-yeast extract with glucose (PYG) medium. This medium has been shown to be efficient for mimivirus production and yielded titers that were ~ 6 logarithmic units higher than viral titers produced in Page's amoeba saline (PAS; Abrahão et al., 2014b). This protocol describes mimivirus production using *A. castellanii* cultures. However, this protocol can be used to produce mimivirus stocks in other amoeba species, such as *A. polyphaga*. After reaching confluence, the amoebae should be infected and incubated at 28°C until cytopathic effects (CPE) are induced, such as amoebae rounding, loss of motility, and lysis. To obtain efficient mimivirus replication, a multiplicity of infection (MOI) of 0.01 is recommended since low MOIs produce higher viral titers compared to high MOIs (Abrahão et al., 2014b). Supernatants from the infected amoeba should be collected and submitted to three cycles of freezing and thawing to release viruses from cells (Basic Protocol 2).

NOTE: It is recommended that the procedure be performed using sterile materials in a Class II Biosafety hood. *A. castellanii* cells can be obtained from the American Type Culture Collection (ATCC; ATCC 30234 and ATCC 30010).

Materials

Viral samples to be produced (a previously titrated seed pool; see Basic Protocol 3)
Acanthamoeba castellanii culture grown in tissue culture flasks (see Support Protocol)

Peptone-yeast extract with glucose (PYG) medium (see recipe)

Phosphate-buffered saline (PBS; see recipe)

Incubator (28° to 32°C)

150-cm² cell culture flasks

Refrigerated low-speed table-top centrifuge

50-ml conical centrifuge tubes

1.5-ml microcentrifuge tubes

BASIC PROTOCOL 1

DNA Viruses

14G.1.3

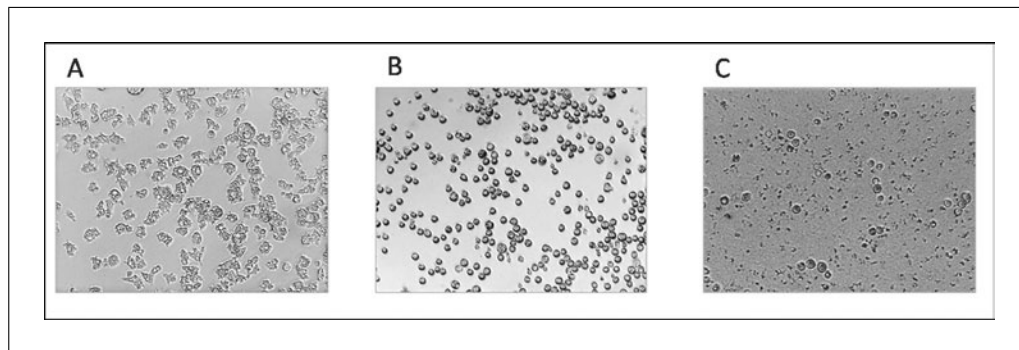


Figure 14G.1.1 Uninfected monolayer of *A. castellanii* (A). Mimivirus production in *A. castellanii* cells showing CPE at 48 hr (B) and 72 hr (C) post-infection.

37°C water bath
Inverted microscope

Mimivirus production in cultures of Acanthamoeba sp.

1. Add 7×10^6 *A. castellanii* cells in PYG medium to 150-cm² cell culture flasks (see Support Protocol).

For biological assays, a total of six 150-cm² cell culture flasks is enough for mimivirus replication. However, the number of culture flasks can be increased according to necessity (e.g., production of virus for genome sequencing usually requires about twenty flasks).

2. Incubate at 28°C, 30 min to allow cells to adhere to the flasks.

*The cell culture flasks could be prepared 24 hr before infection. In this case, 150-cm² cell culture flasks should be prepared by seeding 3×10^6 *A. castellanii* per 150-cm² cell culture flask in 25 ml PYG medium and before the infection, cells should be counted to calculate the MOI.*

3. Inoculate viral samples to be replicated, diluted in PBS, at MOI of 0.01.

Low MOIs produce higher titers of infectious particles than high MOIs, since high MOIs may be related to a higher rate of defective particle formation.

4. Incubate at 28°C, ~72 hr.

Check cells every day under the microscope to verify CPE (see Fig. 14G.1.1).

5. Collect supernatant and cell lysates using a pipet when CPE are observed in ~80% to 90% of cells.

Typically, at MOI of 0.01, 48 hr after infection, all of the cells showed rounding and 72 hr after infection, $\geq 90\%$ of the cells presented cell lysis; most of the cells have detached from the monolayer and lysed (see Fig. 14G.1.1).

6. Submit infected cells to three cycles of freezing at –80°C and thawing at room temperature to release the virus.

To make the process faster, freezing could be performed in liquid nitrogen and thawing in a 37°C water bath. Alternatively, a hypotonic lysis buffer could be used to promote lysis of the remaining amoeba cells.

7. Freeze tubes in a –80°C freezer for storage until purification (*Basic Protocol 2*).

If the virus will not be purified, the supernatant and cell lysates should be centrifuged at $600 \times g$ for 5 min at 4°C. After that the debris should be discarded and the supernatant stored at –80°C.

MIMIVIRUS PURIFICATION

Sucrose cushions are sufficient to concentrate viral stocks, increase viral titer, and remove non-viral elements from the stock. For most of the biological and molecular experiments involving mimiviruses, including animal experimentation, this level of purification (sucrose cushion at 24%) is sufficient, and will be presented here. Also, if required, a simple filtration of virus-containing cell lysates through a 0.8- μm filter has been empirically tested, and shown to eliminate traces of the host genome.

In this protocol, the mimivirus-rich supernatants from the infected amoebae obtained during the mimivirus replication (Basic Protocol 1) were submitted to several rounds of homogenization in a Dounce, and purified by ultracentrifugation through a sucrose cushion (24%), followed by homogenization in PBS or Page's amoeba saline (PAS), and stored at -80°C .

Materials

- Viral samples to be purified (see Basic Protocol 1)
- 24% sucrose solution (see recipe)
- Phosphate-buffered saline (PBS; see recipe, or Page's amoeba saline [PAS; see recipe])

- Dounce homogenizer, glass, with tight pestle
- 50-ml conical centrifuge tubes
- Refrigerated low-speed table-top centrifuge
- 1.2- μm pore syringe filter
- Ultracentrifuge (Sorvall Combi OTD or equivalent)
- Beckman ultracentrifuge polypropylene tubes
- 0.6-ml microcentrifuge tubes

Mimivirus purification by sucrose cushion

1. Submit viral samples to be purified (see Basic Protocol 1) to 80 homogenization cycles in a Dounce homogenizer.

Although not essential, this step is important to disrupt remaining amoeba cells and also to homogenize the solution.

2. Filter supernatant and cell lysates through a 1.2- μm syringe filter to remove amoeba debris.

Although filtration allows purer viral stocks to be obtained, some particles may be retained in the filter, causing a decrease of viral titer.

3. Slowly layer 25 ml filtrate onto a 10-ml 24% sucrose cushion (see recipe) in ultracentrifuge tubes (see Fig. 14G.1.2).

This protocol used a 24% sucrose cushion; a 22% sucrose cushion can also be used with success.

4. Balance centrifuge tubes.
5. Centrifuge at $35,250 \times g$, 30 min at 4°C in an ultracentrifuge.

An easily visualized pellet will be formed (see Fig. 14G.1.2).

6. Homogenize pellet with a pipet in 500 μl PBS.

This step should be performed on ice.

7. Store 5 to 10 μl aliquots (or in an appropriate volume according to specific needs) in 0.6-ml microcentrifuge tubes at -80°C ; and then titrate virus (see Basic Protocol 3).

**BASIC
PROTOCOL 3**

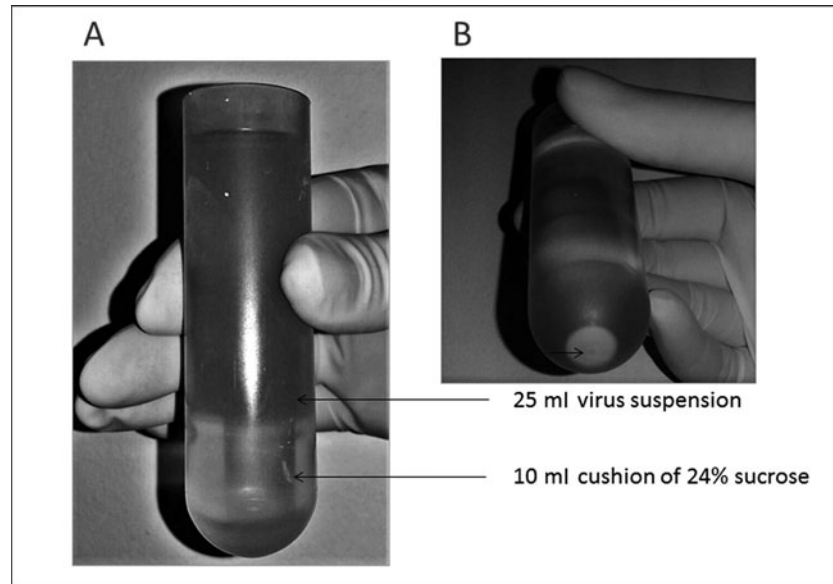


Figure 14G.1.2 Ultracentrifuge tube with 24% sucrose cushion prepared with virus overlay prior to centrifugation (A) and mimivirus pellet after ultracentrifugation (B).

MIMIVIRUS TITER CALCULATION BY END-POINT DILUTION ASSAY

End-point dilution assays are commonly performed to determine the viral titer of viruses that do not form plaques, such as mimiviruses, in *Acanthamoeba* sp. cells. This protocol describes the mimivirus end-point dilution assays. The procedure involves performing serial dilutions of the viral solution and inoculating in *A. castellanii* previously plotted on 96-well plates. After incubation, CPE are observed under an optical microscope and the titer (TCID₅₀) is calculated as described by Reed and Muench (1938).

Materials

- Viral samples to be quantified
- Acanthamoeba castellanii* culture grown in tissue culture flasks (see Support Protocol)
- Peptone-yeast extract with glucose (PYG) medium (see recipe)
- Phosphate-buffered saline (PBS; see recipe, or Page's amoeba saline [PAS; see recipe])

- Incubator (28°C)
- 96-well plates
- 75-cm² tissue culture flasks
- Transfer pipet
- 1.5-ml microcentrifuge tubes (for serial dilutions of virus)
- Inverted microscope

A. *castellanii* cells preparation

1. Setup 4×10^4 *A. castellanii* cells in 96-well plates in 100 μ l PYG medium per well (see Support Protocol).
2. Prepare cells in PYG medium to a final volume of 11 ml for one 96-well plate.
3. Pipet 100 μ l cell mixture into each well of a 96-well tissue culture plate.

	1	2	3	4	5	6	7	8	9	10	11	12
A	10 ⁻¹	10 ⁻²	10 ⁻³	10 ⁻⁴	10 ⁻⁵	10 ⁻⁶	10 ⁻⁷	10 ⁻⁸	10 ⁻⁹	10 ⁻¹⁰	10 ⁻¹¹	Uninfected controls
B	10 ⁻¹	10 ⁻²	10 ⁻³	10 ⁻⁴	10 ⁻⁵	10 ⁻⁶	10 ⁻⁷	10 ⁻⁸	10 ⁻⁹	10 ⁻¹⁰	10 ⁻¹¹	Uninfected controls
C	10 ⁻¹	10 ⁻²	10 ⁻³	10 ⁻⁴	10 ⁻⁵	10 ⁻⁶	10 ⁻⁷	10 ⁻⁸	10 ⁻⁹	10 ⁻¹⁰	10 ⁻¹¹	Uninfected controls
D	10 ⁻¹	10 ⁻²	10 ⁻³	10 ⁻⁴	10 ⁻⁵	10 ⁻⁶	10 ⁻⁷	10 ⁻⁸	10 ⁻⁹	10 ⁻¹⁰	10 ⁻¹¹	Uninfected controls
E	10 ⁻¹	10 ⁻²	10 ⁻³	10 ⁻⁴	10 ⁻⁵	10 ⁻⁶	10 ⁻⁷	10 ⁻⁸	10 ⁻⁹	10 ⁻¹⁰	10 ⁻¹¹	Uninfected controls
F	10 ⁻¹	10 ⁻²	10 ⁻³	10 ⁻⁴	10 ⁻⁵	10 ⁻⁶	10 ⁻⁷	10 ⁻⁸	10 ⁻⁹	10 ⁻¹⁰	10 ⁻¹¹	Uninfected controls
G	10 ⁻¹	10 ⁻²	10 ⁻³	10 ⁻⁴	10 ⁻⁵	10 ⁻⁶	10 ⁻⁷	10 ⁻⁸	10 ⁻⁹	10 ⁻¹⁰	10 ⁻¹¹	Uninfected controls
H	10 ⁻¹	10 ⁻²	10 ⁻³	10 ⁻⁴	10 ⁻⁵	10 ⁻⁶	10 ⁻⁷	10 ⁻⁸	10 ⁻⁹	10 ⁻¹⁰	10 ⁻¹¹	Uninfected controls

Figure 14G.1.3 Schematic figure to prepare 96-well plaque for mimivirus titration by end-point dilution assay.

*One 75-cm² tissue culture flask, when confluent, contains $\sim 1.5 \times 10^7$ cells, and each well of the 96-well plate should be seeded with 4×10^4 *A. castellanii*. Therefore, a single 75-cm² tissue culture flask is needed to prepare four 96-well plates.*

- Incubate at 28°C, 30 min to adhere the cells.

*The 96-well plates could be prepared 24 hr before infection. In this case, the 96-well plates should be prepared by seeding 3×10^4 *A. castellanii* per well in 100 μ l of PYG medium.*

- Visualize *A. castellanii* cells using a microscope.

The cells should be 80% to 90% confluent.

Cell infection

- If the sample to be titrated is directly derived from mimivirus production (see Basic Protocol 1), submit samples to three cycles of freezing and thawing to release viruses trapped in the cells. If the sample to be titrated is derived from mimivirus purification (Basic Protocol 2) dilute samples directly.
- For each sample to be titrated, perform serial ten-fold dilutions (from 10⁻¹ to 10⁻¹¹) of the virus final volume of 500 μ l in PBS (or PAS), in microtubes.

During the dilution it is important to pipet from the surface of the sample to be diluted and dispense the sample on the tube wall of the next tube. It is necessary to change tips between dilutions.

- Then add directly onto the amoebae monolayer with 100 μ l medium, 100 μ l of each dilution to a single well in the plate, as shown in Figure 14G.1.3.

Each dilution is usually titrated in duplicate.

- Inoculate one row of each plate with PBS (or PAS) to serve as uninfected controls, as shown in Figure 14G.1.3.
- Incubate samples at 28°C, 96 hr and observe CPE in an inverted microscope.

It is recommended CPE be observed in each well daily.

For mimiviruses the CPE are rounding, loss of motility, and cell lysis of amoebae.

- Calculate titer as described by Reed and Muench (1938).

GROWTH AND PASSING OF ACANTHAMOEBA CULTURE

Amoebae of the *Acanthamoeba* genus are mimivirus hosts. The first mimivirus was originally isolated from *A. polyphaga*, but in the laboratory, the following can also be cultured: *A. castellanii*, *A. griffin*, *A. lenticulata*, and *A. quina* cultures. *A. polyphaga* or *A. castellanii* cells are the most widely used for mimivirus replication. In this protocol, the *A. castellanii* are cultivated at 28°C in PYG medium and subcultured until confluent cell monolayers are obtained. The amoebae should be counted when splitting.

Materials

Acanthamoeba castellanii cells (ATCC; ATCC 30234 and ATCC 30010)
Peptone-yeast extract with glucose (PYG) medium (see recipe)
Ice

Incubator (28°C)
25-, 75-, and 150-cm² tissue culture flasks
Neubauer chamber and glass cover (for cell counting)
1.5-ml microcentrifuge tubes
50-ml tubes
Inverted microscope

NOTE: Preparation of *A. castellanii* cultures: All solutions and equipment coming into contact with *A. castellanii* cultures must be sterile, and aseptic technique should be used accordingly.

1. Maintain *A. castellanii* cultures at 28°C in 75-cm² tissue culture flasks containing 15 ml PYG medium.

Cell splitting

2. Incubate cell culture flasks containing *A. castellanii* culture in an ice bath 5 min to detach the cells.
3. Gently knock flask to detach cells and observe under an inverted microscope
4. Determine cell count using a Neubauer chamber.

For counting, a dilution of the cells should be prepared. Typically, the concentration range for a cell count with a Neubauer chamber is between 250,000 cells/ml and 2.5 million cells/ml. The Neubauer chamber should be loaded with 10 µl of the dilution with a micropipet.

5. Subculture cells in a new tissue culture flask, adding 100,000; 500,000; and 1,000,000 cells to 25-, 75-, and 150-cm² tissue culture flasks containing 5 ml, 15 ml, and 25 ml PYG medium, respectively, according to requirement.
6. Incubate at 28°C until cell confluence is reached.

Perform cell splitting at least three times weekly.

The same procedure should be used to prepare plates of cells for titration (see Basic Protocol 3).

REAGENTS AND SOLUTIONS

Use deionized, distilled water in all recipes and protocol steps unless noted otherwise. For common stock solutions, see APPENDIX 2A.

NOTE: Media recipes were calculated for 1 liter but can be modified for smaller or larger volumes.

NOTE: Solutions should be prepared in sterile ultrapure water.

Page's amoeba saline (PAS)

Solution A:

1.20 g NaCl

0.04 g MgSO₄·7H₂O

1.42 g Na₂HPO₄

1.36 g KH₂PO₄

Dissolve in distilled water (dH₂O) to a final volume of 100 ml.

Solution B:

0.04 g CaCl₂·2H₂O.

Dissolve in dH₂O to final volume of 100 ml.

For 1 liter:

Add 10 ml of solution A and 10 ml of solution B to 980 ml dH₂O.

Check pH and adjust to pH 6.91 if necessary, using NaOH 10 M or HCl 4 M.

Autoclave for 20 min.

Store at room temperature or at 4°C after opening for up to 6 months.

Peptone-yeast extract with glucose (PYG) medium

Solution A:

Dissolve the following components in 300 ml ultrapure H₂O:

0.98 g MgSO₄·7H₂O

0.06 g CaCl₂

9.0 g glucose (C₆H₁₂O₆)

0.02 g ammonium iron(II) sulfate hexahydrate ((NH₄)₂Fe(SO₄)·6H₂O)

0.40 g Na₂HPO₄·7H₂O

0.34 g KH₂PO₄

1.00 g sodium citrate tribasic dihydrate (C₆H₅Na₃O₇·2H₂O)

Solution B:

Dissolve 20.0 g Bacto-peptone extract in 200 ml ultrapure H₂O.

Solution C:

Dissolve 2.0 g yeast extract in 200 ml ultrapure H₂O.

Combine solutions A, B, and C, mix well, and add ultrapure H₂O to a final volume of 1 liter. Check pH; adjust to pH 6.5 if necessary, using 10 M NaOH or 4 M HCl. Autoclave at 121°C for 20 min and allow to cool. Filter the medium; add fetal bovine serum, antibiotics, and fungicides to the medium at the following concentrations:

7% FBS

25 mg/ml amphotericin B

500 U/ml penicillin

50 mg/ml gentamicin

Store at 4°C for up to 6 months.

Phosphate-buffered saline (PBS)

For 1 liter:

8 g NaCl (137 mM)

1.44 g Na₂HPO₄ (10 mM)

0.2 g KCl (2.7 mM)

0.24 g KH₂PO₄ (2 mM)

Dissolve in 900 ml ultrapure H₂O.

Check pH and adjust to pH 7.4 if necessary, using NaOH 10 M or HCl 4 M.

Make up volume to 1 liter with ultrapure H₂O.

Autoclave in 500-ml bottles for 20 min.

Store at room temperature or at 4°C after opening for up to 6 months.

Sucrose, 24% (w/v)

For 1 liter:

240 g sucrose

Dissolve in 800 ml ultrapure H₂O, mixing well on a magnetic stirrer.

Adjust volume to 1 liter.

Prepare immediately or store in 250-ml aliquots at 4°C for up to 3 months.

COMMENTARY

Background Information

The first mimivirus was isolated in 1992 and has been investigated as a putative etiological agent of pneumonia (La Scola et al., 2003, 2005). However, its characterization as a virus occurred only in 2003. The study of this sample was delayed for a decade due to difficulty in characterization of the mimivirus, which was initially thought to be a bacterium. In addition, its size was unexpected for a viral particle, which may have delayed its isolation, consequent discovery, and study. Traditionally, viruses were thought to pass through 0.2- μ m filters in which this virus is retained. The difficulty of characterizing the mimivirus was mainly due to the fact that these viruses have unique characteristics that differentiate them from most viruses described to date. Among these features are its extensive size (~700 nm) and genome (~1.2 million base pairs). These viruses show an extensive gene content that had not previously been attributed to any virus. These and other features make the mimivirus one of the most complex viruses described to date.

Electron microscopy was one of the main techniques responsible for solving the mystery surrounding the mimivirus. Because of their unique morphological features, microscopy has also been a very important tool in the characterization of these viruses. Since the discovery and characterization of the first *Mimivirus*, the search for mimiviruses has been conducted in different environments and clinical samples, and the mimivirus replication in the laboratory has been performed in amoebae of the *Acanthamoeba* genus, its natural host, as described in this section.

Mimivirus study is an open field for basic and applied studies. However, to improve research involving the characterization of these viruses as well as elucidating their clinical and environmental significance, it was necessary to establish and improve the protocols for their study; for example, to test and determine the best conditions for viral isolation and replication. Analyzing growth conditions, obtaining purified virus at high titers as well as searching for fast, efficient, and inexpensive viral

production strategies are sine qua non points in the scientific routine, and are directly linked to further understanding the biology of viruses (Kusnetsov et al., 2010; Mutsafi et al., 2013), but require a standardization process. Most of the newly identified mimiviruses have been successfully replicated, purified, and titrated using the methods described here. However, due to the increasing number of *Mimivirus* isolates, it is necessary for these protocols to be routinely assessed for their suitability for new samples that have been isolated. The interest in *Mimivirus* continues to increase among researchers worldwide, creating the need to establish methods and descriptions to improve *Mimivirus* study and provide a basis for their study in the laboratory.

Critical Parameters and Troubleshooting

As in other cell cultures, the *Acanthamoeba* sp. cultures are very susceptible to contamination with bacteria, filamentous fungus, and yeast. To overcome this critical parameter and to minimize contamination, preventive measures such as the use of medium containing large amounts of antimicrobial agents have been taken (mainly when isolating viruses from environmental samples). However, in specific cases, the antimicrobial agents can be reduced or even eliminated.

All protocols described here involving cell culture must be performed in a biosafety cabinet and with aseptic technique. Furthermore it is essential that the cabinet and the work surfaces are cleaned with 70% ethanol. The PYG medium should be autoclaved and can be filtered after the autoclave step to remove salt crystals. Another critical point to consider in preparation of *Acanthamoeba* sp. cultures is the procedure in step 2 of the Support Protocol, in which the amoeba cultures are kept in an ice bath to aid detachment. It is essential that the time of 5 min is followed because amoeba cultures maintained in an ice bath for a longer time period could encyst due to physiological stress. A second critical parameter is the cultivation atmosphere because the *Acanthamoeba* culture should be incubated

without additional CO₂. It is essential that the plates and flasks containing *Acanthamoeba* sp. cultures be carefully maintained, completely sealed, and closed.

Mimivirus replication and titration by end-point dilution assays are very sensitive and reliable. However, the success of these techniques depends on the state of the *Acanthamoeba* sp. cultures used. During repeated subculture of *Acanthamoeba* sp., passage modifications may occur, which affect virus production. Therefore, we recommend *Acanthamoeba* sp. cultures be grown for no more than ten passages to try to reduce variability, and keep a stock of *Acanthamoeba* cysts to be excysted when necessary.

For mimivirus production and titration, it is necessary to prepare the culture plates and flasks in advance and wait for cells to adhere. Furthermore, at this step it is essential to seed a consistent number of cells because this is a critical parameter for titration by end-point dilution assays. The seeding of 4×10^4 cells per well in 96-well plates for mimivirus titration and 7×10^6 cells per culture flasks for mimivirus production is ideal when cells are infected on the same day. If necessary the cells can be prepared ~24 hr before infection, as described in step 2 of Basic Protocol 1 and step 4 of Basic Protocol 3. However, in this case, it is necessary to add a lower concentration of cells per well. One of the most important parameters for mimivirus production is the MOI. Thus, the cell count is a critical parameter to obtain an MOI of 0.01.

One of the critical parameters for mimivirus purification is the quality of the sample to be purified. It is therefore very important that the viral production protocol is carried out properly and that the viral titer is high enough. Furthermore, during the procedure of placing the virus over the sucrose solution, it is important not to disturb the sucrose solution. It is also important to handle the ultracentrifuge tube carefully after the addition of the viral solution.

Anticipated Results

After mimivirus production (from a viral seed pool; Basic Protocol 1) the titers obtained in the laboratory typically ranged between 10^6 and 10^7 TCID₅₀/ml. Also, after 48 to 72 hr of incubation, at an MOI of 0.01, ≥90% of the cells presented CPE with most of the cells having detached from the monolayer. The CPE most commonly observed in amoeba infected with mimivirus are amoebae rounding, loss of motility, and lysis (see Fig. 14G.1.1). The titers can be increased by

purifying the produced virus. Viral purification by sucrose cushion (Basic Protocol 2) results in the formation of easily visualized pellets, as shown in Figure 14G.1.2. After viral purification, titers typically range between 10^9 and 10^{11} TCID₅₀/ml. As described, mimivirus can be titrated by the end-point dilution assay (Basic Protocol 3). When the growth and splitting of amoebae in culture are performed using the specific conditions and amoeba concentration indicated in Support Protocol (every 2 days), the amoebae monolayer quickly becomes confluent and can be counted, split, and used to prepare plates.

Time Considerations

It generally takes 1 to 2 hr to split and prepare the amoebae culture for infection. Preparation of the plate to perform titration generally takes 1 to 2 hr. For PYG medium preparation, a complete day is necessary, since the medium is autoclaved and only after it is cold should it be filtered. However, PYG medium can be prepared and stored at 4°C until use.

In successful experiments, it generally takes 4 days to propagate mimivirus (Basic Protocol 1), a single day for mimivirus purification (Basic Protocol 2), and another 5 days to determine the titer (Basic Protocol 3). The infection for mimivirus replication generally takes ~72 hr, since the infection is performed by the inoculation of the samples in the amoebae monolayer at adequate MOI. After mimivirus production, the sample can be purified on the same day or stored at -80°C until purification. Amoeba cells infected with mimivirus at an MOI of 0.01 generally show CPE 24 to 72 hr after infection. The time of incubation can vary among the different isolates of mimivirus. Samples with decreased rates of growth can be incubated as early as 72 hr. Then, in ~3 days, the virus can be collected.

Mimivirus purification (Basic Protocol 2) generally takes about 8 hr to perform. This protocol involves homogenizing with a Dounce tissue grinder, centrifugation, and 30 min of ultracentrifugation through a sucrose cushion. All of these steps can be performed in a single day.

The mimivirus titration of the viral sample by end-point dilution assay is done over several days (5 days), but the plates can be prepared and infected in about 30 min on the first day of the procedure (Basic Protocol 3). For example, on day 1, cells are seeded into a 96-well dish and incubation of ~30 min is maintained; after this, the virus is diluted and added to the plate. This process takes ~1 hour.

In this case, most of the time will be spent waiting for cell seeding. While the amoebae are being incubated to adhere to the plate, samples can be diluted for titration. The analyses and titer calculations can be performed in ~1 hr.

Acknowledgements

We thank our colleagues from Laboratório de Vírus of Universidade Federal de Minas Gerais and the research team of URMITE, Aix Marseille Université for their excellent support. We would also like to thank Conselho Nacional de Desenvolvimento Científico e Tecnológico (CNPq), Coordenação de Aperfeiçoamento de Pessoal de Nível Superior (CAPES), Fundação de Amparo à Pesquisa do Estado de Minas Gerais (FAPEMIG), and Pro-Reitoria de Pesquisa da Universidade Federal de Minas Gerais (PRPq-UFMG) for the financial support.

Literature Cited

- Abrahão, J.S., Dornas, F.P., Silva, L.C., Almeida, G.M., Boratto, P.V.M., Colson, P., La Scola, B., and Kroon, E.G. 2014a. Acanthamoeba polyphaga mimivirus and other giant viruses: An open field to outstanding discoveries. *Viol. J.* 11:120. doi: 10.1186/1743-422X-11-120.
- Abrahão, J.S., Boratto, P.V.M., Dornas, F.P., Silva, L.C., Campos, R.K., Almeida, G.M., Kroon, E.G., and La Scola, B. 2014b. Growing a giant: Evaluation of the virological parameters for mimivirus production. *J. Virol. Methods* 207:6-11. doi: 10.1016/j.jviromet.2014.06.001.
- Andrade, K.R., Boratto, P.V.M., Rodrigues, F.P., Silva, L.C., Dornas, F.P., Pilotto, M.R., La Scola, B., Almeida, G.M., Kroon, E.G., and Abrahão, J.S. 2015. Oysters as hot spots for mimivirus isolation. *Arch. Virol.* 160:477-82. doi: 10.1007/s00705-014-2257-2.
- Arslan, D., Legendre, M., Seltzer, V., Abergel, C., and Claverie, J. 2011. Distant Mimivirus relative with a larger genome highlights the fundamental features of Megaviridae. *Proc. Natl. Acad. Sci. U.S.A.* 108:17486-17491. doi: 10.1073/pnas.1110889108.
- Boughalmi, M., Saadi, H., Pagnier, I., Colson, P., Fournous, G., Raoult, D., and La Scola, B. 2012. High-throughput isolation of giant viruses of the Mimiviridae and Marselleviridae families in the Tunisian environment. *Environ. Microbiol.* 53:344-353. doi: 10.1111/1462-2920.12068.
- Bousbia, S., Papazian, L., Saux, P., Forel, J.M., Auffray, J.P., Martin, C., Raoult, D., and La Scola, B. 2013. Serologic prevalence of amoeba-associated microorganisms in intensive care unit pneumonia patients. *PLoS One* 8:e58111. doi: 10.1371/journal.pone.0058111.
- Boyer, M., Madoui, M.A., Gimenez, G., La Scola, B., and Raoult, D. 2010. Phylogenetic and phyletic studies of informational genes in genomes highlight existence of a 4 domain of life including giant viruses. *PLoS One* 5:e15530. doi: 10.1371/journal.pone.0015530.
- Campos, R.K., Boratto, P.V., Assis, F.L., Aguiar, E.R.G.R., Silva, L.C.F., Albarnaz, J.D., Dornas, F.P., Trindade, G.S., Ferreira, P.C.P., Marques, J.T., Roberts, C., Raoult, D., Kroon, E.G., La Scola, B., and Abrahao, J.S. 2014. Samba virus: A novel mimivirus from a giant rain forest, the Brazilian Amazon. *Viol. J.* 11:95. doi: 10.1186/1743-422X-11-95.
- Claverie, J.M., Grzela, R., Lartigue, A., Bernadac, A., Nitsche, S., Vacelet, J., Ogata, H., and Abergel, C. 2009. Mimivirus and Mimiviridae: Giant viruses with an increasing number of potential hosts, including corals and sponges. *J. Invertebr. Pathol.* 101:172-180. doi: 10.1016/j.jip.2009.03.011.
- Colson, P., La Scola, B., and Raoult, D. 2013. Giant viruses of amoebae as potential human pathogens. *Intervirology* 56:376-385. doi: 10.1159/000354558.
- Dornas, F.P., Rodrigues, F.P., Boratto, P.V., Silva, L.C., Ferreira, P.C., Bonjardim, C.A., Trindade, G.S., Kroon, E.G., La Scola, B., and Abrahao, J.S. 2014a. Mimivirus circulation among wild and domestic mammals, Amazon Region, Brazil. *Emerg. Infect. Dis.* 20:469-472. doi: 10.3201/eid2003.131050.
- Dornas, F.P., Silva, L.C., de Almeida, G.M., Campos, R.K., Boratto, P.V., Franco-Luiz, A.P., La Scola, B., Ferreira, P.C., Kroon, E.G., and Abrahão, J.S. 2014b. Acanthamoeba polyphaga mimivirus stability in environmental and clinical substrates: Implications for virus detection and isolation. *PLoS One* 9:e87811. doi: 10.1371/journal.pone.0087811.
- Ghedini, E., and Claverie, J.M. 2005. Mimivirus relatives in the Sargasso sea. *Viol. J.* 2:62. doi: 10.1186/1743-422X-2-62.
- Ghigo, E., Kartenbeck, J., Lien, P., Pelkmans, L., Capo, C., Mege, J.L., and Raoult, D. 2008. Ameobal pathogen mimivirus infects macrophages through phagocytosis. *PLoS Pathog.* 4:e1000087. doi: 10.1371/journal.ppat.1000087.
- Khan, M., La Scola, B., Lepidi, H., and Raoult, D. 2007. Pneumonia in mice inoculated experimentally with *Acanthamoeba polyphaga mimivirus*. *Microb. Pathog.* 42:56-61. doi: 10.1016/j.micpath.2006.08.004.
- King, A.M.Q., Adams, M.J., Carstens, E.B., and Lefkowitz, E.J. 2012. Virus Taxonomy: Classification and Nomenclature of Viruses: Ninth Report of the International Committee on Taxonomy of Viruses. Elsevier, New York.
- Kusnetsov, Y.G., Xiao, C., Sun, S., Raoult, D., Rossmann, M., and McPherson, A. 2010. Atomic force microscopy investigation of the giant mimivirus. *Virology* 404:127-137. doi: 10.1016/j.virol.2010.05.007.
- La Scola, B., Marrie, T.J., Auffray, J.P., and Raoult, D. 2005. Mimivirus in pneumonia patients. *Emerg. Infect. Dis.* 11:449-452. doi: 10.3201/eid1103.040538.

- La Scola, B., Audic, S., Robert, C., Jungang, L., de Lamballerie, X., Drancourt, M., Birtles, R., Claverie, J.M., and Raoult, D. 2003. A giant virus in amoebae. *Science* 299:2033. doi: 10.1126/science.1081867.
- Legendre, M., Arslan, D., Abergel, C., and Claverie, J.M. 2012. Genomics of Megavirus and the elusive fourth domain of Life. *Commun. Integr. Biol.* 5:102-106. doi: 10.4161/cib.18624.
- Marciano-Cabral, F. and Cabral, G. 2003. *Acanthamoeba* spp. as agents of disease in humans. *Clin. Microbiol. Rev.* 16:273-307. doi: 10.1128/CMR.16.2.273-307.2003.
- Monier, A., Larsen, J.B., Sandaa, R.A., Bratbak, G., Claverie, J.M., and Ogata, H. 2008. Marine mimivirus relatives are probably large algal viruses. *Viol. J.* 5:12. doi: 10.1186/1743-422X-5-12.
- Moreira, D., and Brochier-Armanet, C. 2008. Giant viruses, giant chimeras: The multiple evolutionary histories of mimivirus genes. *BMC Evol. Biol.* 8:12. doi: 10.1186/1471-2148-8-12.
- Mutsafi, Y., Shimon, E., Shimon, A., and Minsky, A. 2013. Membrane assembly during the infection cycle of the giant mimivirus. *PLoS Pathog.* 9:5. doi: 10.1371/journal.ppat.1003367.
- Raoult, D., Audic, S., Robert, C., Abergel, C., Renesto, P., Ogata, H., La Scola, B., Suzan, M., and Claverie, J.M. 2004. The 1.2-megabase genome sequence of mimivirus. *Science* 306:1344-1350. doi: 10.1126/science.1101485.
- Raoult, D., and Forterre, P. 2008. Redefining viruses: Lessons from mimivirus. *Nat. Rev. Microbiol.* 6:315-319. doi: 10.1038/nrmicro1858.
- Raoult, D., Renesto, P., and Brouqui, P. 2006. Laboratory infection of a technician by mimivirus. *Ann. Intern. Med.* 144:702-703. doi: 10.7326/0003-4819-144-9-200605020-00025.
- Reed, L.J., and Muench, H., 1938. A simple method of estimating fifty percent endpoints. *Am. J. Hyg.* 27:493-497.
- Saadi, H., Pagnier, I., Colson, P., Cherif, J.K., Beji, M., Boughalmi, M., Azza, S., Armstrong, N., Robert, C., Fournous, G., La Scola, B., and Raoult, D. 2013a. First isolation of *Mimivirus* in a patient with pneumonia. *Clin. Infect. Dis.* 57:127-134. doi: 10.1093/cid/cit354.
- Saadi, H., Reteno, D.G., Colson, P., Aherfi, S., Minodier, P., Pagnier, I., Raoult, D., and La Scola, B. 2013b. Shan virus: A new mimivirus isolated from the stool of a Tunisian patient with pneumonia. *Intervirology* 56:424-429. doi: 10.1159/000354564.
- Santos Silva, L.K., Arantes, T.S., Andrade, K.R., Lima Rodrigues, R.A., Miranda Boratto, P.V., de Freitas Almeida, G.M., Kroon, E.G., La Scola, B., Clemente, W.T., and Santos Abrahão, J. 2015. High positivity of mimivirus in inanimate surfaces of a hospital respiratory-isolation facility, Brazil. *Clin. Virol.* 66:62-65. doi: 10.1016/j.jcv.2015.03.008.
- Shah, N., Hülsmeier, A.J., Hochhold, N., Neidhart, M., Gay, S., and Hennet, T. 2013. Exposure to mimivirus collagen promotes arthritis. *J. Virol.* 88:838-845. doi: 10.1128/JVI.03141-13.
- Silva, L.C., Almeida, G.M., Oliveira, D.B., Dornas, F.P., Campos, R.K., La Scola, B., Ferreira, P.C., Kroon, E.G., and Abrahao, J.S. 2013. A resourceful giant: APMV is able to interfere with the human type I interferon system. *Microbes Infect.* 16:187-195. doi: 10.1016/j.micinf.2013.11.011.
- Williamson, S.J., Allen, L.Z., Lorenzi, H.A., Fadrosch, D.W., Brami, D., Thiagarajan, M., McCrow, J.P., Tovchigrechko, A., Yooseph, S., and Venter, J.C. 2012. Metagenomic exploration of viruses throughout the Indian Ocean. *PLoS One* 7:e42047. doi: 10.1371/journal.pone.0042047.
- Xiao, C., Chipman, P.R., Battisti, A.J., Bowman, V.D., Renesto, P., Raoult, D., and Rossmann, M.G. 2005. Cryo-electron microscopy of the giant mimivirus. *J. Mol. Biol.* 353:493-496. doi:10.1016/j.jmb.2005.08.060.
- Yamada, T. 2011. Giant viruses in the environment: Their origins and evolution. *Curr. Opin. Virol.* 1:58-62. doi: 10.1016/j.coviro.2011.05.008.

Natural *Vaccinia Virus* Infection: Diagnosis, Isolation, and Characterization

Erna Geessien Kroon,¹ Jônatas Santos Abrahão,¹ Giliane de Souza Trindade,¹ Grazielle Pereira Oliveira,¹ Ana Paula Moreira Franco Luiz,¹ Galileu Barbosa Costa,¹ Mauricio Teixeira Lima,¹ Rafael Silva Calixto,¹ Danilo Bretas de Oliveira,² and Betânia Paiva Drumond¹

¹Laboratório de Vírus, Departamento de Microbiologia, Instituto de Ciências Biológicas, Universidade Federal de Minas Gerais, Belo Horizonte, Brazil

²Faculdade de Medicina de Diamantina, Universidade Federal dos Vales do Jequitinhonha e Mucuri, Diamantina, Brazil

Natural infections of *Vaccinia virus* (VACV)—the prototype species of the *Orthopoxvirus* genus, from the family *Poxviridae* and subfamily *Chordopoxvirinae*—cause an occupational emergent zoonotic disease that is primarily associated with the handling of infected dairy cattle. In humans, VACV infection is characterized by skin lesions, primarily on the hands, and accompanied by systemic symptoms such as fever, myalgia, headache, and lymphadenopathy. The diagnosis of VACV is usually performed according to the methods described for other orthopoxviruses. This unit describes the methods utilized to obtain clinical samples, the serological and molecular techniques used for diagnosis, and the isolation methods and techniques used for molecular and biological characterization of the viruses. © 2016 by John Wiley & Sons, Inc.

Keywords: vaccinia virus • orthopoxvirus • natural vaccinia virus infection

How to cite this article:

Geessien Kroon, E., Santos Abrahão, J., de Souza Trindade, G., Pereira Oliveira, G., Moreira Franco Luiz, A.P., Barbosa Costa, G., Teixeira Lima, M., Silva Calixto, R., de Oliveira, D.B., and Drumond, B.P. 2016. Natural *Vaccinia virus* infection: Diagnosis, isolation, and characterization. *Curr. Protoc. Microbiol.* 42:14A.5.1-14A.5.43. doi: 10.1002/cpmc.13

INTRODUCTION

Vaccinia virus (VACV) is involved in zoonosis as bovine vaccinia (BV) in South America and as buffalopox (a possible variant of VACV) in Asia. It affects mainly milking cows and the dairy workers who have direct contact with those cows. VACV infection has also been detected in cattle, humans, rodents, monkeys, and horses, both with and without clinical manifestations. In humans, VACV infection is characterized by the development of skin lesions, principally on the hands, that appear as itchy nodular swellings. Lesions have also been described on the nasal vestibule, periorbital and intraorbital areas, face, legs, arms, scrotum, mouth, and vulva. The nodular swellings evolve from papules with local edema to umbilicated pustules that are surrounded by evidence of a strong inflammatory response. After ~2 weeks, the lesions turn into necrotic and painful ulcers, and later scabs. Exanthema is coincident with the development of peripheral lymphangitis and lymphadenopathy. The disease progression is accompanied by systemic influenza-like symptoms including headache, myalgia, and fever. The systemic symptoms are



Table 14A.5.1 Summary of the Protocols Described in This Unit^a

Technique	Protocol title	Protocol number
Sample collection	Selection of samples for diagnosis	Basic Protocol 1
Serological	Indirect ELISA	Basic Protocol 2
	Plaque reduction neutralization test	Basic Protocol 3
	VACV replication	Support Protocol 1
	Titration of VACV by plaque assay	Support Protocol 2
	VACV purification	See Basic Protocol 6 of <i>UNIT 14A.3</i> and Earl et al., 2001
Molecular	DNA extraction from clinical samples and infected cells	Support Protocol 3
	PCR amplification of the C11R gene	Basic Protocol 4
	Agarose gel electrophoresis	Support Protocol 4
	Polyacrylamide gel electrophoresis	Support Protocol 5
	qPCR of the C11R gene	Alternate Protocol 1
Viral isolation	Isolation of VACV in Vero cell lines	Basic Protocol 5
	Isolation of VACV in primary chicken embryo fibroblast cells	Basic Protocol 6
	Isolation of VACV in chicken chorioallantoic membrane	Basic Protocol 7
	Establishment of primary chicken embryo fibroblasts	See Basic Protocol 4 of <i>UNIT 14A.3</i> and Earl et al., 2001
	Plaque purification of VACV isolates	Basic Protocol 8
Viral characterization	qPCR to amplify the A56R (hemagglutinin) gene	Basic Protocol 9
	PCR for A56R gene	Basic Protocol 10
	PCR for A26L gene	Alternate Protocol 2
	PCR for C23L gene	Alternate Protocol 3
	Sequencing and sequence analysis of PCR-amplified DNA fragments	Basic Protocol 11
	Biological characterization of virulence in mouse models	Basic Protocol 12
	Biological characterization of plaque phenotypes in cell culture	Basic Protocol 13

^aSee Figure 14A.5.1 for a flowchart of protocols.

present 3 to 20 days after infection for ~2 to 5 days. Other symptoms include anorexia, dehydration, arthralgia, nausea, and sudoresis. Secondary bacterial infections have also been described.

VACV is the prototype species of the *Orthopoxvirus* (OPV) genus (family *Poxviridae*; subfamily *Chordopoxvirinae*), which also includes the *Variola virus* (VARV), *Cowpox virus* (CPXV), *Monkeypox virus* (MPXV), *Ectromelia virus* (ECTV), *Camelpox virus* (CMLV), *Raccoonpox virus*, *Taterapox virus*, and *Volepox virus*. The VACV genome is composed of a single linear double-stranded DNA molecule of ~200 kilobase pairs (kbp) with a hairpin loop at each end. Consistent with its large size, VACV encodes more than 200 genes that function in viral RNA synthesis, genome replication, virus assembly, and host defense. The viral particle contains ~75 proteins, of which one-third

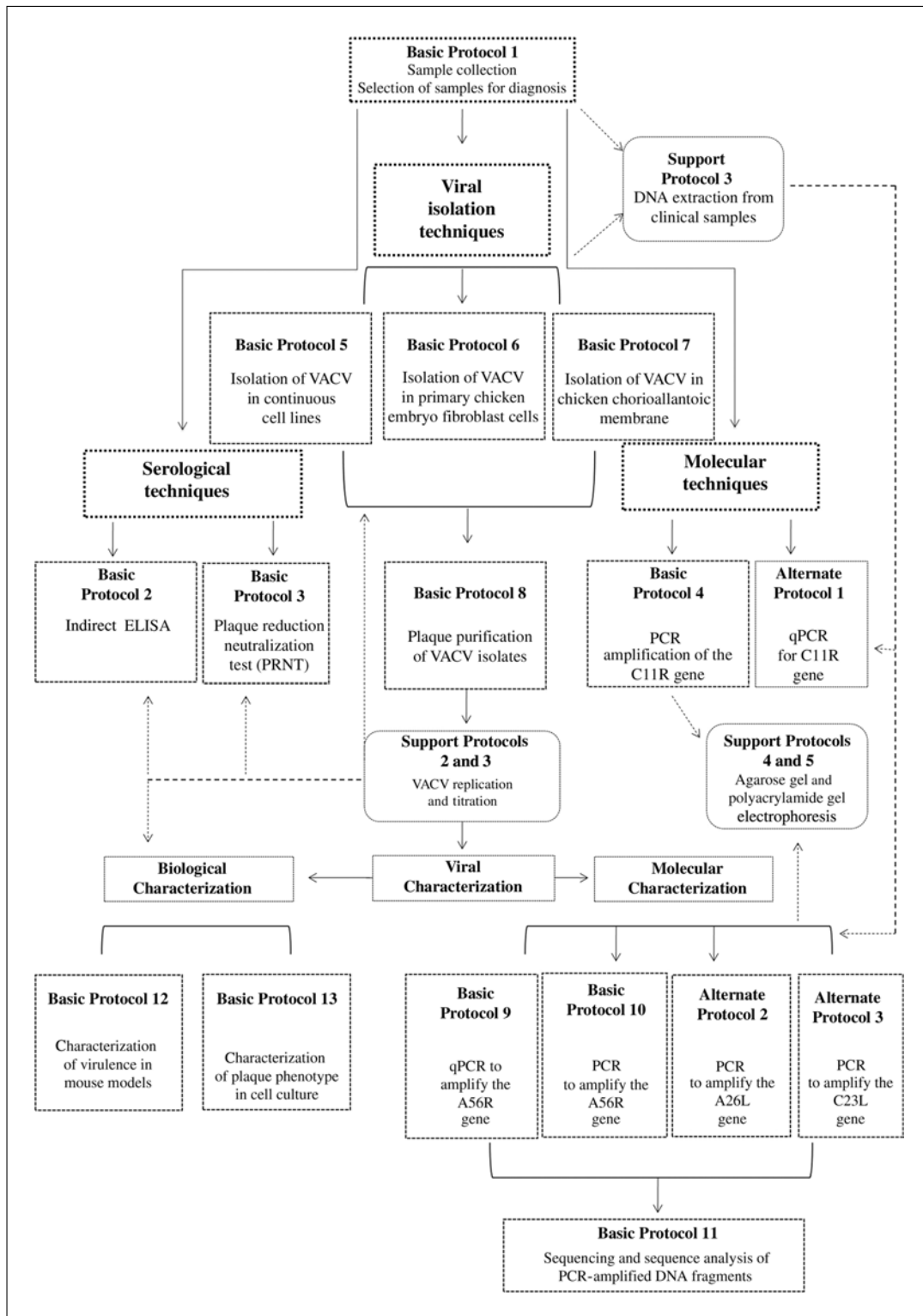


Figure 14A.5.1 Flowchart of the methodology and protocols in this unit.

are enzymes involved in early mRNA synthesis, one-quarter are membrane proteins, and the remainder are non-membrane structural proteins. Morphologically, VACV is a brick-shaped structure with dimensions of $360 \times 270 \times 250$ nm.

The diagnosis of VACV infection is usually performed using methods described for other OPVs. VACV diagnosis involves clinical, serological, viral, microscopic, and molecular techniques. Due to the robust humoral immune response caused by VACV, antibodies

can be detected with ELISA or plaque reduction neutralization tests (PRNT). Viruses can be isolated from vesicle secretions and from scabs by inoculation of permissive cell lines or the chorioallantoic membrane of embryonated hen eggs. Molecular techniques, including real-time, nested, and semi-nested PCR have been widely applied in diagnosis of VACV infection. During the last decade, several novel VACVs have been isolated and characterized. This has demonstrated that there is diversity among natural infecting VACVs and that there is a clear phenotypic and genetic dichotomy among the viruses. Several genes have been used to characterize viral isolates, including those encoding viral growth factor (VGF; i.e., C11R), thymidine kinase (TK; i.e., J2R), interferon resistance (i.e., E3L), extracellular enveloped (EEV) surface glycoprotein (i.e., B5R), A-type inclusion (ATI) body gene (i.e., A26L), and type I interferon-binding protein (i.e., B18R). The most widely used genetic marker in VACV studies, however, is the gene encoding the viral hemagglutinin (i.e., A56R).

This unit describes the methods utilized to obtain clinical samples and the serological and molecular techniques required for diagnosis. Procedures for viral isolation in different cells, as well as other useful molecular and biological techniques for viral characterization, are also provided. See Table 14A.5.1 and Figure 14A.5.1 for a summary of the methodology and protocols described in this unit.

CAUTION: *Vaccinia virus* is a biosafety level 2 (BL-2) organism. Proceed carefully and follow BL-2 practices when working with standard *Vaccinia virus* [see UNIT 14A.3 (Cotter et al., 2015)]. Carry out all procedures utilizing virus and clinical samples in an appropriate safety cabinet. Wear personal protective equipment, including gloves and lab coat, during handling of samples.

BASIC PROTOCOL 1

SAMPLE COLLECTION: SELECTION OF SAMPLES FOR DIAGNOSIS

VACV can be detected during symptomatic infection by detection of the viral genome or isolation of virus or retrospectively, by detection of anti-OPV antibodies using serological tests. Clinical samples for viral genome detection or viral isolation include crusts, tissue, vesicle fluid, lesion swabs, whole blood, serum, or plasma.

Materials

- Sample of interest (i.e., solid tissue, vesicle fluid, lesion swab, whole blood, plasma, or serum)
- Phosphate buffered saline (PBS; see recipe) containing antimicrobial agents: penicillin (200 U/ml), amphotericin B (4 µg/ml), and gentamicin (100 µg/ml)
- 1.5-ml microcentrifuge tube, sterile
- Scissors, sterile
- Tweezers, sterile
- Mortar and pestle
- Liquid nitrogen
- Homogenizer (e.g., Polytron Handheld Homogenizer)
- Vortex
- Sonicator (e.g., Unique Ultrasonic Cleaner, USC-2850A)
- Refrigerated centrifuge and microcentrifuge
- Anticoagulant-treated tubes (e.g., BD Vacutainer, cat. no. 367863)
- Dry tubes *or* serum clot activator tubes (e.g., BD Vacutainer, cat. no. 367815)

Solid tissue: lesion biopsies, scabs

- 1a. Collect a piece of tissue weighing around 0.05 g in a sample collection tube using sterile scissors and tweezers.

- 2a. Add 100 to 200 μl PBS containing antimicrobials, and macerate sample in a mortar containing liquid nitrogen with a pestle or in a homogenizer at room temperature.

To improve the conservation of samples, they should be collected in sterile tubes and stored at room temperature without buffer or medium. The addition of PBS must be done just at the moment that the diagnosis will be performed.

- 3a. Return remaining tissue to its original tube and store at 4°C.
- 4a. Freeze the homogenate at -20°C for 5 min, and then thaw for 5 min. Repeat two additional times.
- 5a. Vortex sample.
- 6a. Sonicate 30 sec, and then cool on ice 30 sec. Repeat two additional times.

CAUTION: *Be sure to wear hearing protectors and safety goggles when operating the sonicator.*

- 7a. Clarify the homogenate by centrifugation 3 min at $2000 \times g$, room temperature.
- 8a. Collect the supernatant and discard the pellet.

Vesicle fluids

- 1b. Bring the volume of clinical sample up to 200 μl using PBS containing antimicrobials.

To improve the conservation of samples, they should be collected and stored at room temperature without buffer or medium. The addition of PBS must be done just at the moment that the diagnosis will be performed.

- 2b. Sonicate 30 sec, and then cool on ice 30 sec. Repeat two additional times.

CAUTION: *Be sure to wear hearing protectors and safety goggles when operating the sonicator.*

- 3b. Clarify by centrifugation 3 min at $2000 \times g$, room temperature.
- 4b. Collect the supernatant and discard the pellet.

Dry swabs

- 1c. Cut the shaft of the swab with the sample close to the top of the cotton, and place in a sterile 1.5-ml microcentrifuge tube.

To improve the conservation of samples, they should be collected and stored without buffer or medium. The addition of PBS must be done just at the moment that the diagnosis will be performed.

- 2c. Add 250 μl PBS containing antimicrobials to the tube containing the swab, and incubate at room temperature for 10 min.
- 3c. Freeze the homogenate for 5 min, and then thaw for 5 min. Repeat two additional times.

It is important for the swab to stay inside the tube during the freeze-thaw process.

- 4c. Sonicate for 30 sec, and then cool on ice 30 sec. Repeat two additional times.

CAUTION: *Be sure to wear hearing protectors and safety goggles when operating the sonicator.*

- 5c. Centrifuge 1 min at $2000 \times g$, room temperature, to rinse the swab. Collect the eluate and transfer to a new sterile tube.
- 6c. Transfer the swab back to its original tube using tweezers, and keep the original swab at -20°C .

Whole blood or plasma

- 1d. Collect whole blood into anticoagulant-treated tubes (e.g., EDTA-treated tube).

Whole blood can be used for DNA extraction or to obtain plasma samples.

- 2d. Thoroughly homogenize the blood by gently inverting the tube four times.
- 3d. Centrifuge whole blood 10 min at 1000 to 2000 × g, 4°C, to removed cells from plasma.

Avoid higher centrifugation time as it depletes platelets in the plasma sample.

- 4d. Transfer plasma into a sterile 1.5-ml microcentrifuge tube.

Plasma should be maintained at 2°C to 8°C while handling. If the plasma is not analyzed immediately, it should be stored at or below –20°C. It is important to avoid freeze-thaw cycles. Samples which are hemolyzed, icteric, or lipemic can invalidate some tests.

Serum

- 1e. Collect whole blood into dry tubes or serum clot activator tubes.
- 2e. After collection, allow the blood to clot by leaving it undisturbed at room temperature for 15 to 30 min.
- 3e. Remove the clot by centrifuging 10 min at 1000 to 2000 × g, 4°C.
- 4e. Transfer the serum into a sterile 1.5-ml microcentrifuge tube.

Keep serum samples at 2°C to 8°C while handling. If the serum is not analyzed immediately, it should be stored at or below –20°C. It is important to avoid freeze-thaw cycles. Samples which are hemolyzed, icteric, or lipemic can invalidate some tests.

SEROLOGICAL TECHNIQUE: INDIRECT ELISA

The indirect enzyme-linked immunosorbent assay (ELISA) has been used as an important tool in diagnostic virology. It allows rapid screening and quantification of specific viral antibodies in a large number of samples. However, it is important to remember that VACV, the prototype of the genus OPV, exhibits serological cross-reactivity with other OPV species. The assay is useful to screen populations for specific anti-OPV IgG and to confirm the circulation of the virus in a population (Silva-Fernandes et al., 2009; Mota et al., 2010).

Materials

- Purified VACV (see Support Protocol 1, *UNIT 14A.3*, or Earl et al., 2001)
- Coating buffer (see recipe)
- PBST: 0.05% (v/v) Tween 20 in PBS (see recipe)
- Blocking buffer: 5% (w/v) dry-fat milk in PBST
- Test serum or plasma samples (see Basic Protocol 1)
- Positive and negative sera, for controls
- Serum diluent: 0.5% (w/v) dry-fat milk in PBST
- Secondary antibody: rabbit anti-bovine IgG or rabbit anti-human IgG antibody conjugated to horseradish peroxidase (e.g., Sigma Aldrich)
- 3,3',5,5'-tetramethylbenzidine (TMB) Substrate Reagent Set (e.g., BD Biosciences)
- 1 M sulfuric acid

- Bath sonicator (e.g., Unique Ultrasonic Cleanser, USC-2850A)
- Reagent reservoir or petri dish
- UV light (15 Watts)
- 96-well ELISA plate
- ELISA washer

37°C incubator
ELISA microplate reader

Prepare VACV

1. Sonicate purified VACV for 30 sec at 25 kHz, and then cool on ice 30 sec. Repeat two additional times.

CAUTION: Be sure to wear hearing protectors and safety goggles when operating the sonicator.

2. Dilute VACV to a concentration of 10^6 plaque forming unit/ml (PFU/ml) in coating buffer.
3. Place the solution in a reagent reservoir (i.e., petri dish).
4. Place the diluted VACV under a UV light for 20 min to inactivate.

Use a minimum distance of 15 cm from UV light.

It is recommended to check virus inactivation status (as described in Support Protocol 2) before proceeding to the ELISA.

Prepare plate

5. Coat ELISA plates with 100 μ l inactivated diluted VACV, and incubate at 4°C overnight.
6. Wash the plate three times with 200 μ l PBST using the ELISA washer.
7. Add 200 μ l blocking buffer to each well, and incubate at 37°C for 2 hr.
8. Wash the plate three times with 200 μ l PBST using the ELISA washer.
9. Dilute the test serum samples 1:100 in serum diluent in microcentrifuge tubes. Also dilute the positive and negative controls 1:100 in serum diluent in microcentrifuge tubes.
Positive and negative controls are determined by other serological techniques such as the plaque reduction neutralization test.
10. Add 100 μ l diluted test serum to duplicate wells, and include wells without serum and with positive and negative controls.
11. Incubate at 37°C for 1 hr.
12. Wash the plate three times with 200 μ l PBST using the ELISA washer.
13. Add 100 μ l secondary antibody diluted 1:10,000 in serum diluent.
14. Incubate at 37°C for 1 hr.
15. Wash the plate five times with 200 μ l PBST using the ELISA washer.

Develop and analyze plate

16. After the last wash cycle, to develop the plates add 50 μ l TMB solution and incubate for 10 min at room temperature in the dark.
17. Stop the reaction by adding 50 μ l of 1 M sulfuric acid.
18. Immediately measure optical density (OD) values at 450 nm.
19. Analyze ELISA results and determine the cut-off.

Cut-off is equal to the mean OD of the negative samples plus three standard deviations.

Interpretation of results: All values above 10% of the cut-off point may be considered potentially positive.

**SEROLOGICAL TECHNIQUE: PLAQUE REDUCTION NEUTRALIZATION
TEST**

The plaque reduction neutralization test (PRNT) is used to detect and quantify the titer of neutralizing antibodies for a specific virus. The serum sample or antibody to be tested is diluted and mixed with a specific viral suspension. The mixed solution is incubated to allow the antigen-antibody reaction to proceed and then inoculated on a confluent monolayer of host cells. The concentration of plaque forming units (PFU) can be estimated by the number of plaques (cytopathic effect [CPE] on infected cells) formed after a few days. The test serum samples, which reduce the number of plaques by 50% compared to the serum-free virus (virus control), gives the measure of antibody concentration. Currently, PRNT is considered to be the “gold standard” for detecting and measuring antibodies that can neutralize viruses. The test can be used to confirm positivity in ELISA (Basic Protocol 2), although nonconcordant results may occur between ELISA and PRNT as the ELISA has a higher sensitivity in detecting all antibodies classes, while PRNT detects antibodies with neutralizing activity. Hence, it is possible that some samples contain low levels of antibodies with neutralizing activity which are undetectable in PRNT and only detectable by ELISA.

Materials

Trypsin/EDTA solution (see recipe)
BSC-40 cells (ATCC #CRL-2761)
Minimum essential medium (MEM; e.g., Gibco, cat. no. 11700-077) with and without 5% (v/v) fetal bovine serum (FBS)
Test serum samples (see Basic Protocol 1)
Purified VACV (see Support Protocol 1, *UNIT 14A.3*, or Earl et al., 2001)
10% formalin in PBS (see recipe)
1% (w/v) crystal violet (see recipe)

37°C, 5% humidified incubator
Hemocytometer
6-well tissue culture plates
1.5-ml microcentrifuge tubes
56°C water bath
Sonicator
Aspirator

Prepare cells

1. Trypsinize confluent BSC-40 cells by adding trypsin/EDTA solution to the culture for 5 min at 37°C in a 5% humidified incubator. Then, mix in MEM with 5% FBS.
2. Count cells using a hemocytometer.

To count the cells, a dilution is prepared. Typically, the starting concentration range for a cell count is between 250,000 cells/ml and 2,500,000 cells/ml. The hemocytometer should be loaded with 10 μ l of the cell dilution using a pipettor (see APPENDIX 4A).

3. Plate 5×10^5 cells/well in a 6-well tissue culture plate (2 ml final volume per well). Incubate until the monolayer is confluent.

Reaching confluence should take <24 hr.

The assay should be performed in triplicate.

Prepare diluted serum samples

4. Aliquot 25 μ l of the serum samples into a sterile 1.5-ml microcentrifuge tube.
5. Heat the serum samples at 56°C for 30 min in a water bath to denature complement proteins.

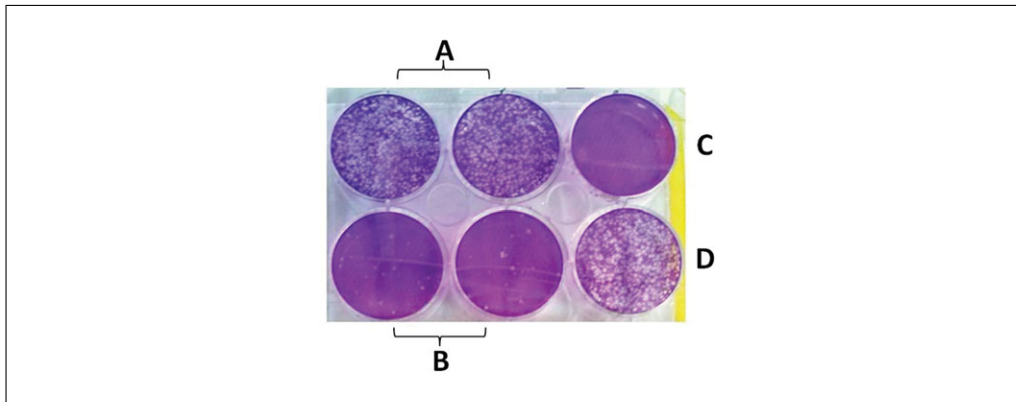


Figure 14A.5.2 Plaque reduction neutralization test (PRNT) in a (A) seronegative sample, (B) seropositive sample, (C) cell control, and (D) virus control. Note that the seronegative sample is similar to the virus control in number of PFUs (~225 PFUs), while the seropositive sample has around 20 PFUs, which means a reduction of 91.1%.

- Dilute serum samples 1:20 in MEM without FBS to a final volume of 0.5 ml.

Prepare diluted virus

- Sonicate the purified virus for 30 sec, and then place on ice for 30 sec. Repeat two additional times.

CAUTION: Be sure to wear hearing protectors and safety goggles when operating the sonicator.

VACV is usually at a titer of 2×10^9 PFU/ml, but may be significantly lower depending on the cells in which it was produced.

- Dilute the stock virus to between 100 and 300 PFU/ml in MEM.

Neutralize

- Mix 0.5 ml of the diluted test serum with 0.5 ml of the diluted virus into a 1.5-ml sterile microcentrifuge tube, and incubate at 37°C for 16 hr.

Perform assay

- Remove medium from BSC-40 cell monolayers from step 3, and infect cells in duplicate wells with 0.4 ml of the mixed solution (diluted virus + diluted serum) from step 9. Place the cells in a CO₂ incubator at 37°C for 1 hr, rocking the dish at 15-min intervals to spread virus uniformly.

Remember to reserve one well in the 6-well plate for a cell control (without virus) and one well for a virus control (a seronegative sample with virus solution).

- Cover cells in each well with 2 ml MEM with 2% of FBS, and place in a CO₂ incubator at 37°C for 2 days.
- Remove medium and add 0.5 ml of 10% formalin to each well. Incubate for 30 min at room temperature.
- Remove the 10% formalin, and add 0.5 ml of 1% crystal violet to each well. Incubate 15 min at room temperature.
- Aspirate crystal violet, wash the plates with water, and allow wells to dry.
- Count the number of plaques in the virus control well and compare with the number of plaques in test samples.

The serum samples are considered positive when the average number of plaques corresponds to a reduction of 50% in the plaque count (Fig. 14A.5.2).

Titrate positive samples

16. Prepare diluted serum samples as described in steps 4 to 6.
17. Dilute serum samples using two-fold serial dilutions from 1:20 to 1:5120.
18. Prepare diluted virus solution as described in steps 7 and 8.
19. Perform the assay as described in steps 10 to 15.
20. Determine the last positive dilution, as in step 15, in which 50% PFU reduction is observed using the number of plaques counted in virus control well as a reference.
21. Calculate the value of neutralizing units (NU) per milliliter (NU/ml).

This value is obtained by dividing 1 ml by the volume of virus/serum solution inoculated in the 6-well plate (0.4 ml) and multiplying it by the inverse of the last positive serum dilution value.

SUPPORT PROTOCOL 1

VACV REPLICATION

VACV can be replicated in Vero cells cultured in MEM. After reaching confluence, the Vero cells should be infected and incubated at 37°C with 5% CO₂ until the formation of lysis plaques due to the development of CPE. To obtain efficient VACV replication, a multiplicity of infection (MOI) of 0.01 is recommended. After the development of plaques, infected Vero cells should be scraped using a cell scraper and submitted to three cycles of freezing in liquid nitrogen or at -80°C and thawing in a 37°C water bath to release viruses from cells.

Materials

Vero cells (ATCC #CCL-81)
MEM (e.g., Gibco, cat. no. 11700-077) with and without 1% (v/v) and 5% (v/v)
FBS
PBS (see recipe)
Trypsin/EDTA solution (see recipe)
Viral samples to be replicated (see Support Protocol 2)

Tissue culture flasks
37°C, 5% humidified incubator
Aspirator
Inverted microscope
Hemocytometer
Cell scraper
Liquid nitrogen
37°C water bath
Centrifuge

Prepare cells

1. Grow Vero cells to a confluent monolayer in MEM in tissue culture flasks.
2. Remove the MEM from Vero cell monolayer, and wash the cells twice with PBS.
3. Add trypsin/EDTA solution to the Vero cell monolayer (~1.5 ml for a 150-cm² flask), and incubate the cells at 37°C for ~2 min.
4. Aspirate the trypsin and gently knock flask to detach cells. Verify that all of the cells have detached using an inverted microscope.
5. Add 2 ml MEM with 5% FBS, and pipet up and down ten times to disrupt cell clumps.

6. Count cells using a hemocytometer.

To count the cells, a dilution is prepared. Typically, the concentration range for a cell count is between 250,000 cells/ml and 2,500,000 cells/ml. The hemocytometer should be loaded with 10 μ l of the cell dilution using a pipettor.

7. Add 8×10^6 Vero cells in MEM with 5% FBS to a 150-cm² cell culture flask.

8. Incubate the flasks at 37°C with 5% CO₂ for ~24 hr.

9. Before the infection, count the cells to calculate the MOI. For counting, prepare an extra flask at the same density.

MOI is the multiplicity of infection, calculated as the infectious particles per cell.

Infect Vero cells

10. Dilute the virus to be replicated in MEM without FBS at an MOI of 0.01.

11. Inoculate 2 ml of the diluted virus in a 150-cm² culture flask containing the Vero cell monolayer.

12. Incubate cells at 37°C with 5% CO₂ for 1 hr. Rock the flask manually at 10 min intervals.

13. Bring up to a final volume of 25 ml using MEM with 1% FBS.

14. Incubate the cells at 37°C with 5% CO₂ for ~48 hr.

Check cells every day under the inverted microscope. Typically at an MOI of 0.01, 48 hr after infection ~90% of the cells present CPE. If necessary the virus can be collected 72 hr after infection.

15. Remove the supernatant when ~90% of the cells present CPE, and scrape the cell monolayer using a cell scraper.

16. Prepare virus stocks (for future viral replication). After removing the supernatant of infected cells, add 2 mL MEM to each 150-cm² culture flask and subject the infected cells to three cycles of freezing in liquid nitrogen or at –80°C and thawing in a 37°C water bath to release the virus.

Virus stocks should not be purified.

If the viruses will be submitted for purification (see Support Protocol 1, UNIT 14A.3, or Earl et al., 2001) after scraping, they should not be subjected to freeze-thaw cycles. Instead, collect the infected cells and store at –80°C until purification.

17. Centrifuge the lysed cells 5 min at 600 \times g, 4°C, and freeze supernatant at –80°C.

TITRATION OF VACV BY PLAQUE ASSAY

The VACV titer is determined by plaque assays. The procedure consists of performing serial dilutions of the virus and inoculating it in Vero cells grown on 6-well plates. After incubation, the cells are stained with crystal violet and the titer calculated. This assay is based on a previously described method (Campos and Kroon, 1993) with modifications.

Additional Materials (also see Support Protocol 1)

- Virus to be titrated
- 10% formalin in PBS (see recipe)
- 1% (w/v) crystal violet (see recipe)

- 6-well tissue culture dish
- 37°C, 5% humidified incubator
- Sonicator

**SUPPORT
PROTOCOL 2**

DNA VIRUSES

14A.5.11

Prepare cells

1. Perform steps 1 through 6 of Support Protocol 1.
2. Set up 6×10^5 Vero cells per well in 6-well plates to a final volume of 2 ml using MEM with 5% FBS.
3. Incubate at 37°C with 5% CO₂ for ~24 hr.
4. Check cells using an inverted microscope.

The cells should be 80% to 90% confluent for infection.

Infect cells

5. Sonicate the virus 20 to 30 sec on ice, and prepare ten-fold serial dilutions down to 10^{-10} , in MEM without FBS.

CAUTION: *Be sure to wear hearing protectors and safety goggles when operating the sonicator.*

During the dilution it is important to pipet from the surface of the sample to be diluted (so that excess sample does not cling to the outside of the pipet tip) and to dispense the sample on the tube wall in the next tube. It is necessary to change tips and mix well between dilutions.

6. Remove the medium from the 6-well plates.
7. Add 300 µl of each virus dilution directly to the cell monolayer of a single well in the plate to infect confluent Vero cell monolayers.

Each dilution is usually titrated in duplicate or triplicate.

One well of each 6-well plate should be inoculated only with MEM without FBS to serve as an uninfected control.

8. Incubate at 37°C with 5% CO₂ for 1 hr. Rock the plates manually at 10 min intervals to spread virus uniformly.
9. Cover cells in each well by bringing up to a final volume of 2 ml with MEM with 1% FBS.
10. Incubate samples at 37°C with 5% CO₂ for 48 hr, and observe CPE on an inverted microscope (see Fig. 14A.5.3).

It is recommended to observe the CPE in each well daily.

11. Add 0.5 ml of 10% formalin, and incubate at least 30 min at room temperature for fixation.
12. Remove medium containing formalin, and add 0.5 ml of 1% crystal violet to each well. Incubate at least 15 min at room temperature. Aspirate the crystal violet solution, wash twice with deionized water, and allow wells to dry upside down.
13. Calculate the titer in PFU/ml. Count plaques in wells that contains between 20 and 80 plaques and multiply by the dilution factor (DF) and conversion factor (CF) which equals 1 ml over the volume of the inoculum.

MOLECULAR TECHNIQUE: DNA EXTRACTION FROM CLINICAL SAMPLES AND INFECTED CELLS

DNA extraction from clinical samples can be done using phenol/chloroform/isoamyl alcohol. This protocol is useful for extraction of VACV DNA in clinical samples, including crusts, tissue, vesicular fluid, lesion swabs, whole blood, serum, and plasma. In addition, this protocol can be used to extract DNA from VACV-infected cell cultures.

SUPPORT PROTOCOL 3

Natural Vaccinia Virus Infection: Diagnosis, Isolation, and Characterization

14A.5.12

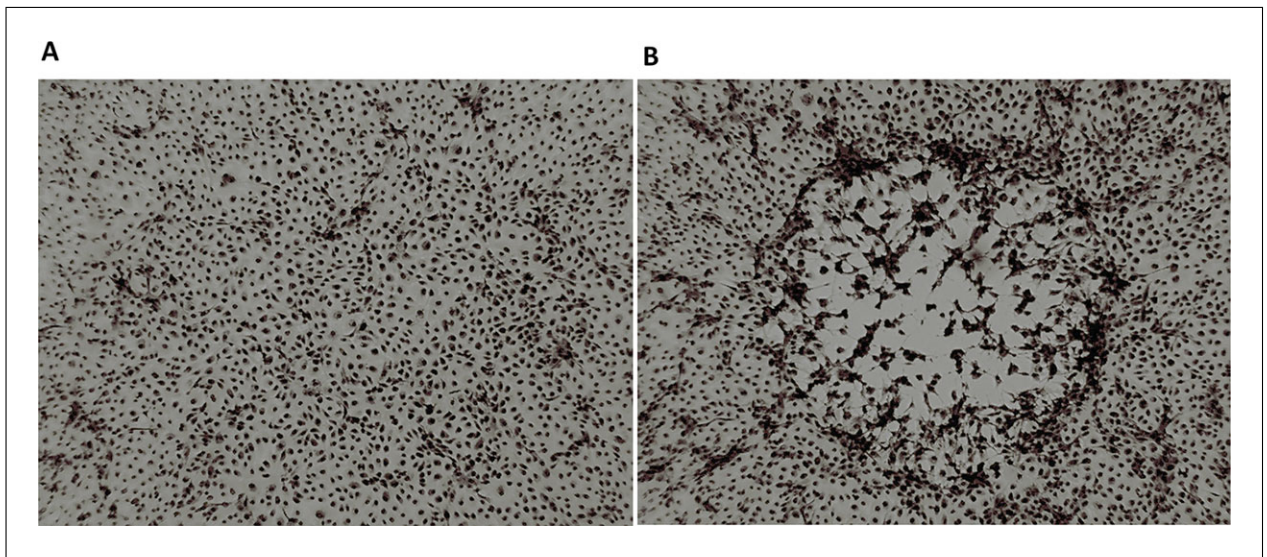


Figure 14A.5.3 Cytopathic effect (CPE) on Vero cells. (A) Uninfected monolayer of Vero cells. (B) VACV replication on Vero cells monolayer showing CPE 48 hr after infection.

Materials

Samples to be extracted (see Basic Protocol 1)
 PBS (see recipe)
 25:24:1 phenol (pH 8.0)/chloroform/isoamyl alcohol
 96% to 100% ethanol, ice cold
 3 M sodium acetate, pH 5.5
 Nuclease-free water

37°C and 75°C incubator
 1.5-ml polypropylene microcentrifuge tubes
 Vortex
 Centrifuge with refrigeration capabilities

CAUTION: Perform phenol manipulation in a fume hood. Wear gloves, safety glasses, and a lab coat at all times.

Extract with phenol

1. Incubate the samples to be extracted at 75°C for 1 hr.
2. Prepare 400 μ l of each sample in a 1.5-ml polypropylene microcentrifuge tube. For samples <400 μ l, bring to 400 μ l with PBS.
3. Add an equal volume of phenol/chloroform/isoamyl alcohol solution to the nucleic acid solution.
4. Mix using a vortex for 10 sec.
5. Centrifuge 1 min at top speed ($\sim 16,000 \times g$), room temperature.

The aqueous phase (upper) and organic phase (lower) should be well separated.

6. Incubate 10 min at room temperature

In this step it is possible to visualize the volume changes in the upper aqueous phase.

7. Collect the aqueous phase and put in a new tube.

Precipitate with ethanol

8. Add 2.5 vol ice-cold 96% to 100% ethanol and 0.1 vol of 3 M sodium acetate.

9. Mix gently by inverting tube five times.
10. Centrifuge 5 min at top speed ($\sim 16,000 \times g$), 4°C.
11. Discard the supernatant, and dry the pellet in 37°C incubator until the tube is completely dry.
12. Dissolve the dry pellet in 50 μ l nuclease-free water heated to at least 37°C.

MOLECULAR TECHNIQUE: PCR AMPLIFICATION OF THE C11R GENE

For OPV diagnosis, a highly sensitive, conventional semi-nested PCR technique was developed to amplify a region of the C11R gene (viral growth factor; vgf) directly from dried scabs, vesicular contents, and serum samples. The C11R gene has been used as a marker for sample screening by PCR because it is conserved among OPV members and is duplicated in most OPV genomes. In this protocol, the C11R semi-nested PCR method does not require viral isolation or DNA extraction, and therefore it can be useful for unsophisticated routine clinical diagnostic laboratories as a rapid screening tool for OPV (Abrahão et al., 2010).

Materials

- 10 \times PCR buffer (see recipe)
- 10 mM dNTP mix
- 25 mM MgCl₂
- 1 μ g/ μ l bovine serum albumin (BSA)
- 2 U/ μ l Taq DNA polymerase
- Primers (10 μ M):
 - vgfF: 5'-CGCTGCTATGATAATCAGATCATT-3'
 - vgfR: 5'-GATATGGTTGTGCCATAATTTTAT-3'
 - vgfF2: 5'-ACACGGTGACTGTATCCA-3'
 - vgfR2: 5'-CTAATACAAGCATAATAC-3'
- Nuclease-free water
- Extracted DNA (50 to 100 ng; see Support Protocol 3) *or* processed sample (see Basic Protocol 1)
- Positive (VACV DNA) and negative control samples

- 0.2-ml thin-walled PCR tubes
- Thermal cycler

1. Prepare a master mix by combining the following components:

- 2.0 μ l of 10 \times PCR buffer
- 0.4 μ l of 10 mM dNTP mix
- 1.6 μ l of 25 mM MgCl₂
- 0.5 μ l of 1 μ g/ μ l BSA
- 0.3 μ l of 2 U/ μ l Taq DNA polymerase
- 0.2 μ l of 10 μ M vgfF primer
- 0.2 μ l of 10 μ M vgfR primer
- 12.8 μ l nuclease-free water (to a final volume of 18 μ l)

Volumes given are for one reaction; scale up as required.

VACV primers are generally synthesized commercially. When ready to use, an aliquot should be thawed and diluted to the appropriate working concentration.

For a nested PCR use nested VACV primers (vgfF2 and vgfR2).

2. Distribute 18 μ l/tube of the master mix into PCR tubes.

3. Add 2 μ l DNA (50 to 100 ng) solution or processed sample to each tube.

Also prepare positive and negative control samples.

4. Cap the tubes, mix gently, and place on ice.
5. For VGF primer mix, carry out PCR as follows:

Initial step	9 min	94°C	(initial denaturation)
30 cycles	1 min	94°C	(denaturation)
	1 min	45°C	(annealing)
	1 min	72°C	(extension)
Final extension	10 min	72°C	(final extension)
Final step	Indefinitely	4°C	(hold)

For a nested PCR, the same chemical and thermal conditions must be used but with nested VACV (vgfF2 and vgfR2) primers.

6. Remove 10- μ l aliquots for 8% polyacrylamide gel electrophoresis (PAGE; Support Protocol 5).

After PCR, fragments of 381 bp in the positive control and positive samples are expected, but not in the negative control. After semi-nested PCR, a fragment of 170 bp is expected in the positive reactions.

MOLECULAR TECHNIQUE: AGAROSE GEL ELECTROPHORESIS

The final step in PCR testing is to separate the PCR products according to their size by electrophoresis using either agarose or polyacrylamide gel electrophoresis (PAGE; Support Protocol 5). The choice depends on the quantity of DNA product and the fragment size. Agarose gel electrophoresis is an effective way of fractionating DNA fragments of sizes ranging from 100 bp to 25 kbp. SYBR Safe is added to the agarose gel so that, once fractionated, the DNA fragments can be visualized under UV light, and a permanent record can be obtained.

Materials

Agarose (e.g., Sigma)
10 \times TAE buffer (see recipe)
SYBR Safe DNA Gel Stain (e.g., Thermo Fisher Scientific, cat. no. S33102)
DNA Ladder (e.g., Promega)
PCR-amplified DNA samples (see Basic Protocol 4)
6 \times DNA loading buffer (see recipe)

Erlenmeyer flask
Gel casting platform (e.g., BIO-RAD Wide Mini Handcasting Kit, cat. no. 1704497)
Horizontal gel electrophoresis system (e.g., BIO-RAD Wide Mini-Sub Cell GT System, cat. no. 1704405EDU)
DC power source
UV imaging platform (e.g., UVItec Cambridge Essential V4)

Prepare agarose gel

1. Weigh 1.5 g of agarose.

Agarose gels are commonly used in concentrations ranging between 0.7% and 2% depending on the size of DNA bands to be separated. Using the protocols presented in this unit, we detect amplified DNA from 170 to 900 base pairs, and we therefore use 1.5% agarose gels. To make gels at different concentrations, simply adjust the amount of starting agarose appropriately (e.g., 2 g agarose per 100 mL will give you a 2% gel).

SUPPORT PROTOCOL 4

DNA VIRUSES

14A.5.15

2. Put agarose powder into a microwavable flask and add 100 ml of 1× TAE.
Prepare 1× TAE by diluting 10 ml of 10× TAE in 90 ml water.
3. Microwave for 1 to 3 min (until the agarose is completely dissolved). Add water to adjust back to 100 ml to compensate for evaporation.
4. Let agarose solution cool down to 60°C.
This can be done at room temperature, but it may take more than 5 min. Alternatively, the flask can be placed in water for 3 to 5 min.
5. Add SYBR Safe to a final dilution of 1:10,000 (10 µl stock solution per 100 ml gel).
SYBR Safe stain is specifically formulated to be a less hazardous alternative to ethidium bromide and can bind to the DNA allowing it to be visualized by UV excitation.
6. Pour the liquid agarose into a gel tray with a well comb in a gel box.
Pour slowly to avoid bubbles which will disrupt the gel. Any bubbles can be pushed away from the well comb and towards the edges of the gel with a pipet tip.
7. Place newly poured gel at room temperature for 20 to 30 min, until it is completely solidified. Then, carefully remove the well comb.
If you are in a hurry, the gel tray can be placed at 4°C before making the gel so that it is already cold when the gel is poured into it.
8. Mix the DNA samples and ladders with 2 µl loading buffer.
9. Place the solidified gel in the electrophoresis system, and fill the gel electrophoresis apparatus with 1× TAE until the gel is covered.
Prepare 1× TAE by diluting 1 vol of 10× TAE in 9 vol water.

Perform electrophoresis

10. Load a DNA ladder into the first well, and load the DNA samples into the remaining wells using a micropipet equipped with a drawn-out plastic tip.
Do not insert the entire tip into the gel; avoid piercing the gel to avoid sample leak.
11. Connect the electrodes of the power source to the gel box, turn on the power, and begin electrophoresis.
Agarose gels are usually run at 100 volts.
12. Run the gel until the marker dyes have migrated the desired distance.
Usually a 30 min run is sufficient. If necessary, the gel can be run for around 1 hr.
13. Expose gel to a device that has UV light to visualize and image DNA fragments.

SUPPORT PROTOCOL 5

MOLECULAR TECHNIQUE: POLYACRYLAMIDE GEL ELECTROPHORESIS

An alternative to agarose gel electrophoresis is polyacrylamide gel electrophoresis (PAGE). The choice depends on the quantity and the fragment size of DNA product. Indeed, PAGE is more sensible than agarose, because it has very high resolution power for small DNA fragments. Once separated, the PCR products can be visualized by either silver nitrate or SYBR Gold staining, and a permanent record can be obtained.

Materials

- 5× TBE buffer (see recipe)
- Acrylamide solution (see recipe)

TEMED (e.g., Thermo Fisher Scientific, cat. no. 17919)
10% (w/v) ammonium persulfate
PCR-amplified DNA samples (see Basic Protocol 4)
6× DNA loading buffer (see recipe)
DNA ladder (e.g., Promega)
Fixer 1 solution (see recipe)
Fixer 2 solution (see recipe)
1× oxidant solution (see recipe)
0.2 % (w/v) silver nitrate
Developer solution (see recipe)
Dry solution (see recipe)
SYBR Gold Nucleic Acid Gel Stain (10,000× concentration in DMSO; e.g.,
Thermo Fisher Scientific, cat. no. S11494)

Gel casting platform (e.g., BIO-RAD Mini-PROTEAN Tetra Cell Casting Module)
Bulldog clips
Vertical gel electrophoresis apparatus (e.g., BIO-RAD, cat no. 1658040EDU)
Electrophoresis electrode assembly (e.g., BIO-RAD Mini-PROTEAN Tetra
Electrode Assembly)
DC power source
Spacer or plastic wedge, to separate glass plates of casting platform
Cellophane
Blue light transilluminator (e.g., Thermo Fisher Scientific Safe Imager 2.0, cat. no.
G6600EU)

Prepare PAGE

1. Clean the glass plates and spacers of the gel casting platform thoroughly. Rinse the plates with deionized water and ethanol, and set them aside to dry.

The glass plates must be free of grease spots to prevent air bubbles from forming in the gel.

2. Assemble gel casting apparatus by clamping two glass plates in the gel caster.
3. Prepare the gel solution using the following for one gel:

3.6 ml water
1.4 ml of 5× TBE
1.86 ml acrylamide solution
0.1 ml of 10% ammonium persulfate
7 μl TEMED

Work quickly after addition of TEMED to complete the gel before the acrylamide polymerizes. The final concentration of the gel is 8.0%.

Ammonium persulfate is used as a catalyst for the co-polymerization of acrylamide and bisacrylamide gels. The polymerization reaction is driven by free radicals that are generated by an oxidation-reduction reaction in which a diamine (e.g., TEMED) is used as the adjunct catalyst.

4. Immediately insert the appropriate comb into the gel.

Be careful not to allow air bubbles to become trapped under the teeth. The tops of the teeth should be slightly higher than the top of the glass. Clamp the comb in place with bulldog or binder clips. If necessary, use the remaining acrylamide gel solution to fill the gel mold completely. Make sure that no acrylamide solution is leaking from the gel mold.

5. Allow the acrylamide to polymerize for 10 to 30 min at room temperature.

6. When ready to proceed with electrophoresis, remove gel plates from the gel caster, carefully remove the combs, and attach the gel plates into a gel box. Add 1 × TBE buffer into the gel box and between the gel plates.

Polyacrylamide gels are poured and run in 1 × TBE at low voltage (1 to 8 V/cm) to prevent denaturation of small fragments of DNA by heating. Other electrophoresis buffers such as 1 × TAE can be used, but they are not as good as TBE. The gel must be run more slowly in 1 × TAE, which does not provide as much buffering capacity as TBE.

To ensure adequate buffering power during vertical electrophoresis, TBE buffer is used for PAGE at a working strength of 1 ×. Lower dilutions of the buffer or the use of TAE buffer may cause gels to overheat and result in band smearing throughout the gel.

7. Mix the DNA samples with 1 μl loading buffer.

Run PAGE

8. Load the DNA ladder and the DNA samples into the wells using a micropipet equipped with a drawn-out plastic tip.

Do not attempt to expel all the sample from the loading device, as this almost always produces air bubbles that blow the sample out of the well. However, it is important not to take too long to complete loading the gel; otherwise, the samples will diffuse from the wells.

9. Connect the electrodes to a power source, turn on the power, and begin the electrophoresis.

Nondenaturing polyacrylamide gels are usually run at 100 volts.

10. After the DNA has sufficiently separated, turn off the power, disconnect the leads, and discard the electrophoresis buffer from the reservoirs.

11. Remove the glass plates from the assembly, and place them on the benchtop. Use a spacer or plastic wedge to lift a corner of the upper glass plate. Check that the gel remains attached to the lower plate. Pull the upper plate smoothly away, and remove the spacers.

12. Proceed to step 13a or 13b to stain gels with silver nitrate or SYBR Gold, respectively.

Stain polyacrylamide gel

Silver nitrate staining

- 13a. Add 100 ml fixer 1 solution and incubate 1 hr or overnight at room temperature, with rocking.
- 14a. Discard fixer 1 solution and incubate in 100 ml fixer 2 solution for 30 min, with rocking.
- 15a. Discard fixer 2 solution, and incubate in 100 ml of 1 × oxidant solution, with rocking.
- 16a. Wash gel with water for 5 min twice. If necessary wash a third time.
- 17a. Discard water and, to stain gel, incubate in 100 ml of 0.2% silver nitrate solution for 20 min, with rocking.
- 18a. Discard silver nitrate in an appropriate waste container, and wash gel with water to remove silver nitrate excess.
- 19a. Discard wash water and add 50 ml developer solution. Mix well and then discard developer solution.

- 20a. Add 150 ml developer solution and keep rocking until the bands are visualized.
- 21a. To stop staining, incubate in 100 ml fix 1 solution and fix 2 solution prepared at a 1:1 ratio for 10 min.
- 22a. Discard stop solution, and add dry solution for 10 min.
- 23a. Cover the gel with cellophane and allow the gel to dry completely.

SYBR Gold staining

SYBR Gold staining is the most sensitive fluorescent stain for detection of nucleic acids. It is 25 to 100 times more sensitive than ethidium bromide and much more sensitive than silver staining for the detection of double-stranded DNA in native polyacrylamide gels. It is capable of detecting as little as 25 pg of DNA.

- 13b. Add 100 ml of 1× oxidant solution, with rocking.
- 14b. Wash gel with water for 5 min twice. Repeat if necessary.
- 15b. Discard water and, to stain gel, incubate in 100 ml SYBR Gold for 30 min, with rocking.

SYBR Gold Nucleic Acid Gel Stain is at 10,000× concentration. To use for gel staining, it is necessary dilute it to 1× using deionized/Milli-Q water.

- 16b. Expose gel to a blue light transilluminator to visualize the DNA fragments.

MOLECULAR TECHNIQUE: qPCR OF THE C11R GENE

Alternate Protocol 1 describes an alternative to PCR for C11R that is more sensitive, faster, and able to quantify the viral DNA.

Materials

Power SYBR Green PCR Master Mix (e.g., Thermo Fisher Scientific)

Primers (10 μM):

VGF forward: 5'-CGCTACAACAGATATTCCAGCTATCAG-3'

VGF reverse: 5'-AGCGTGGATACAGTCACCGTGTA-3'

Nuclease-free water

Extracted DNA (10 to 50 ng; see Support Protocol 3) *or* processed sample (see Basic Protocol 1)

Real-time PCR plate *or* 0.2-ml PCR tubes

Centrifuge

Real-time PCR system and analysis software

1. Prepare PCR master mix by combining the following:

5.0 μl Power SYBR Green PCR Master Mix

0.8 μl VGF forward primer

0.8 μl VGF reverse primer

1.4 μl nuclease-free water

Volumes given are for one reaction. Scale up as required.

2. Add 8 μl of the master mix to each well of a real-time PCR plate or real-time PCR tube.
3. Add 2 μl sample to each well or tube.

Samples should be run in duplicate or triplicate.

ALTERNATE PROTOCOL 1

DNA VIRUSES

14A.5.19

Prepare appropriate controls, including a VACV positive control and negative control that consists of mix with nuclease-free water

4. Cap tubes or seal the PCR plate and label (according to instrument requirements).
5. Briefly centrifuge (quick spin) the plates or tubes at room temperature.
6. Program the standard real-time PCR system as follows:

1 cycle	10 min	95°C
40 cycles	10 sec	95°C
	40 sec	58°C
Melting curve analysis	15 sec	95°C
	15 sec	58°C
	Every 2 sec	Increase 1°C , from 60°C to 95°C
	15 sec	95°C
7. After qPCR is finished, remove the tubes or plate from the machine, and analyze the results with real-time PCR system software.
8. Check the negative control wells for any amplification.
9. Check the wells for samples that amplify until threshold cycle <38 and have a melting curve the same value as the positive control.

There should be no amplification in the negative control.

Those that amplify until threshold cycle (tc) <38 and have a melting curve with the same value as the positive control ($\pm 1^\circ\text{C}$) are positive samples.

Samples that amplify in only one replica can be considered suspect and should be repeated or subjected to another target gene.

BASIC PROTOCOL 5

VIRAL ISOLATION TECHNIQUE: ISOLATION OF VACV IN VERO CELL LINES

VACV can be replicated in a large variety of cell lines; however, Vero cells are the most suitable cell lines for VACV isolation. VACV should be isolated in Vero cells cultured in minimum essential medium (MEM). During outbreaks, cows and milkers are affected and may present with lesions mainly in teats and hands, respectively. The lesions present with high viral load compared to other clinical specimens (e.g., serum). Thus scabs and swabs from lesions are better specimens for VACV isolation (Basic Protocol 1).

This protocol describes VACV isolation in Vero cell culture. However, this protocol can be applied to isolation in other cell lines, such as BSC-40 cells. After reaching confluence, the cells should be infected, and then after an adsorption step they are incubated at 37°C with 5% CO₂ for 48 hr or until appearance of CPE. If in the first infection (first passage) the cell monolayer does not present with CPE, a second or third round of infection should be done. For the second and third passages, cells and supernatants should be collected and submitted to three cycles of freezing and thawing to release viruses from cells.

Materials

Vero cells
MEM (e.g., Gibco, cat. no. 11700-077) with 5% and 2% (v/v) FBS
Processed clinical samples (see Basic Protocol 1)

25-cm² tissue culture flasks
37°C, 5% humidified incubator
Inverted microscope
Liquid nitrogen

**Natural Vaccinia
Virus Infection:
Diagnosis,
Isolation, and
Characterization**

14A.5.20

37°C water bath
Refrigerated centrifuge

1. Add 10⁶ Vero cells in 25-cm² cell culture flasks using MEM with 5% FBS.

For VACV isolation, one 25-cm² cell culture flask for each sample plus one flask for the cell control is generally sufficient.

2. Incubate at 37°C for 24 hr until the monolayer reaches 90% to 95% confluence.
3. Inoculate with 400 µl processed samples.
4. For adsorption, incubate the inoculated cells for 1 hr, rocking it gently every 10 min.
5. Add 4.6 mL MEM with 2% FBS, and incubate at 37°C and 5% CO₂ for ~48 hr.

Check cells every day under the microscope to verify CPE (see Fig. 14A.5.3).

6. If CPE is not observed after 48 hr infection, remove 4.5 ml supernatant and submit the infected cells to three cycles of freezing and thawing to release viruses from cells. Collect the cell lysate and supernatant (~500 µl). Repeat the process until the appearance of CPE or third passage.

To make the process faster, scrape the cells and collect the cells plus supernatant. Then place in a cryovial for freezing in liquid nitrogen and thawing in a 37°C water bath.

If CPE is not observed after three passages, the cells should be collected and virus detected by PCR targeting the vgf gene (Basic Protocol 4). In the case of positive detection, one more passage can be done.

7. When CPE is observed, scrape the cells and submit the supernatant and cells to three cycles of freezing in liquid nitrogen or at -80°C and thawing in a 37°C water bath to release viruses from cells. Collect the cell lysate and supernatant.

After the cells are disrupted through the freeze-thaw cycles, the viruses will be released into the supernatant.

8. Centrifuge 3 min at 2000 × g, 4°C, to remove the cellular debris. Then aliquot and store the isolated virus.
9. Freeze tubes in a -80°C freezer for storage until purification (see Basic Protocol 8, UNIT 14A.3, or Earl et al., 2001).

VIRAL ISOLATION TECHNIQUE: ISOLATION OF VACV IN PRIMARY CHICKEN EMBRYO FIBROBLAST CELLS

**BASIC
PROTOCOL 6**

Cultured cells are the host system most often used for virus replication. Primary cell culture stands out because it is extremely efficient. A primary cell culture is defined as a culture of cells obtained from the original tissue that have been cultivated in vitro for the first time and that have not been subcultured. They are obtained from the original tissue and have higher identity with the original tissue as they have been grown in vitro for the first time. Thus, this host system presents a higher sensitivity for virus isolation compared with other cell systems.

A primary culture widely used for VACV isolation is chicken embryonic fibroblasts (CEF). CEF cells are produced by maceration of embryonic tissue and subsequent enzymatic cell disruption (using proteases and/or collagenases), generating individualized cells which are grown in suitable containers with appropriate culture medium.

This protocol describes VACV isolation in CEF cells. After the obtained CEFs reach a confluence of 90% to 100%, the cells should be infected, and, after an adsorption

DNA VIRUSES

14A.5.21

step, incubated at 37°C with 5% CO₂ for 72 hr or until appearance of CPE. If in the first infection (first passage) the cell monolayer presents CPE, a second or third round of infection should be done. For the second and third passages, cells and supernatants should be collected and submitted to three cycles of freezing and thawing to release viruses from cells.

Materials

CEF cells

MEM (e.g., Gibco, cat. no. 11700-077) containing 10% FBS

Additional reagents and equipment for isolating VACV in cells (Basic Protocol 5)

1. Add 10⁶ CEF in 25-cm² cell culture flasks using MEM with 10% FBS.

For VACV isolation, one 25-cm² cell culture flask for each sample plus one flask for the cell control is generally sufficient.

2. Incubate at 37°C for 24 hr until the monolayer reaches 90% to 100% of confluence.
3. Perform steps 3 through 9 of Basic Protocol 5.

BASIC PROTOCOL 7

VIRAL ISOLATION TECHNIQUE: ISOLATION OF VACV IN CHICKEN CHORIOALLANTOIC MEMBRANE

The use of eggs for virus propagation was first demonstrated by Woodruff, Goodpasture, and Burnet in 1930. Much of the early progress in the field of virology was due to the use of this system since many viruses known at that time were able to grow in embryonic eggs. With the advent of cell culture in 1950, the use of embryonated eggs decreased and have been almost wholly replaced by cell culture techniques. However, they are still the most convenient method for growing high titer stocks of some viruses and thus continue to be used both in research laboratories and for vaccine production. Because of this, the use of embryonated eggs is, in some cases, the most sensitive method for virus isolation.

This protocol describes the use of chicken embryonated eggs for isolation of VACV from clinical samples. Embryonated eggs of 9 or 10 days old are used to inoculate a processed clinical specimen into the chorioallantoic membrane. After 72 hr the eggs are opened and the membrane collected. The virus isolation is verified by “pock” formation in the membrane (Fig. 14A.5.4).

Materials

9- or 10-day-old embryonated eggs

70% ethanol

Processed clinical sample (see Basic Protocol 1)

PBS (see recipe) containing penicillin (200 U/ml), amphotericin B (1.5 µg/ml), and gentamicin (40 µg/ml)

Cotton

Egg box

Egg piercer

Small catheter

Vacuum/pressure bulb (e.g., Thomas Scientific, cat. no. HS20631B)

1-ml syringe with 25-G, 16-mm needle

Tape *or* melted wax

1.5-ml microcentrifuge tubes

1. Swab the eggs to be inoculated with 70% ethanol using cotton. Allow the alcohol to evaporate.

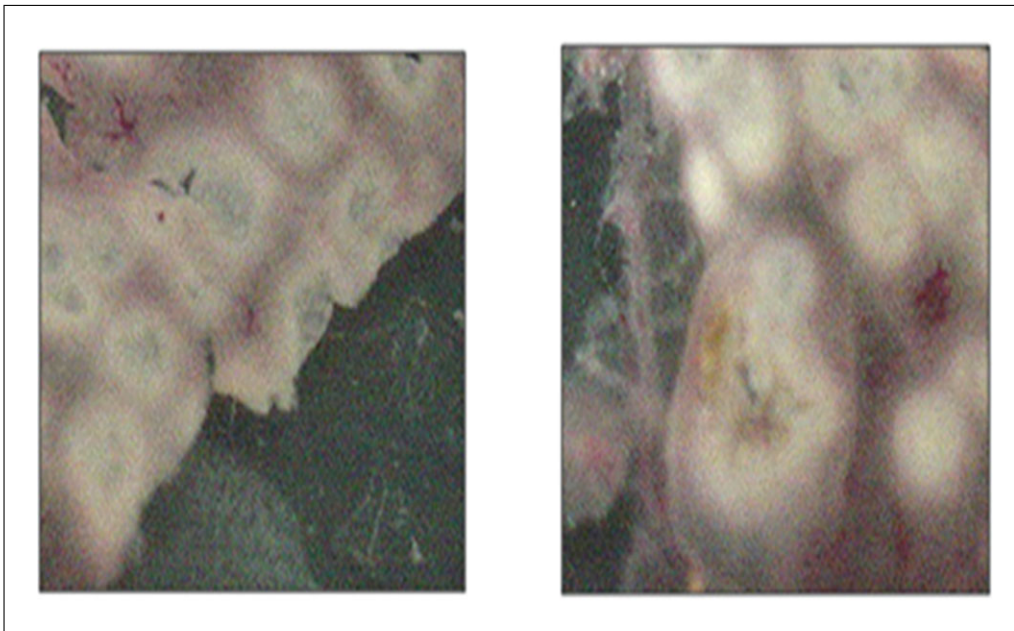


Figure 14A.5.4 Isolation of VACV in chorioallantoic membrane forming “pocks” (right panel). VACV were inoculated in 9–day-old embryonated eggs (left panel), and after 72 hr of incubation the membrane was removed and observed.

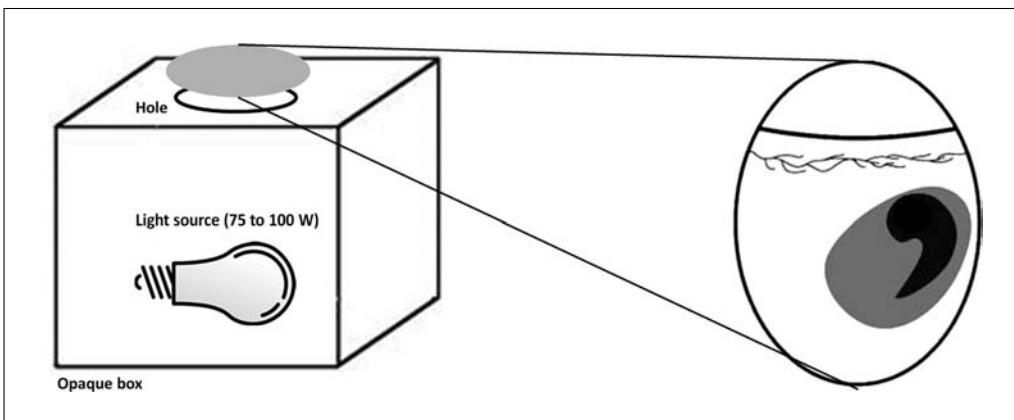


Figure 14A.5.5 Equipment used to make the egg box in order to visualize the embryo inside the egg.

2. Visualize the embryonated eggs using the egg box, and mark the embryo, air sac, and inoculation site with a pencil.

The egg box is a piece of equipment used to visualize the embryo inside the egg. It is an opaque box with a hole to put the egg in and a strong light source (75 to 100 W) inside (Fig. 14A.5.5).

3. Pierce a hole in the egg shell at the marked inoculation site (Fig. 14A.5.6).
4. Create negative pressure in the air sac using a small catheter and vacuum/pressure bulb to shift it (Fig. 14A.5.6B).

The chorioallantoic membrane will peel off the egg shell at the inoculation point following displacement of the air sac, which allows inoculation of the clinical sample.

5. Keeping the needle and syringe vertical, place the needle through the hole in the egg shell, and inject 0.1 ml processed clinical sample into the egg (Fig. 14A.5.6C).

The sample should be injected in the air sac between the egg shell and chorioallantoic membrane.

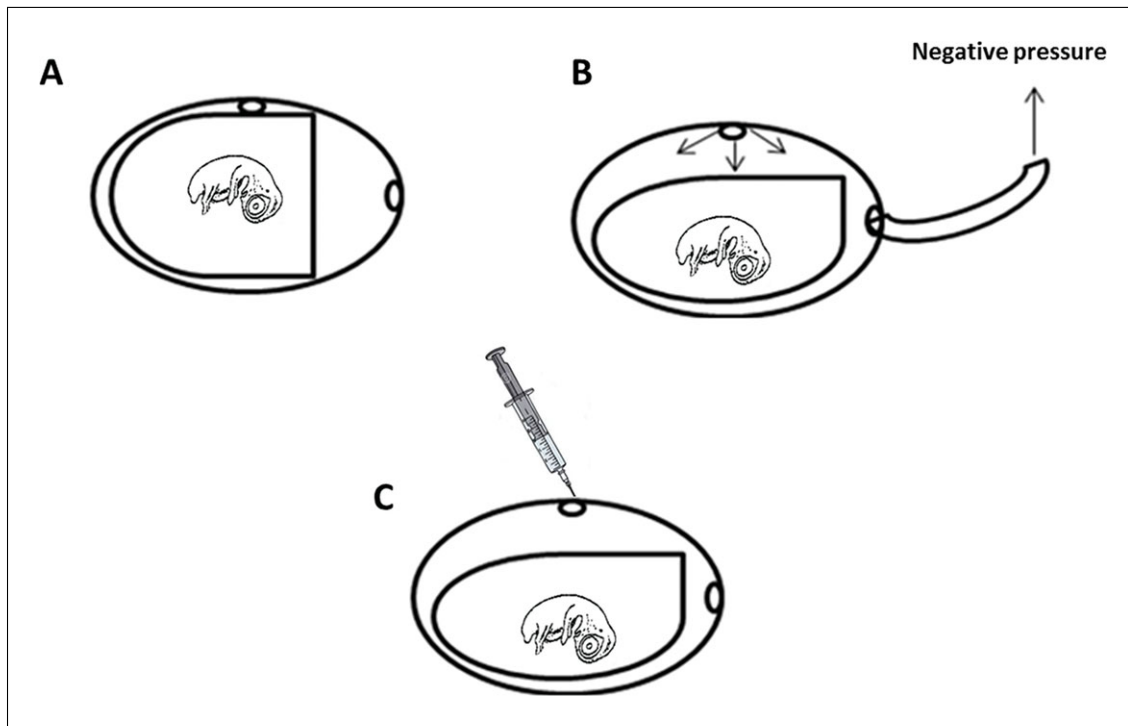


Figure 14A.5.6 Poxvirus inoculation in chorioallantoic membrane. **(A)** Holes are made in the air sac and at the inoculation point. **(B)** Displacement of the air sac. **(C)** Inoculation of clinical sample in chorioallantoic membrane.

6. Seal the hole in the shell with tape or melted wax.
7. Incubate at 37°C for 72 hr.

Look at the eggs every day with the egg box (Fig. 14A.5.5) to check the viability of the embryo. If any embryo is dead, put in cold storage until opening the other eggs. Eggs should have thick veins and should present movement if turned.
8. After 72 hr place the eggs in a 4°C refrigerator.
9. Open the eggs by cutting the shell starting at the inoculation point and removing the shell from air sac.
10. Remove the embryo and embryonic attachments being careful so that the chorioallantoic membrane does not also come out.
11. Remove the chorioallantoic membrane, and wash it with PBS. Cut out the region in which the “pock” appeared (near the inoculation site).
12. Keep the chorioallantoic membrane with “pocks” in 1.5-ml microcentrifuge tubes with PBS (100 μ l) at -70°C .

**BASIC
PROTOCOL 8**

**Natural Vaccinia
Virus Infection:
Diagnosis,
Isolation, and
Characterization**

VIRAL ISOLATION TECHNIQUE: PLAQUE PURIFICATION OF VACV ISOLATES

To obtain purified plaques containing a single VACV particle it is essential to perform plaque purification using BSC-40 cells. Co-circulation and co-infection with different clades of VACV have been described, reinforcing the importance of this procedure. For this protocol, serial dilutions of the isolated VACV (Basic Protocols 5 to 7) are used to infect BSC-40 cells, and after 48 hr the plaques are collected and submitted to rounds of purification.

14A.5.24

Materials

BSC-40 cells at confluent monolayer grown in tissue culture flasks
MEM (e.g., Gibco, cat. no. 11700-077) with and without 5% (v/v) FBS
Agarose (e.g., Promega)
MEM (2× concentrated; e.g., Gibco, cat. no. 11700-077) with 2% (v/v) FBS
Isolated VACV to be plaque purified (see Basic Protocols 5 to 7)
PBS (see recipe)

6-well tissue culture plate
37°C, 5% humidified incubator
Inverted microscope
37°C and 56°C water bath

Set up the plates

1. Set up 6×10^5 BSC-40 cells in 6-well plates at final volume of 2 mL MEM with 5% FBS per well.
2. Incubate at 37°C with 5% CO₂ for ~24 hr.
3. Visualize cells using an inverted microscope.

The cells should be 80% to 90% confluent at moment of infection.

Prepare medium containing agarose

4. Make a 2% agarose solution with water as diluent. Keep agarose in a 56°C water bath until use, to prevent solidification. Heat 2× MEM in a 37°C water bath prior to use.
5. Combine equal volumes (1:1) of the agarose solution and 2× MEM.

Keep solution in a 37°C water bath until use, to prevent solidification

Perform plaque purification assay

6. Dilute the isolated virus using ten-fold serial dilutions from 10^{-1} through 10^{-5} using 1× MEM without FBS.
7. Remove the culture medium from the 6-well plates.
8. Wash twice with PBS and remove any excess solution.
9. Add 300 µl of each virus dilution into the wells.
10. Incubate at 37°C for 1 hr. Rock the plates manually every 10 min.
11. Remove the virus dilution, and add 2 ml of 1:1 agarose/MEM solution to each well.
12. Incubate at 37°C with 5% CO₂ for 48 hr.
13. View with an inverted microscope. Select and delimit with a pen the plaques to be collected.

Select the most separated plaques as possible.

14. Collect the plaques using a P10 or P100 pipet tip.
15. Dilute the collected plaques in MEM with 5% FBS.

This procedure should be repeated at least three times to ensure the purity of the collected viral plaques.

16. Store the purified plaques at –80°C.

VIRAL CHARACTERIZATION

Several molecular methods to detect and subtype viruses of the genus OPV exist. These first generation techniques are based on standard PCRs to amplify conserved or variable DNA sequences. PCR to amplify variable DNA sequences uses primers that are able to detect signature deletions or variable-sized amplified fragments, thus allowing the discrimination of different VACV. C11R has been widely used to diagnose OPV, but it is not used for characterization. For this, A56R, A26L, and C23L genes are good targets because these genes are able to identify and differentiate the different OPVs (Fig. 14A.5.7). Moreover, these genes and others can be used to differentiate VACV isolates from Brazil (Br-VACV). Br-VACVs are divided into two main groups based on genetic diversity in plaque assays and virulence in animal models (BALB/c mice): group 1 (non-virulent in mouse models) and group 2 (virulent in mouse models; Trindade et al., 2006; Ferreira et al., 2008; Kroon et al., 2011; Oliveira et al., 2015). Viral characterization is essential for studying VACV epidemiology and evolution. Molecular findings are used in phylogenetic analysis based on comparison of the new sequence with the sequences of known viruses. The reliability of analysis depends on the length of the sequence obtained and sequenced quality.

Molecular Characterization: qPCR to Amplify the A56R (Hemagglutinin) Gene

Real-time PCR (quantitative PCR; qPCR) approaches combine the detection of target template with quantification by recording the amplification of a PCR product via a corresponding increase in the fluorescent signal associated with product formation during each cycle in the PCR. The A56R (hemagglutinin) gene has been the most widely used gene marker in genetic analyses for VACV differentiation. In 2000, it was demonstrated that VACV Cantagalo (group 1) has an 18-nucleotide deletion in A56R. With the discovery of new VACV isolates in Brazil, A56R proves to be even more interesting because some group 2 isolates do not have this particular 18-nucleotide deletion in A56R.

The following protocol identifies variants of VACV based on a specific 18-nucleotide deletion found in A56R of VACV group 1. The primers (HA-gen F and HA-gen R) were designed to amplify all VACV, and the combination of HA-BVV-nDEL F (hybridization in the deletion) with HA-gen R differentiates the two groups (de Souza Trindade et al., 2008).

Materials

Power SYBR Green PCR Master Mix (e.g., Thermo Fisher Scientific)

Primers (0.2 μ M):

HA-gen F: 5'-CATCATCTGGAATTGTCACTACTAAA-3'

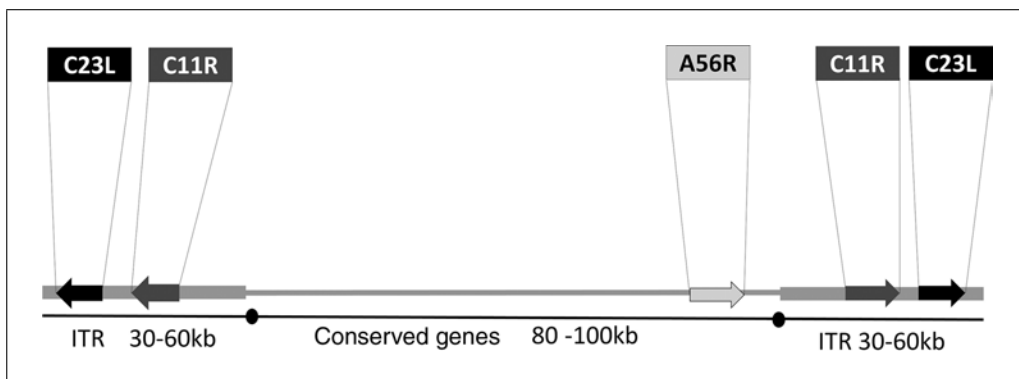


Figure 14A.5.7 Vaccinia virus genome structure. The genome structure of VACV is represented showing the localization of amplified genes.

HA-gen R: 5'-ACGGCCGACAATATAATTAATGC-3'
HA-BVV-nDEL F: 5'-GCGGATCTTTATGATACGTACAATG-3'

Nuclease-free water

Extracted DNA sample (10 to 100 ng; see Support Protocol 3)

Positive control: DNA of VACV group 1 and 2

Real-time PCR plate *or* thin-walled, 0.2-ml PCR strip tubes with real-time grade optical strip cap

Real-time PCR system and analysis software

1. Prepare master mix:

5.0 μ l Power SYBR Green PCR Master Mix
0.2 μ l HA-gen F primer
0.2 μ l HA-gen R primer
3.6 μ l nuclease-free water

Volumes given are for one reaction and should be multiplied by the number of samples to be analyzed.

2. Add 9 μ l master mix to each well of a real-time PCR plate or real-time PCR tube.

3. Add 1 μ l template DNA (10 to 100 ng; see Support Protocol 3, UNIT 14A.3, or Earl et al., 2001) to each well or tube.

It is necessary to use appropriate controls including a negative control of nuclease-free water, a positive control containing DNA of VACV group 1, and another positive control containing DNA of VACV group 2. Samples should be run in duplicate or triplicate. The real-time PCR plate or real-time PCR tubes should be briefly centrifuged (quick spin) before the run.

4. Program the standard real-time PCR system as follows:

1 cycle	10 min	95°C
40 cycles	10 sec	95°C
	40 sec	58°C
Melting curve analysis	15 sec	95°C
	15 sec	58°C
	Every 2 sec	Increase 1°C, from 60°C to 95°C
	15 sec	95°C

5. After qPCR is finished, remove the tubes or plate from the machine and analyze the results using real-time PCR system software.

6. Check the negative control wells for any amplification.

There should be no amplification in the negative controls.

7. Check the wells for samples that amplify until threshold cycle <38 and have a melting curve the same value of the positive control.

Those that amplify until threshold cycle <38 and have a melting curve the same value as the positive control ($\pm 1^\circ\text{C}$) are positive samples.

The reaction is not able to identify the VACV-Br groups using only qPCR peak fluorescence due deletion of 18 nucleotides in A56R. In the generic PCR (using HA-gen F and HA-gen R), the fluorescence peaks within 0.5°C, making it difficult to rely on the melting curve (T_m) as a unique identifier for each PCR product (T_m group 1 = 75.8°C; T_m group 2 = 76.3°C).

Using primers for BVV-nDEL (HA-BVV-nDEL F and HA-gen R), T_m for group 2 = 75.1°C, and group 1 is not amplified.

Molecular Characterization: PCR for the A56R (Hemagglutinin) Gene

In addition to qPCR, the A56R amplified product can be subjected to sequencing to differentiate between isolates of VACV (Ropp et al., 1995).

Materials

10× PCR buffer (see recipe)

10 mM dNTP mix

25 mM MgCl₂

5 U/μl Taq DNA

Primers (10 μM):

EACP1: 5'-ATGACACGATTGCCAATAC-3'

EACP2: 5'-CTAGACTTTGTTTTCTG-3'

Nuclease-free water

Extracted DNA (100 ng; see Support Protocol 3)

Positive control: VACV DNA

Thin-walled, 0.2-ml PCR tubes

Thermal cycler

Additional reagents and equipment for electrophoresis (Support Protocols 4 and 5)

1. Prepare a master mix by combining the following volumes below per reaction:

2 μl of 10× PCR buffer

0.4 μl of 10 mM dNTP mix

1.6 μl of 25 mM MgCl₂

0.3 μl of 5 U/μl Taq DNA polymerase

0.2 μl of 10 μM primer EACP-1

0.2 μl of 10 μM primer EACP-2

13.3 μl nuclease-free water (to a final volume of 18 μl)

2. Distribute 18 μl of the master mix per reaction into PCR tubes.
3. Add 2 μl DNA (100 ng) solution to each tube.

Prepare appropriate positive and negative controls.

4. Cap the tubes, mix gently, and place on ice.
5. For A56R primer mix, program the PCR thermal cycler as follows:

Initial step	9 min	94°C	(initial denaturation)
25 cycles	1 min	94°C	(denaturation)
	2 min	55°C	(annealing)
	3 min	72°C	(extension)
Final extension	10 min	72°C	(final extension)
Final step	Indefinitely	4°C	(hold)

6. Load the tubes and run the program.
7. Remove 10-μl aliquots and use for electrophoresis (Support Protocols 4 and 5).

Fragments of 960 bp in the positive control and positive samples are expected but not in negative control. Keep positive samples stored at -20°C, and sequence as described in Basic Protocol 11.

Molecular Characterization: PCR for the A26L Gene

The A26L (ATI) gene has been used for the molecular characterization of Br-VACV due to the large polymorphisms between different isolates. This reaction was set for the detection of Brazilian examples of group 1 that have the full gene. Group 2 Brazilian samples do not have this gene, with the exception of VACV-SAV (SpAn232 virus) and SH2V (SerroHumano 2). However, these samples show some differences from group 1 genes.

Materials

10× PCR buffer (see recipe)

10 mM dNTP mix

25 mM MgCl₂

5 U/μl Taq DNA polymerase

Primers (10 μM):

ATI-iF/1: 5'-ACCACGTCTACTCTCGGCGA-3'

ATI-iR/2: 5'-TGCATCGAGAGCGGAGGAGGA-3'

ATI-iR/3: 5'-CGATGCCAAGTACATCGACGA-3'

Nuclease-free water

Extracted DNA (100 ng; Support Protocol 3)

Positive control: VACV DNA

Thin-walled, 0.2-ml PCR tubes

Thermal cycler

Additional reagents and equipment for electrophoresis (Support Protocols 4 and 5)

1. Prepare a master mix by combining the following volumes per reaction:

2 μl of 10× PCR buffer

0.4 μl of 10 mM dNTP mix

1.6 μl of 25 mM MgCl₂

0.3 μl of 5 U/μl Taq DNA polymerase

0.2 μl of 10 μM primer ATI-iF/1

0.2 μl of 10 μM primer ATI-iR/2

11.3 μl nuclease-free water (to a final volume of 18 μl)

For the semi-nested step, use internal primers ATI-iF/1 and ATI-iR/3.

2. Distribute 18 μl of the master mix per reaction into PCR tubes.

3. Add 1 μl DNA (100 ng) solution to each tube.

Prepare appropriate positive and negative controls.

4. Cap the tubes, mix gently, and place on ice.

5. For A56R primer mix, program the PCR thermal cycler as follows:

Initial step	9 min	94°C	(initial denaturation)
25 cycles	1 min	94°C	(denaturation)
	2 min	55°C	(annealing)
	3 min	72°C	(extension)
Final extension	10 min	72°C	(final extension)
Final step	Indefinitely	4°C	(hold)

For the semi-nested step, 1 μl of undiluted product from the initial PCR is used as template; the same chemical and thermal conditions are used, but with internal VACV primers (ATI-iF/1 and ATI-iR/3).

Table 14A.5.2 Expected DNA Fragment Size to Identify Group 1 or Group 2 VACV

Reaction	Primers	Group 1 size (bp)	Group 2 size (bp)
Initial PCR	ATI-iF/1: 5'-ACCACGTCTACACTCGGCCGA-3' ATI-iR/2: 5'-TGCATCGAGAGCGGAGGAGGA-3'	787	753
Semi-nested PCR	ATI-iF/1: 5'-ACCACGTCTACACTCGGCCGA-3' ATI-iR/3: 5'-CGATGCCAAGTACATCGACGA-3'	166	145

6. Load the tubes, and run program.
7. Remove 10- μ l aliquots and use for electrophoresis (Support Protocols 4 and 5).

Table 14A.5.2 shows the expected sizes of amplified DNA to detect group 1 or 2 viruses.

ALTERNATE PROTOCOL 3

Molecular Characterization: PCR for the C23L Gene

The C23L (chemokine binding protein) gene is another gene that may elucidate the Br-VACV dichotomy, depending on its variability in other OPV genomes. Analysis of the C23L gene sequence, based on VACV-WR annotation, revealed the presence of a ten-nucleotide deletion, resulting in a frameshift mutation that creates a stop codon. In Br-VACV, only group 1 isolates had the ten-nucleotide deletion in C23L in contrast with C23L of group 2 isolates. Thus, C23L can be used to segregate Br-VACV into group 1 or 2. The forward and reverse primers (C23LF and C23LR) were designed to amplify all VACV, and the combination of C23LRD (hybridization in the deletion) with C23LF differentiates the two groups.

Materials

10 \times PCR buffer (see recipe)
 10 mM dNTP mix
 25 mM MgCl₂
 5 U/ μ l Taq DNA polymerase
 Primers (10 μ M):
 C23LF: 5'-GCGTGTCCCCAGGACAAGGT-3'
 C23LR: 5'-ATGTCGCTGTCTTTCTCTTCTTCGC-3'
 C23LRD: 5'-CTGGATGGGTCTTG-3'

Nuclease-free water
 Extracted DNA (100 ng; see Support Protocol 3)
 Positive control: VACV DNA

Thin-walled, 0.2-ml PCR tubes
 Thermal cycler

Additional reagents and equipment for electrophoresis (Support Protocols 4 and 5)

1. Prepare a master mix by combining the following volumes below per reaction:

2 μ l of 10 \times PCR buffer
 0.4 μ l of 10 mM dNTP mix
 1.6 μ l of 25 mM MgCl₂
 0.3 μ l of 5 U/ μ l Taq DNA polymerase
 0.2 μ l of 10 μ M primer C23LF
 0.2 μ l of 10 μ M primer C23LR
 11.3 μ l nuclease-free water (to a final volume of 18 μ l)

To test for the deletion, use primers C23LF and C23LRD.

2. Distribute 18 μ l of the master mix per reaction into PCR tubes.
3. Add 2 μ l DNA (100 ng) solution to each tube.

Prepare appropriate positive and negative controls.

4. Cap the tubes, mix gently, and place on ice.
5. For C23L primer mix, program the PCR thermal cycler as follows:

Initial step	9 min	94°C	(initial denaturation)
25 cycles	1 min	94°C	(denaturation)
	2 min	55°C	(annealing)
	3 min	72°C	(extension)
Final extension	10 min	72°C	(final extension)
Final step	Indefinitely	4°C	(hold)

6. Load the tubes and run program.
7. Remove 10- μ l aliquots and use for electrophoresis (Support Protocols 4 and 5).

Using the first primer set, fragments of 124 bp are expected in the positive control and positive samples but not in negative control. In the differentiation reaction, fragments of 138 bp are expected in the samples from group 2 (without deletion). Samples from group 1 show no amplification in the latter PCR (with deletion).

Molecular Characterization: Sequencing and Sequence Analysis of PCR-amplified DNA Fragments

PCR products can be directly sequenced without the need for cloning the fragment, but it is crucial to check the PCR product for its band size and quality. To obtain high-quality sequencing data, it is necessary that only one purified PCR fragment is used as template for sequencing reactions. First, it is important to check if you have a single and specific amplified DNA band or if unspecific amplified DNA bands and/or a background smear is present. Second, while PCR uses two primers for DNA amplification, the dideoxy sequencing reaction (Sanger et al., 1977) utilizes only one primer at a time. In that way, all primers as well as unincorporated nucleotides must be removed before the PCR product is sequenced. After sequencing, the raw data must be analyzed in order to get a consensus sequence of good quality. In order to compare the obtained sequences to each other or with other sequences, a dataset containing aligned nucleotide sequences has to be constructed before analysis. Several programs are available for different purposes, and it is recommended to spend some time looking for the programs that best fit your goals.

Materials

- Isolated PCR product (see Basic Protocols 4 or 10 or Alternate Protocols 2 or 3) or PCR product run on agarose gel (see Support Protocol 4)
- ExoSAP-IT PCR Product Cleanup (e.g., Affymetrix)
- MinElute PCR Purification Kit (e.g., Qiagen) containing:
 - Buffer QG
 - Buffer PE
 - Buffer EB
 - Spin column
 - 2-ml collection tube
- 3 M sodium acetate, pH 5.0
- Isopropanol
- Forward and reverse primers

BASIC PROTOCOL 11

DNA VIRUSES

14A.5.31

0.5-ml and 1.5-ml microcentrifuge tubes (DNase-free)

Vortex

Scalpel

Centrifuge

DNA sequencing facility

Computer with Internet access and SeqTrace (or equivalent) software (available at <http://seqtrace.googlecode.com>) and MEGA 6.0 software (available at <http://www.megasoftware.net>)

Additional reagents and equipment for PCR (Basic Protocols 4 and 5 and Alternate Protocols 2 and 3) and agarose gel electrophoresis (Support Protocol 4)

Prepare PCR gene products for sequencing

1. Run PCR reaction (Basic Protocols 4 or 10 or Alternate Protocols 2 or 3) and carry out agarose gel electrophoresis (Support Protocol 4). After staining the gel, if only one specific and strong band (of expected size) is observed then proceed to step 2a (direct cleanup of PCR products); if unspecific bands or a background smear is observed, proceed to step 2b (cleanup of PCR products from agarose gel).

Directly clean up PCR products

Several commercial kits are available for PCR clean up and sequencing, based on standard spin columns or magnetic beads. Here we describe a single-step, enzymatic cleanup of PCR products, based on exonuclease I and shrimp alkaline phosphatase (SAP) activities. Exonuclease I removes unincorporated single-stranded primers and any extra single-stranded DNA produced by the PCR process. SAP destroys any remaining dNTPs.

- 2a. Transfer 5.0 μ l of the aqueous phase of PCR product to a 0.5-ml microcentrifuge tube.
- 3a. Remove ExoSAP-IT reagent from -20°C freezer and keep it on ice. Add 2.0 μ l ExoSAP-IT reagent to the tube containing 5.0 μ l PCR product.

When treating PCR product volumes greater than 5 μ l, increase the amount of ExoSAP-IT reagent proportionally.

- 4a. Vortex the mixture, and incubate 15 min at 37°C .
- 5a. Incubate 15 min at 80°C , to completely inactivate both enzymes.

Treated PCR product is ready for downstream sequencing reactions, or it may be stored at -20°C until required.

- 6a. Proceed to step 19.

Clean up PCR products from agarose gel

Several commercial kits are available. Clean-up using a MinElute Gel Extraction Kit (Qiagen) is presented here.

- 2b. Cut the desired DNA band from the gel using a new scalpel blade, and place it into a 1.5-ml microcentrifuge tube.
- 3b. Weigh the gel slice in a colorless tube. Add 3 vol of Buffer QG to 1 vol of gel (100 mg corresponds to ~ 100 μ l).
- 4b. Incubate the tube 10 min at 50°C or until the gel slice has completely dissolved. During incubation, vortex the tube every 2 to 3 min to help dissolve the gel.
- 5b. At the end of incubation, check if the gel is completely dissolved and if the mixture is yellow. If the mixture presents an orange or violet color, add 10 μ l of 3 M sodium acetate, and mix.

- 6b. Add 1 vol isopropanol to the sample and vortex the mixture.
- 7b. Place a MinElute spin column into a 2-ml collection tube, and transfer the sample (up to 700 μ l) to the column.
- 8b. Centrifuge 1 min at 16,000 \times *g*, room temperature.
- 9b. Discard the flow-through in the collection tube, and place the column back into the same collection tube.
- 10b. Transfer the remaining sample to the column, and repeat steps 8b and 9b.
- 11b. Add 500 μ l Buffer QG to the column, and repeat steps 8b and 9b.
- 12b. Add 750 μ l Buffer PE to the column, and let it stand 5 min at room temperature.
- 13b. Centrifuge 1 min at 16,000 \times *g*, room temperature.
- 14b. Discard the flow-through in the collection tube, and place the column back into the same collection tube.

Residual ethanol from Buffer PE will not be completely removed unless the flow-through is discarded before step 15b.

- 15b. Centrifuge the tube 1 min at 16,000 \times *g*, room temperature.
- 16b. Place the column into a new 1.5-ml microcentrifuge tube. Add 10 to 20 μ l Buffer EB to the column, and let it stand 5 min at room temperature.

Make sure that Buffer EB is dispensed directly onto the membrane for complete elution of bound DNA. Do not touch the membrane of the column. The volume of Buffer EB to elute the DNA will depend on the concentration of your sample DNA.

- 17b. Centrifuge 1 min at 16,000 \times *g*, room temperature, and collect the flow-through.

The flow-through contains the purified PCR product.

- 18b. Proceed to step 19.

Verify the quality and concentration of purified PCR product

19. Run an aliquot (1 to 2 μ l) of purified PCR product in an agarose gel with a DNA ladder for quantification and size determination.
20. Estimate the DNA concentration on an agarose gel (Support Protocol 4).

DNA concentration can be determined after gel electrophoresis is complete by comparing the sample DNA intensity to that of the DNA ladder for quantification and size determination. You can also estimate DNA concentration by spectrophotometry at 260 nm.

21. Prepare a mix containing the desired amount of DNA and the primer (usually 10 pmol). Prepare at least one mix with forward primer and one mix with reverse primer. Submit the mix for DNA sequencing.

Check with the DNA sequencing facility for the amount of DNA and primer required. Usually protocols for sequencing PCR fragments recommend using 10 ng of PCR fragment per 100 bp of fragment size.

Overconcentrating the template will not give you a better sequencing result.

Analyze sequences

22. After getting the results from the sequencing facility, use the reads of each PCR product to create a consensus sequence using SeqTrace or equivalent software.

Table 14A.5.3 Genes Used to Distinguish Between Group 1 and Group 2 Brazilian Vaccinia Virus

Group	Strain	Gene		
		A56R	C23L	A26L
1	Araçatuba (ARAV)	AY523994	JX678776	DQ516057
1	Guarani P2 (GP2V)	DQ206437	JX678772	DQ516058
1	Passatempo (PSTV)	DQ516060	JX678773	DQ516060
1	Serro human2 virus (SH2V)	JQ361130	JX678778	JQ361140.1
1	Pelotas 2 (P2V)	GU183770	JX678774	
1	Mariana (MARV)	GQ226040	JX678775	
1	Cantagalo (CTGV)	AY354514		
1	Maranhão	KF273984		
1	Diamantina (DMTV)		JX678777	
2	Pelotas 1 (P1V)	GU183769	JX678770	
2	Guarani P1 (GP1V)	DQ206436	JX678771	DQ516061
2	Belo Horizonte (VBH)	DQ206435	JX678779	AF501620
2	BeAn58058 (BAV)	DQ206442		DQ516062

Several programs can be used to work with raw sequence data. Here we suggest SeqTrace, which is freely available (<http://seqtrace.googlecode.com>) and runs on most popular operating systems (Stucky, 2012). The software features a graphical interface including a chromatogram viewer and sequence editor with tools to align, compute consensus sequences using forward and reverse traces, filter low-quality base calls, and eliminate primer sequences.

To compare nucleotide sequences to check for the presence of molecular signatures and to perform further analyses, you need to create a file containing the desired gene sequences. Here we suggest the analysis of the A56R, A26L, and C23L genes, since those have genetic markers that can differentiate VACV groups or strains (see Basic Protocol 10 or Alternate Protocols 2 or 3).

To create the file containing nucleotide sequences to be analyzed, we suggest including sequences obtained from different species of Orthopoxvirus (*Variola virus*, *Cowpox virus*, *Camelpox*, *Monkeypox virus*, *Rabbitpox virus*, *Horsepox virus*, *Buffalopox virus*) and different sequences of VACV, including Br-VACV from groups 1 and 2 (see Table 14A.5.3; Drumond et al., 2008; Campos et al., 2011; Assis et al., 2012).

- To obtain the desired nucleotide sequences, perform a search in a nucleotide database such as GenBank (<http://www.ncbi.nlm.nih.gov/genbank/>), European Nucleotide Archive (EMBL-EBI; <http://www.ebi.ac.uk/>), or DNA Data Bank of Japan (<http://www.ddbj.nig.ac.jp/>).

You can perform the search using the name of the gene and of the organism/strain or using sequence accession numbers (for some examples see Table 14A.5.3; Drumond et al., 2008; Campos et al., 2011; Assis et al., 2012). You can also retry sequences after a similarity search using each of your consensus sequences (after BLASTn or FASTAn analysis).

- Using the consensus sequence, perform an initial analysis using BLASTn and/or FASTAn. Then perform a search for similar sequences using tools such as FASTA (http://fasta.bioch.virginia.edu/fasta_www2/fasta_list2.shtml; Pearson, 2013) or BLAST (<http://blast.ncbi.nlm.nih.gov/Blast.cgi>; Altschul et al., 1990)

BLASTn and FASTAn find regions of local and global similarity, respectively, between your DNA sequences and sequences deposited in the DNA databases. Tutorials for these tools are available online (<http://www.ncbi.nlm.nih.gov/books/NBK1734/> and http://fasta.bioch.virginia.edu/fasta_www2/fasta_guide.pdf; Pearson, 2004; Ladunga, 2009). This initial analysis gives an idea of sequences that are more similar to the query (your sequence). Review the results and the alignments. Determine if the query is similar to the plus (5' to 3' strand; strand = plus/plus) or minus (3' to -5' strand; strand = plus/minus) strand. Observe the similarity between the obtained sequences and sequences deposited into databases.

BLASTx and FASTAx analysis can also be performed to have an idea of the deduced amino acid sequence coded by your nucleotide sequence. These tools translate the query DNA sequence in six reading frames, and the resulting six-protein sequences are then compared to protein sequences in the database.

BLAST and FASTA have different tools to compare nucleotide or protein sequences to sequences in a database and calculate the statistical significance of the matches. Different tools can be tried.

25. Download the sequences in FASTA format, and create a FASTA file (*.fas) containing all sequences to be analyzed.

Information about FASTA format is available at <http://blast.ncbi.nlm.nih.gov/blastcgihelp.shtml>.

26. Align the sequences using ClustalW or Muscle algorithms implemented in MEGA 6.0.

A tutorial (Assembling Data for Analysis: Building Sequence Alignments) is available at <http://www.megasoftware.net/webhelp/helpfile.htm>.

Several programs and tools are available to perform phylogenetic and evolutionary analyses. Here we use MEGA 6.0 (Molecular Evolutionary Genetics Analysis; Tamura et al., 2013), available for download at <http://www.megasoftware.net/>.

If you are working with protein coding sequences and if they are in the right frame, you can align the sequences as the translated codon to amino acids usually give better results (options “Align by ClustalW codons” or “Align by Muscle codons”).

27. Visually inspect the alignment, and if necessary edit it to improve the alignment quality. Check the alignment for the presence of molecular signatures of other polymorphisms.

28. Export the alignment.

The alignment can be saved in different formats: mega (.meg), fasta (*.fas), or nexus (*.nex).*

29. Open the alignment in mega format in MEGA 6.0. To reconstruct a phylogenetic tree, go to “Model,” and choose the option “Find best DNA/Protein Models.”

30. After choosing the model that best fit the data, under “Phylogeny” choose “Construct/Test Neighbor-joining Tree” or “Construct/Test Maximum Likelihood Tree” to perform phylogenetic inferences based on distance and maximum likelihood methods, respectively.

Tutorials are available at <http://www.megasoftware.net/webhelp/helpfile.htm>.

31. Analyze the trees and perform other analyses within the several evolutionary analysis tools.

Tutorials for “Evolutionary Analysis” are available at <http://www.megasoftware.net/webhelp/helpfile.htm>. You can also try different tools and programs available online.

Biological Characterization of Virulence in Mouse Models

Based on the virulence profile in BALB/c mouse models, VACV can be grouped into two groups as also observed in phylogenetic studies. Group 2 viruses cause disease and death in infected BALB/c mice, but group 1 viruses do not cause any clinical signs or death in infected mice. This protocol describes a biological characterization for VACV based on virulence in BALB/c mice. VACV samples are used to infect BALB/c mice intranasally with 10 μ l of viral suspensions containing 10⁶ PFU. The mice are weighed daily, and clinical signs are recorded for 10 days post infection.

Materials

- 4- to 6-week-old male BALB/c mice
- Viral samples to be inoculated previously purified and titrated (see Support Protocols 1 and 2)
- PBS (see recipe)
- Ketamine/xylazine in PBS (see *APPENDIX A.3N*)
- Positive control: VACV Western Reserve strain

- Mouse housing facility
- Insulin syringe with 12.7-mm needle
- Petri dish
- Scale, to weigh mice

NOTE: All protocols using live animals must first be reviewed and approved by an Institutional Animal Care and Use Committee (IACUC) and must conform to governmental regulations regarding the care and use of laboratory animals.

Maintain mice

1. Maintain 4- to 6-week-old male BALB/c mice in filter-top microisolator cages.

The microisolator cages should be located in a ventilated animal caging system with controlled light (12 hr light and 12 hr dark), humidity (60% to 80%), and temperature (22 \pm 1°C).

Provide the mice with commercial mouse food and water ad libitum. Clean the cages and replace water at least two times a week or according to need.

Prepare inoculation

2. Dilute the viral samples to be inoculated at 10⁶ PFU in a final volume of 10 μ l/mouse using PBS as diluent.
3. Anesthetize mouse by i.p. injection of ketamine and xylazine with an insulin syringe.

*An appropriate dose for anesthesia is 80 to 120 mg/kg (see *APPENDIX A.3N*).*

Wait until the animals are completely anesthetized before infection.

Infect mice by intranasal inoculation

4. Place 10 μ l containing 10⁶ PFU of test viral suspension in a petri dish.
5. Inoculate the mice intranasally with a drop of viral suspension.

The animals should be arranged vertically at a 60° to 90° angle to the drop and placed in contact with the drop until it's completely inhaled.

Groups of at least 5 mice are suggested for this assay.

6. Inoculate the uninfected control group with 10 μ l PBS.

The VACV Western Reserve strain can be used as a positive control, as it is pathogenic for BALB/c mice.

7. Weigh the mice daily, and register clinical signs such as ruffling fur, arching back, periocular alopecia, and penile balanoposthitis for 10 days post infection.

Mice that lose >25% of their initial weight should be euthanized. To analyze VACV tropism in mice, the organs (trachea, lungs, heart, kidneys, liver, brain, and spleen) can be aseptically removed after euthanasia.

Biological Characterization of Plaque Phenotype in Cell Culture

VACV show a biological diversity that allows for separating the viruses into different groups, and they can be characterized in many different ways. The VACV strain shows plaque phenotypes that differ in size such that group 2 VACV have larger plaques than group 1 VACV. This protocol describes a biological characterization for VACV based on plaque phenotype assays in cell culture. VACV previously isolated (Basic Protocol 5 to 7), plaque purified (Basic Protocol 8), replicated (Support Protocol 1), and titrated (Support Protocol 2) are used to infect BSC-40 cells. After 48 hr the cells are stained with crystal violet.

Materials

BSC-40 cells grown to 80% to 90% confluence in 6-well tissue culture plates (see Basic Protocol 8, steps 1 through 3)

Agarose

2× MEM (e.g., Gibco, cat. no. 11700-077) with 2% (v/v) FBS

VACV to be assayed

1× MEM (e.g., Gibco, cat. no. 11700-077)

PBS (see recipe)

10% formalin in PBS

1% (w/v) crystal violet (see recipe)

37°C and 56°C water bath

37°C, 5% humidified incubator

Aspirator

Plate preparation

1. Grow BSC-40 cells to 80% to 90% confluence in a 6-well culture plate (see Basic Protocol 8, steps 1 through 3).
2. Make a 1% agarose solution with water as diluent. Prewarm 2× MEM in a 37°C water bath.

Keep agarose in a 56°C water bath and 2× MEM in a 37°C water bath until use, to prevent solidification.

3. Combine the agarose solution and the 2× MEM at a 1:1 ratio.

Keep final solution in a 37°C water bath until use, to prevent solidification

Perform plaque phenotyping in cell culture

4. Dilute the virus to be assayed using MEM without FBS so that ~50 PFU per 300 µl can be added to each well of the 6-well tissue culture plates.
5. Remove the culture medium from the BSC-40 plates.
6. Wash twice with PBS, and remove any excess liquid.
7. Add 300 µl of virus containing 50 PFU into each well.
8. Incubate 1 hr at 37°C. Rock plates every 10 min.
9. Remove the virus and add 2 ml of 1:1 agarose/MEM solution to each well.

10. Incubate 48 hr at 37°C with 5% CO₂.
Check under the microscope daily.
11. Add 0.5 ml of 10% formalin, and incubate at least 2 hr at room temperature for fixation.
Greater fixation times are required to allow penetration of formalin in medium containing agarose.
12. Remove medium with formalin and add 0.5 ml of 1% crystal violet to each well. Incubate at least 15 min at room temperature.
13. Aspirate crystal violet, wash with water, and allow wells to dry for plaque phenotype analysis.

The expected plaque phenotypes differ in size such that group 2 VACV have larger plaques than group 1 VACV (Campos et al., 2011). The appearance of the plaque when viewed with an inverted microscope is similar to that demonstrated in Figure 14A.5.3.

REAGENTS AND SOLUTIONS

Use deionized, distilled water in all recipes and protocol steps. When working with DNA, prepare all reagents using nuclease-free water. For common stock solutions, see APPENDIX 2A.

Acrylamide/bisacrylamide solution (29:1), 30%

290 g acrylamide
10 g *N,N'*-methylbisacrylamide
600 ml water
Adjust the final volume to 1 liter with water
Filter sterilize (0.45- μ m pore size) and adjust pH to 7.0 with 10 M NaOH
Store in dark bottles at 2°C to 8°C for up to 6 months

Heating may be necessary to dissolve the acrylamide.

Coating buffer, pH 9.6

0.01 M sodium carbonate (Na₂CO₃)
0.01 M sodium bicarbonate (NaHCO₃)
Adjust pH to 9.6 with 10 M NaOH
Store up to 2 months at 4°C

Crystal violet solution, 1%

Dissolve 10 g crystal violet in 1 liter of 20% ethanol to obtain a stock solution. To obtain a working solution, mix 96 ml stock solution, 190 ml of 95% ethanol, and 714 ml water or PBS. Store indefinitely at room temperature.

Developer solution

5.9 g sodium carbonate (Na₂CO₃; e.g., Millipore, cat. no. 207-838-8)
0.1 g paraformaldehyde (CH₂O)_n (e.g., Millipore, cat. no. 30525-89-4)
Dissolve in water and bring final volume to 200 ml with water
Prepare fresh

DNA loading buffer, 6 \times

60 ml glycerol
6 ml 1 M Tris·Cl, pH 8.0 (APPENDIX 2A)
1.2 ml 25 mM EDTA, pH 8.0
60 mg bromophenol blue or 100 mg Orange G

Dissolve in 32.8 ml water
Adjust pH to 8.3 with HCl
Store at 4°C for up to 6 months

Dry solution

500 ml 99.8% ethanol
50 ml glycerol
50 ml glacial acetic acid
400 ml water
Store at room temperature for up to 6 months

Fixer 1 solution

400 ml 99.8% methanol
100 ml glacial acetic acid
500 ml water
Store at room temperature for up to 6 months

Fixer 2 solution

100 ml 99.8% ethanol
50 ml glacial acetic acid
500 ml water
Store at room temperature for up to 6 months

Oxidant solution, 10×

5 g potassium dichromate (34 mM final)
1.1 ml nitric acid (32 mM final)
Dissolve in water and bring final volume 500 ml with water
Store at 4°C for up to 6 months

Oxidant solution should be diluted to a 1× concentration prior to use.

PBS

8 g NaCl (137 mM final)
1.44 g Na₂HPO₄ (10 mM final)
0.2 g KCl (2.7 mM final)
0.24 g KH₂PO₄ (2 mM final)
Dissolve in 900 ml water
Adjust pH to 7.4 using 1 M NaOH or 1 M HCl if necessary
Bring final volume to 1 liter with water
Autoclave in 500-ml bottles for 20 min
Store indefinitely at room temperature or at 4°C after opening

PCR buffer, 10×

0.1 M Tris·Cl, pH 8.3
0.5 M KCl
0.1% (v/v) Triton X-100
Store at -20°C for up to 1 year

TAE buffer stock solution, 10×

48.4 g Tris base
11.42 ml glacial acetic acid
20 ml 25 mM EDTA
Dissolve in water and bring final volume to 1 liter with water

continued

DNA VIRUSES

14A.5.39

Autoclave in 500-ml bottles for 20 min
Store indefinitely at room temperature or at 4°C after opening

TAE should be diluted to 1× prior to use for electrophoresis.

TBE buffer stock solution, 5×

54 g Tris base
27.5 g boric acid
20 ml 25 mM EDTA

Dissolve in water and bring final volume to 1 liter with water

Adjust pH to 8.3 with 10 M NaOH

Autoclave in 500-ml bottles for 20 min

Store indefinitely at room temperature or at 4°C after opening

TBE should be diluted to 1× prior to use for electrophoresis.

Trypsin/EDTA solution

40 g NaCl

2 g KCl

5 g glucose

2.9 g NaHCO₃

2.25 ml 1% (w/v) phenol red

5.3 ml 0.5 M EDTA

2.5 g trypsin, 1:250 (e.g., BD Difco)

Add NaCl, KCl, glucose, NaHCO₃, and phenol red in a 5-liter volumetric flask

Add 1 liter water

Add 0.5 M EDTA

Dissolve the trypsin in 20 ml water with use of a mortar and pestle. Slowly bring final volume to 100 ml with water and add to solution.

Bring final volume to 5 liter with water

Filter using a 0.22- μ m membrane in a biological flow hood

Aliquot and store for 1 year at –20°C

COMMENTARY

Background Information

VACV, the prototype species of the OPV genus, causes an occupational zoonotic disease that is primarily associated with the handling of infected dairy cattle. In humans, VACV infection is characterized by the development of skin lesions, principally on the hands, that appear as itchy nodular swellings. Other localizations of the lesions have been described. After a few days, the nodular swellings become papules, and local edema appears. The lesions evolve into umbilicated pustules surrounded by a strong inflammatory response. Approximately 12 days after the initial appearance of the lesions, they turn into necrotic and painful ulcers; after a short period of time, all the lesions develop into scabs, most of which slough off. Exanthema is coincident with the development of peripheral lymphangitis and lymphadenopathy. The disease progression is accompanied by systemic influenza-like symptoms including headache, myalgia, and fever. The sys-

temic symptoms are present for ~2 to 5 days within the third and twentieth day after the onset of symptoms. Other symptoms include anorexia, dehydration, arthralgia, nausea, and sudoresis (Silva-Fernandes et al., 2009).

The exact incubation period of the infection is difficult to determine, but it has been described as 3 to 5 days. The whole progression of the disease takes 4 weeks (Silva-Fernandes et al., 2009).

Diagnosis can be done by detecting the virus in the lesions and also confirming the presence of antibodies in unvaccinated individuals (Mota et al., 2010; Costa et al., 2013). Isolation of viruses from lesions is frequently very efficient as there are a lot of viral particles in lesions. DNA can also be detected from viruses in blood of patients during the systemic period confirming that it is not only a localized infection (Abrahão et al., 2010).

During the last decade, several natural infecting VACVs were isolated and characterized in Brazil (Damaso et al., 2000;

Trindade et al., 2003). When outbreak notifications first began, diagnosis of the etiologic agent was the priority. Today, however, reasonable amounts of genetic and biological data allow a wider view of the viral polymorphisms and the relationships among these viruses.

The most important finding about the diversity of Br-VACV is that there is a clear phenotypic and genetic dichotomy among the viruses (Trindade et al., 2006; de Souza Trindade et al., 2008; Trindade et al., 2008; Oliveira et al., 2015), which has been supported by studies of the partial genomic sequencing of these viruses and by in vivo virulence studies (Ferreira et al., 2008).

Critical Parameters and Troubleshooting

VACV is stable when stored at -20°C , but it is safer to store the viruses at -80°C with desiccation in the form of crusts, biopsies, or dry swabs. It is important to add PBS or medium to the samples only just before performing any procedure.

VACV replicates efficiently in human cells, mouse cells, and avian cells. During our studies we observed that, in some cellular types, there was a selection of a group of viruses. Therefore, we have used Vero cells to avoid this.

To avoid mutations it is important to make a virus seed stock for virus replication and to reduce the number of passages in culture in order to maintain the natural characteristics of the virus.

As the virus charge of the lesions or culture is high, it is important to avoid cross contamination by using a biological safety cabinet which should be efficiently decontaminated.

Anticipated Results

Basic Protocol 4 and Alternate Protocol 1 are very sensible methods to detect viral genome in clinical samples and helpful for a rapid diagnosis. The amplified DNA can be sequenced and the virus characterized as an OPV or VACV (Basic Protocol 11). Isolation of the virus (Basic Protocols 5, 6, or 7) can be obtained in the first passage in culture, though sometimes one or more blind passages are needed. The replication of VACV obtained from clinical samples after the third or fourth passage produces titers around 10^4 to 10^6 PFU/ml. After isolation a cleaning procedure is used to proceed to plaque purification (Basic Protocol 8). Characterization can be obtained using Basic Protocols 9 or 10 or

Alternate Protocols 2 or 3. Biological characterization (Basic Protocols 12 and 13) can confirm the group of VACV. For serological techniques (Basic Protocols 2 and 3), it is recommended to use the purified virus with titers around 10^9 PFU/ml.

Time Considerations

The molecular technique (Basic Protocol 4) takes around 4 hr to obtain the diagnosis. To use this protocol DNA can be extracted or the sample can be diluted in water. If DNA is extracted we can use qPCR (Alternate Protocol 1) with results in 2 hr. The isolation takes a minimum of 48 hr (Basic Protocols 5, 6, or 7) and needs further characterization which takes at least 2 hr.

Acknowledgements

We thank our colleagues from Laboratório de Vírus of Universidade Federal de Minas Gerais for their excellent support. We would also like to thank CNPq, CAPES, FAPEMIG and Pro-Reitoria de Pesquisa da Universidade Federal de Minas Gerais (PRPq-UFMG) for financial support.

Literature Cited

- Abrahão, J.S., Drumond, B.P., Trindade, G.E.S., da Silva-Fernandes, A.T., Ferreira, J.M., Alves, P.A., Campos, R.K., Siqueira, L., Bonjardim, C.A., Ferreira, P.C., and Kroon, E.G. 2010. Rapid detection of orthopoxvirus by semi-nested PCR directly from clinical specimens: A useful alternative for routine laboratories. *J. Med. Virol.* 82:692-699. doi: 10.1002/jmv.21617.
- Altschul, S.F., Gish, W., Miller, W., Myers, E.W., and Lipman, D.J. 1990. Basic local alignment search tool. *J. Mol. Biol.* 215:403-410. doi: 10.1016/S0022-2836(05)80360-2.
- Assis, F.L., Almeida, G.M., Oliveira, D.B., Franco-Luiz, A.P., Campos, R.K., Guedes, M.I., Fonseca, F.G., Trindade, G.S., Drumond, B.P., Kroon, E.G., and Abrahão, J.S. 2012. Characterization of a new Vaccinia virus isolate reveals the C23L gene as a putative genetic marker for autochthonous group 1 Brazilian Vaccinia virus. *PLoS ONE* 7:e50413. doi: 10.1371/journal.pone.0050413.
- Campos, M.A.S. and Kroon, E.G. 1993. Critical period of irreversible block of VACV replication. *Braz. J. Microbiol.* 24:104-110.
- Campos, R.K., Brum, M.C., Nogueira, C.E., Drumond, B.P., Alves, P.A., Siqueira-Lima, L., Assis, F.L., Trindade, G.S., Bonjardim, C.A., Ferreira, P.C., Weiblen, R., Flores, E.F., Kroon, E.G., and Abrahão, J.S., 2011. Assessing the variability of Brazilian Vaccinia virus isolates from a horse exanthematic lesion: Coinfection with distinct viruses. *Arch. Virol.* 156:275-283. doi: 10.1007/s00705-010-0857-z.

- Costa, G.B., Moreno, E.C., de Souza Trindade, G., and Studies Group in Bovine Vaccinia. 2013. Neutralizing antibodies associated with exposure factors to orthopoxvirus in laboratory workers. *Vaccine* 31:4706-4709. doi: 10.1016/j.vaccine.2013.08.023.
- Cotter, C.A., Earl, P.L., Wyatt, L.S., and Moss, B. 2015. Preparation of cell cultures and vaccinia virus stocks. *Curr. Protoc. Microbiol.* 39:14A.3.1-14A.3.18. doi: 10.1002/9780471729259.mc14a03s39.
- Damaso, C.R.A., Esposito, J.J., Condit, R.C., and Moussatché, N., 2000. An emergent poxvirus from humans and cattle in Rio de Janeiro State: Cantagalo virus may derive from Brazilian smallpox vaccine. *Virology* 277:439-449. doi: 10.1006/viro.2000.0603.
- de Souza Trindade, G., Li, Y., Olson, V.A., Emerson, G., Regnery, R.L., da Fonseca, F.G., Kroon, E.G., and Damon, I. 2008. Real-time PCR assay to identify variants of vaccinia virus: Implications for the diagnosis of bovine vaccinia in Brazil. *J. Virol. Methods* 152:63-71. doi: 10.1016/j.jviromet.2008.05.028.
- Drumond, B.P., Leite, J.A., da Fonseca, F.G., Bonjardim, C.A., Ferreira, P.C., and Kroon, E.G. 2008. Brazilian Vaccinia virus strains are genetically divergent and differ from the lister vaccine strain. *Microbes Infect.* 10:185-197. doi: 10.1016/j.micinf.2007.11.005.
- Earl, P.L., Moss, B., Wyatt, L.S., and Carroll, M.W. 2001. Generation of recombinant vaccinia viruses. *Curr. Protoc. Mol. Biol.* 43:16.17.1-16.17.19. doi: 10.1002/0471142727.mb1617s43.
- Ferreira, J.M., Drumond, B.P., Guedes, M.I., Pascoal-Xavier, M.A., Almeida-Leite, C.M., Arantes, R.M., Mota, B.E., Abrahão, J.S., Alves, P.A., Oliveira, F.M., Ferreira, P.C., Bonjardim, C.A., Lobato, Z.I., and Kroon, E.G. 2008. Virulence in murine model shows the existence of two distinct populations of Brazilian Vaccinia virus strains. *PLoS ONE* 8: e3043. doi: 10.1371/journal.pone.0003043.
- Ladunga, I. 2009. Finding similar nucleotide sequences using network blast searches. *Curr. Protoc. Bioinform.* 26:3.3.1-3.3.26. doi: 10.1002/0471250953.bi0303s26.
- Mota, B.E., Trindade, G.S., Diniz, T.C., da Silva-Nunes, M., Braga, E.M., Urbano-Ferreira, M., Rodrigues, G.O., Bonjardim, C.A., Ferreira, P.C., and Kroon, E.G. 2010. Seroprevalence of orthopoxvirus in an amazonian rural village, acre, Brazil. *Arch. Virol.* 155:1139-1144. doi: 10.1007/s00705-010-0675-3.
- Oliveira, G., Assis, F., Almeida, G., Albarnaz, J., Lima, M., Andrade, A.C., Calixto, R., Oliveira, C., Neto, J.D., Trindade, G., Ferreira, P.C., Kroon, E.G., and Abrahão, J. 2015. From lesions to viral clones: Biological and molecular diversity amongst autochthonous Brazilian Vaccinia virus. *Viruses* 7:1218-1237. doi: 10.3390/v7031218.
- Pearson, W. 2004. Finding protein and nucleotide similarities with FASTA. *Curr. Protoc. Bioinform.* 8:3.9.1-3.9.23. doi: 10.1002/0471250953.bi0309s04.
- Pearson, W.R. 2013. An introduction to similarity ("homology") searching. *Curr. Protoc. Bioinform.* 42:3.1.1-3.1.8. doi: 10.1002/0471250953.bi0301s42.
- Ropp, S.L., Jin, Q.I., Knight, J.C., Massung, R.F., and Esposito, J.J. 1995. PCR Strategy for identification and differentiation of small pox and other orthopoxviruses. *J. Clin. Microbiol.* 33:2069-2076.
- Sanger, F., Nicklen, S., and Coulson, A.R. 1977. DNA Sequencing with chain-terminating inhibitors. *Proc. Natl. Acad. Sci. U.S.A.* 74:5463-5467. doi: 10.1073/pnas.74.12.5463.
- Silva-Fernandes, A.T., Travassos, C.E., Ferreira, J.M., Abrahão, J.S., Rocha, E.S., Viana-Ferreira, F., dos Santos, J.R., Bonjardim, C.A., Ferreira, P.C., and Kroon, E.G. 2009. Natural human infections with vaccinia virus during bovine Vaccinia outbreaks. *J. Clin. Virol.* 44:308-313. doi: 10.1016/j.jcv.2009.01.007.
- Stucky, B.J. 2012. SeqTrace: A graphical tool for rapidly processing DNA sequencing chromatograms. *J. Biomol. Tech.* 23:90-93. doi: 10.7171/jbt.12-2303-004.
- Tamura, K., Stecher, G., Peterson, D., Filipski, A., and Kumar, S. 2013. MEGA6: Molecular evolutionary genetics analysis version 6.0. *Mol. Biol. Evol.* 30:2725-2729. doi: 10.1093/molbev/mst197.
- Trindade, G.S., da Fonseca, F.G., Marques, J.T., Nogueira, M.L., Mendes, L.C., Borges, A.S., Peiró, J.R., Pituco, E.M., Bonjardim, C.A., Ferreira, P.C., and Kroon, E.G. 2003. Araçatuba virus: A Vaccinia-Like virus associated with infection in humans and cattle. *Emerg. Infect. Dis.* 9:155-160. doi: 10.3201/eid0902.020244.
- Trindade, G.S., Lobato, Z.I.P., Drumond, B.P., Leite, J.A., Trigueiro, R.C., Guedes, M.I.M.C., da Fonseca, F.G., Santos, J.R.D., Bonjardim, C.A., Ferreira, P.C.P., and Kroon, E.G. 2006. Isolation of two Vaccinia virus strains from a single bovine Vaccinia outbreak in rural area from Brazil: Implications on the emergence of zoonotic orthopoxviruses. *Am. J. Trop. Med. Hyg.* 75:486-490.

Key References

- Abrahão, J.S., Guedes, M.I., Trindade, G.S., Fonseca, F.G., Campos, R.K., Mota, B.E., Lobato, Z.I., Fernandes, A.T., Rodrigues, G.O., Lima, L.S., Ferreira, P.C., Bonjardim, C.A., and Kroon, E.G. 2009. One more piece in the VACV ecological puzzle: Could peridomestic rodents be the link between wildlife and bovine Vaccinia outbreaks in Brazil? *PLoS ONE* 4:1-7. doi: 10.1371/journal.pone.0005361.
- This manuscript describes the circulation of VACV in bovines and peridomestic rodents.*

- Damon, I. 2013. Poxviridae and their replication. *In* Fields Virology, 6th ed. (B.N. Fields, D.M. Knipe, and P.M. Howley, eds.) pp. 2129-2159.

Lippincott, Williams, and Wilkins, Philadelphia.
A useful book chapter with basic virology information on poxviruses.

Kroon, E.G., Mota, B.E., Abrahão, J.S., da Fonseca, F.G., and de Souza Trindade, G. 2011. Zoonotic Brazilian Vaccinia virus: From field to therapy. *Antiviral Res.* 92:150-163. doi: 10.1016/j.antiviral.2011.08.018.

An extensive review about the Brazilian VACV, from discovery to diagnosis.